UNIVERSITY OF SOUTHAMPTON

The Interaction between Light and Gibberellin in the Regulation of Wheat Architecture

Bethany Day Wallace

Doctor of Philosophy

FACULTY OF NATURAL AND ENVIRONMENTAL SCIENCES

September 2017

UNIVERSITY OF SOUTHAMPTON

ABSTRACT

NATURAL AND ENVIRONMENTAL SCIENCES

Biological Sciences

Doctor of Philosophy

THE INTERACTION BETWEEN LIGHT AND GIBBERELLIN IN THE REGULATION OF WHEAT ARCHITECTURE

Bethany Day Wallace

DELLA proteins are repressors of plant height that act in the gibberellin-response pathway. The Green Revolution saw DELLA variants exploited in wheat breeding, causing a dwarf phenotype that reduced lodging and increased grain numbers, greatly improving yields. However, the wheat DELLA *Rht-1* mutant lines also display adverse pleiotropic affects such as reduced grain size and reduced seedling vigour. Therefore, the identification of new targets which act downstream of RHT-1 in the regulation of stem elongation could provide a method to increase yields avoiding these pleiotropic effects. Phytochrome Interacting Factors (PIFs) are transcription factors that repress light responses in plants, leading to the promotion of hypocotyl elongation in Arabidopsis. DELLAs repress the transcriptional activity of PIFs through a direct physical interaction. This highlights a role for PIFs in regulating growth in response to gibberellin. Furthermore, a recent paper indicated that a rice PIF homologue, OsPIL1, is an important regulator of stem elongation. PIF-like proteins have not been previously identified in wheat, and the interaction between PIFs and DELLAs has not been demonstrated in any cereals. The evidence indicates that *PIF*s may act downstream of DELLAs in the GA response pathway, and are therefore make a promising target for modifying stem height in wheat, with the potential benefit of avoiding the pleiotropic effects associated with *Rht-1* mutations.

Each of the genomes in hexaploid bread wheat contain one DELLA gene, *RHT-1*. In contrast, bioinformatic analysis has identified three wheat paralogues of OsPIL1, named *TaPIL1*, *TaPIL2* and *TaPIL3*, each with three homoeologues. RHT-D1a was shown to interact with TaPIL1, TaPIL2 and TaPIL3 in a yeast two-hybrid screen. A yeast two-hybrid library screen identified twelve proteins of interest which interact with RHT-1 in the wheat stem including bHLH proteins, ethylene response elements, and indeterminate domain proteins. *TaPIL1* overexpression and RNAi lines demonstrated a role for TaPIL1 in the regulation of flowering time, stem elongation and ear length. Transgenic expression of OsPIL1 in wheat caused an increase in stem elongation and ear length, and delayed flowering time. TILLING lines were used to produce triple mutants of TaPIL1 and TaPIL3. Knockout of both genes displayed a reduced stem elongation phenotype, and the TaPIL3 triple mutant also displayed a reduced tiller phenotype, indicating that TaPIL1 and TaPIL3 promote stem elongation and that TaPIL3 also promotes tillering. These results suggest that the TaPILs are promising targets for downstream regulation of GA mediated of stem elongation.

Contents

List of figures

List of tables

UNIVERSITY OF Southampton

Academic Thesis: Declaration Of Authorship

I, Bethany Day Wallace

declare that this thesis and the work presented in it are my own and has been generated by me as the result of my own original research.

The interaction between Light and Gibberellin in the Regulation of Wheat Architecture.

I confirm that:

1. This work was done wholly or mainly while in candidature for a research degree at this University;
2. Where any part of this thesis has previously been submitted for a degree or any other qualification at this University or any other institution, this has been clearly stated;
3. Where I have consulted the published work of others, this is always clearly attributed;
4. Where I have quoted from the work of others, the source is always given. With the exception of such quotations, this thesis is entirely my own work;
5. I have acknowledged all main sources of help;
6. Where the thesis is based on work done by myself jointly with others, I have made clear exactly what was done by others and what I have contributed myself;
7. Either none of this work has been published before submission, or parts of this work have been published as: [please list references below]:

Signed: ……

Date: 27/09/2017

ACKNOWLEDGEMENTS:

Firstly, I would like to thank my supervisors, Peter Hedden, Steve Thomas, Andy Phillips and Matthew Terry for all their expertise and guidance throughout my studies. You have all helped me immensely and this project would not have been as interesting or enjoyable without your support.

I would also like to thank all the past and present members of the lab group during the time I have been at Rothamsted Research for making the lab such a pleasant place to work and for all the help and advice they have given me.

The Rothamsted students also deserve thanks for making my time at Rothamsted so enjoyable, especially my wonderful friends Lucy and Sofia for always cheering me up and taking me for a coffee break when I needed one. And thank you to Lucy, Sofia, Joe and Will for all the fun nights in the Pavilion when we needed something a bit stronger than coffee!

Finally, I would like to thank my family for all their love and support thoughout by studies, especially my amazing husband Alastair who has always been there to keep me motivated.

This work was funded by the Doctoral Training Partnership (DTP) BBSRC studentship programme.

ABBREVIATIONS:

3-AT	3-Amino-1,2,4-triazole
ABA	Abscisic acid
AD	Activation domain
ALA	δ-aminolevulinic acid
ALC	ALCATRAZ
ANOVA	Analysis of variance
APB	Active phytochrome binding
ARF	Auxin response factor
BAC	Bacterial artificial chromosome
bHLH	Basic helix-loop-helix
BiFC	Bimolecular Fluorescence Complementation
BOI	Botrytis susceptible1 interactor
BR	Brassinosteroid
BRG	BOI related
bZIP	basic leucine zipper
BZR1	Brassinazole-resistant 1
cDNA	Coding DNA
ChIP	Chromatin immunoprecipitation
CIMMYT	Centre for wheat and maize improvement in Mexico
CE	Controlled environment
CO	CONSTANS 1
COP1	Constitutive photomorphogenic 1
CPS	Copalyl diphosphate synthase
CRY	Cryptochrome
CT	Cytokinin
CTD	C terminal domain
CVA	Canonical variates analysis
D8	Dwarf-8-1
D9	Dwarf 9-1
DNAB	DNA binding
EMS	Ethyl methanesulfonate
ER	Endoplasmic reticulum
ERF	Ethylene-responsive element binding factors
EST	Expressed Sequence Tags
ET	Ethylene
FAD	Flavin adenine dinucleotide
FAR	Far-red-impaired response
FHL	FHY1-like
FHY1	Far-red elongated Hypocotyl 1
FKPM	Fragments per kilo base per million reads mapped
FLT	Flowering locus C
FR	Far red
FT	Flowering Locus T
GA	Gibberellin
GAI	Gibberellic acid insensitive
GAMT	GA methyl transferases

GAMyb GA-induced Myb-like protein
gDNA Genomic DNA
GFP Green fluorescent protein
GGPP *Trans*-geranylgeranyl diphosphate
GID1 Gibberellin insensitive dwarf 1
GUS Glucuronidase reporter gene
h Hour
HFR1 Long hypocotyl in far-red
HY5 Elongated hypocotyl 5
IDD INDETERMINATE DOMAIN
IWGSC International Wheat Genome Sequencing Consortium
JAJ Jasmonic acid
JAZ Jasmonate-ZIM domain
KAO *ent*-kaurenoic acid oxidase
KNOX1 KNOTTED1-like homeobox
KO *ent*-kaurene oxidase
KS *ent*-kaurene synthase
LHR Leucine heptad repeat
LSD Least significant difference
miRNA micro RNA
MY Million years
MYA Million years ago
NLS Nuclear localisation signal
NTD N terminal domain
P Phosphate
PAC Paclobutrazol
PCD Programmed cell death
PHOT Phototropin
phyA Phytochrome A
phyB Phytochrome B
PIF Phytochrome interacting factor
PIL PIF-like
PTGS Post transcriptional gene silencing
R Red
RAP Related to APETALA
RGA Repressor of ga1-3
RGL RGA-like
RNAi RNA interference
SAM Shoot apical meristem
SCF Skp1-cullin-F-box
SCL SCARECROW-like
SCR SCARECROW
SED Standard error of the mean
SLR Slender rice 1
SLR1 Slender 1
SLY1 Sleepy 1
SNP single nucleotide polymorphism
SOC1 SUPPRESSOR OF OVEREXPRESSION OF CONSTANS1

SPL	squamosa promoter binding-like
SPT	SPATULA
SRL	Short under red light
TILLING	Targeting Induced Local Lesions IN Genomes
UTR	Untranslated region
WGS	Whole genome shotgun
YA	Years ago

DEFINITIONS:

Chronic hunger	Undernourishment caused by not ingesting enough energy to lead a normal, active life.
Etiolation	Growth of a flowering plant in the dark.
Homologue	Two related sequences.
Orthologue	Two genes in different species which evolved from a common ancestral gene.
Paralogue	Two genes in the same species that are derived from the same ancestral gene.
Photomorphogenesis	The development of a seedling in the light.
Polyploid	Nuclei containing more than two homologous sets of chromosomes, i.e. more than two copies of each gene.
Skotomorphogenesis	The development of a seedling in the dark.

Chapter 1: Food security and the importance of wheat

1.1.1 Food security

The world population is rapidly increasing and is expected to reach somewhere between nine and eleven billion by 2050 (Lele, 2010). This constitutes an increase of six million people per month (Beddington, 2010), providing huge challenges in terms of food security. The number of people who are chronically hungry i.e. consistently failing to consume enough calories to lead a normal active life, has risen since the start of the millennium (Parry and Hawkesford, 2010). The FAO estimated that in 2009, one billion people went hungry, the highest number ever recorded (Chakraborty and Newton, 2011), and currently 840 million people worldwide suffer from chronic hunger (FAO 2013). In 2011 12% of the world population were undernourished (FAO, 2013) and more than one in seven people worldwide do not have access to a diet containing adequate protein and energy (Godfray et al., 2010). In low-middle income countries 26% of children are malnourished, which is a serious problem as under-nutrition in children causes 3.1 million deaths/year (Lancet, 2013). Food insecurity is also problematic in the developed world with 16 million people from developed nations being under-nourished; i.e. failing to receive enough nutrients from food for a good health and condition (FAO 2013). The number of people who were undernourished increased sharply in 2007, by 75 million, due to low grain yields which led to a price spike (Beddington, 2010). This demonstrates the large number of people who are vulnerable to changes in food availability, which is likely to become more common in the coming years as the world population increases.

The projected population increase therefore suggests that unless food production can be improved the number of people who are chronically hungry and malnourished could rise. Competition for land usage is another compounding factor that will cause instabilities in food supply. Currently there is increasing demand for meat, dairy products and biofuels (Godfray et al., 2010); by 2030 the demand for production of livestock is expected to increase by 40%. Currently 1.6 billion hectares of land are used in agriculture worldwide (Beddington, 2010) with croplands covering 12% of the earth's ice free terrestrial surface. In addition, land devoted to pasture covered 26% of the earth's ice free land, meaning that in total, food production encompasses 38% of the earth's terrestrial surface (Foley et al., 2011). Without considering impacts on biodiversity, ecosystems and climate change, the FAO has predicted that 2.4 billion hectares of new land could be suitable for agriculture. However other studies

have predicted only 50-1600 million hectares of available land, demonstrating that the figure is not easily determined (Beddington, 2010).

Worldwide, agriculture has already caused the clearing or conversion of 70% of the total grassland, 50% of the savannah, 45% of the deciduous forests and 27% of the tropical forests for farming. Currently agriculture is mainly expanding in the tropics where 80% of new cropland has replaced native tropical forest (Foley et al. 2011). Sustainable development requires that increases in agricultural production are not at the expense of biodiversity and ecosystems. In addition, forests have proven to be instrumental in combating climate change (Godfray et al. 2010), and it is estimated that the clearing of tropical forest for agriculture causes 12% of the annual anthropogenic CO_2 emissions (Foley et al. 2011), making their destruction highly undesirable. Therefore, it is likely that in the future more food will need to be produced on the same or a smaller amount of land than is currently available (Godfray et al. 2010). In addition to the lack of land availability, agriculture is facing serious pressures from other areas of production. Water availability is increasingly becoming a problem worldwide, with 80-90% of consumed water being devoted to irrigation. The need to increase crop production means that water use will need to become more sustainable in the future (Morison et al., 2008). Another area that is putting strain on global food production is fertiliser availability. Agriculture depends on the application of fertilisers containing phosphate (P), nitrogen and potassium to sustain yields. Modern agriculture is reliant on P from phosphorus rock, a non-renewable and dwindling resource. Reserves of P rock are predicted to be depleted within the next 50-100 years. Additionally, the quality of the remaining rock is declining. All these factors are set to cause a P crisis, in which availability of P falls well below the amount required to sustain yields (Cordell et al., 2009).

By 2050, global food demand is projected to increase by at least 60%, compared to demand in 2006. To meet this demand, annual world production of crops and livestock will need to be 60% higher than production in 2006. Around 80% of this increase needs to result from increases in crop yields (FAO, 2016).Modern agriculture is also facing challenges in all areas from increasing demand, climate change, water and fertiliser availability and restraints on land use. A drastic change involving higher yielding crop varieties and more sustainable farming methods is required, if we are to feed a growing population.

1.1.2 The importance of wheat

Wheat is grown in many areas of the globe as a vital staple food. The worldwide consumption of wheat was 680 mega tonnes in 2013, and 217 million hectares of wheat were planted in 2010, making it the most widely grown crop and accounting for 32% of the global area planted with staple crops (maize, rice, barley & sorghum) (Wheat Initiative 2013).

Globally, there are 1.2 billion 'wheat dependent' people who rely on wheat as their main source of calories and protein (CIMMYT, 2011). Worldwide, wheat provided 18.8% of the total energy supply in diets in 2009, making it second only to rice in terms of calories/capita/day(Dixon, 2009). Wheat also provides 20.4% of total protein supply, meaning that is the most important single source of protein globally (Shiferaw et al., 2013). Despite its wide-reaching importance to daily diets, wheat production is not consistently reaching demand; production has only met demand in 5 of the last 15 years (Wheat Initiative 2013). It has been predicted that for wheat production to match the strains of the increasing population, there needs to be a 60% increase by 2050 (CIMMYT 2011). However, in the past decade, production has only increased by 1.1% per year (Reynolds et al., 1999), see **Figure 1.1** (Wheat Initiative 2013), meaning that much needs to be done to prevent wheat production falling catastrophically below the levels of demand. As the amount of land available for agricultural practices is predicted to remain the same size or decrease (Wheat Initiative 2013), the yield of the existing wheat plots needs to be increased.

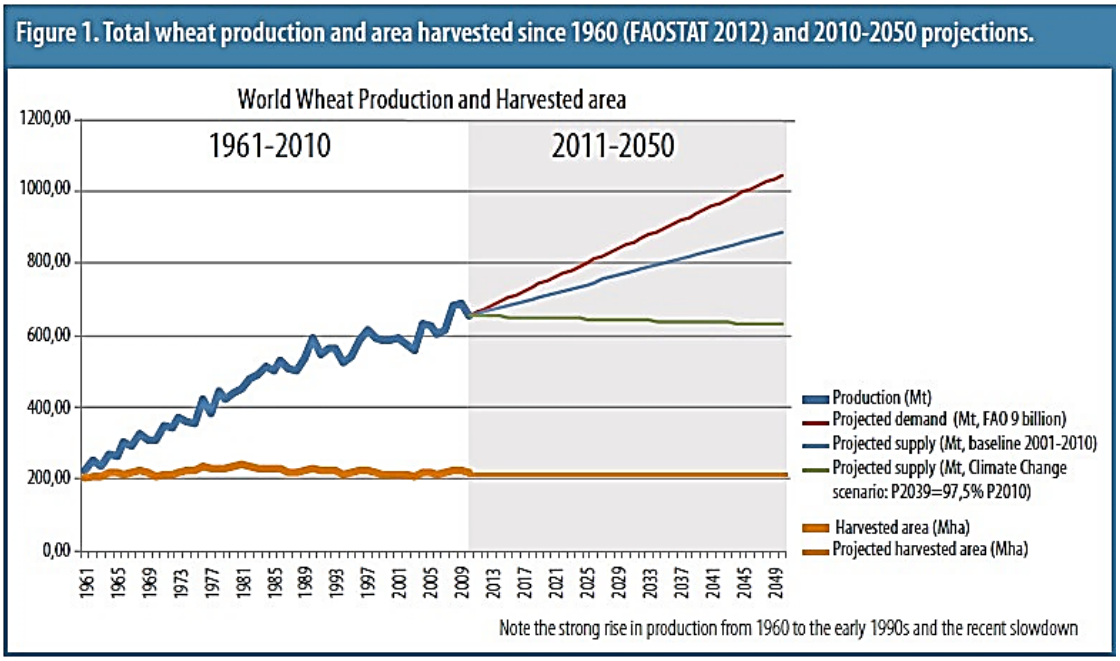

Figure 1.1 Wheat Production and Harvested Area since 1950 with 2050 Predictions (reproduced from Wheat Initiative 2013). Wheat production is shown by the bold blue line and harvested area is indicated by the bold orange line. Projected supply and projected harvested area are shown by thin blue and orange lines respectively. Projected demand is shown by the red line, and projected supply considering the effects of climate change is shown in green.

1.1.3 The Green Revolution

During the 1960s and 70s there were large increases in the yield of wheat. This was due to the cultivation of new high-yielding varieties in combination with increased use of fertiliser and pesticides. The new varieties had shorter, stronger stems that allowed the plants to accommodate the heavier ears with reduced risk of lodging in wind and rain (Evenson and Gollin, 2003). Furthermore, these semi-dwarf varieties allocated more assimilate to the grain improving their harvest index due to the production of larger numbers of slightly smaller grain (Flintham et al., 1997b, Peng et al., 1999).

The dwarfing gene in the green revolution crops originated in Japan, where a semi-dwarfing variety called Daruma was crossed with high yielding varieties of American wheat, which produced Norin10 lines. Norin10 was then used in breeding programmes in the USA to yield high yielding semi-dwarf wheat cultivars. One cross, called Norin10-Brevor14, was sent to Normal Borlaug at the International Centre for Wheat and Maize Improvement in Mexico (CIMMYT) (Hedden, 2003) where breeders incorporated dwarfing alleles into widely grown wheat varieties for tropical and sub-tropical regions; mainly spring wheat lines that could be grown in warmer climates. The new varieties of wheat were readily adopted by farmers in tropical and subtropical regions who had access to good irrigation systems or reliable rainfall.

The success of these new varieties was the beginning of the 'Green Revolution' (Evenson and Gollin 2003). The Norin10 dwarfing genes were so successfully adopted, that they can be found in over 70% of the current commercial wheat cultivars grown world-wide (Hedden 2003). The phenotype of these new wheat varieties was due to their abnormal response to gibberellin (GA), a plant hormone that is involved in many processes, including the control of plant height. The dwarf wheat plants had a mutation in their DELLA protein, discussed in section 1.4.1, which is involved in negatively regulating GA signalling. This prevents the stem from elongating in response to GA (Peng et al. 1999).

These green revolution crops have now reached the limits of their productivity, and so if we are to increase production to meet the growing demands for food, we need a new green revolution, generating novel high yielding wheat varieties.

1.1.4 Structure and origins of the wheat genome

A large proportion of the crop species grown today have genomes that originate from polyploidization events, meaning that these species contain multiple closely related genomes which result in multiple homoeologous copies of each gene (Edwards et al., 2013a). Polyploidization has also lead to chromosomal rearrangements, and long stretches of repetitive DNA, which means that analysis of the genome or identifying specific genes is difficult (Brenchley et al., 2012). The wheat genome consists of three sets of each chromosome pair which originate from three distinct diploid genomes; A, B and D. Each diploid genome contains seven chromosome pairs, meaning that there are 21 chromosome pairs within each genome, and six copies of each genome, leaving each wheat genome containing six sets of 21 chromosomes (Edwards et al. 2013; Marcussen et al. 2014).

Modern agriculture was first developed in the Fertile Crescent around 10,000 years ago (YA), which was a crucial advance in human history. In early farming, wild diploid wheat varieties such as *Aegilops* and *Triticum* species were grown, and as agriculture developed these wild species were replaced with domesticated diploid and tetraploid varieties (International Wheat Genome Sequencing, 2014).

The hexaploid wheat genome was thought to originate from two separate interspecies hybridisation events (**Figure 1.2**). Firstly, a hybridisation between *T. uratu* (AA) and an unknown relative of *Aegilops spelttoides* (BB), which gave rise to a quadraploid (AABB) species. A second hybridisation between the quadraploid *T. turgidum* (AABB) and *Ae. Tauschii* (DD)

then transpired to produce the hexaploid *T. aestivum* (AABBDD) (Brenchley et al. 2012; Edwards et al. 2013; Petersen et al. 2006), which makes up 95% of the bread wheat grown worldwide today (Marcussen et al. 2014). Petersen et al. (2006) isolated two single copy nuclear genes; *DCMI* and *EF-G* from each of the subgenomes. Phylogenetic analysis of these genes was used to demonstrate that the A genome originated from *Triticum uratu*, the B genome from an unknown but closely related relative of *Aegilops speltoides* and the D genome from *Aegilops tauschii*, supporting the theory of multiple hybridisations. Modern bread wheat was therefore thought to have arisen around 10,000 years ago as a result of a second hybridisation (Marcussen et al. 2014).

In 2014, the IWGSC used genome sequences from the A, B and D subgenomes, and 5 diploid relatives, to estimate the phylogenetic history of A, B and D. It was found that A and B are less similar to each other than they are to D, which suggests that D could have been formed from a hybridisation event between A and B. The phylogenetic evidence demonstrated that the initial divergence between *Aegilops* and *Triticum* occurred around 7 million years ago (Marcussen et al. 2014). The divergence between A-D and B-D was found to be around 1.2 million years (MY) later than the A-B divergence. In addition, the divergence between A–D is slightly later than between B-D, suggesting that gene flow between A and D continued after it had stopped between B and D. Using the phylogenetic evidence, it is thought that the hybridisation between *T. uratu* (AA) and *A. spelttoides* (BB) occurred somewhere between 0.58 and 0.82MYA, and the second hybridisation to give hexaploid wheat occurred 0.23-0.43MYA (**Figure 1.2**). Put together this new phylogenetic evidence demonstrates that bread wheat is a product of both hybridisation/polyploidization of the A, B and D genomes, along with ancestral hybridisation events (Marcussen et al. 2014).

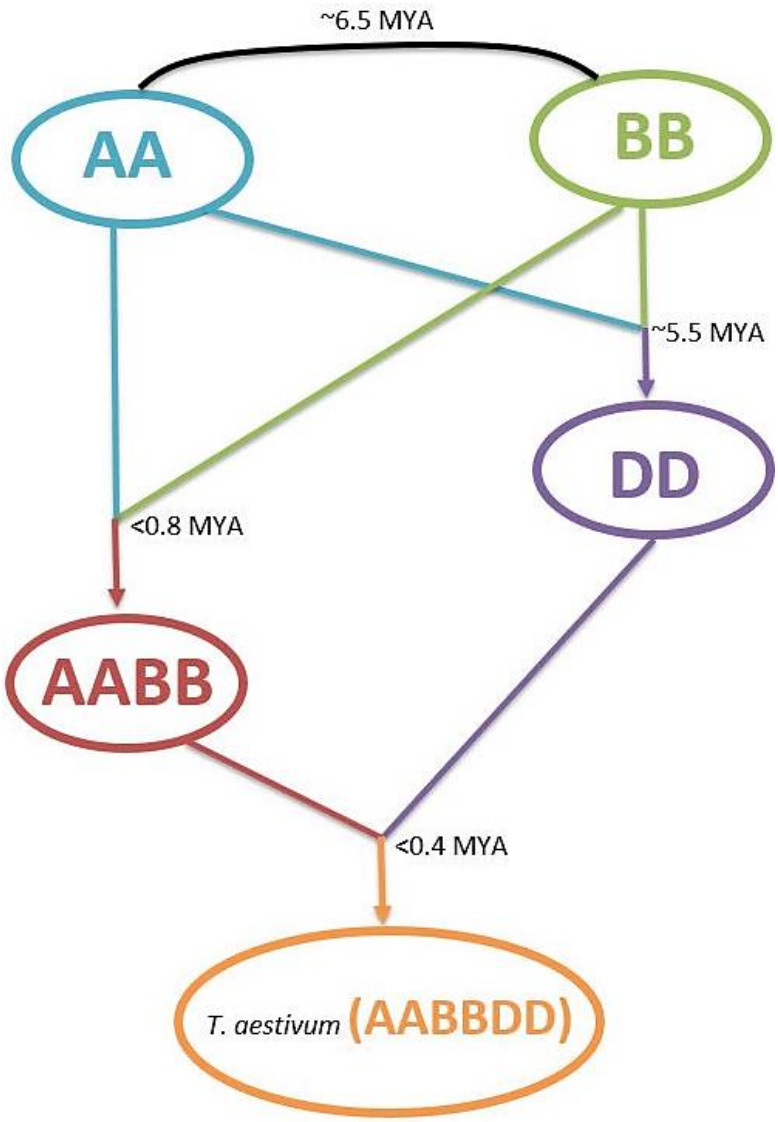

Figure 1.2 The hybridisation events leading to hexaploid bread wheat. The (AA) close relative of *T. uratu* is shown in blue, The (BB) relative of *Ae. speltoides* is shown in green. The (DD) close relative of *Ae. tauschii* is shown in purple. The (AABB) *T. turgidum* is shown in red, and hexaploid (AABBDD) T. aestivum is shown in orange. Ages of the hybridizations are shown in the figure in million years ago (MYA).

Polyploidy has been a driving evolutionary mechanism for the success of many of the domesticated species grown today (Edwards et al. 2013). The success of wheat is due to its adaptability to a wide range of climatic conditions, and large grain size, which are both down to its hexaploid genome (Marcussen et al., 2014). The cereals rice, maize, barley and wheat evolved from a common ancestor around 70-55MYA; however, genome size varies greatly between these species, with the wheat genome being eight-fold larger than maize and 40-fold larger than rice (Moolhuijzen et al., 2007). Most *Triticeae* species have a haploid genome size which is almost twice that of the human genome containing at least 80% repetitive sequences (Wicker et al., 2011).

1.2 Plant growth in response to light and hormones

Plants are sessile organisms that have developed mechanisms to detect changes in their environment and alter their physiology to bring about adaptive responses. Changing light quality and quantity provides plants with information about their surrounding environment, and allows adaptation to a wide range of habitats e.g. forest floors and open fields. These changes in light conditions are detected by photoreceptors. Developmental changes within the plant in response to these changing environments are regulated by plant hormones. In all stages of plant development, light and hormones interact to regulate developmental changes. The main plant hormones are gibberellin (GA), auxin, ethylene (ET), abscisic acid (ABA), jasmonic acid (JA), cytokinin (CT), brassinosteroids (BR) and strigolactones (Vanneste and Friml, 2009, Ballare et al., 1989, de Wit et al., 2016, Warpeha and Montgomery, 2016, Clouse and Sasse, 1998, Brewer et al., 2013).

1.2.1 Germination

Plant seeds contain an embryo surrounded by covering layers, which protect the embryo from damage before growth. Germination begins with the uptake of water or imbibition of the dry seed, followed by expansion of the growing embryo. This causes rupture of the covering layers, allowing the final step in the germination process to take place; emergence of the radicle. To ensure that the seeds do not germinate in unfavourable conditions, a period of seed dormancy must be overcome before germination. This process is tightly controlled by light and hormone signalling (Kucera et al., 2005, de Wit et al., 2016, Warpeha and Montgomery, 2016).

ABA is the plant hormone involved in promoting seed dormancy and inhibiting germination. ABA is accumulated in dormant seeds, and as ABA levels decline the seeds become non-dormant. This is usually associated with a period of after-ripening i.e. storage of freshly harvested grain in dry conditions, which results in an alleviation of dormancy (Kucera et al., 2005). As ABA levels decline, GA levels rise and are associated with dormancy release, promotion of germination and are required to break through the seed covering tissues (Yamaguchi and Kamiya, 2001). GA promotes the expression of an *α-amylase* gene through the expression of a GA-induced Myb-like protein (GAMyb) that binds to a GA response element on the *α-amylase* promoter. ABA is able to repress this interaction via an ABA-induced Ser/Thr protein kinase, PKABA1 (Gomez-Cadenas et al., 2001), and two WRKY transcriptional regulators, which repress the expression of both GAMyb and α-amylase (Xie et al., 2006). ABA and GA are active at different locations and times within the seeds lifetime to ensure

germination at the correct stage. Disruption in either of these hormone signalling pathways causes defects in germination timing (Kucera et al., 2005). A number of other hormones also play a role in germination. ET counteracts the negative effects of ABA on germination by interfering with ABA signalling (Kucera et al., 2005). Auxins are involved in promoting cellular elongation and root initiation after germination and during seedling establishment. CTs are involved in regulating embryo development (Warpeha and Montgomery, 2016).

Light is also a major regulator of germination. Plant species either produce seeds that germinate near the soil surface, or in the dark i.e. submerged in soil. Light signalling affects these germination processes in different ways (de Wit et al., 2016). Germination in the light is induced by the detection of red (R) light, and can be quickly reversed by a subsequent irradiation with far-red (FR) light. The inhibiting FR light pulse has been associated with a correlating ABA pulse, which prevents germination (Lee et al., 2012). Detection of R light promotes GA biosynthesis and relieves repression of the GA signalling pathway, promoting germination (Oh et al., 2007). A summary of the germination regulation by light and hormones is shown in **Figure 1.3**.

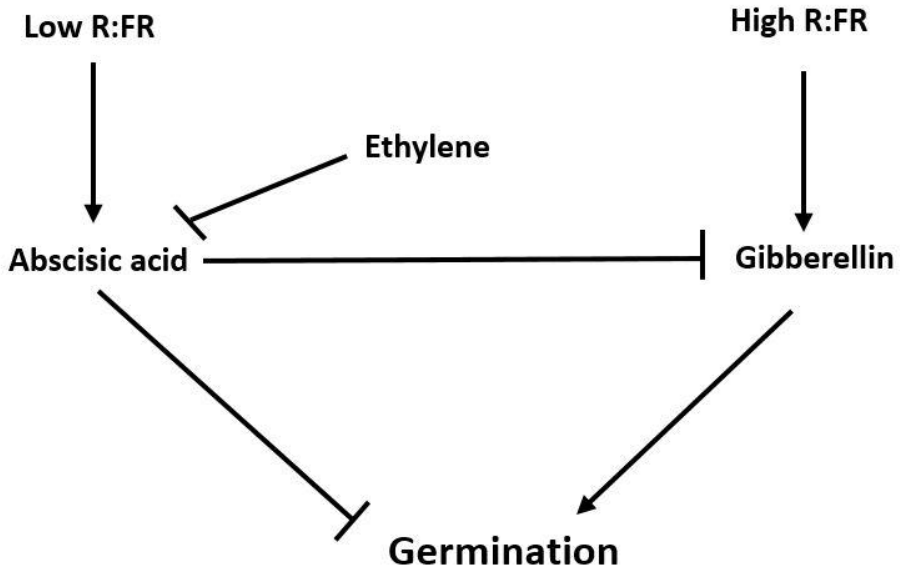

Figure 1.3 The regulation of germination by light and hormones. A summary of how germination is regulated by the red to far red ratio (R:FR) is shown. In low R:FR ratio, abscisic acid inhibits germination and gibberellin biosynthesis. In high R:FR light, gibberellin promotes germination, and ethylene inhibits abscisic acid signalling.

1.2.2 Seedling development

Germination in the dark involves etiolated growth of the seedling in a process called skotomorphogenesis. This consists of elongation of the hypocotyl and the formation of an apical hook. During this process, development of the cotyledons, the apical meristem and growth of the root system is inhibited. The apical hook and closed cotyledons protect the shoot apical meristem from mechanical damage. Once the hypocotyl reaches the surface and perceives light, the photomorphogenic growth process is induced. The dark environment during germination ensures that photomorphogenic growth processes are repressed (de Wit et al., 2016).

ET is involved in ensuring etiolated growth. ET is accumulated when etiolated growth is physically obstructed, resulting in shorter, thicker hypocotyls and roots, along with an exaggerated apical hook. The amount of ET detected in etiolated seedlings was directly correlated with the depth of the seeds and the firmness of the soil (Goeschl et al., 1966, Harpham et al., 1991). The induction of the apical hook by ET also requires the action of GA. Vriezen et al. (2004) found that when *Arabidopsis* seedlings were treated with the GA biosynthesis inhibitor paclobutrazol (PAC) apical hook formation was prevented, even in constitutive ET response (*crt1-1*) mutants. Two other hormone classes have been linked to promotion of skotomorphogenesis; BR and GA. BR-deficient mutants of several plant species display a constitutive photomorphogenic phenotype, involving de-etiolation, hypocotyl elongation and increased expression of genes involved in photomorphogenesis. GA-deficient mutants in *Arabidopsis* show a similar phenotype, suggesting that both these hormones are involved in a regulatory switch between skoto and photomorphogenesis (Alabadi et al., 2009). *Arabidopsis* mutants with elevated levels of endogenous CK, have also been shown to have a constitutive photomorphogenic phenotype in the dark, suggesting a role for CT in regulating this switch (Chaudhury et al., 1993, Chin Atkins et al., 1996).

Once seedlings emerge from the dark conditions of the soil, they switch to photomorphogenic development, which is characterised by short hypocotyls, expanded cotelydons and an accumulation of chlorophyll resulting in greening. The apical meristem produces the first pair of true leaves and the hypocotyls re-orientate their cotyledons toward the light due to positive phototrophic and negative gravitropic cues. This allows optimal exposure for light to enhance photosynthesis (von Arnim and Deng, 1996). This process of bending toward the light is called positive phototropism. Phototropism occurs at all stages of plant development, and is not limited to newly germinated seedlings. During phototropism, the plant detects directional light

using its phototropins; this then promotes auxin accumulation on the shaded side of the plant, causing increased growth on the shaded side, which leads to bending toward the light. Red light has been shown to enhance blue light mediated phototropism if applied 1-2 hours prior to the blue light stimulus (de Wit et al., 2016, Briggs, 2014).

1.2.3 Shade avoidance

During growth and development, plants may need to compete with their neighbours for light. During this competition, a size difference or delayed growth are disadvantageous. Plants must adjust their growth to stay as tall as their neighbours at a minimum. This process, called shade avoidance, occurs in both adults and seedlings, and involves directing energy into stem elongation at the expense of leaf development and seed set. The shade avoidance phenotype involves elongated hypocotyls and stem, hyponastic leaves, enhanced apical dominance and early flowering (de Wit et al., 2016, Franklin, 2008). Plants are able to detect shading from other plants through changes in the R:FR ratio. Shading results in a reduction in the R:FR ratio because green leaves absorb R light and reflect FR light. Many different hormones play a role in shade avoidance, including GA, ET, auxin, BR, CT and JA. The hormone with the most dominant role is auxin (de Wit et al., 2016). **Figure 1.4** shows a summary of the regulation of shade avoidance.

Auxin response mutants and inhibitors of auxin biosynthesis have been used to demonstrate that auxin is laterally redirected to allow increased elongation of the expanding organs. During the detection of a low R:FR ratio, auxin is generated in the cotyledon and transported to the hypocotyl, allowing a rapid rise in auxin levels, causing increased stem elongation (Friml et al., 2002, de Wit et al., 2016, Tao et al., 2008). Auxin also promotes GA production in the stem to promote growth of the soot apical meristem (SAM). When pea (*Pisum sativum*) and tobacco (*Nicotiana tabacum*) shoots were decapitated, reduced levels of active GAs were detected in the stems. This effect was reversed by auxin application, suggesting that auxin causes an increase in GA (Ross et al., 2000). In *Arabidopsis* this effect was explained by the discovery that auxin can induce the expression of the GA biosynthetic gene GA20ox (Frigerio et al., 2006). Similarly, in pea, auxin was shown to induce expression of the GA biosynthetic gene *GA3ox* and suppress the expression of GA de-activation gene *GA2ox* (O'Neill and Ross, 2002).

Arabidopsis plants with mutations in their GA-response pathway display a reduced response to low R:FR ratio, and therefore an impaired shade avoidance response. In addition the detection of a reduced R:FR light ratio is accompanied by an increase in GA levels, suggesting that GA is

required for the promotion of the shade avoidance response (Djakovic-Petrovic et al., 2007). Studies have demonstrated that the shade avoidance response requires BR synthesis (Luccioni et al., 2002), and the transcription factor BRASSINAZOLE-RESISTANT 1 (BZR1). BZR1 interacts with the light responsive transcription factor, PIF4, to synergistically regulate the expression of genes involved in the shade avoidance response. Genes targeted include those involved in stem elongation (Oh et al., 2012). Strigolactones have also been implicated in the shade avoidance response. Strigolactones and phytochrome double mutants suggest that strigolactones act downstream of the PHYB-dependent response to high R:FR to promote the shade avoidance response (Finlayson et al., 2010). Both GA and CT are also required for normal SAM function, and act antagonistically to regulate SAM development. (Sakamoto et al., 2001). Proteins from the KNOTTED1-like homeobox (KNOXI) family have been shown to regulate SAM function through the induction of the CT biosynthesis gene *ISOPENTENYL TRANSFERASE7* which causes CT to accumulate in the meristem (Yanai et al., 2005). Proteins from the KNOXI family are also involved in negatively regulating the GA level in the SAM by repressing the expression of *GA20ox* (Sakamoto et al., 2001). Furthermore, both KNOXI and CT induce the expression of GA2ox, the GA-deactivation enzyme, in the base of the SAM (Jasinski et al., 2005).

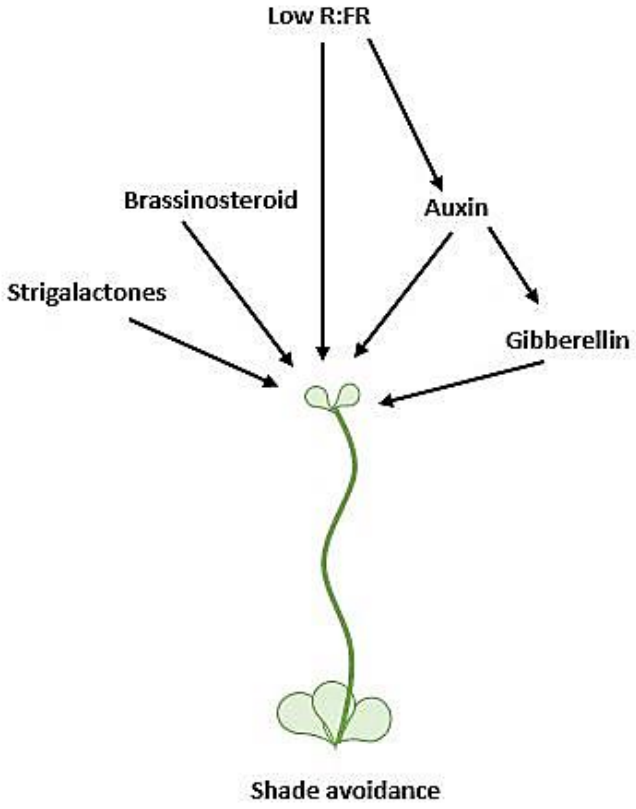

Figure 1.4 The regulation of shade avoidance by light and hormones. A summary diagram of the light signals and hormones involved in the promotion of shade avoidance is shown. In a low red to far red (R:FR) light ratio shade avoidance is promoted. Auxin, gibberellin, brassinosteroid and Strigalactones also promote this response.

1.2.4 Flowering

Flowering at the correct time is essential for successful reproduction, particularly in plants that are self-incompatible and therefore rely on pollinators, or those that inhabit climates with strong seasonal changes. To ensure the energy-expensive process of flowering occurs when conditions are favourable, the induction of flowering is tightly controlled by environmental cues. One important flowering cue is the detection of light quality and photoperiod (de Wit et al., 2016). Many different hormones are involved in the control of flowering. Mutants with altered GA signalling pathways flower incorrectly in both short and long day conditions, suggesting that GA is essential for the regulation of flowering in response to these cues. GA has also been shown to control the expression of flowering time genes (de Wit et al., 2016).

ET regulates the transition to flowering antagonistically to GA. This interaction between GAs and ET involves the repression of GA signalling by ET, mediated by an interaction with the GA-

repressive DELLA proteins (Achard et al., 2003). In *Arabidopsis*, several GA-responsive genes displayed enhanced expression in the ET-resistant mutant *etr1* or when plants were pre-treated with the ET perception inhibitor 1-methylcyclopropene (De Grauwe et al., 2007). During flowering, ET has been shown to repress GA signalling through an interaction with DELLAs and through the manipulation of GA biosynthesis. The repression of GA signalling causes reduced expression of two central flowering genes, *LEAFY* and *SUPPRESSOR OF OVEREXPRESSION OF CONSTANS1 (SOC1)*, preventing the transition into flowering (Achard et al., 2007). Auxin is also involved in correct flower development. Studies have demonstrated that a local application of auxin triggers flower formation in the shoot apex, suggesting that auxin plays a critical role in the initiation of the floral organ (Tanaka et al., 2006).

In *Arabidopsis*, BR deficient or insensitive mutants have a well-established delayed flowering phenotype, suggesting an involvement of BR in regulating flowering time. The transmembrane receptor kinase, brassinosteroid-insensitive1 has been shown to promote flowering in *Arabidopsis* through its interaction with FLOWERING LOCUS C (FLC), explaining the delayed flowering phenotype in BR mutants (Domagalska et al., 2007). CTs also regulate flowering time and *Arabidopsis* mutants with increased levels of endogenous CT showed an early flowering phenotype (Chaudhury et al., 1993).

1.2.5 Senescence

Under stress conditions it can be beneficial for a plant to senesce leaves that are no longer photosynthetically productive, making resources available for other organs. The tightly co-ordinated process of leaf senescence involves the dismantling of cellular components to remobilize plant resources and is fundamental to plant life (Liebsch and Keech, 2016, Gan and Amasino, 1995, Buchanan Wollaston, 1997).

Light plays an important role in the regulation of senescence. The detection of shading or darkness by the plant leads to rapid senescence, especially if only part of the plant is affected. R light pulses have been shown to delay senescence, whereas pulses of FR light can promote senescence, and counteract the effect of R light pulses, informing the plant of a change in light quality (Liebsch and Keech, 2016).

CTs have been shown to delay leaf senescence in numerous plant species. Increasing CT levels causes a delayed onset of senescence, and studies have shown that a reduction of CT in the leaves leads to senescence. When CT levels rise above a certain level, the expression of

senescence-related genes has been shown to be inhibited. The control of senescence by CTs is therefore likely to be at the level of transcriptional control (Gan and Amasino, 1995, Buchanan Wollaston, 1997). ET has also been implicated in the regulation of senescence in some plant species. In contrast to CT, ET has some effect on senescence, but is not an essential regulator of the process. Disruptions in ET biosynthesis, resulting in reduced levels of ET cause delays in senescence, but not complete disruption, suggesting that ET is more important for the timing of senescence (Buchanan Wollaston, 1997).

1.2.6 The effect of light and gibberellin on monocots.

Both light and GA affect the growth and development of monocots. A change in the R/FR light ratio can dramatically affect the morphology of monocot plants, with changes to tillering, stem elongation and leaf development (Casal et al., 1985, Barnes and Bugbee, 1991, Deregibus et al., 1983). A schematic of wheat morphology is shown in **Figure 1.5**. Higher R/FR ratios were found to promote increased tillering along with increased number and area of leaves in *L. perenne* (perennial ryegrass) (Deregibus et al., 1983). In contrast lower R/FR light ratios cause a 50% reduction in tillering, along with a slightly higher rate of leaf development and an increase in the length of leaf sheaths in wheat (Barnes and Bugbee, 1991). In *Lolium multiflorum* (ryegrass), lower R/FR ratio causes an increase in the number of fertile tillers on each plant along with longer leaf sheaths, blades and reproductive shoots (Casal et al., 1985). These results indicate that a lower R/FR ratio caused by shading represses tillering, and the promotes the growth of taller fertile tillers with longer leaves to compete for sunlight. GA also promotes a similar morphological response in monocots. When a maize *GA20ox* gene was expressed in *Panicum virgatum L.* (switchgrass), plants exhibited longer leaves, internodes and tillers, which resulted in a twofold increased biomass (Do et al., 2016). In rice, higher levels of GA_1 and GA_4 have been associated with increased internode elongation, which is abolished if GA levels are reduced (Ayano et al., 2014). In wheat GA is associated with increased leaf elongation (Xu et al., 2016), and stem elongation (Peng et al., 1999). GA therefore promotes stem, internode and leaf elongation in monocots.

Red light alone has an inhibitory effect on wheat development. When grown under red light, wheat plants have lower levels of main culm development; shoot dry matter and net rate of photosynthesis (Goins et al., 1997). Seedlings whose shoot bases were exposed to red light did not accumulate chlorophyll or carotenoids and only accumulated 50% of the δ-aminolevulinic acid (ALA) found in control plants (Sood et al., 2005). Wheat plants treated with pulses of R, green or FR light were shown to have rapid inhibition of stem elongation (Smith and Jackson, 1987). When wheat grown under red light received 10% blue light supplementation, the plants

recovered similar growth rates to those grown under white light. Blue light supplementation reversed the negative impact of red light on shoot and main culm dry matter, subtiller number, seed yield seed number, carotenoid accumulation, ALA accumulation and chlorophyll accumulation (Goins et al., 1997, Sood et al., 2005). A reduction in GA levels is also accompanied by a reduction in chlorophyll production in rice (Jiang et al., 2012). Red light has been shown to cause swelling of protoplasts and unrolling of wheat leaves (Beevers et al., 1970). This process was also promoted by GA application (Blakeley et al., 1983).

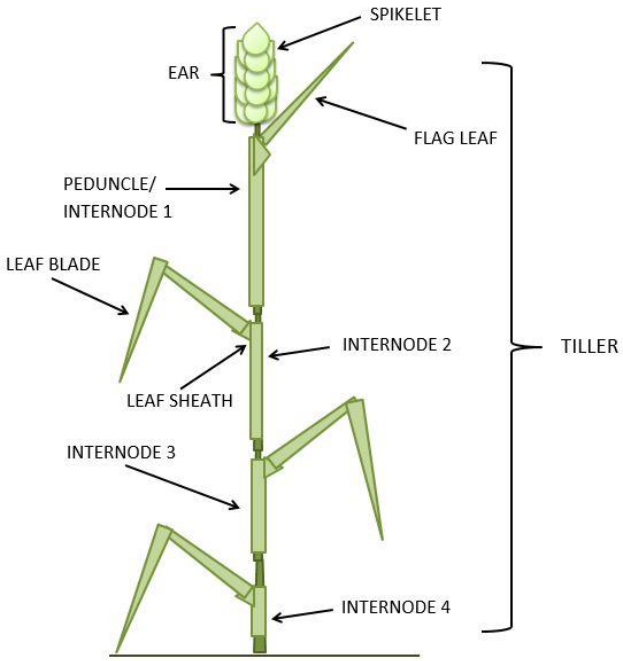

Figure 1.5 Wheat morphology. A schematic diagram of a wheat tiller is shown, with each aspect of wheat morphology labelled.

1.3 Gibberellin

The GAs are tetracyclic diterpenoid hormones that have an important role in ensuring normal plant growth and development (Fu et al., 2001). GA was first identified in the pathogenic fungus *Gibberella fujikuroi*, which is responsible for causing 'foolish-seedling' disease of rice. Infected plants become extremely tall and often fall over as the elongated stem cannot take the weight of the grain (Yabuta and Sumiki, 1938).

Over 130 GAs have been identified in plants, fungi and bacteria; however only a small proportion of GAs have biological activity, the major bioactive forms are GA_1, GA_3, GA_4 and GA_7 (Yamaguchi, 2008). Many non-bioactive GAs exist in plants in the form of either precursors or de-activated metabolites. Active GAs are created from a basic diterpenoid carboxylic acid skeleton, and usually have a hydroxyl group at the C3 position (Yamaguchi, 2008, Daviere and

Achard, 2013). GA_1 and GA_4 occur universally in plants as the main bioactive forms (Hedden and Thomas, 2012) and their structures are shown in **Figure 1.6**. GAs stimulate organ growth by promoting cell elongation or division and act as developmental switches in the plant life cycle. Through these mechanisms GAs affect a wide range of processes, such as seed germination, seed growth, hypocotyl and stem elongation, leaf expansion, trichome development, pollen maturation, flower induction and fruit growth (Richards et al., 2001).

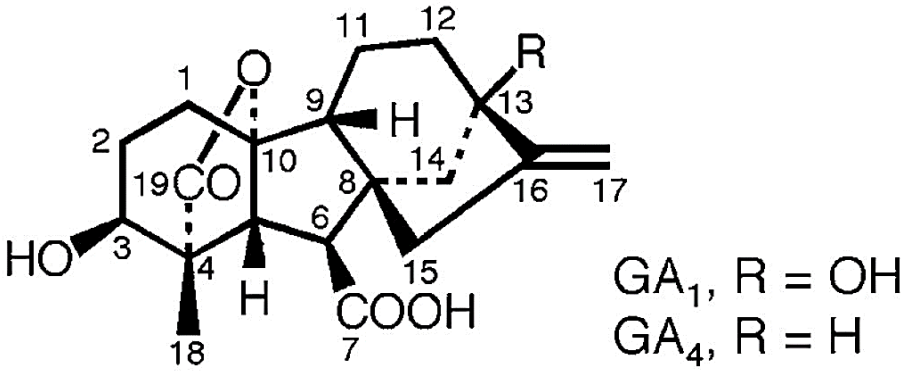

Figure 1.6 The structure of biologically active GA_1 and GA_4 (taken from Zhu et al., 2006). The structure of the biologically active GA_1 and GA_4 is shown with carbons numbered. The R group takes the form of an OH group in GA_1 or a H in GA_4

1.3.1 Gibberellin biosynthesis

As shown in **Figure 1.7**, the GA biosynthesis pathway can be split up into three main processes: the synthesis of *ent*-kaurene, the conversion of *ent*-kaurene to GA_{12} by cytochrome P450 enzymes and the metabolism of GA_{12}/GA_{53} to biologically active GAs (Mizutani and Ohta, 2010). The methylerythritol pathway makes up the main mode of GA synthesis in higher plants (Kasahara et al., 2002). The first step in this process involves the formation of *ent*-kaurene from *trans*-geranylgeranyl diphosphate (GGPP) in proplastids (Aach et al., 1997); *ent*-kaurene is synthesised in a two-step process: firstly GGPP is converted to *ent*-copalyl diphosphate via *ent*-copalyl diphosphate synthase (CPS) and then to *ent*-kaurene by *ent*-kaurene synthase (KS). *Arabidopsis* contains single copies of KS and CPS, which produce severe GA-deficient phenotypes when mutated (Koornneef and Vanderveen, 1980). In cereals more than one copy of each gene has been identified. Wheat contains three CPS genes; *TaCPS1*, *TaCPS2* and *TaCPS3*. Only *TaCPS3* is involved in GA biosynthesis, while *TaCPS1* and *TaCPS2* are involved in phytoalexin biosynthesis (Toyomasu et al., 2009). A family of *KS-like* genes has been described in rice (Xu et al., 2007).

The next stage in GA biosynthesis involves the conversion of *ent*-kaurene (**Figure 1.7**) into GA_{12} within the endoplasmic reticulum (ER), which involves six oxidative steps (Mizutani and Ohta, 2010). *ent*-kaurene oxidase (KO) catalyses three steps from *ent*-kaurene to *ent*-kaurenoic acid (Helliwell et al., 1999). *ent*-kaurenoic acid is then converted into GA_{12} by a cytochrome P450 (Helliwell et al., 2001). GA_{12} is a common precursor for all plant GAs (Hedden and Phillips, 2000) and at this point, the GA biosynthesis branches into two reaction routes. GA_{12} can be directly oxidised by GA20ox and subsequently converted into GA_4, or it can be first converted into GA_{53} and then to GA_1 and in some cases also GA_3 (Hedden and Thomas, 2012).

The final stage in the GA biosynthetic pathway involves the production of bioactive GAs through the processing of inactive precursors (**Figure 1.7**). GA20ox oxidises the C20 position of both GA_{12} and GA_{53}, which are converted into GA_9 and GA_{20}, respectively. In parallel pathways in a 3 or 4 step process (Hedden, 1997), GA_9 and GA_{20} are then converted into GA_4 and GA_1, respectively, via 3β-hydroxylation by GA3ox. GA_{20} can also be oxidised into GA_3 by GA3ox (Hedden and Thomas, 2012).

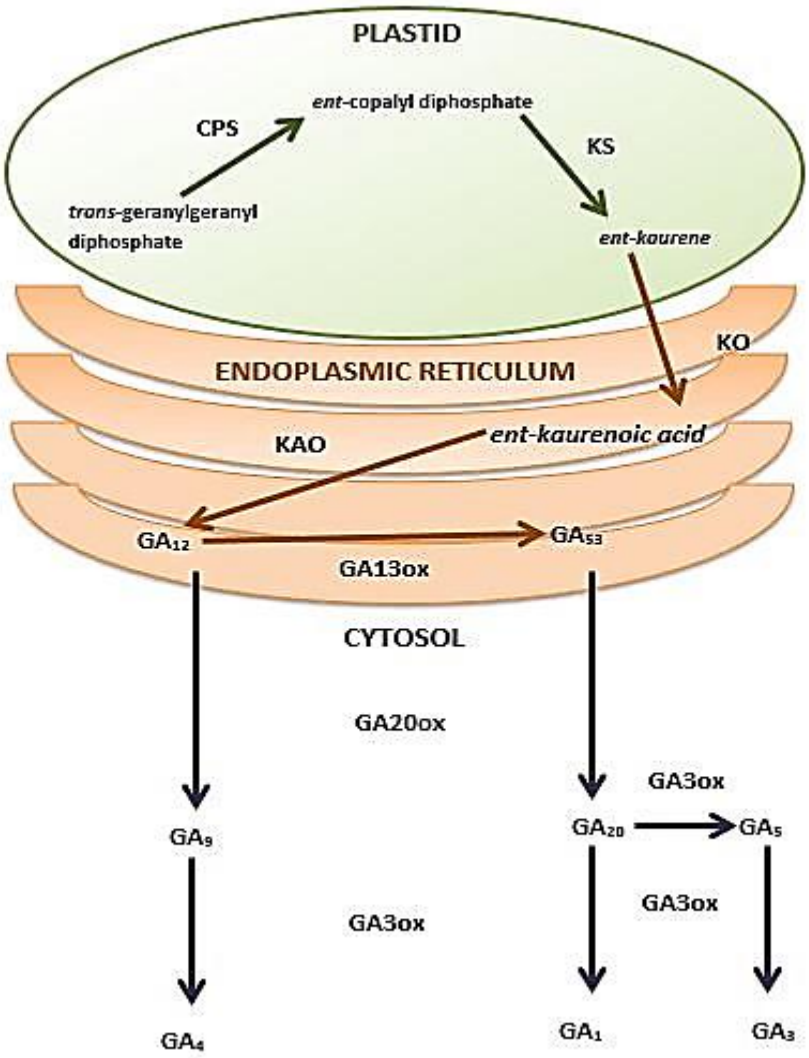

Figure 1.7 The GA biosynthesis pathway. The GA biosynthesis pathway from *trans*-geranylgeranyl diphosphate to bioactive GA is shown. CPS, copalyl diphosphate synthase; KS, *ent*-kaurene synthase; KO, *ent*-kaurene oxidase; KAO, *ent*-kaurenoic acid oxidase.

1.3.2 Sites of GA biosynthesis and transport

The location and concentration of bioactive GA must be rapidly altered to allow the plant to regulate development and respond to the environment. This occurs through the regulation of GA biosynthesis and inactivation.

In vegetative tissues, the highest levels of biologically active GA are found in growing organs, such as the developing leaves, but the highest levels of GA are found in developing seeds and anthers. Smith et al. (1992) found that growing regions of pea accumulated GA_{20} and its metabolites, with very low amounts in the mature vegetative tissues. Similarly, on the basis of reporter gene expression, GA biosynthesis was shown to occur at the site of action in growing organs of rice (Kaneko et al., 2003). GA biosynthesis and signalling were detected in growing

organs and in inflorescence/floral stages, although not in the aleurone cells of the endosperm, which is a major site of GA action in germinating cereal grain (Kaneko et al., 2003).

Different reactions within the GA biosynthesis pathway can also occur in different tissues, meaning that intermediates need to move between cells to complete the pathway. Yamaguchi et al. (2001) demonstrated that in germinating seeds, GA biosynthesis takes place in two separate locations, with the early step involving CPS in the provasculature and the later steps involving KO and GA3ox taking place in the cortex and endodermis (Yamaguchi et al., 2001). GA biosynthesis has also been detected in mature tissues. Silverstone et al. (1997) found that the *KS (GA1)* gene was expressed at the highest levels in rapidly growing tissues, but was also active in vascular tissue in some non-growing organs such as expanded leaves. Ross et al. (2003) found that while pea plants expressed *CPS* in mature tissue, these tissues contained low levels of GA_1 and GA_{20} due to their rapid oxidation to inactive GAs (Silverstone et al., 1997).

There is evidence that GA is capable of moving between tissues within the plant in order to induce physiological changes. In *Arabidopsis* GA_4 is exported from the leaves to the shoot apex to induce flowering under short day conditions (Eriksson et al., 2006). Similarly, in *Lolium temulentum* GA_5 and GA_6 are exported from the leaves to the shoot apex to induce flowering in long day conditions (King et al., 2001). In some instances, tissues with high levels of GA biosynthesis act as sources of GA for neighbouring tissues. In germinating cereal grains GA is exported from the sculletum epithelium to the aleurone cells, which causes the aleurone to export hydrolytic enzymes and undergo programmed cell death (PCD) (Kaneko et al., 2003). The tissues with the highest GA concentrations within flowers are the anthers with the main site of GA production being the tapetum. GA made in the anthers is transported to the petals, which do not synthesise GA, meaning the anthers act as a major source of GA within the flower (Hu et al., 2008). GA can be transported between plant tissues in the regulation of GA biosynthesis. GA_{12} can undergo long distance transport from root to shoot and visa versa through the plant vascular system. This allows the relocation of precursors from production sites to recipient tissues (Regnault et al., 2016). Several GA transporters have been identified, which belong to the NITRATE TRANSPORTER1/PEPTIDE TRANSPORTER FAMILY (NPF) (Regnault et al., 2016, Chiba et al., 2015, Saito et al., 2015). The NPFs represent a large family of membrane proteins which are capable of transporting a variety of compounds across the cell membrane, such as, nitrate, peptides and phytohormones. Recent studies have revealed that NPF proteins are capable of transporting GA_3, providing a mechanism by which biologically active GA can be moved between tissues (Saito et al., 2015, Chiba et al., 2015).

1.3.3 Regulation by GA inactivation

The inactivation of GA allows the plant to regulate homeostasis and permits the concentration of GA to fall rapidly when required (Hedden and Thomas, 2012). There are various mechanisms by which GA can be deactivated, the most common being 2β-hydroxylation, which is carried out by GA 2-oxidases. Two groups of GA 2-oxidases are present in plants, which act on either C_{19}-GAs or C_{20}-GAs (Thomas et al., 1999, Schomburg et al., 2003). A 2β-hydroxylase from runner beans was found to act on C_{19}-GAs, converting GA_9 to GA_{51} and a GA_{51} catabolite, preventing the synthesis of biologically active GA_4. This 2β-hydroxylase also acts on GA_4, GA_{20} and GA_1 to prevent the accumulation of active GAs (Thomas et al., 1999). Two 2β-hydroxylases have been identified in *Arabidopsis* that act on C_{20}-GAs, but not on C_{19}-GAs (Schomburg et al., 2003). The GA 2-oxidases form a large gene family including separate clades of C_{20} and C_{19}-GA enzymes. GA2ox, GA3ox and GA20ox belong to the 2OG-Fe(II)oxygenase superfamily, in which all three enzymes are encoded in different gene families (Han and Zhu, 2011).

Another mechanism of GA inactivation involves a cytochrome P450 mono-oxygenase, which in rice is encoded by *ELONGATED UPPERMOST INTERNODE* (EUI). In vitro studies have demonstrated that EUI is capable of 16α, 17-epoxidation of GA_4, GA_9 and GA_{12} (Zhu et al., 2006). The GAMT (GA methyl transferases) provide a further mechanism of GA inactivation. GAMT1 and GAMT2 in *Arabidopsis* encode enzymes that catalyse the modification of active GA by the formation of methyl esters, which is thought to cause their deactivation and initiate their degradation (Varbanova et al., 2007).

1.3.4 Regulation of GA biosynthesis

Along with regulation of sites of synthesis, transport and de-activation, individual steps in the GA biosynthesis pathway can also be regulated to manipulate levels within the plant. This regulation can either be by environmental signals, other hormones, or self-regulation from GA responsive genes (Hedden and Thomas, 2012).

1.3.4.1 GA biosynthesis regulation in response to light

Changes in light quantity, quality or duration can affect GA biosynthesis resulting in increased or decreased GA content. Two photoreceptors, phytochrome and cyptochrome, are responsible for the regulation of GA levels (Foo et al., 2006, Oh et al., 2006). Phytochrome regulates GA biosynthesis through its interaction with the basic helix-loop-helix (bHLH) transcripton factor PHYTOCHROME INTERACTING FACTOR 1 (PIF1). PIF1 positively regulates transcription of the GA inactivation gene *GA2ox2* and negatively regulates transcription of the

GA biosynthesis genes *GA3ox1* and *GA3ox2* (Oh et al., 2006). Blue light causes a reduction in the levels of bioactive GAs in plants. This process is mediated by both cryptochrome (cry1) and phytochrome A (phyA), and leads to a decrease in the level of bio-active GA_1 and an increase in the levels of the inactive catabolite GA_8. In pea Cry1 and phyA have been shown to suppress the transcript level of *PsGA3ox1*, the product of which catalyses the conversion of GA_{20} to GA_1. In addition phyA and cry1 upregulate the expression of *PsGA2ox2* under blue light, which encodes a GA 2-oxidase that converts GA_1 to inactive GA_8 (Foo et al., 2006). The effect of this light-mediated regulation is a reduction in bio-active GA in response to both red and blue light.

1.3.4.2 GA biosynthesis regulation in response to hormones

Auxin has been shown to positively regulate GA biosynthesis genes. Auxin response proteins AUX/IAA and AUXIN RESPONSE FACTOR (ARF) have been shown to directly increase expression of two biosynthesis genes, *GA20ox1 amd GA20ox2*, and repress the expression of GA de-activation genes *GA2ox2, GA2ox3, GA2ox6,and GA2ox8* in *Arabidopsis*. In auxin overexpression mutants, this regulation of GA biosynthesis causes an increase in levels of bio-active GA (Frigerio et al., 2006).

ABA regulates GA biosynthesis during seed development through the CHOTTO1 transcription factor. CHOTTO1 inhibits GA biosynthesis through suppression of the GA biosynthesis gene *AtGA3ox2*, which causes a corresponding enhancement in dormancy due to reduced GA levels. The expression of *CHOTTO1* requires ABA signalling, demonstrating a mechanism by which ABA regulates GA levels (Yano et al., 2009).

1.3.4.3 GA biosynthesis homeostasis.

GA biosynthesis is also regulated in a negative feedback loop by which GA biosynthesis genes are repressed when GA levels are high and vice versa. In *Arabidopsis* three *GA20ox* genes (*GA20ox1, GA20ox2* and *GA20ox3*) and a single *GA3ox* (*GA3ox1*) biosynthesis gene have highly elevated expression levels when bioactive GA levels are low, but rapidly decrease expression when plants are treated with exogenous GA (Phillips et al., 1995, Mitchum et al., 2006). In addition, increased GA signalling leads to transcriptional upregulation of the GA de-activation enzyme GA2ox (Rieu et al., 2008).

The GA response repressing DELLA proteins have been shown to promote the expression of GA biosynthesis genes. In pea, the DELLA proteins LA and CRY promote the expression of the GA synthesis genes *GA3ox1* and *GA3ox2*, and inhibit the repression of de-activation genes

GA2ox1 and *GA2ox2* (Weston et al., 2008). In *Arabidopsis* 14 GA biosynthesis genes have been identified as targets of DELLAs, including *AtGA20ox2* and *AtGA3ox1 (Hou et al., 2008)*. In *gai*, a constitutively active DELLA mutant line, levels of bio-active GAs are elevated, and are unaffected by endogenous application of GA, demonstrating that DELLAs are required for GA homeostasis (Talon et al., 1990). Although DELLAs activate the expression of GA biosynthesis genes, no direct binding to the promoter of biosynthesis genes can be identified, suggesting that instead, DELLAs alter expression through interaction with transcription factors (Talon et al., 1990). Multiple transcription factor families have been shown to be involved in the regulation of GA biosynthesis results in either upregulation or downregulation of biosynthesis or de-activation genes.

AGF1, an AT-hook motif protein, has been identified as a GA biosynthesis regulator in *Arabidopsis* (Matsushita et al., 2007). AGF1 is involved in the upregulation of the biosynthesis gene *AtGA3ox1* in response to a decrease in GAs, but had no effect on the expression of the *AtGA20ox* genes. AGF1 has been shown to bind a 43 bp cis-element located in the *AtGA3ox1* promoter, called the *GNFEI.* This interaction allows the upregulation of *AtGA3ox* (Matsushita et al., 2007). The YABBY1 (YAB1) C2C2 zinc finger transcription factor transcription factor acts downstream of DELLA to regulate GA biosynthesis in rice. GA treatment was found to cause a rapid increase in *OsYAB1* transcripts, while treatment with the GA inhibitor PAC had the opposite effect. YAB1 binds to the GA responsive element located in the *GA3ox2* promoter, repressing *GA3ox2* expression and indicating that YAB1 regulates *OsGA3ox2* directly (Dai et al., 2007). In tobacco, RSG, a basic leucine zipper (bZIP) domain transcriptional activator, has been implicated in the regulation of GA biosynthesis. An RSG-binding sequence has been identified in the promoter region of *NtGA20ox1*. Binding of RSG to this region *in vivo* occurs in response to a decrease in GA levels, causing increased *GA20ox* expression. In contrast, an increase in GA levels abolishes this binding, demonstrating that RSG is involved in regulating *GA20ox* expression levels in tobacco (Fukazawa et al., 2011, Fukazawa et al., 2010). The Arabidopsis INDETERMINATE DOMAIN (IDD) protein, GAF1 has been shown to interact with Arabidopsis DELLAs. This interaction forms a transcriptional activation complex which drives the expression of GA biosynthesis genes., forming a further mechanism for feedback regulation (Fukazawa et al., 2014).

1.3.5 GA dependent regulation of plant growth and development

The roles of GA in plant development can be demonstrated by the phenotype of the *ga1-3* mutant, which is defective in a CPS enzyme, meaning it cannot synthesise GA. The *ga1-3*

mutant displays a dwarf phenotype, with dark green leaves (Koornneef and Vanderveen, 1980), delayed flowering in short day conditions (Wilson et al., 1992), male sterillity and failure to germinate unless the seed coat is removed (Koornneef and Vanderveen, 1980). Addition of exogenous GA restores all these mutant phenotypes, suggesting that GA plays a role in stem elongation, leaf development, germination, flowering and production of reproductive organs (Koornneef and Vanderveen 1980).

The role of GA in seed development was uncovered in pea plants with a mutation in the *LH* locus, which encodes a KO enzyme. Homozygous *lh-2* plants were found to have a 50% seed abortion rate, and seeds that did survive were lighter and smaller than wild type, demonstrating that GA is essential for normal seed development (Swain et al., 1995). One specific area of seed development regulated by GA in cereals is the production of α-amylase by the aleurone. GA controls transcription of α-amylase and its secretion from the aleurone, the α-amylases then hydrolyse the starch in the endosperm to feed the growing embryo and promote germination (Bethke et al., 1997). GA also promotes the expression of protease genes and acidification within the developing embryo to promote breakdown of the aleurone (Dominguez and Cejudo, 1999).

The effect of GA on floral initiation is dependent on species; however, the effects in *Arabidopsis* and many other rosette species are obvious for flowering time and morphology. Applying exogenous GA in short day conditions leads of early flowering (Langridge, 1957). Whereas mutants with low levels of endogenous GA e.g. the *ga1-3* mutant, have later flowering than wild-type under long day conditions and fail to flower in short days (Blazquez et al., 1998). GA regulates floral initiation through induction of the LEAFY transcription factor. Blazquez et al. (1998) found that constitutive expression of LEAFY could restore flowering in the *ga1-3* mutant.

GA has also been implicated in meristem function. There are many genes involved in shoot apical meristem (SAM) function, including the *KNOTTED-like 1 homeobox (KNOX1)* gene family. Expression of *KNOX* in tobacco caused a reduction in the expression of *GA20ox* leading to lower endogenous GA levels (Hay et al., 2004). This localised reduction in GA is an important step in the production of complex leaf shapes and meristem function. This is demonstrated in *Arabidopsis* via the expression levels of *GA5*, which encodes AtGA20ox1. *GA5* expression is not detected in the shoot apical meristem, consistent with low GA levels being important for meristem maintenance. However *GA5* is highly expressed in developing leaf primordia,

indicating the importance of GA levels in leaf initiation and development (Swain and Singh, 2005).

1.4 Gibberellin signalling pathway

1.4.1 DELLAs: negative regulators of the GA response.

DELLA proteins are involved in the cellular response to GA. They are localised to the nucleus and act to modify the transcription of genes involved in plant growth. In the presence of GA, DELLA proteins are degraded, relieving their effect on transcription (Daviere and Achard, 2013, Claeys et al., 2014). Various mutants in GA signalling were used to identify DELLA proteins and downstream signalling components; **Table 1.1** gives an overview of all these mutants and their phenotype

Table 1.1 Gibberellin response mutants of Arabidopsis and cereal crops

Plant species	Mutant	Phenotype	Role in GA response	Reference
Arabidopsis	*gai* - Gibberellic acid insensitive	Gain-of-function. Dwarf, unable to respond to GA.	DELLA	Peng and Harberd (1993)
Arabidopsis	rga: Repressor of *ga1-3*	Partially supresses the *gai1-3* (GA-deficient) phenotype	DELLA	Silverstone et al. (1997)
Arabidopsis	rgl1-2: RGA like 1 and 2	Able to germinate in the presence of paclobutrazol	DELLA	Hussain et al. (2005)
Rice	*Slr1*: slender	Tall, elongated stem with reduced root lengths and numbers	DELLA	Ikeda et al. (2001)
Barley	*Sln1:* Slender 1	Tall, elongated stems and leaves, insensitive to GA	DELLA	Fu et al. (2002)
Arabidopsis	*sly1*: Sleepy1	Recessive, GA insensitive dwarf mutants with RGA accumulation	F-box – E3 Ligase	McGinnis et al. (2003)
Rice	*gid2*: GA insensitive dwarf 2	GA insensitive, dwarf phenotype with wide leaf blades and dark green leaves	F-box – E3 Ligase	Sasaki et al. (2003)
Rice	*gid1:* Gibberellin insensitive dwarf 1	GA insensitive dwarf phenotype with wide leaf blades and dark green leaves	GA Receptor	Ueguchi-Tanaka et al. (2007)
Arabidopsis	*gid1a, b and c:* Gibberellin insensitive dwarf 1	GA insensitive dwarf phenotype	GA Receptor	Griffiths et al. (2006)
Wheat	*RHT-1:* Reduced height 1	Gain-of-function. Short, dwarfed stems, resistance to lodging, increased gain numbers, gain-of-function	DELLA	Peng et al. (1999)
Maize	*Dwarf-8*	GA-unresponsive, dominant dwarf	DELLA	Winkler and Freeling (1994)
Maize	*Dwarf-9*	GA-unresponsive, dominant dwarf	DELLA	Winkler and Freeling (1994)

1.4.1.1 *Arabidopsis* DELLAs: GAI, RGA and RGL1-3

The first DELLA mutant identified in *Arabidopsis* was the *gai* (gibberellic acid insensitive) mutant. The *gai* plants have a dwarf phenotype with dark green leaves and reduced apical dominance (Peng et al., 1997, Koornneef et al., 1985). This mutant resembles others that are defective in GA biosynthesis, however, unlike other mutants, *gai* is unable to respond to

exogenous application of GA and accumulates intracellular GA to higher levels than wild type. This demonstrates that the *gai* mutation affects a gene that is involved in negatively modulating growth in response to GA (Peng and Harberd, 1993).

Examination of the wild-type and mutant GAI sequences revealed that the *gai* mutant contains an in-frame 51-bp deletion close to the amino terminus of the predicted protein resulting in a 17 amino acid deletion (Peng et al., 1997). Sequence analysis also revealed that the GAI sequence contains a nuclear localisation signal (NLS) along with motifs that are involved in mediating the binding of transcription co-activators and nuclear receptors: Leucine heptad repeats (LHR), SAW and PFYRE – named for their amino acid sequences (Hirsch et al., 2009). In addition, sequence data indicated that GAI has a region homologous to the VHIID domain of the VHIID family of regulatory proteins (Peng et al., 1997), and an amino acid motif named DELLA (**Figure 1.8**). This information suggested that GAI functioned in the nucleus potentially as a negative transcriptional regulator of GA responsive genes (Peng et al., 1997).

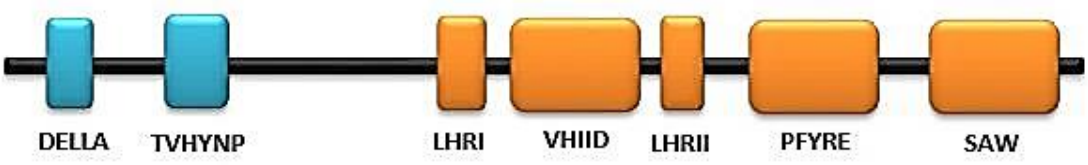

Figure 1.8 DELLA protein domains. A schematic diagram of the domains presents in DELLA proteins. The C terminal domains, required for protein-protein interactions, are labelled in orange; Leucine heptad repeat I (LHRI), VHIID, Leucine heptad repeat II (LHRII), PFYRE and SAW. Labelled in blue are the conserved N terminal domains, DELLA and TVHYNP.

Another *Arabidopsis* mutant *repressor of ga1-3 (rga)* was found to partially suppress the *ga1-3* mutant phenotype (Silverstone et al., 1998). Sequence analysis showed that RGA and GAI have 82% identical amino acid sequences (Dill et al., 2001) and examination of the RGA amino acid sequence revealed that like GAI, RGA contains C-terminal regulatory regions and an N terminal DELLA domain (**Figure 1.8**). These data indicated that RGA and GAI must play very similar, if not overlapping roles to negatively regulate the GA signalling pathway (Dill et al., 2001, Silverstone et al., 1998). The *rga* mutant sequence contains a premature stop codon at the C terminal of the protein, meaning the truncated product is able to respond to GA, but is unable to interact with other proteins to repress growth (Silverstone et al., 1998). Pysh et al. (1999) found that the amino acid sequences of RGA and GAI were very similar in their carboxyl-termini to the *Arabidopsis SCARECROW (SCR)* locus and SCR-like genes. Due to this similarity, RGA and GAI were grouped into the GRAS (GAI, RGA, SCR) family of proteins (Pysh et al., 1999).

The 17-amino acid deletion present in *gai* mutants was reproduced in the RGA sequence (**Figure 1.9**). Expression of the *rga*-Δ17 sequence in *Arabidopsis* caused a GA-unresponsive severe dwarf phenotype, similar to that of *gai*, supporting their role as redundant repressors of GA response (Dill et al., 2001). The DELLA domain is essential for response to GA. Both wild-type and mutant *rga*-GFP fusion proteins were able to localise to the nucleus of cells. However, GA application caused the disappearance of wild type but not mutant RGA fusion proteins. This suggested that the DELLA domain is needed for GA induced degradation (Dill et al., 2001).

Analysis of the *Arabidopsis* genome revealed three additional genes with high homology to *RGA* and *GAI*; *RGL1, RGL2* and *RGL3* (*RGA-like 1, 2 and 3*) (Dill et al., 2001). The RGL proteins have similarities to GAI and RGA in both the C and N termini. In the N terminal domain (NTD), many regions that have been implicated in GA response such as the DELLA domain are conserved (**Figure 1.9**), suggesting that the RGL proteins may play similar roles to GAI and RGA in GA signalling. Mutant analysis demonstrated that RGL2 plays a role in GA response in germinating seeds. Germination of wild-type seeds is completely inhibited by PAC whereas loss-of-function *rgl2* mutant seeds were able to germinate in the presence of PAC, suggesting that RGL2 is a GA responsive negative regulator of seed germination (Lee et al., 2002). When the DELLA domain of RGL2 is deleted it ceases to disappear in the presence of GA, indicating that it is also regulated by GA and that its DELLA domain is required for this response. It is thus likely to have a similar or redundant role to GAI and RGA (Hussain et al., 2005).

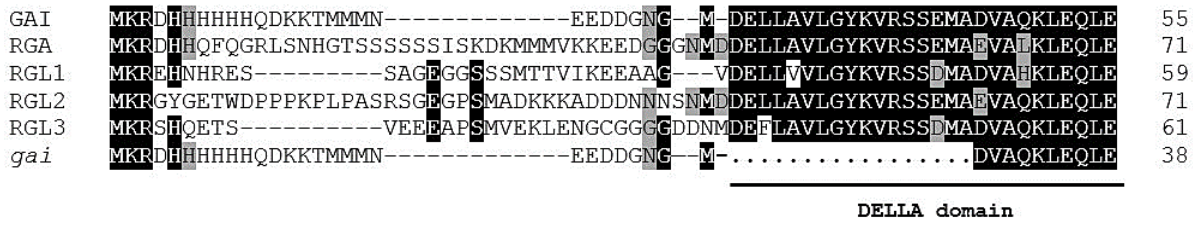

Figure 1.9 The *Arabidopsis* DELLA domain. The *Arabidopsis* DELLA sequences are compared with the mutant *gai* sequence. Identical residues are shown in reverse and similar residues are shown in grey. The DELLA domain is labelled with a bold black line beneath the sequences. The DELLA domain is highly conserved between the *Arabidopsis* DELLA sequences. The *gai* mutant contains a 17-amino acid deletion within the DELLA domain. The deletion is marked with dots in place of the deleted residues.

1.4.1.2 SLR1: the rice DELLA

The rice *slender* (*SLR1)* gene was identified because mutant *slr1* plants had an elongated phenotype, similar to wild-type plants that had been saturated with GA (Ikeda et al., 2001). The *slr1* phenotype is caused by a single recessive mutation in the *SLR1* gene and produces a

constitutive GA response phenotype, including reduced root lengths and numbers. Treatment with the GA biosynthesis inhibitor, uniconazole, did not affect the elongation of the plant, suggesting that the phenotype was not due to high endogenous GA levels (Ikeda et al., 2001). Molecular analysis of the SLR1 amino acid sequence revealed that it is orthologous to GAI and contains many of the same motifs including a DELLA domain, an NLS and a C terminal regulatory region. Mutant alleles of *SLR1* were found to have either a single bp mutation in the NLS motif or premature stop codons. To confirm SLR1's role as a GAI orthologue its 17-amino acid DELLA domain was deleted, which produced a dwarf phenotype much like the *gai1-3* mutant (Ikeda et al., 2001). In addition, Hirano et al. (2012) established that the N terminal DELLA domain of SLR1 possesses transactivation activity. Fusion of SLR1 to GFP demonstrated that SLR1 localises to the nucleus, and disappears after GA treatment (Itoh et al., 2002), indicating that SLR1 plays the same role in rice GA signalling as GAI does in Arabidopsis. Itoh et al. (2002) also produced a truncated SLN1 protein, lacking the C terminal domain. The resulting plants had a very similar phenotype to the *sln1* mutant, suggesting that the VHIID, LHR, PFYRE and SAW domains are required for interaction with other proteins, such as transcription factors, to allow repression of plant growth in response to GA (Itoh et al., 2002).

1.4.1.3 SLN1: The barley DELLA

The *SLENDER 1* (*SLN1*) gene in barley confers a tall elongated stem and leaf phenotype when mutated and is insensitive to external GA application. This phenotype is similar to the *slr1* mutant in rice, and therefore suggested that the *SLN1* gene was involved in GA signalling (Foster et al., 1977). When wild-type barley is treated with the GA biosynthesis inhibitor ancymidol, shoot elongation is severely disrupted, whereas *sln1* mutants are unaffected, demonstrating that the mutants are not responsive to endogenous GA levels. Analysis of the SNL1 amino acid sequence revealed that it is closely related to GAI and RGA and contains a DELLA motif in its NTD (Fu et al., 2002). Several mutant *sln1* alleles have been identified, with differing mutations that all cause dwarf or slender phenotypes. The *sln1b* mutant displays a dwarf phenotype, due to a single nucleotide frameshift mutation which causes a premature stop codon in the N terminal. The *sln1c* allele shows a slender phenotype, caused by an early termination codon at the extreme C terminal, resulting in loss of the final C terminal 17 amino acids. The *sln1d* mutant encodes a G-A substitution within the DELLLA domain of SLN1, resulting in a dominant dwarf phenotype (Chandler et al., 2002).

1.4.1.4 The maize DELLA proteins D8 and D9

The *Dwarf-8-1 (D8)* and *Dwarf 9-1 (D9)* genes in maize have been identified as the maize DELLA proteins. The phenotype of *d8* and *d9* mutant plants is a dominant dwarf, GA non-responsive phenotype, similar to that of the *gai* mutants in *Arabidopsis*. Multiple *d8* mutant alleles have been identified, which produce a range of dwarf phenotypes, ranging from mild to severe (Winkler and Freeling, 1994). The similarities between the *d8* and *gai* mutant phenotypes suggest that these genes could be orthologous. Comparison of the amino acid sequences reveal that D8 and GAI contain the same conserved C terminal domains, characteristic of the SCR family of proteins. In addition, both GAI and D8 contain conserved DELLA and TVHYNP domains in the N terminal. All the *d8* mutant alleles contain deletions, insertions or substitutions within these conserved N terminal regions, much like the *gai* mutant, suggesting that D8 does act as a maize DELLA protein (Peng et al., 1999). The mutant *d9-1* allele contains a number of nucleotide substitutions in the N terminal and a C terminal E-K substitution which was sufficient to produce a dwarfing and early flowering phenotype in *Arabidopsis* (Lawit et al., 2010).

1.4.1.5 Wheat RHT-1

Mutations of the *Rht-1* gene in wheat produce a range of dwarf phenotypes that are unresponsive to GA (Pearce et al., 2011). The similarities between this phenotype and other DELLA mutants, suggested that RHT-1 could be the wheat DELLA protein. Sequence analysis revealed that regions of wheat chromosomes 4A, 4B and 4C have a similar sequence to the *GAI* gene, and amino acid sequence examination showed that the DELLA and TVHYNP domains from the N terminal region of both GAI and RHT-1 were conserved (Peng et al., 1999).

RHT-1 was identified as the gene that is mutated in the semi-dwarf green revolution wheat lines and numerous mutant alleles of *Rht-1* have been identified that produce dwarf lines with a variety of different heights. Six mutant alleles of *Rht-1* have been identified with four on chromosome 4B and two on chromosome 4D (Borner et al., 1996). The height differences between the mutant alleles can be seen in **Figure 1.10**. Currently no dwarf alleles of *Rht-A1* have been described in the literature. However, Pearce et al. (2011) found that *Rht-A1* is expressed at the same levels as *Rht-B1* and *Rht-D1*, and contains all the conserved domains found in a functional DELLA protein (Pearce et al., 2011).

Rht-B1b (formerly Rht1) and *Rht-D1b* (Rht2) both have a similar height that is about 80% of the tall control (Flintham et al., 1997b). The *Rht-B1c* (Rht3) and *Rht-D1c* (Rht10) alleles give a

more severe phenotype of less than half the size of the tall control plants. These differences in height are due to different mutations within the *Rht-B1* and *Rht-D1* homoeologous sequences. Less severe dwarfing mutants *Rht-B1d* and *Rht-B1e*, along with *Rht-B1b and Rht-D1b* are caused by a premature stop codon within the coding region, which produces an N terminally truncated product that is no longer able to bind to the GA receptor GID1 (see section 1.4.2), *The Rht-B1c* mutation was found to be a 90-bp insertion within the N terminal DELLA domain, again disrupting its ability to bind GID1. The extreme dwarf phenotype from *Rht-D1c* is caused by multiple copies of the *Rht-D1b* mutant allele (**Figure 1.11**) (Pearce et al., 2011). Pearce et al. (2011) demonstrated that all mutant alleles of RHT-B1 were unable to interact with TaGID1 in a yeast two hybrid screen. Pearce et al. (2011) therefore suggested that the semi-dwarf phenotype of *Rht-B1d*, *Rht-B1e*, *Rht-B1b and Rht-D1b* is due to inefficient re-initiation of translation, meaning reduced levels of N-terminally truncated GA-insensitive DELLAs being produced. However, Wu et al. (2011) used yeast two-hybrid assays to show that while *Rht-B1c* is unable to interact with TaGID1, *Rht-B1b* only has a reduced interaction with TaGID1.

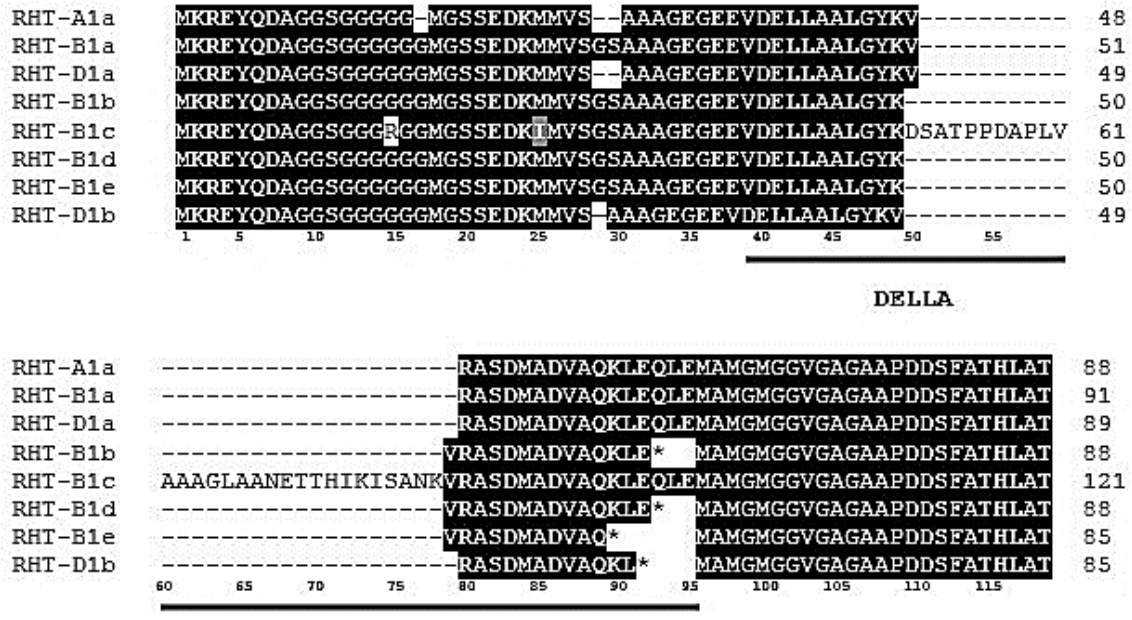

Figure 1.10 Alignment of the *RHT-1* alleles. A comparison of the wild-type and mutant *Rht-1* alleles. Identical residues are shown in reverse. The DELLA domain is shown by a bold black line beneath the sequences. The *Rht-B1b* and *Rht-B1d* mutant alleles contain an identical premature stop codon at E93, marked with an asterisk, which is predicted to re-initiate at M95. The *Rht-B1e* mutant allele has a premature stop codon after Q89. The *Rht-D1b* mutant sequence contains a premature stop codon at L91. The *Rht-B1c* sequence contains a 30 amino acid insertion from V49 which disrupts the DELLA domain.

The semi dwarfing *Rht-B1b* and *Rht-D1b* alleles are found in the majority of wheat varieties grown for food worldwide (Pearce et al., 2011) and give the highest yields of all the *Rht-1* mutant alleles. The semi-dwarfing alleles cause increased yield due to an increased harvest index, high spikelet fertility, a larger number of seeds per ear and the ability to partition more resources to the developing ear rather than to the stem. The best results for the semi-dwarfing genes can be observed in winter wheat varieties, and increases in yield are less obvious or completely absent under heat or drought stress (Flintham et al., 1997b). Shorter *Rht-1* mutant alleles such as *Rht-B1c* or *Rht-D1c* have not been exploited for agricultural use. Studies have shown that although the severe mutants can yield the same or more than the semi-dwarf varieties when conditions are favourable, they yield less under stressful conditions, making them less reliable (Flintham et al., 1997b).

Figure 1.11 Height differences between *RHT-1* mutant alleles. The height of different *Rht-1* mutant alleles was compared to the wild-type RHT-1, taken from Pearce et al. (2011).

1.4.2 The GA receptor: GID1

The GA receptor was first identified in rice through the isolation of the *gid1* mutant, which had a dwarf, GA-insensitive phenotype (Ueguchi-Tanaka et al., 2005). The GIBBERELLIN INSENSITIVE DWARF 1 (GID1) protein is able to bind GA, which causes a conformational change that allows GID1 to interact with DELLA proteins (**Figure 1.12**) and facilitate the downstream response to GA (Murase et al., 2008).

The sequence of the rice gene *GID1* was found to have similarities to hormone-sensitive lipases indicating potential for hormone interaction. Furthermore, the GA-insensitive phenotype of *gid1* mutants is consistent with GID1 having a role in GA signalling. Double mutants of *gid1slr1* exhibit a phenotype matching that of the *slr1* single mutant, suggesting that GID1 acts upstream of SLR1 in the same GA response pathway (Ueguchi-Tanaka et al., 2007). GFP-SLR1 was degraded in response to GA in wild-type, but not in *gid1* mutant cells, demonstrating that GID1 is essential for SLR1 degradation. Further pull down experiments showed that SLR1 could only be pulled down by GID1 in the presence of active GA, showing that GA is required for this interaction (Ueguchi-Tanaka et al., 2005).

Arabidopsis contains three GID1 homologues, GID1a GID1b and GID1c, which seem to play similar roles to GID1 in rice. When expressed in *E. coli* all three *Arabidopsis* GID1 paralogues bound GA with the same affinity as rice GID1, and expression of the *Arabidopsis GID1* genes in rice rescues the *gid1* phenotype (Nakajima et al., 2006). A triple *gid1* mutant displayed a severe dwarf phenotype, with a large reduction in root radius and length compared to the wild-type (Griffiths et al., 2006). Much like rice GID1, *Arabidopsis* GID1 paralogues were also shown to require the DELLA domain of RGA for interaction. In addition, yeast two-hybrid and pull-down experiments demonstrated that the presence of GA enhances the interaction between RGA and GID1, indicating that GID1 binds GA which then promotes its interaction with RGA.

The crystal structure of GID1 bound to the DELLA N-terminus was able to show the structure of the GA-GID1-DELLA complex (Murase et al., 2008, Shimada et al., 2008). This allowed the physical interaction between GA, GID1 and DELLAs to be investigated. GID1 is a monomeric protein, comprising an α/β core domain and an N terminal extension. The crystal structure demonstrates that GID1 and not the DELLA protein is responsible for the interaction with GA, with GA binding GID1 directly. GID1 contains a central deep pocket which binds active GAs. GA_4 is held in the binding pocket by several hydrogen bonds or indirectly by means of a water molecule (Shimada et al., 2008). Once GA has bound the pocket, the flexible N terminal extension forms a lid that is held over the top of the binding pocket, covering GA (**Figure 1.12**). The N terminal domain of the DELLA protein is then able to interact with GID1-GA via the N terminal lid (Murase et al., 2008).

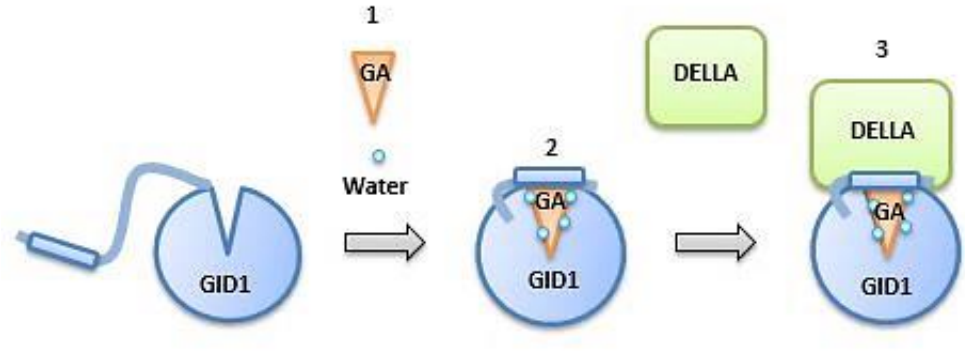

Figure 1.12 The GA-GID1-DELLA Interaction. The interaction between DELLA and GIBBERELLIN ACID INSENSITIVE (GID1) in response to gibberellin (GA) is shown. GA binds GID1 via the GID1 binding pocket (1), which causes the N terminal extension to form a lid (2). GID1 is then able to interact with DELLA via the N terminal extension (3).

1.4.3 F-box proteins involved in DELLA degradation

After interaction with GID1, DELLAs are marked for degradation by interactions with DELLA specific F-box proteins, which recruit the E3 ubiquitin ligase complex (McGinnis et al., 2003) (**Figure 1.13**).SLY1 (SLEEPY) from *Arabidopsis* and GID2 from rice have both been found to be positive regulators of GA signalling, and mutants display phenotypes that are associated with a disrupted GA response, such as dwarfing, increased seed dormancy, delayed flowering, and reduced fertility (McGinnis et al., 2003, Sasaki et al., 2003). Sequence analysis of SLY1 revealed that it has homology to F-box proteins (McGinnis et al., 2003)

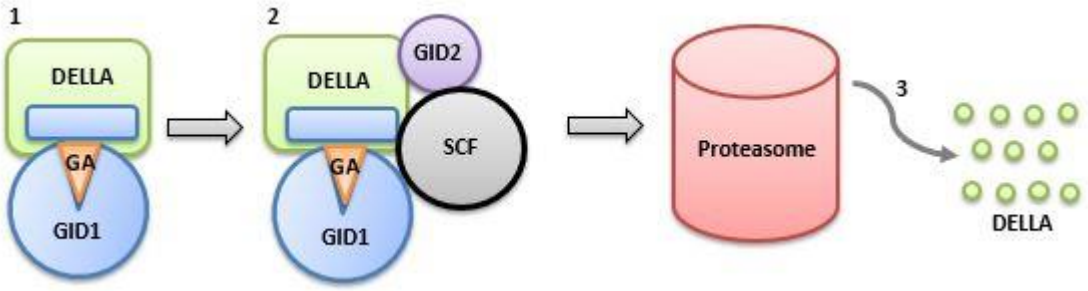

Figure 1.13 The GA response pathway. The pathway leading to DELLA degradation by the proteasome is shown. GID1; GIBBERELLIN INSENSITIVE DWARF1, SCF; SKP, Cullin, Fbox. (1) GID1 binds DELLA via its the N terminal extension, (2) this then recruits the F-box protein GID2 and the SCF complex, leading to degradation of DELLA by the proteasome (3).

F-box proteins are part of the degradation complex in eukaryotic cells that binds proteins destined for degradation by the proteasome and recruits an E3 ubiquitin ligase family termed the SCF (Skp1-cullin-F-box) (**Figure 1.13**). The SCF is made up of the SKP1 linker protein, the CDC53/CUL1 scaffold protein and the RBX1/ROC1/HRT1 RING domain protein which interact

with a suite of F-box proteins. The F-box proteins recruit E3 ubiquitin ligases that mark the substrate for degradation by the proteasome (Willems et al., 2004). Components of the SCF have been identified in wheat. Hong et al. (2012b) identified an F-box protein termed the *Triticum aestivum* cyclin F-box domain (TaCFBD). Six *SKP-like* genes have also been isolated in wheat, termed *TaSKP1-6*. A yeast two-hybrid experiment demonstrated that different combinations of SKP proteins were able to interact with TaCFBD and wheat cullin (TaCullin) homologues, with TaSKP1, TaSKP5 and TaSKP6 acting as a bridge between F-box proteins and cullin proteins (Hong et al., 2013). In addition, a yeast two-hybrid library identified an E3-ubiquitin ligase-like protein (TaRMD5) that interacted with TaCullin (Hong et al., 2014).

Examination of the GID2 protein sequence indicated that it also contains conserved F-box motifs, and has similarities to SLY1 (Gomi et al., 2004, McGinnis et al., 2003). In both sequences, mutations were found in the carboxyl terminal domain (CTD) rather than the F-box domain, suggesting that the CTD is important for GA signalling. The phenotype of mutants lacking these proteins is a dwarf plant with no response to GA application. A series of deletions in GID2 demonstrated that all three conserved CTD motifs are required for GID2 function (Gomi et al., 2004). These results indicate that both SLY1 and GID2 may act as F-box proteins in the GA signalling pathway (Gomi et al., 2004, McGinnis et al., 2003, Sasaki et al., 2003).

Examination of *sly1* mutants revealed that RGA accumulation was increased to similar levels as in the *rga* constitutively-active mutant, suggesting that SLY1 could have a role in regulating RGA degradation (McGinnis et al., 2003). GFP-SLR1 was degraded after GA application in wild-type, but not in *gid2* mutant cells, suggesting that GID2 plays a vital role in the regulation of SLR1 degradation (Gomi et al., 2004). To further investigate this interaction, double mutants of *rga* and *sly1* were produced. The *rga* mutation was able to rescue the *sly1* mutant phenotype, demonstrating that RGA acts downstream of SLY1 in the GA signalling pathway (McGinnis et al., 2003). Similar results were obtained in rice. When a *gid2-slr1* double mutant was produced, the *gid2* mutant phenotype was rescued and the plant resembled the tall-elongated *slr1* mutant. This indicates that SLR1 acts downstream of GID2 in the GA response pathway (Sasaki et al., 2003).

A screen for proteins that bound GID2 identified a Skp-1 homologue, OsSKP15. When the F-box domain of GID2 was mutated the interaction with OsSKP15 was abolished, demonstrating that GID2 binds via its F-box domain to Skp1 (Gomi et al., 2004). In addition, yeast two-hybrid experiments also demonstrated that GID2 interacts with OsSKP1 (Sasaki et al., 2003). Further supporting the role of GID2 as an SCF component, immunoprecipitation experiments showed

co-precipitation of GID2 with OsSKP15 and OsCUL1 proteins, demonstrating that GID2 can interact with various components of the E3 ligase to promote DELLA degradation (Gomi et al., 2004).

1.4.4 DELLA degradation by the proteasome

The method by which GA causes the disappearance of DELLA proteins was discovered to be degradation by the proteasome (**Figure 1.13**). Fu et al. (2002) found that the disappearance of GFP fused SLN1 was inhibited in the presence of proteasome inhibitors, but unaffected by inhibitors of proteases, suggesting that the proteasome is responsible for the degradation of SLN1. RGL2 similarly fails to disappear in the presence of proteasome inhibitors, but disappeared in the presence of protease inhibitors, supporting the findings for SLN1 and showing that RGL2 also seems to be degraded by the proteasome (Hussain et al., 2005). In addition, proteasome inhibitors were shown to block GA induced α-amylase activity in aleurone cells, demonstrating that this proteasome-mediated degradation of DELLA does affect downstream signalling (Hussain et al., 2007). The current model for GA response is as follows; when GA present, it is able to bind its receptor GID1, which then undergoes a conformational change which allows binding of GID1 to DELLAs (Murase et al., 2008). This binding promotes the recruitment of a DELLA-specific F-box protein and associated E3 ubiquitin ligase (McGinnis et al., 2003), which marks DELLAs for degradation by the proteasome (Hussain et al., 2007) (**Figure 1.13**).

1.4.5 Downstream regulators of the GA response through DELLA-protein interactions

DELLAs act as negative regulators of the GA response through their interaction with various proteins including transcription factors. In the GA dependent regulation of flowering time, both GAI and RGL1 have been shown to interact with the transcription factors WRKY12 and WRKY13 in *Arabidopsis*. This interaction was found to disrupt the transcriptional activity of the WRKY transcription factors (Li et al., 2016c). CONSTANS 1 (CO) and FLOWERING LOCUS T (FT) are transcription factors that integrate the GA and vernalisation pathways to correctly regulate flowering time. FLOWERING LOCUS 1 (FLC) is a transcriptional repressor that interacts with both SOC1 and FT in the control of flowering time. DELLAs have been shown to interact with FLC via their LHR1 domains to modulate this interaction (Li et al., 2016b). Another group of transcription factors that interact with DELLAs are the ET responsive element binding (ERF) family. Both RELATED TO APETALA2.3 (RAP2.3). RAP2.3 and RAP2.12 were able to interact with GAI and RGA in a yeast two-hybrid screen (Marin-de la Rosa et al., 2014). Another screen was

able to demonstrate that ERF11, ERF4, ERF8 and ERF10 also interacted with the GRAS domain of RGA (Zhou et al., 2016). The interaction between GAI and RAP2.3 was shown to repress the ability of RAP2.3 to bind to and promote the expression of its target genes. One process shown to be regulated by this interaction was apical hook development in seedlings. RAP2.3 promotes the expression of Apical hook genes in the presence of ethylene, whereas GAI represses RAP2.3 activity in the absence of GA to repress apical hook formation (Marin-de la Rosa et al., 2014).

In *Arabidopsis* BOTRYTIS SUSCEPTIBLE1 INTERACTOR (BOI) and BOI related (BRG) proteins 1-3 have been shown to interact with DELLAs (Park et al., 2013). BOIs interact with DELLAs via their RING domain, which allows the DELLA-BOI complex to target the promoters of a subset of GA responsive genes (Park et al., 2013). Altering BOI expression in *Arabidopsis* results in GA response phenotypes (Park et al., 2013). Single *boi* mutants had no effect on the GA response, but the quadruple *boiQ* mutant lines displayed phenotypes typical of enhanced GA signalling. In contrast *BOI* overexpression lines demonstrated phenotypes associated with reduced GA signalling. *Arabidopsis* BOI proteins have been shown to be involved multiple processes in plant growth, including the regulation of pathogen response (Luo et al., 2010), germination and flowering (Nguyen et al., 2015). DELLAs interact with the zinc finger INDETERMINATE DOMAIN (IDD) family in a similar manner (Yoshida et al., 2014). IDDs are C2H2 zinc finger proteins which have a wide range of role in the regulation of plant development such as flowering time in response to sugar metabolism, gravitropic response and root development (Morita et al., 2006, Seo et al., 2011). *Arabidopsis* IDDs 3, 4, 5, 9 and 10 were shown to interact with the GRAS domain of RGA. The IDD proteins were also shown to bind the promoter sequence of *SCARECROW-LIKE3 (SCL3),* which is positively regulated by DELLAs. The interaction between DELLAs and IDDs in *Arabidopsis* results in the formation of a complex able to bind to the promoter of *SCL3* and drive its expression.

The bHLH transcription factor ALCATRAZ (ALC) has also been shown to interact with DELLAs. ALC is required for the regulation of fruit patterning in *Arabidopsis*. During fruit patterning, valve margins differentiate into a lignification layer (LL) and a separation layer (SL). ALC is required for SL specification (Rajani and Sundaresan, 2001). In yeast two-hybrid experiments, ALC was shown to bind to GAI, RGA and RGL2, in an interaction which represses ALC transcriptional activity (Arnaud et al., 2010). This provides a model whereby in the absence of GA, DELLAs repress SL specification by repressing ALC transcriptional activity, whereas an increase in GA concentration would promote SL specification by releasing ALC from DELLA repression (Arnaud et al., 2010). DELLAs have been shown to interact with another branch of the bHLH superfamily called the PHYTOCHROME INTERACTING FACTORS (PIFs). Both PIF3 and

PIF4 have been shown to directly bind to DELLAs in *Arabidopsis*, with the result of repression of PIF transcriptional activity (Feng et al., 2008, de Lucas et al., 2008). See **section 1.6** for a detailed discussion of PIF protein function.

1.4.5.1 The role of DELLAs in other hormone response pathways

Along with DELLA interactions with transcription factors to modify gene expression, DELLAs are also capable of interacting with other proteins. DELLAs have been shown to interact with signalling components of other plant hormone response pathways to facilitate crosstalk between GA and other plant hormones. One example is the interaction with components of the auxin response pathway to regulate shoot growth. Previous experiments have demonstrated that when the shoot apex of GA-deficient dwarf mutant pea plants was removed, the shoot failed to elongate in response to GA, indicating that an intact shoot apex is required for normal GA response. Recent experiments have shown that the GA response of *ga1-3* seedlings in *Arabidopsis* can be restored with the addition of auxin to the shoot apex, suggesting that auxin promotes the GA response in some way (Fu and Harberd, 2003). GFP labelled RGA failed to disappear in response to GA in decapitated seedlings. Application of auxin to the decapitated shoot apex resulted in the disappearance of GFP labelled RGA at a similar rate to that in intact seedlings in response to GA. These results indicated that auxin is required for the GA-induced disappearance of RGA. The auxin transport inhibitor 1-N-naphthylphthalamic acid (NPA; a specific inhibitor of auxin efflux20) prevented exogenous GA from restoring normal growth to *ga1-3* roots, supporting the findings that auxin is required for GA induced RGA degradation, and therefore GA response (Fu and Harberd, 2003).

DELLAs have also been shown to interact with components of the JA response pathway (Xie et al., 2016). Anthocyanin accumulation is a detectable biomarker of environmental stress in plants. The expression of anthocyanin-specific genes is regulated by the MBW complex, which consists of MYB, bHLH and WD40 subunits. The activity of MBW is repressed by MYBL2 and JAZ family proteins via sequestration of the bHLH and MYB subunits. The *Arabidopsis* DELLAs, RGA and GAI, have both been shown to bind MYBL2 and JAZ in pull down assays. This binding releases the sequestered bHLH and MYB subunits, allowing the formation of an active MWB complex, which in turn activates the anthocyanin biosynthetic response pathway in response to environmental stress (Xie et al., 2016). DELLAS have also been shown to regulate the activity of the *Arabidopsis* MCY2, MYC3 and MYC4 bHLH transcription which are factors are involved in the promoting the expression of genes involved in the JA response. The *Arabidopsis* MCY2 transcription factor has been shown to bind directly to all five *Arabidopsis* DELLAs in a

yeast two-hybrid screen (Hong et al., 2012a). The binding of DELLAs to MYC2 causes the sequestration of MYC2, and therefore repression of the plant-insect interaction response. This provides a mechanism by which GA can positively regulate this response by promoting the degradation of DELLAs, freeing the MYC transcription factors from repression and allowing the synthesis of pollinator attracting substances. (Hong et al., 2012a). JA signalling components have also been shown to promote DELLA expression. This promotion is dependent on the F-box protein CORONATINE INSENSITIVE1 and MYC transcription factor JASMONATE INSENSITIVE1 (JIN1/MYC2). MYC2 has been shown to bind directly to the RGL3 promoter in *Arabidopsis*, and RGL3 has been shown to bind JAZ proteins. These results indicate that the MYC2 dependent accumulation of RGL3 causes a repression of JAZ activity, leading to an increase in expression of JA responsive genes, and therefore promoting the JA response. In the *rgl3-5* mutant, JA responsive genes have reduced expression, and conversely, in *RGL3* overexpression lines expression of JA responsive genes is enhanced, supporting a role for RGL3 in the JA response (Wild et al., 2012).

Crosstalk between the BR and GA response pathways has also demonstrated via an interaction between DELLAs and the BR activated transcription factor BZR1 (Li et al., 2012d). BZR1 is a positive regulator of BR signalling, which when de-phosphorylated can bind to the promoters of BR response genes and promote their expression. BZR1 has also been shown to regulate the activity of DELLA family members (Sun et al., 2010). BZR1 was shown to interact with all five members of the Arabidopsis DELLA family; GAI, RGA and RGL1-3. A close homolog of BZR1; BES1 which also positively regulates BR signalling was also capable of binding RGA. The interaction between BZR1 and the DELLAS was reliant on the BIN2 phosphorylation domain of BZR1 and the LHR1 domain of the DELLAs. The interaction between BZR1 and DELLAs occurs when BZR1 is de-phosphorylated and therefore active, providing a means by which low GA levels can inhibit BR mediated cell elongation. In the presence of BR, the de-phosphorylated form of BZR1 was also capable of binding and sequestering DELLAs to enhance GA mediated growth. This interaction therefore provides a mechanism through which the GA and BR response pathways can interact (Li et al., 2012d).

1.5 Light regulation of plant development

Plants have the capacity to detect, calculate and respond to changes in the quality, quantity and direction of light which allows them to maximise photosynthetic potential and correctly time developmental processes such as flowering or seed germination. The changes in light are detected through photoreceptors (Briggs and Olney, 2001). A photoreceptor is a light sensitive

molecule that undergoes a conformational/energetic change in response to the absorption of light energy; it forms the interface between light and signal transduction in plants. There are different families of photoreceptors that absorb and respond to different wavelengths of light: R, FR, blue and UV-B light have important roles in photomorphogenesis. This project will focus on the role of phytochromes in regulating plant development. The phytochrome family of photoreceptors respond to R/FR light (Bae and Choi, 2008).

1.5.1 Phytochromes

Phytochromes are dimeric proteins that consist of two identical apoprotein chains, each attached to a chromophore (Rockwell et al., 2006). The chromophore responds to light signals by undergoing isomerisation, which causes a conformational change in the phytochrome (Lagarias and Mercurio, 1985). Absorption of red light converts phytochromes from the Pr to the Pfr form. The Pfr form of phyB can then enter the nucleus due to the NLS in its CTD and interact with transcription factors such as the PIFs to alter gene expression (Nagatani, 2004). phyA requires two small plant-specific proteins FAR-RED ELONGATED HYPOCOTYL 1 (FHY1) and FHY1-LIKE (FHL) to enter the nucleus (Zhou et al., 2005).

There are various forms of phytochrome with different roles in the response to light. *Arabidopsis* contains five different phytochromes: A, B, C, D and E (Clack et al., 1994). phyA accumulates to high levels in dark-grown etiolated seedlings, the levels of phyA then decline in light-grown plants by three mechanisms. Firstly, *PHYA* transcription is repressed, secondly, *PHYA* mRNA is degraded and thirdly, phyA Pfr is ubiquitinated and degraded. phyB, phyC, phyD and phyE are all present at lower, but more stable levels in the plant and transcription and protein levels of these phytochromes are not dramatically affected by light (Duek and Fankhauser, 2005).

The basic model of phytochrome-PIF signalling is as follows (**Figure 1.14**): Phytochrome is activated by absorption of light in the cytoplasm, undergoing a conformational change that enables it to enter the nucleus (Nagatani, 2004). Once in the nucleus, phytochrome is able to interact with PIFs and promote their degradation, thereby relieving repression of genes involved in photomorphogenesis and repressing expression of genes involved in skotomorphogenesis (Jeong and Choi, 2013). Different PIFs can act on different groups of genes. For example, PIF3 is the major regulator involved in promoting hypocotyl elongation in the dark (Soy et al., 2012) and regulating chloroplast development (Ni et al., 1998), whereas PIF4 and PIF5 regulate genes involved in leaf senescence (Sakuraba et al., 2014), phototropism

(Sun et al., 2013) and stem elongation (Brock et al., 2010, Kunihiro et al., 2010, Huq et al., 2004b). PIF1 regulates genes involved in chloroplast development and seed germination in the dark (Huq et al., 2004b)

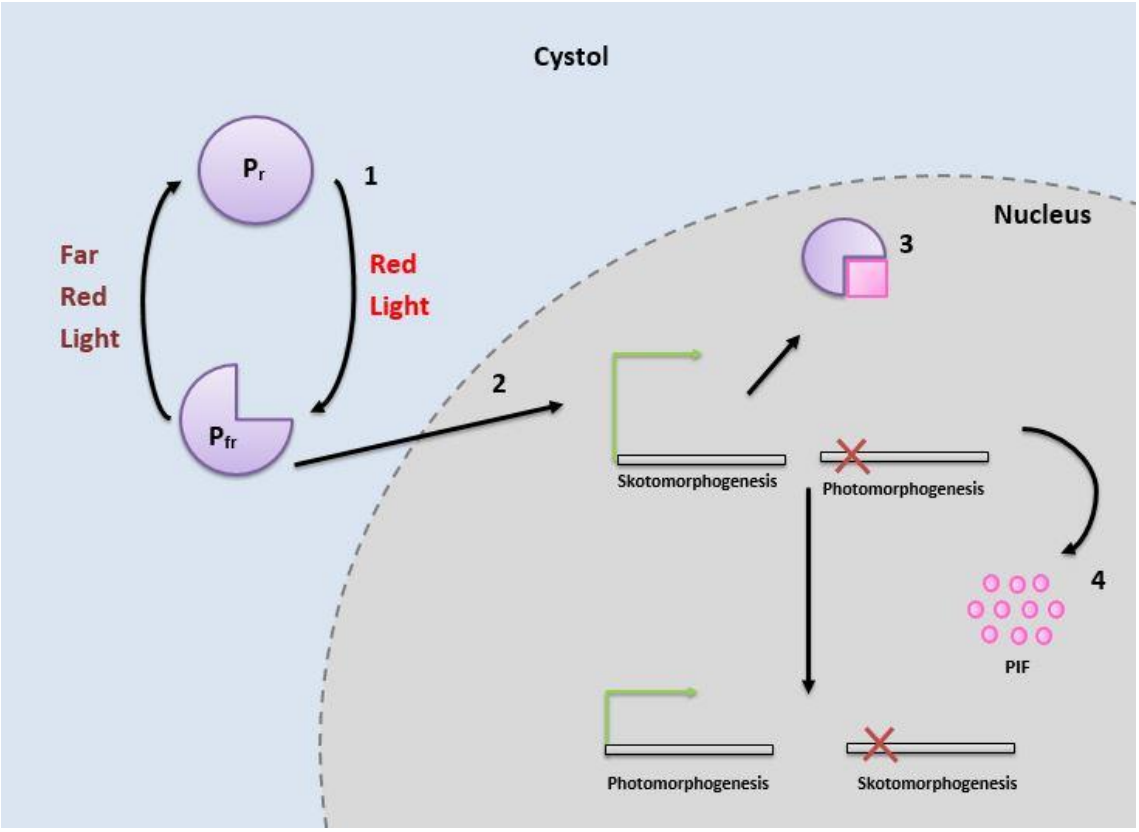

Figure 1.14 Phytochrome-PIF Signalling. (1) In response to red light phytochrome undergoes a conformational change from Pr to Pfr. (2) Pfr is able to translocate into the nucleus and interact with PIFs, repressing their activity by (3) sequestration and (4) degradation.

Phytochromes also regulate the expression of light-regulated genes through the CONSTITUTIVE PHOTOMORPHOGENIC 1 (COP1)- ELONGATED HYPOCOTYL 5 (HY5) pathway (Osterlund et al., 2000). COP1 is a conserved RING finger ubiquitin ligase that is involved in a variety of processes in multiple species from plant development to mammalian cell survival (Yi and Deng, 2005). COP1 was identified in *Arabidopsis* as a repressor of photomorphogenesis, and acts by promoting the degradation of several photomorphogenesis promoting proteins, including HY5 (Deng et al., 1992). HY5 is a nuclear localised bZIP transcription factor which promotes photomorphogenesis under a wide range of wavelengths including R, FR, B and UV-B. The abundance of HY5 has been shown to directly correlate with the extent of photomorphogenesis development, suggesting it is a central regulator of this process (Osterlund et al., 2000). In response to light, HY5 is responsible for both upregulation and

downregulation of gene expression (Lee et al., 2007), and multiple photoreceptors including phytochromes promote the accumulation of HY5 under a range of light conditions by reducing the nuclear abundance of COP1 (Osterlund et al., 2000). COP1 binds directly to HY5 via its WD40 repeat domain, and targets HY5 for degradation by the proteasome, preventing the promotion of photomorphogenesis (Osterlund et al., 2000). A HY5 homologue in *Arabidopsis* called HY5 HOMOLOG (HYH) has also been shown to be a target of COP1 (Osterlund et al., 2000). This COP1-HY5 interaction comprises another mechanism by which phytochrome regulates plant growth in response to light (Chen and Chory, 2011). In addition, COP1 regulates the activity of LONG HYPOCOTYL IN FAR-RED (HFR1) (Duek et al., 2004). HFR1 is a bHLH protein, closely related to PIF1, PIF3 and PIF4, which acts downstream of phyA to regulate development in far red light. In the dark HFR1 is present in an unstable phosphorylated form which is rapidly degraded. The interaction between COP1 and HFR1 promotes this degradation, allowing COP1 to promote the de-etiolation response (Duek et al., 2004).

The phytochrome family has also been identified in monocot and cereal species such as maize and rice. Where *Arabidopsis* has been shown to encode five phytochromes, from phyA to phyE, some monocots only contain three phytochromes; phyA, phyB and phyC (Mathews and Sharrock, 1996). The rice genome contains single copies of *PHYA, PHYB* and *PHYC* (Kay et al., 1989, Dehesh et al., 1991, Basu et al., 2000). Each rice phytochrome has a distinct role in photomorphogenesis, much like *Arabidopsis*. phyA is the most abundant phytochrome present in etiolated rice seedlings, and is involved in regulating development in response to far-red light (Takano et al., 2001). phyB is the most abundant phytochrome in rice under white light conditions, and is involved in various plant processes such as seedling establishment and plant architecture along with stress and hormone responses (Liu et al., 2012). phyC is the least abundant phytochrome present in rice, with a low constitutive expression profile. Rice phyC requires phyB for function. phyC is principally found as a heterodimer with phyB, and is responsible for regulating seedling etiolation under R and FR light (Xie et al., 2014).In maize two copies of the *PHYA*, *PHYB* and *PHYC* genes have been identified (Christensen and Quail, 1989, Sheehan et al., 2004). phyA and phyB are expressed at higher levels in dark-grown seedlings than light-grown plants, whereas phyC is expressed at similar levels in both conditions.

1.5.2 Cryptochromes

Cryptochromes are the photoreceptors responsible for detecting blue light and UV-A radiation. The *Arabidopsis* genome encodes 2 cryptochrome photoreceptors, *CRY1* and *CRY2*. CRY1 and

CRY2 are localised to the nucleus and cytoplasm (Yu et al., 2007, Wu and Spalding, 2007) and are involved in the regulation of numerous aspects of plant growth, such as plant height, apical dominance and flowering (Liu et al., 2011).

The CRY apoprotein is made up of two domains: the N terminal photolyase homologous region (PHR) domain, and the C terminal cryptochrome containing domain, termed the C terminal extension (CCE) domain (Sang et al., 2005). The PHR domain is the domain that interacts with chromophores, non-covalently binding to both flavin adenine dinucleotide (FAD) and a pterin. When oxidised, FAD can absorb significant amounts of blue light, allowing it to act as a chromophore (Lin et al., 1995). In the dark CRYs are bound to oxidised FAD, which is reduced upon blue light absorption, causing a conformational change of the CRY protein into an open conformation and allowing it to interact with other signalling components and cause alterations in gene expression (Bouly et al., 2007). Photoactivation also causes changes in phosphorylation, with CRY2 but not CRY1 being phosphorylated and subsequently degraded in blue light, and de-phosphorylated and stable in the absence of blue light (Shalitin et al., 2002). The conformational change CRY2 undergoes after absorption of blue light allows it to interact with the bHLH transcription factor CIB1. In association with CRY2, CIB1 positively regulates floral initiation via binding to the promoter of the *FLOWERING LOCUS T (FT)* gene (Liu et al., 2008). CRYs also interact with COP1. In blue light, CRY1 interacts with COP1 to prevent it from degrading HY5 and HFR1, thereby promoting seedling growth in response to blue light (Saijo et al., 2003).

In rice, three cryptochrome genes have been identified; *OsCRY1a, OsCRY1b* and *OsCRY2* (Hirose et al., 2006, Matsumoto et al., 2003). The amino acid sequences of the OsCRY sequences contain a photolyase-like domain in their N terminal, and are homologous to *Arabidopsis* CRY1 and CRY2. The OsCRY proteins are localised to both the nucleus and cytoplasm, much like the cryptochromes in *Arabidopsis* (Matsumoto et al., 2003). Two cryptochrome genes have been identified in wheat: *TaCRY1a* and *TaCRY2 (Xu et al., 2009)*. TaCRY1a is orthologous to OsCRY1a and OsCRY1b with 82 and 72% identify respectively. TaCRY2 is orthologous to OsCRY2 with a sequence identity of 80%. The similarity between TaCRY1a and OsCRY2 or TaCRY2 and OsCRY1a or OsCRY1b is less than 48%. Both TaCRY proteins contain the photolyase-like domain in their N terminal, typical of cryptochromes. Expression of TaCRY1a is most abundant in seedling leaves, but very low in roots and germinating embryos. Expression levels of TaCRY2 were much higher than TaCRY1a in developing embryos. Upon transition from dark to light, there was a slight change in TaCRY1a and TaCRY2 expression, whereas transition to red light caused a stronger induction of TaCRY1a

than TaCRY2. The cellular localisation of TaCRY1a mirrors that of the *Arabidopsis* CRY proteins (Xu et al., 2009).

1.5.3 Phototropins

Phototropins are blue light-responsive photoreceptors that mediate phototropism, chloroplast migration, stomatal opening and stem growth (Briggs and Christie, 2002). Phototropins were identified from the observation that blue light activates phosphorylation of a plasma membrane protein in etiolated pea seedlings (Gallagher et al., 1988). Mutations in this protein impair the phototropic response and plants with this mutation were termed *non-phototropic hypocotyl* (*nph*) mutants (Liscum and Briggs, 1995). The CTD of this protein was found to be a serine threonine kinase, which was mutated in all *nph* mutants, suggesting that the kinase activity was essential for function. The NTD contained two repeat domains that have homology to other signalling proteins, termed the LOV domains. The LOV domain was found to bind the chromophore flavin mononucleotide (FMN), indicating the role of NPH as a photoreceptor, causing it to be renamed as PHOTOTROPIN 1 (PHOT 1) (Christie et al., 1999).

Two phototropins have been identified in *Arabidopsis*: PHOT1 and PHOT2. PHOT2 also contains two LOV domains which interact with FMN and a kinase domain which undergoes light activated autophosphorylation. Both PHOT1 and PHOT2 act redundantly to regulate phototropism. While *phot1* mutants still retain phototropic responses at higher intensities of blue light, the *phot1phot2* double mutants lose all response at high intensities. This suggests that PHOT1 acts to promote phototropic responses at low intensities of blue light, while PHOT2 acts to promote phototropism at high blue light intensities (Sakai et al., 2001).

1.5.4 UVR8

UVR8 is a β-propeller protein that was originally identified in an *Arabidopsis* screen of mutants that were hypersensitive to UV-B light (Kliebenstein et al., 2002). UVR8 is localised to the cytoplasm and nucleus under normal conditions. After UV-B irradiation the levels of UVR8 do not change, but it accumulates in the nucleus (Kaiserli and Jenkins, 2007). UVR8 is present in the cell in its inactive homodimer form and after UV-B irradiation, UVR8 monomerises into its active state. UVR8 has not been found to bind any putative chromophores, like cryptochromes or phototropins, but instead UVR8 contains 14 UV-absorbing tryptophans, which localise to the top surface of UVR8 (Kliebenstein et al., 2002) and are conserved from algae to higher plants. The tryptophans are thought to act as the chromophore of UVR8s (Christie et al., 2012). UVR8

regulates the transcriptional activity of HY5. Mutation of HY5 was found to prevent transcriptional activation of some UV-B induced genes, several of which are associated with UV-B tolerance. in addition, *hy5* null mutants have reduced UV-B tolerance, suggesting that UVR8 is involved in regulating UV-B tolerance by promoting HY5 transcriptional activation of UV-B tolerance genes (Oravecz et al., 2006). UVR8 is also involved in various other UV-B induced developmental changes such as hypocotyl growth, leaf morphogenesis, stomata differentiation and cotyledon expansion (Heijde and Ulm, 2012).

1.6 Phytochrome interacting factors

PIFs are bHLH transcription factors that are involved in phytochrome signalling. Over 150 bHLH transcription factors have been identified in *Arabidopsis* (Bailey et al., 2003, Toledo-Ortiz et al., 2003), and the PIFs all belong to one evolutionary subclass of bHLH transcription factors that contain an active phytochrome binding (APB) domain, enabling them to interact with phytochrome B. In *Arabidopsis* this group includes PIF1, PIF3, PIF4, PIF5, PIF6, PIF7 and PIF8 (Khanna et al., 2004). Rice contains six PIF-like bHLH proteins, designated as OsPIL11-16 that contain similar motifs to the *Arabidopsis* PIFs, including an APB domain (**Figure 1.15**) (Nakamura et al., 2007b). As PIF proteins are present in both monocot and dicot plants it suggests that they play an important role in shaping development and signalling in a wide range of plant species.

Table 1.2 shows all the PIFs in *Arabidopsis*, rice and maize.

Table 1.2 Phytochrome interacting factors (PIFs) and PIF-like (PIL) proteins in *Arabidopsis*, Rice, and Maize.

PIF/PIL	Gene number	Publications	Species
PIF1 (PIL5)	AT2G20180.2	Huq et al. (2004b)	*Arabidopsis*
PIF3	AT1G09530.1	Ni et al. (1998)	*Arabidopsis*
PIF4	AT2G43010.1	Huq and Quail (2002a), Huq et al. (2004a)	*Arabidopsis*
PIF5 (PIL6)	AT3G59060.2	Khanna et al. (2004)	*Arabidopsis*
PIF6 (PIL2)	AT3G62090.2	Khanna et al. (2004)	*Arabidopsis*
PIF7	AT5G61270.1	Leivar et al. (2009)	*Arabidopsis*
PIL1	AT2G46970.1	Salter et al. (2003)	*Arabidopsis*
OsPIL11	Os12g0610200	Li et al. (2012a), Nakamura et al. (2007a)	Rice
OsPIL12	Os03g0639300 LOC_Os03g43810.1	Nakamura et al. (2007a)	Rice
OsPIL1 (OsPIL13)	Os03g0782500 LOC_Os03g56950.2	Nakamura et al. (2007a), Todaka et al. (2012)	Rice
OsPIL14	Os07g0143200 LOC_Os07g05010.1	Nakamura et al. (2007a)	Rice
OsPIL15	Os01g0286100	Nakamura et al. (2007a) , Zhou et al. (2014b)	Rice
OsPIL16	Os05g0139100 LOC_Os05g04740.1	Nakamura et al. (2007a)	Rice
ZmPIF3.1	GRMZM2G387528	Kumar et al. (2016)	Maize
ZmPIF3.2	GRMZM2G115960	Kumar et al. (2016)	Maize

1.6.1 Identification of the PIF family in *Arabidopsis*

The first PIF to be identified was PIF3, which was discovered in a yeast two-hybrid screen for proteins that bound to the C-terminal of phyB. Further yeast two-hybrid experiments demonstrated that PIF3 was also able to bind the C terminals of AtPpyA and OsphyB, and the N terminal of *At*phyB. This suggested that PIF3 is capable of interacting with both the N and C termini of phytochromes (Ni et al., 1998). PIF4 was identified from *short under red light* (*srl2*) mutants, in which the *SRL2* gene, involved in response to red light, was found to encode the PIF4 protein. Sequence examination revealed that the PIF4 protein sequence had homology to the bHLH superfamily and contained two NLS sequences, one of which was very similar to the NLS found in PIF3. The *slr2* mutant produces a truncated version of PIF4 that does not contain the bHLH domain and cannot bind its DNA target site, producing the short mutant phenotype (Huq and Quail, 2002a). PIF5 and PIF6 were identified by Khanna et al., (2004) in a screen for proteins that interacted specifically with the Pfr form of phyB. PIF1 was first characterised by Huq et al. (2004a) who demonstrated that it negatively regulates chlorophyll biosynthesis and interacts with both phyA and phyB (Huq et al., 2004). Investigation into the role of PIFs in plant growth and development has demonstrated that they have numerous roles in modulating the response of plants to light, via an interaction with phytochrome.

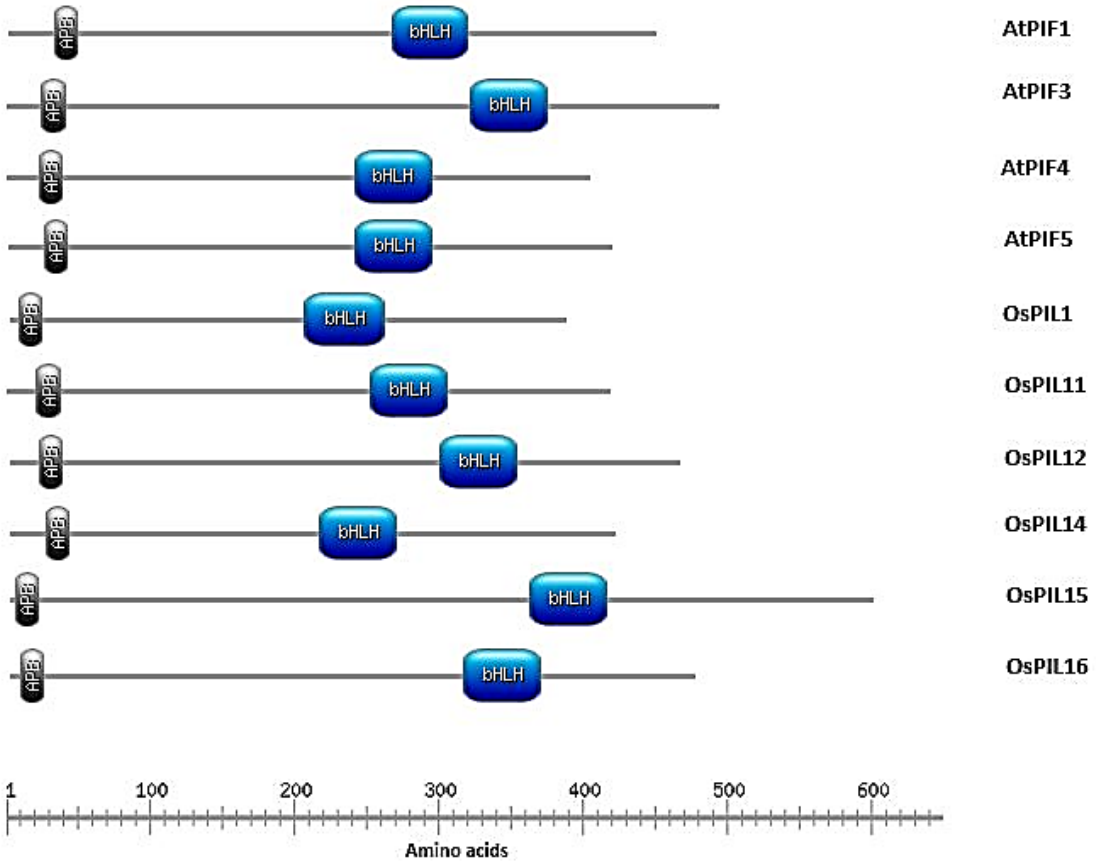

Figure 1.15 Domain positions in phytochrome-interacting factor (PIF) proteins from Arabidopsis and rice. The positions of the basic helix-loop helix (bHLH) and active phytochrome binding (APB) domains are shown in a schematic diagram is blue and grey respectively.

1.6.2 The role of PIFs in light signalling

PIFs are involved in responses to a variety of different light wavelengths and cause a wide range of phenotypic effects. In *Arabidopsis,* PIFs largely play a negative role in phytochrome-mediated signalling in response to red light. This is exemplified by the phenotypes of single or multiple *pif* mutants, which generally display exaggerated photomorphogenic phenotypes characteristic of light-grown seedlings, in the dark. The roles of the various *Arabidopsis* PIFs are much better characterised than in any other species and in many cases individual functions have been assigned (Jeong and Choi, 2013).

PIF3 has been shown to be involved in photo-responsiveness in response to R light. Antisense *PIF3* lines had a significantly reduced response to R and FR light, demonstrating that PIF3 has a role in the regulation of photo-responses to changes in the R:FR ratio (Ni et al., 1998). PIF3 also represses chloroplast development (Stephenson et al., 2009) a process which is promoted by Arabidopsis DELLAS (Cheminant et al., 2011). PIF4 was also shown to be sensitive to red light.

The *pif4* mutants were hypersensitive to a wide range of red light fluence rates, suggesting that PIF4 must act to negatively control the plant response to red light (Huq & Quail, 2002). Both PIF4 and PIF5 are involved in the regulation of red light induced anthocyanin accumulation in Arabidopsis (Liu et al., 2015). Red light was found to induce anthocyanin accumulation in wild-type Arabidopsis, while this response was enhanced in *pif4* and *pif5* mutants and impaired in PIF4 and PIF5 overexpression lines. The transcript levels of several anthocyanin biosynthesis genes was enhanced in *pif4* and *pif5* mutants, which PIF4 and PIF5 were shown to repress the expression of. PIF4 and PIF5 therefore act as repressors of anthocyanin accumulation in red light via the repression of anthocyanin biosynthesis genes (Liu et al., 2015). PIF4 and PIF5 promote the expression of *ETHYLENE INSENTITIVE 3 (EIN3)* which is a transcription factor involved in promoting ethylene induced senescence, and two ABA induced promoters of senescence; *ABA INSENSITIVE 5 (ABI5)* and *ENHANCED EM LEVEL (EEL)*. PIF4, PIF5, EIN3, ABI5 and EEL then activate the expression of the major senescence-promoting NAC transcription factor ORESARA1 (Sakuraba et al., 2014). Senescence is another developmental response which requires PIF4 and PIF5 (Sakuraba et al., 2014).

The high temperature response is regulated by PIF4. The expression of two homologous genes; LONGIFOLIA1 (LNG1) and LONGIFOLIA2 (LNG2) is promoted by PIF4, and Chromatin immunoprecipitation (ChIP) experiments demonstrated a direct interaction between the promoter sequences and PIF4. LNG1 and LGN1 are activated in response to high temperature, and this response is impaired in pif4 mutants, demonstrating the role of PIF4 in this process (Hwang et al., 2017). PIF4 has also been shown to promote flowering in response to high temperature (Kumar et al., 2012), ChIP demonstrated that PIF4 could bind the transcriptional start site of FT to promote expression, and that this binding was temperature dependent (Kumar et al., 2012). PIF4 also regulates the stomatal index in response to phytochrome B signalling (Casson et al., 2009)

A quadruple *pif* mutant, *pif1pif3pif4pif5* (*pifQ*), displays a constitutive photomorphogenic phenotype, including short hypocotyls, open cotyledons and disrupted gravitropism when grown in the dark. In addition, microarray analysis showed that gene expression is similar in the *pifQ* dark-grown mutant, and light-grownwild-type plants (Shin et al., 2009). This demonstrates that these four PIFs are involved in negative regulation of photomorphogenesis in the dark. The plant response to light is allowed by the elimination of PIFs that promote the expression of genes involved in skotomorphogenesis or the repression of genes that promote photomorphogenesis (Leivar et al., 2009).

PIF4 and PIF5 have also been shown to respond to blue light (Kunihiro et al., 2010). Both *pif4* and *pif5* mutants have shorter hypocotyls than wild-type plants under blue light, although there is no alteration in the transcription profiles or the protein levels of PIF4 or PIF5 under blue light, demonstrating that the phenotypic effect is not due to reduced transcription or degradation of PIF4 or 5 under blue light. However, blue light did cause a decrease in the intracellular levels of bioactive GA. The *pif4* and *pif5* mutants were insensitive to external GA application, suggesting that the mutant phenotype is due to an inability of *pif4/5* mutants to respond to blue light-mediated reduction of GA levels. These results indicate that the blue light receptor CRY1 regulates hypocotyl elongation in seedlings by modulating the intracellular GA levels, which then affects the activity of PIF4 and PIF5 (Kunihiro et al., 2010). There are also proteins homologous to PIFs which cannot interact with phytochrome. SPATULA (SPT) is a non-phytochrome binding PIF3 homologue, which is involved in regulating seed dormancy in response to light and temperature through the regulation of GA production (Penfield et al., 2005). The non-phytochrome binding SPT can participate in phytochrome signalling by dimerizing with other members of the PIF family (Toledo-Ortiz et al., 2003). SPT is regulated post-transcriptionally by the DELLA protein GAI which promotes the degradation of SPT mRNA. This provides a mechanism by which an increase in GA levels can promote light signalling by relieving the DELLA mediated repression of SPT (Josse et al., 2011)

1.6.3 Action of PIFs as transcription factors

Both PIF3 and PIF4 contain NLSs and have been shown to localise to the nucleus of cells, consistent with their role in cellular signalling within the nucleus. In addition, PIF1, PIF3, PIF4 and PIF7 can bind to G-box DNA motifs as homodimeric complexes. This homodimeric binding is characteristic of bHLH proteins, and allows the PIFs to alter the transcription of these genes (Huq and Quail, 2002a, Ni et al., 1998, Huq et al., 2004a, Leivar et al., 2008b). However, G box-bound PIF3 is able to interact with phyB (Martinez-Garcia et al., 2000), whereas PIF4 bound to G box motifs is not, demonstrating differences in PIF4 and PIF3 control of gene expression (Huq and Quail, 2002a).

1.6.4 Interaction between phytochrome and PIFs

The largely negative action of PIFs on photomorphogenesis is alleviated by phytochrome in two ways: firstly phytochrome promotes the phosphorylation and subsequent degradation of PIFs by the proteasome, and secondly, phytochrome has been shown to bind PIFs and prevent their interaction with the G-box of promoters (Jeong and Choi, 2013).

phyB has been shown to specifically bind PIF3 upon its conversion from Pr to its active Pfr form. phyA is also able to selectively and reversibly bind to PIF3 after it is converted into Pfr, although its affinity for PIF3 is around 10 times lower than that of phyB (Zhu et al., 2000). PIF4, PIF5 and PIF6 were also shown to have binding affinity for phyB (Casson et al., 2009, Khanna et al., 2004). A sequence motif termed the ACTIVE PHYTOCHROME BINDING (APB) domain was identified in the N terminus of all phy-interacting bHLH proteins including PIFs 3-6. Mutation of the APB domain renders the transcription factor unable to interact with phyB, demonstrating the importance of this domain. The expression of APB-containing PIF4 constructs in a *pif4* null mutant rescued the phenotype, whereas the expression of a PIF4 construct with specific mutations in its APB was unable to rescue the *pif4* mutant phenotype, indicating that this domain is essential for PIF4 function (Khanna et al., 2004). The APB sequence in rice and *Arabidopsis* is shown in **Figure 1.16**.

In support of the APB being essential for PIF4 function, phyB activity was also shown to be necessary for correct PIF4 signalling. Double *pif4phyB* and *pif4phyA* mutants were produced. The *pif4phyA* double mutant displayed no difference to the hypersensitive in red light phenotype of the *pif4* mutant, demonstrating that PhyA has a minimal role in this process (Huq and Quail, 2002a). However, *pif4phyB* double mutants had a phenotype that resembled the *phyB* single mutant, indicating that PIF4 and phyB act in the same signalling pathway. Similarly to PIF3, PIF4 was shown to have weak interaction with phyA, but to preferentially bind to PHYB. PIF4 had no detectable interaction with phyC, phyD or phyE (Huq and Quail, 2002a).

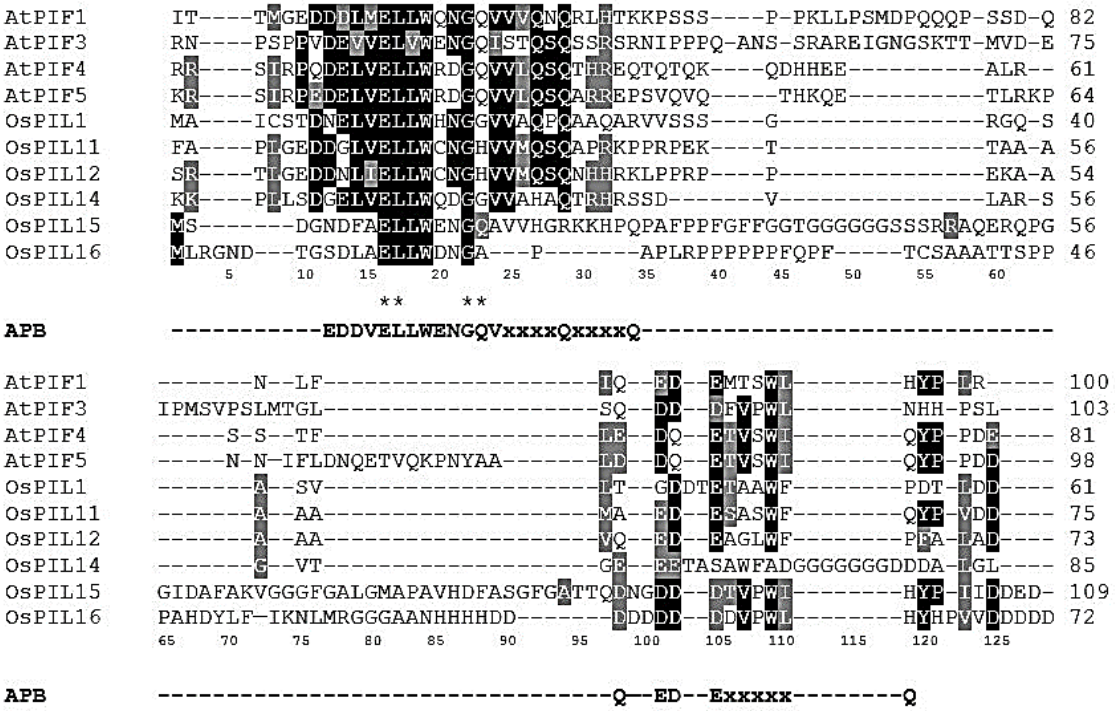

Figure 1.16 The APB domain of PIF/PILs in *Arabidopsis* and rice

The APB domains of AtPIF1-5 and the rice OsPILs are aligned. Similar residues are marked in a grey box, and identical residues are shown in reverse. The APB consensus sequence is shown in bold below the alignment, with residues essential for APB binding marked with an asterisk ((Khanna et al., 2004)). Of these essential residues, the E16, L17 and G22are conserved between *Arabidopsis* and rice. The essential Q23 residue is present in all *Arabidopsis* sequences, but only in the OsPIL15 sequence from rice.

1.6.4.1 Phytochrome-mediated PIF degradation

One method by which phytochrome represses the activity of PIF proteins is to promote their degradation by the proteasome. PIF3 has been shown to be degraded after its interaction with phyA or phyB. Park et al. (2004) found that PIF3 was rapidly degraded after transfer of *Arabidopsis* from red to far red light, and that active phyB was required for this degradation to occur, suggesting that phyB binding of PIF3 triggers this degradation. Additionally, when plants were treated with proteasome inhibitors, the degradation of PIF3 was no longer observed, indicating that the proteasome is responsible for PIF3 degradation (Bauer et al., 2004, Leivar et al., 2008a, Park et al., 2004). PIF3 was found to be phosphorylated before its degradation by the proteasome, with phyA and phyB being redundantly required for this process (Al-Sady et al., 2006).

PIF5 is also degraded during light signalling. Exposure to continuous red light causes a rapid reduction in endogenous PIF5 levels, preceded by phosphorylation, showing that PIF5 turnover works in a similar way to PIF3 (Shen et al., 2007). Mutation of phyA, B and D demonstrated their role in this process. Double *phyAphyB* mutants had a marked decrease in PIF5 degradation, although there was still a small amount occurring. The *phyAphyBphyD* triple mutant had no detectable levels of PIF5 degradation, indicating that phytochromes act redundantly to promote PIF5 degradation, but that phyA and phyB are the most important. These data demonstrate that PIF5 signalling involves rapid phosphorylation and degradation after interaction with phyA, phyB and phyD, in a process very similar to that of PIF3 (Shen et al., 2007).

Ni et al. (2013), used mass spectrometry to identify multiple serine and threonine phosphorylation sites in PIF3. Missense point mutations were introduced to these sites, using site directed mutagenesis, which demonstrated that these sites were necessary for phosphorylation and degradation in response to red light, and allowed a pattern of phosphorylation sites to be identified (Ni et al., 2013).Phosphorylation at these sites was found to induce the recruitment of a light response Bric-a-brack/Tramtrack/Broad (LRB) E3 ubiquitin ligase to the PIF3-phyB complex, and promote PIF3 degradation by the proteasome. An immunoprecipitation assay showed that PIF3 and LRB interact more in red light than in the dark. Furthermore, mutation of the phosphorylation sites in PIF3 abolished LRB binding, demonstrating that LRB interacts with phosphorylated PIF3 in response to red light. There is also evidence for an interaction between LRB and PHYB. Pull-down assays showed co-immunoprecipitation of PIF3 and phyB when LRB was used as bait. phyB alone also shows some affinity for LRB, but this interaction is enhanced by the presence of PIF3 (Ni et al., 2014). The identification of LRB as a component of the machinery responsible for degradation of PIF3, suggests the following pathway: Light activated phyB induces multisite phosphorylation of PIF3, which enhances the binding of LRB to PIF3. This then binds CUL3 and forms an active E3 ligase complex which ubiquitinates PIF3 and phyB, which are subsequently degraded by the 26S proteasome (Ni et al., 2014). Ni et al. (2017) demonstrate another group of protein kinase which appear to promote PIF3 degradation in response to PhyB. Photo-regulatory Protein Kinases (PPK1–4) were shown to interact with PIF3 and phyB in a light-induced manner in vivo, and were shown to be essential for normal light-induced phosphorylation and degradation of PIF3. These data indicate that PKKS promote degradation of PIFs in response to photoactivated phyB (Ni et al., 2017). In contrast Shin et al. (2016) identified that PhyA can act as a protein kinase to promote PIF degradation in *Avena sativa* (oat). The photosensory core region of AsPhyA was shown to be essential for the kinase activity, and transgenic plants expressing

mutant versions of AsphyA lacking the photosensory domain displayed a significant reduction in PIF3 phosphorylation and degradation. These results suggest that phytochrome is capable of acting as a protein kinase that directly promotes the degradation of PIFs (Shin et al., 2016). It is therefore unclear if phytochromes directly phosphorylate PIFs, or if phytochrome promotes the phosphorylation and degradation of PIFs through third-party kinases. The findings of Kim et al. (2016) support the hypothesis that phytochromes promote the degradation of PIFs though downstream kinase proteins. In this study, epidermal phyB was able to promote the degradation of spatially separated PIF in the endodermis, indicating that downstream kinases must be involved. It is possible that both these models act concurrently in the plant, whereby phyB promotes PIF degradation though both direct phosphorylation and the activation of downstream protein kinases.

There is also evidence of PIFs promoting the degradation of phytochrome. Jang et al. (2010) found that phyB is degraded in the nucleus after its N terminal interacts with COP1, and is subsequently ubiquitinated and degraded by the proteasome. This ubiquitination and degradation of phyB can be enhanced in vitro by the presence of PIFs including PIF3, PIF4 and PIF5. Additionally, phyB accumulated to higher levels within the nucleus in *pif* single and double mutants, as well as in *cop1* mutants. This demonstrates that PIFs are able to negatively regulate phyB levels via the COP1 E3 ligase (Jang et al., 2010). These results demonstrate that all PIFs are regulated by phytochrome-mediated degradation that prevents their transcriptional activation of genes involved in skotomorphogenesis.

1.6.4.2 Sequestration of PIFs by phytochrome

Along with degradation, phytochrome represses PIF activity via sequestration. The interaction between phyB and PIF1/PIF3 has been shown to prevent the transcriptional activity of PIFs by releasing them from G-box promoter regions. Park et al. (2012) demonstrated an N terminal fragment of phyB was not able to promote PIF1 and 3 degradation but could block binding of PIFs to DNA in ChIP analysis. Furthermore, the Pfr forms of full length and N terminal phyB could inhibit the binding of PIFs to DNA in vitro. These data suggest that phytochrome binding of PIFs via the APB domain inhibits their DNA binding ability via the bHLH domain and then promotes their degradation by the proteasome, to release their repression of photomorphogenesis.

1.6.5 Identification of PIF-like proteins in rice and other cereals

Nakamura et al. (2007b) identified and characterised a set of bHLH proteins orthologous to the PIFs in *Arabidopsis*. These rice PIFs were termed rice PIF-like 11-16 (OsPIL11-16). A neighbour joining tree was produced with the bHLH domains of the rice PILs and *Arabidopsis* PIFs 1,3,4,5 and 7. This tree suggested that OsPIL15 and OsPIL16 were orthologous to AtPIF3 and that OsPIL13 and OsPIL14 were orthologous to AtPIF4/PIF5. OsPIL11 and OsPIL12 were found to cluster separately (Nakamura et al., 2007b).

All the OsPILs were assessed for their reaction to light exposure. *OsPIL13* was found to have low expression levels in dark-grown seedlings, and increased levels after exposure to light, suggesting positive regulation in response to light. Conversely, *OsPIL15* had high expression levels in dark-grown seedlings, which rapidly decreased after exposure to light, suggesting that *OsPIL15* is negatively regulated by light. *OsPIL14* levels did not appear to fluctuate in response to light conditions. Overexpression of all OsPILs in *Arabidopsis* caused a long hypocotyl phenotype in early development, demonstrating functional homology to the *Arabidopsis* PIFs (Nakamura et al., 2007b). OsPIL15 was investigated further by Zhou et al. (2014a) who demonstrated that OsPIL15 localised to the nucleus of rice protoplasts, as expected for a bHLH transcription factor. Overexpression of OsPIL15 gave plants in which aerial tissues were shorter in the dark, and with an undeveloped root system. Red light exposure of overexpression lines relieved the growth defects and promoted seedling elongation, suggesting that OsPIL15 represses seedling growth in the dark and is regulated by R/FR light (Zhou et al., 2014a).

Li et al. (2012b) characterised OsPIL11 further. Expression patterns of OsPIL11 were analysed in different organs of transgenic tobacco. OsPIL11 had organ specific expression. In leaves, expression was regulated by leaf development, with mRNA levels accumulating to higher levels in developing leaves than old leaves. However, it is unclear how many conclusions can be drawn from expression patterns in another species. OsPIL11 expression was also under the regulation of some plant hormones including JA, SA and ABA (Li et al., 2012b).

OsPIL13 was investigated by Todaka et al. (2012) under the name OsPIL1. Promoter-GUS analyses were performed to determine the histological localisation of OsPIL1. GUS signal was detected in the leaves, the basal area of the shoots and in the nodal regions during the early heading stage. mRNA levels similarly showed localisation to the nodal regions. GFP-tagged OsPIL1 clearly localised to the nucleus in cells at the basal part of the shoot (Todaka et al., 2012).Overexpression and repression lines of OsPIL1 were produced to investigate its

phenotypic effects. OsPIL1-OX lines had an increase in plant height, whereas OsPIL1-RD lines had a decrease in height, suggesting that OsPIL1 is involved in the control of plant height. At adult stages, these alterations in plant height were exaggerated even further. In both the overexpression and repression lines, the alteration in plant height was due to changes in internode elongation. Transgenic *Arabidopsis* either carrying the over-expression or repression OsPIL1 constructs were shown to have the same alterations in plant height, further verifying OsPIL1s role in controlling plant height (Todaka et al., 2012).To test OsPIL1s transactivation activity, a GUS reporter construct was assembled using a promoter of a downstream gene of OsPIL1 with and without its G-box domain. When the G box domain was present OsPIL1 caused an increase in GUS activity and when the G box was removed, GUS activity was reduced, suggesting that OsPIL1 has transactivation activity and acts in the same way as the *Arabidopsis* PIF proteins (Todaka et al., 2012). OsPIL1 has also been shown to promote chlorophyll biosynthesis (Sakuraba et al., 2017a) and negatively regulate senescence in rice (Sakuraba et al., 2017b).

A PIF3 orthologue has also been identified in maize. The *ZmPIF3* gene was found to be expressed strongly in leaves, and its expression responds to drought stress (induced by polyET glycol), NaCl stress and ABA application, suggesting a role in stress responses (Gao et al., 2015). Transgenic rice plants constitutively expressing ZmPIF3 showed no defect in growth and development under normal conditions although no analysis was done under differing light conditions. However, the transgenic plants did display more tolerance to dehydration and salt stresses than the wild-type plants, which was supported by the finding that ZmPIF3 increased the expression of stress responsive genes (Gao et al., 2015). These results suggest that PIFs could also play a role in stress tolerance as well as response to light conditions.

1.7 DELLAs repress the activity of PIFs

An interaction between DELLAs and PIFs has been characterised in *Arabidopsis* whereby DELLAs bind to and sequester PIF3 and PIF4 repressing their transcriptional promotion and repression of skotomorphogenesis and photomorphogenesis, respectively. In this model PIFs comprise a family of transcription factors that DELLAs target to regulate the GA response (Feng et al., 2008, de Lucas et al., 2008).

ChIP experiments showed that there was no specific binding of the five *Arabidopsis* DELLA proteins to 38 GA-responsive gene promoters (Feng et al., 2008).This suggested that DELLA proteins might instead bind to others factors that then directly bind the DNA and alter

transcription. As light and GA act antagonistically to regulate hypocotyl elongation, PIFs were good candidates for DELLA protein targets. PIF3 was specifically identified as a putative DELLA-interacting transcription factor due to its antagonistic role in promoting hypocotyl elongation in red light and its DNA binding ability. PIF3 overexpression was shown to cause increased hypocotyl elongation, implying that DELLA proteins may be involved in negative regulation of PIF3 action on hypocotyl elongation (Feng et al., 2008). PIF4 was also identified as a DELLA interactor (de Lucas et al., 2008).

Yeast two-hybrid experiments demonstrated that PIF3 can bind all five *Arabidopsis* DELLA proteins, and pull down assays indicated that both PIF3 and PIF4 could bind RGA. In addition, BiFC showed direct binding between RGA and PIF3 or PIF4 in the nuclei of plant cells. Immunoprecipitation experiments indicated that the interaction between RGA and PIF3 was able to take place in dark-grown and red-light exposed seedlings. Co-immunoprecipitation suggested that the binding of RGA to PIF3 and 4 was affected by intracellular GA levels. When RGA concentrations fall after GA application, PIF3 and PIF4 are released, whereas cells treated with PAC have increased RGA abundance causing a greater amount of PIF3 and PIF4 to be sequestered. Phytochrome had no effect on the DELLA-PIF interaction and vice versa, suggesting that DELLA-PIF binding is more likely to affect the transcriptional activity of PIF rather than its stability (de Lucas et al., 2008, Feng et al., 2008).

ChIP experiments demonstrated that PIF3 and PIF4 bind to G box DNA motifs via their bHLH DNA binding domains. Deletion studies revealed that the bHLH domain of PIF3 and PIF4 was required for the interaction between PIF4 and RGA, and that the conserved heptad leucine repeat in the RGA sequence was also necessary to allow PIF4-RGA binding. PAC-induced increases in RGA levels caused a significant reduction in PIF3 and PIF4 promoter binding, and when DELLA levels were lowered by GA treatment, PIF3/PIF4-promoter binding was increased. This demonstrates that DELLA proteins can sequester PIF3 and PIF4 by binding to its DNA binding domain which prevents it from binding its G-box promoter sites (de Lucas et al., 2008, Feng et al., 2008).

PIFs can be integrated into the GA signalling pathway as follows: GA binds GID1, GA-charged GID1 interacts with DELLA proteins and recruits a DELLA specific F box protein which targets them for proteasomal degradation. Once the DELLA protein has been degraded the PIF protein is free to bind the G-box of PIF-regulated promoters and promote or repress transcription. If no GA is present DELLA proteins accumulate and bind PIFs via their DNA binding domain,

which prevents PIFs from interacting with target promoters and therefore altering transcription (**Figure 1.17**).

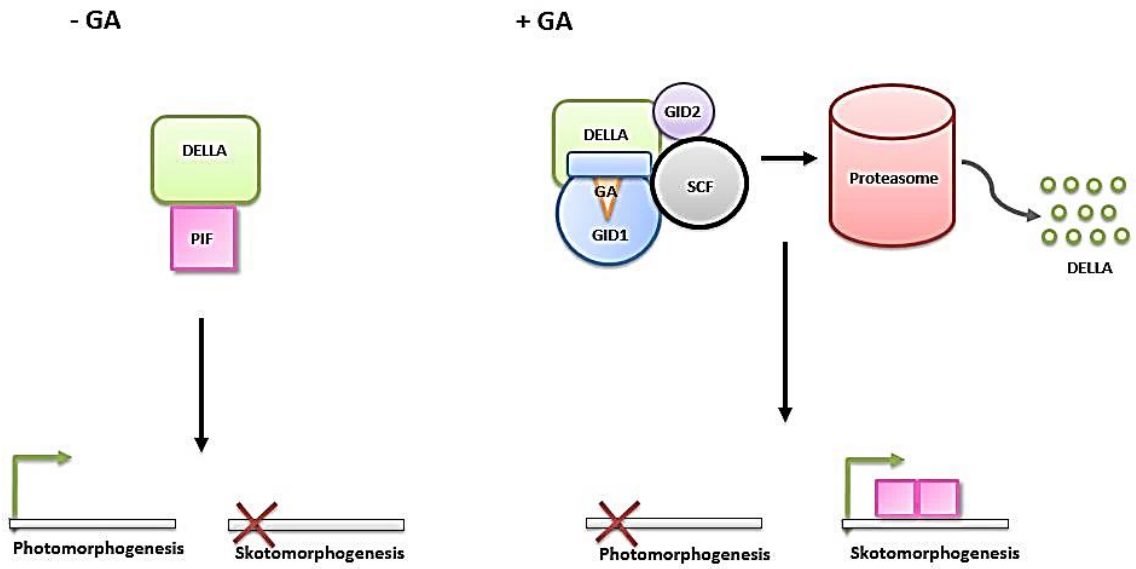

Figure 1.17 The interaction of DELLAs and PIFs in the regulation of gene expression

When GA is absent, DELLAs bind to PIFs via their bHLH domain and sequester them, preventing them from binding to the G-box of promoters to drive the expression of skotomorphogenesis-related genes. When GA is present, DELLAs are degraded, leaving PIFs free to bind promoters and regulate transcription to promote skotomorphogenic growth.

1.8 Overview of project aims

The increases in yield resulting from the *Rht* semi-dwarf lines were instrumental to increasing yields over the past 50 years. However, *RHT-1* mutations also cause pleiotropic affects such as reduced grain size (Flintham et al., 1997a), reduced seedling vigour (Ellis et al., 2004), fertility defects (Alghabari et al., 2014) and reduced root growth (Coelho et al., 2013), which are detrimental to yield. Considering the future challenges to food security, this research aims to identify an alternative target, downstream of RHT-1 in GA signalling, for specifically regulating stem elongation, while avoiding these adverse side effects. The identification of PIFs as downstream targets of DELLAs highlighted their potential for possible intervention to manipulate stem elongation. In addition, the identification of the PIF-like protein OsPIL1 as a regulator of stem elongation in rice make PIF-like proteins in wheat a promising target for precise regulation of stem elongation. At present, the PIF family of proteins have not been identified in wheat, and the interaction between DELLAs and PIFs has not been demonstrated in any cereals. There is also no research on how the PIFs regulate stem elongation and plant

architecture in wheat. The interaction with DELLA indicates that PIFs may act in the GA response pathway to regulate stem elongation. This hypothesis will be investigated in wheat.

The first aim of this research is to identify *PIF-like* genes in wheat that could be potential targets for regulating stem elongation. This will be carried out by using *OsPIL1* to identify homologous sequences in wheat by searching the available wheat sequence databases. Any sequences identified from this search will then be analysed for sequence homology to known PIF proteins to identify PIF domains. The sequences of any wheat PILs identified will then be isolated for use in yeast two-hybrid experiments and transgenic lines.

The second aim of this research is to investigate if an interaction between PIL proteins and DELLAs occurs in wheat. To determine if this interaction occurs, a yeast two-hybrid screen will be employed, with RHT-1 and all wheat PIL sequences identified.

The third aim of this project is to identify additional proteins which interact with RHT-1 in the wheat stem. This could provide alternative targets for manipulating stem elongation which act downstream of RHT-1. A yeast two-hybrid library will be used with RHT-1 as the bait, to screen a library of clones containing cDNAs from the wheat stem. Any cDNAs of interest will have their interaction with RHT-1 confirmed, and have their likely function in wheat investigated by identifying orthologous sequences in other species.

The fourth aim of this research is to investigate the effect on phenotype of altering the expression of wheat PIL sequences. The expression of wheat PIL sequences will be reduced by producing RNAi lines and increased using overexpression lines. Mutagenized TILLING lines will also be used to determine the effect of knockout on phenotype. In particular, any effect on stem elongation will be investigated, as this would provide a means to improve wheat yields though the specific manipulation of stem elongation.

Chapter 2: Plant materials and growth conditions

Triticum aestivum cv. Cadenza plants were grown in individual 15-cm pots using Rothamsted prescription mix compost (75% peat, 12% sterilised loam, 3% vermiculite, 10% grit) in standard glasshouse and controlled environment (CE) growth conditions. Plants in the standard glasshouse growth conditions were 18 – 20°C during the day and 14 – 15°C during the night with a 16-h photoperiod provided by natural light supplemented with banks of Son.T 400 W sodium lamps giving 400-1000 µmol.m^{-2}.s^{-1} PAR total light. CE growth conditions were 20 °C during the day and 15 °C during the night with a 16-h photoperiod provided by tungsten fluorescent lamps providing 500 µmol$m^{-2}s^{-1}$ PAR.

2.1 Screening EMS mutagenized lines and wheat crossing

Mutant *Triticum aestivum* lines for *TaPIL1* and *TaPIL3* were identified through the wheat TILLING website (www.wheat-tilling.com) (Krasileva et al., 2017). These lines contain multiple single nucleotide polymorphisms (SNPs) due to ethyl methanesulfonate (EMS) mutagenesis, and have had their exomes sequenced and mapped to the IWGSC reference sequences to catalogue the mutations. For *TaPIL1* and *TaPIL3*, TILLING lines were selected with premature stop codons or disruption of slice sites. Combinational mutants were produced by manual pollen transfer between flowers on separate plants, both *TaPIL1* and *TaPIL3* TILLING lines went through two crossing cycles. Firstly, the A and D mutant lines were crossed to produce double mutants. The double mutants were then crossed with the B homoeologue mutants, to produce heterozygous triple mutant (AaBbDd) lines. The *TaPIL3* B homoeologue mutant lines underwent a further crossing cycle with wild-type Cadenza, due to an early flowering phenotype associated with the mutation. In general, the success rate per cross was around 10-15 grains per ear. The heterozygous triple mutant lines were then selfed to produce homozygous triple mutant lines.

Buds from the female donor plant were emasculated (**Figure 2.1A**) prior to flower opening and pollen release to prevent self-fertilisation. The glumes of the ear where cut back, as shown in **Figure 2.1B**. The resulting ear was then left for 2-3 days to mature. The emasculated bud was then pollinated with a flowering ear from a separate male donor plant (**Figure 2.1C**). Grain from successful crosses (**Figure 2.1D**) was then harvested. Double and triple mutants were identified in subsequent generations using genotyping by sequencing (2.5.15).

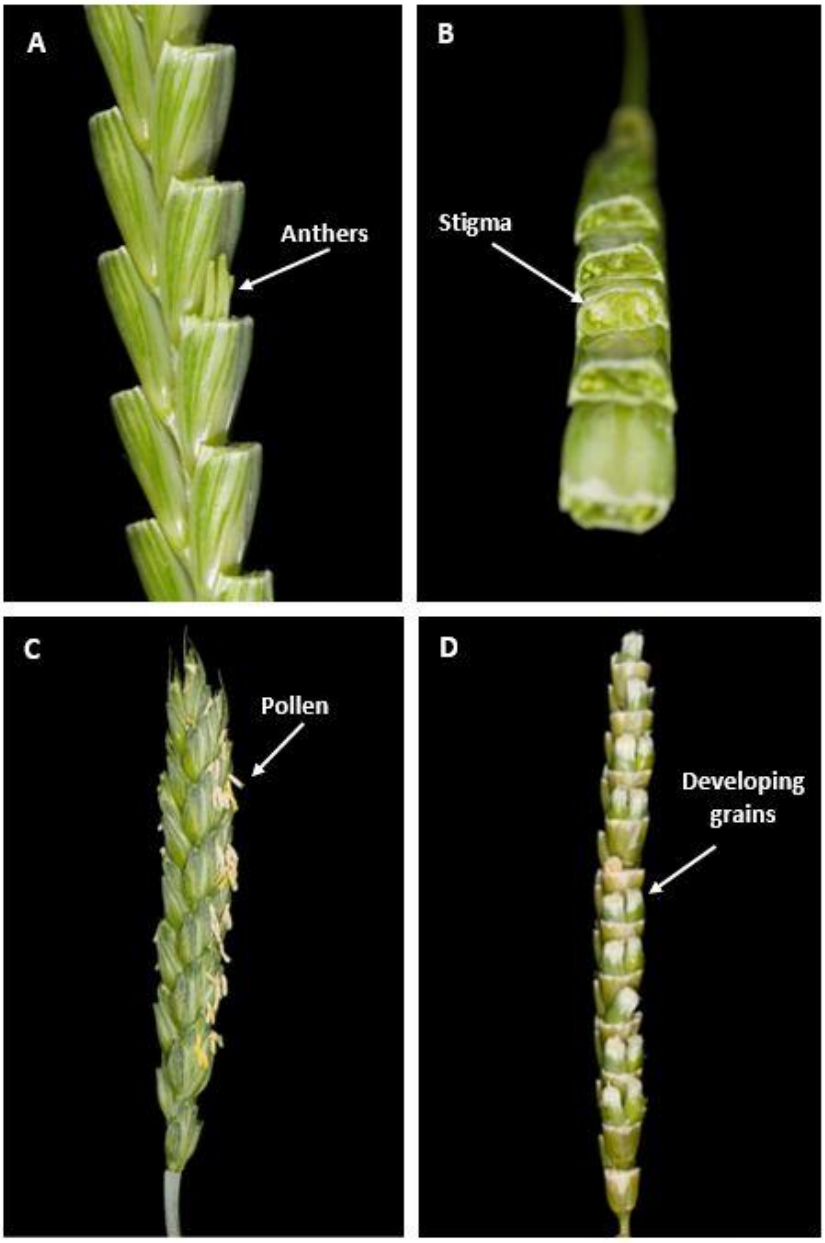

Figure 2.1 Crossing. Panel A shows the three anthers in one wheat floret where the glume has been cut back. Panel B shows a floret where the anthers have been removed leaving only the stigma. Panel C shows a flowering wheat ear which is releasing pollen. Panel D shows grains developing after crossing.

2.2 Generation of transgenic wheat lines

Transgenic *T. aestivum* lines were generated through either Agrobacterium-mediated transformation carried out by NIAB (Cambridge, UK) (Perochon et al., 2015b), or particle bombardment, carried out by the Rothamsted Research Transformation Facility (Harpenden, UK) (Sparks and Jones, 2014). In both cases the variety Cadenza was used.

To generate the *TaPIL1* RNAi line, a section of the *TaPIL1* cDNA was cloned (2.5.7) into *pENTR11.* This construct was then delivered to NIAB where the RNAi trigger sequence was

cloned into the destination RNAi vector, driven by a rice actin promoter, and transformed into Cadenza. T_1 seed produced by NIAB was used for subsequent analysis.

To generate the *TaPIL1* and *OsPIL1* overexpression lines, both cDNA sequences were cloned into the *pRRES14.125* vector, which contains a maize ubiquitin promoter. This vector was then transformed into Cadenza by the Rothamsted Research transformation facility. *TaPIL1* and *OsPIL1* overexpression lines were genotypes at the $_{T1}$ generation to identify homozygous and null lines. *TaPIL1* RNAi lines were genotypes at the T_1 and T_2 generations to identify homozygous and azygous lines.

2.3 Phenotyping experiment

A phenotypic experiment was set up using six *TaPIL1* RNAi lines (3912-1, 3912-4, 3964-3, 3964-8, 4085-3, 4085-6), one *TaPIL1* RNAi azygous line, four *TaPIL1* overexpression lines (C10 and F10) including two azygous (C1 and F11), six *OsPIL1* overexpression lines (A4, C4 and D4) including three azygous (A8, C9 and D9) and a wild-type cadenza control, comprising 18 lines in total. For each line, four individuals were planted, and set up in a four-block system to account for environmental variation within the glasshouse. **Table 2.1** shows a summary of all lines used in the phenotyping experiment. The overexpression and RNAi lines were co-analysed to allow comparisons between the phenotypes of these types of transgenic lines.

Table 2.1 Transgenic lines used in phenotyping experiments.

Transgenic Line	Transformation method
TaPIL1 RNAi 3912-1	Agrobacterium Transformation by NIAB
TaPIL1 RNAi 3912-4	Agrobacterium Transformation by NIAB
TaPIL1 RNAi 3964-3	Agrobacterium Transformation by NIAB
TaPIL1 RNAi 3964-8	Agrobacterium Transformation by NIAB
TaPIL1 RNAi 4085-3	Agrobacterium Transformation by NIAB
TaPIL1 RNAi 4085-6	Agrobacterium Transformation by NIAB
TaPIL1 RNAi azygous	Agrobacterium Transformation by NIAB
TaPIL1 overexpression C10	Particle bombardment by the Rothamsted transformation facility
TaPIL1 overexpression F10	Particle bombardment by the Rothamsted transformation facility
TaPIL1 overexpression azygous C1	Particle bombardment by the Rothamsted transformation facility
TaPIL1 overexpression azygous F11	Particle bombardment by the Rothamsted transformation facility
OsPIL1 overexpression A4	Particle bombardment by the Rothamsted transformation facility
OsPIL1 overexpression C4	Particle bombardment by the Rothamsted transformation facility
OsPIL1 overexpression D4	Particle bombardment by the Rothamsted transformation facility
OsPIL1 overexpression azygous A8	Particle bombardment by the Rothamsted transformation facility
OsPIL1 overexpression azygous C9	Particle bombardment by the Rothamsted transformation facility
OsPIL1 overexpression azygous D9	Particle bombardment by the Rothamsted transformation facility

2.3.1 Phenotype characterisation

Heading was measured as the time point at which the ear first began to emerge from the leaf sheath. Flowering was measured as when the anthers were first visible. Once the plants were fully mature and dried down, the total number of tillers were counted, and the following

length measurements were taken for the three tallest tillers in cm; ear, total stem, internode 1 (peduncle), internode 2, internode 3, internode 4 and internode 5.

2.3.2 Statistical analysis

Measurements from the phenotyping experiments were analysed using a multivariate canonical variates analysis (CVA) (Krzanowski, 2000), and an analysis of variance (ANOVA). The ANOVA allows comparison between lines, whereas the CVA allows a comparison of all lines at the same time. The CVA analysis was carried out as follows; taking the 18 lines as the treatment factor the method works to find linear combinations of the variables that maximises the ratio of the between line variation to the within line variation, thus performing a discrimination between all lines. The fewest number of canonical variates (CVs) are retained that take up the most variation in the data and hence make the most discrimination, subject to the constraint that the maximum possible number of CVs is min (*v*, *g*-1), where *v* is the number of variables and *g* is the number of groups, this minimum being 17 in the present case, as *g* = 18 and *v* = 10. The data are then visualised on the new dimensions, by plotting the canonical variate scores for each sample (i.e. each row of the original data matrix of observations by variables). The mean of canonical variate scores in each dimension, for each genotype, i.e. the canonical variate means, are also plotted. Making the assumption of a multivariate Normal distribution for the data, which, in the present case, is a reasonable assumption for the data on the raw scale, 95% confidence circles can be placed around the canonical variate means for the treatment combinations. It is noted that the radius of these circles is $\sqrt{\chi^2_{2,0.05}} / \sqrt{n}$, where, in the present case, *n* = 4 (the replication) and where $\chi^2_{2,0.05}$ = 5.99, is the upper 5% point of a chi-squared distribution on 2 degrees of freedom. Non-overlapping confidence circles give evidence of significant differences between genotypes at the 5% level of significance. The magnitude of canonical variate loadings (on the variables) can be inspected to see which variables are important in the discrimination in each CV direction, the variables with the large loadings being proposed to be those with most discriminatory power.

The mean for each measurement across the three tillers and the four individuals was calculated and used in an analysis of variance (ANOVA). The ANOVA was applied to individual measurements for all the genotypes together from the experiment, taking into account the variation due to the four blocks and testing (F-tests) the difference between the wild-type Cadenza verses all other lines, the difference between the backgrounds (RNAI, *TaPIL1* overexpression, *OsPIL1* overexpression and Cadenza), the difference between the types (3912, 3964, 4085, null, cadenza, *TaPIL1*-C, *TaPIL1*-F, *OsPIL1*-A, *OsPIL1*-C, *OsPIL1*-D) and the difference

between all individual lines in consecutive order using a nested treatment structure. Particular contrasts of pairs of lines of interest, such a transgenic to its corresponding null, or between two transgenic in the same background were made (F-tests). The standard error of the difference (SED) or the residual degrees of freedom (DF) from the ANOVA were output along with the F-statistics and p-values. The least significant difference (LSD) at the 5% level of significance was used to compare between transgenic and corresponding nulls where there was more than one transgenic for the azygous line. The GenStat statistical package (17th edition, 2014, ©VSN International, Hemel Hempstead, UK) was used for the analysis. No transformation of data was required, plots of residuals were produced showing that there was good conformation to the assumptions of the analysis (normal distribution, additivity of effects and constant variance over the lines).

2.4 Molecular Biology

Unless stated otherwise, all chemicals used in the creation of solutions, buffers, media etc. were purchased from Sigma Aldrich (Sigma-Aldrich Company Ltd., Dorset, U.K.).

2.4.1 DNA extraction

Genomic DNA (gDNA) was extracted from single leaves of individual *T. aestivum* plants using the PVP DNA extraction method. Harvested leaf tissue was lyophilised using the Edwards Mondulyu RV8 Freeze Dryer (Crawley, Sussex, UK). Lyophilised tissue was then homogenised using the 2010 Geno/Grinder® (SPEX SamplePrep, New Jersey, USA), using stainless steel ball-bearings to disrupt tissues. The homogenate was incubated in 600 µl of PVP DNA extraction buffer (see below) at 65°C for 60 minutes. 200µL 5M KAc was then added to the homogenate and then centrifuged at 13,000 rpm for 4 minutes to bring down the cell debris. The supernatant (600 µl) was then mixed with 300 µl chilled isopropanol, incubated at room temperature for 10 minutes and then centrifuged (13,000 rpm, 4 minutes) to pellet the DNA. The pelleted DNA was washed in 1 ml 70% EtOH and re-collected by centrifugation (13,000 rpm, 2 minutes), the supernatant then discarded and the DNA pellet air dried. The gDNA was resuspended in 200 µl 1XTE buffer containing 50 µg/ml RNase A (Melford, UK), and incubated at 50°C for 60 minutes. DNA was quantified and stored at -20°C prior to use.

DNA Extraction Buffer, final concentrations:
100mM Trizma Base (Tris Base)
1M KCl
10mM EDTA pH 8.0
pH adjusted to 9.5 using 1M NaOH
0.18mM PVP-40
34.6mM Sodium bisulphite

1 X TE buffer final concentrations:
10mM Tris-HCl pH7.5
1mM EDTA

2.4.2 RNA extraction

RNA was extracted from Cadenza leaf tissue using the QIAGEN RNAeasy® Plant Mini Kit (Qiagen, Hilden, Germany). Seeds were germinated on 3-mm Whatman filter paper soaked with 2 ml dH2O in 10 mm Petri dishes covered in two layers of aluminium foil. The seeds were cold treated at 5°C for 3 days, and then moved to a growth room at 22°C, 16 hr light, for 5 days. The entire shoot was then harvested into sterile microcentrifuge tubes and immediately frozen in liquid nitrogen. Tissues were homogenised whilst frozen using a 2010 Geno/Grinder® (SPEX SamplePrep, New Jersey, USA) with stainless steel ball-bearings to disrupt tissues. Once homogenized, plant material was stored at -80°C or used immediately.

RNA was extracted from 50-100 mg homogenised tissue using the QIAGEN RNAeasy® Plant Mini Kit (Qiagen, Hilden, Germany) following the supplied protocol. RNA concentration was quantified using a Nanodrop™ ND-1000 spectrophotometer (LabTech International Ltd., U.K.). A 2-µg aliquot of purified RNA per sample was subsequently DNase-treated using the RQ1 RNAse free DNase (Promega, USA). The RNA was first made up t0 16µl, and incubated with 2µl DNsse and 2µl DNsse buffer (final concentration 1x) and incubated at 37°C for 60 minutes. 2µl of DNase stop solution was then added and the reactions were incubated at 65°C for 10 minutes.

2.4.3 cDNA synthesis

DNase-treated RNA (1. 6 µg) was used as a template for cDNA synthesis, using the SuperScript™ III reverse transcription PCR method with oligo(dT) primers, according to the supplied protocol (Invitrogen™ California, USA). The remaining 0.4 µg DNase-treated RNA was used as a negative control for qPCR.

2.4.4 Polymerase Chain Reaction (PCR)

PCR-based techniques were used during this project for genotyping by sequencing from genomic DNA, and for amplification of target DNA sequences from cDNA for the purpose of confirming sequence and cloning. A table of PCR primers are shown in Appendix **Table S.1.**

PCR reactions were carried out using a number of different Taq polymerases; Phusion (Finnzymes - New England Biolabs, Massachusetts, USA), GoTaq (Promega, Wisconsin, USA), Pfu (Promega, Wisconsin, USA), and HotShot (Clent Life Science, Stourbridge, UK). All PCR

reactions were carried out on a BIO-RAD C1000™ Thermal Cycler (California, USA) comprising two 48-well heat blocks and a heated lid. PCR reactions and conditions were as follows:

Phusion Polymerase:

Reagent	**Volume (µl)**	**Concentration**
5x/GC Buffer	4	1x
dNTPs	0.4	200 µM of each
F primer	0.25	0.125 µM
R Primer	0.25	0.125 µM
DMSO (optional)	0.4	3%
$MgCl_2$ (optional)	0.5	2.0 µM
Phusion Polymerase	0.2	0.02U/µl
cDNA	1	30 ng
Sterile Distilled Water	Make up volume to 20 µl	

Initial Denaturation - 98°C for 15 seconds	1 cycle
Denaturation (98°C for 10 seconds), Annealing (X°C for 30 seconds) Extension (72°C for Y seconds)	40 cycles
Final Extension - 72°C for 5 minutes	1 cycle

GoTaq Polymerase:

Reagent	Volume (µl)	Concentration
5X GoTaq Buffer	5	1x
dNTPs	0.5	0.25 mM each
F primer	0.5	0.25 µM
R Primer	0.5	0.25 µM
$MgCl_2$	1.2	1.5 mM
GoTaq Polymerase	0.15	0.5 U
cDNA	1	30 ng
Sterile Distilled Water	Made up to 20 µl	

Initial Denaturation - 98°C for 15 seconds	1 cycle
Denaturation (98°C for 10 seconds), Annealing (X°C for 30 seconds) Extension (72°C for Y seconds)	40 cycles
Final Extension - 72°C for 5 minutes	1 cycle

Pfu Polymerase:

Reagent	Volume (µl)	Concentration
10x Buffer	5	1x
dNTPs	1	200 µM of each
F primer	1.5	0.3 µM
R Primer	1.5	0.3 µM
Pfu Polymerase	0.5	0.025 U/µl
cDNA	1	30ng
Sterile Distilled Water	Up to 50 µl	

Initial Denaturation - 98°C for 15 seconds	1 cycle
Denaturation (98°C for 10 seconds), Annealing (X°C for 30 seconds) Extension (72°C for Y minutes)	35 cycles
Final Extension - 72°C for 5 minutes	1 cycle

HotShot Polymerase:

Reagent	**Volume (µl)**	**Concentration**
2XHotShot Master Mix	10	1X
F primer	4.5	0.25 µM
R Primer	4.5	0.25 µM
cDNA	1	30 ng

Initial Denaturation - 95°C for 5 minutes	1 cycle
Denaturation (95°C for 30 seconds), Annealing (X°C for 30 seconds) Extension (72°C for Y minutes)	35 cycles
Final Extension - 72°C for 5 minutes	1 cycle

Temperature X is determined by the Tm of the primers used and time Y is determined by the length of the PCR product. The extension profiles of the polymerases discussed are:

Phusion	1 kb/minute
GoTaq	1.5 kb/minute
Pfu	0.5 kb/minute
HotShot	1 kb/minute

All primers were synthesised by Eurofins Genomics (Luxembourg).

2.4.4.1 Primer design

PCR primers were designed using the Primer3Plus plugin interface in Geneious (v. 8.1.3, Biomatters Ltd, Auckland, New Zealand). Optimal primer conditions were set to 58 - 60 °C T_m, 30-80% GC content and 18 - 26 bp size. A table of primers used in the project can be found in Appendix **Table S.1**.

2.4.5 Agarose gel electrophoresis

Completed PCR reactions were mixed with 1X Loading Dye containing bromophenol blue and xylene cyanol FF, (Thermo Scientific, Hemel Hempstead, U.K) and run on TBE-buffered (45 nM Tris-borate, 1 mM EDTA, pH 8.3) 1 % agarose-TBE gel matrix (Fisher Scientific, Loughborough, U.K.) containing 0.5 µg/µl Ethidium bromide. A 1 kb or 100bp DNA ladder (Thermo Scientific, Hemel Hempstead, U.K.) was run alongside products for band size estimation. Electrophoresis was usually carried out at 120 mV for 35 minutes. PCR products were visualised by ethidium bromide fluorescence under UV light using the SynGene GelDoc imaging system (Synoptics Ltd, Cambridge, U.K.).

2.4.6 PCR purification

PCR products were purified either from the PCR mix using the QIAquick PCR Purification kit (Qiagen, Hilden, Germany), or from bands extracted from agarose gels (agarose-TBE gel matrix) using the Qiagen Gel Extraction kit. Products were purified according to the protocols given with the retrospective kits. Purified PCR products were quantified using the Nanodrop™ ND-1000 spectrophotometer (LabTech International Ltd., U.K.).

2.4.7 Cloning

Purified PCR products were cloned into either the *pGEM-T-Easy* (Promega Corporation, Wisconsin, U.S.A.) or *pSC-Blunt* (Stratagene, California, U.S.A.) plasmids, depending on if they were produced using a non-proof-reading or proof-reading polymerase, respectively, in each case following the protocol supplied with the kit, including a kit-supplied ligation step. pSC-Blunt ligation reactions were transformed into kit-supplied competent cells following a supplied protocol, whereas pGEM-T Easy ligations were transformed (2.5.9) into *DH5-α* cells. In both cases, successful ligations were selected on the basis of antibiotic resistance.

Cloning into gateway vectors or plasmids for overexpression was carried out by a restriction digest and ligation protocol. All Restriction endonucleases were sourced from New England Biolabs UK (Hitchin, U.K.), Fermentas (Maryland, U.S.A.) or Promega (Wisconsin, U.S.A.), and reactions were carried out using the supplied buffers and following the recommended digest conditions. In all cases, two incompatible restriction sites were used at each cloning step to ensure ligation of DNA fragments in the correct orientation. Restriction digest reactions were typically incubated at 37°C for 2-3 hours. Digested products were separated using a 1% electrophoresis gel (agarose-TBE gel matrix), and extracted by the method detailed in section (2.5.6)

Ligation of digested products was carried out using T4 DNA ligase (Fermentas Inc., Maryland, U.S.A.), using kit-supplied buffer and protocols. Ligation reactions were carried out with a 3:1 molar ratio of insert to vector, and typically 40-50 ng of vector was used. The calculation for the 3:1 ratio is as follows:

((*a* ng vector DNA x *b* kb insert DNA)/ *c* kb of vector DNA) x 3 = ng of insert DNA

Where *a* refers to the chosen ng of vector, and the values for *b* and *c* refer to the specific length in kb of the insert and vector used, respectively. Ligations were transformed (2.5.9) into DH5α ultracompetent cells, with transformants selected on the basis of antibiotic resistance when grown in plates containing 100µg/ml of carbenicillin or 50µg/ml of kanamycin. The success of each cloning step was confirmed using diagnostic digestion (see above) of miniprep DNA (2.5.12).

Cloning from gateway vectors into destination vectors was carried out using the Gateway™ LR Clonase™ II Enzyme Mix (Thermo-fisher Scientific, California, USA), following the supplied protocol. 15µl reactions containing 50-150µg pENTR11 containing the gene of interest, 150µg destination vector (pDEST32/pDEST22), 2µl LR clonase II, and made up to 15 µl with TE buffer. Reactions were incubated at room temperature for >1hour, after which the reaction was terminated by adding 2µl of proteinase K and incubating at 37°C for 10 minutes. Ligations were then transformed into DH5α E. coli as described in section 2.5.9.

2.4.8 Recipes for media

SOC media (1L):
0.5% Yeast Extract
2% Tryptone
10 mM NaCl
2.5 mM KCl
10 mM MgCl2
10 mM MgSO4
20 mM Glucose

2x YT Media (1L):
1.6% Tryptone
1% Yeast extract
25mM NaCl

YPD (1L):
5% YPD
2% agar

SD dropout media (1L): 2.69% SD
2% agar
0.062% -leu/-trp OR 0.064% -leu/trp/-his

Table 2.2 Plasmids using during this project

Plasmid	Selection	Purpose
pSC-b	Carbenicillin, LacZ	Blunt-end PCR cloning
pGEM-T Easy	Carbenicillin	PCR cloning
pEX-K4	Kanamycin	TaPIL2/3 synthesis
pUC57	Carbenicillin	TaPIL1/OsPIL1 synthesis
pENTR11	Kanamycin, chloramphenicol	Gateway vector
pDEST22	Carbenicillin, chloramphenicol	Yeast two-hybrid (prey)
pDEST32	Gentamycin, chloramphenicol	Yeast two-hybrid (bait)
pRRES14.125	Carbenicillin	Overexpression vector

Table 2.3 Bacterial and yeast strains used in this project.

Strain	Species	Genotype	Supplier	Purpose
DH5α	*E. coli*	F– endA1 glnV44 thi1 recA1 relA1 gyrA96 deoR nupG purB20 ϕ80dlacZΔM15 Δ(lacZYA-argF)U169, hsdR17(rK–mK+), λ–	Invitrogen Corporation, California, U.S.A.	Routine cloning
Mav203	*S. cerevisiae*	MATα; leu2-3,112; trp1-901; his3Δ200; ade2-101; cyh2R; can1R; gal4^{R}; gal80^{R}; GAL1::lacZ; HIS3UASGAL1::HIS3@LYS2; SPAL10::URA3.	Invitrogen Corporation, California, U.S.A.	Yeast two-hybrid
StrataClone SoloPack	*E. coli*	Tet^{r}. Δ(mcrA)183 Δ(mcrCB-hsdSMR-mrr)173, *endA1, supE44, thi-1, recA1,* gyrA96, *relA1, lac,* Hte [F´*proAB, lacI^{q}ZΔM15,* Tn*10,* (Tet^{r}), Amy, Cam^{r}]	Stratagene, San Diego, California, U.S.A	Cloning
NEB® 10-beta Competent	*E. coli*	Δ(ara-leu) 7697 araD139 fhuA ΔlacX74 galK16 galE15 e14- φ80dlacZΔM15 recA1 relA1 endA1 nupG rpsL (StrR) rph spoT1 Δ(mrr-hsdRMS-mcrBC)	New England Biolabs, Massachusetts, U.S.A	Yeast two-hybrid library screen

2.4.9 Bacterial transformation

Plasmids were introduced into competent *E. coli* cells using a heat-shock transformation protocol.

In most cases (excluding pSC-Blunt reactions, which were transformed into kit-supplied competent cells (**Table 2.3**)), 50-µl aliquots of *DH5α* ultracompetent cells (**Table 2.3**) (Invitrogen Corporation, California, U.S.A.) were incubated with 2-µl of plasmid on ice for 20 mins. The cell-plasmid mix was then heat-shocked at 42°C for 45 seconds before a second incubation on ice of 2-3 minutes. The cells were then recovered in 250 µl of SOC media, on a 37°C incubated shaker at 250 rpm for 1-2 hours. Typically, 100-µl and 20-µl volumes of transformation were spread on separate 2xYT agar media (Formedium, Hunstanton, U.K.) plates containing the appropriate antibiotic selection for that plasmid. The plates were incubated at 37°C overnight to allow colonies to grow.

2.4.10 Preparation of yeast competent cells

Mav203 was streaked into YPD media and incubated at 30°C for 48 hours. 100 ml YPD liquid media was then inoculated with the *Mav203* and incubated at 160 rpm, 30°C overnight. Once the OD600 reaches 1-1.5, the cells were harvested at 8000 rpm for 5 minutes, then resuspended in 10 ml sterile distilled H_20 twice, this process was repeated once. The cells were then spun down at 8000 rpm and resuspended in 10 ml LiAc, then incubated at 30°C,160 rpm for 1 hour

2.4.11 Yeast transformation

Plasmids were introduced into yeast competent cells using a heat shock protocol. 150 µl of *Mav203* competent yeast cells (**Table 2.3**) (section 2.5.10) (Thermo-fisher Scientific, California, USA), were incubated at 30°C with 1 µg of each plasmid, 2 µl of 10 mg/ml sheared salmon sperm DNA (Thermo-fisher Scientific, California, USA) and 350 µl 50% polyethylene glycol (PEG) for 1 hour. Reactions were then chilled on ice for 2-3 minutes, and spun down at 14,500 rpm for 1 minute in a table top centrifuge to isolate the transformed yeast cells. The cell pellet was then re-suspended in 100 µl sterile distilled water. Typically, 100 µl of cells were spread onto 10mm SC-leu/-trp plates, and incubated at 30°C for 48-72 hours.

2.4.12 Bacterial minipreps

Transformed bacteria were cultured from colonies grown on 2x YT media plates. Typically, one colony was used to inoculate 5 ml of 2x YT liquid media, containing an appropriate antibiotic. The 5 ml cultures were incubated at 37°C at 200 rpm in a heated shaker overnight, giving time for the cultures to grow.

Once the cultures had grown overnight, the culture (typically 4 ml) was spun down by centrifugation (2mins, 10,000 rpm) to isolate a cell pellet. The pellet was then used to extract plasmid DNA using the Qiagen QIAprep Spin Miniprep Kit (Qiagen, Hilden, Germany), following the kit-supplied protocol. Bacterial plasmid minipreps were quantified using the Nanodrop™ ND-1000 spectrophotometer. Where appropriate, plasmid DNA was sequenced by Eurofins Genomics (Luxembourg, Luxembourg). Preparation of the sample was carried out according to their specifications.

2.4.13 Yeast minipreps

Transformed yeast was cultured from single colonies grown on SC-leu/-trp plates. Colonies were inoculated into 5 ml SC-leu/-trp liquid medium, and incubated at 30°C at 200 rpm in a heated shaker overnight.

Once the cultures had grown up overnight, typically 4 ml was spun down by centrifugation (2 mins, 10,000rpm) to isolate a cell pellet. The pellet was then suspended in 200 µl of P1 lysis buffer from the Qiagen QIAprep Spin Miniprep Kit. Glass beads were then added to the lysis solution, and the mixture was homogenised at 1750 rpm for 5 minutes in the 2010 Geno/Grinder®. The subsequent steps were then carried out according to the Qiagen QIAprep Spin Miniprep Kit manufacturer's protocol to isolate the plasmid DNA.

2.4.14 Gene synthesis

Genes were synthesised by Eurofins Genomics (Luxembourg, Luxembourg) and Genscript (New Jersey, USA), and were provided as a construct in pUC57 and pEX-K4, respectively.

2.4.15 Genotyping

TILLING lines were genotyped using either gDNA or KASP assays.

DNA was extracted (2.5.1) from approximately 1g leaf tissue and used as a template for a HotShot polymerase PCR with a primer pair which targeted the region of interest. PCR products were purified following the protocol in section 2.5.6. Purified products were sequenced by Eurofins Genomics (Luxembourg, Luxembourg). Typically, 15 µl of PCR product was combined with 2 µl of 10 pmol/µl of the corresponding primer. Sequencing results were compared to the WT *TaPIL* sequences using the map to reference function in Geneious (Auckland, New Zealand), to identify lines containing the desired SNP.

KASP primers were designed by LGC genomics (Middlesex, UK), to amplify the D genome homoeologue mutation for *TaPIL1* and *TaPIL3*. KASP assays were carried out using the KASP Master mix (LGC genomics, Middlesex, UK) according to the manufacturer's instructions. Reactions were set up as follows:

Reagent	**Volume**	**Concentration**
DNA	5 µl	25 ng/µl
Primer	0.15 µl	30µM
Ready Mix	5 µl	2x

The reactions were loaded into a 96-well plate (4titude Ltd., Surrey, UK), and sealed with clear caps (4titude Ltd., Surrey, UK). The plate was spun down using Labnet MPS 1000 Mini plate spinner (Sigma-Aldrich Company Ltd., Dorset, U.K.). The KASP reaction was carried out using a BIO-RAD C1000™ Thermal Cycler (California USA) comprising one 96-well heat block and a heated lid. Reaction conditions were as follows:

95°C	15 minutes	1 cycle
95°C	20 seconds	
61°C	1 minute	10 cycles
95°C	20 seconds	36 cycles
55°C	1 minute	

Completed reactions were analysed with the 7500 Real Time PCR system (Applied Biosystems, California, USA), using the allelic discrimination settings. The results from this run were then analysed using the KlusterCaller™ software (LGC, Teddington, UK), which discriminates between homozygous, heterozygous and wild-type samples.

Transgenic lines were genotyped by iDNAgenetics with a qPCR based method (Norwich, UK), using supplied genomic DNA samples at the T0 and T1 generations.

2.4.16 Quantitative PCR

qPCR was carried out using the SYBR® Green JumpStart™ *Taq* ReadyMix™ (Sigma-Aldrich Company Ltd., Dorset, U.K.), according to the manufacturer's instructions. All reactions contain three reference gene primer pairs and one target primer pair. The reactions were set up as follows:

SYBR Green:

Reagent	**Volume**	**Concentration**
cDNA	5 µL	5 ng/ul
Primers	5 µl	0.25mM
SYBR Green ReadyMix	10 µl	1X

The reactions were loaded onto a 96-well plate (4titude Ltd., Surrey, UK), and sealed with clear caps (4titude Ltd., Surrey, UK). The plate was spun down using Labnet MPS 1000 Mini plate spinner (Sigma-Aldrich Company Ltd., Dorset, UK). The qPCR was run on a 7500 Real Time PCR system (Applied Biosystems, California, USA), with the following PCR conditions, including a melting curve.

95°C	10 minutes	1 cycle
95°C	15 seconds	40 cycles
60°C	1 minute	
95°C	15 seconds	1 cycle
60°C	1 minute	
95°C	15 seconds	
60°C	15 seconds	

2.4.17 qPCR Analysis

The melting curve was used to identify any secondary products or primer dimers, which were detected by the presence of more than one peak. If only one peak was present, further analysis was carried out on the reaction.

Analysis was carried out by comparing the PCR efficiency and threshold cycle (Ct) value for the target and reference genes in both control and treatment samples. The Ct and PCR efficiency values were calculated by the LinRegPCR software (Heart Failure Research Centre, Netherlands). Typically, PCR efficiency values ranged from 1.5-2.0, and Ct values from 18-40.

Results were analysed using the CT and efficiency values as follows:

$$\text{ratio} = \frac{(E_{\text{target}})^{\Delta \text{CP}_{\text{target}}(control - sample)}}{(E_{\text{ref}})^{\Delta \text{CP}_{\text{ref}}(control - sample)}}$$

ΔCP_{target} refers to the Ct value of the target gene in the control condition minus the Ct value of the same gene in the target sample. $\Delta CT_{reference}$ refers to the Ct value of the reference gene in the control minus the treatment sample. These expression ratios were calculated for the target gene compared to all three reference genes. These values were then used to assess gene expression in transgenic lines.

2.4.18 Yeast two-hybrid assays

To test for self-activation levels, yeast transformed with the bait plasmid and an empty prey vector were grown on SD media lacking leucine, tryptophan and histidine with increasing concentrations of 3-amino-1,2,4-triazole (3-AT), a competitive inhibitor of the *HIS3* gene. A 1M solution of 3-AT was added to liquid -leu/trp/his media to produce final 3-AT concentrations of 10 mM, 15 mM, 20 mM, 30 mM, 40 mM and 50 mM. Typically, one colony of yeast was inoculated into 200 µl sterile distilled water, and 5µl of this was spotted onto the plates. Three biological repeats for each strain were plated in a grid format. Once the culture had dried onto the plates, they were incubated at 30°C for 48 hours. Assays were scored based on the levels of visible growth for each strain.

Once an appropriate minimum 3-AT concentration was identified, the specific screen was run. In this case, the assay was set up in the same was as described above with 3-AT concentrations ranging from the minimum to inhibit self-activation to 50 mM. Each plate contained a negative

control with empty prey and bait vectors, a positive control with known interactors, GAI and ARF19, the test prey plasmid with an empty bait vector, the test bait plasmid with an empty prey vector, and the test prey and bait plasmids. Plates were photographed after 48 hours at 30°C, and assessed for differences in growth levels.

Interaction was also detected using a LacZ filter lift assay. The same colonies as described above, were streaked onto 10 mm x 10 mm YPD plates, with a 100 mm x 100 mm Amersham Protran supported 0.2 um nitrocellulose membrane (GE healthcare life sciences, Buckinghamshire, UK), and incubated at 30°C for 24 hours. After incubation, the nitrocellulose membranes were frozen in liquid nitrogen for 30 seconds to lyse the yeast cells. The membrane was then placed on 2-mm filter paper in a 10 mm Petri dish, soaked in 5 ml of Z buffer (1 µg/ml ortho-nitrophenyl-β-galactoside (ONPG)) and 30µl 2-Mercaptoethanol and incubated at 37°C for 24 hours. Colour was assessed visually at 2, 4 and 24 hours.

Z Buffer (IL): 60 mM Na2HPO4
40 mM NaH2PO4
10 mM KCl
1 mM MgSO4
Adjust pH to 7.0 and filter sterilize

2.4.19 Yeast two-hybrid library screen

The RHT-D1A bait plasmid was tested for self-activation as described above (2.5.18). A 250µl aliquot (over 1×106 transformants) of Library scale *Mav203* competent cells (Thermo-fisher Scientific, California, USA) was combined with the *RHT-D1a* (10 µg) bait plasmid and a wheat stem prey library (10 µg) and 1.5ml PEG/LiAc solution. The reaction was incubated at 30°C, then mixed with 88µl DMSO and heat-shocked at 42°C for 20 minutes. Cells were spun down at 1800rpm, 5mintes, and resuspended in 8ml 0.9% NaCl. Transformed cells were then plated out onto 15-cm SC-leu-trp-his agar 15mM 3-AT plates in 400µl aliquots and incubated at 30°C for 3 days.

After three days, single colonies were patched onto SC-leu/trp master plates and incubated at 30°C for 48 hours. These master plates were then used to create 30% glycerol stocks (made up a 200µl suspension of the yeast colony in sterile distilled water mixed with 200µl of 60% glycerol) of all library plasmids.
Plasmid DNA was extracted from the yeast colonies following the protocol described above (2.5.13). This plasmid DNA was then used in a PCR using GoTaq polymerase following the

protocol described in section 2.5.4, but with 10 µl DNA rather than 1 µl. The PCR was run with the following conditions:

Initial Denaturation - 98°C for 15 seconds	1 cycle
Denaturation (98°C for 10 seconds), Annealing (60°C for 30 seconds) Extension (72°C for 90 seconds)	40 cycles
Final Extension - 72°C for 5 minutes	1 cycle

The PCR products were examined using an electrophoresis gel. For colonies which had more than one band visible on an electrophoresis gel, and therefore more than one insert, DNA was used to transform *NEB® 10-beta* competent *E. coli* (**Table 2.2**) as described in section 2.5.9. Three colonies per transformation were selected to extract plasmid DNA, following the bacterial miniprep protocol described in section 2.5.12. Plasmid DNA was sequenced by Eurofins Genomics (Luxembourg, Luxembourg) using *pDEST22* forward and reverse primers.

Sequencing results were aligned to the Gal4 DNA binding domain and *aatB* motif of *pEXP22*, using the map to reference tool in Geneious (Auckland, New Zealand), to identify the cDNA sequence. The cDNA sequences were the used in a DeCypher® Terra-Blast™ N search of an *Oryza sativa*, and TGAC *T. aestivum* cDNA database, to identify the sequence.

cDNAs of interested were transformed into yeast *Mav203* competent cells (section 2.5.11) with the *RHT-D1a* bait plasmid to confirm to interaction using a 3-AT assay (section 2.5.18).

2.5 Bioinformatics

2.5.1 Sequence data

Nucleotide to nucleotide blast searches were carried out using the Tera-Blast™ N function in DeCypher® (Time Logic, California, USA), within the *T. aestivum* TGAC Ensemble, *O. sativa* phytozome, *Brachipodium distachyon* phytozome and *Arabidopsis thaliana* Ensemble coding sequence databases with the default settings. Tera-Blast™ N searches were also carried out using the w7984 genomic database, the ensemble TGAC genomic database and the ensemble IWGSC database.

Protein to protein searches were carried out using the Tera-Blast™ P function in DeCypher® (Time Logic, California, USA), within the *T. aestivum* TGAC Ensemble, *O. sativa* phytozome, *B.*

distachyon phytozome and *A. thaliana* ensemble protein sequence databases with the default settings.

2.5.2 Identifying coding sequences.

Once putative *T. aestivum* coding sequences were identified using the Tera-Blast™ N function in Decypher, RNAseq reads from a Chinese Spring dataset (PRJDB2496) (Oono et al., 2013) were mapped to the scaffold sequences to identify the exon coding regions.

RNAseq reads from *T. aestivum* root and shoot were mapped to the scaffold sequences using the TopHat2 function in Galaxy (Penn State, John Hopkins University, Oregon Health and Science University, USA), using default settings. The Cufflinks program was then used to assemble the transcript sequence, using default settings. The start and stop codon of the assembled transcript was then identified using the identify open reading frame function in Geneious (Auckland, New Zealand).

2.5.3 Identifying protein domains.

To identify the APB domain in the wheat PIL sequences, the APB consensus sequence (EDVVELLWENGQ) was used in the search for motif function in Geneious, with the default settings, except, the maximum number of mismatches set to 8-10.

To identify the bHLH domain in the wheat PIL sequences, the bHLH consensus sequence Motif (HVLAERKRREKLNERFxxLRSLVPxxxxxxxxKMDKASILGDxIxYLKxLxxKVxE) was used in the search for motif program in Geneious. All settings were default, except the maximum number of mismatches, which was set to 26.

2.5.4 Comparing expression between homoeologues

To compare expression between homoeologues sequences, RNAseq reads were mapped to the three homoeologues sequences to calculate a fragments per kilobase, per million reads mapped (FKPM) value.

Leaf RNAseq data (International Wheat Genome Sequencing, 2014) were mapped to a file containing all the IWGSC *T. aestivum* cDNA sequences, using the BWA-MEM mapping tool in Galaxy community hub (NSF, NHGRI, The Huck Institutes of the Life Sciences, The Institute for CyberScience at Penn State, and Johns Hopkins University), with the default settings. These data were then analysed by the eXpress program in Galaxy, using the default settings, to give an FKPM value for each cDNA sequence.

2.5.5 Sequence alignments and phylogenetic trees

Nucleotide sequences were aligned using the MUSCLE alignment tool in Geneious, with the default settings.

Protein sequence alignments were created using the ClustalW Blosum alignment tool in Geneious, using the default settings. Trees were produced from the sequence alignment using the neighbour joining tree method in Geneious.

Chapter 3: Identifying PIF-like Genes in Wheat with a Putative Role in the Regulation of Stem Elongation.

3.1 Introduction

3.1.1 Wheat sequence databases

The wheat genome is extremely complex due to its three homoeologous genomes and large sections of repetitive DNA. This has made efforts to sequence or identify genes extremely difficult; however new advances in sequencing technology have provided new insights.

The wheat genome displays a reasonable amount of synteny with other grasses, but has a higher amount of repetitive sequences and transpositions (Edwards et al., 2013b). This makes up 75-90% of the genome, which has caused it to expand to around 40 times the size of the rice genome. In addition, the multiple homoeologous copies of each gene mean that assembling and analysing the genome is very difficult (Edwards et al., 2013b). Because a complete genome sequence for wheat has not been available, the gene content and order of *Triticeae* genomes have been inferred from comparisons with the model grass species that have been fully sequenced. Rice, sorghum, maize and Brachipodium make up the model grass species, with Brachipodium being the closest *Triticeae* relative. Between rice and Brachipodium, 80% of the genes are conserved in syntenic positions, and so a higher level of conservation can be expected for Brachipodium and wheat, since they are more closely related than wheat and rice (Wicker et al., 2011).

Rough drafts of a genome can be produced by whole genome shotgun (WGS) sequencing, which produces assemblies made up of many small contigs that can be separated by gaps of unknown size. A reference sequence that represents a near complete genome can only be achieved with clone-by-clone sequencing. The human WGS assembly and other mammalian genomes have been successfully produced, but they still rely on some form of physical map to help assemble the chromosomes. Large WGS assemblies have been attempted, such as for Norway spruce, which is around 20 Gbp in length, but the resulting assemblies are fragmented and have not been organised into chromosomes (Chapman et al., 2015).

In 2003 a consortium was established to begin the international wheat genome sequencing project, with a bacterial artificial chromosome (BAC) by BAC approach. This comprised a five-year project to produce a physical map of the genome with anchored BACs. In 2004 the International Wheat Genome Sequencing Consortium (IWGSC) was established, with the aim of producing a complete and annotated genome sequence for *T. aestivum* cv. Chinese Spring. By 2011, the IWGSC had successfully produced BAC libraries for all individual wheat chromosome arms (Edwards et al., 2013b).

Brenchley et al. (2012) published an analysis of the wheat genome using a WGS sequencing approach. Chinese Spring wheat DNA was sequenced using the Roche 454 pyrosequencing technology, which generated a five-fold coverage of the 17Gb genome. The A, B and D genomes were separated by comparisons to the genomes of the A, B and D donor species. This sequencing identified between 94,000 and 96,000 genes, two thirds of which were assigned to one of the subgenomes. Comparison to other grass species revealed many small disruptions in gene order. In addition, the genome was found to be highly dynamic, with many gene family members lost during polyploidization. However, there was also significant expansion of gene families associated with crop productivity, including energy harvesting, metabolism and growth. This sequencing project provided a means for gene discovery in wheat (Brenchley et al., 2012).

In 2014 significant progress was made with the publication of the 'chromosome based draft sequence of the wheat genome' by the IWGSC. The 17 giga-base hexaploid genome was produced by sequencing each chromosome arm separately; arms were purified by flow cytometry and sequenced to a depth of between 30x and 241x with Illumina technology. Paired end sequence reads were then assembled, and assessed for quality by mapping them to the virtual barley genome and bin-mapped Expressed Sequence Tags (ESTs), which are short sequences isolated from expressed genes mapped to chromosome arms (International Wheat Genome Sequencing, 2014, Qi et al., 2004). Sequencing of the wheat genome revealed around 160,000 functional protein coding genes, with each diploid genome estimated to contain between 32-38,000 genes. The distribution of genes between the subgenomes was slightly uneven; A 33%, B32%, D 35%, but there is no global dominance between homoeologues (International Wheat Genome Sequencing, 2014).

Another wheat genome assembly was produced by Chapman et al. (2015) from the synthetic wheat variety; W7984; a reconstitution of hexaploid bread wheat produced by hybridising tetraploid *Triticum turgidum* (AABB) and diploid *Aegilops tauschii* (DD). This study combined a

WGS assembly and genome-wide genetic mapping to sequence hexaploid wheat. Sequencing produced a 30-fold coverage of W7984, which was assembled using an updated version of the assembly program 'Meraculus', which can efficiently assemble large, repetitive datasets (Chapman et al., 2015).

Comparisons of the W7984 genome assembly and the IWGSC consortium sequence were carried out by Chapman et al. (2015) to see if there were any differences in coverage. Six known sequences; the homoeologues of *Rht-1* and the GA biosynthesis enzyme *KAO*, were compared between the two databases. In the W7984 assembly, all these genes were found within six scaffolds, whereas in the IWGSC assembly one gene was not found and the others were spread across multiple scaffolds. This suggests that the W7984 assembly may be more complete (Chapman et al., 2015). Both the IWGSC and W7984 databases capture around 3/4 of the known genes, identified in the Triticeae Full-Length CDS Database (TriFLDB) (Mochida et al., 2009), in a somewhat complete form (>50% of translated sequence in one scaffold); however, they do not completely overlap, so the databases can be complementary to one another. Together the databases contain 93% of the known genes (Chapman et al., 2015).

In 2016 the TGACv1 sequence assembly was released (Clavijo et al., 2017). This assembly was produced using whole-genome shotgun sequencing of the Chinese Spring wheat variety. This involved an open source approach, which consisted of mapping of Illumina paired end reads to libraries using newly developed 'w2rap' assembly software, designed to deal with large and complex genomes (Clavijo et al., 2017). The TGACv1 sequence assembly is the most complete so far, with more than 78% of the genome covered. In comparison, the IWGSC and W7984 assemblies only cover 48.9% and 48.2% respectively. The scaffold sizes of the TGACv1 assembly are also much larger than the IWGSC or W7984 assemblies, with the average scaffold length being around 88.8 kb (Clavijo et al., 2017).

These new advances in sequencing the wheat genome have made it possible to identify and investigate wheat genes.

3.1.2 A rice PIL, OsPIL1 regulates stem elongation in rice.

The overriding aim of this project was to identify an alternative means to control stem elongation in wheat for the purpose of increasing wheat yields, while avoiding the pleiotropic effects associated with *Rht* mutant lines (Ellis et al., 2004, Alghabari et al., 2014, Coelho et al., 2013, Flintham et al., 1997b).

Phytochrome interacting factors (PIF)s are a family of light responsive transcription factors that have been shown to interact with GA-responsive DELLA proteins in *Arabidopsis*. In this interaction, DELLAs bind to and sequester PIF proteins in the absence of GA, preventing them from regulating plant growth (Feng et al., 2008, de Lucas et al., 2008, Li et al., 2016a). This interaction makes PIFs a good candidate for specific regulation of plant growth during the GA response.

A rice PIF-like (PIL) protein, OsPIL1, has been shown to play a key role in the regulation of stem elongation. Overexpression of OsPIL1 in rice caused an elongated stem phenotype, whereas repression of OsPIL1 expression, caused a short, dwarf-like phenotype (Todaka et al., 2012). These data suggested that OsPIL1 could specifically regulate stem elongation in rice. For this reason, identifying orthologous sequences in wheat could provide strong candidates for regulating the GA response, and more specifically, stem elongation. Disruption of OsPIL1 orthologues in wheat could provide a means to alter plant height while avoiding the *Rht* pleiotropic effect, resulting in increases to wheat yield. Currently no PIF-like proteins have been identified in wheat. In order to investigate the hypothesis that wheat PIF-like proteins interact with RHT-1 to regulate GA medicated stem elongation, the family of wheat PILs need to be identified. The recent advances in sequencing of the large and complex wheat genome has made identifying putative wheat genes possible. This project will utilise all available wheat sequencing databases; IWGSC, W7984 and TGACv1, to identify putative wheat PIL genes.

The *OsPIL1* cDNA sequence was used to search the wheat databases for homologous sequences using a Terra-blast-N search in DeCypher. The putative orthologous sequences identified were analysed to identify coding sequences using RNA-seq data, and their protein sequences were subsequently analysed for consensus PIF domains. This search has identified three putative wheat *PIL* genes – *TaPIL1*, *TaPIL2* and *TaPIL3.*

3.2 Results

3.2.1 Identification of *OsPIL1* orthologues in wheat

3.2.1.1 Identifying scaffolds containing sequences orthologous to *OsPIL1*

An aim of this project is to identify an alternative means to *Rht-1* mutations by which stem elongation in wheat can be specifically regulated, avoiding the pleiotropic affects associated with the *Rht-1* mutant lines. As explained above, *PIF-like* genes are a good candidate for this, with *OsPIL1* orthologues of particular interest since OsPIL1 has been shown to regulate stem growth in rice. Therefore, the *OsPIL1* sequence was used to search wheat sequencing databases for homologous sequences. At the time this project started, only the IWGSC sequence database was available, so the initial identification of *OsPIL1* homologues was completed using this database only. Once the W7984 and TGAC databases became available, they were also searched with *OsPIL1* to confirm the identified sequences, and to identify homoeologous sequences not present in the IWGSC database.

The rice *OsPIL1* (LOC_Os03g56950) cDNA sequence was used in a blastn search of the IWGSC wheat sequence database (IWGSC 2014). This search identified three scaffolds from chromosome five (scaffolds 1404752, 10924907 and 4583931) with sequence identities of 86%, 90% and 87% with *OsPIL1* respectively. Three scaffolds from chromosome two were also identified (Scaffolds 6420388, 8024059 and 9884497), all with 88% sequence identify with *OsPIL1*. These scaffolds were thought to correspond to the three A, B and D homoeologues of two separate genes. Other scaffolds were also identified from this search, but were eliminated when very few RNA-seq reads mapped to the sequences, suggesting that they were not expressed.

Since Brachipodium is more closely related to wheat than rice, Brachipodium sequences were also used to search the IWGSC database to identify more wheat PILs. First, Brachipodium orthologues of *OsPIL1* were identified in a blastn search of a Brachipodium cds database, which revealed three genes: *Bradi1g06670, Bradi1g58230* and *Bradi1g13980, with* sequence identities of 84%, 86% and 91%, respectively. Each Brachipodium gene was then used in a blastn search of the IWGSC database. Searching with *Bradi1g58230* or *Bradi1g06670* detected the previously identified chromosome two and chromosome five scaffolds, respectively. This suggests that these Brachipodium genes could be orthologous to the genes already identified in wheat. Finally, searching with the third Brachipodium gene - *Bradi1g13980* – identified a third set of chromosome scaffolds, which made up the top eight hits from the blast search. The

scaffolds identified (scaffolds 10820313 and 4549919) were from chromosome five and had sequence identities of 98%. These results included a scaffold from the B and D genomes, but not the A genome. See **Table 3.1** for scaffold identities.

Table 3.1 Scaffold identities of the wheat PIL homoeologous sequences in the IWGSC, W7984 and TGACv1 assemblies

Wheat Sequence	IWGSC Scaffold	W7984 Scaffold	TGACv1 Scaffold
TaPIL1 5AL	1404752	1209428	-
TaPIL1 5BL	10924907	895801	404326
TaPIL1 5DL	4583931	4238176	435807
TaPIL2 5AL	-	-	375250
TaPIL2 5BL	10820313	524452	404326
TaPIL2 5DL	4549919	1410488	435807
TaPIL3 2AL	6420388	3818900	092984
TaPIL3 2BL	8024059	56664	131229
TaPIL3 2DL	9884497	862036	157972

3.2.1.2 Identifying genomic sequences within the scaffolds

To identify regions of the scaffolds that are expressed in wheat, RNAseq reads were mapped to the scaffold to visualise the coding regions. Root and shoot RNAseq data (PRJDB2496) from the Chinese Spring *T. aestivum* variety was used in this process. These reads were published in a study to investigate the effect of phosphorus starvation on the wheat transcriptome. This RNA-seq dataset was created using high-quality reads obtained from RNAseq libraries, which were used in *de novo* assembly of the RNAseq dataset (Oono et al., 2013).

RNAseq reads from Chinese Spring root and shoot data were mapped to the scaffold sequences using the TopHat2 programme in Galaxy. RNAseq reads which were homologous to areas of the scaffold sequence aligned to their corresponding regions, giving a visualisation of the regions of the scaffold that contained coding exon sequence, and confirming the exon-

intron boundaries. The exon sequence in each scaffold was therefore identified, and the genomic sequence of each gene was extracted, resulting in the identification of three *PIF-like* genes.

For the first set of scaffolds from chromosome 5 (scaffolds 1404752, 10924907 and 4583931), the 5DL and 5BL sequences revealed genes with a similarly sized, seven exon structure. However, the 5AL scaffold only contained a partial sequence of the gene. The exon sequences of the complete 5BL and 5DL sequences were compared, revealing over 96.5% identity (**Table 3.2**), confirming that these sequences are homoeologues. The 5BL and 5DL sequences were used in blastn searches of both the W7984 (Chapman et al., 2015) and TGACv1 (Clavijo et al., 2016) assemblies, in order to try to identify a full 5AL sequence. The W7984 database contained a scaffold which covered the full seven exon 5AL sequence. Predictive software in Geneious was used to identify an open reading frame of approximately 1.2 kb for each homoeologous sequence. The genomic sequences of the A, B and D homoeologues are 1.93 kb. The exon structure is shown in **Figure 3.1**, and the sizes on introns and exons are shown in **Table 3.3**. These three sequences were termed the A, B and D homoeologues of *TaPIL1*. Full cDNA sequences are shown in Appendix **Figure 7.1.**

Table 3.2 Sequence identities between the TaPIL1 homoeologues. The sequence identities between each pair of TaPIL1 homoeologues is shown.

	TAPIL1 5AL	**TAPIL1 5BL**	**TAPIL1 5DL**
TAPIL1 5AL		95.8%	96.3%
TAPIL1 5BL	95.8%		95.6%
TAPIL1 5DL	96.3%	95.6%	

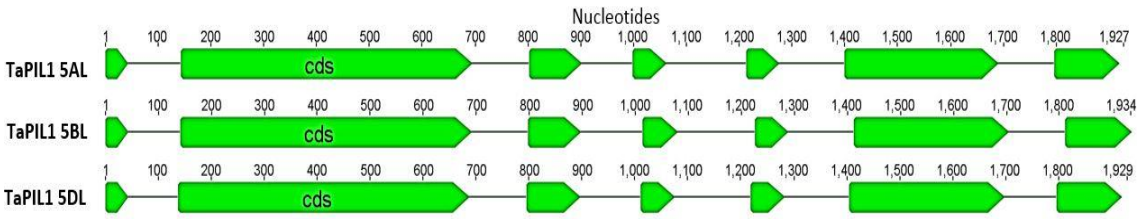

Figure 3.1. The genomic structure of *TaPIL1*. The genomic sequences of the three A, B and D homoeologues of TaPIL1 are shown. Sequence length is indicated by the nucleotide label above the sequences. Exon coding sequence is indicated by green arrows.

Table 3.3 The exon and intron sizes for TaPIL1. The exon and intron sizes in bp are given for the three homoeologous sequences.

	TAPIL1 5AL	**TAPIL1 5BL**	**TAPIL1 5DL**
Exon 1	44 bp	44 bp	44bp
Intron 1	100 bp	98bp	94 bp
Exon 2	551 bp	551 bp	551 bp
Intron 2	110 bp	106 bp	109 bp
Exon 3	100 bp	100 bp	100 bp
Intron 3	96 bp	118 bp	114 bp
Exon 4	65 bp	65 bp	65 bp
Intron 4	151 bp	146 bp	143 bp
Exon 5	64 bp	64 bp	64 bp
Intron 5	123 bp	123 bp	123 bp
Exon 6	292 bp	292 bp	292 bp
Intron 6	107 bp	108 bp	100 bp
Exon 7	123 bp	123 bp	123 bp

The second set of chromosome 5 scaffolds (scaffolds 10820313 and 4549919) both contained genes with a five-exon structure. The exon sequences of these genes were compared, revealing a sequence identity of 88.2% (**Table 3.4**), which is slightly lower than expected for

homoeologous sequences. However, there is a ~30 bp insertion within the 5BL sequence, which is responsible for this low ID. Therefore, these sequences are likely to be homoeologous. The TGACv1 database was searched with the 5BL and 5DL sequences to identify the 5AL homoeologue. In this search a scaffold (scaffold 375250) was identified that contained the full five-exon 5AL sequence. The genomic sequences of the A B and D homoeologues are 1.85. 1.72 and 1.86 kb respectively. The open reading frames of the sequences were predicted in Geneious, with the 5AL, 5BL and 5DL homoeologues containing 1.5, 1.34 and 1.46 kb sequences respectively. The exon structures are shown in **Figure 3.2**, and the intron and exon sizes are shown in **Table 3.5**. These three sequences were designated as the A, B and D homoeologues of *TaPIL2*. Full cDNA sequences are shown in Appendix **Figure S.2.**

Table 3.4 The sequence identity between the TaPIL2 homoeologues. The sequence identity between each pair of TaPIL2 A, B and D homoeologues is shown.

	TAPIL2 5AL	**TAPIL2 5BL**	**TAPIL2 5DL**
TAPIL2 5AL		86.5%	94.9%
TAPIL2 5BL	86.5%		88.2%
TAPIL2 5DL	94.9%	88.2%	

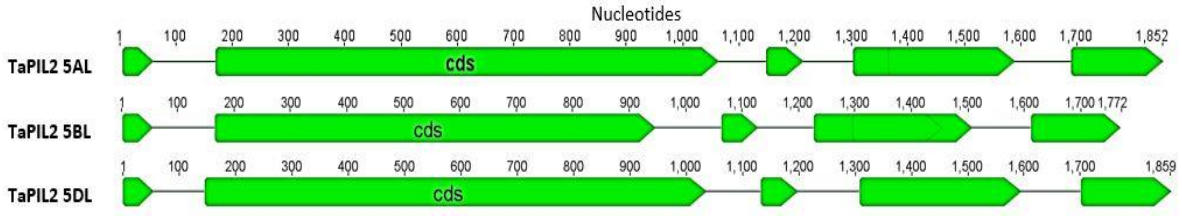

Figure 3.2. The Exon Structure of *TaPIL2.* The genomic sequence of the three A, B and D homoeologues of TaPIL2 are shown. Length of the sequences is shown by a nucleotide scale above the sequences. Exon coding sequence is labelled by green arrows.

Table 3.5 The intron and exon sizes of *TaPIL2.* The exon and intron sizes are given in bp for the three homoeologous sequences

	TAPIL2 5AL	**TAPIL2 5BL**	**TAPIL2 5DL**
Exon 1	55 bp	55 bp	55 bp
Intron 1	112 bp	110 bp	90 bp
Exon 2	892 bp	781 bp	892 bp
Intron 2	86 bp	118 bp	96 bp
Exon 3	65 bp	65 bp	65 bp
Intron 3	89 bp	99 bp	109 bp
Exon 4	287 bp	281 bp	287 bp
Intron 4	101 bp	105 bp	106 bp
Exon 5	162 bp	159 bp	159 bp

The set of chromosome 2 scaffolds (scaffolds 6420388, 8024059 and 9884497) all contained genes with a seven-exon structure; comparison of the exon structures revealed a sequence identity of over 94.5% between each pair of sequences (**Table 3.6**), confirming that these sequences are the A, B and D homoeologues of the same gene. The A, B and D homoeologues had a genomic sequence of 1.65, 1.63 and 1.63 kb, respectively. The open reading frames were predicted using Geneious, with all three homoeologues containing a coding sequence of approximately 1 kb. The exon structure is shown in **Figure 3.3**, and the intron and exon lengths are shown in **Table 3.7**. These three sequences have been designated as the A, B and D homoeologues of *TaPIL3*. Full cDNA sequences are shown in Appendix **Figure 7.3.**

Table 3.6 The sequence identity between the TaPIL3 homoeologues. The sequence identities between each pair of A, B and D homoeologues of TaPIL3 are show.

	TAPIL3 2AL	TaPIL3 2BL	TaPIL3 2DL
TaPIL3 2AL		94.6%	94.7%
TaPIL3 2BL	94.6%		98.4%
TaPIL3 2DL	94.7%	98.4%	

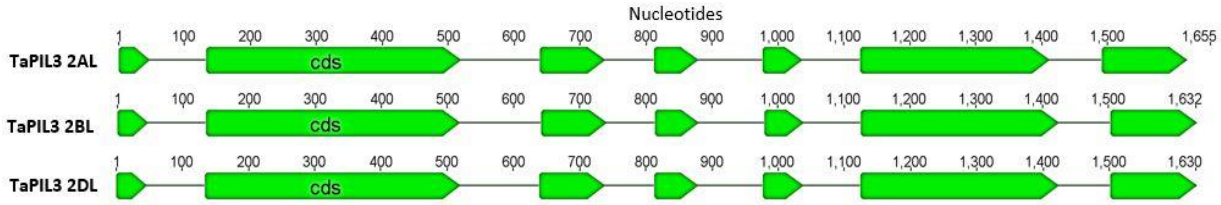

Figure 3.3. The Exon Structure of *TaPIL3*. The genomic sequences of TaPIL3 are shown. Sequence length is indicated by a nucleotide scale above the sequence. Coding exon sequence is indicated by the green arrows.

Table 3.7 The intron and exon sizes of TaPIL3. The exon and intron sizes are given in bp for the three homoeologous sequences.

	TaPIL3 2AL	TaPIL3 2BL	TaPIL3 2DL
Exon 1	47 bp	47 bp	47 bp
Intron 1	85 bp	87 bp	87 bp
Exon 2	386 bp	383 bp	383 bp
Intron 2	119 bp	123 bp	120 bp
Exon 3	100 bp	100 bp	100 bp
Intron 3	74 bp	73 bp	74 bp
Exon 4	65 bp	64 bp	65 bp
Intron 4	99 bp	99 bp	99 bp
Exon 5	62 bp	62 bp	62 bp
Intron 5	87 bp	86 bp	86 bp
Exon 6	285bp	297 bp	297 bp
Intron 6	96 bp	78 bp	78 bp
Exon 7	114 bp	132 bp	132 bp

3.2.2 The *TaPIL1*, *TaPIL2* and *TaPIL3* genes encode predicted proteins containing active phytochrome binding and basic helix-loop-helix domains

PIF proteins contain a conserved active phytochrome binding (APB) domain at their N terminus, which is required for the interaction with Phytochrome B. When the plant detects red light, phytochrome is converted from the Pr to the Pfr form, which allows it to translocate into the nucleus of cells, and bind to PIFs via their APB domain. The binding of Phytochrome B to the PIFs is essential for the sequestration and degradation of PIFs which causes the plant to switch to photomorphogenic growth (Khanna et al., 2004). Therefore, any functional PIF-like protein would be expected to contain this domain. An APB consensus sequence was described by Khanna et al. (2004) (**Table 3.9**).

PIF proteins also contain a basic helix-loop-helix (bHLH) domain, which allows them to bind the G-box of promoters to regulate gene expression (Huq and Quail, 2002b). A bHLH consensus sequence in plants was described by Heim et al. (2003), shown in **Table 3.9**.

The *TaPIL* cDNA sequences were translated into protein sequences to compare amino acid sequences between the PIL genes and their homoeologues. The homoeologous sequences of all the TaPILs encode proteins of a similar length, and share a high degree of similarity. The TaPIL1 A, B and D homoeologues encode protein sequences of 412, 410 and 414 amino acids, respectively, with over 94% identity between each pair of homoeologues. The TaPIL2 A, B and D homoeologues encode proteins with 486, 447 and 486 amino acids, respectively, and the homoeologues share at least 85.5% identity between each pair of homoeologues. The TaPIL3 A homologue encodes a protein of 352 amino acids, and the B and D homoeologues both encode proteins of 361 amino acids. The homoeologues of TaPIL3 share at least 91.9% identity between each pair of homoeologues. Sequence identities are shown in **Table 3.8**.

A comparison of the three TaPIL genes revealed a sequence identity of less than 45% between each pair of TaPIL genes (**Table 3.8**). An examination of the alignment (**Figure 3.4**) revealed that only two regions of the sequences contain a high degree of conservation: a small region at the N-terminus of the proteins, consistent with the location of a putative APB domain, and a larger region toward the C-terminal of the proteins, consistent with a putative bHLH domain. The remainder of the sequence shares little conservation between the *TaPIL* genes, suggesting that the conserved APB and bHLH domains are most likely to be important for function. The consensus sequence of these domains is shown in **Table 3.9**. Both the bHLH and APB domains were identified within the conserved regions of the TaPIL sequences, in the same locations that they occur in other PIL proteins. **Figure 3.5** shows the locations of these domains within the TaPIL sequences. The TaPIL1, TaPIL2 and TaPIL3 protein sequences are shown in Appendix **Figure 7.4, 7.5** and **7.6** respectively

Table 3.8 The sequence identities between the TaPIL1, TaPIL2 and TaPIL3 protein sequences. The sequence identify between each pair of TaPIL sequences is shown. Numbers shaded in grey are identities between homoeologues of the same protein, and white background indicates sequence identities between different TaPIL proteins.

	TaPIL1 5AL	**TaPIL1 5BL**	**TaPIL1 5DL**	**TaPIL2 5AL**	**TaPIL2 5BL**	**TaPIL2 5DL**	**TaPIL3 2AL**	**TaPIL3 2BL**	**TaPIL3 2DL**
TaPIL1 5AL		94.9%	96.9%	30.7%	33.2%	30.9%	41.9%	43.1%	42.3%
TaPIL1 5BL	94.9%		95.7%	31.1%	33.3%	31.1%	43.3%	44.4%	44.0%
TaPIL1 5DL	96.9%	95.7%		30.7%	33.6%	30.9%	42.5%	43.7%	43.0%
TaPIL2 5AL	30.7%	31.1%	30.7%		85.5%	92.7%	24.9%	25.3%	25.3%
TaPIL2 5BL	33.2%	33.3%	33.6%	85.5%		87.5%	26.6%	27.0%	27.0%
TaPIL2 5DL	30.9%	31.1%	30.9%	92.7%	87.5%		24.5%	24.9%	24.9%
TaPIL3 2AL	41.9%	43.3%	42.5%	24.9%	26.6%	24.5%		93.1%	91.9%
TaPIL3 2BL	43.1%	44.4%	43.7%	25.3%	27.0%	24.9%	93.1%		93.4%
TaPIL3 2DL	42.3%	44.0%	43.0%	25.3%	27.0%	24.9%	91.9%	93.4%	

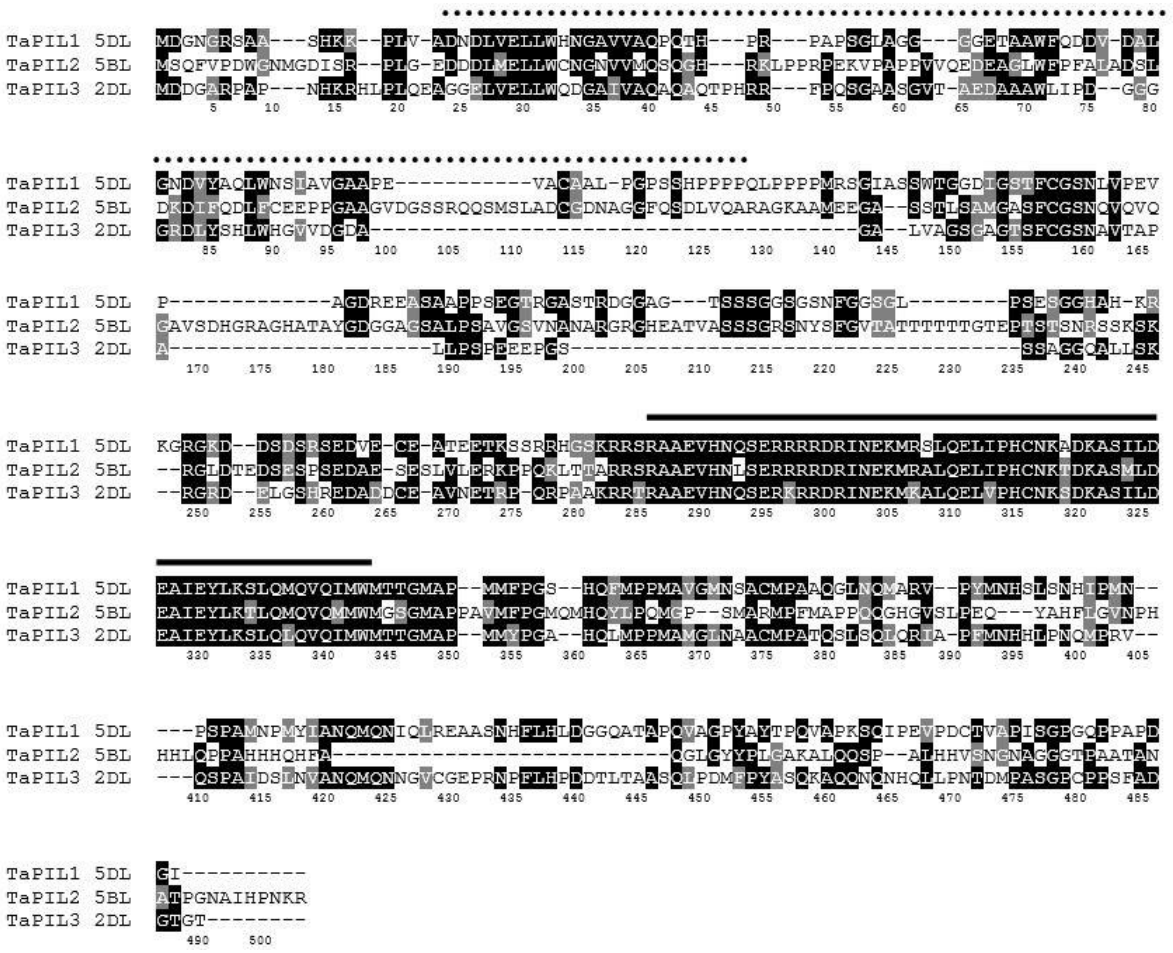

Figure 3.4 Alignment of the TaPIL protein sequences. The TaPIL1 5DL, TaPIL2 5BL and TaPIL3 2DL protein sequences were aligned using the T-coffee tool. The APB motif is labelled with a dotted line above the sequences, and the bHLH domain is labelled with a solid line above the sequences.

Table 3.9 The APB and bHLH consensus sequences. The active phytochrome binding, and basic helix-loop-helix domains described in Khanna et al. (2004) and Heim et al. (2003) are shown.

ACTIVE PHYTOCHROME BINDING (APB)	EDDVVELLWENGQVxxxxQxxxxQxxxxxxxxxxxxxxxxxxxxxxxxxxxxxxxxx QxxxxQEDExxxxxxxxxxxD
bHLH	xxxxHVLAERKRREKLNERFxxLRSLVPxxxxxxxxKMDKASILGDxIxYLKxLxxKVxEL

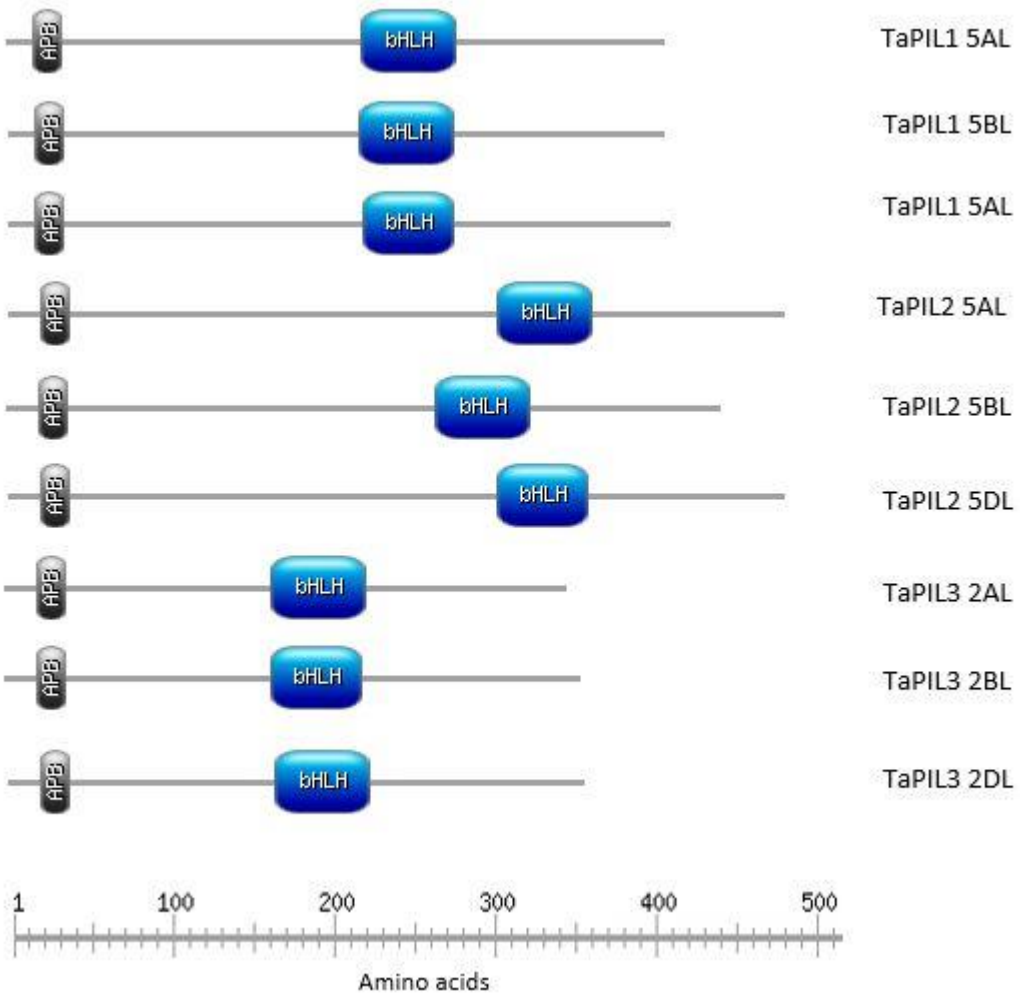

Figure 3.5. Domain positions within the TaPIL sequences. The positions of the highly conserved region of the putative APB and bHLH domains within the TaPIL sequences were identified, and shown diagrammatically. The APB appears at the extreme N terminal of all the TaPILs, labelled in grey. The bHLH domain occurs at the C terminal end of each protein, labelled in blue.

3.2.2.1 The APB domain

An APB consensus sequence was identified by Khanna et al. (2004) from an alignment of 12 *Arabidopsis* bHLH proteins, including the *Arabidopsis* PIFs 1-6. This consensus sequence was compared to the TaPIL sequences in a motif search in Geneious. In all three TaPIL proteins, a similar motif was identified at the N terminus (**Figure 3.6**.). Other than the bHLH domain, this is the only other region that is highly conserved between the wheat PILs, suggesting that it is important for function.

The APB domains identified in the wheat PILs have conserved amino acids with respect to those found in *Arabidopsis*. In *Arabidopsis* the E8, L9, G14 and Q15 residues marked by an

asterisk in **Figure 3.6**., are the most important for PhyB binding. Three of these residues, the E8, L9 and G14 are conserved in all three PILs. In addition, TaPIL1 and TaPIL2 have conservation of a further six residues compared to the consensus sequence, while TaPIL3 has conservation of only three in addition to the E8, L9 and G14. In the wheat PILs, only the first section of the APB domain appears to be conserved, while the later QxxxxQEDE sequence is not.

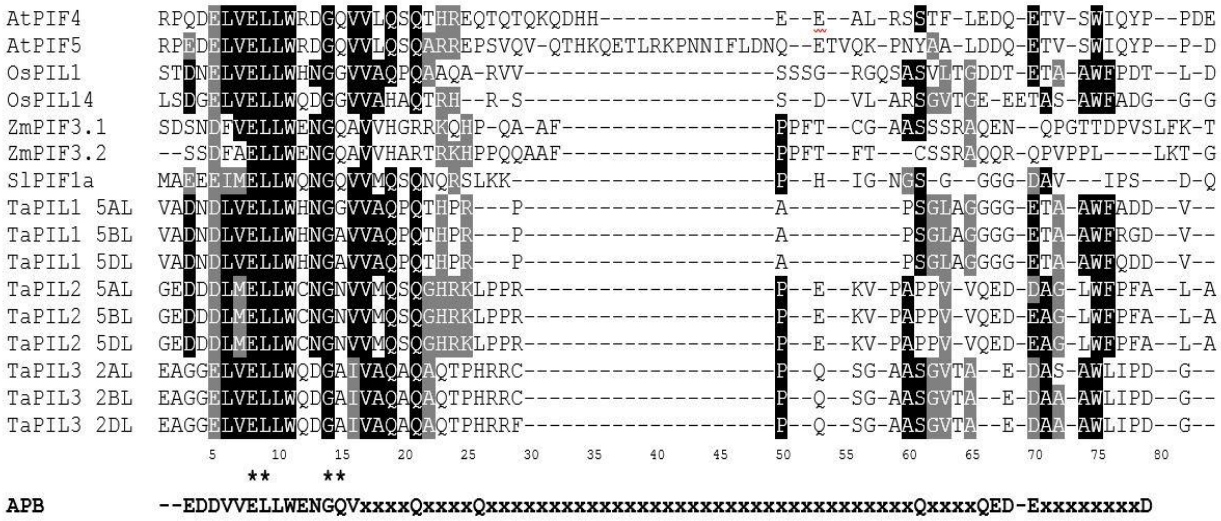

Figure 3.6. The APB motif within the TaPIL sequences. Using the T-Coffee alignment tool, the three homoeologous protein sequences of TaPIL1, 2 and 3, the *Arabidopsis* protein sequences of PIF4 and PIF5, the rice OsPIL1 and OsPIL14, the maize ZmPIF3.1 and ZmPIF3.2 and the tomato SlPIF1a amino acid sequences were compared to the APB consensus sequence domain (shown in bold below the alignment) described in Khanna et al. (2004). Residues shown in reverse are highly conserved among the sequences, and residues shown in grey are similar. The residues of the consensus sequence marked with an asterisk are required for APB function in *Arabidopsis*.

3.2.2.2 The bHLH Domain

A bHLH consensus sequence in plants was described by Heim et al. (2003). However, this is not specific for PIF proteins. The rice OsPIL and Arabidopsis PIF1-7 sequences were aligned to identify a more accurate bHLH consensus sequence, shown underneath the alignment in **Figure 3.7**. This sequence differs from the bHLH consensus described by Heim et al. (2003), but is likely to be more accurate for PIF-like sequences. Residues shown in bold are conserved among all sequences, and residues marked with an asterisk were also shown to be important for function by Heim et al. (2003). This bHLH consensus domain was compared to the conserved region within the homoeologous protein sequences of TaPIL1, TaPIL2 and TaPIL3, along with *Arabidopsis* PIF4 and PIF5 and rice OsPIL1, OsPIL12 and OsPIL14 (**Figure 3.8**). In all TaPIL sequences, a highly conserved bHLH domain was identified, with a high degree of

similarity to the *Arabidopsis* and rice sequences. Between the TaPIL sequences almost all amino acid residues were conserved.

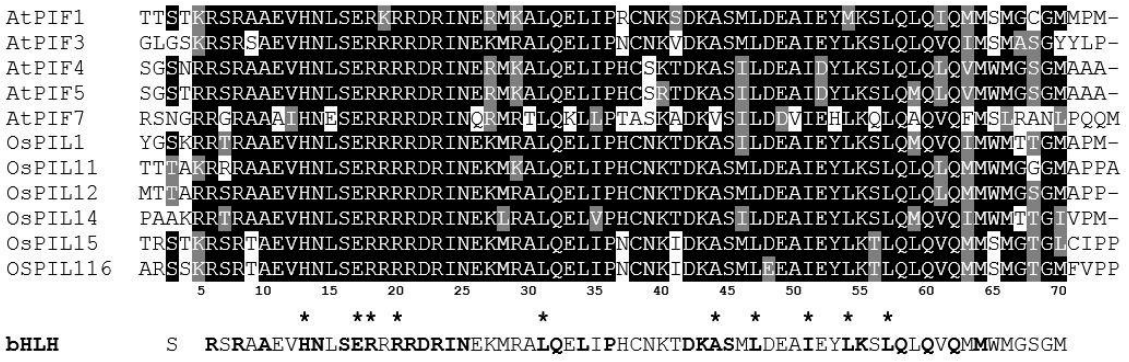

Figure 3.7 The bHLH consensus sequence among rice and Arabidopsis PIF and PIL proteins. The rice OsPIL proteins and the *Arabidopsis* PIF protein bHLH sequences were aligned using the T-coffee programme. Residues that are highly conserved are shown in reverse, and similar residues are shown in grey. The consensus sequence of the bHLH domain from these sequences is shown below the alignment. Consensus residues shown in bold are conserved in all sequences. Residues marked with an asterisk were shown to be important for protein or DNA binding by Heim et al. (2003).

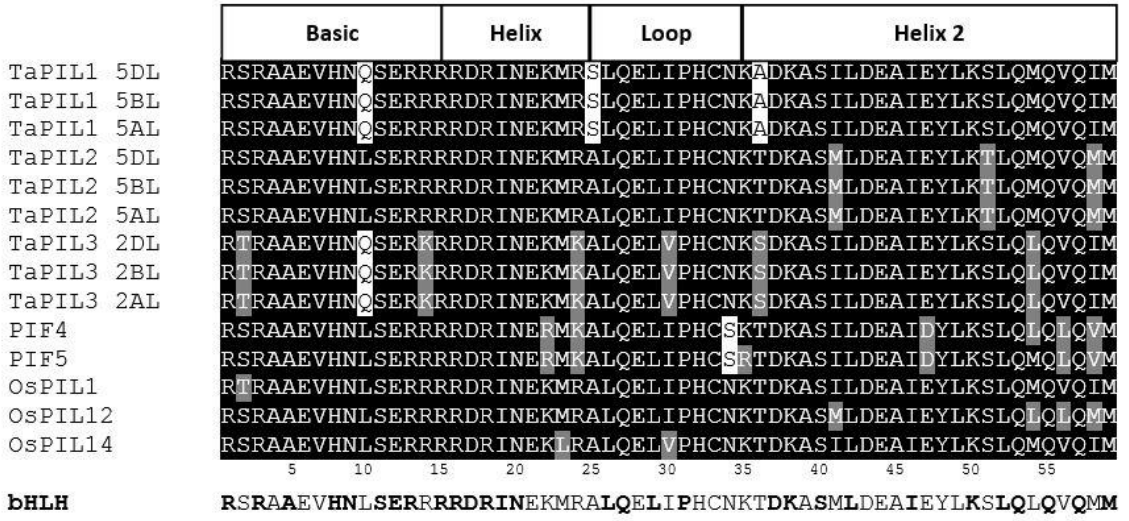

Figure 3.8. A comparison of the bHLH domains from the wheat TaPIL, *Arabidopsis* PIF4 and PIF5, and the rice OsPIL1, OsPIL12 and OsPIL14 protein sequences. The three homoeologous protein sequences of TaPIL1, TaPIL2 and TaPIL3 were aligned with the *Arabidopsis* PIF4 (At2g43010) and PIF5 (AT3G59060), and the rice OsPIL1 (Os03g0782500), OsPIL12 (Os03g0639300) and OsPIL14 (Os07g0143200) protein sequences in a T-coffee Clustal-W alignment. The consensus bHLH sequence is shown below the alignment. Residues which are highly conserved between PIF proteins are shown in bold.

3.2.3 Phylogenetics identify that the TaPILs are related to *Arabidopsis* PIF4 and PIF5.

Once the wheat TaPIL sequences had been identified, phylogenetic analysis was used to identify which TaPIL was the most closely related to OsPIL1, and therefore most likely to regulate stem elongation in the same way. Relationships between the wheat PILs and *Arabidopsis* were also investigated. The *Arabidopsis* PIF proteins have functions that are much better understood than the rice PILs. Therefore, identifying an *Arabidopsis* homologue could provide an insight into the function of the wheat PILs. The TaPIL protein sequences were used in a neighbour joining tree with the *Arabidopsis* PIF sequences, the maize PIF3 sequences, the rice PIL sequences, the maize PIF3.1 and PIF3.2 protein sequences, tomato SlPIF1a, *Physcomitrella* PIF1-4 and *Marchantia* Mp-PIF. A summary of this selection, along with accession numbers can be found in **Table 3.10**. The full protein sequence was used in each case.

Protein sequences were aligned using the Clustal-W BLOSUM alignment tool in Geneious. These alignments were then used to create a neighbour joining tree in Geneious, shown in **Figure 3.9**. The *Arabidopsis* PIF sequences which have been grouped most closely to the TaPIL sequences are PIF4 and PIF5, suggesting that the three TaPIL proteins could be related to PIF4 and PIF5 in *Arabidopsis*. The other *Arabidopsis* PIFs were clustered separately to the wheat sequences, suggesting that these PIF sequences are not related. Each wheat PIL has also been grouped with a different rice PIL. TaPIL2 is grouped with OsPIL11 and OsPIL12, TaPIL1 is grouped with OsPIL1 and TaPIL3 is grouped with OsPIL14, indicating that these rice sequences could be orthologous. This suggests that TaPIL1 is a promising target for regulation of wheat stem elongation. Between the wheat PILs, there appears to be a stronger relationship between TaPIL1 and TaPIL3 than with TaPIL2, which is also supported by the more similar gene structures and sequence identities between TaPIL1 and TaPIL3.

Table 3.10. The Accession numbers of rice, maize, tomato, *Marchantia, Physcomitrella* and *Arabidopsis* PIF protein sequences used to construct the phylogenetic tree shown in Figure 3.9.

Species	Name	Accession Number
Arabidopsis	AtPIF1	AT2G20180
Arabidopsis	AtPIF3	AT1G09530
Arabidopsis	AtPIF4	AT2G43010
Arabidopsis	AtPIF5	AT3G59060
Arabidopsis	AtPIF7	AT5G61270
Rice	OsPIL1	Os03g0782500
Rice	OsPIL11	Os12g0610200
Rice	OsPIL12	Os03g0639300
Rice	OsPIL14	Os07g0143200
Rice	OsPIL15	Os01g0286100
Rice	OsPIL16	Os05g0139100
Maize	ZmPIF3.1	GRMZM2G387528
Maize	ZmPIF3.2	GRMZM2G115960
Tomato	SlPIF1a	Solyc09g063010
Marchantia	MpPIF	Mapoly0039s0059
Physcomitrella	PpPIF1	Pp1s68_85V6.1
Physcomitrella	PpPIF2	Pp1s69_37V6.1
Physcomitrella	PpPIF3	Pp1s84_22V6.1
Physcomitrella	PpPIF4	Pp1s147_126V6.1

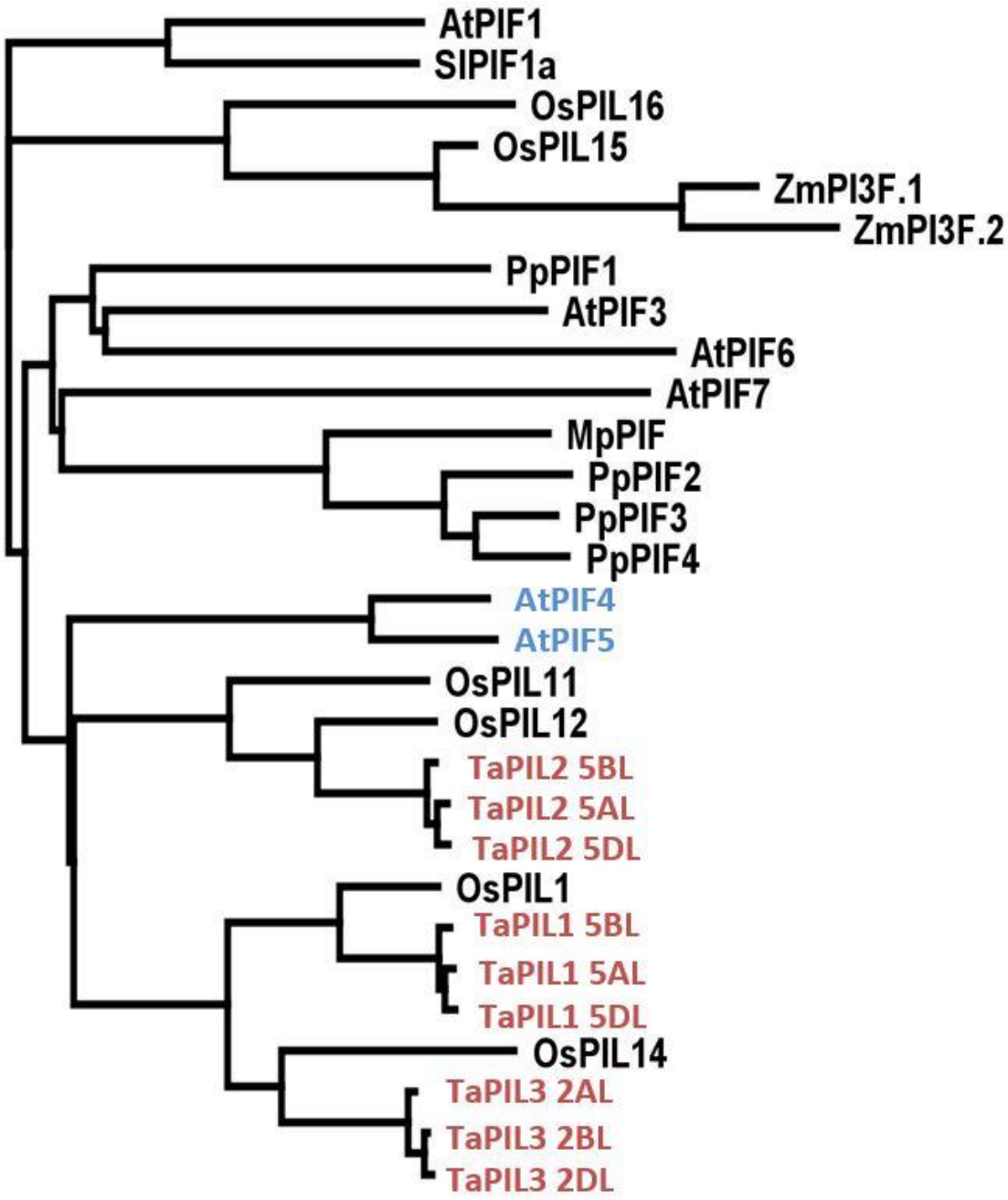

Figure 3.9. The relationship between TaPIL sequences and *Arabidopsis* and rice orthologues. A neighbour joining tree was produced using the wheat, rice, maize, tomato, *Marchantia, Physcomitrella* and *Arabidopsis* PIF and PIL protein sequences. The *Arabidopsis* PIF4 and PIF5 sequences are shown in blue and the wheat PILs in red.

3.2.4 Expression Profiles of the TaPIL sequences.

To give more insight into the functional role for the TaPIL sequences, their expression profile in a variety of tissues was examined, using existing RNAseq data database (International Wheat Genome Sequencing, 2014). This allowed visualisation of the tissues in which each *TaPIL* was most highly expressed, and therefore, the tissues in which the genes are most likely to

function. Files containing every cDNA sequence isolated from the IWGSC and the TGACv1 database were used as templates for RNAseq mapping. In each case the RNAseq reads from the Choulet database (International Wheat Genome Sequencing, 2014), which includes RNAseq reads from five different tissues (root, leaf, stem, spike and grain) at three different developmental stages of Chinese Spring, were used. The reads were mapped using the BWA-MEM tool in Galaxy, which resulted in fragments per kilobase per million reads mapped (FKPM) values for each gene. The FKPM value refers to the number of RNAseq reads which map to an exon sequence. The higher the FPKM value the more highly expressed this sequence is.

The *TaPIL1* homoeologues were extracted from the results in each case. The 5DL homoeologue was absent from the IWGSC cDNA file, and the 5AL homoeologous sequence was absent from the TAGACv1 cDNA file. In both cases, the tissue with the highest *TaPIL1* expression level is the leaf. Expression is also present in the stem, spike and grain. However very low levels were detected in the roots.

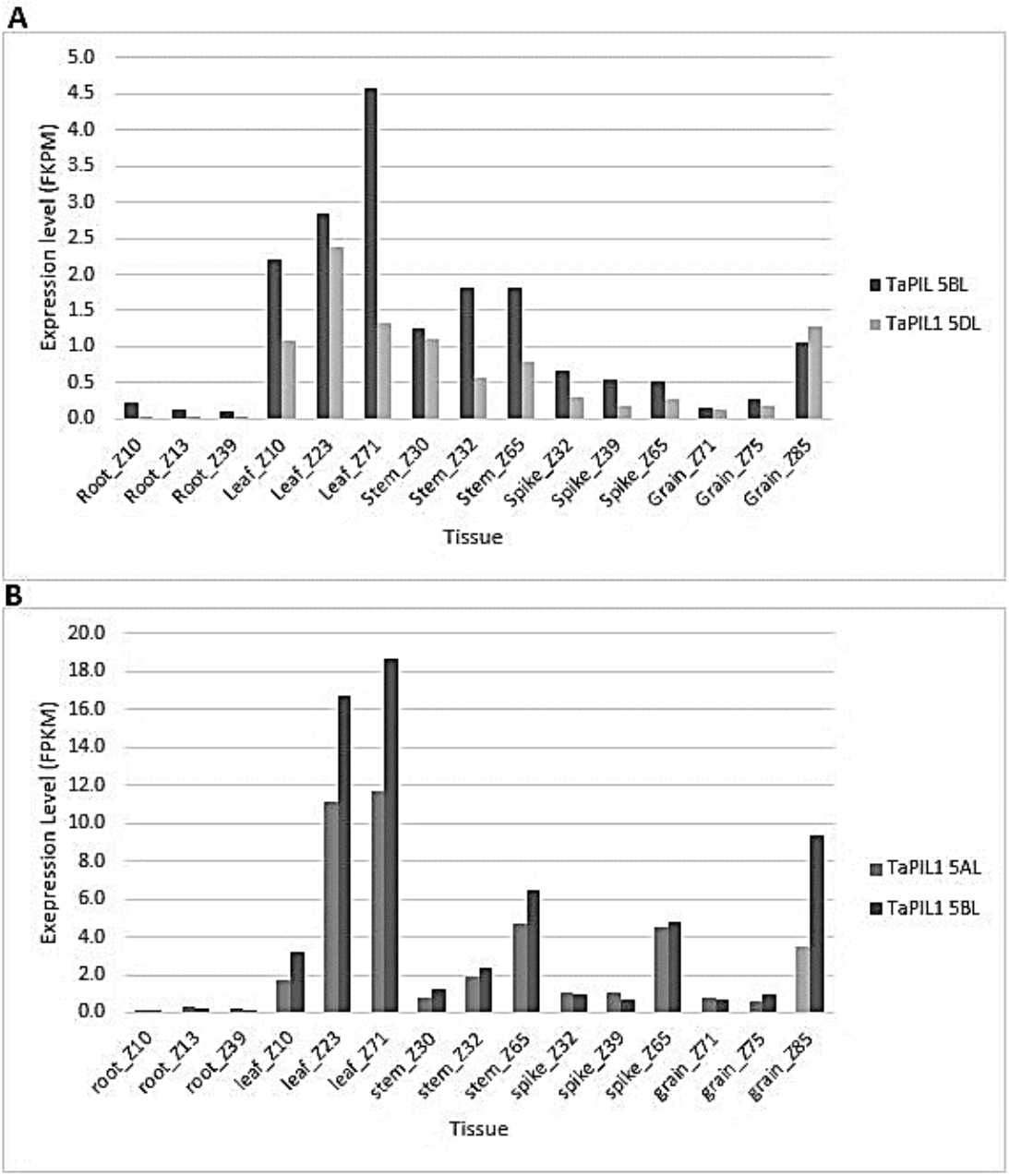

Figure 3.10. Expression levels of TaPIL2. A file containing all TGACv1 cDNAs (A) and IWCSC cDNAs (B) was used as a template for RNAseq mapping with the Choulet (International Wheat Genome Sequencing, 2014) tissue specific dataset, containing RNAseq reads from five different tissues (root, leaf, stem, spike and grain) at three different developmental stages, indicated by the Zadoks scale (Z) number indicated in each tissue. Reads were mapped using the BWA-MEM function in Galaxy. FKPM values for each gene are shown for each tissue.

The TaPIL2 homoeologous sequences were also extracted from both data-sets. The 5AL homoeologue is not present in the IWGSC database, and is therefore not present in the analysis. In both databases, the TaPIL2 sequences are most highly expressed in the leaf. Expression is also present at higher levels in the stem and grain. Lower levels of expression were detected in the spike. Root tissue showed very low levels of TaPIL2 expression.

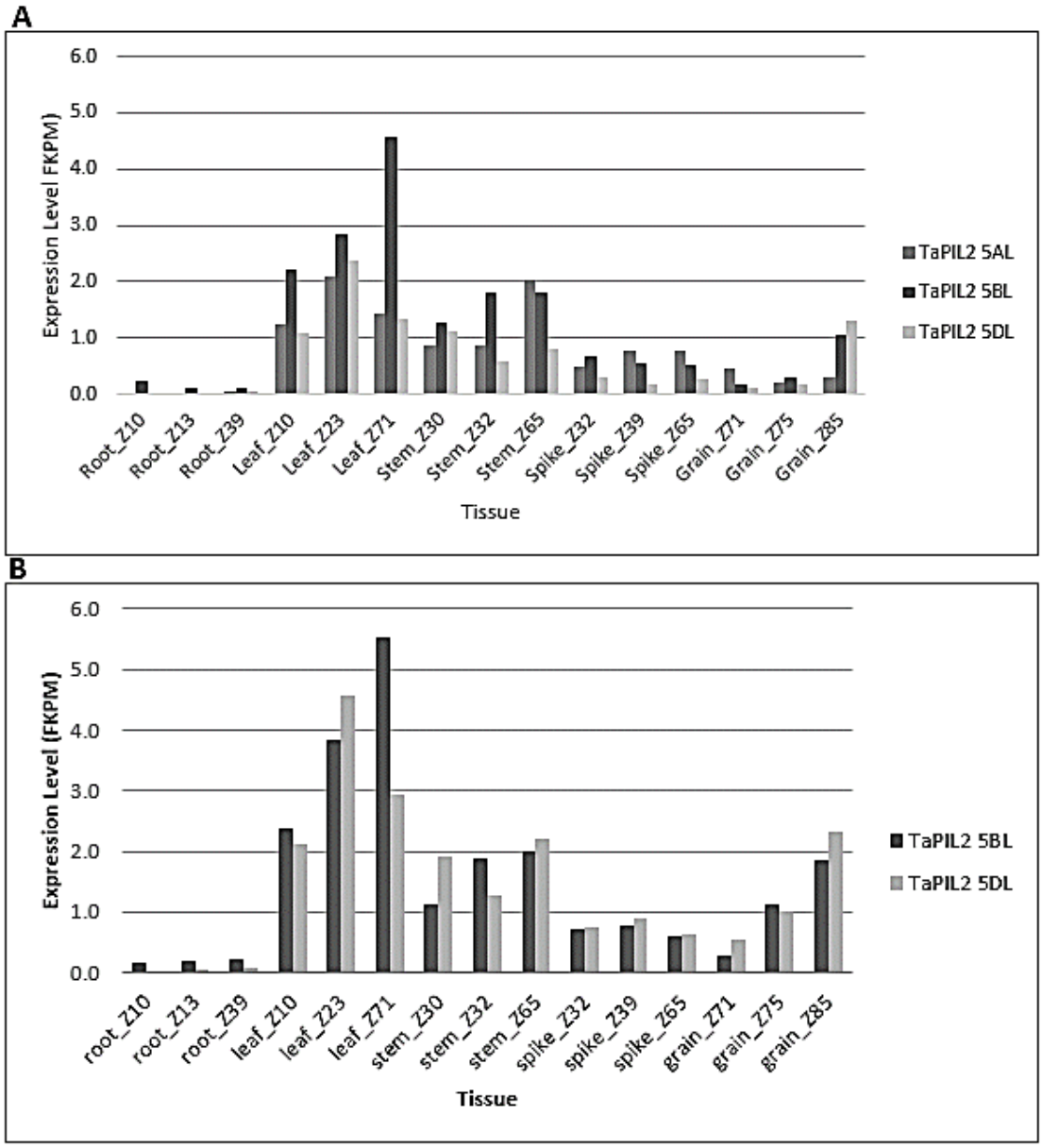

Figure 3.11 Expression levels of TaPIL2. A file containing all TGACv1 cDNAs (A) and IWCSC cDNAs (B) was used as a template for RNAseq mapping with the Choulet (International Wheat Genome Sequencing, 2014) tissue specific dataset, containing RNAseq reads from five different tissues (root, leaf, stem, spike and grain) at three different developmental stages, indicated by the Zadoks scale (Z) number indicated in each tissue. Reads were mapped using the BWA-MEM function in Galaxy. FKPM values for each gene are shown for each tissue.

The *TaPIL3* homoeologous sequences were extracted from both datasets. There are more discrepancies between the way the RNAseq reads mapped to the *TaPIL3* sequences from the IWGSC and TGAC datasets, than there were for either *TaPIL1* or *TaPIL2*. In the TGACv1 dataset, the *TaPIL3* 5DL homoeologue appears to have much higher expression than the other homoeologues, whereas the IWGSC dataset shows similar expression profiles for the three homoeologues.

The distribution of expression amongst the tissues is also different in the two datasets. In the TGACv1 dataset, expression is highest in leaf tissue, whereas the IWGSC dataset shows highest expression in grain and stem. The IWGSC data also suggests that *TaPIL3* is expressed in roots at similar levels to other tissues, whereas expression in roots is shown as very low using the TGACv1 data. Taken together, these data suggest that *TaPIL3* is expressed at high levels in leaf, stem and spike tissue, with possible high expression in the grain, and some expression in roots.

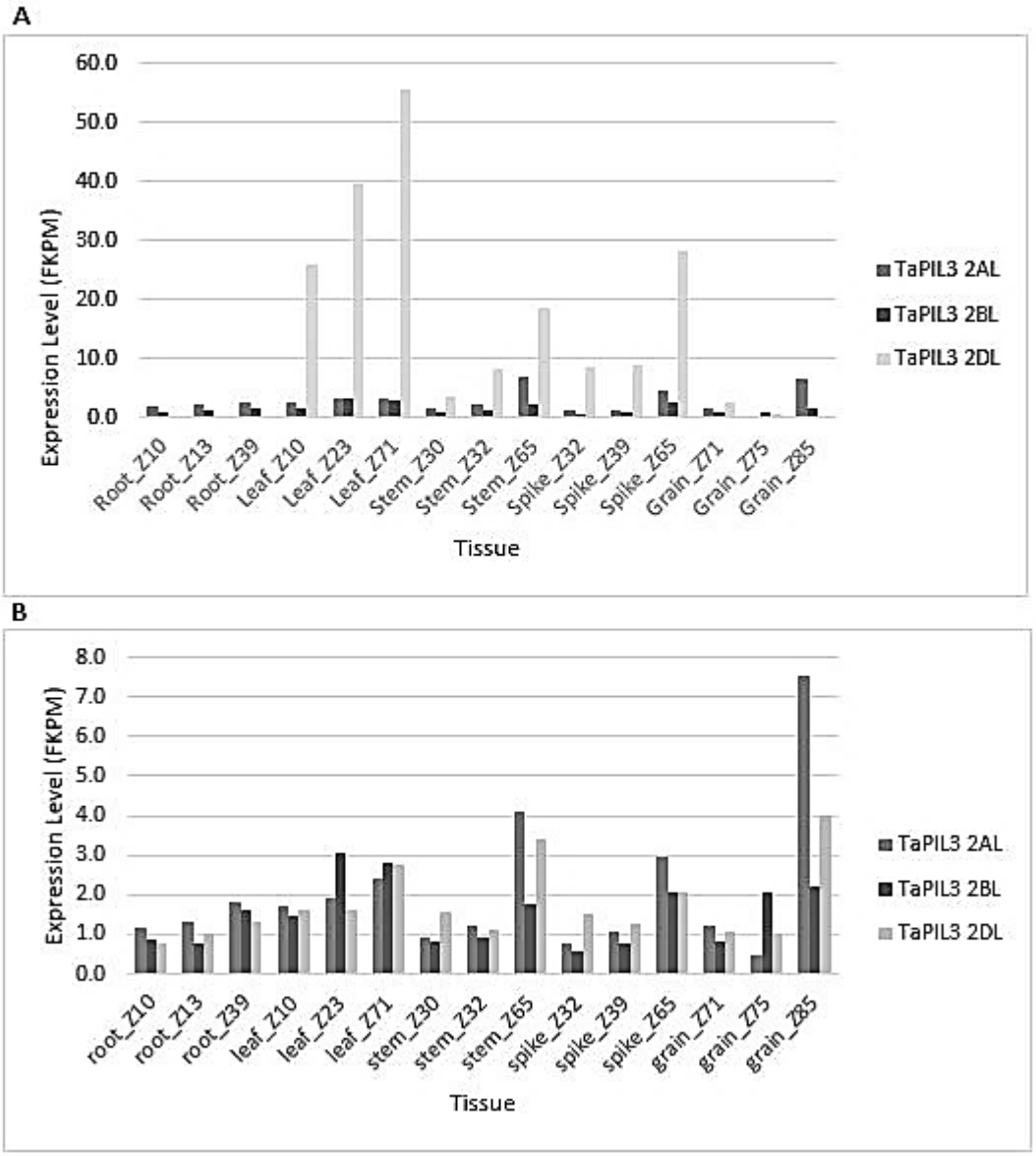

Figure 3.12 Expression levels of TaPIL3. A file containing all TGACv1 cDNAs (A) and IWCSC cDNAs (B) was used as a template for RNAseq mapping with the Choulet (International Wheat Genome Sequencing, 2014) tissue specific dataset, containing RNAseq reads from five different tissues (root, leaf, stem, spike and grain) at three different developmental stages, indicated by the Zadoks scale (Z) number indicated in each tissue. Reads were mapped using the BWA-MEM function in Galaxy. The resulting data included FKPM values for each gene in each separate tissue.

3.2.5 Cloning of the wheat *PIL* cDNA sequences

To confirm the *TaPIL* sequences in the Cadenza background used in this study and to clone *TaPIL*s for overexpression studies, a PCR approach was taken to obtain the full-length cDNAs. A cDNA template was used so that the amplified sequence would be coding exon sequence only, which is easier to amplify, and more useful for future cloning. Two sets of primers were designed for each *TaPIL* gene, one set to amplify the full-length cDNA, and another set to amplify a smaller 3' fragment. The primers for the short segment were designed because amplification of a small product should be easier, and therefore the product could be used to confirm that the cDNA sequence is present in leaf tissue, and the 3' fragment could be used for the RNAi trigger sequence (chapter 5 section 5.2.1.1), while the full-length PCR was being optimised.

3.2.5.1 Amplifying *TaPIL1, TaPIL2* and *TaPIL3* from leaf tissue

Primers to amplify a 3' 400 bp 3' fragment of *TaPIL1* were designed. The 5' forward primer TaPIL1 F2 anneals at around 800 bp downstream of the start codon, and the reverse primer, TaPIL1 R binds the final 20 bp at the 3' end of the coding sequence. PCRs were performed using cDNA from leaf tissue isolated from 3-week old plants of the wheat variety Cadenza. This tissue and stage was chosen as this is when the TaPILs are consistently highly expressed.

This fragment of the *TaPIL1* sequence was successfully amplified from wheat leaf cDNA as shown in **Figure 3.13**. Sequencing of the PCR products confirmed that they were successful amplifications of the 3' *TaPIL*1 sequence (**Figure 3.14**). Comparison with the IWGSC, TGACv1 and W7984 *5DL* sequences revealed only 3 base pair changes within the PCR product, which could be down to either varietal change between Cadenza and Chinese Spring, or due to sequencing error.

The TaPIL1 R primer was used also with another F primer: TaPIL1 F that binds to the first 20 bp of the *TaPIL1* sequence, to allow amplification of the full-length sequence. Additional forward primers, TaPIL1 F3 and TaPIL1 F4 and TaPIL1 F5 were also designed to amplify 550 bp, 650 bp and 1 kb products respectively. Primers were also designed to anneal to the 5' and 3' UTR, called TaPIL1 UTR F and TaPIL1 UTR R (**Figure 3.15**)

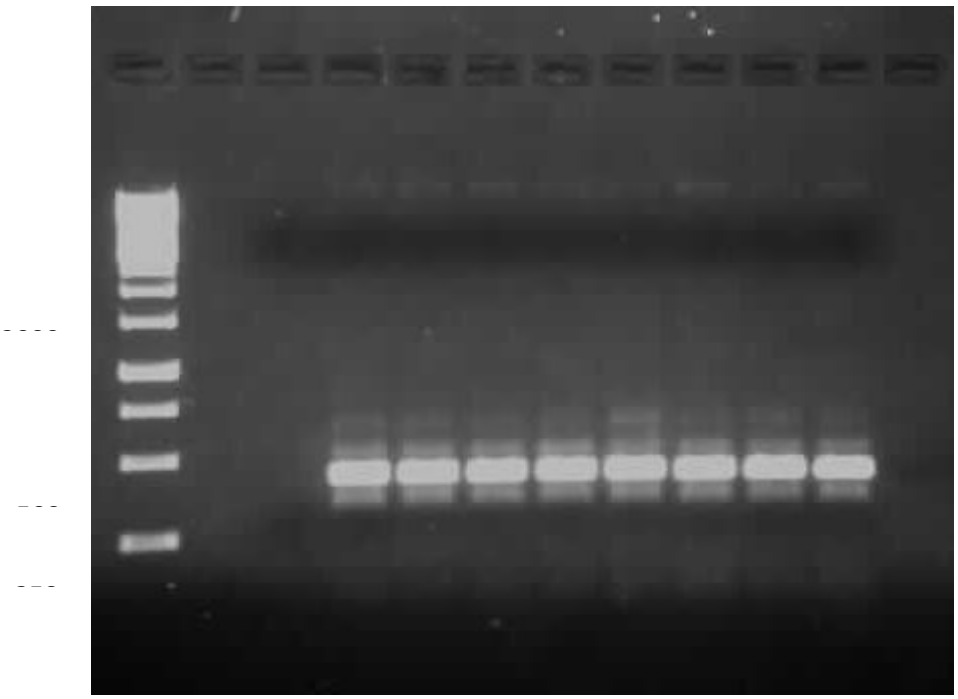

Figure 3.13. Amplification of a 3' fragment of *TaPIL1*. A 400-bp 3' fragment of *TaPIL1* was amplified using PCR and run on an electrophoresis gel. The PCR products were run in lanes 4-11, against a 1 kb ladder shown in lane 1. Lane 3 contained a water negative control. Lanes 4-11 contain wheat leaf cDNA.

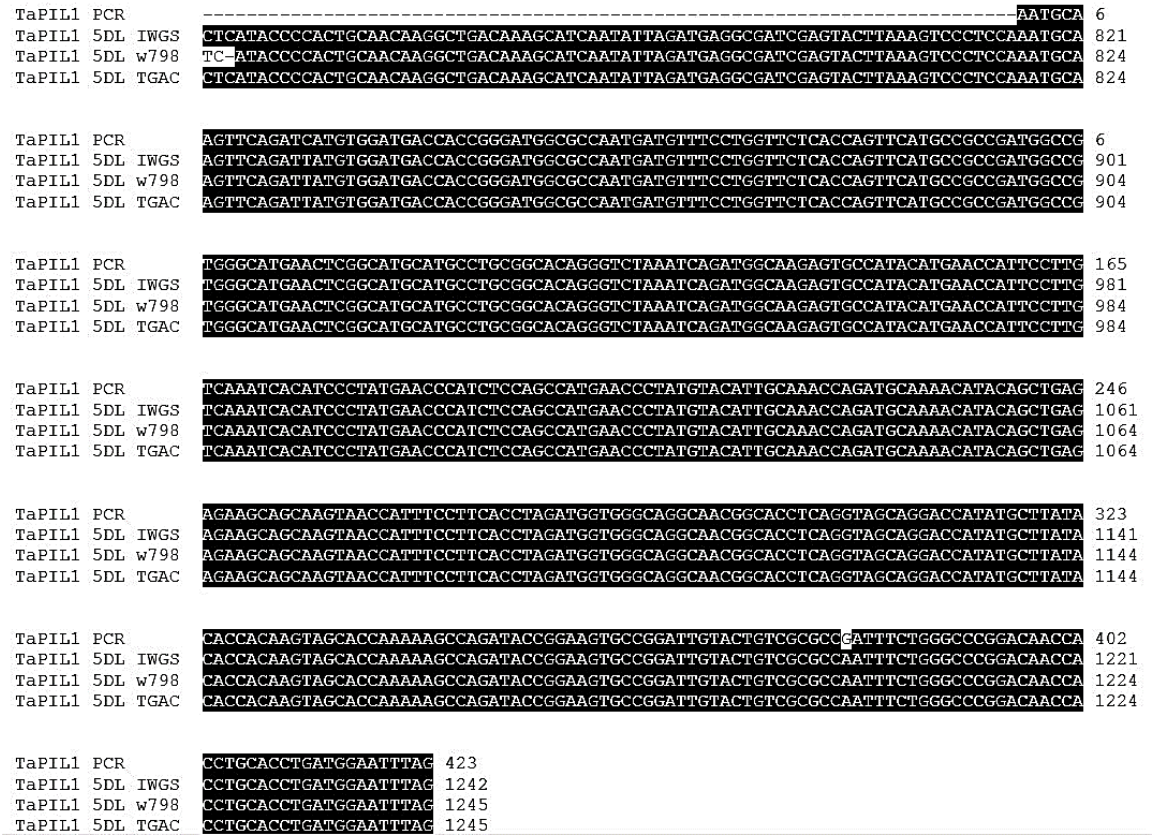

Figure 3.14 Sequence of the *TaPIL1* 3' PCR product. The purified PCR product shown in **Figure 3.13** was sequenced. The sequencing data was aligned with the IWGSC, TGACv1 and W7984 *TaPIL1 5DL* sequences using T-coffee. Identical residues are shown in reverse.

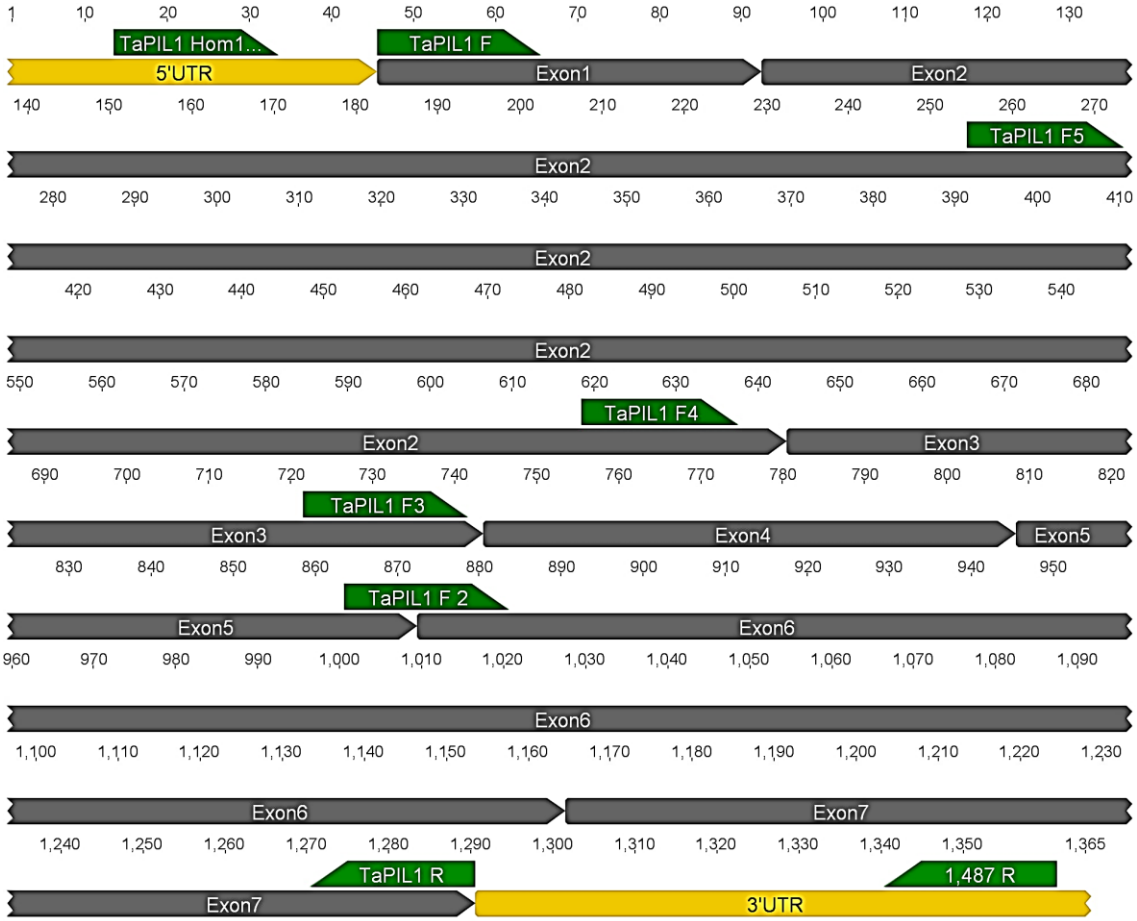

Figure 3.15 Primer binding positions within the *TaPIL1* sequence. Primer binding positions are marked onto the coding sequence of *TaPIL1*. Exon positions are shown in dark grey, untranslated regions (UTR)s are shown in yellow and primer positions are marked in green.

Primers were designed to amplify the full length *TaPIL2* sequence, with the 5' forward primer, TaPIL2 F, binding to the first 21 bp of the sequence and the reverse primer, TaPIL2 R, binding to the final 23 bp of the *TaPIL2* sequence. Two more forward primers, TaPIL2 F2 and TaPIL2 F3, were designed to amplify 400 bp and 600 bp 3' fragmented, respectively. Primers were also designed to anneal to the 5' and 3' UTR, called TaPIL2 UTR F and TaPIL2 UTR R (**Figure 3.16**).

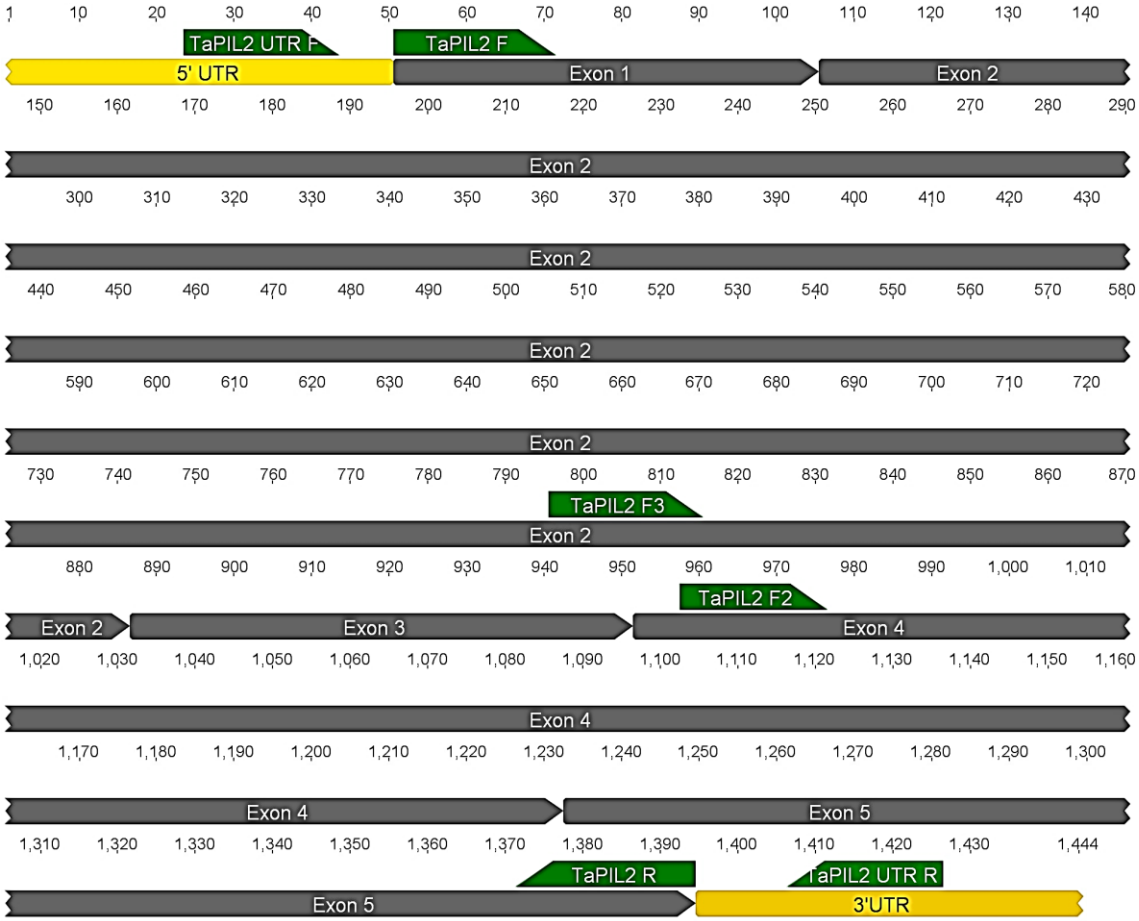

Figure 3.16 Primer positions within the *TaPIL2* sequence. Primer binding positions are marked onto the coding sequence of *TaPIL2*. Exon positions are shown in dark grey, untranslated regions (UTR)s are shown in yellow and primer positions are marked in green.

Primers were designed to amplify the full length *TaPIL3* sequence, with the 5’ forward primer, TaPIL3 F, binding to the first 19 bp of the sequence and the reverse primer, TaPIL3 R, binding to the final 23 bp of the *TaPIL3* sequence. Two more forward primers, TaPIL3 F2 and TaPIL3 F3, were designed to amplify 400bp and 600 bp 3’ fragments, respectively. Primers were also designed to anneal to the 5’ and 3’ UTR, called TaPIL3 UTR F and TaPIL3 UTR R (**Figure 3.17**).

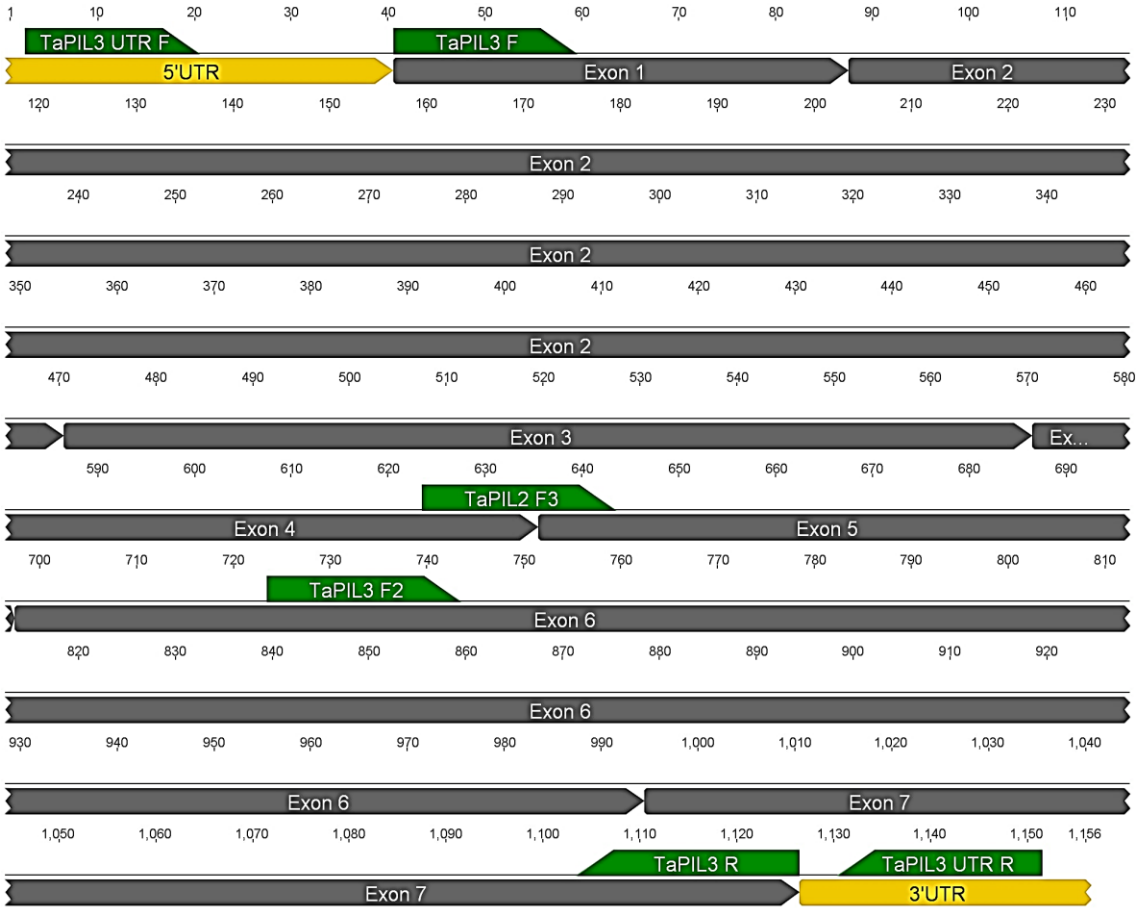

Figure 3.17 Primer positions within the *TaPIL3* sequence. Primer biding positions are marked onto the coding sequence of *TaPIL3*. Exon positions are shown in dark grey, untranslated regions (UTR)s are shown in yellow and primer positions are marked in green.

The full length *TaPIL1*, *TaPIL2* and *TaPIL3*, and the 3' *TaPIL2* and *TaPIL3* transcripts could not be amplified from wheat tissue. Four different polymerases were tried: Phusion, GoTaq, HotShot and Pfu. In each case, alternative reaction buffers were tested. For Phusion reactions the high GC content buffer was trialled, along with the addition of DMSO. For GoTaq reactions the standard and flexi buffer were trialled, and the magnesium content was increased.

PCR conditions were also varied. The denaturation temperature was increased from 95°C to 98°C to increase the chance of denaturation for high GC templates. Each primer pair was run on an annealing temperature gradient ranging from 50-70°C. The extension time was also varied for each primer pair and for each polymerase.

Amplification was also attempted from genomic DNA extracted from Cadenza leaf and immature floral tissues. However, none of these strategies enabled the full length *TaPIL* products, or the *TaPIL2* and *TaPIL3* 3' products to be amplified. It is unclear why PCR

amplification of the three wheat TaPIL sequences was not achievable. It is possible that the difficulties were due to the high GC content of wheat genes. The homoeologues of *TaPIL1*, *TaPIL2* and *TaPIL3* have GC contents of approximately 63%, 68%, and 62%, respectively. These GC contents are high enough to cause problems such as high melting temperature and formation of secondary structures.

3.2.5.2 Synthesis of *OsPIL1*

Because of the difficulties in amplifying the full-length wheat *PIL* sequences, it was decided that the full length *OsPIL1* sequence should be synthesised and used in an overexpression construct in wheat, to investigate the effect of *OsPIL1* overexpression on wheat stature.

The *OsPIL1* cDNA sequence (Os03g0782500) was synthesised. Restriction sites *Nco*I and *Eco*RV were chosen to flank the *OsPIL1* sequence at the 5' and 3' ends respectively, which would allow cloning into Gateway vectors and the overexpression vector. To allow detection of OsPIL1 in the overexpression lines, the protein was tagged with a c-myc tag. The c-myc-tag is an antibody epitope of eleven amino acids (EQKLISEEDL) which can be fused to proteins of interest and confer detection by the 9E10 immunoglobulin antibody (Terpe, 2003). The c-myc tag can be attached either to the N or C terminal of the protein. In the case of OsPIL1, the C terminal was chosen (**Figure 3.18**), as this terminal is the furthest from either the APB or bHLH domain. The c-myc-tag has been used previously to tag PIF proteins in *Arabidopsis*, and the c-myc-tag had no effect on PIF function (Park et al., 2004). For this reason, it would not be expected that the c-myc-tag would have any effect on function.

NcoI

CCATGGATGGCAATGCGAGATCGGCGGCGAATCAGACGAAGCAAATCGTCACGGACAACGAGC 64

TGGTGGAGCTGCTATGGCACAACGGCGGCGTCGTGGCGCAGCCGCAGGCGGCGCAGGCGAGG 126

GTCGTCTCCTCCTCCGGCCGCGGCCAGAGCGCCAGCGTGCTCACCGGCGACGACACGGAGACCG 189

CCGCGTGGTTCCCGGACACCCTCGACGACGCGCTGGAGAAGGACCTCTACACGCAGCTCTGGCG 254

CAGCGTCACCGGCGACGCGTTCCCGGCGGCCGCGGCGGCGGGGCCGAGCTCTCACCACGCTCC 317

GCCGCCGGACTTGCCGCCCCCGGCGGCGAGGCCGCCGATGAGGAGCGGCATCGGGTCGAGCTG 380

GACCGGCGACATCTGTTCGGCCTTCTGCGGCAGCAACCACATCCCGGAGACGGCGGCGCAGCGC 444

TGCCGGGACGCCGGCGCGGCATTGCCGCCGGAGCGGCCGCGCCGGTCGAGCACCCACGACGGC 507

GCCGGCACGTCGTCGTCGGGCGGCTCCGGCAGCAACTTCGGCGCTTCCGGCTTGCCCAGCGAGA 571

GCGCCAGTGCCCACAAGAGGAAAGGCAGAGAAGATTCAGACAGTCGCAGTGAGGATGCTGAAT 634

GCGAGGCAACCGAAGAGACCAAATCGTCGTCGCGGCGATATGGATCAAAGAGGAGAACTCGTG 697

CAGCTGAAGTTCATAACCTGTCAGAGAGGAGAAGAAGGGATCGGATCAACGAGAAGATGCGCG 760

CATTGCAAGAACTCATACCTCATTGCAACAAGACCGACAAGGCATCTATATTAGATGAAGCAATC 825

GAGTATCTGAAGTCACTCCAAATGCAAGTTCAGATCATGTGGATGACTACTGGGATGGCACCAA 889

TGATGTTCCCTGGTGCTCACCAGTTCATGCCACCAATGGCCGTGGGCATGAATTCTGCGTGCATG 954

CCTGCGGCACAAGGCCTAAGTCACATGTCAAGATTGCCATACATGAACCATTCTATGCCAAATCA 1019

CATCCCTCTAAATTCATCTCCAGCTATGAACCCAATGAATGTTGCAAACCAGATGCAGAACATTCA 1085

ACTGAGAGAGGCAAGCAATCCCTTCCTTCACCCAGATGGCTGGCAAACAGTGCCACCACAGGT 1148

ATCAGGACCATATGCTTCTGGGCCTCAAGTAGCACAGCAAAACCAGATACCGAAAGCGTCAGC 1211

TAGCACTGTTCTGCCAAATTCTGGGGCTGAACAACCACCAACCTCTGATGGAATTGAACAAAAAC 1276

TTATTTCTGAAGAAGATCTGTAGGATATC 1305

Myc EcoRV

Figure 3.18 The *OsPIL1* construct synthesized for expression studies. The full length *OsPIL1* coding sequence was flanked with an *Nco*I restriction site at the 5' end and an *Eco*RV restriction site at the 3' end. A myc tag was added to the 3' end of the sequence before the stop codon. The restriction sites are labelled with a bold line above or below the sequence, and the myc tag is labelled with a dashed line.

3.2.6 Synthesis of the *TaPIL* sequences

The full length TaPIL1, TaPIL2 and TaPIL3 sequences were required for a yeast two-hybrid screen to test their interaction with RhtD1a. The TaPIL1 was also needed, along with the full length OsPIL1 sequence to produce overexpression lines to assess the effect of overexpression on stem elongation. As PCR amplification of full length *TaPIL* cDNA sequences was not successful , these sequences were synthesised. For each *TaPIL* gene, there are three slightly

different homoeologous sequences, one of which needed to be selected for synthesis. In most cases, these differences consist of single base-pair changes, which can lead to amino acid changes. In some instances, the sequence differences are more drastic, for example the TaPIL2 5BL sequence contains a 30-bp deletion not present in the A or D homoeologous sequences, and the TaPIL3 2AL homoeologue contains a 12bp deletion not present in either of the other homoeologues. Not only are the sequences different, but the expression levels of the homoeologues can vary. For this reason, the homoeologue with the highest expression level in leaf and stem tissue was selected in each case, as this homoeologue is likely to be the dominant contributor to the growth phenotype.

3.2.6.1 Synthesis of *TaPIL1*

The expression levels of the A, B and D homoeologues of *TaPIL1* were compared. RNAseq data from two sets of leaf and stem data (International Wheat Genome Sequencing, 2014) were mapped to the three homoeologous sequences. The results were then processed to give a fragments per kilobase per million reads mapped (FKPM) value for each homoeologue, shown in **Table 3.11**. The *TaPIL1 5DL* sequence appears to be the most highly expressed across the four datasets. Restriction sites *Nco*I and *Eco*RV were chosen to flank the *TaPIL1 5DL* sequence at the 5' and 3' ends, respectively. These sites were chosen to allow cloning of *TaPIL1* into appropriate vectors for yeast two-hybrid assays and overexpression. A myc-tag was also added to the 3' end of the sequence, to allow detection of the protein in overexpression lines (**Figure 3.19**).

Table 3.11. Expression levels of *TaPIL1, TaPIL2* and *TaPIL3* homoeologues in leaves and stems. The three homoeologous coding sequences of each *TaPIL* sequence were used as a template for RNAseq mapping with two sets of Chinese Spring leaf and stem data. The results were processed to give a fragments per-kilobase per-million reads mapped (FKPM) value for each homoeologue.

***TaPIL1* homoeologue**	**FKPM value (Leaf Z71 1)**	**FKPM Value (Leaf Z71 2)**	**FKPM value (Stem Z65 1)**	**FKPM Value (Stem Z65 2)**
TaPIL1 5AL	9.46	9.36	9.46	9.36
TaPIL1 5BL	4.76	10.27	10.45	10.27
TaPIL1 5DL	10.04	9.20	10.04	8.92
TaPIL2 5BL	5.81	5.25	5.81	5.25
TaPIL2 5DL	3.02	2.82	3.02	2.82
TaPIL3 2AL	2.39	2.42	2.42	2.39
TaPIL3 2BL	2.55	3.00	3.00	2.55
TaPIL3 2DL	2.64	3.00	3.00	2.64

NcoI

CCATGGACGGCAATGGGAGATCGGCGGCGAGCCACAAGAAGCCTCTCGTCGCGGACAACGACC 63

TGGTGGAGCTGCTGTGGCACAACGGGGCGGTCGTCGCGCAGCCGCAGACGCACCCGAGGCCGG 126

CGCCCAGCGGCCTCGCCGGCGGTGGCGGGGAGACGGCCGCGTGGTTCCAGGACGACGTCGACG 187

CGCTGGGGAACGACGTCTACGCACAGCTCTGGAACAGCATTGCGGTGGGCGCCGCCCCGGAGG 252

TCGCGTGCGCGGCGCTCCCGGGGCCCAGCTCCCACCCTCCCCCGCCGCAGCTGCCGCCGCCGCC 316

GATGCGGAGCGGCATCGCCTCCAGCTGGACCGGGGGCGACATCGGCTCCACCTTCTGCGGCAG 379

CAACCTGGTCCCGGAGGTGCCGGCGGGGGACAGAGAGGAGGCGAGCGCCGCGCCGCCGTCGG 441

AGGGGACGCGCGGGGCGAGCACGCGCGACGGCGGCGCCGGCACCTCGTCGTCCGGCGGGTCC 503

GGGAGCAACTTCGGGGGCTCCGGCCTGCCGAGCGAGAGCGGCGGCCATGCCCACAAGAGGAA 565

GGGGAGGGGCAAAGACGACTCCGATAGCCGCAGCGAGGATGTGGAGTGTGAGGCGACCGAG 626

GAGACCAAATCGTCGAGGCGGCACGGGTCGAAGCGGAGGAGCAGGGCAGCTGAGGTTCATAA 688

CCAGTCAGAGAGGAGGCGAAGGGACCGGATCAACGAAAAGATGCGGTCGTTGCAAGAACTCAT 751

ACCCCACTGCAACAAGGCTGACAAAGCATCAATATTAGATGAGGCGATCGAGTACTTAAAGTCCC 816

TCCAAATGCAAGTTCAGATTATGTGGATGACCACCGGGATGGCGCCAATGATGTTTCCTGGTTCT 881

CACCAGTTCATGCCGCCGATGGCCGTGGGCATGAACTCGGCATGCATGCCTGCGGCACAGGGTC 945

TAAATCAGATGGCAAGAGTGCCATACATGAACCATTCCTTGTCAAATCACATCCCTATGAACCCAT 1011

CTCCAGCCATGAACCCTATGTACATTGCAAACCAGATGCAAAACATACAGCTGAGAGAAGCAGC 1075

AAGTAACCATTTCCTTCACCTAGATGGTGGGCAGGCAACGGCACCTCAGGTAGCAGGACCATAT 1139

GCTTATACACCACAAGTAGCACCAAAAAGCCAGATACCGGAAGTGCCGGATTGTACTGTCGCGC 1203

CAATTTCTGGGCCCGGACAACCACCTGCACCTGATGGAATTGAACAAAAACTTATTTCTGAAGAA 1268

GATCTGTAGGATATC 1283

Myc **EcoRV**

Figure 3.19 The *TaPIL1* construct synthesized for over-expression. The full length TaPIL1 cDNA sequence was flanked with an *Nco*I restriction site at the 5' end and an *Eco*RV restriction site at the 3' end. A myc tag was added to the 3' end of the sequence before the stop codon. The restriction sites are labelled with a bold line above or below the sequence, and the myc tag is labelled with a dashed line.

3.2.6.2 Synthesis of *TaPIL2*

Expression levels of the *TaPIL2* homoeologues were compared to identify which homoeologue of *TaPIL2* to select for synthesis. At the time of synthesis, the TGACv1 annotation was not available, so only the expression of the B and D homoeologues were compared, which were

identified from the IWGSC database. RNAseq data from two leaf and stem data sets were mapped to the *TaPIL2* B and D homoeologues. The FKPM values are shown in **Table 3.11**. Both homoeologues are highly expressed in both datasets; however the 5BL homoeologue appears to be the more highly expressed and was chosen for synthesis. Restriction sites *Bam*HI and *Xho*I were chosen to flank the 5' and 3' ends of the sequence, respectively, to allow cloning into gateway vectors.

3.2.6.3 Synthesis of TaPIL3

Expression levels of the *TaPIL3* A, B and D homoeologues were compared in order to identify which homoeologous sequence to have synthesised. RNAseq reads from two leaf and stem, data sets were mapped to the *TaPIL3* homoeologues. The FKPM values from this analysis are shown in **Table 3.11**. All three homoeologues are expressed at similar levels in both data sets; however, the 2DL sequence is most highly expressed, so this homoeologue was chosen for synthesis. Restriction sites *Bam*HI and *Xho*I were chosen to flank the 5' and 3' ends of the sequence, respectively, to allow cloning into Gateway vectors.

3.2.7 Cloning *OsPIL1*, *TaPIL1, TaPIL2* and *TaPIL3* into gateway vectors

The synthesised products were supplied already cloned into a plasmid. Both *OsPIL1* and *TaPIL1* were supplied cloned into *pUC57*, while *TaPIL2* and *TaPIL3* were supplied in *pEX-K4*. The plasmids containing the synthesised inserts along with the entry vector *pENTR11* were digested with the appropriate restriction enzymes. *pENTR11* was used to allow gateway cloning into the necessary destination vectors for yeast two-hybrid experiments. The products were run on an electrophoresis gel, and the digested bands were extracted.

The digested products were then ligated into the digested *pENTR11* vector using a T4 DNA ligase reaction. The ligation product was then transformed into *E. coli* DH5α cells, and the plasmids from these cells were extracted using a miniprep protocol. The resulting plasmids were analysed by restriction digests to confirm the presence of the inserts, and were then sequenced to confirm their identity.

3.3 Discussion

3.3.1 Identifying three PIF-like genes, *TaPIL1*, *TaPIL2*, and *TaPIL3* within the wheat sequence databases.

The first objective of this project was to identify PIF-like sequences within the wheat genome which could be potential candidates for regulating stem elongation. Sequences with high similarity to *OsPIL1* were of particular interest as putative stem elongation regulators. Three PIF-like genes with similarity to *OsPIL1* were identified from the wheat genome sequence databases: *TaPIL1*, *TaPIL2* and *TaPIL3*. These three sequences all possess the PIF-specific APB domain as well as a bHLH domain, suggesting that they do function as wheat PIF-like proteins. *TaPIL1* has the highest similarity to *OsPIL1*, indicating that this sequence could be a promising target for regulating stem elongation.

The full sequences of the three *TaPIL* genes were obtained primarily from the available sequence databases, rather than by amplification from biological material. Amplification of sequences from wheat is difficult due to the high GC content, and previous projects have experienced difficulties in PCR amplification from wheat (personal communication, Dr. Stephen Thomas, Dr. Andy Phillips). Amplification of the Rht-1 homoeologues from wheat gDNA was complex, and only achieved through amplifying overlapping 5' and 3' fragments (Pearce et al., 2011). The inability to amplify the sequences did cause some doubt as to their validity, and raised questions about their expression levels in vivo. However, their presence in multiple databases, and the RNAseq mapping support the validity of the sequences. All three *TaPIL* genes had at least two of their three homoeologous sequences identified in all three databases, with very few variances in their sequence, which can be put down to differences in the wheat variety used for generating each database. The 3' *TaPIL1* sequence obtained by PCR, was highly similar to the *TaPIL1* homoeologous sequences from the IWGSC, W7984 and TGACv1 sequence databases (The 5DL sequence alignment is shown in **Figure 3.14**), indicating that the sequences from these databases are biologically relevant. In addition, all the TaPIL coding sequences had high FKPM values when used as a template for RNAseq mapping with leaf and stem reads, indicating that these genes are expressed.

Analysis of the *TaPIL* sequences identified from the wheat sequencing databases enabled a high level of confidence in their accuracy. *The TaPIL1 5DL*, *TaPIL2 5BL* and *TaPIL3 2DL* sequences were therefore synthesised and cloned into a gateway vector for use in experiments described in the following chapters.

3.3.2 TaPIL1 is orthologous to OsPIL1, and all three TaPIL proteins are orthologous to *Arabidopsis* PIF4/PIF5.

A phylogenetic analysis of the three wheat PIF-like proteins, TaPIL1, TaPIL2 and TaPIL3, was carried out. The aim of this analysis was to discover which TaPIL was the most closely related to OsPIL1, and therefore most likely to be involved in stem elongation. The *Arabidopsis* PIF sequences were also included in the analysis to ascertain which *Arabidopsis* PIF was the most closely related to the wheat sequences. As the *Arabidopsis* PIF proteins have well characterised functions, identifying *Arabidopsis* orthologues could also give a good indication of function for the wheat PILs.

The TaPIL1 sequence was grouped closely with OsPIL1, suggesting that the genes are orthologous to each other. This data suggests that TaPIL1 is the best candidate for manipulation of stem elongation in wheat. On the basis of published work with OsPIL1, it could be expected that overexpressing or knocking down TaPIL1 expression could lead to a corresponding increase or decrease in stem length, respectively. TaPIL2 and TaPIL3 were grouped with separate OsPIL proteins. TaPIL2 was grouped closely with OsPIL11 and OsPIL12, suggesting that these sequences are orthologous to each other. The TaPIL3 sequence was grouped most closely with OsPIL14, suggesting that these sequences are also orthologous. Less data is available for the function of these rice PILs; however this orthology could indicate a role in de-etiolation in red light for TaPIL2 (Peng, 2012). In terms of the relationship between wheat and rice PILs, the phylogenetic tree suggests that each wheat PIL is orthologous to one or two rice PILs. This indicates that the function of these wheat and rice genes could be conserved between these species. None of the wheat PILs were grouped with the maize, tomato, *Marchantia* or *Physcomitrella* PIL protein families, which makes drawing parallels between the protein functions difficult.

In addition to phylogeny and identification of protein domains, the expression pattern of the *TaPIL* genes was also used to gain more information about their function. Analysis of public RNAseq data ((International Wheat Genome Sequencing, 2014), was used to identify in which tissues the *TaPIL* genes were most highly expressed. The *TaPIL1* homoeologues were most highly expressed in leaf tissue, followed by stem and grain. The *TaPIL2* genes showed a similar expression profile, with the highest level of expression in leaf, followed by stem and grain. The *TaPIL3* expression pattern was more difficult to determine, due to differences in the way the RNAseq data mapped, depending on whether the IWGSC or TGACv1 reference sequences were used. However, expression also seems to be high in leaf, stem and grain.

To determine which *TaPIL* gene has the expression profile most like that of *OsPIL1*, the expression pattern of *OsPIL1* was analysed in various tissues. A public rice gene expression dataset (http://rice.plantbiology.msu.edu/expression.shtml) was used for this analysis (**Figure 3.20**). The results are not directly comparable to wheat, as the tissues represented in the RNAseq data differ, but broad parallels can be drawn. *OsPIL1* is also expressed at a high level in leaf tissue, much like *TaPIL1* and *TaPIL2*. In addition, expression is also detected in the shoot and developing grain which correlates with the expression profiles of all the wheat PILs. The main difference is that this rice expression data does not indicate expression of *OsPIL1* in mature stem, whereas all three wheat PILs are expressed in the stem. This is an unexpected result, as OsPIL1 primarily affects stem elongation, so expression in the stem would be anticipated. However, expression would be expected to be highest in young elongating stem rather than fully extended mature stem. The results indicate that *OsPIL1* has a similar expression profile to all three *TaPIL* sequences, and particularly with *TaPIL1* due to the high level of expression in leaves, supporting the orthologous relationship between *TaPIL1* and *OsPIL1*.

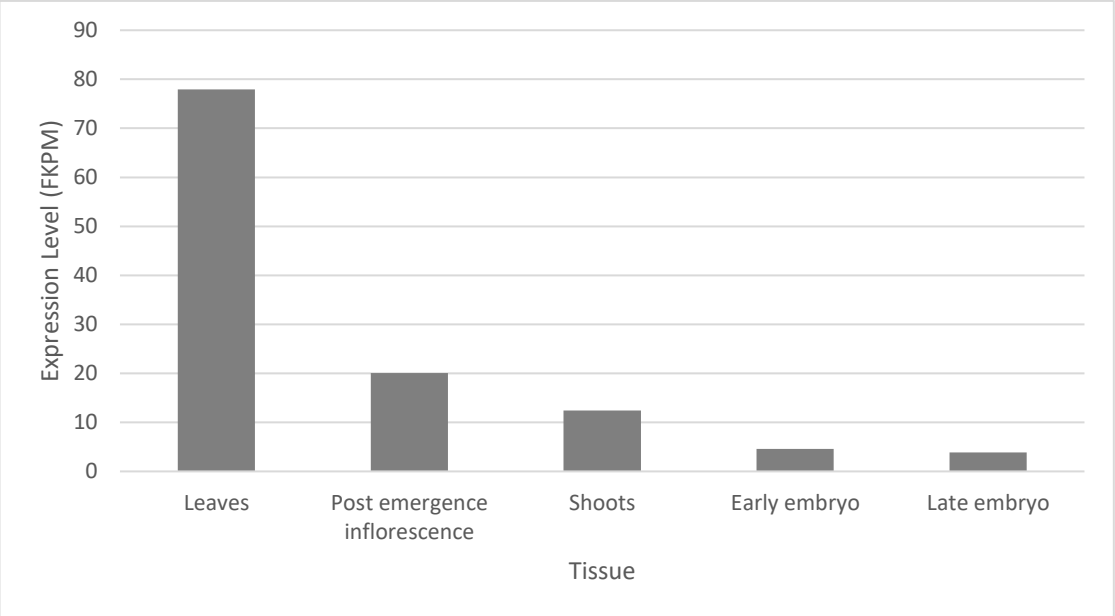

Figure 3.20 Expression levels of *OsPIL1*. The level of *OsPIL1* expression in 5 different tissues from a publicly available rice expression dataset (http://rice.plantbiology.msu.edu/expression.shtml) is shown.

The phylogenetic tree produced with the rice, wheat and *Arabidopsis* PIF and PIL proteins indicated that the three TaPILs could be orthologous to *Arabidopsis* PIF4 and PIF5. If this is the case, the wheat PILs could be expected to play roles in stem elongation, sensitivity to red and blue light, and flowering time (Huq and Quail, 2002b, Kunihiro et al., 2011). These findings are

consistent with those found by Nakamura et al. (2007a), that OsPIL1, OsPIL12 and OsPIL14 are all homologous to *Arabidopsis* PIF4 and PIF5.

In most species, a family of PIL proteins are present which redundantly regulate growth. In *Arabidopsis*, each PIF plays a distinct, yet overlapping role in light response, and only quadruple *pifQ* mutants show a completely constitutively photomorphogenic phenotype (Leivar et al., 2009, Shin et al., 2009). Tomato encodes a family of eight PIL proteins, although the function of only one of these , SlPIF1a, has been characterised. SlPIF1a has been shown to act in a similar maner to Arabidopsis PIFs, being degraded in response to red light, and can restore hypocotyl elongation in dark-grown *pifQ Arabidopsis* mutant seedlings to *pif3/4/5* triple mutant levels (Llorente et al., 2016). *P. patens* also has a family of PIL proteins: PpPIF1-4, which interact with PhyA and PhyB (Possart et al., 2017). In contrast *Marchantia* has only one PIF-like protein, MpPIF which appears to play a similar role to all the Arabidopsis PIFs in light response (Inoue et al., 2016). It is not clear how the functional roles of the wheat PILs will be divided in comparison to those of other species. Each TaPIL could play a distinct role, or the three wheat PILs could all play redundant or overlapping roles in developmental light responses. Each *Arabidopsis* PIF appears to have one or two orthologous PIL genes in rice. The fact that two *Arabidopsis* PIFs are orthologous to three wheat PILs would suggest some overlap of function.

The phylogenetic tree also gives some indication about the relationship between the wheat PILs. The tree suggests that TaPIL1 and TaPIL3 are more closely related to each other than they are to TaPIL2. This could indicate that TaPIL1 and TaPIL3 play a similar functional role. Although TaPIL1 is the only wheat PIL that appears to be orthologous to OsPIL1, TaPIL2 and TaPIL3 will also be selected for further analysis. The overlapping roles of the PIFs in *Arabidopsis* suggest that some redundancy between the TaPILs is likely, and therefore TaPIL2 and TaPIL3 could also have roles in stem elongation, even if they are less important than TaPIL1. In addition, the fact that all three TaPILs have been grouped with *Arabidopsis* PIF4 and PIF5, suggest that these TaPILs could have similar functions to the *Arabidopsis* PIFs, including control of stem elongation. However, the close homology of TaPIL1 with OsPIL1 does define TaPIL1 as the most promising candidate for regulating stem elongation. Therefore, this TaPIL will be the main focus for altering expression.

All three wheat PIL sequences contain the conserved APB and bHLH domains expected in PIF-like proteins. Three of the four residues shown to be essential for APB function in *Arabidopsis* are conserved in the wheat PILs, suggesting that this domain would be functional. The

alignment shown in **Figure 3.6** demonstrates that known phytochrome interacting PIL proteins maize ZmPIF3.1 and ZmPIF3.2 (Kumar et al., 2016) and tomato SlPIF1a (Llorente et al., 2016), have all four conserved residues important for function in Arabidopsis. OsPIL1 also contains a conserved APB domain with three conserved essential residues, like the wheat PILs. However, Todaka et al. (2012) reported that OsPIL1 did not interact with phytochrome B in a yeast two-hybrid assay. This could indicate that OsPIL1 does not contain a functional APB domain. If this is the case, it is possible that the APB domains present in the TaPIL sequences are also non-functional, suggesting that the TaPILs may not act as phytochrome interacting factors. However, OsPIL14 has been shown to interact with rice PhyB (Cordeiro et al., 2016), and only has conservation of three of the four essential residues, the same as OsPIL1, suggesting that the wheat PILs could have functional APB domains. TaPIL3 was shown to be orthologous to OsPIL14 in the phylogenetic analysis, indicating that at least TaPIL3 may have a functional APB domain required for PhyB interaction.

Chapter 4: Identification of RHT-1 interacting proteins using the yeast two-hybrid system

4.1 Introduction

4.1.1 DELLA proteins interact with Phytochrome Interacting Factors

DELLAs are repressors of GA signalling that act by binding to transcription factors and modulating their activity. When GA is present in the cell, DELLAs are degraded, relieving their repressive activity on growth. If GA concentration is low, DELLAs accumulate and can repress GA-regulated growth by interacting with various groups of transcription factors (Li et al., 2016c, Li et al., 2016b, Hong et al., 2012a, Marin-de la Rosa et al., 2014).

One group of transcription factors that have been shown to interact with DELLAs in *Arabidopsis* are the phytochrome interacting factors (PIFs). Both PIF3 and PIF4 have been shown to interact with the *Arabidopsis* DELLA RGA (Feng et al., 2008, de Lucas et al., 2008). This interaction was demonstrated using yeast two-hybrid, bimolecular fluorescence complementation (BiFc), and pull-down assays, and was also shown to be affected by GA levels. The region of the PIF proteins required for this interaction was the bHLH domain. The model of interaction suggested by these results indicated that when DELLAs accumulate in the absence of GA, they bind the PIF proteins via their bHLH domain, preventing them from binding to promoters and regulating transcription of their target genes. Conversely, when GA is present, DELLAs are degraded and PIFs are released, allowing them to regulate transcription (Feng et al., 2008, de Lucas et al., 2008).

This interaction between DELLAs and PIFs has not been demonstrated in any cereals. The interaction between DELLAs and PIFs in Arabidopsis indicates that wheat PILs may regulate stem elongation in response to GA though an interaction with RHT-1. To test this hypothesis, it is necessary to demonstrate the PIF-DELLA interaction in wheat. To this end, a yeast-two-hybrid assay was used to determine whether TaPIL1, TaPIL2 and TaPIL3 can interact with the wheat DELLA protein RHT-D1A. Previous research also suggests that DELLAs are capable of interacting with numerous proteins, and therefore regulating multiple response pathways. This led to the hypothesis that RHT-1 may regulate stem elongation by interacting with multiple binding partners in the wheat stem. This will be investigated by using RHT-1 to screen a library of wheat stem cDNAs.

4.1.2 The yeast two-hybrid system allows the detection of an interaction between proteins

The yeast two-hybrid system, first described by Fields and Song (1989), allows the detection of an interaction between two proteins by exploiting the DNA binding and activation domains of GAL4, a yeast transcription factor involved in positively regulating the expression of galactose-induced genes. The two coding sequences encoding the proteins of interest are cloned into bait and prey constructs containing the DNA-binding domain and activation domain of GAL4, respectively. These constructs are then transformed into yeast. If an interaction occurs between the two proteins of interest, the DNA-binding and activation domains of GAL4 come together and drive the expression of yeast reporter genes. The expression of these genes can be detected by the growth of yeast on media lacking a particular amino acid or a LacZ induced colour change. This system has already been used successfully to demonstrate an interaction between DELLAs and PIFs in *Arabidopsis* as explained above.

4.1.3 Using the yeast two-hybrid system to screen a library of putative interactors

The yeast two-hybrid system can also be used in a library screen to identify proteins that interact with a protein of interest. This approach was first described by Chien et al. (1991), who used the library approach to screen a library of yeast genomic fragments with SIR4, a protein involved in the transcriptional repression of yeast mating type, as the bait. This screen pulled out a plasmid carrying a fragment of the SIR4 gene, which demonstrated that SIR4 produces homodimers. This method has been very successful in the identification of interacting proteins, and has become the method of choice as an alternative to more complex biochemical methods such as protein arrays. In the yeast two-hybrid library screen system, the protein of interest is cloned into the bait plasmid containing the DNA binding domain of GAL4. A cDNA library is prepared and then cloned into the prey plasmid, containing the GAL4 activation domain. Yeast cells are transformed with the bait plasmid and prey library, and grown on media lacking amino acids which can be synthesised if the yeast contains both the bait and prey plasmids. Colonies able to grow after this transformation should contain prey proteins that interact with the bait protein of interest. Proteins from these colonies are then further characterised to confirm putative interactions. This method has been used successfully to identify novel interactors with known proteins. Kim et al. (1997) used this method to screen an *Arabidopsis* cDNA library with IAA1 as the bait, allowing the identification of novel members of the *AUX/IAA* gene family, including IAA24, a protein with similarities to AUXIN RESPONSE FACTOR 1 (ARF1). Niu et al. (2011) used the JASMONATE ZIM-DOMAIN-1 (JAZ-1) protein to screen an *Arabidopsis* cDNA library which allowed the identification of two new bHLH

transcription factors involved in jasmonate signalling. The yeast two-hybrid library system has also been used to identify GA-responsive factors by Robertson (2004), who used the system to identify proteins that interacted with the negative GA response regulator SPINDLY (SPY) in barley. DELLA proteins have also been previously used as bait in yeast two-hybrid library screens. Marin-de la Rosa et al. (2014) used the *Arabidopsis* DELLA GAI to screen a library of transcription factors, in order to identify classes of GA responsive transcription factors such as the ethylene responsive element binding (ERF) family, basic helix-loop-helix (bHLH) and zinc finger transcription factors.

4.2 Results

4.2.1 RHT-1 interacts with TaPIL1, TaPIL2 and TaPIL3 in yeast two-hybrid assays

The rice PIL protein OsPIL1 was shown to positively regulate stem elongation (Todaka et al., 2012). The homology of the TaPIL proteins to this rice protein marked them as promising targets for regulating stem elongation in wheat. The documented interaction between DELLAs and PIFs in *Arabidopsis* (de Lucas et al., 2008, Feng et al., 2008) would suggest that in wheat, RHT-1 may bind to and inhibit the activity of TaPIL1 to prevent stem elongation. Therefore, the next aim of the project was to determine whether or not TaPIL proteins interact with RHT-1, and are therefore downstream regulators of the GA response. The interaction between DELLAs and PIFs has only been shown in *Arabidopsis*, so this interaction must be assessed in wheat.

Interactions between RHT-1 and PILs were tested using the Invitrogen ProQuest™ Two-Hybrid System. This system used the expression of the reporter genes *LacZ* and *HIS3.* The bait and prey plasmids provide the genes required for growth on media lacking leucine and tryptophan, respectively. When using the yeast two-hybrid system, the protein cloned into the bait plasmid containing the DNA binding domain of GAL4 must be tested for self-activation (see **Figure 4.2** in section 4.2.1.1). Self-activation can occur if the protein of interest is able to either non-specifically trans-activate the reporter genes or interact with the nuclear localisation signal (NLS) or GAL4 activation domain present in the prey plasmid. This is a common problem with DELLAs, which may act as transcriptional activators. In other experiments, this problem has been avoided by expressing only the C terminal GRAS domain (de Lucas et al., 2008). The self-activation of the *HIS3* reporter gene is assessed by quantifying the concentration of the HIS3 inhibitor, 3-amino-1,2,4-triazole (3-AT) needed to repress growth on media lacking histidine. All bait constructs used for this project were tested for self-activation before use in specific or library two-hybrid screens.

4.2.1.1 Constructs used in the yeast two-hybrid screen

The full length RHT-D1A protein causes a very high level of self-activation, characterised by strong growth on media lacking histidine when no protein of interest is present in the prey plasmid. For this reason, a C-terminal truncated RHT-D1A product was used in the screen. This truncated RHT-1 protein consists of the C-terminal 401 acids, lacking 217 amino acids from the N-terminus. The truncated product contains the C-terminal domains required for protein-protein interactions, but lacks the N terminal DELLA and HYNP domain. The encoded protein expressed from the yeast bait expression construct begins with the amino acid sequence PALPV at position 218 (**Figure 4.1**).

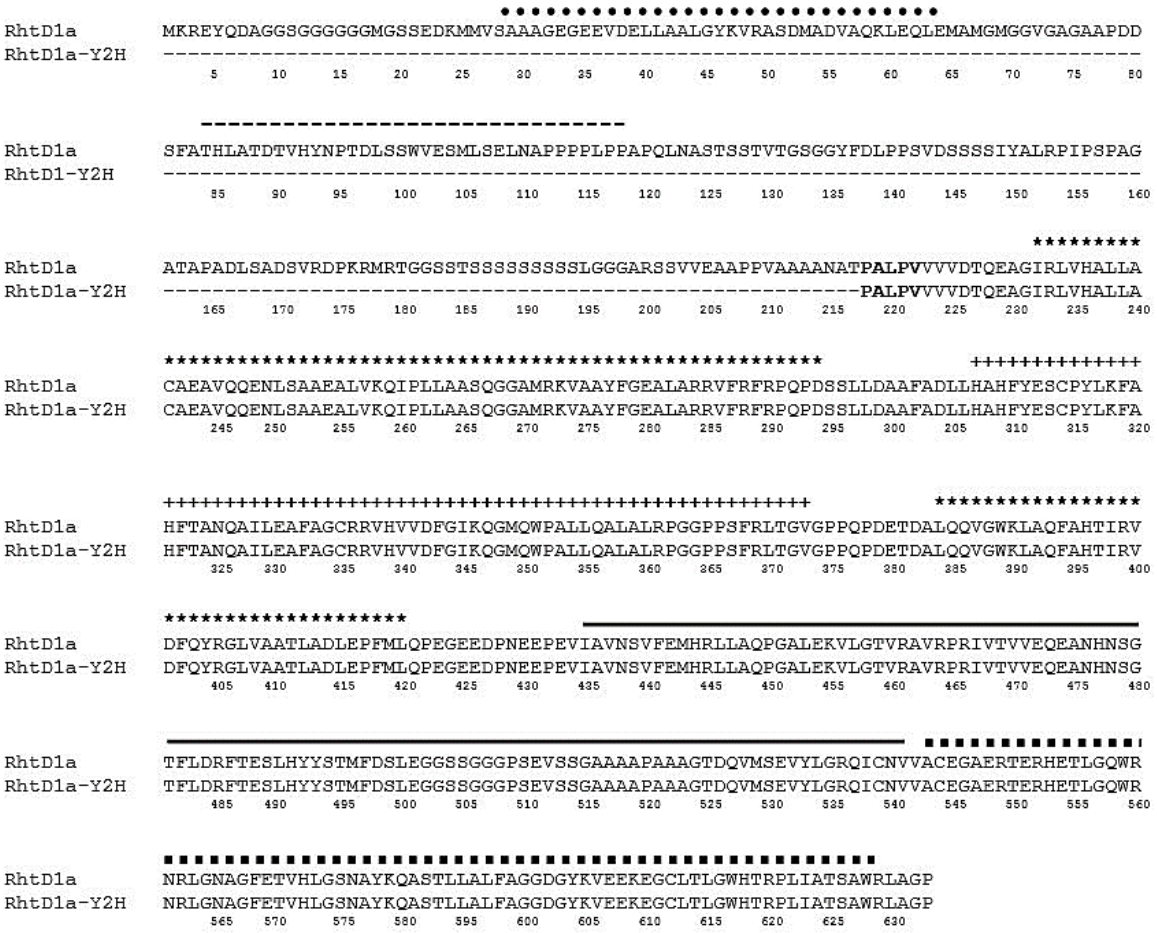

Figure 4.1 Protein sequence of the RHT-D1A yeast two-hybrid construct. The protein sequences of the full length RHT-D1A and the N-terminal truncated yeast two-hybrid RHT-D1A construct are shown. The yeast two-hybrid construct is labelled as RHT-D1a-Y2H, and begins with the residues PALPV (shown in bold). Domains are indicated by lines above the sequence. The DELLA domain is marked by the round dotted line, the HYNP domain is shown by the dashed line, the two leucine heptad repeat domains are marked by a line of asterisks, the VHIID domain is indicated by a line of plus symbols, the PFYRE domain is shown by the solid black line, and the SAW domain is labelled with a square dotted line. The yeast two-hybrid construct begins at the amino acid sequence 218P, 219A, 220L, 221P, and lacks the N terminal DELLA and HYNP domains.

The truncated RHT-D1A encoding sequence was amplified by PCR and cloned into pDEST32 bait plasmid using the LR clonase reaction, and was then transformed into yeast competent cells with an empty pDEST22 prey plasmid. Yeast were also transformed with empty bait and prey vectors, for use as a negative control. For a positive control, yeast was transformed with a bait plasmid containing the *Arabidopsis* DELLA GAI and a prey plasmid containing the *Arabidopsis* auxin response factor (ARF19). These proteins have previously been shown to interact in this yeast two-hybrid system (Dr Stephen Thomas, personal communication). The

Arabidopsis DELLA RGA has previously been shown to interact with ARF8 (Oh et al., 2014), which belongs to the same group as ARF19.

Transformed yeast were spotted onto -Leu/-Trp/-His media containing 3-AT, at increasing concentrations of 0 mM, 10 mM, 20 mM, 30 mM, 40 mM, 50 mM and 100 mM. The yeast strain Mav203 used in these experiments expresses a basal level of *HIS3*, and most bait proteins do contain a level of transcriptional activity. As such, even negative control strains will initiate some transcription of *HIS3*. 3-AT can inhibit *HIS3* in a dose dependent manner, determining the baseline level of 3-AT resistance allows detection of slight increases in HIS3 expression in test strains. The plates were incubated for 48 h and then assessed for yeast growth. The colony containing empty prey with the RHT-D1A bait did show some self-activation at up to 20 mM of 3-AT, but the level of growth was noticeably lower than the positive control, indicating that this construct can be used at a concentration ≥15mM 3-AT (**Figure 4.2**).

Because the RHT-D1A yeast two-hybrid construct had a level of self-activation, the TaPIL sequences were also cloned into the pDEST32 bait plasmid and tested for self-activation. In each case the full-length coding sequence was used. The constructs were tested at the same 3-AT concentrations used for RHT-D1A. TaPIL2 and TaPIL3 caused a very high level of self-activation, up to 50 mM 3-AT, when growth was indistinguishable from that of the positive control, meaning neither TaPIL2 or TaPIL3 could be expressed as bait constructs. However, the TaPIL1 bait construct caused a very low level of self-activation which was not detectable at 20 mM 3-AT. The self-activation tests indicated that both the RHT-D1A bait construct and TaPIL1 bait construct could be used in the screen. Therefore, pDEST22 prey constructs were produced containing the full-length RHT-D1A, TaPIL2 and TaPIL3 sequences. The prey constructs were also transformed into yeast with the empty bait vector to check for self-activation, and spotted into –leu/-trp/-his 3-AT media to test for self-activation, however none was detected in any case (**Figure 4.2**)

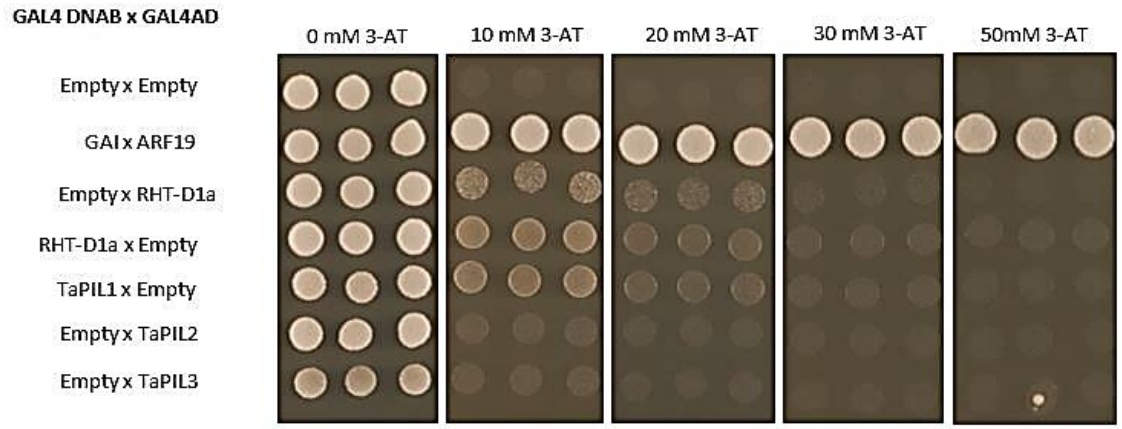

Figure 4.2 Yeast two-hybrid screen detecting the expression of *HIS3*, demonstrating the levels of self-activation. Mav203 competent yeast were transformed with GAL4 DNA-binding bait (GAL4 DNAB) and GAL4 activation domain (GAL4 AD) prey vectors containing proteins labelled under the GAL4 DNAB and GAL4 AD headings at the left of the figure. These strains were spotted onto –Leu/-Trp/-His media containing concentrations of 3-AT ranging from 0-50mM. Strains were spotted onto each plate with three technical replicates shown in each panel of the figure.

4.2.1.2 TaPIL1 interacts with RHT-D1A

Mav203 competent yeast cells were transformed with the TaPIL1 bait plasmid and the full length RHT-D1A prey plasmid. The yeast strains shown in **Table 4.1** were spotted onto -Leu/-Trp/-His media containing concentrations of 3-AT ranging from 0 mM to 50 mM.

Table 4.1 Yeast strains used in the TaPIL1-RHT-D1A yeast two-hybrid screen, indicating the bait and prey constructs present in each strain

Strain	Bait	Prey	
1	Empty	Empty	Negative Control
2	GAI	ARF19	Positive Control
3	Empty	RHT-D1a	Negative control
4	TaPIL1	Empty	Self-activation control
5	TaPIL1	RHT-D1a	Test

At 0 mM 3-AT all five yeast strains were able to grow, including the negative controls. By 10 mM 3-AT, the negative control yeast strains containing the empty bait and prey vectors, and the empty bait and RHT-D1a prey had very low levels of detectable growth, as did the empty prey, TaPIL1 bait self-activation control. The level of growth in the GAI-ARF19 and the TaPIL1-

RHT-D1a strains was strong up to 50 mM 3-AT, and was visibly much higher than the control strains from 10 mM 3-AT (**Figure 4.3**). The level of growth detected in the TaPIL1-RHT-D1a strain was much higher than the RHT-D1a bait self-activation control, and was equivalent to the positive control, suggesting that TaPIL1 and RHT-D1a are interacting.

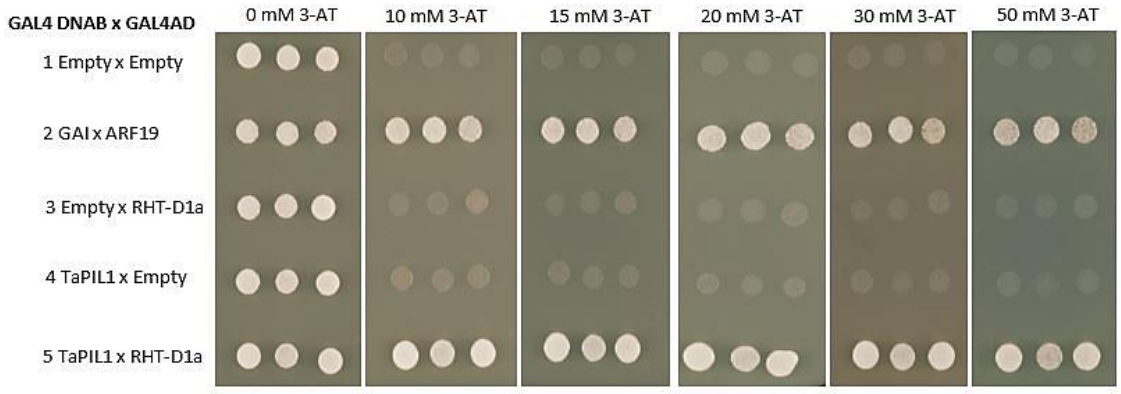

Figure 4.3 Yeast two-hybrid screen demonstrating the interaction between TaPIL1 and RHT-D1a. Mav203 competent yeast were transformed with GAL4 DNA-binding bait (GAL4 DNAB) and GAL4 activation domain (GAL4 AD) prey vectors containing proteins labelled under the GAL4 DNAB and GAL4 AD headings at the left of the figure. Expression of *HIS3* was detected by spotting strains onto –Leu/-Trp/-His media containing concentrations of 3-AT ranging from 0-50mM. Strains were spotted onto each plate with three technical replicates shown in each panel of the figure.

To provide more evidence of the interaction between TaPIL1 and RHT-D1A, the activity of a second reporter gene, *LacZ*, was tested. The same strains as the 3-AT assay, shown in **Table 4.1** were patched onto YPD media, covered with a nitrocellulose membrane, lysed and incubated with X-gal to detect a white to blue colour change, indicative of an interaction. If the *LacZ* reporter gene is expressed, a white-blue colour change will be observed, due to the activity of the *LacZ* gene product, ß-galactosidase on X-gal. This colour change was assessed at 4 h and 24 h during a 24-h incubation.

After 4 h of incubation the empty bait and prey negative control and the empty bait RHT-D1A prey negative control gave no detectable colour change. The TaPIL1 bait with empty prey self-activation control also showed no detectable colour change after 4 h.The GAI bait, ARF19 prey positive control showed a strong blue colour change at this time-point. The TaPIL1 bait, RHT-D1A prey strain displayed a clear blue colour change, similar to that seen in the positive control (**Figure 4.4**). At 24 h, the same results were obtained, but with a stronger blue colour observed in the ARF1-GAI positive control and the TaPIL1-RHT-D1A test strain (**Figure 4.4**). These results support the findings of the 3-AT assay, that TaPIL1 does interact with RHT-D1A in this yeast assay.

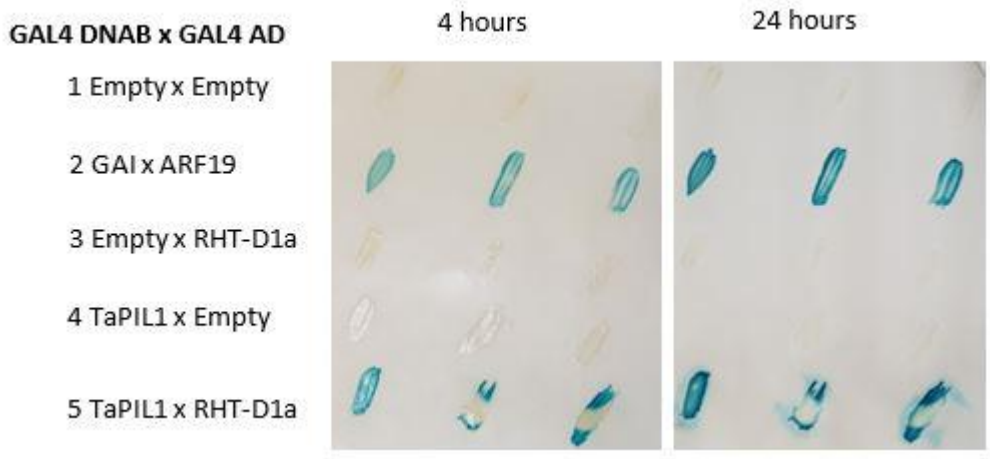

Figure 4.4 TaPIL1 interacts with RHT-D1a in a yeast two-hybrid screen detecting the expression of *LacZ.* Mav203 competent yeast were transformed with GAL4 DNA-binding bait (GAL4 DNAB) and GAL4 activation domain (GAL4 AD) prey vectors expressing proteins labelled under the GAL4 DNAB and GAL4 AD headings at the left of the figure. These strains were streaked onto a nitrocellulose membrane on YPD media in three technical replicates, which are shown in each panel of the figure. The plates were incubated for 24 h, then lysed and incubated with X-gal for 24 h. The white-blue colour change was assessed at 4 and 24 h.

4.2.1.3 TaPIL2 and TaPIL3 Interact with RHT-D1a

Mav203 competent yeast cells were transformed with the RHT-D1a bait plasmid and both the TaPIL2 and TaPIL3 prey plasmids. The yeast strains shown in **Table 4.2** were spotted onto -Leu/-Trp/-His media, containing concentrations of 3-AT ranging from 0 mM to 50 mM.

Table 4.2 Yeast strains used in the RHT-D1a-TaPIL2 and RHT-D1a-TaPIL3 yeast two-hybrid assays, indicating the bait and prey constructs.

Strain	Bait	Prey	
1	Empty	Empty	Negative Control
2	GAI	ARF19	Positive Control
3	Empty	TaPIL2	Negative Control
4	Empty	TaPIL3	Negative Control
5	RHT-D1a truncated	Empty	Self-activation control
6	RHT-D1a truncated	TaPIL2	Test
7	RHT-D1a truncated	TaPIL3	Test

At 0 mM 3-AT all yeast strains were able to grow, including the negative controls. By 10 mM 3-AT, the negative control yeast strains containing the empty bait and prey vectors, and the empty bait and TaPIL2/TaPIL3 prey had very low levels of growth. Growth was detectable in the self-activation control strains containing the empty prey vector and RHT-D1a up to 20 mM 3-AT, as expected from the self-activation tests. The level of growth in the GAI-ARF19 and the RHT-D1a-TaPIL2 strains was strong up to 50 mM 3-AT, and was visibly much higher than the negative controls from 10 mM 3-AT (**Figure 4.5**). The level of growth detected in the RHT-D1a-TaPIL2 and RHT-TaPIL3 strains was much higher than the RHT-D1a bait self-activation control, and was equivalent to the positive control, suggesting that RHT-D1a is interacting with both TaPIL2 and TaPIL3 in these yeast assays.

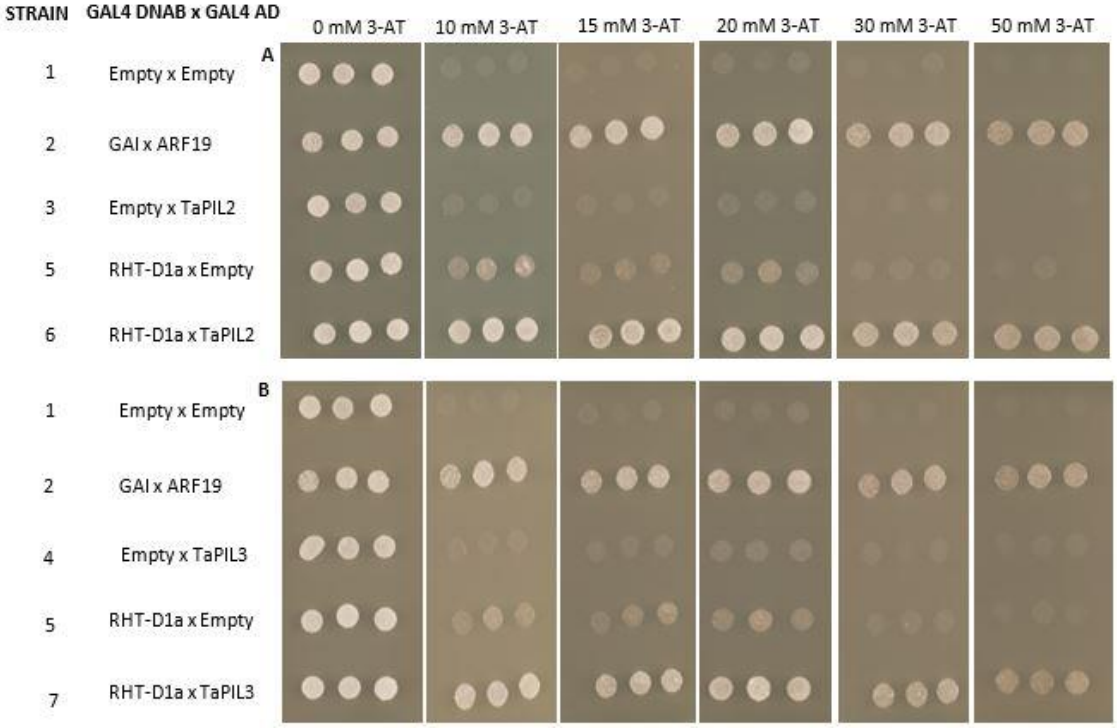

Figure 4.5 Yeast two-hybrid screen detecting the expression of *HIS3*, demonstrating the interaction between RHT-D1a and both TaPIL2 (A) and TaPIL3 (B). Mav203 competent yeast were transformed with GAL4 DNA-binding bait (GAL4 DNAB) and GAL4 activation domain (GAL4 AD) prey vectors containing proteins labelled under the GAL4 DNAB and GAL4 AD headings at the left of the figure. These strains were spotted onto –Leu/-Trp/-His media containing concentrations of 3-AT ranging from 0-50 mM. Strains were spotted onto each plate with three technical replicates shown in each panel of the figure.

To confirm the interaction of RHT-D1a with TaPIL2 and TaPIL3, the activity of the second reporter gene, LacZ, was also assessed. The same strains as the 3-AT assay were patched onto

a nitrocellulose membrane, lysed and incubated with X-gal to detect a white to blue colour change, indicative of an interaction. This colour change was assessed at 4 h and 24 h.

After 4 h of incubation, the RHT-D1a bait empty prey self-activation control showed a slight colour change. The RHT-D1a bait, TaPIL2/TaPIL3 prey strain had a definite blue colour change, stronger than the self-activation control, but weaker than the positive control (**Figure 4.6**). By 24 h, the same results were observed, with a stronger blue colour change in the positive control and test strains (**Figure 4.6**). These results support the findings of the 3-AT assay, that TaPIL2 and TaPIL3 interact with RHT-D1a.

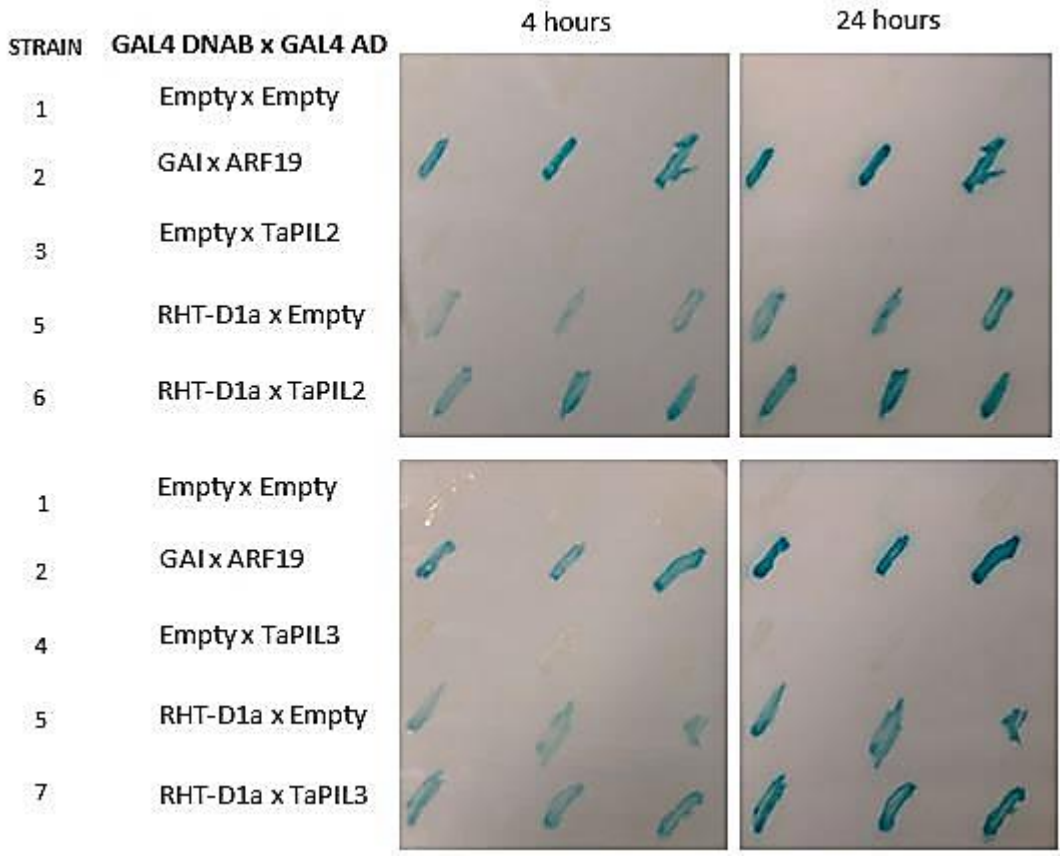

Figure 4.6 TaPIL2 and TaPIL3 interact with RHT-D1a in a yeast two-hybrid screen detecting the expression of *LacZ.* Mav203 competent yeast were transformed with GLA4 DNA-binding bait (GAL4 DNAB) and GAL4 activation domain (GAL4 AD) prey vectors containing proteins labelled under the GAL4 DNAB and GAL4 AD headings at the left of the figure. These strains were streaked onto a nitrocellulose membrane on YPD media in three technical replicates, which are shown in each panel of the figure. The plates were incubated for 24 h, then lysed and incubated with X-gal for 24 h. The white-blue colour change was assessed at 4 and 24 h.

4.3 Identification of putative RHT-D1a interactors using a yeast two-hybrid wheat stem library screen

Along with demonstrating an interaction between RHT-1 and the TaPIL proteins, a further aim of this project was to identify proteins that interact with Rht-1 in the wheat stem. This could allow the identification of further targets which act downstream of RHT-1 in the regulation of stem elongation during the GA response. Identification of such proteins could provide more foci for the specific manipulation of stem elongation, bypassing the pleiotropic effects present in the *Rht-1* mutant lines.

4.3.1 A yeast two-hybrid library screen identified 486 putative RHT-D1a interactors

A yeast two-hybrid screen with the RHT-D1a bait construct described in section 4.1.1, was used to screen a library of prey plasmids containing a cDNA library from the wheat stem. The library was constructed by Dr. Stephen Thomas from elongating peduncle tissue at Zadoc stage Z31 taken from Cadenza plants grown under standard conditions in a glasshouse. The number of clones in the primary library was 30 million, and the average insert size was 1.6 kb. The screen was carried out using 20 mM 3-AT, due to the self-activation activity of the truncated RHT-D1A bait construct described in section **4.2.1.1.**

Mav203 library scale competent cells were transformed with the RHT-D1A bait construct, and the wheat stem prey cDNA library. Transformed cells were grown on –Leu/-Trp/-His 20 mM 3-AT plates for 36 h. At this point all colonies present on the plates were selected and transferred to master plates for further testing and characterisation. This screen identified 486 strains that grew under the selection conditions and therefore contained putative RHT-D1a interactors.

These strains of interest were then tested to confirm their status as legitimate RHT-D1a interactors and eliminate false positives. All 486 strains were patched onto –leu/-trp/-his media with 3-AT concentrations ranging from 10 mM to 50 mM 3-AT, along with a positive control containing the known interactors GAI and ARF19, and a negative self-activation control containing the empty prey plasmid and the RHT-D1a bait. All colonies had a higher level of growth than the self-activation control at all 3-AT concentrations, suggesting that all strains collected from the screen did not grow solely as a result of RHT-D1a self-activation.

The *LacZ* assay was also used to confirm that these 486 yeast strains contain proteins that interact with RHT-D1a. The 486 library yeast strains and control strains were patched onto a nitrocellulose membrane and lysed before incubation with X-gal to detect GUS activity by a

white to blue colour change. All 486 strains had a stronger blue colour change than the self-activation control, indicating that all colonies do contain proteins that interact with RHT-D1a.

4.3.2 Sequencing of the cDNA clones identified in the library screen reveals twelve proteins of interest.

Once strains containing proteins that interact with RHT-D1a were identified, the cDNA inserts were sequenced. Prey plasmids were isolated from yeast colonies using a yeast miniprep protocol. Once isolated, plasmids were used as a template for PCR with primers (pDEST22 F and pDEST22 R) designed to amplify the insert of pDEST22 prey plasmids downstream of the cDNA insert (**Figure 4.7**). PCRs were carried out with GoTaq polymerase, with an annealing temperature of 60°C, an extension time of 1 minute, and a cycle number of 35. To visualise the PCR products, 5 µl of the reactions were separated on an electrophoresis gel. Strains with a single cDNA insert, *i.e*. those with only one detectable band, were then purified and sequenced with the pEXP22 F primer. Plasmids from strains with more than one cDNA clone were transformed into *E. coli* competent cells, from which plasmids were extracted from three colonies per transformation and sequenced, to account for the multiple inserts.

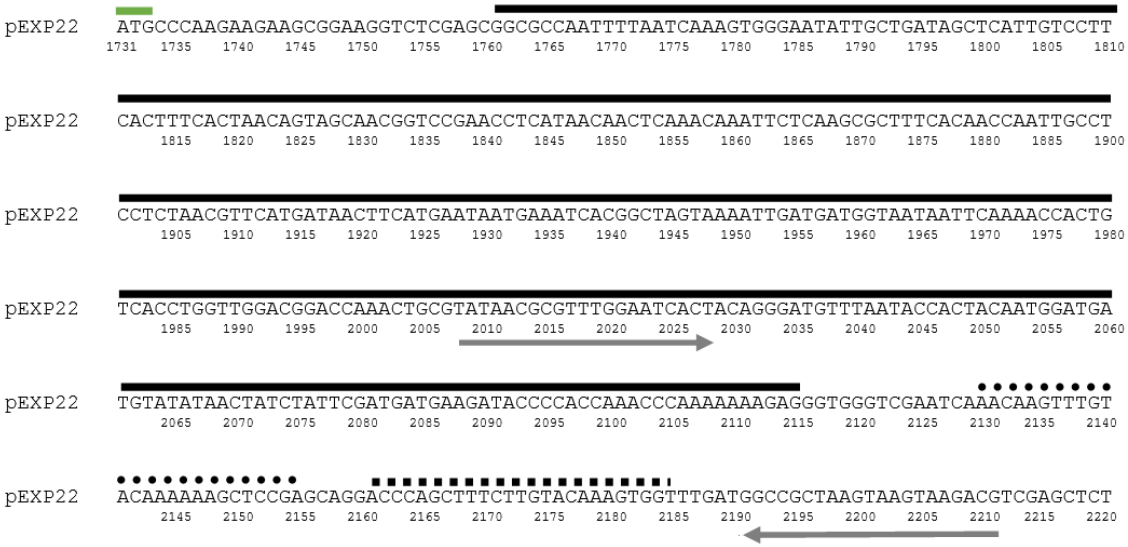

Figure 4.7 The sequence of the *pEXP22* cDNA cloning region. The sequence of the *pEXP22* cDNA cloning region is shown. The ATG start codon is marked by a green solid line, the *GAL4* activation domain is shown by a solid black line, the *aatB1* site is indicated by a circular dotted line and the *aatB2* site is marked by a square dotted line. The cDNA sequence is cloned into *pEXP22* using an LR clonase reaction between the *aatB1* and *aatB2* sites. The forward and reverse primers to amplify the cDNA sequence are marked by grey arrows below the sequence.

In order to identify the cDNA inserts, the sequences were blasted against an *O. sativa* CDS database and the *T. aestivum* TGACv1 cDNA database. Close homologues in the rice database gave an indication of the likely function for each sequence. The TGACv1 database allowed

identification of the wheat cDNAs, and also gave a predicted function for each cDNA based on the protein sequence. The full table of sequenced clones is shown in appendix **Table S.3.** Twelve clones were selected for further characterisation because the encoded proteins already had an interaction with DELLAs documented in Arabidopsis, or because the encoded proteins have a role in hormone or light signalling. The selected clones are shown in **Table 4.3**.

Table 4.3 Clones of interest identified in an RHT-D1A yeast two-hybrid library screen

Library Strain	TGACv1 cDNA	Predicted Role	Rice Orthologue	Function	Number of clones
51	*TRIAE_CS42_2BS_TGACv1_146333_AA0462840*	Rho GTPase-activating 7-like	LOC_Os07g46450	Rho GTPase activation protein (RhoGAP)	2
59	*TRIAE_CS42_4DL_TGACv1_344008_AA1142470*	Probable BOI-related E3 ubiquitin- ligase 3	LOC_Os03g15730	S-ribonuclease binding protein 1	2
65	*TRIAE_CS42_7AS_TGACv1_570423_AA1835500*	Ethylene-responsive element binding	LOC_Os02g54160	Related to AP2 12	3
91	*TRIAE_CS42_5BL_TGACv1_404297_AA1294450*	GATA transcription factor 16-like isoform X2	LOC_Os01g74540	GATA transcription factor 16	1
137	*TRIAE_CS42_5BL_TGACv1_406028_AA1339440*	Squamosa promoter-binding 18 isoform X1	LOC_Os08g41940	Squamosa promoter-binding protein-like	1
143	*TRIAE_CS42_U_TGACv1_642981_AA2125590*	FAR1-RELATED SEQUENCE 5-like	-	-	1
202	*TRIAE_CS42_3AS_TGACv1_210742_AA0678170*	Transcription factor bHLH35-like	LOC_Os04g23550	Basic helix-loop-helix (bHLH) DNA-binding	2
220	*TRIAE_CS42_4AS_TGACv1_307707_AA1022890*	ETHYLENE INSENSITIVE 3-like 1	LOC_Os03g20780	Ethylene insensitive 3 family protein	1
221	*TRIAE_CS42_4DL_TGACv1_343378_AA1133790*	Defensin 1	LOC_Os03g03810	Low-molecular-weight cysteine-rich 69	2
236	*TRIAE_CS42_7DL_TGACv1_603063_AA1974950*	bHLH DNA-binding domain superfamily	LOC_Os01g70310	basic helix-loop-helix (bHLH) DNA-binding	1
297	*TRIAE_CS42_5AL_TGACv1_377393_AA1246520*	Squamosa promoter-binding 18	LOC_Os08g41940	Squamosa promoter-binding protein-like	1
444	*TRIAE_CS42_4BS_TGACv1_330766_AA1108750*	Zinc finger	LOC_Os08g45040	Zinc finger (C2H2 type) family protein	1

4.3.3 Characterization of putative RHT-D1A interactors identified from the wheat stem library screen

Once the colonies of interest were identified, the sequences of the prey clones were analysed to discover which portion of the protein was present in the clone, and if the cDNA sequence was in-frame. To find the start of the cDNA sequence, and to check if the insert is in-frame, the sequencing results were mapped to the pEXP22 cDNA cloning region shown in **Figure 4.7**, including the GAL4 activation domain and *aatB* sites. Strains containing a cDNA insert show an unknown sequence between the *aatB* sites, beginning after the *aatB1* sequence (ACAAGTTTGTAAAAAAAGCTCCGA). To be in-frame, the first codon of the cDNA sequences must be in-frame with the ATG at the start of the cDNA cloning region shown in **Figure 4.7**.

The interaction between the prey plasmids of interest and RHT-D1A was tested by the expression of the *HIS3* and *LacZ* reporter genes. For each clone of interest, Mav203 yeast strains were transformed with the library prey plasmid and the RHT-D1a bait plasmid. The resulting yeast strains were then used in both a HIS3/3-AT and X-gal assay to detect the activity of reporter genes and confirm the interactions. Strains shown in **Table 4.4** were used in each case. **Table 4.5** shows a summary of the selected library strains, including the reason they were selected, method for confirmation of interaction with RHT-1 and co-expression with *RHT-1*.

Table 4.4 Yeast strains used to test the interaction between RHT-D1a and the library proteins of interest in the 3-AT and X-gal assays.

Yeast Strain	Bait	Prey	
1	Empty	Empty	Negative Control
2	GAI	ARF19	Positive control
3	Empty	Library protein of interest	Negative Control
4	RHT-D1a	Empty	Self-activation control
5	RHT-D1a	Library prey clone of interest	Test

Table 4.5 Summary table of library strains.

Strain	Putative role	Reason for selection	Frame	Interaction confirmation	Co-expression with *RHT-1*
51	Rho GTPase-activating 7-like protein	Multiple clones, role in hormone signalling	In-frame	3-AT, X-gal	Root, leaf, stem, spike, grain
59	BOI-related protein	Multiple clones, interaction with DELLAs	In-frame	3-AT	Root, leaf, stem, spike, grain
65	Ethylene-responsive element binding protein	Multiple clones, interaction with DELLAs	In-frame	3-AT	Root, leaf, stem, spike, grain
91	GATA transcription factor	Role as transcription factor	Not in-frame	-	-
137	SPL protein	Two homoeologues identified, interaction with DELLA	In-frame	3-AT	Spike. stem, grain
297	SPL protein	Two homoeologues identified, interaction with DELLA	In-frame	3-AT	Spike. stem, grain
143	FAR-1 related protein	Role as transcription factor and in light signalling.	In-frame	3-AT	Root, leaf, stem, spike, grain
202	bHLH transcription factor	Multiple clones, interaction with DELLA	Not in-frame	-	-
220	Ethylene insensitive protein	Role in hormone signalling.	Not in-frame	-	-
221	Defensin-1 related protein	Multiple clones, role in hormone signalling	In-frame	3-AT	Root, leaf, stem, spike, grain
236	bHLH transcription factor	Role as transcription factor, interaction with DELLA	In-frame	3-AT	Root, leaf, stem, spike, grain
444	Zinc finger family/IDD	Interaction with DELLAs	Unsure	3-AT, X-gal	Root, leaf, stem, spike, grain

4.3.3.1 Yeast Strain 51 contains a Rho GTPase-activating 7-like protein.

Yeast strain 51 was chosen as a strain of interest because this cDNA sequence was identified in two separate yeast library strains, while two further strains contained related Rho GTPase-activating 7-like proteins. In plants, Rho GTPases have been characterised as major regulators of cell polarity, giving them important roles in many different processes including Ca^{2+} signalling gradients, vesicle trafficking and cytoskeletal processes. There has also been some evidence that Rho GTPases have a role in hormone signalling. In *Arabidopsis* Rho GTPases activated by auxin are involved in the promotion of leaf development (Xu et al., 2010), and have been shown to have a role in crosstalk between the auxin and ABA signalling pathways (Nibau et al., 2013). Sequencing revealed that the *library cDNA 51* sequence was in-frame with the *GAL4* start codon (**Figure 4.8**) and encodes an N-terminal truncated product of TRIAE_CS42_2BS_TGACv1_146333_AA0462840 consisting of the C-terminal 400 amino acids of the protein sequence (**Figure 4.9**).

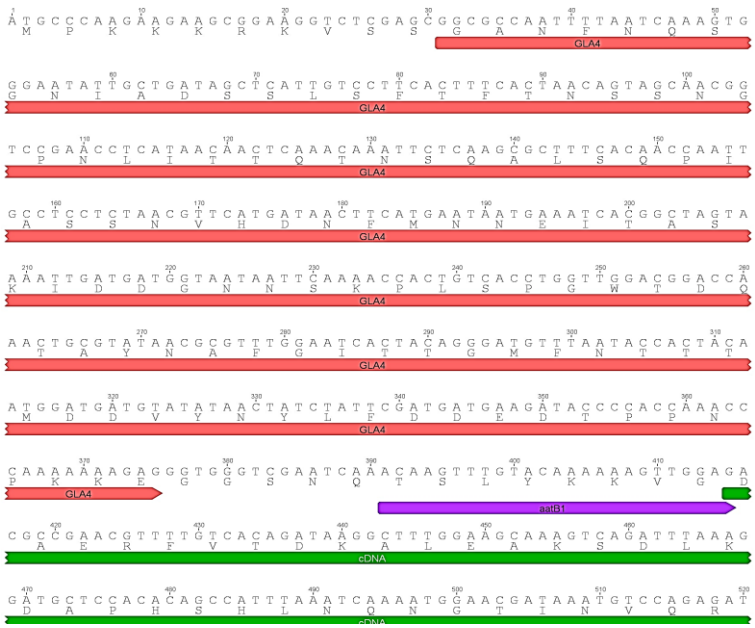

Figure 4.8 The *library cDNA 51* is in-frame with the *GAL4* start codon. The library strain 51 prey plasmid was sequenced to identify if the cDNA is in-frame with the *GAL4* start codon. The sequence is shown in the figure, beginning at the *GAL4 ATG* start codon, running into the *library cDNA 51* sequence. The GAL4 activation domain is labelled in red under the sequence. The aatB1 sequence is labelled with purple under the sequence. The *library cDNA 51* sequence is labelled with green under the sequence.

Figure 4.9 The protein sequence of library strain 51, a Rho GTPase-activating 7-like protein. The cDNA sequence present in the prey plasmid of library strain 51 was translated into the amino acid sequence. This library protein 51 sequence is aligned to the full length TRIAE_CS42_2BS_TGACv1_146333_AA0462840 sequence (labelled in the figure as TGACv1) of this protein using the T-coffee alignment tool. This figure shows residues 321-860 of the full length TGACv1 sequence. Residues shown in reverse are shared between the two sequences.

The 3-AT assay testing the interaction between RHT-D1a and library protein 51 is shown in **Figure 4.10**. The RHT-D1a-library protein 51 strain grew at a similar level to the positive control at all 3-AT concentrations, and was visibly much stronger than the self-activation control. These results indicate that *library cDNA 51* encodes an RHT-D1A interacting protein in yeast.

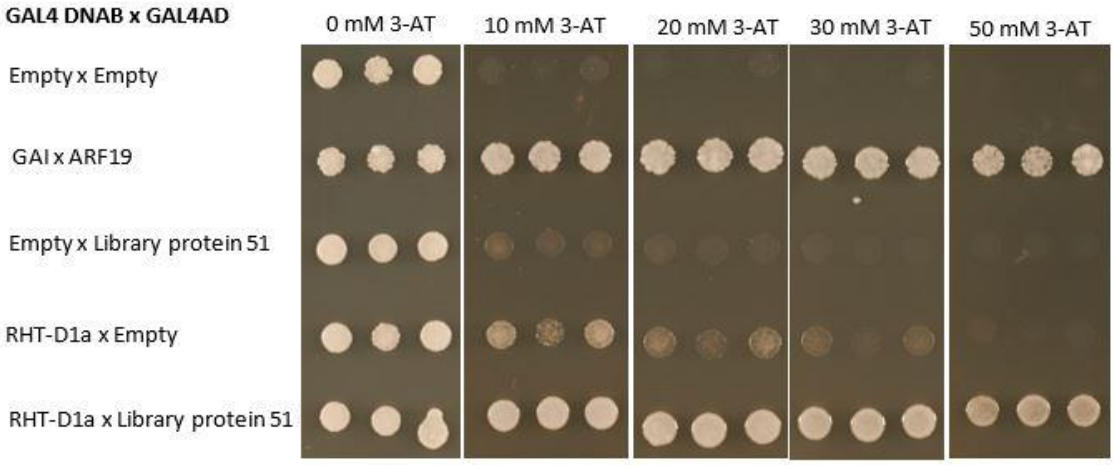

Figure 4.10 Yeast two-hybrid screen detecting the expression of HIS3 demonstrating the interaction between RHT-D1a and library protein 51. Mav203 competent yeast were transformed with GAL4 DNA-binding bait (GAL4 DNAB) and GAL4 activation domain (GAL4 AD) prey vectors containing proteins labelled under the GAL4 DNAB and GAL4 AD headings at the left of the figure. These strains were spotted onto –Leu/-Trp/-His media containing

concentrations of 3-AT ranging from 0-50 mM. Strains were spotted onto each plate with three technical replicates shown in each panel of the figure.

The X-gal assay to confirm the interaction between RHT-D1a and library protein 51 is shown in **Figure 4.11**. After 4 h, the RHT-D1a bait, library protein 51 prey strain showed a blue colour change, which was slightly stronger than the self-activation control strain. At 24 h of incubation, the same results were obtained, but with a stronger blue colour change in the positive control, self-activation control and test strain. The interaction between library protein 51 and RHT-1 is therefore confirmed by the X-gal assay.

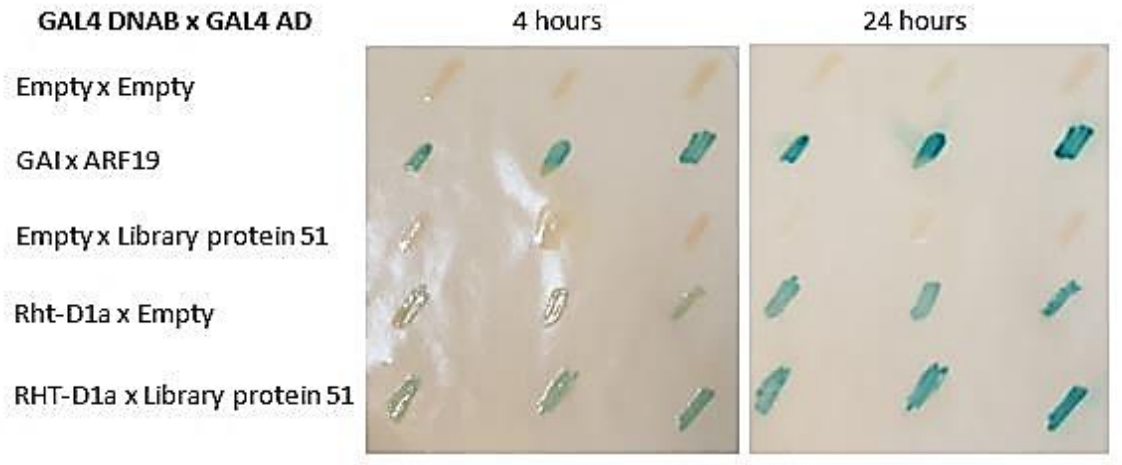

Figure 4.11 A yeast two-hybrid screen detecting the expression of the *LacZ* indicates an interaction between library protein 51 and RHT-D1a. Mav203 competent yeast were transformed with GAL4 DNA-binding bait (GAL4 DNAB) and GAL4 activation domain (GAL4 AD) prey vectors containing proteins labelled under the GAL4 DNAB and GAL4 AD headings at the left of the figure. These strains were streaked onto a nitrocellulose membrane on YPD media in three technical replicates, which are shown in each panel of the figure. The plates were incubated for 24 h, then lysed and incubated with X-gal for 24 h. The white-blue colour change was assessed at 4 and 24 h.

The expression pattern of *library cDNA 51* was compared to that of *RHT-D1a* (**Figure 4.12**) to confirm that the two proteins are expressed in the same tissues, and could therefore theoretically interact in vivo. The TGACv1 were used as a template for RNAseq mapping using reads from 5 different tissues; root, leaf, stem, spike and grain, at three different Zadoks developmental stages, from the wheat variety Chinese spring (International Wheat Genome Sequencing, 2014). The reads were mapped using the BWA-MEM tool in Galaxy, which resulted in fragments per kilobase per million reads mapped (FKPM) values for each gene. The FKPM value therefore indicates the number of RNAseq reads that map to an exon sequence and the higher the FPKM value, the more highly expressed the sequence is. *Library cDNA 51* is expressed in all tissues tested, with the highest expression levels in elongating stem and spike. *RHT-D1a* is also highly expressed in these tissues, indicating that these proteins have the opportunity to interact in vivo.

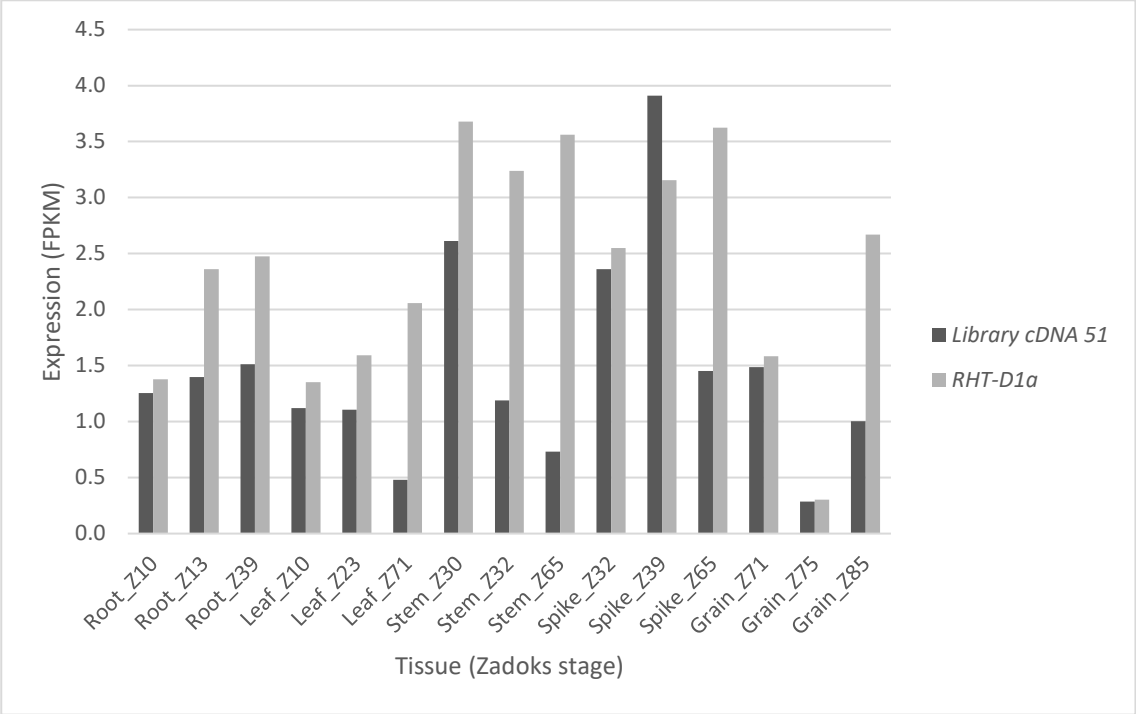

Figure 4.12 Expression levels of *library cDNA 51* compared to *RHT-D1a*. A file containing all TGACv1 cDNAs was used as a template for RNAseq mapping with the Choulet (International Wheat Genome Sequencing, 2014) tissue specific dataset, containing RNAseq reads from five different tissues (root, leaf, stem, spike and grain) at three different developmental stages, indicated by the Zadoks scale (Z) number for each tissue. Reads were mapped using the BWA-MEM function in Galaxy. FKPM values for each gene are shown for each tissue.

4.3.3.2 Yeast library strain 59 contains a Probable BOI-related E3 ubiquitin-ligase 3 protein.

Yeast strain 59 contains a probable BOTRYTIS SUSCEPTIBLE1 INTERACTOR (BOI)-related E3 ubiquitin- ligase 3 protein. This strain was chosen for further characterization because this cDNA was identified in two separate yeast strains from the library screen, and because BOI and the BOI-related proteins, BRG1-3, have been shown to interact with DELLAs in *Arabidopsis* (Park et al., 2013). BOI and BRGs were shown to repress seed germination, the juvenile-to-adult phase transition, and flowering via their interaction with DELLAs. The interaction between DELLAs and BOIs does not affect the stability of either protein, but instead they interact to form a complex that targets the promoters of a subset of GA responsive genes to regulate their expression. The RING domain of the BOIs is necessary for this interaction (Park et al., 2013). Previous studies demonstrated that BOI proteins are involved in the plant response to pathogens, and knockdown of BOI expression caused *Arabidopsis* to be more susceptible to bacterial pathogens (Luo et al., 2010). A recent study revealed a role for BOIs in

the repression of flowering through their interaction with FLOWERING LOCUS T (FT) (Nguyen et al., 2015).

Sequencing revealed that this cDNA sequence was in-frame with the GAL4 start codon (**Figure 4.13**) and encodes the full-length TRIAE_CS42_4DL_TGACv1_344008_AA1142470 protein (**Figure 4.14**).

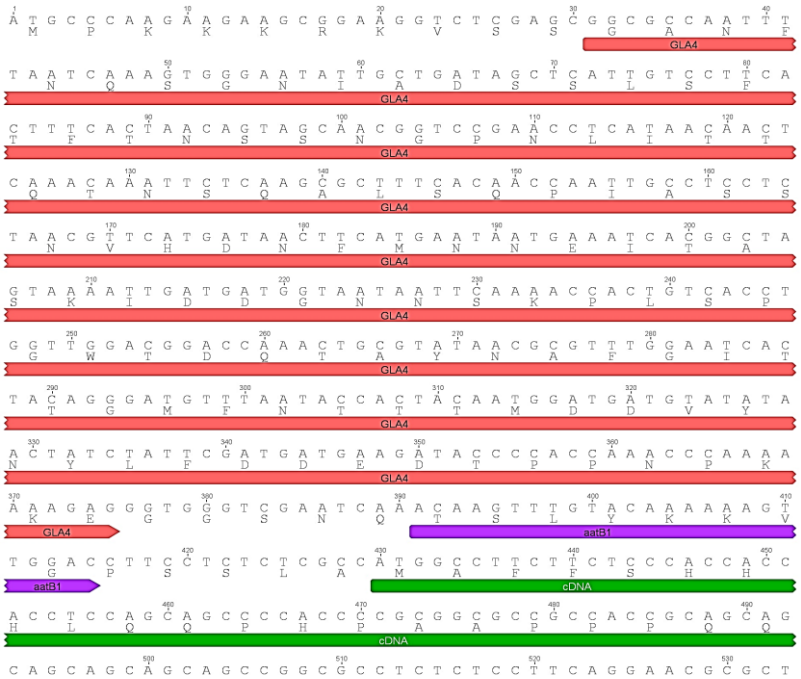

Figure 4.13 The *library cDNA 59* sequence is in frame with the GAL4 start codon. The library strain 59 prey plasmid was sequenced to identify if the cDNA is in-frame with the GAL4 start codon. The sequence is shown in the figure, beginning at the GAL4 ATG start codon, running into the 59 cDNA sequence. The GAL4 activation domain is labelled in red under the sequence. The aatB1 sequence is labelled with purple under the sequence. The *library cDNA 59* sequence is labelled with green under the sequence.

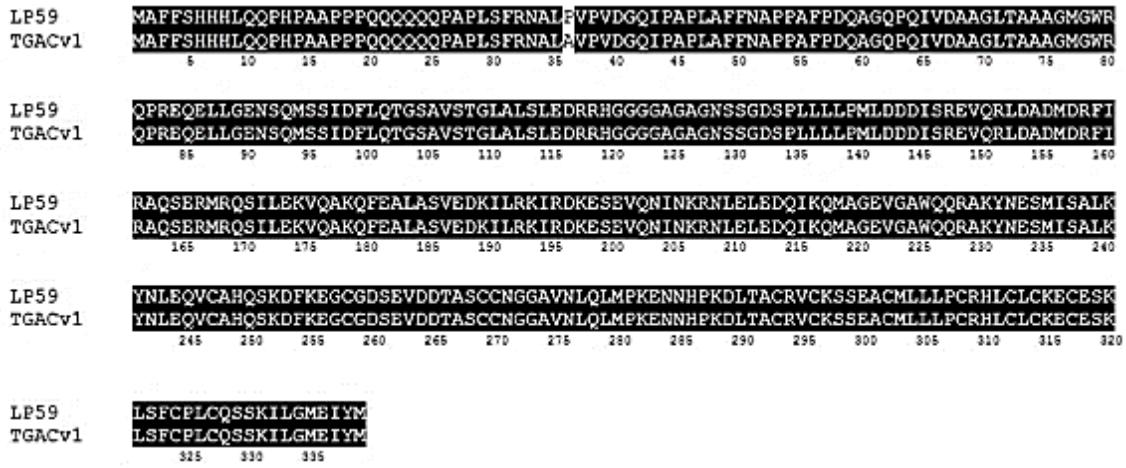

Figure 4.14 The protein sequence of library strain 59, a probable BOI-related E3 ubiquitin-ligase 3. The cDNA sequence present in the prey plasmid of library strain 59 was translated into the amino acid sequence. This library protein 59 sequence (LP59) was aligned to the full length TRIAE_CS42_4DL_TGACv1_344008_AA1142470 sequence (labelled in the figure as TGACv1) of this protein using the T-coffee alignment tool. Residues shown in reverse are shared between the two sequences.

The 3-AT assay testing the interaction between RHT-D1a and library protein 59 is shown in **Figure 4.15**. The RHT-D1a-library protein 59 grew at a similar level to the positive control at all 3-AT concentrations, and was visibly much stronger than the self-activation control. These results indicate that library protein 59 is interacting with RHT-D1a.

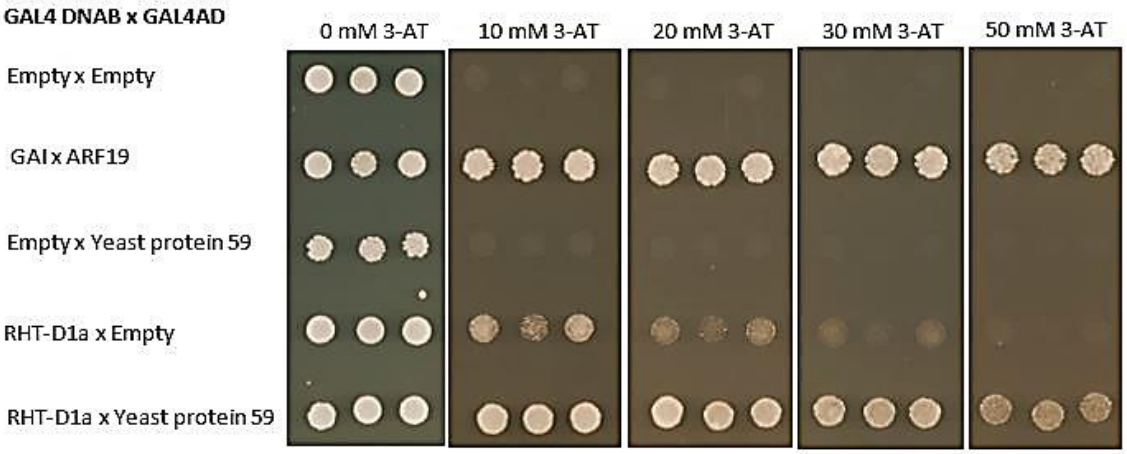

Figure 4.15 Yeast two-hybrid screen detecting the expression of HIS3 demonstrating the interaction between RHT-D1a and library protein 59. Mav203 competent yeast were transformed with GAL4 DNA-binding bait (GAL4 DNAB) and GAL4 activation domain (GAL4 AD) prey vectors containing proteins labelled under the GAL4 DNAB and GAL4 AD headings at the left of the figure. These strains were spotted onto –Leu/-Trp/-His media containing concentrations of 3-AT ranging from 0-50 mM. Strains were spotted onto each plate with three technical replicates shown in each panel of the figure.

The X-gal assay to confirm the interaction between RHT-D1a and library protein 59 is shown in **Figure 4.16**. After 4 h, the RHT-D1a bait, library protein 59 prey strain showed a blue colour change, which was indistinguishable from the colour change detected in the self-activation control strain. At 24 h of incubation, the same results were obtained, but with a stronger blue colour change in the positive control, self-activation control and test strain. The interaction between library protein 59 and RHT-1 is therefore likely to be a weak interaction which is distinguishable by the 3-AT assay, but not the less sensitive X-gal assay. Therefore, the X-gal assay did not confirm the interaction between library protein 59 and RHT-D1a indicated by the 3-AT assay (**Figure 4.15**).

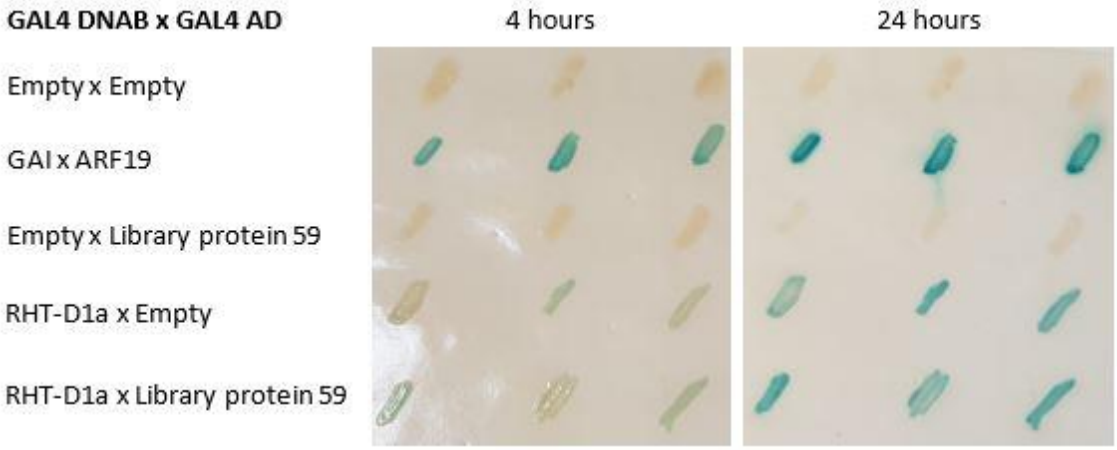

Figure 4.16 A yeast two-hybrid screen detecting the expression of the *LacZ* reporter gene does not indicate an interaction between library protein 59 and RHT-D1a. Mav203 competent yeast were transformed with GAL4 DNA-binding bait (GAL4 DNAB) and GAL4 activation domain (GAL4 AD) prey vectors containing proteins labelled under the GAL4 DNAB and GAL4 AD headings at the left of the figure. These strains were streaked onto a nitrocellulose membrane on YPD media in three technical replicates, which are shown in each panel of the figure. The plates were incubated for 24 h, then lysed and incubated with X-gal for 24 h.The white-blue colour change was assessed at 4 and 24 h

Once library protein 59 had been identified as an Rht-D1a interactor, phylogenetic analysis was carried out to identify closely related sequences from other species which could give an indication of function. The BOI and BOI-related genes identified as DELLA interactors by Park et al. (2013) were used to construct a Clustal W BLOSUM alignment with library proteins. No BOI or BOI-related genes from maize or rice have been characterized, so this analysis was limited to *Arabidopsis* sequences. This alignment was used to produce a PHYML WAG tree shown in **Figure 4.17**. The *Arabidopsis* sequence most closely related to library protein 59 is BRG3 (At3g12920).

An alignment of the RING domain required for the interaction between BOIs and DELLAs is shown in **Figure 4.18**. The *Arabidopsis* BOI and BRG RING domain sequences were aligned to the RING domain of library protein 59. The residues marked with an asterisk show the conserved metal ligand positions. Library protein 59 has conservation of all 8 positions.

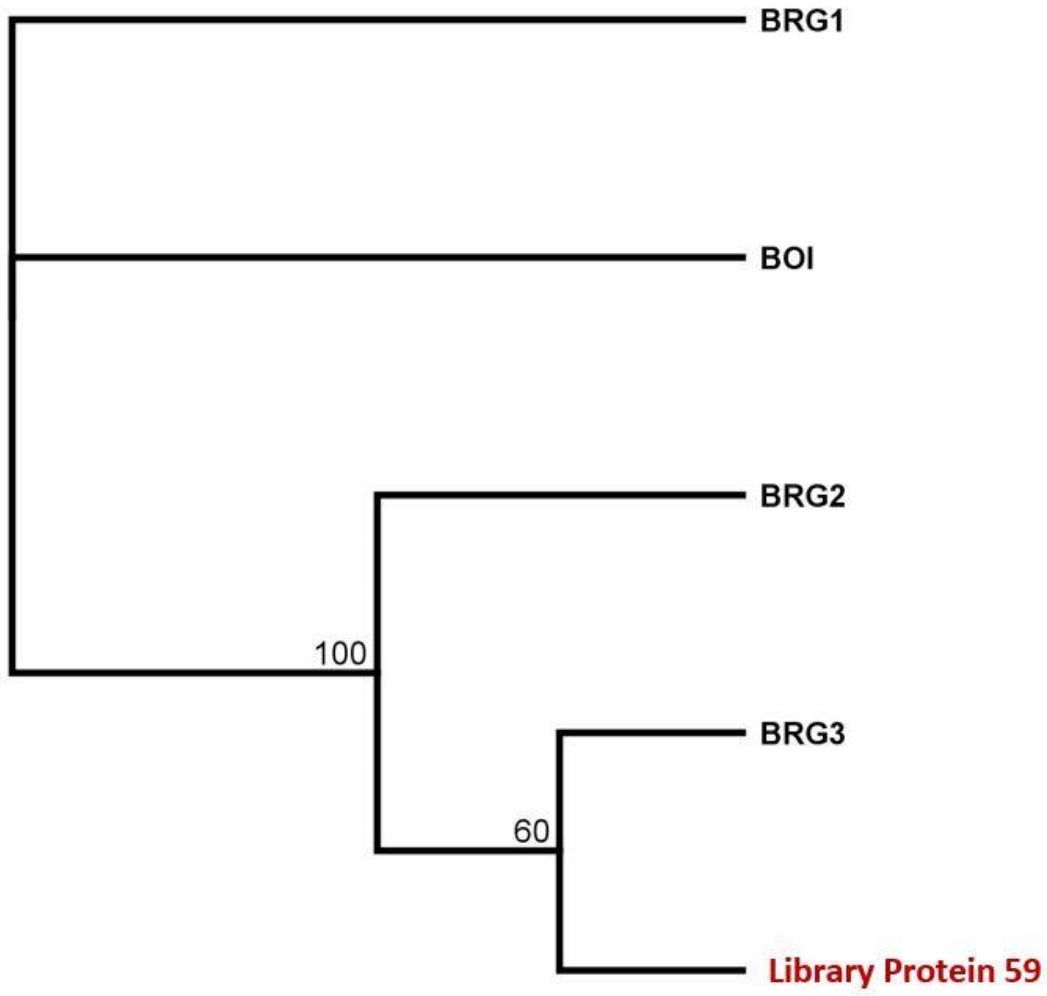

Figure 4.17 The relationship between library protein 59 and *Arabidopsis* BOI-related proteins. Library protein 59 and the *Arabidopsis* BOI (At4g19700) and BRG1-3 (At5g45100, At1g79110, At3g12920) were aligned using the ClustalW BLOSUM alignment tool in Geneious. This alignment was used to create a PHYML WAG tree. Bootstrapping values are shown at the branch points of the tree.

Figure 4.18 An alignment of the RING domain of the *Arabidopsis* BOIs with library protein 59. The amino acid sequence of the RING domain of the *Arabidopsis* BOI (At4g19700) and BRG1-3 (At5g45100, At1g79110, At3g12920) was aligned with the library protein 59 (LP59) ring domain sequence using the T-coffee alignment tool. Residues shown in reverse are highly conserved, residues in grey are similar. Residues marked by an asterisk below the alignment show the conserved metal ligand positions.

Comparison of *library cDNA 59* and *RHT-D1a* expression levels (**Figure 4.19**) demonstrated that *library cDNA 59* is highly expressed in all tissues, suggesting that it would have the opportunity to interact with RHT-D1a in vivo.

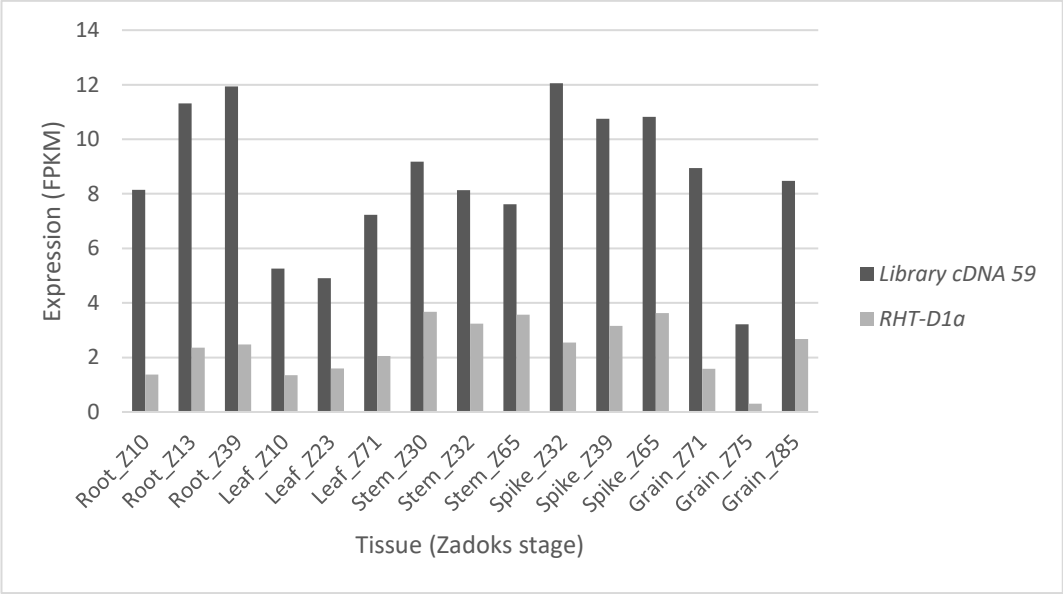

Figure 4.19 Expression levels of *library cDNA 59* compared to *RHT-D1a*. A file containing all TGACv1 cDNAs was used as a template for RNAseq mapping with the Choulet (International Wheat Genome Sequencing, 2014) tissue specific dataset, containing RNAseq reads from five different tissues (root, leaf, stem, spike and grain) at three different developmental stages, indicated by the Zadoks scale (Z) number indicated in each tissue. Reads were mapped using the BWA-MEM function in Galaxy. FKPM values for each gene are shown for each tissue.

4.3.3.3 Yeast Strain 65 contains an ethylene-responsive element binding protein.

Yeast strain 65 encodes an ethylene-responsive element binding protein. This strain was chosen for further characterization because of the protein's probable role in hormone

signalling, and because three library strains encoded this protein. In *Arabidopsis*, RELATED TO APETALA2.3 (RAP2.3) an ethylene responsive element binding protein from the ERF-VII family has been shown to interact with the DELLA protein GAI. This interaction causes repression of ethylene responsive element activity in regulating transcription (Marin-de la Rosa et al., 2014). Deletion studies identified that the N-terminal and AP2 domain of RAP2.3 are required for binding to GAI. The interaction between GAI and the AP2 domain prevents the binding of RAP2.3 to target genes. The inhibition of RAP2.3 by DELLAs is involved in the regulation of apical hook formation, during which ethylene promotes RAP2.3 regulation of genes involved in apical hook formation. Marin-de la Rosa et al. (2014) also demonstrated that another ERF family protein, RAP2.12, was able to interact with GAI and RGA, suggesting that the interaction with DELLAs can occur in all ERF-VII family proteins. RAP2.3 has also been shown to promote low oxygen, oxidative and osmotic stress responses in *Arabidopsis* (Papdi et al., 2015).

Sequencing revealed that the *library cDNA 65* sequence was in-frame with the GAL4 start codon (**Figure 4.20**) and encodes the full-length TRIAE_CS42_7AS_TGACv1_570423_AA1835500 protein (**Figure 4.21**).

Figure 4.20 The *library cDNA 65* sequence is in frame with the GAL4 start codon. The library strain 65 prey plasmid was sequenced to identify if the cDNA is in-frame with the GAL4 start codon. The sequence is shown in the figure, beginning at the GAL4 ATG start codon, running into the 65 cDNA sequence. The GAL4 activation domain is labelled in red under the sequence. The aatB1 sequence is labelled with purple under the sequence. The *library cDNA 65* sequence is labelled with green under the sequence.

Figure 4.21 The protein sequence of library protein 65; an ethylene responsive element binding protein. The cDNA sequence present in the prey plasmid of library strain 65 was translated into the amino acid sequence. This library protein 65 (LP65) sequence was aligned to the full length TRIAE_CS42_7AS_TGACv1_570423_AA1835500 sequence (labelled in the figure as TGACv1) of this protein using the T-coffee alignment tool. Residues shown in reverse are shared between the two sequences.

The 3-AT assay testing the interaction between RHT-D1a and library protein 65 is shown in **Figure 4.22**. The RHT-D1a-LP65 strain was able to grow at all 3-AT concentrations at a visibly higher level than the self-activation control, demonstrating that library protein 65 is interacting with RHT-D1a.

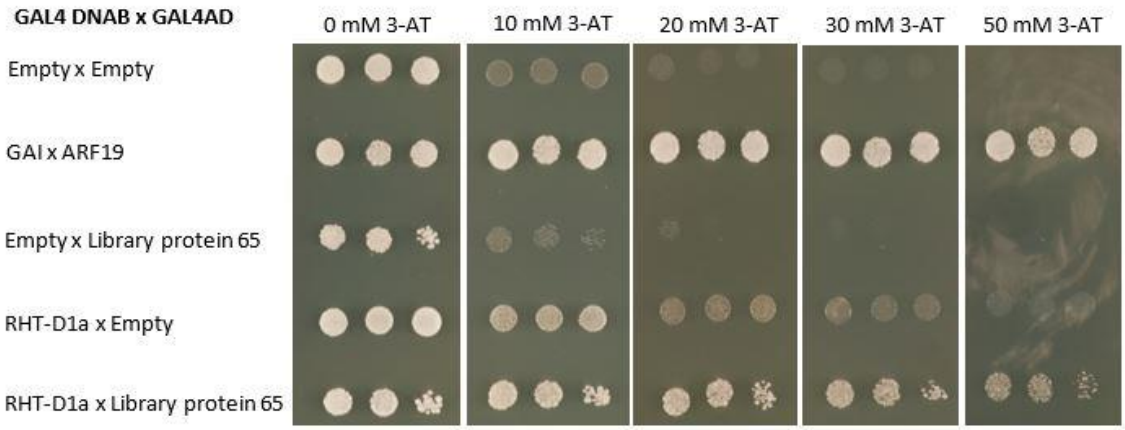

Figure 4.22 Yeast two-hybrid screen detecting the expression of *HIS3* demonstrating the interaction between RHT-D1a and library protein 65. Mav203 competent yeast were transformed with GAL4 DNA-binding bait (GAL4 DNAB) and GAL4 activation domain (GAL4 AD) prey vectors containing proteins labelled under the GAL4 DNAB and GAL4 AD headings at the left of the figure. These strains were spotted onto –Leu/-Trp/-His media containing concentrations of 3-AT ranging from 0-50 mM. Strains were spotted onto each plate with three technical replicates shown in each panel of the figure.

The X-gal assay to confirm the interaction between RHT-D1a and library protein 65 is shown in **Figure 4.23**. After 4 h, the RHT-D1a bait, library protein 65 prey strain showed a blue colour change, which was indistinguishable from the colour change detected in the self-activation

control strain. At 24 h of incubation, the same results were obtained, but with a stronger blue colour change in the positive control, self-activation control and test strain. The interaction between library protein 65 and RHT-1 is therefore likely to be a weak interaction, which is distinguishable by the 3-AT assay, but not the less sensitive X-gal assay. Therefore, the X-gal assay was unable to confirm the interaction between library protein 65 and RHT-D1a shown in the 3-AT assay (**Figure 4.22**).

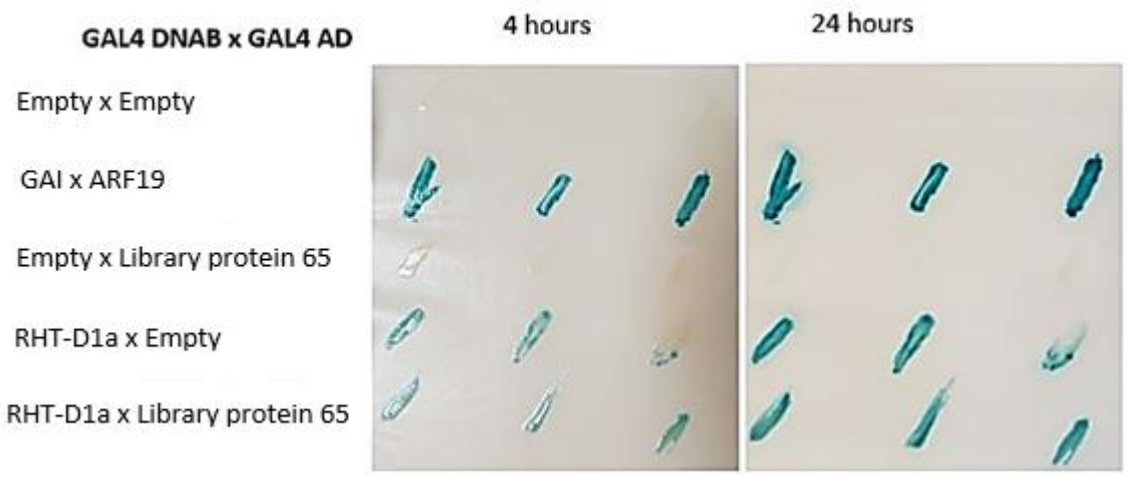

Figure 4.23 A yeast two-hybrid screen detecting the expression of the *LacZ* reporter gene does not indicate an interaction between library protein 65 and RHT-D1a. Mav203 competent yeast were transformed with GAL4 DNA-binding bait (GAL4 DNAB) and GAL4 activation domain (GAL4 AD) prey vectors containing proteins labelled under the GAL4 DNAB and GAL4 AD headings at the left of the figure. These strains were streaked onto a nitrocellulose membrane on YPD media in three technical replicates, which are shown in each panel of the figure. The plates were incubated for 24 h, then lysed and incubated with X-gal for 24 h. The white-blue colour change was assessed at 4 and 24 h.

Comparison of *library cDNA 65* and *RHT-D1a* expression levels (**Figure 4.24**) demonstrated that *library cDNA 65* is highly expressed in all tissues, suggesting that it would have the opportunity to interact with RHT-D1a in vivo.

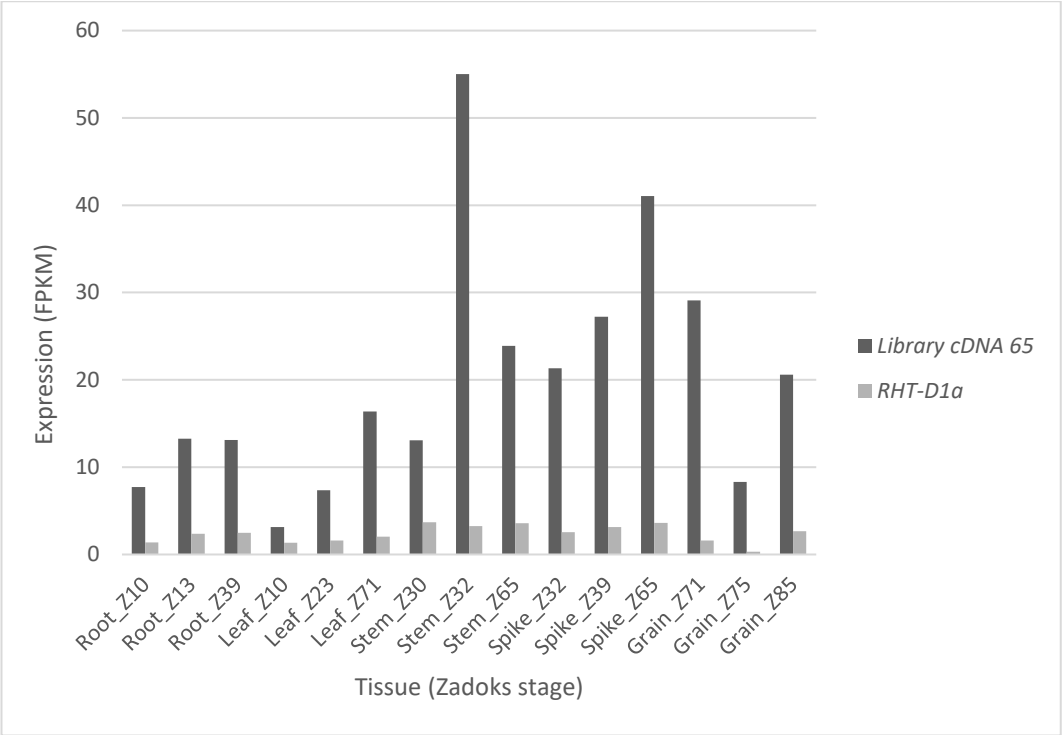

Figure 4.24 Expression levels of *library cDNA 65* compared to *RHT-D1a.* A file containing all TGACv1 cDNAs was used as a template for RNAseq mapping with the Choulet (International Wheat Genome Sequencing, 2014) tissue specific dataset, containing RNAseq reads from five different tissues (root, leaf, stem, spike and grain) at three different developmental stages, indicated by the Zadoks scale (Z) number indicated in each tissue. Reads were mapped using the BWA-MEM function in Galaxy. FKPM values for each gene are shown for each tissue.

4.3.3.3 Library strains 137 and 297 contain squamosa promoter-binding proteins.

Yeast strains 137 and 297 encode the B and A homoeologues of a SQUAMOSA PROMOTER BINDING LIKE (SPL) protein, respectively. SPLs are involved in the regulation of flowering under short days through their interaction with micro RNAs (miRNA). As the plant ages, the levels of miRNA156 decline, allowing SPL levels to increase and promote the juvenile to adult phase transition and flowering through their activation with miR172, MADS box genes, and the transcription factor LEAFY (Wang et al., 2009, Wu et al., 2009, Yamaguchi et al., 2009). The yeast strains 137 and 297 were chosen for further characterisation because two homoeologues were isolated in the library, and because DELLAs have been shown to directly bind to and moderate the activity of squamosa promoter binding transcription factors in *Arabidopsis* (Yu et al., 2012). The interaction between DELLA and SPL inhibits SPL transcriptional activation of MADS box genes and miR172. Yeast two-hybrid experiments demonstrated that the C terminal of SPL9 was required for RGA binding, and that constructs containing only the SPB DNA binding domain or the N terminal domain of SPL9 could not interact with RGA. These results demonstrated that SPLs interact with DELLAs through their C terminal domains (Yu et al., 2012).

Sequencing of *library cDNAs 137* and *297* confirmed that they are in-frame with the GAL4 start codon (**Figure 4.25**, **Figure 4.26**) and both encode N-terminally truncated products of TRIAE_CS42_5BL_TGACv1_406028_AA1339440 TRIAE_CS42_5AL_TGACv1_377393_AA1246520, missing the N terminal 175 amino acids and 137 amino acids respectively (**Figure 4.27**).

Figure 4.25 *Library cDNA 137* is in-frame with the GAL4 start codon. The library strain 137 prey plasmid was sequenced to identify if the cDNA is in-frame with the GAL4 start codon. The sequence is shown in the figure, beginning at the GAL4 ATG start codon, running into the 137 cDNA sequence. The GAL4 activation domain is labelled in red under the sequence. The *aatB1* sequence is labelled with purple under the sequence. The *library cDNA 137* sequence is labelled with green under the sequence.

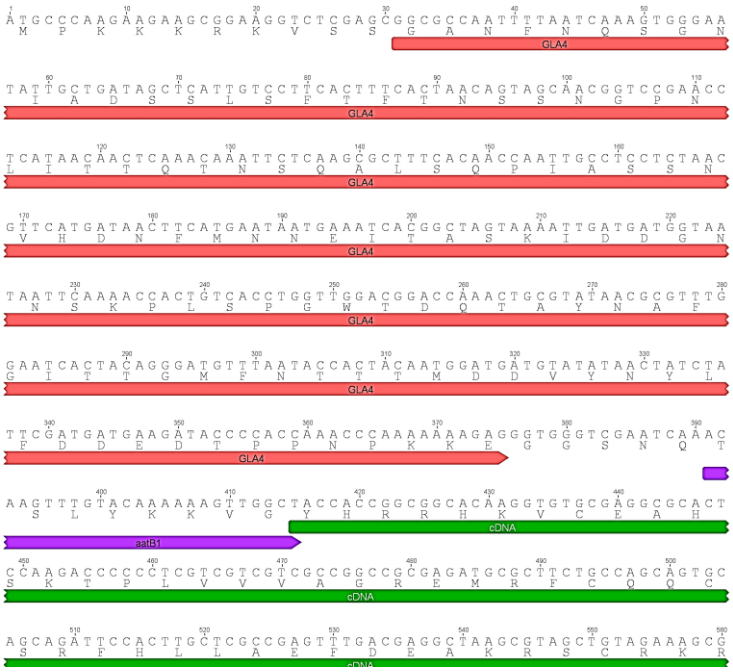

Figure 4.26 The *library cDNA 297* sequence is in-frame with the GAL4 start codon. The library strain 297 prey plasmid was sequenced to identify if the cDNA is in-frame with the GAL4 start codon. The sequence is shown in the figure, beginning at the GAL4 ATG start codon, running into the *297 cDNA* sequence. The GAL4 activation domain is labelled in red under the sequence. The *aatB1* sequence is labelled with purple under the sequence. The *library cDNA 297* sequence is labelled with green under the sequence.

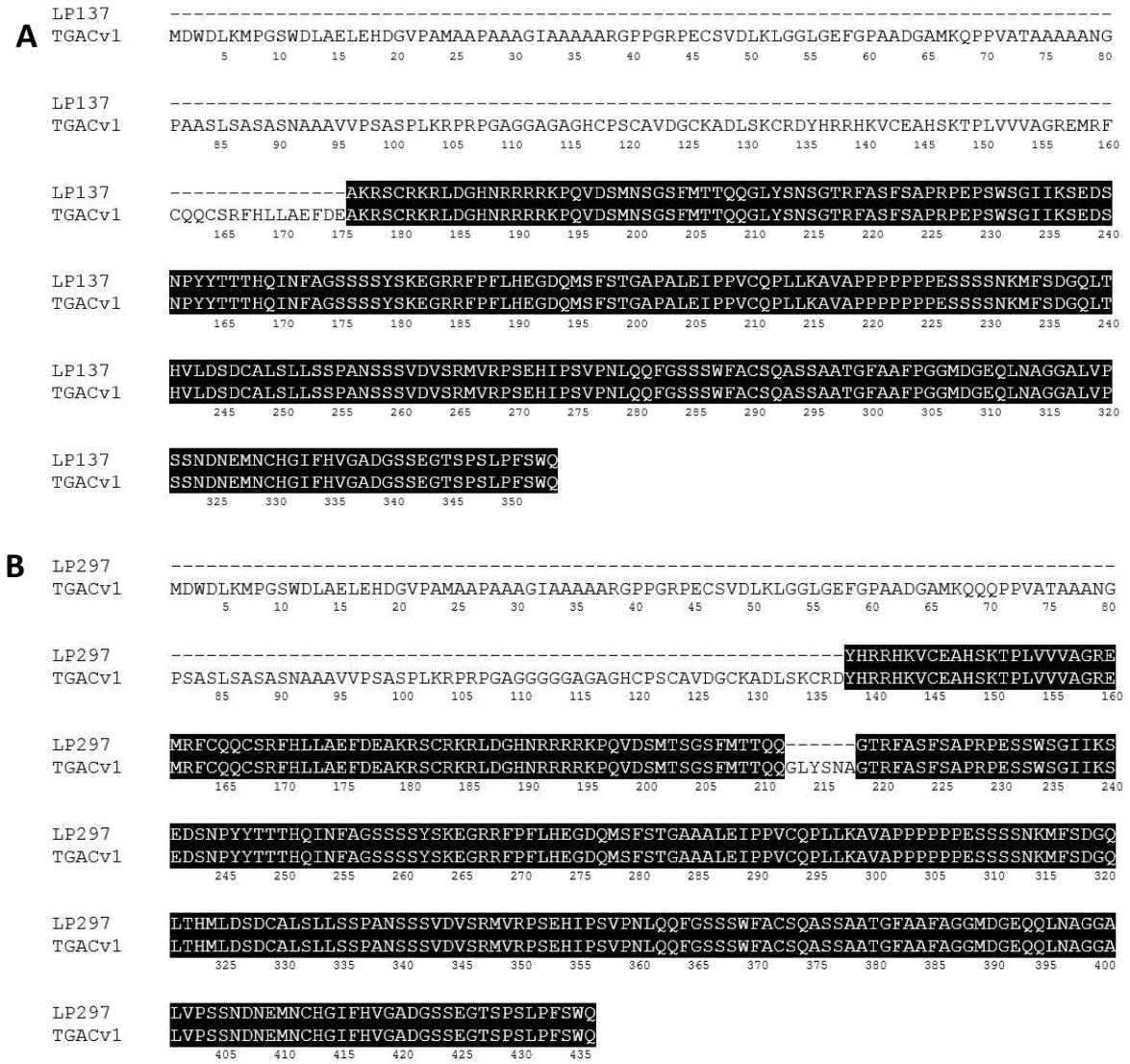

Figure 4.27 Library proteins 137 and 297 encode N-terminally truncated squamosa promoter binding-like proteins. Residues shown in reverse are shared between the two sequences. **(A)** The library protein 137 (LP137) sequence was aligned to the full length TRIAE_CS42_5BL_TGACv1_406028_AA1339440 sequence (labelled in the figure as TGACv1) using the T-coffee alignment tool. **(B)** The library protein 297 (LP297) sequence was aligned to the full-length TRIAE_CS42_5AL_TGACv1_377393_AA1246520 sequence (labelled in the figure as TGACv1) using the T-coffee alignment tool.

The 3-AT assay testing the interaction between RHT-D1a and library proteins 137 and 297 is shown in **Figure 4.28**. The RHT-D1a-library protein 137/297 strain was able to grow at all 3-AT concentrations at a visibly higher level than the self-activation control, demonstrating that proteins 137 and 297 interact with the C terminus of RHT-D1a (**Figure 4.28**).

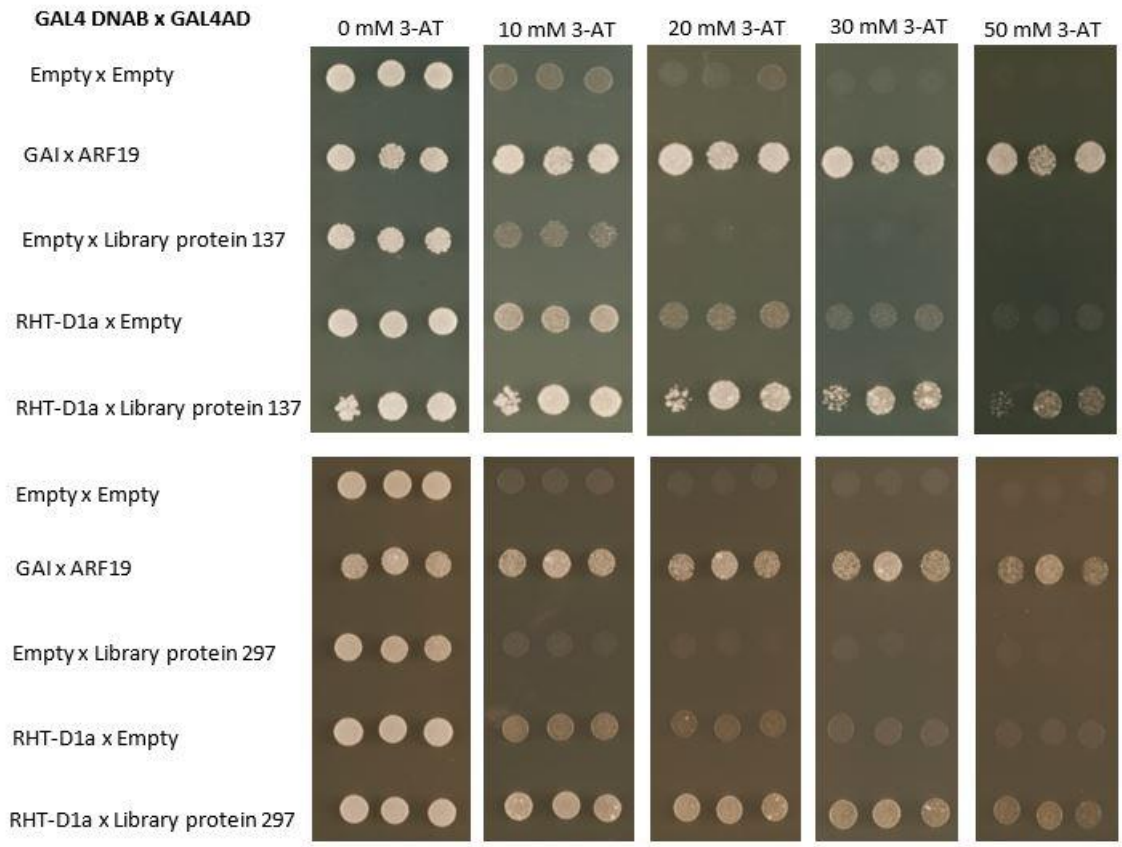

Figure 4.28 Yeast two-hybrid screen detecting the expression of *HIS3* demonstrating the interaction between RHT-D1a and library proteins 137 and 297. MaV203 competent yeast were transformed with GAL4 DNA-binding bait (GAL4 DNAB) and GAL4 activation domain (GAL4 AD) prey vectors containing proteins labelled under the GAL4 DNAB and GAL4 AD headings at the left of the figure. These strains were spotted onto –Leu/-Trp/-His media containing concentrations of 3-AT ranging from 0-50 mM. Strains were spotted onto each plate with three technical replicates shown in each panel of the figure.

The X-gal assay to confirm the interaction between RHT-D1a and library proteins 137 and 297 is shown in **Figure 4.29**. After 4 h of incubation the RHT-D1a bait, library protein 137 prey strain showed a blue colour change, which was indistinguishable from the colour change detected in the self-activation control strain. The library protein 297, RHT-D1a strain did show a slightly stronger blue colour change than the self-activation strain. At 24 h of incubation, the same results were obtained with a stronger blue colour change in the positive control, self-activation control and test strains. The interaction between library proteins 137 and 297 and RHT-1 is therefore likely to be a weak interaction which is distinguishable by the 3-AT assay, but not the less sensitive X-gal assay.

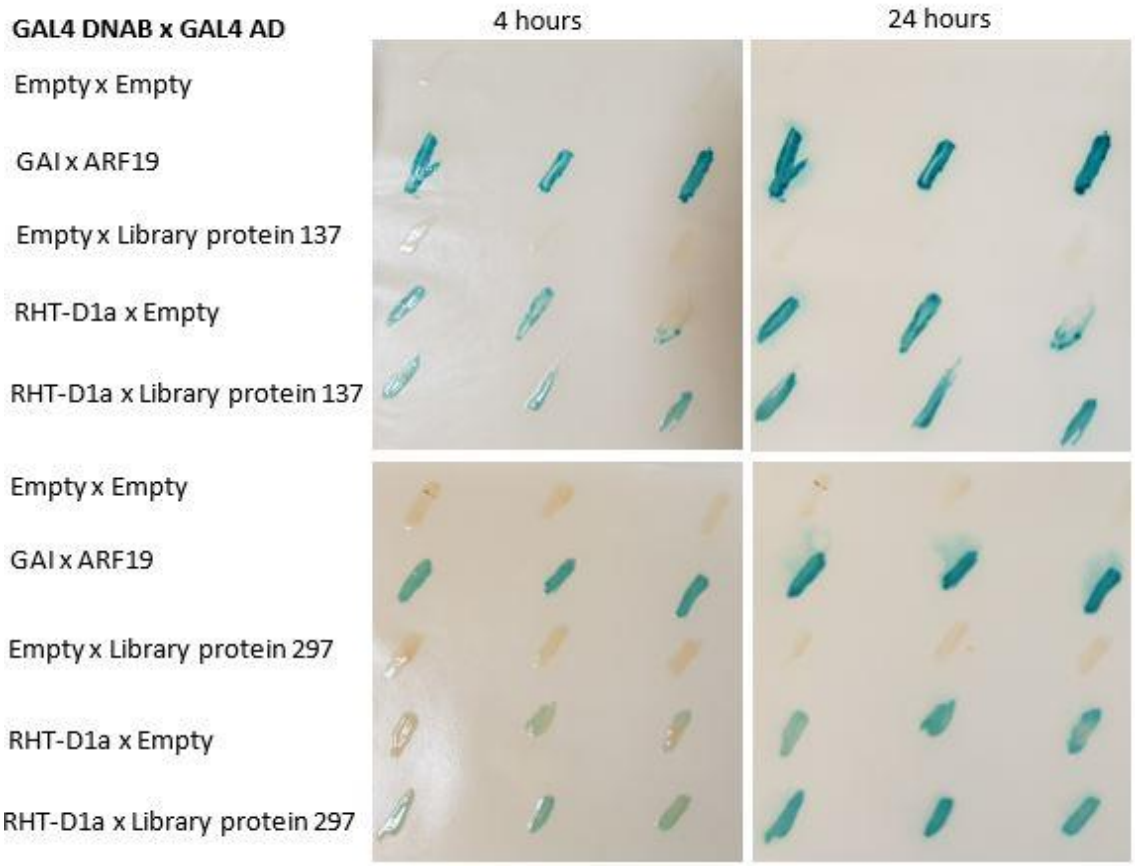

Figure 4.29 A yeast two-hybrid screen detecting the expression of the *LacZ* reporter gene supports an interaction between library protein 297 and RHT-D1a but not library protein 137. Mav203 competent yeast were transformed with GAL4 DNA-binding bait (GAL4 DNAB) and GAL4 activation domain (GAL4 AD) prey vectors containing proteins labelled under the GAL4 DNAB and GAL4 AD headings at the left of the figure. These strains were streaked onto a nitrocellulose membrane on YPD media in three technical replicates, which are shown in each panel of the figure. The plates were incubated for 24 h, then lysed and incubated with X-gal for 24 h.The white-blue colour change was assessed at 4 and 24 h.

Once library protein 137 had been identified as an SPL protein, phylogenetic analysis was carried out to identify closely related sequences from other species which could give an indication of function. *Arabidopsis*, maize and rice SPL proteins with known functions are listed in **Table 4.6**. These proteins were used to produce a neighbour joining tree from a clustalW BLOSUM alignment, shown in **Figure 4.30**. Library proteins 137 and 297 are grouped with rice SPL16, maize TGA1 and *Arabidopsis* SPL10 and SPL11.

Table 4.6 *Arabidopsis*, rice and maize SPL proteins. The accession numbers and references of the *Arabidopsis*, rice and maize SPLs are shown

Species	Name	Accession Number	Reference
Arabidopsis	SPL1	At2g47070	Chao et al. (2017)
Arabidopsis	SPL3	At2g33810	Yamaguchi et al. (2009)
Arabidopsis	SPL4	At1g53160	Wu and Poethig (2006)
Arabidopsis	SPL5	At3g15270	Wu and Poethig (2006)
Arabidopsis	SPL6	At1g69170	Padmanabhan et al. (2013)
Arabidopsis	SLP7	At5g18830	Yamasaki et al. (2009)
Arabidopsis	SPL8	At1g02065	Zhang et al. (2007)
Arabidopsis	SPL9	At2g42200	Schwarz et al. (2008)
Arabidopsis	SPL10	At1g27370	Shikata et al. (2009)
Arabidopsis	SPL11	At1g27360	Shikata et al. (2009)
Arabidopsis	SPL12	At3g60030	Chao et al. (2017)
Arabidopsis	SPL15	At3g57920	Schwarz et al. (2008)
Arabidopsis	SPL19	At3g57920	Schwarz et al. (2008)
Rice	OsSPL13	LOC_Os07g32170 Os07g0505200	Si et al. (2016)
Rice	OsSPL14	LOC_Os08g39890 Os08g0509600	Luo et al. (2012) Miura et al. (2010)
Rice	OsSPL16	LOC_Os08g41940 Os08g0531600	Wang et al. (2012)
Rice	OsSPL17	LOC_Os09g31438 Os09g0491532	Wang et al. (2015b), Wang et al. (2015a)
Maize	ZmTGA1	AAX83875.1	Wang et al. (2005a)

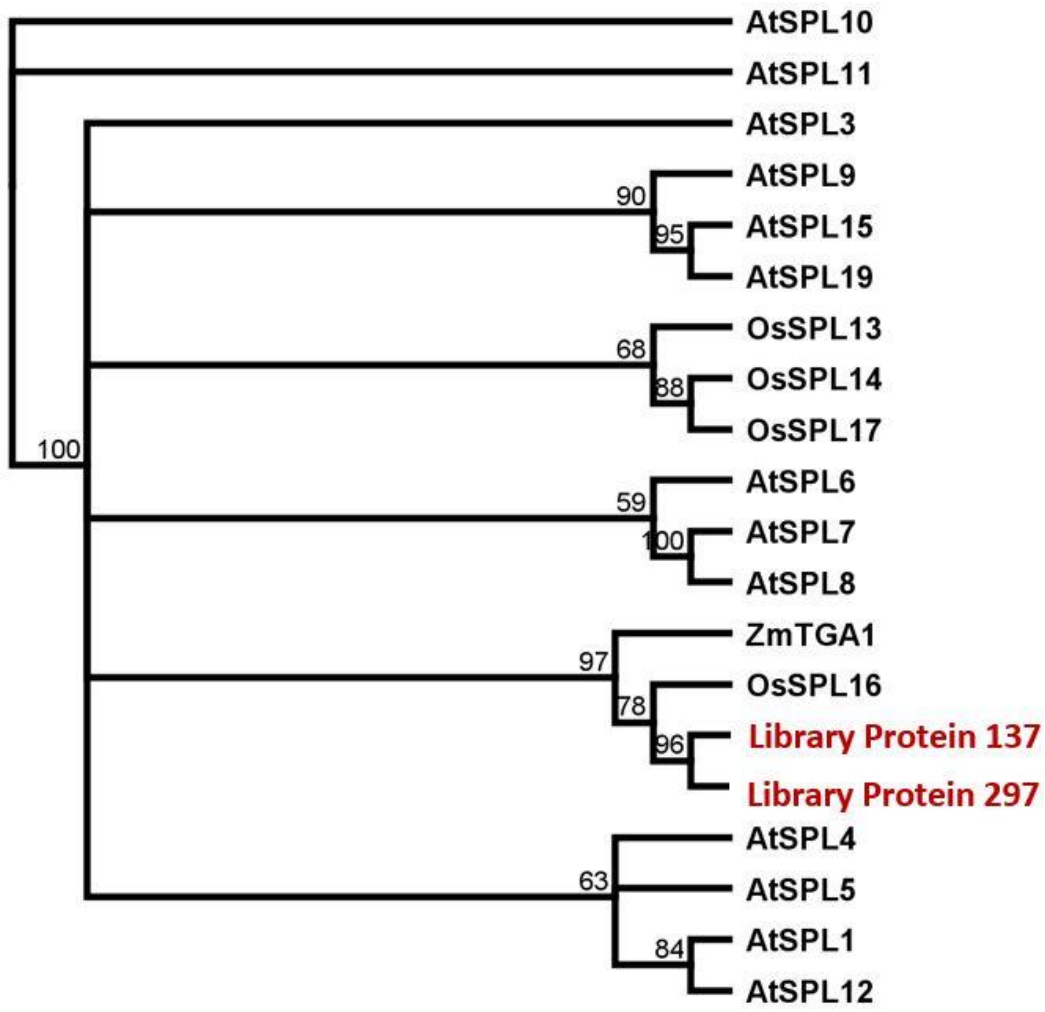

Figure 4.30 The relationship between library proteins 137 and 297 with rice, maize and *Arabidopsis* SPL proteins. Library proteins 137 and 297 were aligned with *Arabidopsis*, rice and maize SPL proteins using the ClustalW BLOSUM alignment tool in Geneious. A neighbour joining tree was then produced from this alignment. Bootstrapping values are shown at the branch points of the tree.

A Comparison between the expression levels of *library cDNAs 137, 297* and *RHT-D1a* (**Figure 4.31**) demonstrated that both *137* and *297* were expressed at high levels in the spike, and had low levels of expression in the elongating stem and developing grain. The results indicate that there is opportunity for an interaction with RHT-D1a in these tissues.

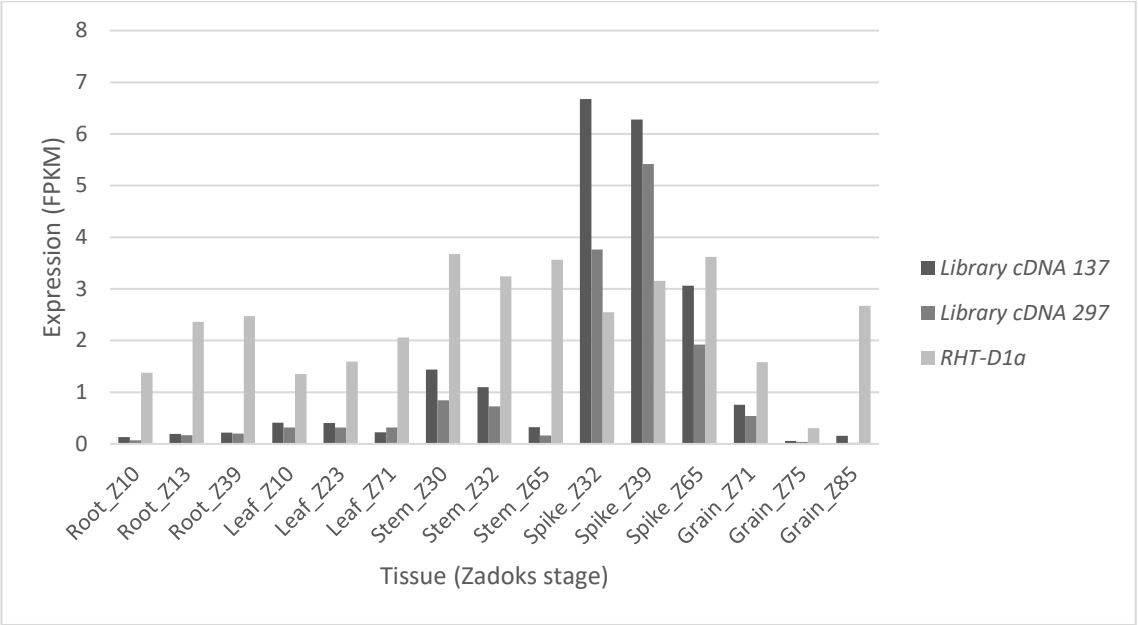

Figure 4.31 Expression levels of *library cDNAs 137* and *297* compared to *RHT-D1a.* A file containing all TGACv1 cDNAs was used as a template for RNAseq mapping with the Choulet (International Wheat Genome Sequencing, 2014) tissue specific dataset, containing RNAseq reads from five different tissues (root, leaf, stem, spike and grain) at three different developmental stages, indicated by the Zadoks scale (Z) number indicated in each tissue. Reads were mapped using the BWA-MEM function in Galaxy. FKPM values for each gene are shown for each tissue.

4.3.3.4 Library strain 143 contains a FAR1-related sequence.

Yeast strain 143 encodes a FAR RED IMPAIRED RESPONSE (FAR1)--related sequence. This strain was chosen for further characterisation because of the role of the FAR1 transcription factor, which acts downstream of phytochrome in the regulation of light responses (Siddiqui et al., 2016). FAR1 belongs to a family of mutator-like transposases which also includes FAR-RED ELONGATED HYPOCOTYL 3 (FHY3) (Lin and Wang, 2004). FAR1 and FHY3 dimerize (Lin et al., 2007, Ouyang et al., 2011) and positively regulate transcription of genes involved in the inhibition of hypocotyl elongation, opening of apical hook, expansion of cotyledons and greening which are associated with phytochrome-mediated development in response to R and FR light (Deng and Quail, 1999). FAR1 and FHY3 promote phyA signalling by positively regulating the expression of the phyA nuclear importers, FHY1 and FHL (Lin et al., 2007).

Sequencing of *library cDNA 143* confirmed that it is in-frame with the GAL4 start codon (**Figure 4.32**) and encodes a truncated product of TRIAE_CS42_U_TGACv1_642981_AA2125590, missing the N terminal 175 amino acids and the C terminal 47 amino acids (**Figure 4.33**). Some residues at the centre of this clone appear to be different from the TGAC amino acid sequence.

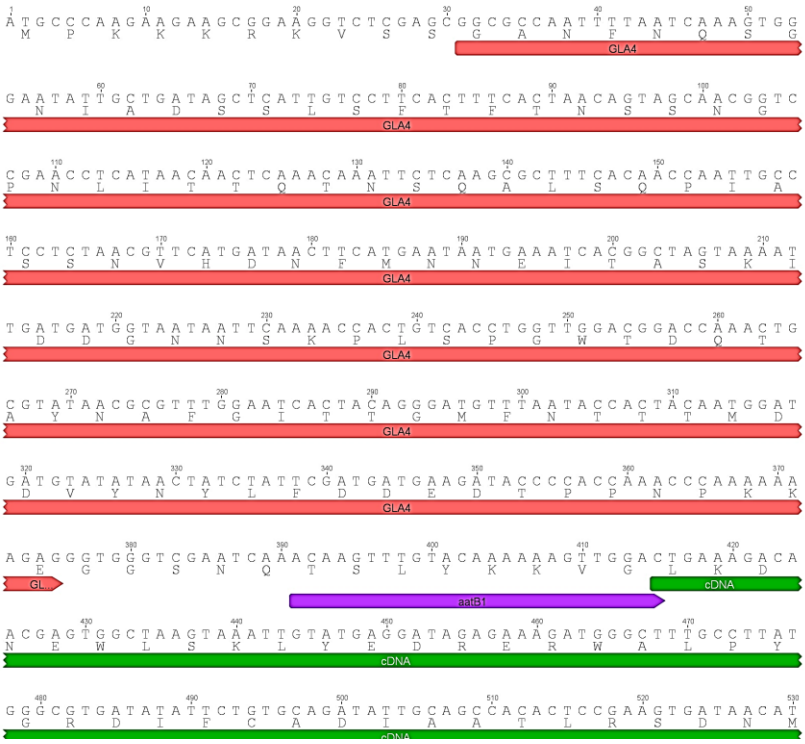

Figure 4.32 The *library cDNA 143* sequence is in-frame with the GAL4 start codon. The library strain 143 prey plasmid was sequenced to identify if the cDNA is in-frame with the GAL4 start codon. The sequence is shown in the figure, beginning at the GAL4 ATG start codon, running into the 143 cDNA sequence. The GAL4 activation domain is labelled in red under the sequence. The aatB1 sequence is labelled with purple under the sequence. The *library cDNA 143 sequence* is labelled with green under the sequence.

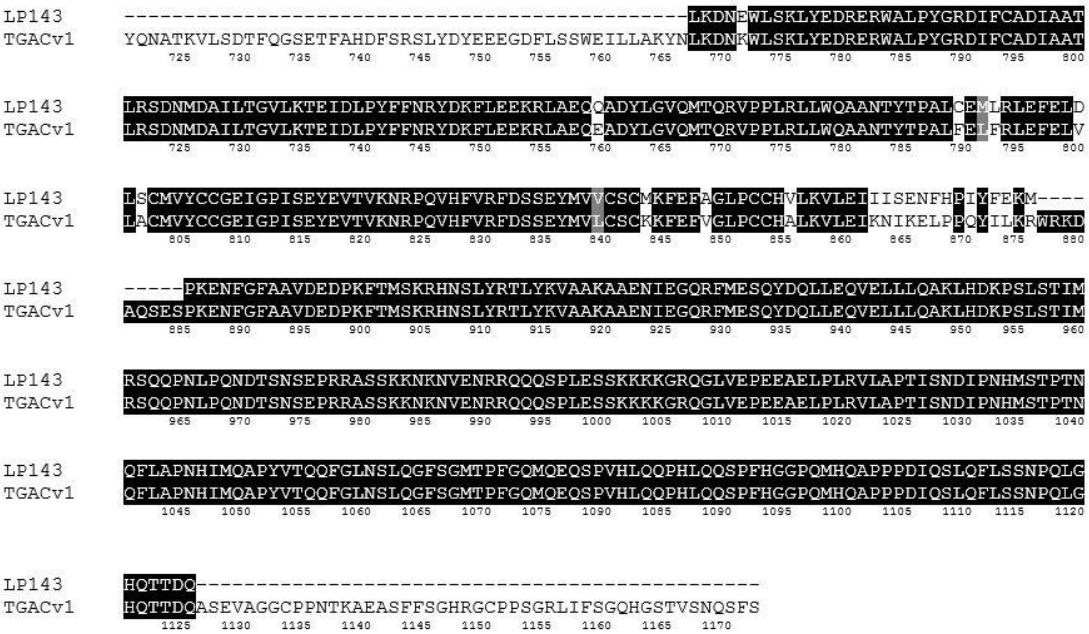

Figure 4.33 The sequence of library protein 143, a truncated FAR1-related sequence. The cDNA sequence present in the prey plasmid of library strain 143 was translated into the amino acid sequence. This library protein 143 (LP143) sequence was aligned to the full-length TRIAE_CS42_U_TGACv1_642981_AA2125590 sequence (labelled in the figure as TGACv1) using the T-coffee alignment tool. This figure shows residues 721-1173 of the full length TGACv1 sequence. Residues shown in reverse are shared between the two sequences.

The 3-AT assay testing the interaction between RHT-D1a and library protein 143 is shown in **Figure 4.34**. The RHT-D1a-library protein 143 strain was able to grow at all 3-AT concentrations at a visibly higher level than the self-activation control, demonstrating that library protein 143 is interacting with RHT-D1a (**Figure 4.34**)

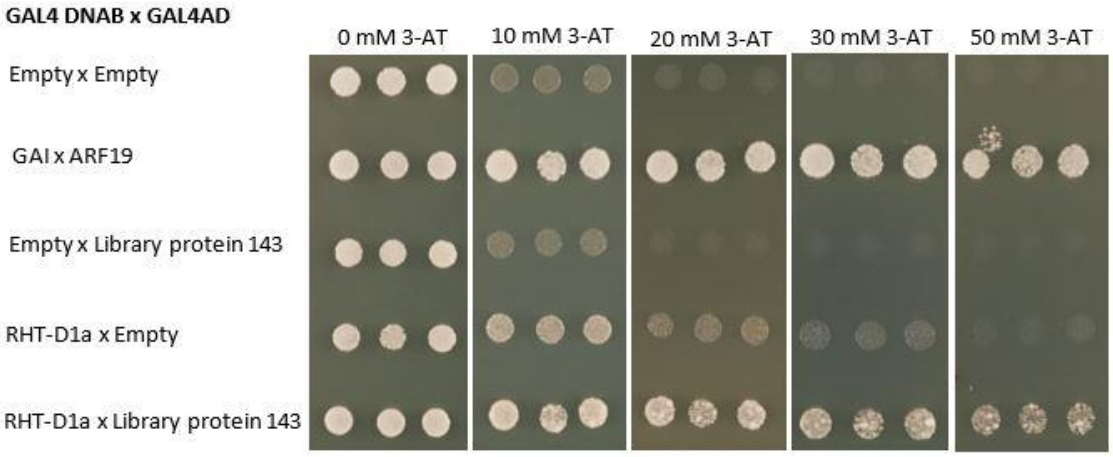

Figure 4.34 Yeast two-hybrid screen detecting the expression of *HIS3* demonstrating the interaction between RHT-D1a and library protein 143. Mav203 competent yeast were transformed with GLA4 DNA-binding bait (GAL4 DNAB) and GAL4 activation domain (GAL4 AD) prey vectors containing proteins labelled under the GAL4 DNAB and GAL4 AD headings at the left of the figure. These strains were spotted onto –Leu/-Trp/-His media containing concentrations of 3-AT ranging from 0-50 mM. Strains were spotted onto each plate with three technical replicates shown in each panel of the figure.

The X-gal assay to confirm the interaction between RHT-D1a and library protein 143 is shown in **Figure 4.35**. After 4h of incubation the RHT-D1a bait, library protein 143 prey strain showed a blue colour change which was indistinguishable from the colour change detected in the self-activation control strain. At 24 h of incubation, the same results were obtained with a stronger blue colour change. These results do not confirm the interaction between library protein 143 and RHT-D1a, demonstrated by the 3-AT assay (**Figure 4.34**).

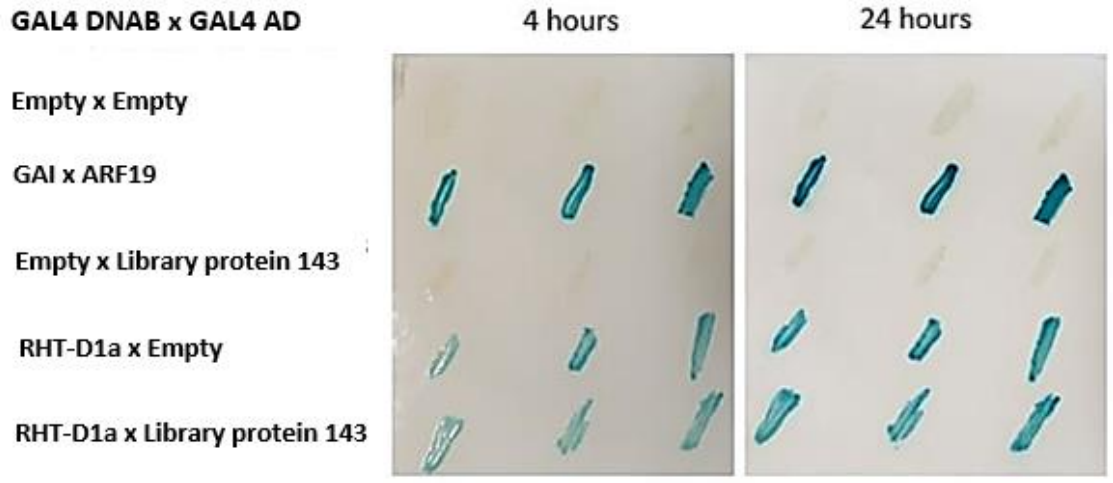

Figure 4.35 A yeast two-hybrid screen detecting the expression of the LacZ reporter gene does not indicate an interaction between library protein 143 and RHT-D1a. Mav203 competent yeast were transformed with GLA4 DNA-binding bait (GAL4 DNAB) and GAL4 activation domain (GAL4 AD) prey vectors containing proteins labelled under the GAL4 DNAB and GAL4 AD headings at the left of the figure. These strains were streaked onto a nitrocellulose membrane on YPD media in three technical replicates, which are shown in each panel of the figure. The plates were incubated for 24 h, then lysed and incubated with X-gal for 24h.The white-blue colour change was assessed at 4 and 24 h.

A Comparison between the expression levels of *library cDNA 143* and *RHT-D1a* (**Figure 4.36**) demonstrated that *library cDNA 143* is expressed at lower levels than RHT-D1a in all tissues, but expression is detectable indicating that an interaction has the potential to occur.

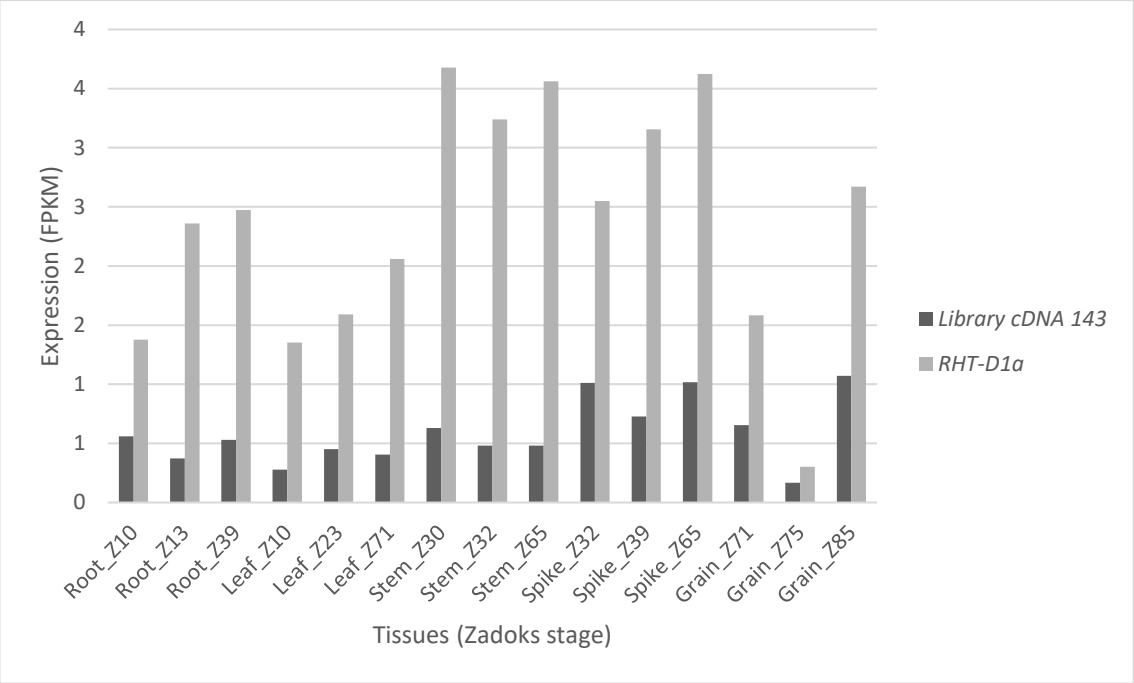

Figure 4.36 Expression levels of *library cDNA 143* compared to *RHT-D1a*. A file containing all TGACv1 cDNAs was used as a template for RNAseq mapping with the Choulet (International Wheat Genome Sequencing, 2014) tissue specific dataset, containing RNAseq reads from five different tissues (root, leaf, stem, spike and grain) at three different developmental stages, indicated by the Zadoks scale (Z) number indicated in each tissue. Reads were mapped using the BWA-MEM function in Galaxy. FKPM values for each gene are shown for each tissue.

4.3.3.5 Library strain 221 encodes a defensin 1-like protein.

Yeast protein 221 was chosen for further characterisation because the protein was identified in two library strains, and because a defensin has been implicated in the jasmonate and ethylene response pathways in *Arabidopsis* (Penninckx et al., 1998). Defensins are small cysteine-rich peptides with antimicrobial activity against a wide range of microorganisms. Most defensins act against fungi including yeast, although a small number can act on bacteria. Defensins generally inhibit pathogens through their functions as protein translation inhibitors, α-amylase and protease inhibitors or ion channel blockers (De Coninck et al., 2013).

Sequencing revealed that this cDNA is in-frame with the GAL4 activation domain start codon (**Figure 4.37**), and encodes the full-length TRIAE_CS42_4DL_TGACv1_343378_AA1133790 protein sequence (**Figure 4.38**).

Figure 4.37 *Library cDNA 221* is in-frame with the GAL4 start codon. The library strain 221 prey plasmid was sequenced to identify if the cDNA is in-frame with the GAL4 start codon. The sequence is shown in the figure, beginning at the GAL4 ATG start codon, running into the 221 cDNA sequence. The GAL4 activation domain is labelled in red under the sequence. The aatB1 sequence is labelled with purple under the sequence. The *library cDNA 221* sequence is labelled with green under the sequence.

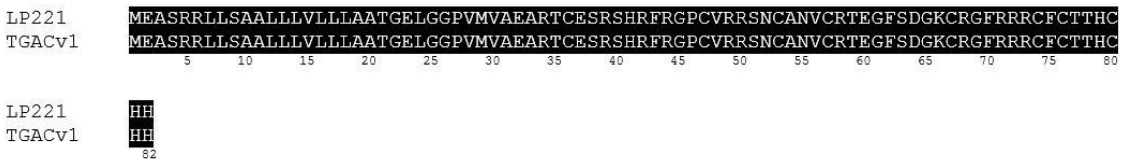

Figure 4.38 The amino acid sequence of library protein 221, a defensin-1 like protein. The cDNA sequence present in the prey plasmid of library strain 221 was translated into the amino acid sequence. This library protein 221 (LP221) sequence was aligned to the full-length TRIAE_CS42_4DL_TGACv1_343378_AA1133790 sequence (labelled in the figure as TGACv1) using the T-coffee alignment tool. Residues shown in reverse are shared between the two sequences.

The 3-AT assay testing the interaction between RHT-D1a and library protein 221 is shown in **Figure 4.39**. The RHT-D1a-library protein 221 strain grew at high levels up to 50mM 3-AT, like the GAI-ARF19 positive control. These results indicate that library protein 221 can interact with RHT-D1a.

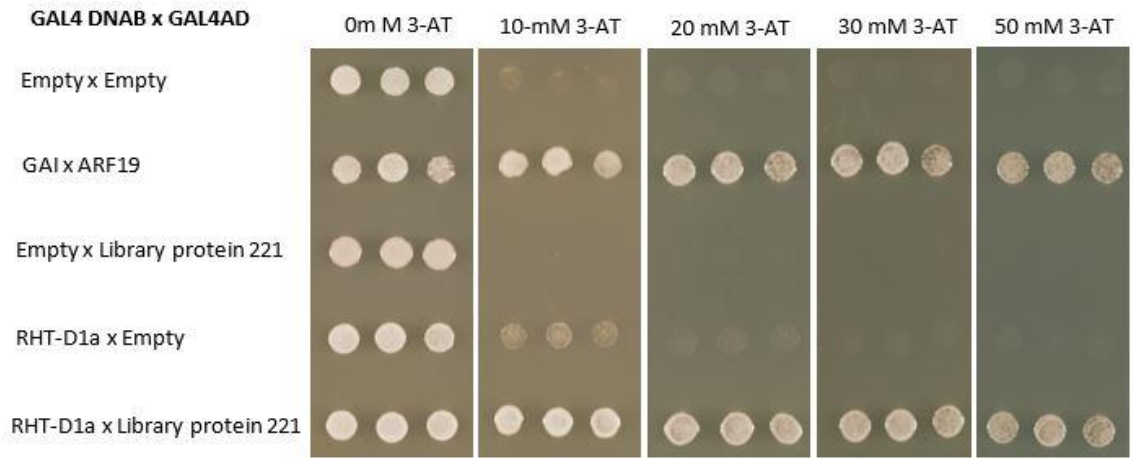

Figure 4.39 Library protein 221 interacts with RHT-D1a. Mav203 competent yeast were transformed with GLA4 DNA-binding bait (GAL4 DNAB) and GAL4 activation domain (GAL4 AD) prey vectors containing proteins labelled under the GAL4 DNAB and GAL4 AD headings at the left of the figure. These strains were spotted onto –Leu/-Trp/-His media containing concentrations of 3-AT ranging from 0-50 mM. Strains were spotted onto each plate with three technical replicates shown in each panel of the figure.

The X-gal assay to confirm the interaction between RHT-D1a and library protein 221 is shown in **Figure 4.40**. After 4 h of incubation the RHT-D1a bait, library protein 221 prey strain showed a blue colour change which was indistinguishable from the colour change detected in the self-activation control strain. At 24 h of incubation, the same results were obtained with a stronger blue colour change. These results are unable to confirm an interaction between library protein 221 and RHT-D1a, demonstrated by the 3-AT assay (**Figure 4.39**).

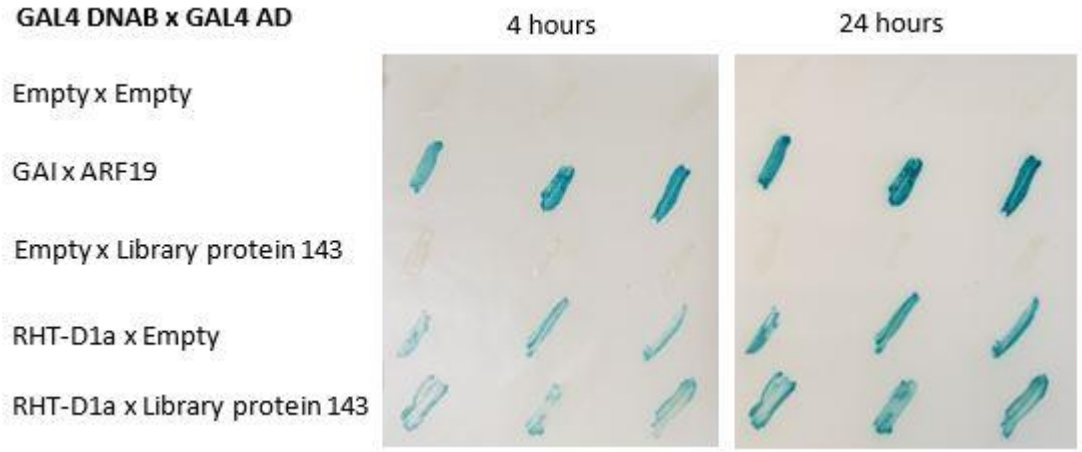

Figure 4.40 A yeast two-hybrid screen detecting the expression of the LacZ reporter gene does not indicate an interaction between library protein 221 and RHT-D1a. Mav203 competent yeast were transformed with GLA4 DNA-binding bait (GAL4 DNAB) and GAL4 activation domain (GAL4 AD) prey vectors containing proteins labelled under the GAL4 DNAB and GAL4 AD headings at the left of the figure. These strains were streaked onto a nitrocellulose membrane on YPD media in three technical replicates, which are shown in each panel of the figure. The plates were incubated for 24 h, then lysed and incubated with X-gal for 24 h. The white-blue colour change was assessed at 4 and 24 h.

A comparison between the expression levels of *library cDNA 221* and *RHT-D1a* (**Figure 4.41**) demonstrated that *library cDNA 221* is expressed at the highest levels in the root, but also has similar expression levels to RHT-D1a in the leaf, stem and spike, suggesting that an interaction could take place in these tissues.

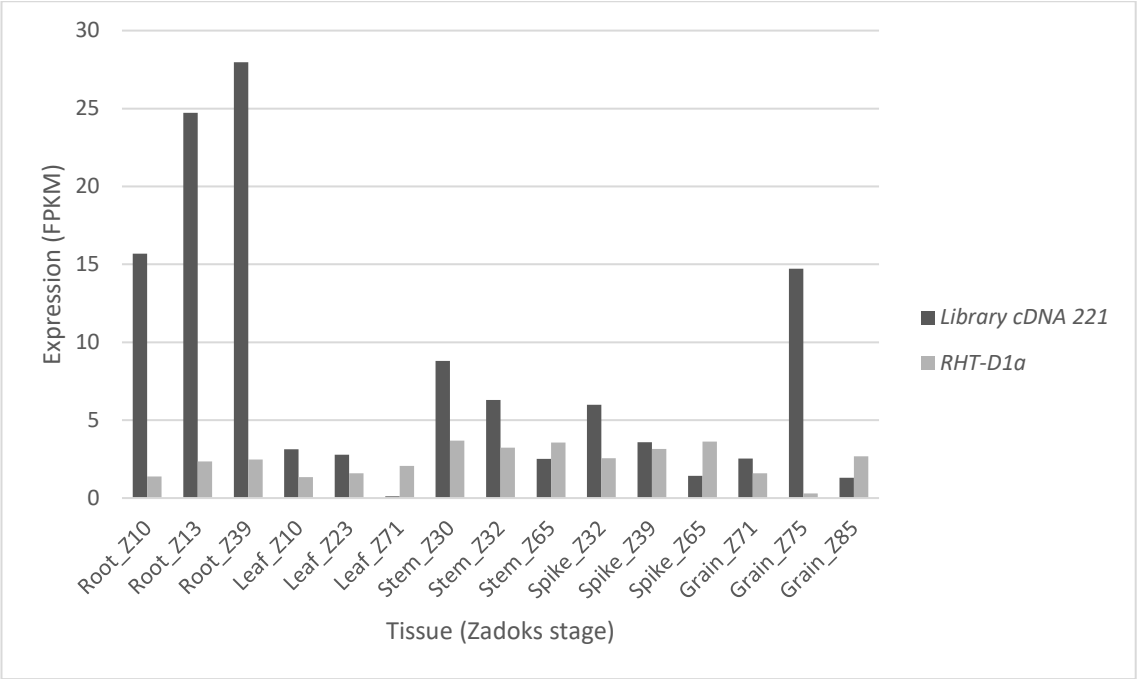

Figure 4.41 Expression levels of *library cDNA 221* compared to *RHT-D1a*. A file containing all TGACv1 cDNAs was used as a template for RNAseq mapping with the Choulet (International Wheat Genome Sequencing, 2014) tissue specific dataset, containing RNAseq reads from five different tissues (root, leaf, stem, spike and grain) at three different developmental stages, indicated by the Zadoks scale (Z) number indicated in each tissue. Reads were mapped using the BWA-MEM function in Galaxy. FKPM values for each gene are shown for each tissue.

4.3.3.6 Library strain 236 encodes a bHLH transcription factor.

Library strain 236 encodes a bHLH transcription factor. This strain was chosen for further characterisation because of its role as a transcription factor, and because of its similarity to PIFs, which also contain a bHLH domain. The bHLH domain proteins form a superfamily of transcription factors that bind as dimers to specific DNA target sites and can form homodimers or heterodimers with related sequences. bHLH domain transcription factors have been identified as regulators of a wide range of responses (Toledo-Ortiz et al., 2003), and interactions between bHLH transaction factors and DELLAs have been documented.

The *Arabidopsis* MCY2 and MYC3 bHLH transcription factors regulate the JA response, and are targeted for repression by the JAZ repressors. MYC2 has been shown to bind directly to all five *Arabidopsis* DELLAs in a yeast two-hybrid screen and deletion analyses revealed that the N terminal of MYC2 was required for this interaction. This interaction demonstrated that DELLAs are capable of repressing the plant defence response, involving the biosynthesis of sesquiterpenes, via their interaction and inhibition of MYC2 (Hong et al., 2012a). The bHLH transcription factor ALCATRAZ (ALC) has also been shown to interact with DELLAs. In yeast two-hybrid experiments, ALC was shown to bind to GAI, RGA and RGL2. DELLAs are thought to

bind to and inhibit the transcriptional activity of ALC to repress valve margin formation in the absence of GA (Arnaud et al., 2010).

Sequencing revealed that the cDNA sequence is in-frame with the GAL4 start codon (**Figure 4.42**), and encodes the full length TRIAE_CS42_7DL_TGACv1_603063_AA1974950 (**Figure 4.43**).

The rice sequence homologous to library protein 236 was used to identify homologous proteins in *Arabidopsis* using a Decypher terra blast-p search. The most closely related *Arabidopsis* sequence identified was At3g26744.1, which is a MYC-like sequence that is part of the group IIIb bHLH transcription factors.

Figure 4.42 *Library cDNA 236* is in-frame with the GAL4 start codon. The library strain 236 prey plasmid was sequenced to identify if the cDNA is in-frame with the GAL4 start codon. The sequence is shown in the figure, beginning at the GAL4 ATG start codon, running into the 236 cDNA sequence. The GAL4 activation domain is labelled in red under the sequence. The aatB1 sequence is labelled with purple under the sequence. The *library cDNA 236* sequence is labelled with green under the sequence.

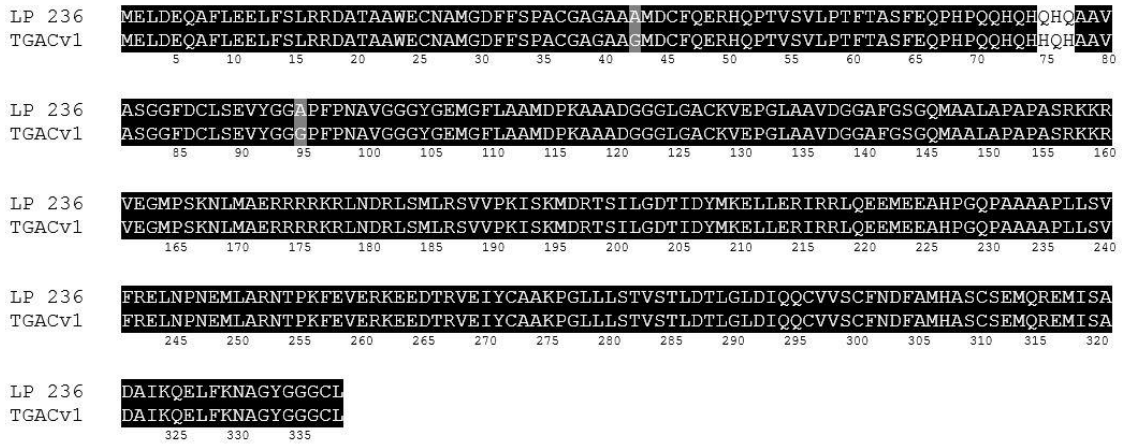

Figure 4.43 The amino acid sequence of library protein 236; a bHLH transcription factor. The cDNA sequence present in the prey plasmid of library strain 236 was translated into the amino acid sequence. This library protein 236 (LP236) sequence was aligned to the full-length TRIAE_CS42_7DL_TGACv1_603063_AA1974950 sequence (labelled in the figure as TGACv1) using the T-coffee alignment tool. Residues shown in reverse are shared between the two sequences.

The 3-AT assay testing the interaction between RHT-D1a and library protein 236 is shown in **Figure 4.44**. The RHT-D1a-library protein 236 strain grew at high levels up to 50mM 3-AT, much stronger than the self-activation control. These results indicate that library protein 236 can interact with RHT-D1a.

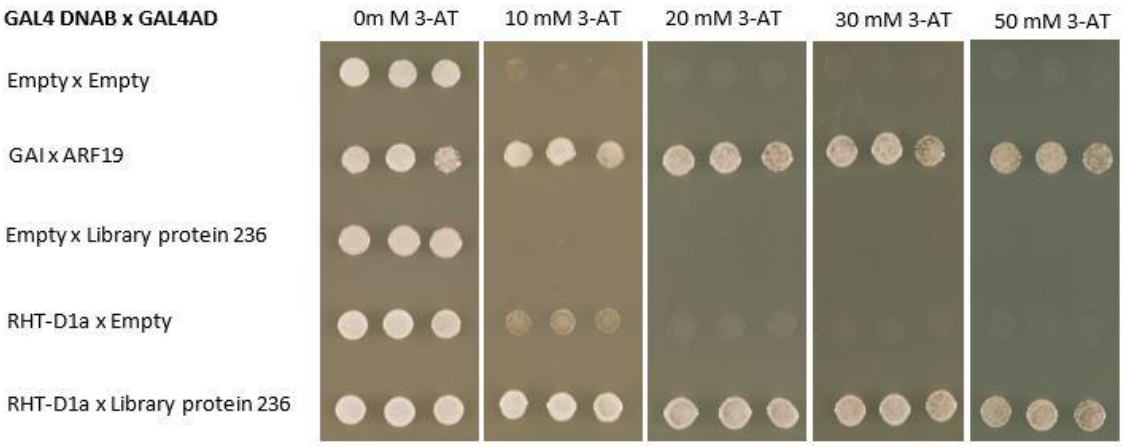

Figure 4.44 Library protein 236 interacts with RHT-D1a. Mav203 competent yeast were transformed with GLA4 DNA-binding bait (GAL4 DNAB) and GAL4 activation domain (GAL4 AD) prey vectors containing proteins labelled under the GAL4 DNAB and GAL4 AD headings at the left of the figure. These strains were spotted onto –Leu/-Trp/-His media containing concentrations of 3-AT ranging from 0-50 mM. Strains were spotted onto each plate with three technical replicates shown in each panel of the figure.

The X-gal assay to confirm the interaction between RHT-D1a and library protein 236 is shown in **Figure 4.45**. After 4 h of incubation the RHT-D1a bait, library protein 236 prey strain showed a blue colour change which was indistinguishable from the colour change detected in the self-activation control strain. At 24 h of incubation there was stronger blue colour change, with the self-activation control displaying similar levels colour change to the positive control. These results cannot confirm the interaction indicated by the 3-AT assay (**Figure 4.44**).

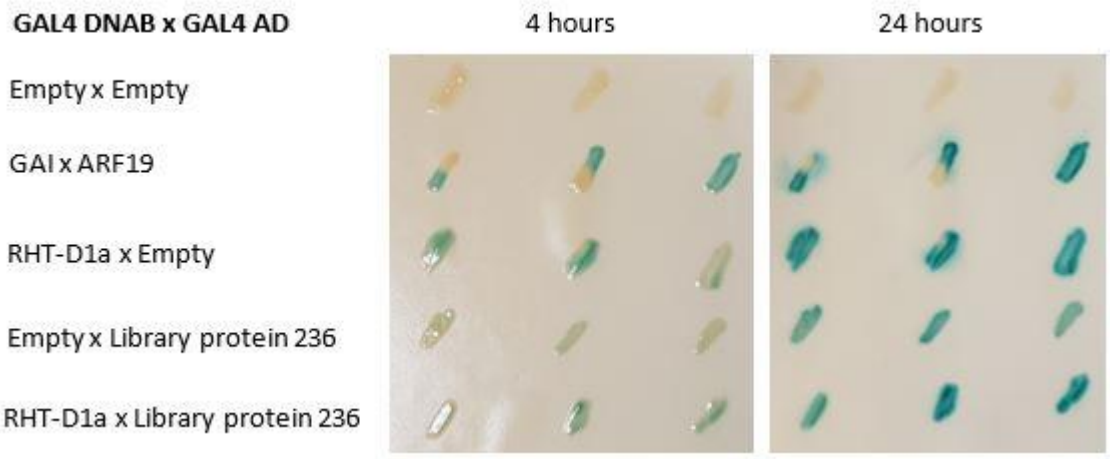

Figure 4.45 A yeast two-hybrid screen detecting the expression of the LacZ reporter gene does not indicate an interaction between library protein 236 and RHT-D1a. Mav203 competent yeast were transformed with GLA4 DNA-binding bait (GAL4 DNAB) and GAL4 activation domain (GAL4 AD) prey vectors containing proteins labelled under the GAL4 DNAB and GAL4 AD headings at the left of the figure. These strains were streaked onto a nitrocellulose membrane on YPD media in three technical replicates, which are shown in each panel of the figure. The plates were incubated for 24 h, then lysed and incubated with X-gal for 24 h. The white-blue colour change was assessed at 4 and 24 h.

A comparison between the expression levels of *library cDNA 236* and *RHT-D1a* (**Figure 4.46**) demonstrated that *library cDNA 236* is expressed at the highest levels in elongating stem, spike and developing grain, indicating that an interaction with RHT-D1a could occur in these tissues in vivo.

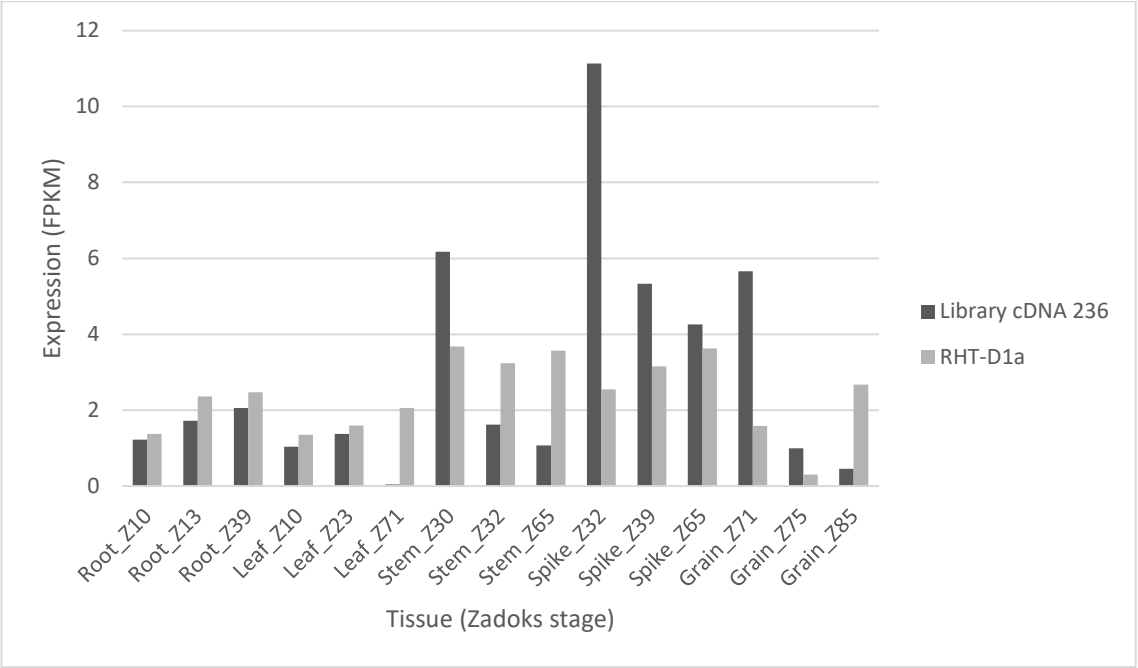

Figure 4.46 Expression levels of *library cDNA 236* compared to *RHT-D1a*. A file containing all TGACv1 cDNAs was used as a template for RNAseq mapping with the Choulet (International Wheat Genome Sequencing, 2014) tissue specific dataset, containing RNAseq reads from five different tissues (root, leaf, stem, spike and grain) at three different developmental stages, indicated by the Zadoks scale (Z) number indicated in each tissue. Reads were mapped using the BWA-MEM function in Galaxy. FKPM values for each gene are shown for each tissue.

4.3.3.7 Library Strain 444 encodes a zinc finger family protein.

Yeast strain 444 encodes a zinc finger family protein. This strain was chosen for further characterisation because an interaction between DELLAs and the zing finger INDETERMINATE DOMAIN (IDD) family proteins has been characterised previously (Yoshida et al., 2014). IDDs have a wide range of roles in the regulation of plant development such as control of flowering time and gravitropic responses (Morita et al., 2006, Seo et al., 2011). *Arabidopsis* IDDs 3, 4, 5, 9 and 10 were shown to interact with the GRAS domain of RGA along with the promoter sequence of a DELLA target gene, SCARECROW-LIKE3 (SCL3). The interaction between the IDDS and RGA was dependent on the C terminal region of the IDDS. This interaction therefore mediates the promotion of SCL3 expression by DELLAs (Yoshida et al., 2014). Another IDD protein, GAI-ASSOCIATED FACTOR1 (GAF1) has also been shown to interact with DELLAs (Fukazawa et al., 2014). GAF1 was shown to interact with all five *Arabidopsis* DELLAs using yeast two-hybrid screens. Deletion studies identified that the SAW domain of GAI and an internal 16 amino (PAM) domain of GAF1 were required for the interaction. The DELLA proteins were shown to act as co-activators of GAF1 function in promoting transcription. In this model, at low GA levels, GAF1 acts with DELLA as a regulator of GA-down-regulated genes,

such as the GA-biosynthetic gene *AtGA20ox2*. Whereas, at high GA levels, DELLAs are degraded, allowing GAF1 to bind TOPLESS RELATED, which suppresses GAF1 activity. (Fukazawa et al., 2014). Thus GAF1 is a major component of the feedback regulation of GA biosynthesis.

Sequencing revealed that this cDNA sequence was not in-frame with the GAL4 start codon **Figure 4.47**, however, the full length TRIAE_CS42_4BS_TGACv1_330766_AA1108750 protein sequence was present (**Figure 4.48**).

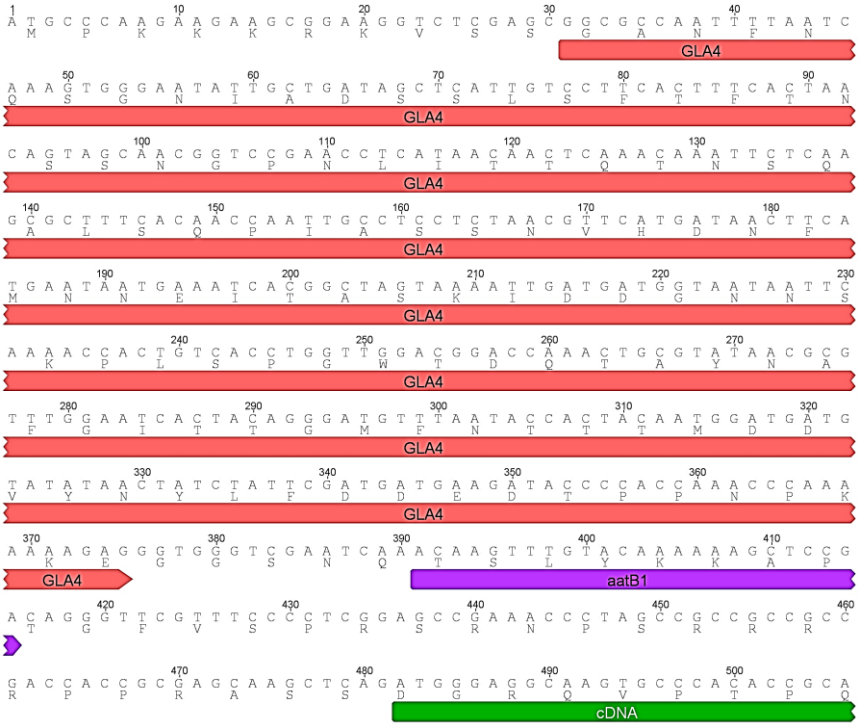

Figure 4.47 *Library cDNA 444* is not in-frame with the GAL4 start codon. The library strain 444 prey plasmid was sequenced to identify if the cDNA is in-frame with the GAL4 start codon. The sequence is shown in the figure, beginning at the GAL4 ATG start codon, running into the 444 cDNA sequence. The GAL4 activation domain is labelled in red under the sequence. The aatB1 sequence is labelled with purple under the sequence. The *library cDNA 444* sequence is labelled with green under the sequence.

```
LS444   MGGKCPHRKVKKRRLNCKQVRRGKFLVKADDAVYDELVKLADQGKDSEGKALPVDEDLPGMGQFYCLHCDRYFADETVKE
TGACv1  MGGKCPHRKVKKRRLNCKQVRRGKFLVKADDAVYDELVKLADQGKDSEGKALPVDEDLPGMGQFYCLHCDRYFADETVKE
        5   10   15   20   25   30   35   40   45   50   55   60   65   70   75   80

LS444   DHYRSKRHKKRVKQLSGPAPHTQIDADLAGGMGMPDNGLKLMSS
TGACv1  DHYRSKRHKKRVKQLSGPAPHTQIDADLAGGMGMPDNGLKLMSS
        85   90   95   100  105  110  115  120
```

Figure 4.48 The protein sequence of library screen 444; a zinc finger protein. The cDNA sequence present in the prey plasmid of library strain 444 (LS444) was translated into the amino acid sequence. This sequence was aligned to the TGACv1 full length sequence (labelled in the figure as TGACv1) of this protein using the T-coffee alignment tool. Residues shown in reverse are shared between the two sequences.

The 3-AT assay testing the interaction between RHT-D1a and library protein 444 is shown in **Figure 4.49**. The RHT-D1a-library protein 444 strain grew at high levels up to 50 mM 3-AT, like the GAI-ARF19 positive control. These results indicate that the protein encoded by library strain 444 can interact with RHT-D1a, and therefore must be expressed in frame. The discrepancy between this result and the sequencing result could either be due to re-initiation, or a sequencing error. Re-sequencing to confirm the frame was not carried out due to time constraints.

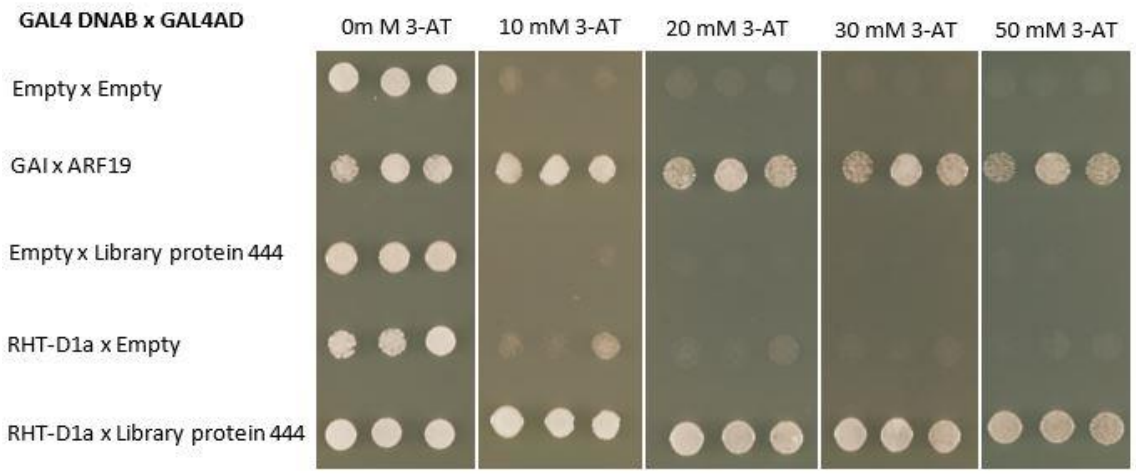

Figure 4.49 Library screen protein 444 interacts with RHT-D1a. Mav203 competent yeast were transformed with GAL4 DNA-binding bait (GAL4 DNAB) and GAL4 activation domain (GAL4 AD) prey vectors containing proteins labelled under the GAL4 DNAB and GAL4 AD headings at the left of the figure. These strains were spotted onto –Leu/-Trp/-His media containing concentrations of 3-AT ranging from 0-50 mM. Strains were spotted onto each plate with three technical replicates shown in each panel of the figure.

The X-gal assay to confirm the interaction between RHT-D1a and library protein 444 is shown in **Figure 4.50**. After 4 h of incubation the RHT-D1a bait, library protein 444 prey strain showed a blue colour change which was slightly stronger than the colour change detected in the self-activation control strain. At 24 h of incubation, the same results were obtained with a stronger blue colour change. These results suggest a weak interaction between library protein 444 and RHT-D1a, which confirms results from the *HIS3* 3-AT assay.

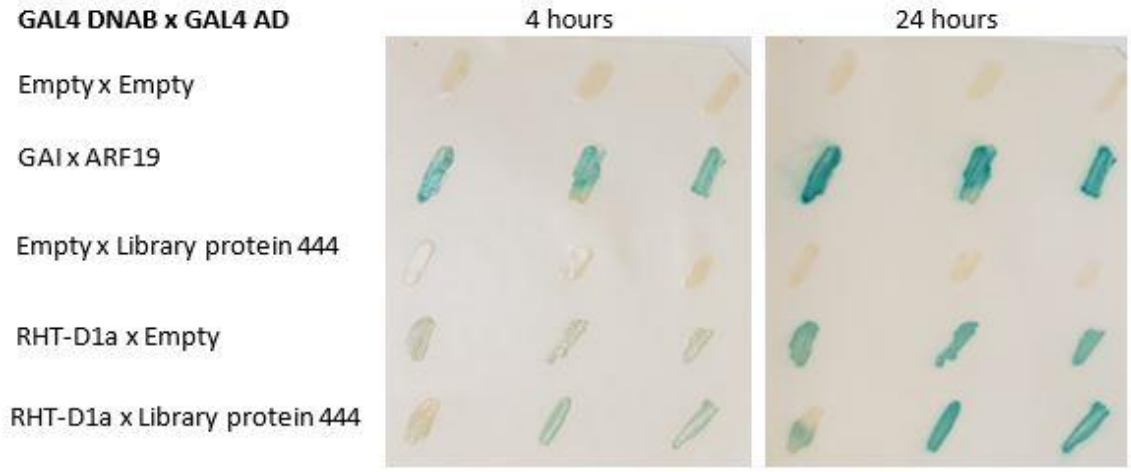

Figure 4.50 A yeast two-hybrid screen detecting the expression of the LacZ reporter gene does not indicate an interaction between library protein 444 and RHT-D1a. Mav203 competent yeast were transformed with GLA4 DNA-binding bait (GAL4 DNAB) and GAL4 activation domain (GAL4 AD) prey vectors containing proteins labelled under the GAL4 DNAB and GAL4 AD headings at the left of the figure. These strains were streaked onto a nitrocellulose membrane on YPD media in three technical replicates, which are shown in each panel of the figure. The plates were incubated for 24 h, then lysed and incubated with X-gal for 24 h. The white-blue colour change was assessed at 4 and 24 h.

Library protein 444 was first aligned with zinc finger domain proteins and IDD proteins. This alignment was used to produce a tree in which library protein 444 was grouped with the *Arabidopsis* IDD proteins. Because library protein 444 only grouped with IDD proteins, a second tree was produced containing only IDD proteins to identify which IDD library protein 444 is most homologous too. Phylogenetic analysis was carried out using IDD proteins from *Arabidopsis*, rice and maize IDD proteins with described functions, listed in **Table 4.7**, with accession numbers and references. Library protein 444 was aligned with these IDD proteins in a Clustal W alignment, which was used to produce a PHML tree shown in **Figure 4.51**. Library protein 444 was grouped with rice regulator of *CBF1* (ROC1), the *Arabidopsis* IDDs 4 and 5, *Arabidopsis* GAF1, and IDD1, and the rice loose plant architecture 1 (LPA1). Library protein 444 appears to be most closely related to OsROC1. The interaction between DELLAs and IDDs described by Yoshida et al. (2014) involved two conserved C terminal domains. These domains could not be identified at the C terminus of library protein 444, and there were no other regions of conservation between the IDD sequences. For this reason, an alignment to compare the sequence of library protein 444 with the other IDDs could not be produced. This suggests that the function of library protein 444 may not be as an IDD, despite homology implied by phylogenetic analysis. It is possible that library protein 444 is a zinc finger protein with an unrelated function to IDDs.

Table 4.7 IDD proteins from *Arabidopsis*, rice and maize. The accession number and references for the intermediate domain (IDD) proteins used in phylogenetic analysis.

Species	Name	Accession Number	Reference
Arabidopsis	AtIDD1	At5g66730	Feurtado et al. (2011)
Arabidopsis	AtIDD3	At1g03840	Yoshida et al. (2014)
Arabidopsis	AtIDD4	At2g02080	Yoshida et al. (2014)
Arabidopsis	AtIDD5	At2g02070	Yoshida et al. (2014)
Arabidopsis	AtIDD9	At3g45260	Yoshida et al. (2014)
Arabidopsis	AtGAF1	At3g50700	Fukazawa et al. (2014)
Arabidopsis	AtMGP	At1g03840	Welch et al. (2007)
Arabidopsis	AtJKD	At5g03150	Welch et al. (2007)
Maize	ZmID1	AAC18941.1	Colasanti et al. (2006)
Rice	EDH2	BAG12102.1	Matsubara et al. (2008)
Rice	OsROC1	LOC_Os09g12770 Os09g0299200	Dou et al. (2016)
Rice	OsLPA1	AFS60115.1	Wu et al. (2013)

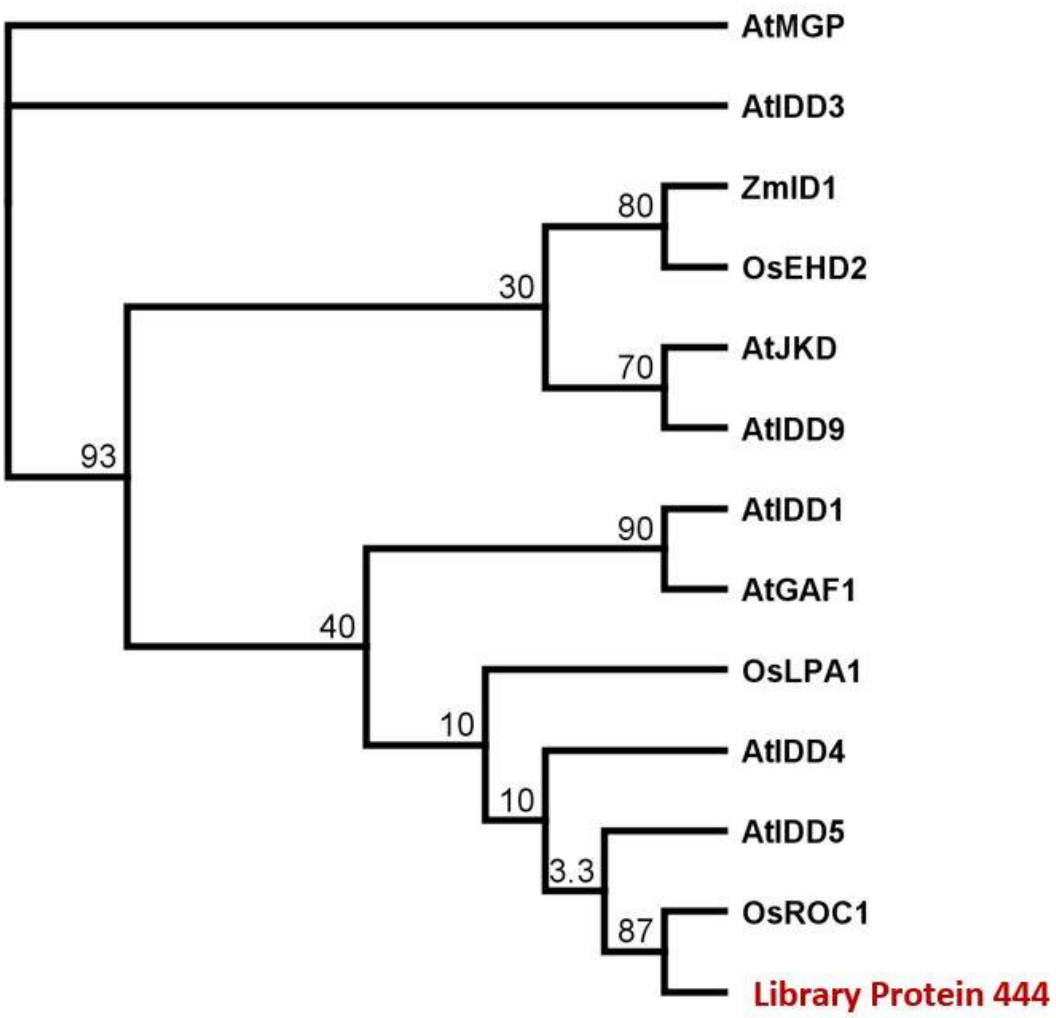

Figure 4.51 The relationship between library protein 444 and IDD proteins. INTERMEDIATE DOMAIN (IDD) proteins from *Arabidopsis*, rice and maize were aligned using the ClustalW tool in Geneious. This alignment was used to produce a PHYML WAG tree. Library protein 444 is labelled in red. Accession numbers shown in **Table 4.7**. Bootstrapping values are shown at the branch points of the tree.

A comparison between the expression levels of *library cDNA 444* and *RHT-D1a* (**Figure 4.52**) demonstrated that *library cDNA 444* is expressed strongly compared to *RHT-D1a* in all tissues tested, indicating that an interaction with RHT-D1a *in vivo* could occur in any of these tissues.

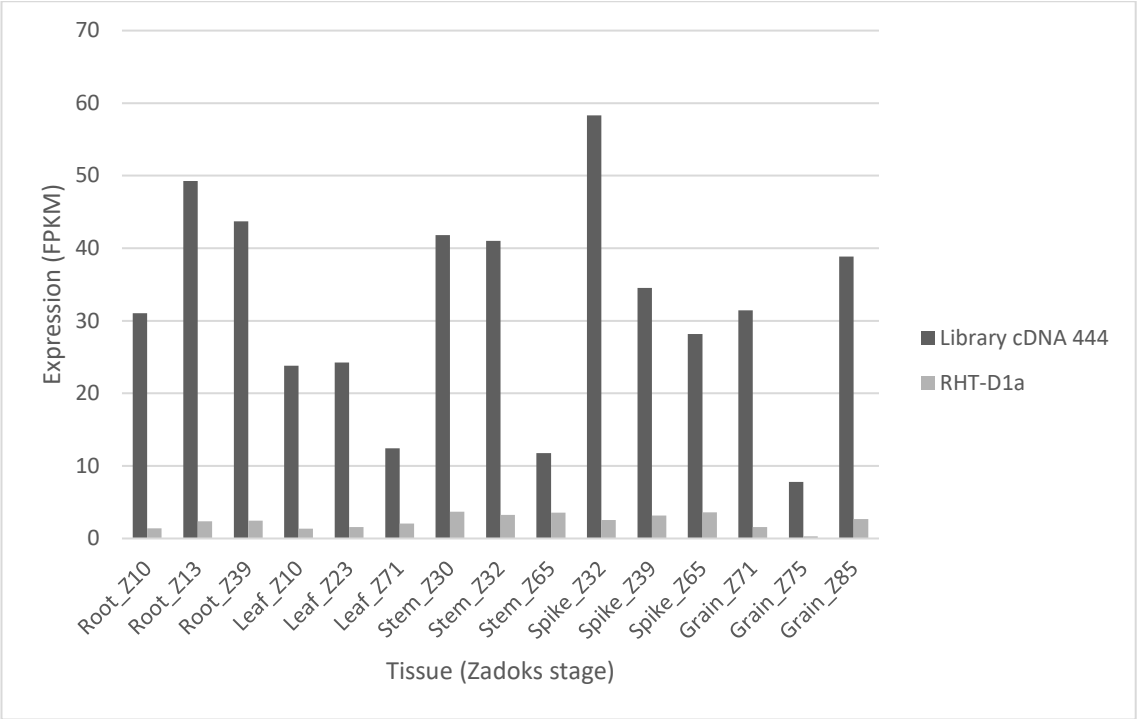

Figure 4.52 Expression levels of *library cDNA 444* compared to *RHT-D1a*. A file containing all TGACv1 cDNAs was used as a template for RNAseq mapping with the Choulet (International Wheat Genome Sequencing, 2014) tissue specific dataset, containing RNAseq reads from five different tissues (root, leaf, stem, spike and grain) at three different developmental stages, indicated by the Zadoks scale (Z) number indicated in each tissue. Reads were mapped using the BWA-MEM function in Galaxy. FKPM values for each gene are shown for each tissue.

4.3.3.8 Library strains 91, 202 and 220 encode proteins that do not interact with Rht-D1a

Yeast strain 91 encodes a GATA transcription factor 16-like isoform, which was not in-frame with the GAL4 start codon. Yeast strain 202 encodes a full-length bHLH transcription factor, and library strain 220 encodes a full-length ethylene insensitive 3-like protein. The 3-AT assay testing the interaction between RHT-D1a and library proteins 91, 202 and 220 is shown in **Figure 4.53**. The RHT-D1a-LP91/LP202/LP220 strains displayed only a very low level of growth at or above 10mM 3-AT, much lower than or equal to the self-activation control. These results indicate that library proteins 91, 202 and 220 do not interact with RHT-D1a.

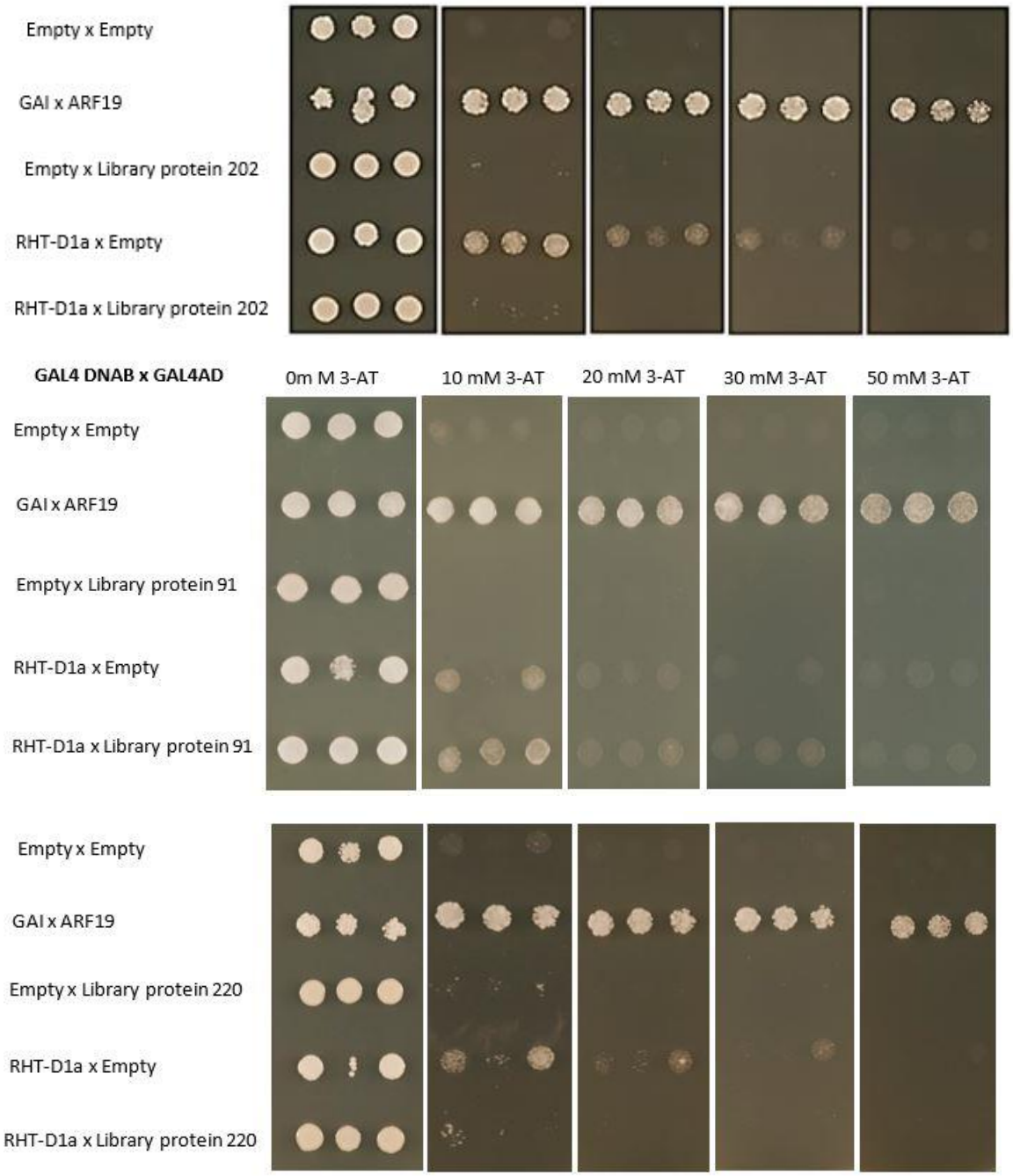

Figure 4.53 Yeast two-hybrid screen detecting the expression of *HIS3* demonstrating that library proteins 91, 202 and 220 do not interact with RHT-D1a.Mav203 competent yeast were transformed with GLA4 DNA-binding bait (GAL4 DNAB) and GAL4 activation domain (GAL4 AD) prey vectors containing proteins labelled under the GAL4 DNAB and GAL4 AD headings at the left of the figure. These strains were spotted onto –leu/-trp/-his media containing concentrations of 3-AT ranging from 0-50mM. Strains were spotted onto each plate with three technical replicates shown in each panel of the figure.

4.4 Discussion

4.4.1 RHT-D1a interacts with all three TaPIL proteins in yeast two-hybrid assays

This project aimed to determine whether or not the wheat DELLA protein RHT-1 interacts with the wheat PIF-like proteins TaPIL1, TaPIL2 and TaPIL3. The interaction between DELLAs and

PIFs has, at this point, only been demonstrated in *Arabidopsis.* To confirm that the TaPILs are potential targets for controlling GA-regulated stem elongation, this interaction must be established in wheat.

The yeast two-hybrid approach used in this project indicated that all three TaPIL sequences have a strong interaction with RHT-D1a. In all cases the growth of yeast strains transformed with both the RHT-D1a and the TaPIL sequences was equivalent to the GAI-ARF19 positive control and much higher than the level of self-activation from the bait plasmids. A C terminal GRAS domain fragment of RHT-D1a was used in this assay because the N-terminal DELLA/TVHYNP motif of the rice DELLA, SLR1, has been shown to possesses transactivation activity, while the C terminal GRAS domain was determined to be responsible for DELLA interactions with other proteins (Hirano et al., 2012). Yoshida et al. (2014) therefore used only a GRAS domain C terminal fragment of RGA to test interaction with members of the IDD family. The truncated RHT-D1a bait construct showed a low level of self-activation up to 20 mM 3-AT, meaning that the C terminal domain of RHT-D1a must either have some transactivation activity, or can interact with the NLS or GAL4 activation domain in the prey plasmid.

TaPIL1 was the only TaPIL which did not self-activate and could therefore be used as a bait protein. Both TaPIL2 and TaPIL3 caused very high levels of self-activation, presumably because of their activity as transcription factors. TaPIL1 contains the same conserved APB and bHLH domains as TaPIL2 and TaPIL3, so it is unclear why TaPIL1 does not cause the same level of self-activation, but this could indicate a difference in function between TaPIL1 and the other TaPILs. TaPIL2 and TaPIL3 may therefore be able to transactivate reporter genes, interact with a NLS or bind to the GAL4 activation domain to provoke the self-activation response.

The yeast two-hybrid assay demonstrated that the interaction between RHT-D1a and all three TaPILs was sufficient to drive the expression of both the *HIS3* and *LacZ* reporter genes. This is a strong indication that an interaction is occurring, although ideally, the interaction would be confirmed with an alternative experimental method such as a pull-down assay. This method also only demonstrates an interaction using two methods in the same system, so using another method such as Bimolecular Florescence Complementation (BiFC) to establish the interaction *in vivo* would be ideal to confirm the interaction.

The interaction between the wheat PILs and RhtD1-a may occur in a similar way to the interaction between DELLAs and PIFs in *Arabidopsis in vivo*. In this case a potential function for the interaction between RHT-D1a and the TaPILs would be the RHT-1 mediated repression of TaPIL activity by sequestration (Feng et al., 2008, de Lucas and Prat, 2014). In terms of the

control of stem elongation, the role of PIFs in the shade avoidance response (Jeong and Choi, 2013), involves their promotion of genes that stimulate stem elongation. In this instance, a reduction in GA concentration would lead to an increase in Rht-1 abundance, so that the TaPILs would be sequestered to prevent their promotion of stem elongation. This would support the role of the TaPILs as potential targets for the specific control of GA-mediated stem elongation. This model should be tested by altering the expression levels of the PILs in wheat to determine the phenotypic effects. The TaPIL sequences could be overexpressed and also repressed through either knockdown with RNAi or repression domains, or knocked out through mutations within the homoeologous sequences. If the TaPILs are involved in the regulation of stem elongation in a similar manner to OsPIL1, it would be expected that overexpression lines would display tall elongated stem phenotypes, while reduced expression lines would show a dwarf-like phenotype. These lines might also display other GA-related phenotypes if TaPILs are involved in modulating the GA response, such as changes in flowering time, fertility defects and reduced apical dominance. It would then be necessary to confirm which genes are targeted by the TaPILs, and if these genes are RHT-1 regulated, which could be accomplished using ChIP seq.

4.4.2 Identification of novel RtD1a interactors in the wheat stem

The yeast two-hybrid library screen aimed to identify proteins that interact with RHT-1 within the wheat stem. Identification of alternative RHT-1 interactors could provide further targets for the manipulation of GA-regulated stem elongation and provide clues to the mechanisms by which RHT-1 regulates stem elongation. The screen was carried out using the Rht-D1a bait construct used in the specific yeast two-hybrid assays. The bait construct displayed a low level of self-activation below 20 mM 3-AT. For this reason, the screen was carried out at 20 mM 3-AT to reduce the background level of colonies growing only because of self-activation. Screening at this level of 3-AT could have excluded strains with prey proteins, which only had a weak interaction with RHT-D1a, so that some interactors were likely to be missed from this screen. Furthermore, the level of self-activation displayed by the RHT-D1a bait may have resulted in false positives by allowing some strains to grow at 20 mM 3-AT even if they did not have an interaction with Rht-D1a. Despite this, the screen identified 486 strains with possible interactors, and from these twelve colonies of interest were chosen for further characterisation. Of particular interest were cDNAs that encoded proteins which could be involved in hormone signalling or regulation of stem elongation. The twelve library proteins were selected for further characterisation because they it into one or more of the following criteria; being identified in multiple clones in the library screen, there was a previous

interaction with DELLAs identified in *Arabidopsis*, they had a role in hormone signalling, or they had a role in light signalling.

Only two of the nine strains which were shown to interact with RHT-D1a in the 3-AT assay were also confirmed using the X-gal assay. In all other cases the level of self-activation in the RHT-D1a control was indistinguishable from the test strain. This is likely to be because the X-gal assay is more sensitive to self-activation, meaning if the interaction between RHT-D1a and the library protein is weak, the colour change will not be detectable. The X-gal assay was able to confirm the interaction between all there TaPILs and RHT-D1a, indicating that these interactions are strong. However, the TaPILs were not picked out of the library screen despite this strong interaction. In addition, the TaPILs are highly expressed in the stem (see **chapter three section 3.2.4**), which would suggest that they are interacting with RHT-D1a in the wheat stem. This could be because the TaPILs are just not present in the 147 clones from the strains which were sequenced (**Appendix Table S.1**). It would therefore be essential to sequence the remaining 300 clones.

Of the twelve strains of interest, three strains, 91, 202 and 220, did not show an interaction in the 3-AT yeast two-hybrid assays. This suggests that these strains were picked up in the library screen due to the self-activation activity of the RHT-D1a bait rather than an interaction between Rht-1 and the library proteins.

4.4.2.1 Library protein 59: BOI related E3 ubiquitin ligase-like

Library cDNA 59 encodes the full length TRIAE_CS42_4DL_TGACv1_344008_AA1142470, which is homologous to BOI-type ring finger E3 ubiquitin ligase-like proteins. In *Arabidopsis* BOI and BOI related (BRG) proteins 1-3 have been shown to interact with DELLAs via their RING domain, which allows the DELLA-BOI complex to target the promoters of a subset of GA responsive genes (Park et al. (2013). *Arabidopsis* BOI proteins have been shown to be involved multiple processes in plant growth, including the regulation of pathogen responses (Luo et al., 2010), germination and flowering (Nguyen et al., 2015), many of which are typical of enhanced GA signalling.

Altering BOI expression in *Arabidopsis* resulted in GA response phenotypes (Park et al., 2013). Single *boi* mutants had no effect on the GA response, but the quadruple *boiQ* mutant lines displayed phenotypes typical of enhanced GA signalling. In contrast, BOI overexpression lines demonstrated phenotypes associated with reduced GA signalling. The *boiQ* mutant showed a 90% germination rate in the presence of the GA biosynthesis inhibitor PAC, whereas overexpression lines showed reduced germination in the presence of PAC, indicating that BOI-

DELLA interaction results in the repression of germination in *Arabidopsis*. BOIs were also shown to inhibit chlorophyll accumulation, a process shown to be inhibited by GA (Park et al., 2013). The *boiQ* mutants displayed significantly reduced chlorophyll accumulation resulting in pale leaves, while overexpression lines had higher chlorophyll levels, demonstrating that BOIs promote chlorophyll accumulation. The *boiQ* mutants also displayed an early juvenile to adult transition, while overexpression delayed the transition, indicating that BOIs are involved in the repression of juvenile to adult transition. Flowering was shown to be induced in the *boiQ* mutants, which displayed an early flowering phenotype while overexpression lines displayed a late flowering phenotype. All these *boiQ* mutant phenotypes were shared by the DELLA pentuple mutant (*dellaP*) mutant which indicates that BOIs and DELLAs regulate the same processes in development (Park et al., 2013).

The BOI proteins identified by Park et al. (2013) were used to produce a phylogenetic tree with library protein 59, shown in **Figure 4.17**. Library protein 59 was grouped with BRG3, suggesting that this could be the most closely related *Arabidopsis* protein. The *Arabidopsis* BOI proteins play a redundant role in the regulation of GA responsive genes, so it is unclear if library protein 59 alone could be involved in BOI mediated regulation of the GA response, or if multiple wheat proteins could be responsible. The RING domains of the *Arabidopsis* BOIs and library protein 59 were compared in a T-coffee alignment (**Figure 4.18**), which demonstrated that library protein 59 contains a conserved RING domain with conservation of 7 of the 8 conserved metal ligand positions. The conserved RING domain supports the role of library protein 59 as a wheat BOI-related protein.

The interaction between library protein 59 and RHT-D1a detected in the yeast two-hybrid screen suggests that DELLAs and BOIs also interact in wheat. It could be hypothesised that in wheat library protein 59 and RHT-D1a interact to form a complex which targets the promoters of genes involved in the GA response, in the same way that this interaction occurs in *Arabidopsis*. If this is the case, library protein 59 could be expected to repress the expression of genes involved in germination, chlorophyll accumulation, juvenile to adult transition and flowering. *Library cDNA 59* was expressed at a high level in all five tissues and developmental stages present in the RNAseq data, supporting the activity of the RHT-1 BOI complex in this variety of plant processes.

4.4.2.2 Library protein 65: An ethylene responsive element binding protein

Library protein 65 encodes the full length TRIAE_CS42_7AS_TGACv1_570423_AA1835500 ethylene-responsive element binding protein, which was shown to interact with Rht-D1a in both the *HIS3* and *LacZ* assays. The interaction between RHT-D1a and library protein 65 is

consistent with the findings of (Marin-de la Rosa et al., 2014), who used a yeast two-hybrid library screen with *Arabidopsis* GAI as the bait to identify an ethylene responsive element binding protein, RELATED TO APETALA2.3 (RAP2.3), as a GAI interactor. Another ERF family protein, RAP2.12, was also able to interact with GAI and RGA, suggesting that the interaction with DELLAs might be able to occur with all ERF-VII family proteins (Marin-de la Rosa et al., 2014). Yeast two-hybrid assays have been used to demonstrate that ERF11, ERF4, ERF8 and ERF10, interact with the GRAS domain of RGA (Zhou et al., 2016).

The interaction between GAI and RAP2.3 was shown to repress the ability of RAP2.3 to bind to and promote the expression of its target genes. One process shown to be regulated by this interaction was apical hook development in seedlings. RAP2.3 promotes the expression of apical hook promoting genes in the presence of ethylene, whereas GAI represses RAP2.3 activity in the absence of GA to repress apical hook formation (Marin-de la Rosa et al., 2014). ERF11 has been shown to promote stem elongation redundantly with other closely related ERFs 4, 8 and 10. Overexpression of ERF11 caused an enhanced GA response phenotype, while single *erf11* mutants had a reduced GA response. The interaction between RGA and ERF11 was shown to repress the activity of DELLAs in promoting expression of their target genes such as *bHLH137*. This model indicates regulated two counteracting processes; Promoting internode elongation by promoting GA biosynthesis at the same time as repressing DELLA activity, which prevents DELLA mediated activation of GA biosynthesis genes. (Zhou et al., 2016). In rice, ERF proteins, OsSUB1A, SNORKEL1 and SNORKEL2 (Hattori et al., 2009, Xu et al., 2006), have been linked to the regulation of stem elongation. However, in rice OsSUB1A has been shown to regulate GA response by affecting the expression levels of the rice DELLA SLR1 (Xu et al., 2006).

The interaction between library protein 65 and RHT-D1a supports the findings that ERF family proteins in *Arabidopsis* are capable of binding DELLAs. Using the interaction between DELLAs and ERFs in *Arabidopsis* as a model, it can be suggested that library protein 65 would have a role in promoting stem elongation. In this case, the interaction between library protein 65 and RHT-D1a would inhibit RHT-D1a activity, thereby preventing the RHT-D1a repression, while also promoting the expression of GA biosynthesis genes. In support of this model, RNAseq data analysis showed that *library cDNA 65* is highly expressed in the stem. These findings suggest that library protein 65 could have a role in regulating stem elongation, and that manipulating its expression could provide a mechanism to regulate plant height without the pleiotropic effects of the *Rht-1* mutants.

4.4.2.3 Library proteins 137 and 297: squamosa promoter binding-like proteins

Library proteins 137 and 297 encode N-terminally truncated versions of TRIAE_CS42_5BL_TGACv1_406028_AA1339440 and TRIAE_CS42_5AL_TGACv1_377393_AA1246520, respectively. These proteins encode the A and B homoeologues of one SPL protein. An interaction between RHT-1 and library proteins 137 and 297 is consistent with findings from *Arabidopsis*, as the DELLA protein RGA has been shown to bind directly to SPLs in a yeast two-hybrid screen (Yu et al., 2012). Because only a C terminal truncated version of the SPL protein was encoded by both library protein 137 and 297, this C terminal region must be the part of the protein required for the interaction between RHT-D1a and the SPL. This is supported by findings of Yu et al. (2012), that if the C terminal of SPL9 is deleted, the interaction between SPL9 and RGA is compromised. SPLs are involved in the regulation of flowering under short days through their interaction with micro RNAs (miRNA). As the plant ages, the levels of miRNA156 decline, allowing SPL levels to increase and promote the juvenile to adult phase transition and flowering through their activation of miR172, MADS box genes, and the transcription factor LEAFY (Wang et al., 2009, Wu et al., 2009, Yamaguchi et al., 2009).

The binding of RGA to SPL9 was found to repress the transcriptional activity of SPL9, which is then unable to promote the expression of the MADS box genes or miR172. Through this mechanism low GA levels lead to RGA-mediated repression of the juvenile to adult phase transition through the repression of SPL activity. In this model, the interaction between RHT-D1a and library proteins 137 and 297 would inhibit their transcriptional activity and repress the juvenile to adult transition in wheat.

SPLs play a wide variety of roles in plant growth and development, so a phylogenetic tree was constructed to ascertain which SPLs were homologous to library proteins 137 and 297. SPL proteins from rice, maize and *Arabidopsis* were used to form a phylogenetic tree shown in **Figure 4.30**. Library proteins 137 and 297 are grouped with rice SPL16, maize TGA1 and *Arabidopsis* SPL10 and SPL11. Both OsSPL16 and ZmTGA1 are involved in the regulation of grain architecture (Wang et al., 2012, Yu et al., 2015), which could indicate a similar role for library proteins 137 and 297. The *Arabidopsis* SPL10 and SPL11 proteins are involved in shoot maturation (Shikata et al., 2009). The *library cDNAs 137* and *297* are most highly expressed in the three spike developmental stages, which include flowering and grain development. Since OsSLP16 is involved in grain architecture, it is possible that this could be determined early in grain development, explaining the high level of library proteins 137 and 297 expression in the spike and low levels in the grain (**Figure 4.31**). This would indicate that library proteins 137 and

297 could be involved in juvenile to adult phase transitions and shoot maturation, similar to the *Arabidopsis* SPLs. In this case RHT-D1a would inhibit the promotion of shoot maturation and flowering by repressing the activity of library proteins 137 and 297.

4.4.2.4 Library protein 236: bHLH transcription factor-like protein.

Library protein 236 (LP236) encodes the full length TRIAE_CS42_7DL_TGACv1_603063_AA1974950 bHLH transcription factor-like protein. The protein was chosen for further characterisation because multiple bHLH domain containing proteins have been shown to interact with DELLAs. The bHLH domain proteins belong to a superfamily of transcription factors which form homo or heterodimers to bind DNA sequences via the bHLH DNA binding domain and regulate transcription. bHLH transcription factors are involved in the regulation of a wide variety of developmental processes (Toledo-Ortiz et al., 2003), and interactions between multiple bHLH transaction factors and DELLAs have been documented.

The *Arabidopsis* MCY2, MYC3 and MYC4 bHLH transcription factors are involved in the regulation of the JA response. The MYC transcription factors promote the expression of genes involved in the JA response, such as genes involved in wounding, flower maturation and herbivore-induced formation of volatiles. The activity of MYC2, MYC3 and MYC4 is repressed through an interaction with the JAZ proteins, which represses the plant JA response by blocking MYC activity. The *Arabidopsis* MCY2 transcription factor has been shown to bind directly to all five *Arabidopsis* DELLAs in a yeast two-hybrid screen (Hong et al., 2012a). This interaction is dependent on the N terminal of MYC2. The binding of DELLAs to MYC2 causes the sequestration of MYC2, and therefore repression plant-insect interactions. This provides a mechanism by which GA can positively regulate this response by promoting the degradation of DELLAs, freeing the MYC transcription factors from repression and allowing the synthesis of pollinator-attracting substances (Hong et al., 2012a). The bHLH transcription factor ALCATRAZ (ALC) has also been shown to interact with DELLAs. ALC is required for the regulation of fruit patterning in *Arabidopsis*. During fruit patterning, valve margins differentiate into a lignification layer (LL) and a separation layer (SL). ALC is required for SL specification (Rajani and Sundaresan, 2001). In yeast two-hybrid experiments, ALC was shown to bind to GAI, RGA and RGL2, in an interaction that represses ALC transcriptional activity (Arnaud et al., 2010). This provides a model whereby, in the absence of GA, DELLAs repress SL specification by repressing ALC transcriptional activity, whereas an increase in GA concentration would promote SL specification by releasing ALC from DELLA repression (Arnaud et al., 2010).

The rice sequence (LOC_Os01g70310) homologous to library protein 236 was used to identify the most closely related *Arabidopsis* sequence, At3g26744.1, which is a MYC-like sequence within the group of IIIb bHLH transcription factors. This group has been described as having involvement in stomatal development (Kanaoka et al., 2008) and the response to cold (Feller et al., 2011). Analysis of public RNAseq data demonstrated that library protein 236 is highly expressed in the elongating stem, spike and grain, which suggests that this bHLH protein would have a role regulating development in these tissues.

Previously described interactions between DELLAs and bHLH transcription factors indicate that library protein 236 is likely to have its transcriptional activity repressed by the interaction with RHT-D1a. The expression pattern of *library cDNA 236* indicates that this repression would prevent library protein 236 from promoting the expression of genes involved in the development of the stem, spike and grain in the absence of GA. The high level of *library cDNA 236* in the stem could indicate that library protein 236 is a promising candidate for the specific regulation of stem elongation.

4.4.2.5 Library protein 444, a zinc finger-like protein

Library protein 444 encodes the full length TRIAE_CS42_4BS_TGACv1_330766_AA1108750, a zinc finger-like protein. Although *library cDNA 444* was not in-frame with the GAL4 start codon, the protein was able to interact with RHT-D1a in both the HIS3 and X-gal assays, suggesting that the cDNA is expressed. Further sequencing would be ideal to confirm the frame of *library cDNA 444*. It is possible that *Library cDNA 444* is out of frame but re-initiation allows transcription of the correct sequence. Library protein 444 was chosen for further characterisation because an interaction between DELLAs and the zing finger INDETERMINATE DOMAIN (IDD) family of proteins has been characterised (Yoshida et al., 2014). IDDs are C2H2 zinc finger proteins that have a wide range of roles in the regulation of plant development such as flowering time in response to sugar metabolism, gravitropic response and root development (Morita et al., 2006, Seo et al., 2011). The first member of the IDD family to be identified was the ID1 protein from maize, which regulates floral initiation (Colasanti et al., 2006).

Arabidopsis IDDs 3, 4, 5, 9 and 10 were shown to interact with the GRAS domain of RGA. The IDD proteins were also shown to bind the promoter sequence of *SCARECROW-LIKE3 (SCL3)* and this activity is positively regulated by DELLAs. The interaction between DELLAs and IDDs in *Arabidopsis* results in the formation of a complex able to bind to the promoter of *SCL3* and drive its expression (Yoshida et al., 2014). Another *Arabidopsis* IDD protein, GAI-ASSOCIATED FACTOR1 (GAF1), was shown to interact with DELLAs in a similar manner (Fukazawa et al., 2014). A yeast two-hybrid screen demonstrated that GAF1 could interact with the all 5

Arabidopsis DELLAs. Mutant screens indicated that GAF1 had a role in regulating flowering, stem elongation and hypocotyl elongation in response to GA, in conjunction with another IDD protein, IDD1/ ENHYDROUS (ENY). GAF1 was also shown to bind TOPLESS (TPL), a transcriptional corepressor. These interactions provide a mechanism by which in the absence of GA, DELLAs bind GAF1 and form a transcriptional activation complex that drives expression of GA biosynthesis genes and the GA receptor *GID1*. When GA levels rise, DELLAs are degraded and GAF1 is instead bound by TPL which forms a transcriptional repressor complex to repress transcription of GA genes (Fukazawa et al., 2014). ENY was also shown to interact with all five *Arabidopsis* DELLAs in a yeast two-hybrid assay and has been shown to promote the expression of GA biosynthesis genes leading to a negative feedback loop.

Library protein 444 was aligned with zinc finger-containing proteins from rice, maize and *Arabidopsis* to determine its likely function. A phylogenetic tree produced with this alignment showed library protein 444 grouped with the IDD proteins, indicating that it would function as an IDD in wheat. A second alignment was then produced with the *Arabidopsis*, maize and rice IDD proteins, which was used to produce the phylogenetic tree shown in **Figure 4.51**. Library protein 444 was grouped with rice regulator of CBF1 (ROC1), rice loose plant architecture 1 (LPA1) and the *Arabidopsis* IDD4, IDD5, GAF1, and IDD1 proteins. The most closely related sequence appears to be OsROC1, which is involved in positive regulation of cold stress responses. However, the conserved C terminal domains present in the *Arabidopsis* IDDs described by Yoshida et al. (2014) could not be identified in library protein 444, meaning its role as an IDD is questionable. It is possible that library protein 444 encodes a zinc finger protein, without IDD domains, meaning the interaction with RHT-1 could represent a novel DELLA-zinc finger interaction.

If library protein 444 does interact with RHT-D1a in the same way as the described IDD-DELLA interactions, it is likely that the library protein 444-RHT-D1a forms a transcriptional activation complex, which drives the expression of DELLA targeted genes. *Library cDNA 444* was expressed in all tissues and developmental stages tested in the public RNAseq data, suggesting that it is present in all tissues.

4.4.2.6 Library protein 51: Rho GTPase-activating 7-like

Library protein 51 encodes an N-terminally truncated version of TRIAE_CS42_2BS_TGACv1_146333_AA0462840 Rho GTPase activating 7-like protein, lacking the N terminal 444 amino acids. This clone was also identified in a yeast two-hybrid library screen of cDNAs from the wheat aleurone, using RHT-D1a as the bait (unpublished, Patrycja Sokolowska). No Interaction has previously been demonstrated between DELLAs and Rho

GTPases, so the interaction between Rht-D1a and library protein 51 could not be predicted. However, Rho GTPases have been implicated in auxin and ABA signalling (Nibau et al., 2013, Xu et al., 2010) with two Rho GTPases activated by auxin to promote cell expansion. Rho-GTPases ROP2 and ROP6 are co-ordinately activated through AUXIN-BINDING PROTEIN 1 to promote the formation of complementary lobes and indentations within leaf epidermal pavement cells (Xu et al., 2010). The Rho-GTPase AtRAC7/ROP9 also functions as a modulator of auxin and abscisic acid (ABA) signalling. When AtRAC7/ROP9 levels were reduced, *Arabidopsis* plants were more sensitive to auxin and less sensitive to ABA. Conversely, overexpression of AtRAC7/ROP9 lead to an activation of ABA-induced gene expression and a repression of auxin gene expression (Nibau et al., 2013). This role of rho-GTPases in the auxin and ABA response pathways could suggest a role in other hormone signalling pathways, including GA.

Library protein 51 was shown to be expressed in the same tissues as RHT-D1a in analysis of public RNAseq data. The analysis also demonstrated that library protein 51 was most highly expressed in elongating stem and developing spike and grain. This could indicate a role for an interaction with RHT-D1a in these tissues with the high level of expression in the elongating stem indicating a possible role for rho GTPases in stem elongation in response to GA.

4.4.2.7 Library protein 143: A FAR1 related protein

Library protein 143 encodes the full length TRIAE_CS42_U_TGACv1_642981_AA2125590 protein, a FAR1 related protein It was selected for further characterisation because in *Arabidopsis* FAR1 has been shown to act downstream of phytochrome in light signalling (Siddiqui et al., 2016). FAR1 belongs to a family of mutator-like transposases, which also include FHY3 (Lin and Wang, 2004). FAR1 functions by dimerizing with FHY3 (Lin et al., 2007, Ouyang et al., 2011), which allows the formation of a complex that positively regulates transcription of genes involved in phyA-mediated development in response to R and FR light, such as the inhibition of hypocotyl elongation, opening of apical hook, expansion of cotyledons and greening (Deng and Quail, 1999). The FAR1-FHY3 complex also promotes phyA signalling by increasing the expression of the phyA nuclear importing proteins, FHY1 and FHL.

No interaction between FAR1 and DELLA proteins or any role in the GA response pathway has been documented, however FAR1 appears to act in a similar manner to PIF proteins in that it is a transcriptional regulator that forms dimers to drive the expression of genes in response to phytochrome signalling. FAR1 has the opposite effect on seedling growth to PIFs, meaning the interaction between FAR1 and DELLAs would be expected to result in the opposite effect. This would indicate that RHT-1 could bind FAR1, and promote its transcriptional activity to inhibit hypocotyl elongation, greening and opening of the apical hook. *Library cDNA 143* was

expressed at lower levels than *RHT-D1a* in all tissues examined; however expression was highest in developing spike and grain, indicating that the interaction would be most likely to be important in these tissues. phy

4.4.2.8 Library protein 221: a Defensin1-like protein

The library protein 221 encodes the full length TRIAE_CS42_4DL_TGACv1_343378_AA1133790, a Defensin1-like protein. Library protein 221 was selected for further characterisation because in *Arabidopsis* defensin has a role in the JA and ET response pathways. Defensins are small cationic cysteine-rich peptides of 45–54 amino acid residues (De Coninck et al., 2013). They are constitutively expressed, and show upregulation in response to pathogen attack, injury and some abiotic stresses (de Beer and Vivier, 2011). Most defensins act against fungi, including yeast, although a small number can act on bacteria. Defensins are thought to interact with negatively charged molecules present at the cell membrane of pathogens, causing the membrane to become permeable and leading to death by necrosis (Hegedus and Marx, 2013).

No interaction between DELLAs and defensins has previously been documented. However, in tomato, a defensin-like protein, TGAS118, was shown to be regulated by GA levels (van den Heuvel et al., 2001). The abundance of *TGAS118* mRNA increased in response to both GA application and wounding or dehydration (van den Heuvel et al., 2001). Although no interaction between defensins and DELLAs has been demonstrated, DELLAS have previously been implicated in plant defence, for example in the interaction between DELLA and JAZ proteins (Xie et al., 2016). A role of GA in defence responses could also explain an interaction between RHT-D1a and library protein 143. GA could promote defence responses through the interaction between RHT-D1a and defensins. In this model, Library protein 221 would be bound by RHT-D1a in the absence of GA, which would repress its activity as a defensin. As GA levels increase RHT-D1a would be degraded, relieving repression of library protein 221. *Library cDNA 221* is expressed at very high levels in the root, but is also expressed at higher levels than *RHT-D1a* in the stem and spike, indicating that an interaction could occur in these tissues.

4.4.2.9 Future work for the yeast two-hybrid library screen

All the proteins identified in this screen must be further characterised to confirm the interaction with RHT-D1a and to characterise the effects of this interaction. Ideally, the interaction with RHT-D1a should be confirmed with alternative in vitro and in vivo methods such as pull-down assays and BiFC experiments. For all sequences, a role in the wheat GA response must be confirmed by altering their expression levels and assessing the associated phenotypes. This could be achieved using RNAi and overexpression lines, or the sequences

could be knocked out using TILLING lines or genome editing. ChIP-seq could then be utilised to confirm which genes are targeted by the library proteins, and how the RHT-1 interaction affects their expression. This work would allow the identification of library proteins with specific roles in stem elongation, which could be manipulated to alter plant height.

Chapter 5: Manipulating the Expression of *PIF-like* genes in Wheat

5.1 Introduction

The 17-Gbp *Triticum aestivum* genome is large and complex, consisting of three homoeologous A, B and D genomes, which are highly similar with extensive stretches of repetitive DNA (Edwards et al., 2013a). These complexities bring challenges when attempting to silence or promote expression of specific genes. Unlike *Arabidopsis*, there are few established resources to rely on for generating loss-of-function mutant lines. The three homologous genomes provide multiple copies of each gene, which may all need to be targeted to assess the effect of knockout or reduced expression. For this reason, the production of traditional single nucleotide polymorphism (SNP) mutants can be complex and time consuming. Newer technologies such as RNAi provide a method to knockdown multiple homoeologous copies at once, but come with their own challenges such as achieving a sufficient level of knockdown to affect expression and phenotypes (Birmingham et al., 2006, Wang et al., 2005b).

The overriding hypothesis of this project was that wheat PILs would regulate stem elongation in response to GA through an interaction with RHT-1. The interaction with RHT-1 has been demonstrated in chapter 4. The next step was therefore to investigate the role of the wheat PILs in the regulation of stem elongation. TaPIL1 was chosen as the primary target for altered expression due to its similarity to OsPIL1 (see chapter 3 section 3.1.2), the expression of which was shown to influence culm height in rice (Todaka et al., 2012). Knockdown of TaPIL1 was attempted using two methods: RNAi and TILLING. Both TaPIL1 and OsPIL1 were used in overexpression constructs. The *OsPIL1* sequence was chosen for overexpression because of initial difficulties in isolating the *TaPIL1* sequence (Chapter 3 section 3.2.5.1). At this point in the project it was decided to overexpress *OsPIL1* to investigate the phenotypic effects in wheat. If the *OsPIL1* and *TaPIL1* overexpression lines produced similar phenotypes in wheat, this would provide evidence that the genes are orthologous.

5.1.1 Methods of altering gene expression in wheat

5.1.1.1 RNA interference

RNA interference (RNAi) is a conserved mechanism of gene regulation which involves the use of small RNAs (sRNA)s to silence of gene expression to produce a loss-of-function phenotype. RNAi was first identified as the mechanism by which exogenously supplied sense and antisense RNAs silenced gene expression in *Caenorhabditis elegans* (Rocheleau et al., 1997). Subsequent studies demonstrated that double stranded RNA corresponding to a target gene in *C. elegans* silenced expression more efficiently than sense or antisense strands individually (Fire et al., 1998). In addition, researchers working with plants and fungi had observed that the introduction of transgenes sometimes induced post transcriptional gene silencing (PTGS) resulting in repression of the transgene and any homologous native sequences, which was termed co-supression (Hammond et al., 2001).

PTGS involves the initial processing or cleavage of dsRNA into 21-25 nucleotide fragments, siRNAs, by an RNAseIII enzyme called Dicer. These siRNAs are then combined into an RNA-induced silencing complex (RISC), which includes an Argonaute protein containing an siRNA-binding domain and endonucleolytic activity (Vaucheret et al., 2001). The RISC complex unwinds the siRNAs, generating sense and antisense strands. The sense strand is subsequently degraded and the antisense strand is used to target complementary mRNA, which is then degraded (Liu and Paroo, 2010). The delivery of RNAi to plants involves the expression of hairpin RNAs, which fold back to create a double stranded region which is targeted by Dicer for cleavage into siRNAs and subsequent targeting of target mRNAs (Helliwell and Waterhouse, 2005, Smith et al., 2000, Wesley et al., 2001).

Using RNAi as a method for knockdown of gene expression holds some advantages when compared to generating mutants with complete loss of function. Firstly, RNAi is dominant, and so the effect on phenotype can potentially be observed in the T1 generation. Secondly knockdown is usually partial, which means a range of phenotypes with differing severities can be observed, and is useful when loss of function is lethal. Thirdly, RNAi can be used to target several related genes at the same time, for example the homoeologous copies of each gene in wheat. This facilitates the knockdown of multiple redundant genes (Small, 2007).

Conversely, there are also disadvantages associated with RNAi. Firstly, knockdown of non-target genes can occur if there are small regions of homology. A homologous sequence of as little as seven nucleotides has been reported to allow recognition of an mRNA molecule by an antisense siRNA, leading to the silencing of non-target genes (Birmingham et al., 2006).

Furthermore, the effect of RNAi inhibition is not always predictable. DNA level mutations such as base changes, deletions or insertion have predictable and irreversible consequences. However, RNAi inhibition can have a variety of effects depending on which gene or the region of the transcript that was targeted, and may vary between plants carrying the same RNAi construct (Wang et al., 2005b). The efficiency of the RNAi silencing may be dependent on how strongly the construct is expressed in the plant cell, and on where the construct is incorporated in the genome. If the construct incorporation disrupts the sequence of another gene, the RNAi may display an unrelated phenotype. The expression of the hairpin RNAi molecules has also been shown to be silenced through an epigenetic mechanism in some cases, leading to a block of the RNAi effects (Yamasaki et al., 2008).

Previous studies have described the successful use of RNAi in wheat to silence target genes. The first stable RNAi line produced in wheat targeted the vernalisation gene *VRN2*, a zinc-finger CCT domain protein, which is downregulated by cold temperatures and short day photoperiods (Loukoianov et al., 2005). *VRN2* was silenced using a 347-bp trigger sequence from the *VRN2* gene. To avoid silencing other genes with homology to *VRN2*, the conserved zinc finger and CCT domains were not included in the trigger sequence. The expression levels of *VRN2* were assessed using quantitative reverse-transcriptase PCR (qRT-PCR), which demonstrated a knockdown to 40% of the expression levels observed in non-transgenic lines. The expression levels of genes with homology to *VRN2* were also analysed to determine the specificity of the trigger sequence. The expression of these conserved sequences was not affected in the RNAi lines (Yan et al., 2004). Another vernalisation gene, *VRN1*, a MADS-box transcription factor that is up-regulated by cold treatment, has also been targeted by RNAi. A 294-bp trigger sequence was designed from the *VRN1* sequence, excluding the MADS and K-box domains. qRT-PCR analysis identified a reduction in *VRN1* expression to 19% of the level observed in the non-transgenic lines (Loukoianov et al., 2005).

The *ETHYLENE INSENSITIVE 2 (EIN2)* gene was used to demonstrate the knockdown of all three homoeologous copies of a gene in wheat using RNAi. A 518-bp section of the B genome *EIN2* sequence was used as the RNAi trigger. This section had 96% identify to the A and D copies of the gene. qRT-PCR analysis revealed that all three copies of *EIN2* were knocked down in transgenic lines, with an average reduction to 30-50% of the level seen in non-transgenic controls. One RNAi transgenic line had a knockdown of expression to only 1% of that observed in control non-transgenic lines (Travella et al., 2006). These results demonstrate that RNAi is a feasible method by which expression of the three homoeologous copies of a target gene can be knocked down in wheat.

5.1.1.2 Targeting Induced Local Lesions IN Genomes (TILLING)

Another method to investigate the role of PILs in wheat architecture is to produce loss-of-function mutants for each wheat *PIL* gene. This is a complex process in wheat due to the large and complex wheat genome, which contains multiple copies of each gene. However, TILLING provides a reverse genetic method that can feasibly be used in wheat.

TILLING involves the induction of high density point mutations from chemical mutagenesis with sensitive mutation detection that allows identification and characterisation of mutants (McCallum et al., 2000a). The potential of TILLING as a reverse genetic tool in plants, was first tested in *Arabidopsis*. DNA from a collection of ethylmethane-sulfonate (EMS)-mutagenized plants was screened for mutations. The mutations identified in this screen were base pair changes causing missense or nonsense changes which could be used in phenotypic analysis (McCallum et al., 2000b).

TILLING has been used successfully in wheat to identify loss-of-function (null) mutants and analyse their phenotype. A screen for mutations in the *WAXY* genes, which encode granule-bound starch synthase I was carried out in bread and durum wheat. 246 alleles of *waxy* were identified in these screens, with a variety of mutations resulting in a gradient of function from wild type to null (Slade et al., 2005). A TILLING population in a tetraploid wheat variety was used to identify wheat lines with truncation mutations in the two homoeologues copies of *VRN1*, resulting in a *vrn-1* null plant. Analysis of these null lines revealed that VRN1 was required to maintain low levels of the flowering repressor VRN2 after vernalisation (Chen and Dubcovsky, 2012). These experiments demonstrate the potential of TILLING as a technique for producing null mutant lines in wheat.

A new wheat TILLING resource consists of TILLING populations in tetraploid 'Kronos' durum wheat and 'Cadenza' hexaploid bread wheat was produced at the University of California at Davis and Rothamsted Research, respectively, as a collaboration between Rothamsted, the John Innes Centre, UC Davis and the Earlham institute. These wheat populations were produced by mutagenesis with EMS, and then the exome sequences of 1,535 Kronos and 1,200 Cadenza M3 lines were sequenced using Illumina next-generation sequencing. These reads were mapped to the IWGSC Chinese Spring Wheat sequencing data to identify the sequence and location of mutations. More than 10 million mutations have been sequenced and catalogued in the protein coding regions of both the tetraploid and hexaploid wheat genomes. This resulted in an average of 23-24 missense and truncation alleles per gene, with 90% of captured wheat genes having at least one truncation or nonsense mutation (Krasileva et al.,

2017). The resulting seed stocks are available in a public collection which can be searched online (http://wheat-tilling.com). The exome capture data for the Cadenza population was searched for lines with truncation or splice site mutations in each homoeologue of *PIL1, PIL2* and *PIL3*.

5.1.1.3 Overexpression

The role of PILs in wheat architecture will also be investigated through the production of overexpression lines. Overexpression lines carry numerous advantages when compared to RNAi or null mutant lines. When gene expression is knocked down, only a low number of mutants show a phenotype. In a study using RNAi in *C. elegans*, only 10% of knockout mutants showed a phenotype (Kamath et al., 2003). This is likely to be due to redundancy, as genes present in a single copy are more than twice as likely to have an RNAi phenotype as those present in multiple copies (Kamath et al., 2003). A problem of redundancy is especially prevalent when studying the role of transcription factors, because they are generally members of large gene families with overlapping function. There have been many cases where knockout of multiple transcription factors has been necessary for phenotypes to be observed (Liljegren et al., 2000, Kumaran et al., 2002).

Overexpression lines provide an alternative and complementary strategy for altering gene expression that is not as vulnerable to functional redundancy, which is particularly important in hexaploid wheat. In numerous cases gene functions that could not be elucidated by knockout lines, were revealed by overexpression (Baima et al., 2001, Fan and Dong, 2002, Pontier et al., 2001). Overexpression does also come with some disadvantages. The abnormally high levels of protein produced by overexpression can lead to atypical effects not associated with the protein's normal function, leading to unrelated phenotypes, particularly if the protein is expressed in tissues where it would not normally be found. When phyA was overexpressed in *Arabidopsis*, results indicated a similar role to phyB in light response (Boylan and Quail, 1991). However, the role of phyA in development is closely linked to its kinetics, meaning overexpression resulted in abnormal functions (Reed et al., 1994). Another issue with overexpression lines is that if the protein is already expressed at a saturating level, overexpression can have no effect on phenotype. Another factor to consider for overexpression lines is post-translational modification. If post-translational modification is required, the excess protein produced by the overexpression vector may not undergo this process and therefore may not function normally in the cell. DELLAs are an example of proteins that undergo post-translational modification. For example, the Arabidopsis DELLA RGA has been shown to be mono-O-fucosylated by SPINDLY. Fucosylation enhances the

activity of RGA by promoting binding to key transcription factors in BR and light-signaling pathways (Zentella et al., 2017). For this reason, overexpression lines will be used in parallel with RNAi and TILLING lines to investigate TaPIL function.

5.2 Results

5.2.1 Knockdown of *TaPIL1* expression using RNAi

5.2.1.1 Design of the RNAi trigger sequence

One aim of this project was to investigate the phenotypic effects of knocking down *TaPIL1*. RNAi lines targeting *TaPIL1* were produced for this purpose. A 300-bp section of the *TaPIL1* sequence was selected for use as the RNAi trigger. This section lies at the 3' end of the sequence, outside of the conserved bHLH domain to avoid silencing of related sequences (**Figure 5.1**). This trigger sequence was designed to silence all three homoeologues of *TaPIL1* by including stretches of identical sequence between the homoeologues of at least 20 bp (**Figure 5.2**). The proposed trigger sequence was used in a blast search of a wheat IWGSC cDNA database to ensure that no other sequences would be silenced; sequences with enough similarities to be silenced by the trigger sequence, i.e. stretches of 20 bp or longer of identical sequence, would be discounted. This RNAi trigger sequence was designed to be specific for *TaPIL1*, so its similarity to the *TaPIL2* and *TaPIL3* sequences was also evaluated. An alignment revealed that the selected sequence is not similar enough to silence *TaPIL2* or *TaPIL3* as there are only short sections of identical sequence (**Figure 5.3**).

Figure 5.1 The position of the RNAi trigger sequence within the *TaPIL1* coding region. The exon sequence of *TaPIL1* is shown, with dark grey arrows indicating the position and size of each exon. The RNAi trigger sequence, positioned at the 3' end of the sequence, covering exons 6 and 7, is indicated by a black arrow. The bHLH domain is indicated by a light grey arrow above exons 3, 5 and 5.

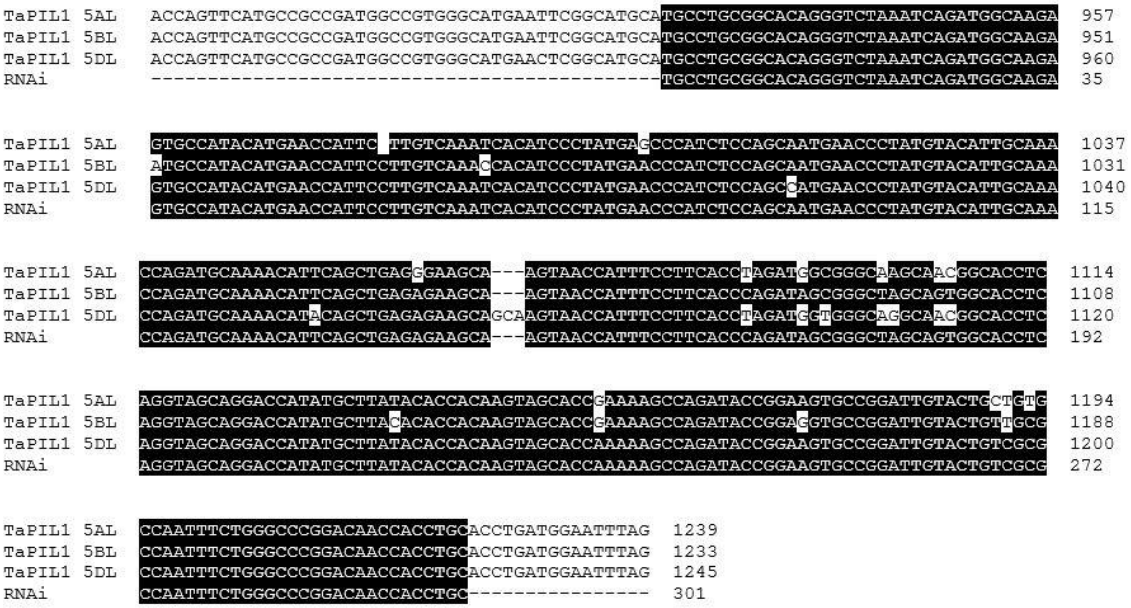

Figure 5.2 The *TaPIL1* trigger sequence aligned to the *TaPIL1* homoeologues. The three homoeologous *TaPIL1* sequences were aligned with the *TaPIL1* RNAi trigger sequence in a T-coffee alignment. Nucleotides shared between the trigger and homoeologous sequences are shown in reverse.

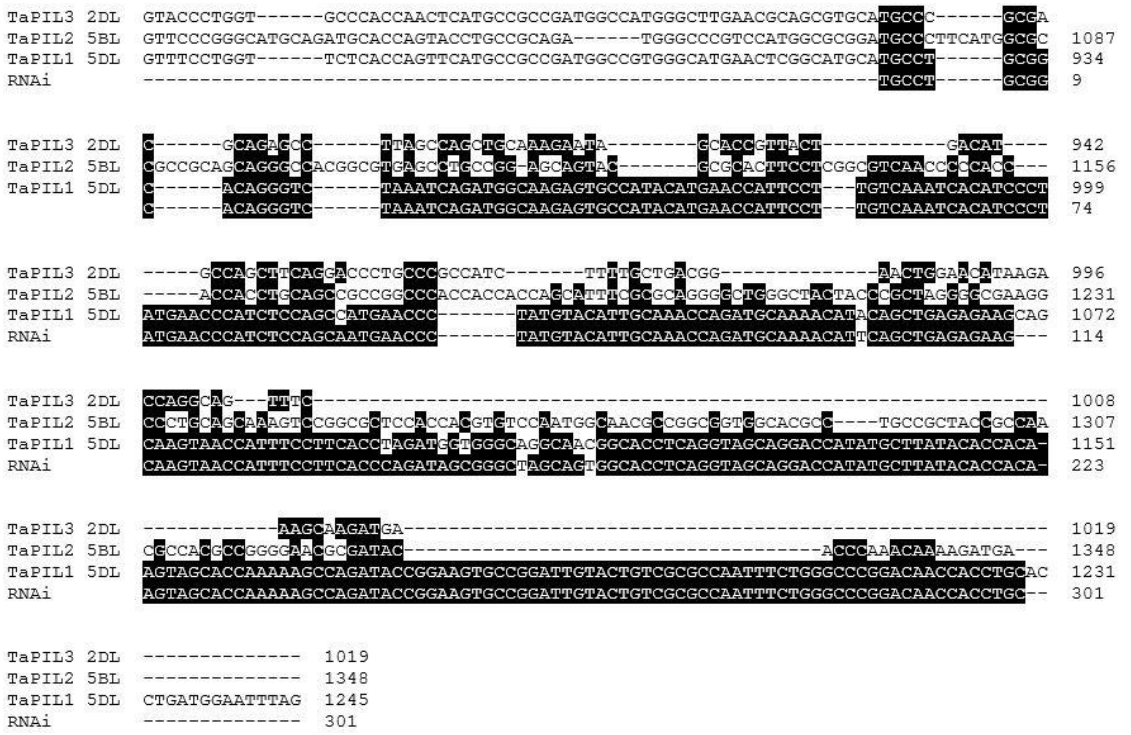

Figure 5.3 The *TaPIL1* RNAi trigger sequence aligned to the *TaPIL2* and *TaPIL3* sequences. The *TaPIL1* RNAi trigger sequence was aligned to a *TaPIL1*, *TaPIL2* and *TaPIL3* sequence in a T-coffee alignment. Nucleotides shared between the trigger and other sequences are shown in reverse.

5.2.1.2 Production of RNAi lines

The *TaPIL1* RNAi trigger sequence was cloned into the *pENTR11* Gateway vector and sent to the National Institute of Agricultural Botany (NIAB) to be transformed into the wheat variety Cadenza (**Figure 5.4**) via *Agrobacterium* transformation (Perochon et al., 2015a). The expression of the RNAi trigger sequence is driven by the rice actin promoter, which has been shown to promote the expression of glucuronidase reporter gene (GUS) in monocot cells (McElroy et al., 1991), and has been used to successfully express transgenes in wheat (Nehra et al., 1994, Takumi et al., 1994). The rice actin promoter has also been shown to constitutively drive the expression of transgenes in vegetative and reproductive tissues of transgenic rice plants (Zhang et al., 1991). T_0 plants were genotyped by NIAB, which provided 29 transgenic lines, each from an independent transformation event, along with three control lines which had not been transformed, but had undergone the same tissue culture process. Seeds from plants with a single insert of the transgene were selected for propagation to the next generation.

Selected T_1 seeds were planted and grown to maturity. Leaf material was harvested and used to extract genomic DNA. The extracted DNA was sent to iDNAgenetics (Norwich U.K) for qRT-PCR-based genotyping. Three homozygous lines were chosen for the T_2 generation, along with one azygous segregant. Eight plants for each of the three homozygous lines were planted and grown to maturity. Leaf material was again harvested and used to extract genomic DNA. Genotyping by iDNAgenetics showed that all lines had two copies and were therefore homozygous. T_3 seed was harvested from these plants. At the T3 generation, six lines were chosen for expression analysis. The lines chosen were 3912-1, 3912-4, 3964-3, 3964-8, 4085-3 and 4085-6, along with one F3 azygous segregant control line.

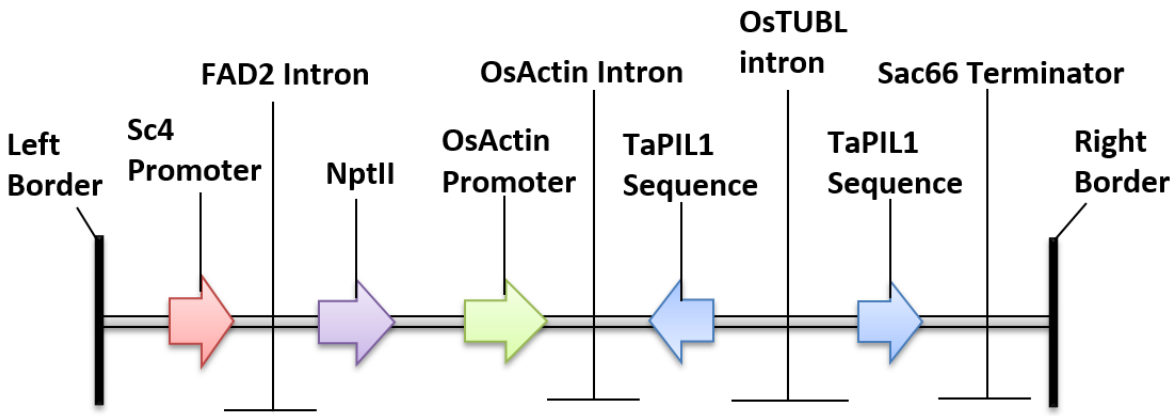

Figure 5.4 The structure of the *TaPIL1* RNAi T-DNA. A schematic representation of the structure of the T-DNA insert in the *TaPIL1* RNAi construct is shown. The *Sc4* promoter is shown in red, the *neomycin phosphotransferase* (*NptII*) gene is shown in purple. The *rice actin* (*OsActin*) promoter is shown in green and the *TaPIL1* sequence is shown in blue. Intron sequences are labelled by a black horizontal line below the sequence.

Six seeds for each RNAi line and the RNAi azygous segregant control were selected and grown for five days in the dark. Shoot tissue was harvested and pooled for RNA extraction. The resulting RNA was then used to synthesise cDNA, which was used as the template for qRT-PCR. A DNase-treated RNA sample was used as a negative control for each line. Four separate cDNA samples were produced from the pooled samples of each line, with three technical replicates in each qRT-PCR. The qRT-PCR was conducted using primers specific for *TaPIL1* and with primers for three reference genes: *Ta2526 (TRIAE_CS42_3AS_TGACv1_211294_AA0688120), TaActin (TRIAE_CS42_5DL_TGACv1_437323_AA1465890)* and *TaCellDevC (TRIAE_CS42_4DL_TGACv1_344906_AA1150440)*. The average CT value and PCR efficiency for each primer was calculated in the transgenic lines and the azygous segregant. The average CT and PCR efficiency values were then used to calculate a fold indication value for *TaPIL1* comparing expression in the RNAi line and azygous segregant control, using each reference for normalisation. These values were then used to produce an average fold induction value per line (**Table 5.1**).

The RNAi lines 3912-1 and 3912-4 have the highest level of expression, with 72% and 39%, respectively, of the expression detected in the azygous segregant line. The lines with the lowest expression are 3964-8 and 4085-3, which have expression levels of 24% and 13%, respectively. These results indicate that a range of *TaPIL1* knockdown is produced through these RNAi Lines.

Table 5.1 Levels of *TaPIL1* expression in RNAi lines. qRT-PCR using cDNA from 5-day old dark-grown seedlings. Four reactions per line were performed, one for *TaPIL1* and three for the reference genes *Ta2526, TaActin, TaCellDevC*. The average PCR efficiency (PCR-EFF) and cycle threshold (CT) for each primer pair per line are shown. The average PCR-EFF and CT were used to calculate a fold induction value, using each reference gene for normalisation. These fold induction values were then used to calculate an average fold induction value for each line. Data for the 6 RNAi lines and the azygous segregant (control) are shown.

	GENE	AVG PCR EFF	AVG CT	FOLD INDUCTION	AVG FOLD INDUCTION
CONTROL	TaPIL1	1.90 ± 0.01	29.54 ± 0.25		
	Ta2526	1.91 ± 0.01	22.59 ± 0.21		
	TaActin	1.90 ± 0.01	20.24 ± 0.24		
	TaCellDevC	1.92 ± 0.01	23.71 ± 0.25		
3912-1	TaPIL1	1.91 ± 0.02	30.42 ± 1.03	0.76	0.72 ± 0.06
	Ta2526	1.90 ± 0.01	23.04 ± 0.77	0.80	
	TaActin	1.88 ± 0.03	20.78 ± 0.73	0.60	
	TaCellDevC	1.90 ± 0.01	23.79 ± 0.70		
3912-4	TaPIL1	1.88 ± 0.02	29.16 ± 0.72		0.39 ± 0.06
	Ta2526	1.91 ± 0.02	20.41 ± 0.70	0.31	
	TaActin	1.96 ± 0.03	18.90 ± 0.63	0.52	
	TaCellDevC	1.93 ± 0.01	21.75 ± 0.65	0.35	
3964-3	TaPIL1	1.89 ± 0.00	31.42 ± 0.75		0.26 ± 0.002
	Ta2526	1.91 ± 0.01	22.33 ± 0.82	0.26	
	TaActin	1.93 ± 0.02	19.98 ± 0.69	0.25	
	TaCellDevC	1.91 ± 0.01	23.50 ± 0.73	0.26	
3964-8	TaPIL1	1.97 ± 0.04	31.66 ± 1.48		0.24 ± 0.02
	Ta2526	1.92 ± 0.01	22.31 ± 0.16	0.20	
	TaActin	1.89 ± 0.01	20.41 ± 0.63	0.26	
	TaCellDevC	1.91 ± 0.00	23.87 ± 0.44	0.26	
4085-3	TaPIL1	1.90 ± 0.01	32.80 ± 0.60		0.13 ± 0.03
	Ta2526	1.94 ± 0.01	22.09 ± 0.44	0.09	
	TaActin	1.93 ± 0.02	20.43 ± 0.44	0.14	
	TaCellDevC	1.94 ± 0.02	24.21 ± 0.52	0.17	
4085-6	TaPIL1	1.89 ± 0.01	31.71 ± 0.87		0.33 ± 0.03
	Ta2526	1.91 ± 0.01	22.87 ± 0.51	0.30	
	TaActin	1.87 ± 0.01	20.89 ± 0.61	0.38	
	TaCellDevC	1.91 ± 0.02	24.00 ± 0.62	0.30	

5.2.2 Overexpression of *OsPIL1* and *TaPIL1* in wheat.

One aim of this project was to investigate the effects of altered *TaPIL* expression on wheat architecture. Overexpression of *OsPIL1* in rice was shown to increase stem height so it was important to confirm that *PIL1* had a similar function in wheat and to investigate other effects of its overexpression. Two overexpression lines were produced, expressing *TaPIL1* and *OsPIL1*. The *TaPIL1* overexpression lines were produced to investigate the effect of increasing

expression of the endogenous *TaPIL1* gene. *OsPIL1* overexpression lines were produced because of initial difficulties isolating the *TaPIL1* sequence (see section 5.1).

The *OsPIL1* and *TaPIL1* coding sequences were synthesised with flanking restriction sites as described in Chapter three, sections 3.2.5.2 and 3.2.6.1, respectively. These restriction sites allowed cloning of the digested *TaPIL1* and *OsPIL1* sequences into the overexpression vector *pRRES14.125* (provided by Dr. Alsion Huttley, Rothamsted Research). This overexpression plasmid contains a maize ubiquitin promoter and Spe-Nos-Nhe terminator to drive constitutive expression of transgenes genes. The maize ubiquitin promoter has been shown to drive the expression of transgenes in wheat (Weeks et al., 1993), with constitutive expression in all tissues and highest activity in young metabolically active tissues (Cornejo et al., 1993, Rooke et al., 2000). The structure of the transgene is shown in **Figure 5.5**. The *OsPIL1* and *TaPIL1* sequences were cloned into the *pRRES14.125* plasmid between *Nco*I and *Eco*RV restriction sites in the multiple cloning site. The ATG in the *Nco*I site acts as the in-frame start codon and can only be used with sequences which begin with ATGG.

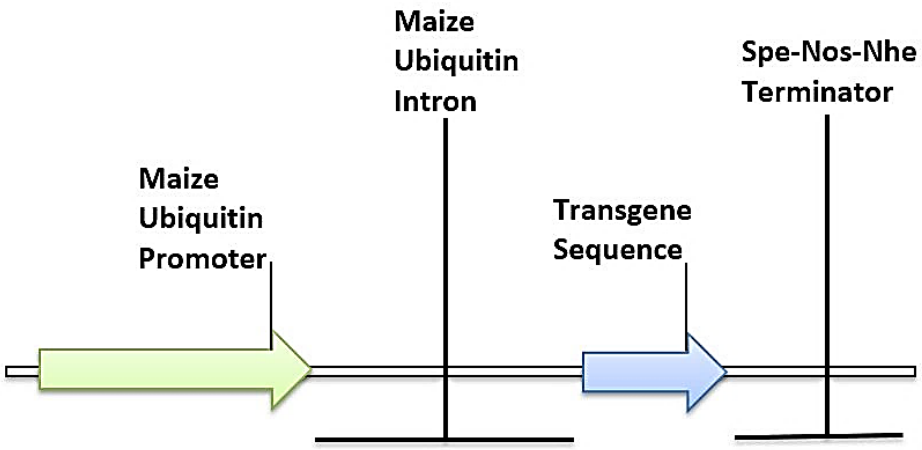

Figure 5.5 The structure of the transgene. The *maize ubiquitin* promoter is indicated by a green arrow. The transgene ORF is indicated by a blue arrow. The *maize ubiquitin* intron and Spe-Nos-Nhe terminator are indicated by a black line.

Once cloned into *pRRES14.124*, the *OsPIL1* and *TaPIL1* overexpression constructs were sequenced to confirm the presence of the cDNA insert. Once the insert was confirmed, plasmid preps were given to the Rothamsted Research transformation facility who used particle bombardment to transform the constructs into wheat cv Cadenza embryos (Sparks and Jones, 2014).

T_1 seed was provided by the transformation facility, comprising 14 transgenic *OsPIL1* overexpression lines, with 4 control lines, and 16 transgenic *TaPIL1* overexpression lines with 4

controls. Six of these transgenic lines were selected for the T1 generation for both the *OsPIL1* and *TaPIL1* overexpression lines. In both cases 12 seeds per line were planted. These plants were grown to maturity, and genomic DNA was extracted from leaf material. This DNA was sent to iDNAgenetics (http://www.idnagenetics.com/) for qRT-PCR-based genotyping to determine transgene copy number. These results were used to select lines to take forward to the next generation.

The *OsPIL1* genotyping results (**Table 5.2**) indicated that three lines, A, C and D, had copy numbers that fell into a 0:1:2 ratio which could be used to determine homozygous, heterozygous and azygous plants. The copy numbers from this transformation are relatively high, probably due to either multiple insertions or tandem repeats; transformation by particle bombardment has been reported to result in a higher copy number than *Agrobacterium* transformation (Li et al., 2017). The F line showed no transgene insertion and the B and E lines showed a more complex insertion pattern. For this reason, azygous segregants and homozygous plants from the A, C and D lines were selected for use in phenotyping experiments with the T_2 generation: A4, A8, C4, C9, D4 and D9 (section 5.2.3).

Table 5.2 Genotyping of T_1 *OsPIL1* overexpression lines. T_1 seeds from 6 T_0 lines were planted, with 12 individuals per line. Leaf tissue was harvested and used for genomic DNA extraction. This DNA was used by iDNAgenetics for qRT-PCR-based genotyping to give a copy number for each plant, which was used to assign plants into azygous (null), heterozygous (Het) and homozygous (Hom) genotypes.

Line	Plant	Copy number	Genotype	Line	Plant	Copy number	Genotype
A	2	27	Hom	D	4	46	Hom
A	4	24	Hom	D	7	30	-
A	3	13	Het	D	3	24	Het
A	10	12	Het	D	11	23	Het
A	5	11	Het	D	10	23	Het
A	8	0	Null	D	9	0	Null
A	9	0	Null	D	12	0	Null
B	11	13	-	E	9	23	-
B	12	0	-	E	7	10	-
B	4	0	-	E	8	8	-
B	5	0	-	E	2	4	-
B	6	0	-	E	10	2	-
				E	3	2	-
C	4	52	Hom	E	11	0	-
C	3	51	Hom				
C	8	48	Hom	F	1	0	Null
C	1	44	Hom	F	10	0	Null
C	11	40	Hom	F	11	0	Null
C	5	23	Het	F	12	0	Null
C	2	21	Het	F	2	0	Null
C	12	0	Null	F	3	0	Null
C	6	0	Null	F	4	0	Null
C	9	0	Null	F	6	0	Null
				F	7	0	Null
				F	9	0	Null

The *TaPIL1* overexpression T_1 genotyping results are shown in **Table 5.3**. Results indicated that two lines, C and F, have copy numbers that fall into a 0:1:2 ratio, allowing the prediction of zygosity. The A, B, D and E lines all have a more complex insertion pattern. For this reason, homozygous and azygous individuals from the C and F lines were selected for use in phenotyping experiments with the T_2 generation (section 5.2.3).

Table 5.3 Genotyping of T_1 *TaPIL1* overexpression lines. Seeds from six T_0 lines were planted, with 12 individuals per line. Leaf material was harvested and used for genomic DNA extraction. The DNA samples were sent to iDNAgenetics for qRT-PCR based genotyping, giving results as copy number per plant, which was used to assign plants into azygous (null), heterozygous (Het) and homozygous (Hom) genotypes.

Line	Plant	Copy number	Genotype	Line	Plant	Copy number	Genotype
A	1	7	-	D	2	10	-
A	6	5	-	D	7	8	-
A	7	5	-	D	6	7	-
A	5	5	-	D	4	6	-
A	3	0	Null	D	12	5	-
A	10	0	Null	D	10	4	-
A	11	0	Null	D	3	4	-
A	2	0	Null	D	11	4	-
A	4	0	Null	D	9	0	Null
A	8	0	Null	D	8	0	Null
A	9	0	Null	D	5	0	Null
				D	1	0	Null
B	7	15	-				
B	2	10	-	E	6	7	-
B	9	8	-	E	1	5	-
B	1	7	-	E	10	5	-
B	5	5	-	E	7	5	-
B	11	5	-	E	3	4	-
B	6	3	-	E	9	4	-
B	3	0	Null	E	2	4	-
B	8	0	Null	E	4	4	-
B	10	0	Null	E	5	3	-
B	4	0	Null	E	8	3	-
C	11	7	Hom	F	10	24	Hom
C	10	6	Hom	F	9	24	Hom
C	7	6	Hom	F	3	23	Hom
C	9	6	Hom	F	4	21	Hom
C	6	3	Het	F	2	11	Het
C	3	3	Het	F	1	10	Het
C	8	3	Het	F	8	10	Het
C	4	3	Het	F	7	10	Het
C	5	0	Null	F	6	10	Het
C	1	0	Null	F	12	9	Null
C	12	0	Null	F	5	0	Null
C	2	0	Null	F	11	0	Null

Homozygous and azygous segregants from the *TaPIL1* and *OsPIL1* overexpression lines were selected for expression analysis and for use in phenotyping experiments. For the *OsPIL1* overexpression lines, the homozygous lines A4, C4 and D4 were selected, along with the corresponding azygous segregants, A8, C9 and D9. For the *TaPIL1* overexpression lines the homozygous lines C10 and F10 were selected, with their corresponding C1 and F11 azygous

segregants. RNA was extracted from six 5-day old dark-grown seedlings and cDNA was synthesised as described previously (see section 5.2.1.2). The cDNA was then used as a template for qRT-PCR with the same reference primers and number of replicates as for the RNAi lines. The average CT value and PCR efficiency was calculated for each transgenic line and azygous segregant. The average PCR efficiency and CT values were used to compare expression of the target gene between samples, using each reference gene for normalisation. These values were used to calculate an average fold-induction value shown in **Table 5.4** (*TaPIL1* overexpression) and **Table 5.5** (*OsPIL1* overexpression). For the *TaPIL1* overexpression lines, the expression of *TaPIL1* in the azygous segregant and transgenic lines was compared to calculate the fold-induction value. For *OsPIL1*, the expression of *OsPIL1* between the three homozygous lines was compared to give a fold induction value in relation to each other because comparisons could not be made to the azygous segregants. The *TaPIL1* C10 and F10 overexpression had 4.2 and 7.3-fold higher expression, respectively, relative to their corresponding C1 and F11 azygous segregant lines. All the *OsPIL1* overexpression lines displayed expression of *OsPIL1*, with a similar CT value to that of *TaPIL1* in the azygous segregant lines shown in **Table 5.1** and **Table 5.4**. Comparison of the level of *OsPIL1* overexpression between the three homozygous overexpression lines showed that A4 had the highest level of expression, and D4 the least. The fold induction values are shown in **Table 5.5**. Some *OsPIL1* amplification was detected in the azygous segregant lines, however the CT values were >34, and were very similar to the DNase treated RNA negative controls, so were likely to be due to low levels of contamination.

Table 5.4 Expression levels of *TaPIL1* in overexpression lines. qRT-PCR using cDNA from 5 day old, dark-grown seedlings with four reactions per line. Each cDNA was amplified with four sets of primers, one for *TaPIL1* and three for the reference genes: *Ta2526, TaActin, TaCellDevC*. The average PCR efficiency (PCR-EFF) and cycle threshold (CT) are shown in the table. The average PCR-EFF and CT were used to compare *TaPIL1* expression level in the overexpression lines and corresponding azygous segregant (null), using each reference gene for normalisation. These fold induction values were then used to calculate an average fold induction value for each line.

	PRIMER	PCR EFF	CT	FOLD INDUCTION	AVG FOLD INDUCTION
C1 (NULL)	TaPIL1	1.90 ± 0.03	32.27 ± 0.51		
	Ta2526	1.91 ± 0.02	22.98 ± 0.25		
	TaActin	1.85 ± 0.03	21.83 ± 0.53		
	TaCellDevC	1.92 ± 0.01	25.34 ± 0.45		
C10	TaPIL1	1.89 ± 0.02	28.64 ± 1.13		
	Ta2526	1.93 ± 0.01	22.15 ± 0.77	5.84	4.15 ± 0.88
	TaActin	1.91 ± 0.04	20.27 ± 1.19	3.67	
	TaCellDevC	1.92 ± 0.01	23.44 ± 1.17	2.92	
F11 (NULL)	TaPIL1	1.88 ± 0.01	29.50 ± 0.75		
	Ta2526	1.93 ± 0.02	22.59 ± 0.86		
	TaActin	1.94 ± 0.03	20.16 ± 0.82		
	TaCellDevC	1.93 ± 0.02	23.58 ± 0.90		
F10	TaPIL1	1.86 ± 0.03	26.95 ± 0.39		
	Ta2526	1.92 ± 0.01	23.27 ± 0.66	7.58	7.29 ± 0.17
	TaActin	1.91 ± 0.03	20.78 ± 0.74	7.27	
	TaCellDevC	1.92 ± 0.01	24.14 ± 0.63	7.01	

Table 5.5 Expression levels of *OsPIL1* in overexpression lines. qRT-PCR using cDNA from 5 day old, dark-grown seedlings with four reactions per line, using primers for *OsPIL1* and for the three reference genes: *Ta2526*, *TaActin*, *TaCellDevC*, respectively The average PCR efficiency (PCR-EFF) and cycle threshold (CT) are shown in the table for the overexpression and azygous segregants (nulls). The fold-induction value for *OsPIL1* was calculated using the average PCR-EFF and CT values, normalised against each reference gene. These values were used to calculate an average fold-induction value.

	PRIMER	PCR-EFF	CT	COMPARISON	AVG FOLD INDUCTION
A4	*OsPIL1*	1.93 ± 0.02	24.70 ± 1.13	C4	9.65 ± 1.66
	Ta2526	1.94 ± 0.02	21.90 ± 0.58	D4	23.16 ± 4.03
	TaActin	1.92 ± 0.04	20.13 ± 0.84		
	TaCellDevC	1.93 ± 0.01	22.85 ± 0.90		
C4	*OsPIL1*	1.91 ± 0.02	27.72 ± 1.86	A4	0.10 ± 0.01
	Ta2526	1.93 ± 0.01	21.91 ± 0.38	D4	2.42 ± 0.02
	TaActin	1.98 ± 0.04	19.25 ± 0.16		
	TaCellDevC	1.94 ± 0.01	22.52 ± 0.16		
D4	*OSPIL1*	1.90 ± 0.01	29.57 ± 1.16	A4	0.05 ± 0.01
	Ta2526	1.91 ± 0.01	22.40 ± 0.44	C4	0.28 ± 0.07
	TaActin	1.94 ± 0.03	19.68 ± 0.57		
	TaCellDevC	1.92 ± 0.00	23.01 ± 0.49		
A8 (NULL)	*OsPIL1*	1.88 ± 0.03	34.14 ± 0.90		
	Ta2526	1.93 ± 0.01	21.54 ± 0.34		
	TaActin	1.92 ± 0.04	19.45 ± 0.65		
	TaCellDevC	1.93 ± 0.01	22.48 ± 0.68		
C9 (NULL)	*OsPIL1*	1.87 ± 0.06	34.19 ± 0.68		
	Ta2526	1.93 ± 0.02	23.23 ± 0.58		
	TaActin	1.94 ± 0.03	19.87 ± 0.82		
	TaCellDevC	1.93 ± 0.01	23.17 ± 0.89		
D9 (NULL)	*OSPIL1*	1.91 ± 0.02	34.53 ± 0.12		
	Ta2526	1.91 ± 0.01	22.81 ± 0.75		
	TaActin	1.91 ± 0.03	20.54 ± 0.77		
	TaCellDevC	1.92 ± 0.01	23.66 ± 0.86		

5.2.3 Phenotyping of the RNAi and overexpression lines

A phenotyping experiment using the RNAi and overexpression lines described in sections 5.2.1.2 and 5.2.2 was set up to analyse the effects of changing *PIL* expression on wheat growth. Four plants of each transgenic line, an azygous segregant RNAi line, the respective azygous segregants for the overexpression lines and the Cadenza wild-type were grown to maturity in a glasshouse, set up in a randomised four block structure to account for environmental variation within the glasshouse compartment. The number of days to heading and anthesis were recorded for the first tiller on each plant. Once the plants were fully mature, the tiller number was recorded, along with the length of the following for the three tallest tillers: ear, total stem, internode 1, internode 2, internode 3, internode 4 and internode 5.

The measurements from the three tallest tillers on each plant were then averaged, to produce one value per plant for each measurement. An analysis of variance (ANOVA) was then applied to all the averaged measurements from this experiment. The ANOVA was used to test (F-test 5%) the difference between Cadenza and all other lines: the backgrounds (Cadenza, RNAi, *TaPIL1* overexpression, *OsPIL1* overexpression), the types (Cadenza; azygous controls; RNAi lines 3912, 3964, 4085; TaPIL1 lines C, and D; OsPIL1 lines A, B and D), and between all the individual lines. Contrasts of pairs of lines of interest were also carried out. Each overexpression line was compared to its azygous segregant, and the pairs of RNAi lines e.g. 3912-1 and 3912-4, were compared to each other. The least significant difference (LSD) values were used to compare each RNAi line to the azygous segregant.

When *OsPIL1* overexpression line A4 was compared to its azygous segregant A8 (**Table 5.6**), there was no significant difference in the number of days to heading or tiller number, but for every other measurement there was a significant difference between the two lines. The difference in length of the total stem and internodes 1-3 was highly significant, with a p value of <0.001. These measurements demonstrate that A4 is significantly taller than the azygous segregant line. When *OsPIL1* overexpression line C4 was compared to its azygous segregant C9 (**Table 5.7**), no significant difference was detected in any measurement. The comparison between *OsPIL1* overexpression line D4 and the azygous segregant D9 (**Table 5.8**), demonstrated that D4 has a significantly longer stem than D9 with a p value of 0.02. No other measurement showed a significant difference.

Table 5.6 Comparison between *OsPIL1* overexpression line A4 and its corresponding azygous segregant A8. An analysis of variance (ANOVA) was applied to measurements from a phenotyping experiment involving *OsPIL1* overexpression line A4 and the azygous segregating line A8. The mean value for each measurement is shown with its standard deviation, along with its standard error of the difference (SED), the F-statistic for each comparison, and the P value. The degrees of freedom for this comparison are 1,51

MEASUREMENT	A4	A8	SED	F STATISTIC	P VALUE
HEADING (DAYS)	55.75 ± 0.48	55.00± 0.41	0.875	0.73	0.395
ANTHESIS (DAYS)	62.75 ± 0.48	61.00 ± 0.41	0.836	4.38	0.041
TILLER NUMBER	5.75 ± 0.85	7.5 ± 0.96	0.908	3.72	0.059
EAR (CM)	11.86 ± 0.15	10.69 ± 0.21	0.419	7.74	0.008
STEM (CM)	94.01 ± 1.37	73.11 ± 2.00	3.342	39.10	<0.001
INTERNODE 1 (CM)	42.68 ± 1.36	34.65 ± 1.42	1.969	16.64	<0.001
INTERNODE 2 (CM)	23.28 ± 0.43	18.06 ± 0.70	0.868	36.16	<0.001
INTERNODE 3 (CM)	14.85 ± 0.34	12.43 ±0.53	0.613	15.65	<0.001
INTERNODE 4 (CM)	9.62 ± 0.39	7.22 ± 0.82	0.859	7.80	0.007
INTERNODE 5 (CM)	3.51 ± 0.72	1.68 ± 0.57	0.780	5.50	0.023

Table 5.7 Comparison between *OsPIL1* overexpression line C4 and its azygous segregant C9. The mean value for each measurement is shown with its standard deviation, along with its standard error of the difference (SED), the F-statistic for each comparison, and the P value. The degrees of freedom for this comparison are 1,51

MEASUREMENT	C4	C9	SED	F STATISTIC	P VALUE
HEADING (DAYS)	57.25 ± 0.85	58.00 ± 0.41	0.875	0.73	0.395
ANTHESIS (DAYS)	64.50 ± 1.04	64.25 ± 0.63	0.836	0.09	0.766
TILLER NUMBER	6.00 ± 0.41	6.25 ± 0.25	0.908	0.08	0.784
EAR (CM)	11.63 ± 0.21	10.89 ± 0.38	0.419	3.13	0.083
STEM (CM)	74.68 ± 2.00	76.25 ± 1.95	3.342	0.22	0.639
INTERNODE 1 (CM)	37.23 ± 0.88	35.96 ± 2.61	1.969	0.41	0.523
INTERNODE 2 (CM)	17.16 ± 0.49	17.74 ± 0.71	0.868	0.45	0.504
INTERNODE 3 (CM)	11.33 ± 0.36	12.43 ± 0.33	0.613	3.22	0.079
INTERNODE 4 (CM)	7.53 ± 0.50	8.25 ± 0.85	0.859	0.71	0.403
INTERNODE 5 (CM)	2.55 ± 0.50	2.18 ± 0.74	0.780	0.23	0.317

Table 5.8 Comparison between *OsPIL1* overexpression line D4 and its azygous segregant D9. The mean value for each measurement is shown with its standard deviation, along with its standard error of the difference (SED), the F-statistic for each comparison, and the P value. The degrees of freedom for this comparison are 1,51

MEASUREMENT	D4	D9	SED	F STATISTIC	P VALUE
HEADING (DAYS)	58.25 ± 0.48	57.75 ± 0.63	0.875	0.33	0.570
ANTHESIS (DAYS)	64.25 ± 0.48	63.25 ± 0.48	0.836	1.43	0.237
TILLER NUMBER	7.25 ± 0.63	7.25 ± 0.75	0.908	0.00	1.000
EAR (CM)	10.08 ± 0.37	9.73 ± 0.26	0.419	0.70	0.408
STEM (CM)	79.39 ± 1.84	71.36 ± 1.81	3.342	0.97	0.020
INTERNODE 1 (CM)	35.43 ± 1.90	32.58 ± 1.34	1.969	2.09	0.154
INTERNODE 2 (CM)	18.33 ± 0.61	17.38 ± 0.42	0.868	1.18	0.283
INTERNODE 3 (CM)	12.69 ± 0.42	11.93 ± 0.41	0.613	1.53	0.222
INTERNODE 4 (CM)	8.90 ± 0.89	8.31 ± 0.77	0.859	0.41	0.494
INTERNODE 5 (CM)	2.60 ± 0.19	1.81 ± 0.56	0.780	1.02	0.317

When the *TaPIL1* overexpression line C10 was compared to its azygous segregant (**Table 5.9**), the overexpression line had a significantly longer ear length than the azygous line, with a p value of 0.024. No other measurements were significantly different between the azygous segregant and overexpression line. The comparison between the *TaPIL1* overexpression line F10 and its azygous segregant F11 (**Table 5.10**) revealed a significantly increased number of days to both heading and anthesis for the transgenic line, with p values of <0.001 and 0.002, respectively.

Table 5.9 Comparison between *TaPIL1* overexpression line C10 and its azygous segregant C1. The mean value for each measurement is shown with its standard deviation, along with its standard error of the difference (SED), the F-statistic for each comparison, and the P value. The degrees of freedom for this comparison are 1,51.

MEASUREMENT	C10	C1	SED	F STATISTIC	P VALUE
HEADING (DAYS)	55.75 ± 0.25	55.25 ± 0.48	0.875	0.33	0.570
ANTHESIS (DAYS)	62.00 ± 0.41	61.5 ± 0.65	0.836	0.36	0.552
TILLER NUMBER	7.00 ± 0.41	6.75 ± 0.85	0.908	0.08	0.784
EAR (CM)	11.43 ± 0.18	10.46 ± 0.20	0.419	5.14	0.024
STEM (CM)	74.03 ± 1.96	75.67 ± 2.19	3.342	0.24	0.627
INTERNODE 1 (CM)	36.73 ± 0.75	34.52 ± 0.94	1.969	1.27	0.266
INTERNODE 2 (CM)	17.98 ± 0.10	18.17 ± 0.61	0.868	0.05	0.826
INTERNODE 3 (CM)	11.34 ± 0.13	12.18 ± 0.20	0.613	1.85	0.180
INTERNODE 4 (CM)	6.97 ± 0.77	8.60 ± 0.25	0.859	3.61	0.063
INTERNODE 5 (CM)	2.12 ± 0.88	2.01 ± 0.37	0.780	0.02	0.890

Table 5.10 Comparison between *TaPIL1* overexpression line F10 and its azygous segregant F11. The mean value for each measurement is shown with its standard deviation, along with its standard error of the difference (SED), the F-statistic for each comparison, and the P value. The degrees of freedom for this comparison are 1,51.

MEASUREMENT	F10	F11	SED	F STATISTIC	P VALUE
HEADING (DAYS)	59.75 ± 0.75	56.50 ± 0.87	0.875	13.79	<0.001
ANTHESIS (DAYS)	66.25 ± 0.63	63.5 ± 0.65	0.836	10.82	0.002
TILLER NUMBER	6.50 ± 0.65	7.00 ± 0.41	0.908	0.30	0.584
EAR (CM)	10.06 ± 0.44	10.63 ± 0.28	0.4193	1.88	0.176
STEM (CM)	79.73 ± 1.22	76.31 ± 1.82	3.342	1.05	0.311
INTERNODE 1 (CM)	37.03 ± 0.83	35.68 ± 0.67	1.969	0.48	0.493
INTERNODE 2 (CM)	19.43 ± 0.15	18.44 ± 0.75	0.868	1.31	0.258
INTERNODE 3 (CM)	12.69 ± 0.10	12.06 ± 0.74	0.613	1.07	0.306
INTERNODE 4 (CM)	8.99 ± 0.22	8.52 ± 0.51	0.859	0.31	0.583
INTERNODE 5 (CM)	2.61 ± 0.31	1.97 ± 0.30	0.780	0.68	0.414

The value for least significant difference (LSD) for each measurement was used to make comparisons between RNAi lines, the RNAi azygous segregant and wild-type Cadenza (**Table 5.11**). Both 3912-1 and 3912-4 had significantly fewer days to anthesis than the RNAi azygous segregant while line 3964-8 had significantly shorter ears than the azygous segregant control. At internode 2, 3964-3 was significantly shorter than the azygous segregant, whereas 3912-4 and 4085-3 were significantly longer. At internode 3, 3964-3 was significantly shorter than the azygous segregant. When compared to wild-type Cadenza, both 3964-3 and 3964-8 had significantly shorter total stem, internode two and internode three lengths. 3964-3 had a shorter internode 4 length. Neither 3912-4 nor 4085-3 had significantly longer internode lengths than wild-type cadenza, despite being significantly longer than the RNAi azygous line.

Table 5.11 A comparison of the means for the RNAi lines and the RNAi Azygous segregant for all measurements. An analysis of variance (ANOVA) was applied to measurements from the RNAi lines 3912-1, 3912-4, 3964-3, 3964-8, 4085-3, 4085-6, the RNAi azygous segregant (control) and wild-type Cadenza. The mean value for each measurement is shown with its standard deviation, along with its standard error of the difference (SED), and the least significant difference (LSD) at the value of 5% for each measurement. Means shown in bold are significantly different from the mean of the control. Means shown underlined are significantly different from Cadenza.

MEASUREMENT	CADEN-ZA	CONTROL	3912-1	3912-4	3964-3	3964-8	4085-3	4085-6	SED	LSD (5%)
HEADING (DAYS)	58.25 ± 0.25	58.5 ± 0.65	55.75 ± 0.63	56.00 ± 0.71	57.75 ± 0.48	58.00 ± 0.91	57.00 ± 0.71	58.00 ± 0.41	0.875	1.757
ANTHESIS (DAYS)	63.75 ± 0.25	63.75 ± 0.25	**61.25 ± 0.63**	**61.75 ± 0.75**	64.25 ± 1.11	63.75 ± 0.48	63.75 ± 0.63	63.25 ± 0.25	0.836	1.678
TILLER NUMBER	7.25 ± 0.48	6.75 ± 1.11	5.75 ± 0.25	6.00 ± 0.71	5.50 ± 0.29	5.75 ± 0.48	7.25 ± 0.75	7.50 ± 0.29	0.908	1.822
EAR (CM)	10.53 ± 0.25	10.23 ± 0.32	10.02 ± 0.36	10.18 ± 0.24	9.70 ± 0.35	**8.96 ± 0.53**	10.19 ± 0.18	9.88 ± 0.19	0.419	0.842
STEM (CM)	75.33 ± 2.73	68.98 ± 1.82	73.78 ± 3.09	79.03 ± 3.67	63.87 ± 2.27	65.82 ± 4.15	77.45 ± 2.5	74.50 ± 1.83	3.342	6.710
INTERNODE 1 (CM)	34.82 ± 0.33	33.53 ± 1.29	35.79 ± 1.86	36.79 ± 1.59	31.38 ± 1.13	30.15 ± 1.93	35.85 ± 1.49	34.16 ± 1.39	1.969	3.953
INTERNODE 2 (CM)	18.43 ± 0.75	17.33 ± 0.95	17.88 ± 0.60	**19.32 ± 1.00**	**13.97 ± 0.78**	16.13 ± 0.81	**19.31 ± 0.85**	18.24 ± 0.58	0.868	1.742
INTERNODE 3 (CM)	12.40 ± 0.65	11.48 ± 0.58	12.06 ± 0.35	12.41 ± 0.60	**9.07 ± 0.2**	10.83 ± 0.56	12.65 ± 0.31	11.88 ± 0.29	0.613	1.231
INTERNODE 4 (CM)	8.26 ± 0.79	7.10 ± 0.54	7.18 ± 0.65	8.48 ± 0.57	5.80 ± 0.39	7.11 ± 0.63	8.17 ± 0.40	8.33 ± 0.35	0.859	1.725
INTERNODE 5 (CM)	2.45 ± 0.48	2.45 ± 0.48	1.83 ± 0.72	2.50 ± 0.43	1.23 ± 0.42	2.42 ± 0.35	2.40 ± 0.43	2.31 ± 0.39	0.780	1.556

The number of days to heading and anthesis for all lines are compared in **Figure 5.6**, which shows F10 clearly has the highest number of days to both heading and anthesis. The length of the stem and ear for all lines was compared in **Figure 5.7**, which clearly shows that OsPIL1 overexpression line A4 has the longest stem. The length of internodes 1-3 for all lines is shown in **Figure 5.8**, which shows that A4 has the longest length for all three internodes. In addition, it is clear that the RNAi line 3964-3 has the shortest lengths for internodes 2 and 3.

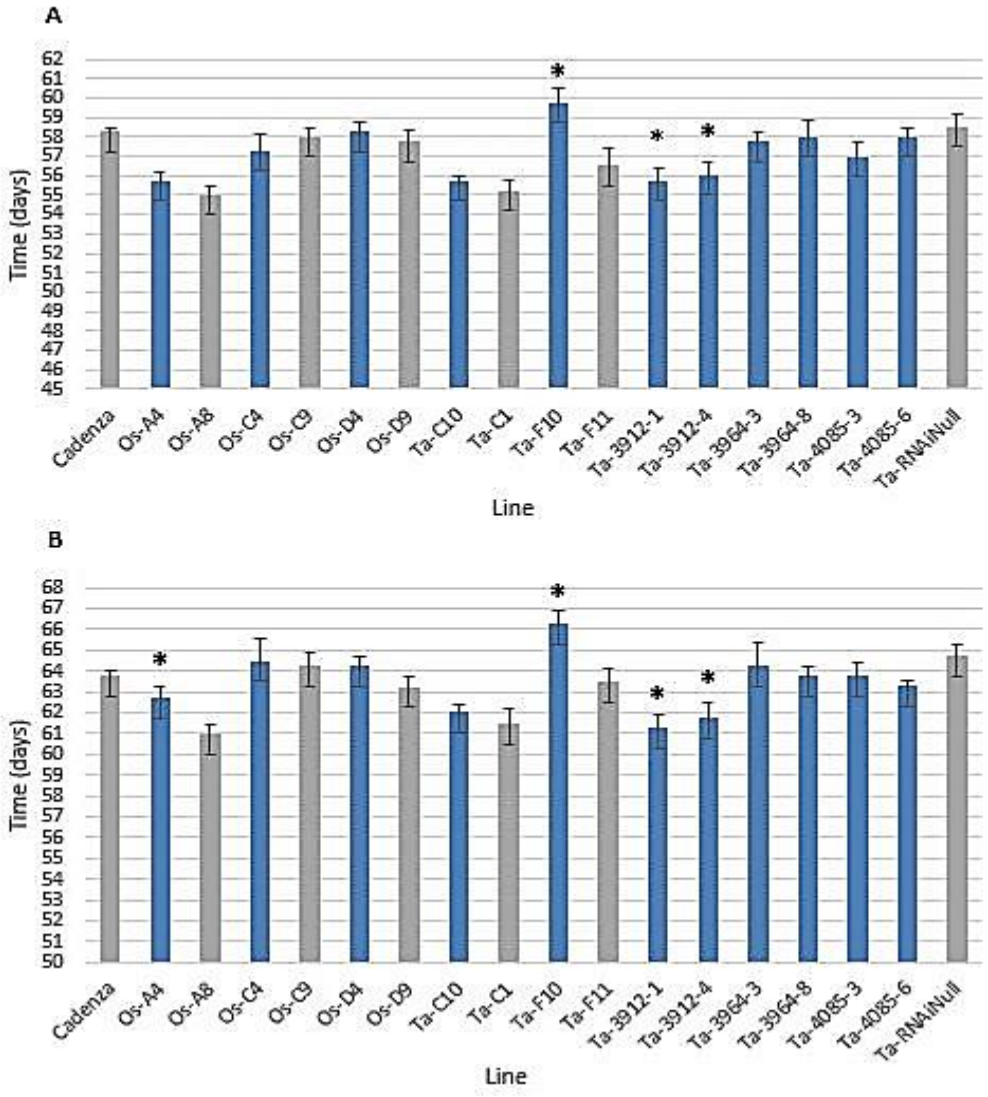

Figure 5.6 Days to heading and anthesis in transgenic RNAi and overexpression lines. The mean values for days to heading **(A)** and anthesis **(B)** for all overexpression, RNAi, azygous segregant (RNAiNull) and wild-type Cadenza lines are shown. All transgenic lines are shown in blue, and wild-type Cadenza are shown in grey. Os-A4, Os-C4 and Os-D4 refer to the *OsPIL1* overexpression lines, with Os-A8, Os-C9 and Os-D9 being their respective azygous segregants. The Ta-C10 and Ta-F10 refer to the *TaPIL1* overexpression lines, with Ta-C1 and Ta-F11 being their respective azygous segregants. Ta-3912-1 to Ta-4085-6 are the RNAi lines. Error bars refer to the standard error (SED). Lines with an asterisk were significantly different from their respective azygous segregant or the wild-type cadenza line.

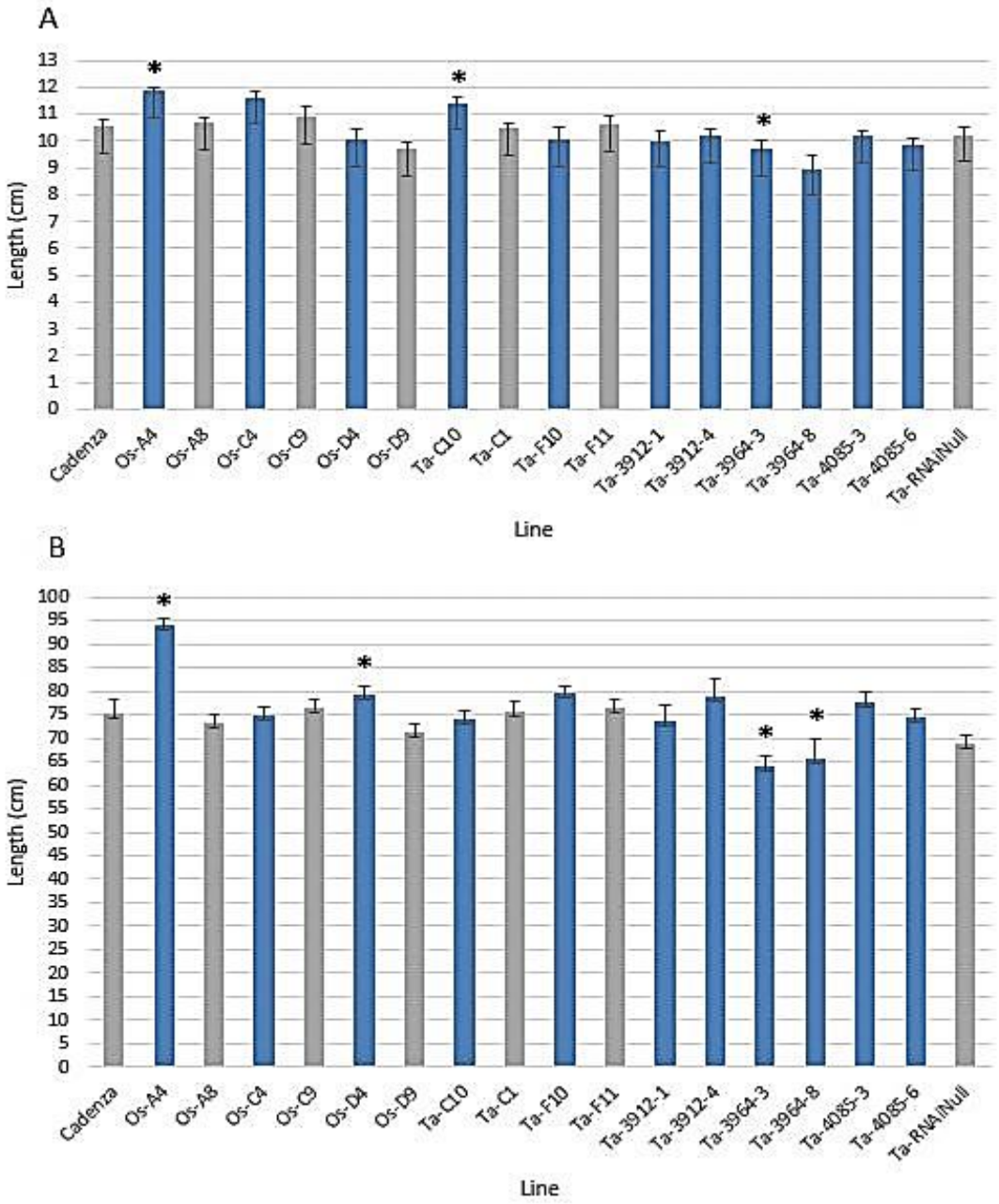

Figure 5.7 Stem and ear length in transgenic RNAi and overexpression lines. The mean values for ear **(A)** and stem **(B)** length for all overexpression, RNAi, azygous segregants (RNAiNull) and wild-type cadenza lines are shown. All transgenic lines are shown in blue, azygous lines and wild-type cadenza are shown in grey. Os-A4, Os-C4 and Os-D4 refer to the *OsPIL1* overexpression lines, with Os-A8, Os-C9 and Os-D9 being their respective azygous segregants. The Ta-C10 and Ta-F10 refer to the *TaPIL1* overexpression lines, with Ta-C1 and Ta-F11 being their respective azygous segregants. Ta-3912-1 to Ta-4085-6 are the RNAi lines. Error bars refer to the standard error (SED). Lines with an asterisk were significantly different from their respective azygous lines or the wild-type cadenza line.

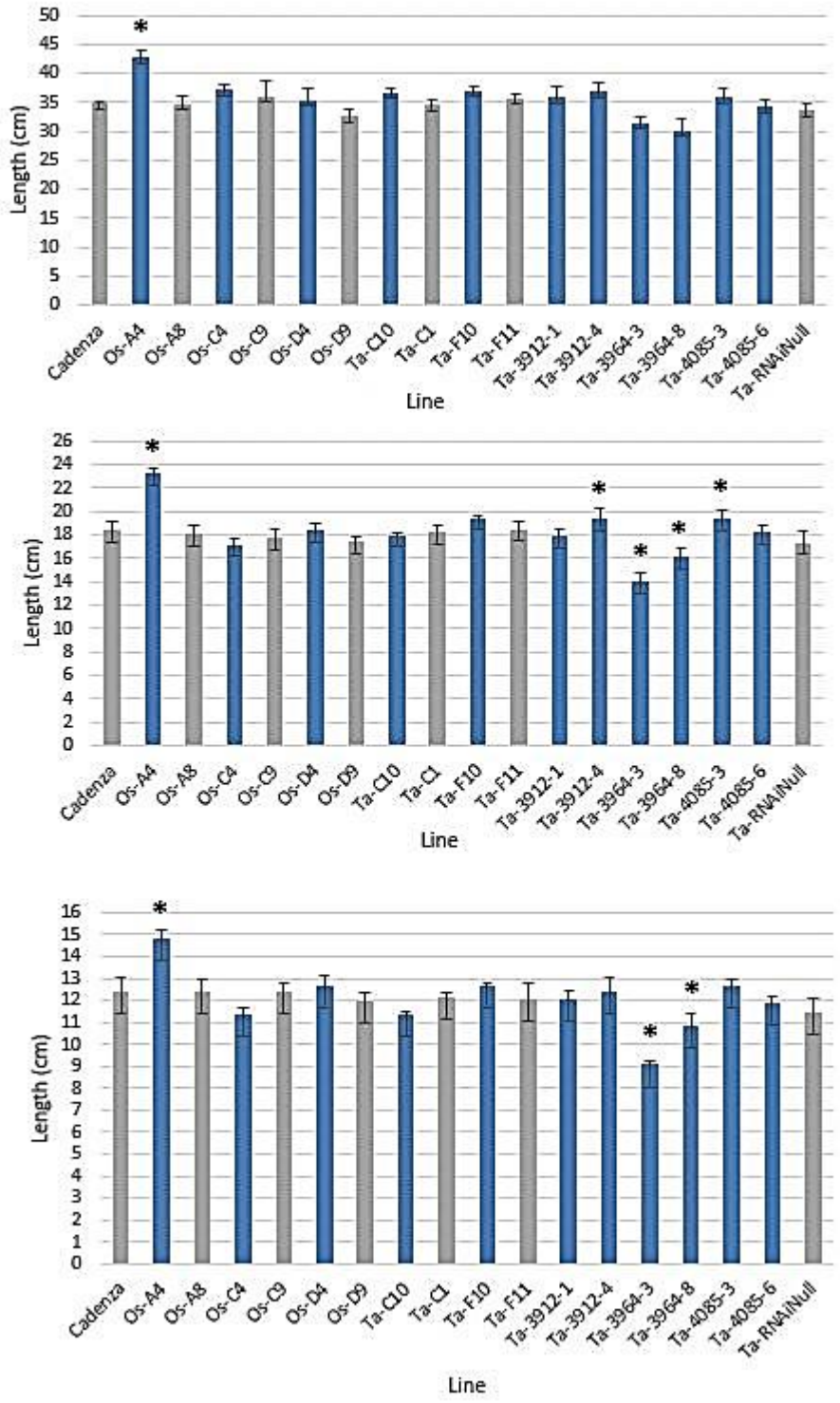

Figure 5.8 Length of internodes 1, 2 and 3 in transgenic RNAi and overexpression lines. The mean values for the lengths of internode 1 **(A)**, internode 2 **(B)** and internode 3 **(C)** for all overexpression, RNAi, azygous segregants (RNAiNull) and wild-type cadenza lines are shown. All transgenic lines are shown in blue, azygous segregants and wild-type cadenza are shown in grey. Os-A4, Os-C4 and Os-D4 refer to the *OsPIL1* overexpression lines, with Os-A8, Os-C9 and Os-D9 being their respective azygous segregants. The Ta-C10 and Ta-F10 refer to the *TaPIL1* overexpression lines, with Ta-C1 and Ta-F11 being their respective azygous segregants. Ta-3912-1 to Ta-4085-6 are the RNAi lines. Error bars refer to the standard error (SED). Lines with

an asterisk were significantly different from their azygous segregant or the wild-type cadenza line.

The increased stem length for *OsPIL1*-overexpression line A4 is also clearly shown in **Figure 5.9A**, in which A4 plants are compared with azygous segregant lines (A8) and Cadenza. **Figure 5.9** also shows images of *OsPIL1*-overexpression lines C4 and D4 alongside their respective azygous segregants and Cadenza in panels B and C, respectively, and examples of the three homozygous lines are compared with Cadenza in panel D. Line D4 is shown to be taller than its azygous segregant line D9.

Images of the fully extended *TaPIL1* overexpression lines are shown in **Figure 5. 10**, which illustrates that there is no height difference between C10 or F10 and their azygous segregant segregants C1 and F11, respectively.

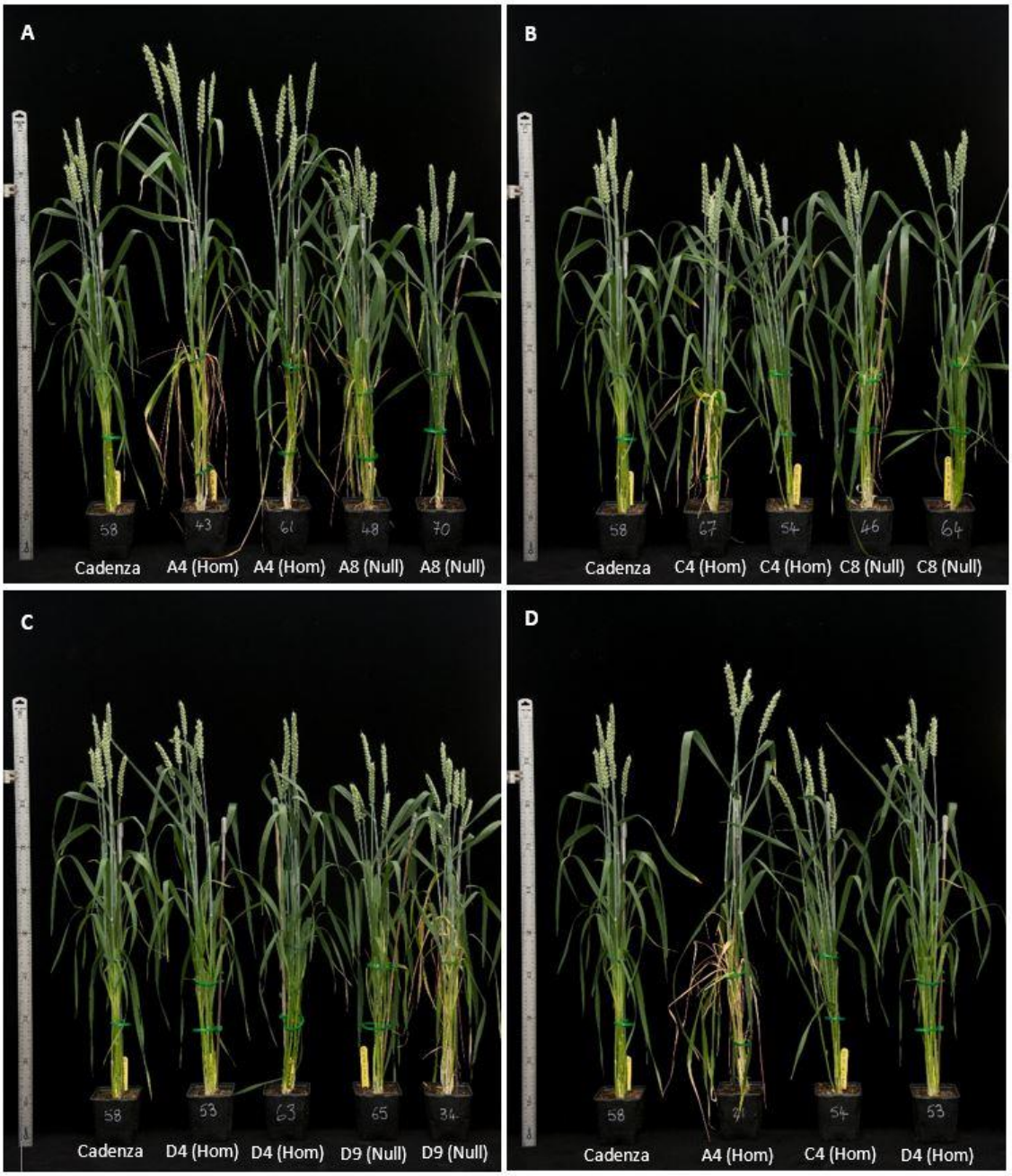

Figure 5.9 The *OsPIL1* overexpression lines. The *OsPIL1* overexpression lines were photographed at approximately 14 days post anthesis. (A) Line A4 with its azygous segregant (null) (line A8) and wild-type Cadenza. (B) Line C4 with the C9 null and Cadenza. (C) Line D4 with the D9 null and Cadenza. (D) The three overexpression lines A4, C4 and D4 with Cadenza. A meter ruler is displayed on the left in each photograph.

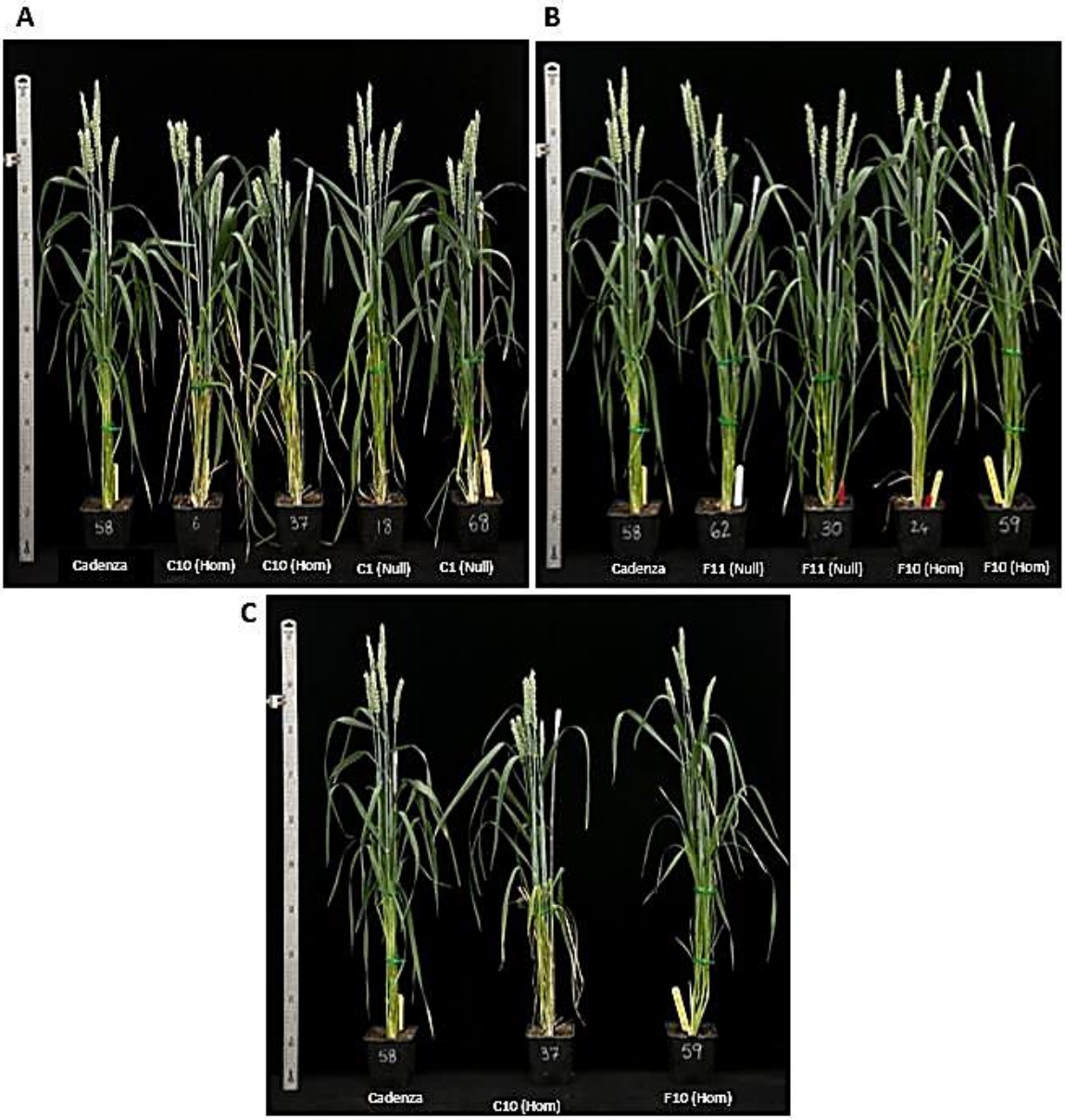

Figure 5. 10 The *TaPIL1* overexpression lines. The *TaPIL1* overexpression lines were photographed at approximately 14 days post anthesis. (A) Line C10 with its azygous segregant (null) (line C1) and wild-type Cadenza. (B) Line F10 with its null (line F11) and wild-type Cadenza. (D) The two TaPIL1 overexpression lines C10 and F10 with wild-type Cadenza. A meter ruler is displayed on the left in each photograph.

Images of the RNAi lines compared with a azygous segregant line and Cadenza are presented in **Figure 5.11**, **Figure 5.12**, **Figure 5.13** and **Figure 5.14**. These images demonstrate the height differences described in the previous analysis (see **Figure 5.7**). **Figure 5.11** demonstrates that neither 3912-1 or 3912-4 are shorter than the azygous segregant line, but that 3912-4 is taller than the azygous segregant line, which could be due to the increased length of internode 2 indicated in **Table 5.11**. **Figure 5.12** shows the reduced height phenotype of 3964-3 compared to Cadenza and the azygous segregant, in agreement with the reduced internode lengths as shown in **Table 5.11**. In **Figure 5.13** it can be seen that the heights of 4085-3 and 4086-6 are

similar to that of the Cadenza and the azygous segregant line. All RNAi lines are compared in **Figure 5.14**, which indicates that 3964-3 is shorter than the other lines.

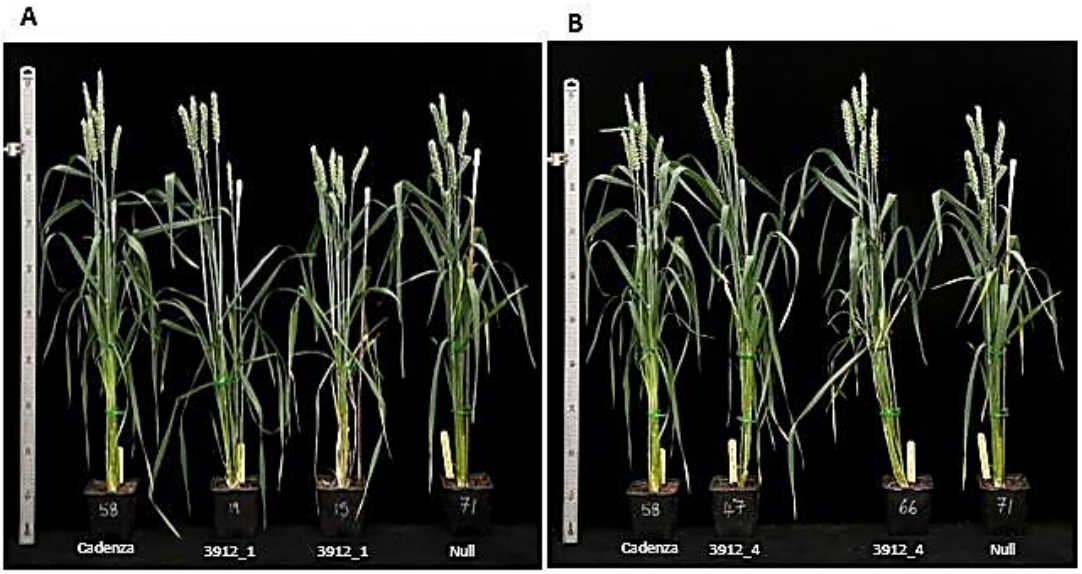

Figure 5.11 The 3912 RNAi lines. The 3912 RNAi lines were photographed when fully extended at approximately 14 days post anthesis. **(A)** 3912-1 RNAi lines with the RNAi azygous segregant (null) and wild-type Cadenza. **(B)** 3912-4 RNAi lines with the RNAi null and Cadenza. A meter ruler is displayed on the left in each photograph.

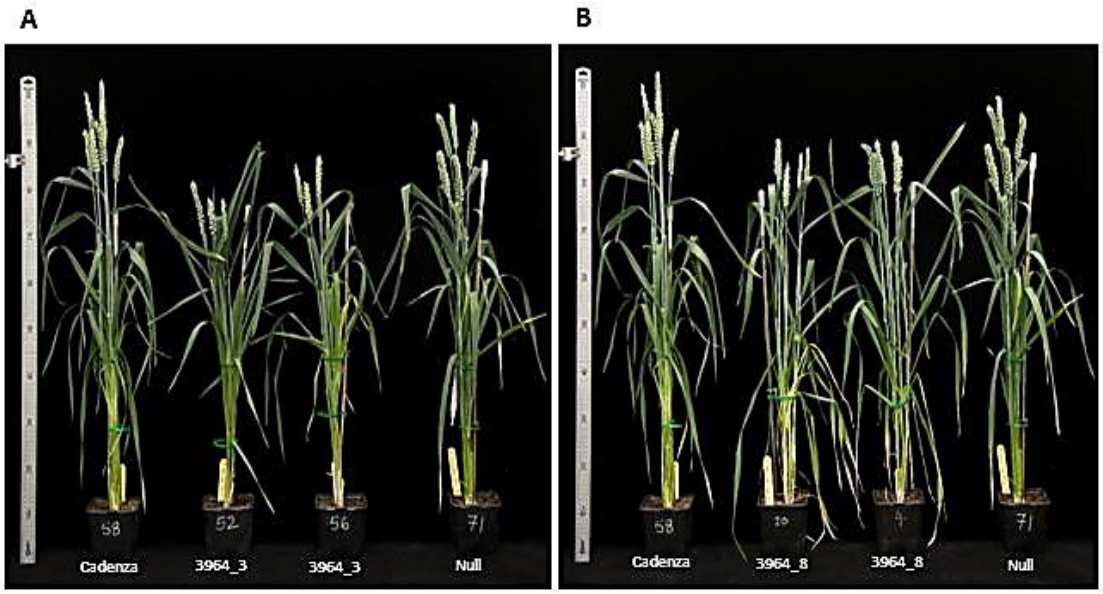

Figure 5.12 The 3964 RNAi lines. The 3964 RNAi lines were photographed when fully extended at approximately 14 days post anthesis. **(A)** 3964-3 RNAi lines with the RNAi azygous segregant (null) and wild-type Cadenza. **(B)** 3964-8 RNAi lines with the RNAi null and Cadenza. A meter ruler is displayed on the left in each photograph.

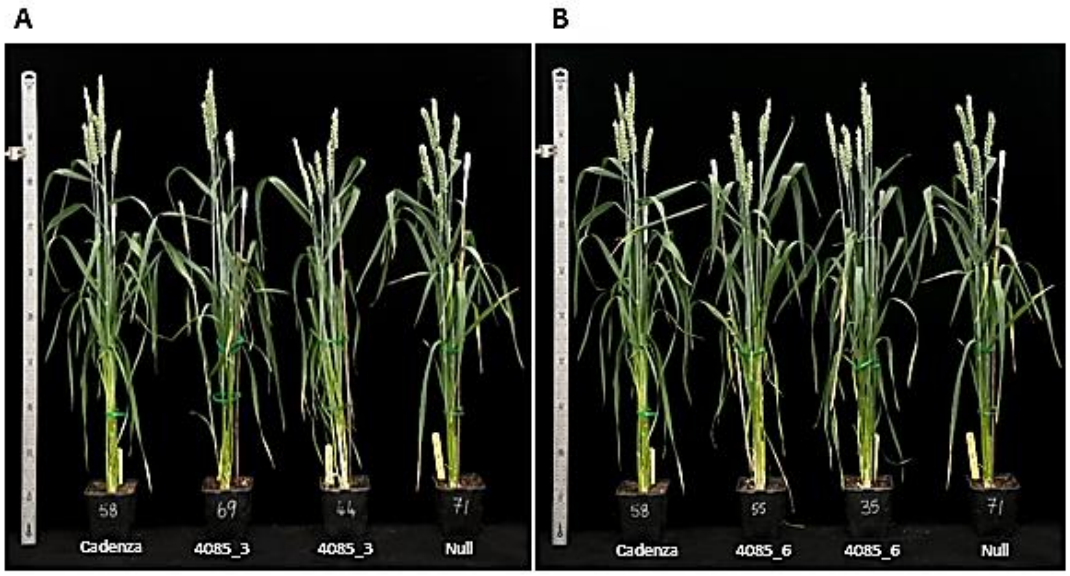

Figure 5.13 The 4085 RNAi lines. The 4085 RNAi lines were photographed when fully extended at approximately 14 days post anthesis. **(A)** 4085-3-3 RNAi lines with the RNAi null and wild-type Cadenza. **(B)** 4085-6 RNAi lines with the RNAi null and Cadenza. A meter ruler is displayed on the left in each photograph.

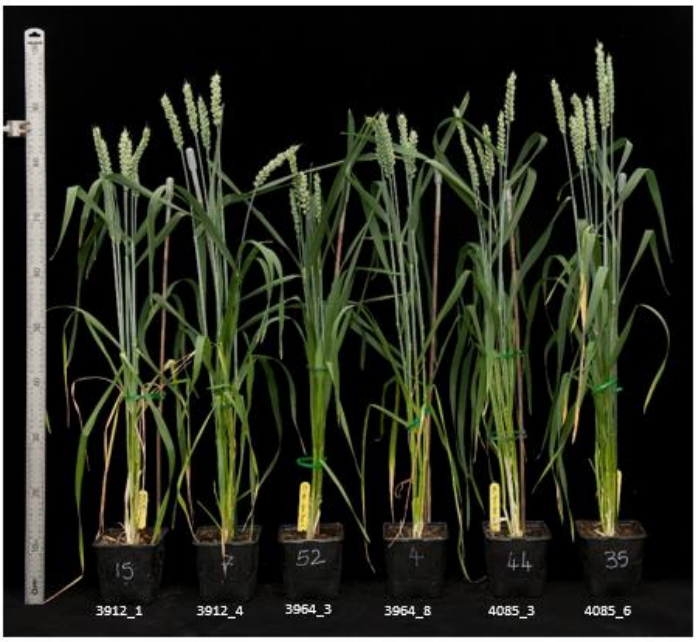

Figure 5.14 The RNAi lines. RNAi lines 3912-1, 3912-4, 3964-3, 3964-8, 4085-3 and 4085-6 were photographed when fully extended at approximately 14 days post anthesis. The six RNAi lines are pictured together with a meter ruler displayed on the left.

5.2.4 A TILLING-based approach to generate knockout mutants of *TaPIL1* and *TaPIL3* in Cadenza.

Two approaches were applied to reduce the expression of *PIL*s in wheat. The first was the use of RNAi as described in section 5.1.1.1, while the second approach was to scrutinise a mutant population for potential knockouts of the *TaPIL* genes. Two approaches were used because RNAi is not always effective due to epigenetic silencing, off-target effects and insufficient

knockdown (see discussion in section 5.1.1.1). A TILLING population of mutagenized Cadenza lines became available during this project. Screening this population provided a potentially more robust method than RNAi for generating loss of function mutants. Utilization of the TILLING lines required the identification of potential loss-of-function mutants of each of the three homoeologues and their combination by crossing. Triple mutant *TaPIL1* and *TaPIL3* plants were produced using TILLING, which were then analysed for alterations in plant height.

5.2.4.1 Identification of mutations within *TaPIL* sequences

The wheat TILLING database (www.wheat-tilling.com) (Krasileva et al., 2017, Clavijo et al., 2017) was used to search for seed stocks with mutations within the wheat *TaPIL1-3* A, B and D homoeologues. Selected mutations either produced nonsense mutations, or affected a splice site. Mutation of the AGGT splice donor site can cause exon skipping, or can cause altered protein sequence from the use of alternative donor sites within the subsequent introns or exons (Lewandowska, 2013). Seeds stocks with stop or splice site mutations in all three homoeologues of *TaPIL1* and *TaPIL3* were identified. For *TaPIL1* (**Figure 5.15**), the A homoeologue has a C/T mutation at position 1352 (**Figure 5.16**), within exon 5 (CAD4-1316), resulting in a Q272* mutation. The *TaPIL1 B* homoeologue has a G/A splice site mutation at position 1205, at the end of exon 4 (CAD4-0743). The *TaPIL1 D* homoeologue has a splice site G/A mutation at position 1818, at the end of exon 6 (CAD4-0917). Mutation positions are shown in **Figure 5.15** and mutant sequences are shown in **Figure 5.16**.

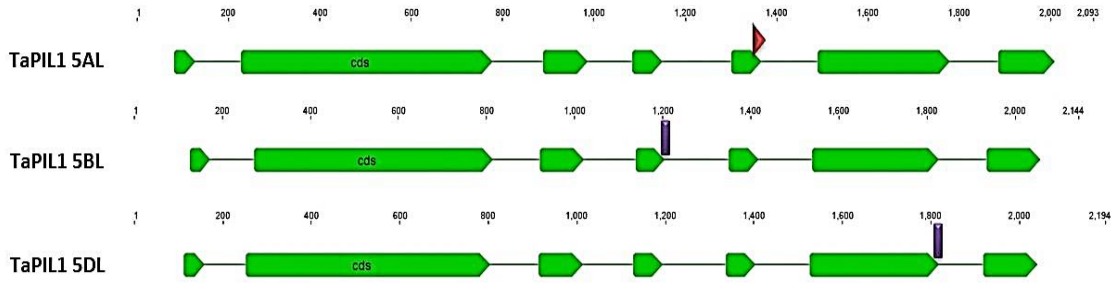

Figure 5.15 Position of mutations within the *TaPIL1* TILLING lines. The position of mutations within the TILLING lines are shown in a schematic of the genomic sequences. The exon sequences are indicated by the green arrows and separated by intron regions. The mutation in the A homoeologue that introduces a stop codon is indicated by a red arrow above the exon annotations, and splice site mutations are shown as a purple line above the exon annotations.

Figure 5.16 The *TaPIL1* A, B and D homoeologue mutations. The sequences of wild-type *TaPIL1* homoeologues were aligned with their corresponding TILLING mutant sequences. Residues shown in reverse are shared between both sequences. Stop codon C/T mutations are indicated by red highlight and splice site G/A mutations are indicated by pink highlight. Exon sequence is indicated by a dashed line below the sequence.

Mutations were detected in the A, B and D homoeologues of *TaPIL3* that introduce a premature stop codon. The A homoeologue contains a C/T mutation at position 1091 that causes a premature stop codon within exon 4 and results in a Q192* mutation (CAD4-0531). The B homoeologue contains a C/T mutation at position 1467, causing a premature stop codon within exon 6, resulting in a Q257* mutation (CAD4-0761). The D homoeologue has a C/T mutation at position 383, causing a premature stop codon within exon 2, resulting in a Q39* mutation (CAD4-1793). The position of the mutations within the genomic sequences is shown in **Figure 5.17** and the sequences indicating the mutation are shown in **Figure 5.18**. The A, B homoeologues of *TaPIL2* had stop codon mutations; however, no stop codon or splice site mutants were identified for *TaPIL2-5DL* so that a triple mutant could not be generated. For this reason, no *TaPIL2* mutants were used.

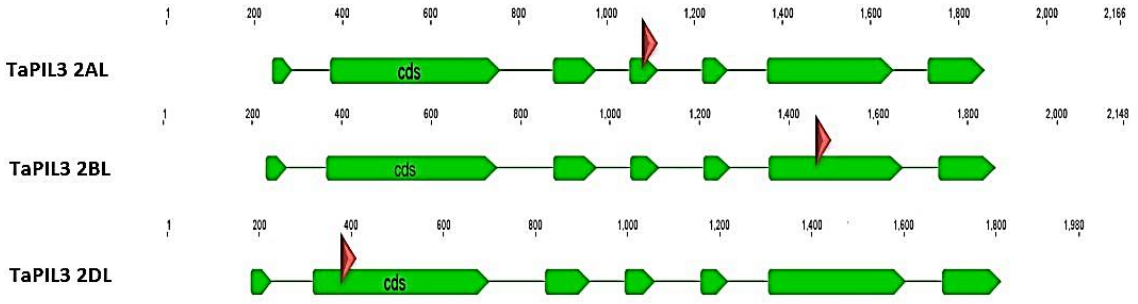

Figure 5.17 Position of mutations within the *TaPIL3* TILLING lines. The position are shown in a schematic of the genomic sequences. The exon sequences are indicated by the green allows, separated by intron regions. Stop codon mutations are indicated by a red arrow above the exon annotations.

Figure 5.18 The *TaPIL3* A, B and D homoeologue mutations. The sequence of the wild type *TaPIL3* homoeologues were aligned with their corresponding mutant sequences. Residues shown in reverse are shared between both sequences and stop codon C/T mutations are indicated by red highlight.

5.2.4.2 Identification of TaPIL1 triple mutants

Seed stocks containing the desired mutations at the M4 generation were ordered and 6 seeds per line were planted. Genomic DNA was extracted from leaf material and mutations within the TILLING lines were identified using genotyping by sequencing. This method involved designing primers to amplify the 200-550 bp region flanking the mutation of interest. Primers were designed to contain homoeologue-specific SNPs within their sequence to allow homoeologue-specific amplification. Using the genomic DNA from the TILLING lines as a template, the primers were used in a HotShot PCR reaction to amplify the region of sequence containing the mutation of interest. PCR products were purified and sequenced by Eurofins Genomics. Resulting sequencing data was aligned with the TILLING mutant sequences to identify wild-type, homozygous and heterozygous mutant lines. Sequence data obtained identified the expected SNPs from the TILLING database sequencing. For both the *TaPIL1* and *TaPIL3* lines, plants with mutations in the A and D homoeologues were crossed together to produce F1 progeny containing both alleles.

The *TaPIL3-B* TILLING line had a late flowering phenotype, probably due to mutations elsewhere in the genome, so these lines were back-crossed with wild type Cadenza to remove this phenotype. The resulting progeny was then planted, and genomic DNA was extracted from leaf material for genotyping by sequencing. Genotyping allowed identification of lines with both an A and D mutant allele, which were then crossed with B homoeologue mutants to stack all three alleles. The resulting heterozygous AaBbDd mutant was identified by sequencing in both the *TaPIL1* and *TaPIL*3 TILLING lines, these were self-pollinated and the triple mutant identified in the F_2 progeny.

A KASP assay (He et al., 2014) was used to identify homozygous triple mutants. KASP assays involve the use of two fluorescently labelled allele-specific primers and one common reverse

primer. Depending which allele-specific primer is able to amplify the sequence, a different fluorescence signal is released, allowing the detection of homozygous, heterozygous and wild-type lines. Homoeologue specific KASP primers were designed by LGC Genomics to allow the detection of the wild-type, heterozygous and homozygous mutant sequences of both *TaPIL1* and *TaPIL3*. Testing of the primers revealed that only the D homoeologue primers were functional for both *TaPIL1* and *TaPIL3*. The D homoeologue-specific primers were used on genomic DNA sampled from selfed heterozygous triple mutant lines. Reactions were analysed to identify homozygous D lines, which were subsequently genotyped by sequencing to identify homozygous mutants for the A and B homoeologues (**Figure 5.19** and **Figure 5.20**).

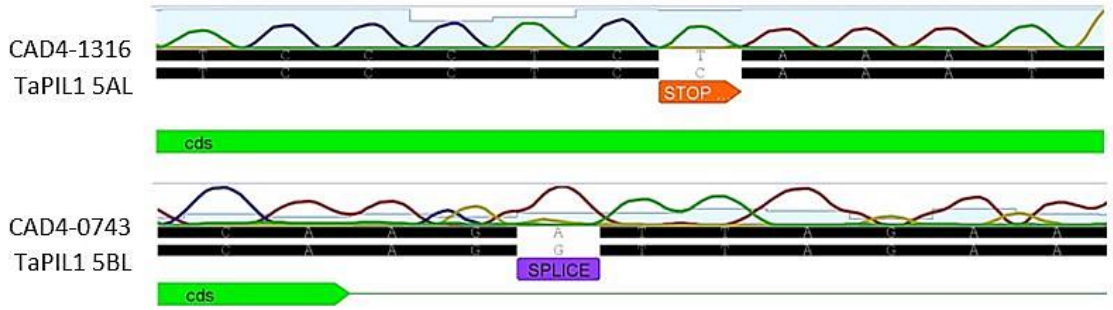

Figure 5.19 Genotyping by sequencing of the TaPIL1 5AL and 5BL homoeologues. Genomic DNA from selfed heterozygous triple TaPIL1 mutants was amplified using homoeologue-specific primers for each mutation of interest. PCR products were sequenced and aligned to the TaPIL1 5AL and 5BL sequence to identify mutations. The coding sequence is indicated in green under the sequence, stop codon mutations are labelled with an orange arrow below the sequence and spice site mutations are labelled with a purple arrow below the sequence. A chromatogram is shown above the sequencing data.

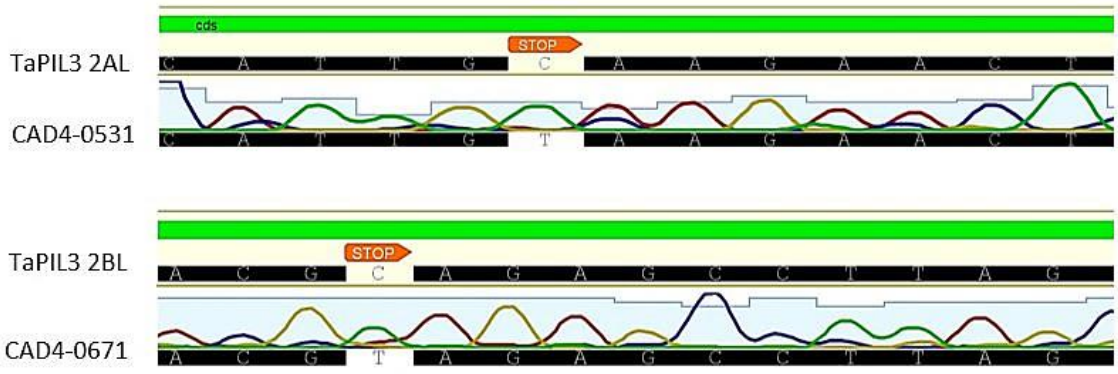

Figure 5.20 Genotyping by sequencing of the TaPIL3 2AL and 2BL homoeologues. Genomic DNA from selfed heterozygous triple TaPIL3 mutants was amplified using homoeologue-specific primers for each mutation of interest. PCR products were sequenced and aligned to the TaPIL3 2AL and 2BL sequence to identify mutations. The coding sequence is indicated in green above the sequence, stop codon mutations are labelled with an orange arrow above the sequence. A chromatogram is shown below the sequencing data.

For *TaPIL1* one homozygous aabbdd triple mutant line (**Figure 5.19**), and one homozygous d mutant line; AABBdd was identified. No wild type D alleles were brought forward, so it was not possible to identify a wild-type segregant. The single and triple mutant lines are shown in **Figure 5.21A**. The comparison between the single and triple mutant lines demonstrated a small reduction in stem elongation in the triple mutant, indicating that TaPIL1 may promote stem elongation. For *TaPIL3* one homozygous aabbdd triple mutant was identified **(Figure 5.20**), along with one wild-type line. When these lines were compared, the triple mutant had fewer tillers and reduced stem elongation, suggesting that TaPIL3 promotes tillering and stem elongation (**Figure 5.21B**).

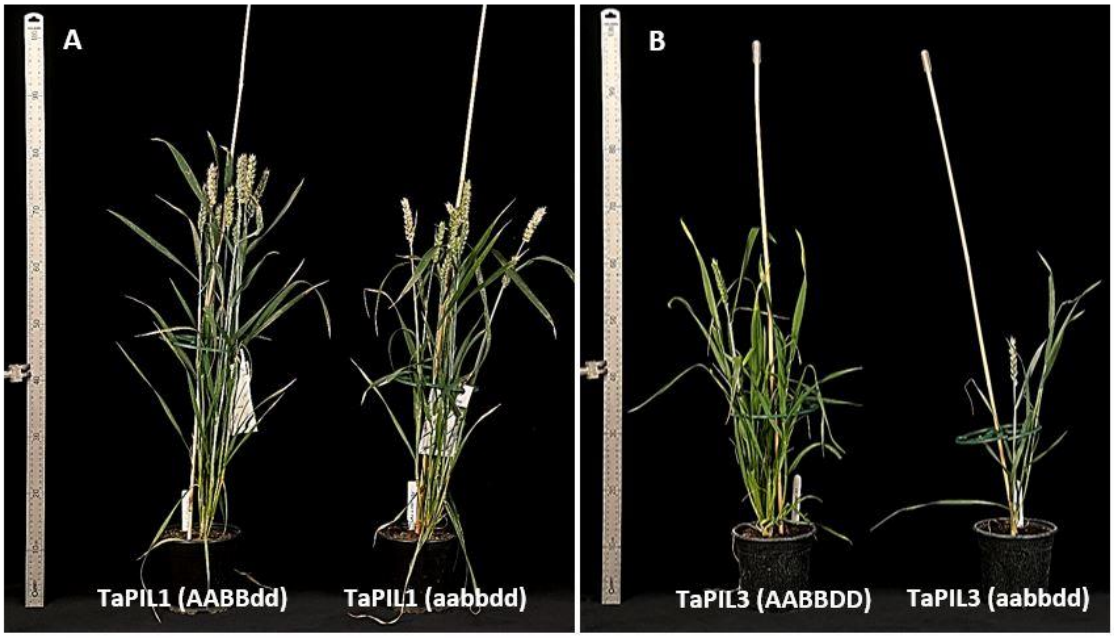

Figure 5.21 Phenotype of *TaPIL1* and *TaPIL3* TILLING mutants. Fully extended *TaPIL1* and *TaPIL3* triple mutants at approximately 14 days after anthesis. In both pictures, a meter ruler is shown on the left. (A) The single *TaPIL1* mutant (AABBdd) is pictured with the triple mutant (aabbddd). (B) The *TaPIL1* wild-type (AABBDD) line is pictured with the *TaPIL3* triple mutant (aabbddd).

5.3 Discussion

The aim of this section of the project was to take a reverse genetics approach to investigating the phenotypic functions of the wheat PILs. Three approaches were used to maximise the potential of successful disruption of PIL function, RNAi, overexpression and knockout using TILLING lines. Producing these lines in wheat has been challenging, mainly due to its hexaploid genome and the long timescale for each generation. The time constrains have prevented the identification of additional mutant TILLING lines, as well as backcrossing and quantitative analysis of the triple mutant TaPIL1 and TaPIL3 lines. However, all three approaches have been successfully utilised to produce transgenic lines with overexpression, knockdown and knockout of the PILs.

5.3.1 Phenotyping of RNAi and overexpression *PIL* lines reveals differences between the lines.

A selection of *TaPIL1* RNAi, *TaPIL1*- and *OsPIL1*-overexpression lines were grown alongside azygous segregant lines and wild-type Cadenza in order to assess the influence of altered *PIL1* expression on phenotype, focussing particularly on plant architecture. A multivariate CVA was carried out to look at broad differences between the means of each line (Appendix **Table S.2** and **Figure S.7**). This analysis indicated that the *TaPIL1* RNAi line 3964-3 and the *OsPIL1*-overexpression line A4 were significantly different from any other line and very different from each other. This is supported by data from the ANOVA comparisons, which demonstrate that line A4 had significantly increased stem elongation compared to the azygous segregant, and that 3964-3 was the shortest RNAi line, with significantly reduced internode elongation. The individual parameters for which differences between lines were found were days to heading, ear length, and the lengths of internodes 2-5. This is supported by ANOVA, which indicated that in these measurements some azygous segregant and transgenic lines were significantly different from each other.

5.3.1.1 Overexpression of OsPIL1 in wheat causes increased stem elongation.

This project aimed to assess the effect of altering *PIL* expression in wheat. Initial difficulties isolating the full *TaPIL1* sequence (described in Chapter 2, Section 3.2.5.1) lead to *OsPIL1* being used for additional overexpression experiments. Todaka et al. (2012) demonstrated that overexpression of *OsPIL1* in rice lead to an increased stem elongation phenotype.

Overexpression lines of *OsPIL1* were produced in wheat to investigate if the same phenotype could be observed.

Two of the three *OsPIL1* overexpression lines; A4 and D4 showed significantly increased stem elongation compared to their azygous segregant. A4 had by far the largest increase in stem elongation, with a p value of >0.001 (**Table 5.6**) when compared to the A8 azygous segregating line. This corresponds well with the analysis of *OsPIL1* expression levels, which demonstrated that the A4 line had the highest level of *OsPIL1* expression, which was 10 times higher than in C4 and 23 times higher than that observed in D4 (**Table 5.5**). The A4 overexpression line also had increased elongation compared to the azygous segregant at every internode. While the D4 line did show a significant increase in stem elongation compared to its azygous segregant, D9 (**Table 5.8**), no significant increase in elongation of any of the internodes was observed, although each internode was slightly longer than in D9. The C4 overexpression line did not display any significant increases in stem length (**Table 5.7**). This is despite the expression analysis, which indicated that expression of OsPIL1 in C4 was 2.4 times higher than that detected in D4 (**Table 5.5**). These discrepancies in expression could be because the expression analysis was carried out on RNA isolated from leaf tissue, and expression of *TaPIL1* may vary between tissues. These results support the findings of Todaka et al. (2012) that overexpression of *OsPIL1* leads to an increase of stem elongation, and demonstrate that OsPIL1 is also capable of causing this phenotypic effect in wheat. This provides more evidence that PIL proteins play an important role in regulating stem elongation, and are therefore promising targets for specific regulation of stem elongation.

5.3.1.2 Overexpression of *TaPIL1* causes a delay in heading and anthesis.

The wheat TaPIL1 protein was found to be the most closely related to OsPIL1, and therefore is likely to play a similar role in regulating stem elongation in wheat. TaPIL2 is most closely related to both OsPIL11 and OsPIL12. OsPIL11 has been shown to regulate red light-induced de-etiolation when transgenically expressed in tobacco (Li et al., 2012c). TaPIL3 is most closely related to OsPIL14, which has been shown to downregulate the expression of *OsDREB1B*, a major regulator of plant stress responses (Cordeiro et al., 2016), indicating that OsPIL14 is involved in cross-talk between light and stress signalling (Cordeiro et al., 2016). Therefore, no role in the regulation of stem elongation has been previously indicated for the TaPIL2/PIL3 orthologous sequences in rice.

For this reason, *TaPIL1* overexpression lines were produced to investigate the resulting phenotypic effects. The *TaPIL1* overexpression C10 and F10 lines displayed an increase in *TaPIL1* expression when compared their respective azygous segregant lines C1 and F11, with

fold increases of 4.2 and 7.3, respectively (**Table 5.4**). Despite these increases in expression, no alterations in stem elongation were detected. This could be because the increases in expression of *TaPIL1* were not sufficient to cause these alternations, or because TaPIL1 does not play as large a role in stem elongation in wheat as OsPIL1 does in rice. Although redundancy between the TaPILs would not be an issue in overexpression lines, it is possible that TaPIL1 forms dimers with other TaPILs to drive the expression of genes involved in stem elongation. In this case overexpression lines of only TaPIL1 would not cause an increase in stem elongation. The Arabidopsis PIFs form heterodimers to regulate some developmental responses e.g. PIF7 forms a heterodimer with PIF4 to redundantly repress the expression of *DREB1* genes (Kidokoro et al., 2009).

Some alterations in the number of days to heading and anthesis were detected in the F10 overexpression line. When compared to its F11 azygous segregant, F10 displayed a significantly increased number of days to both heading and anthesis, with p values of 0.001 and 0.002, respectively (**Table 5.10**). This phenotype was not observed in the C10 line, which could be due to the higher level of TaPIL1 overexpression in F10. These results indicate that TaPIL1 could have a role in regulating the developmental timing of flowering.

While the C10 overexpression line displayed no phenotype for days to heading and anthesis, C10 did display a significantly longer ear than its C1 azygous segregant (**Table 5.9**). However, this phenotype was not displayed in the F10 line. This result indicates a possible role for *TaPIL1* in the regulation of ear length. An alteration in ear length could be due to rachis internode elongation, which occurs during spike development. This would then cause the ear to be elongated. Rachis internode elongation has been shown to be regulated by GA in barley (Nicholls, 1978). Ear length alterations have not been documented in any other species where PIF levels have been altered. There has been a role described for Arabidopsis PIF4 in the promotion of flowering under high temperatures due to temperature-dependent binding to the promoter of flowering genes. Therefore, the role of TaPILs in promoting ear length and repressing flowering time could represent novel PIF-regulated processes (Kumar et al., 2012).

5.3.1.3 Knockdown of TaPIL1 expression using RNAi causes changes in days to heading and anthesis, ear length and stem elongation phenotypes.

The influence of TaPIL1 on phenotype was also investigated by knocking down expression using RNAi. The six RNAi lines included in the phenotyping experiment all showed some decrease in *TaPIL1* expression level compared with an azygous segregant control line, from a 28% knockdown in 3912-1 to an 87% knockdown in 4085-3 (**Table 5.1**).

The 3912 lines both displayed a significantly lower number of days to anthesis than the RNAi azygous segregant, with a p value of <0.05, but no other RNAi lines showed a significant difference in this parameter. RNAi line 3964-8 showed a significantly shorter ear length than the azygous segregant. No RNAi line displayed a significantly reduced overall stem length, although 3964-3 showed a significantly reduced length for internodes 2 and 3 compared to both the azygous segregant and the 3964-8 RNAi line. In contrast, the RNAi lines 3912-4 and 4085-3 both displayed a significant increase in elongation of internode 2 compared to the azygous segregant. These differences in phenotype do not correlate well with the reduction in *TaPIL1* expression level. For example, the line with the lowest *TaPIL1* expression is 4085-3, which actually shows an increase in internode 2 length. In addition, the two 3912 lines displaying the reduced days to anthesis phenotype had the highest level of *TaPIL1* expression. The hypothesis that TaPIL1 is involved in promoting stem elongation would suggest that reducing TaPIL1 expression would cause a reduced stem elongation phenotype. The only lines showing a reduced stem elongation phenotype compared to the azygous segregant was 3964-3, which did have a large reduction in *TaPIL1* expression of 74%, supporting a role for TaPIL1 in promoting stem elongation. However, two RNAi lines also showed increased elongation of one internode: 3912-4 and 4085-3. These lines had reductions in *TaPIL1* expression of 28% and 87% respectively, making the role of TaPIL1 expression in this phenotype unclear.

5.3.1.4 Altering TaPIL1 expression caused a range of phenotypes in wheat

Two phenotypic effects were demonstrated in both the *TaPIL1* overexpression and RNAi lines: the number of days to anthesis and ear length. Both the RNAi 3912 lines and the *TaPIL1* overexpression F10 line displayed a significant difference in the number of days to anthesis, suggesting that TaPIL1 could have a role in regulating this developmental process. However, F10 also had an increase in the number of days to heading, which was not shared by any RNAi line. The *TaPIL1* overexpression line C10 displayed a significant increase in ear length, while the RNAi line 3964-8 showed a significant decrease, suggesting that *TaPIL1* is involved in promoting ear elongation. Neither *TaPIL1* overexpression line displayed the increase/decrease in stem elongation displayed in the RNAi lines.

The *TaPIL*1 RNAi and *TaPIL1* overexpression lines displayed several different phenotypes that were not shared between all lines of each type. The lack of consistency in phenotypic effects of *TaPIL1* expression means that any conclusions about the role of TaPIL1 in wheat development should be drawn with caution. However, the results do suggest a role for TaPIL1 in regulating the timing of ear development, and the elongation of the stem and ear. The role of TaPIL1 in stem elongation may not be as strong as that of OsPIL1 in rice, suggesting that although the

sequences are orthologous, the role of the proteins may differ. However, it should be noted that (Todaka et al., 2012) did not fully confirm the role of OsPIL1 in stem elongation as they did not look at true loss of function mutants. It is also possible that two or more TaPILs regulate stem elongation, meaning single knockdown RNAi lines will not produce a strong phenotype. The PIF4/PIF5 proteins were the most similar Arabidopsis PIFs to TaPIL1 in the phenotypic analysis shown in Chapter 3 (section 3.2.3). TaPIL1 may play a more similar role to AtPIF4 and AtPIF5 in the regulation of wheat development, such as promotion of stem elongation (Koini et al., 2009) or flowering time (Thines et al., 2014) in response to shade or high temperature, rather than a role similar to OsPIL1 in stem elongation (Todaka et al., 2012).

To further investigate the role of TaPIL1 in the regulation of stem elongation more RNAi and overexpression lines could be selected for use in phenotyping experiments. In this project genotyping results from the T_1 generation (**Table 5.3**) only identified two *TaPIL1* overexpression lines with homozygous, heterozygous and azygous individuals. Genotyping of further lines could identify lines with a stronger increase in *TaPIL1* expression and therefore more obvious phenotypic effects. In addition, a more reliable means of reducing expression could be used, such as producing a triple knockout mutant (see section 5.3.2) or using genome editing to be more confident about the results. In future experiments a more dynamic approach to the measurement of ear development and flowering should be used. For example, measurements could be taken at known developmental stages, such as Zadoks stages. This would allow a more detailed analysis of these phenotypes.

5.3.2 Knockout of TaPIL1 and TaPIL3 leads to a reduced stem elongation and reduced tillering phenotype.

Another method of reducing *TaPIL* expression was used to investigate the phenotypic effects. Mutagenized lines with nonsense premature stop codon or splice site mutations within the homoeologous sequences of *TaPIL1* and *TaPIL3* were selected to investigate the effect of *TaPIL* knockout. In each case, homozygous triple mutants were produced by crossing lines with mutations in each homoeologue. The *TaPIL1* mutations include a premature stop codon within exon 5 of the A homoeologue, and splice site mutations at the end of exon 3 and 6 for the B and D homoeologues, respectively. The mutation within the A homoeologue causes a premature stop codon within the bHLH domain which could disrupt the DNA binding ability of the TaPILs. The splice site mutation at the end of exon 3 in the B homoeologue would also disrupt the bHLH domain and prevent DNA binding activity. The splice site mutation within the D homoeologue occurs after the bHLH domain, so may not have a predictable effect on function. The mutant transcripts need to be amplified using RT-PCR to confirm the effect of the

mutations. The *TaPIL3* mutations encode premature stop codons within exons 4, 6 and 2 of the A, B and D homoeologues, respectively. Both the premature stop codons of the A and D homoeologues occur before or within the bHLH domain. However, the B homoeologue mutation occurs after the bHLH domain so may not affect function. The mutant transcript must be confirmed in vivo using RT-PCR.

Genotyping of the TaPIL1 and TaPIL3 lines identified one homozygous triple mutant line (aabbdd), respectively, along with a single mutant (AABBdd) for TaPIL1 and a wild-type line for TaPIL3. Comparison between the homozygous triple mutant and single mutant indicated that TaPIL1 knockout lead to a decrease in stem elongation and tillering. The TaPIL3 triple mutant also displayed reduced stem elongation and tillering in comparison to the wild-type line. However, the wild-type line was visibly shorter than is typical for wild type lines, suggesting that some background mutations could be affecting the phenotypes. Because only one plant of each genotype has been isolated it is not possible to see if the phenotype is consistent across multiple lines, so could be due to variation. It is also possible that because these lines have not been backcrossed, another mutation within the lines is exacerbating the phenotype. Therefore, ideally these lines would be backcrossed to remove additional mutations from the EMS mutagenesis before a comprehensive analysis of their phenotype was undertaken. However, the preliminary results described here do indicate that bothTaPIL1 and TaPIL3 are involved in the promotion of stem elongation and that TaPIL3 promotes tillering.

Chapter 6: General Discussion

6.1.1 Overview of the role of *PIF-like* genes in wheat.

Prior to this research, no PIF-like proteins had been identified in wheat, the interaction between DELLAs and PIFs had not been demonstrated in any cereals and the role of PIFs in the regulation of stem elongation in wheat was unknown. The key hypothesis of this research was that PIF-like proteins in wheat would interact with RHT-1 to regulate stem elongation and plant architecture. The TaPILs would therefore provide an alternative means to Rht-1 mutations to alter plant height, avoiding pleiotropic effects.

The first aim of this project was to identify PIF-like genes in wheat with homology to *OsPIL1* that were therefore potential candidates for the regulation of stem elongation. Three such genes were identified, termed *TaPIL1*, *TaPIL2* and *TaPIL3,* with sequence identities with OsPIL1 of 77%, 49% and 58% at the cDNA level and 62%, 31% and 47% at the protein level,

respectively. Phylogenetic analysis revealed that all three TaPILs were homologues of *Arabidopsis* PIF4 and PIF5, and that TaPIL1 was the likely orthologue of OsPIL1. The second aim of the project was to determine whether wheat PILs interacted with RHT-1. Yeast two-hybrid experiments demonstrate that TaPIL1, TaPIL2 and TaPIL3 are capable of interacting with the C-terminal GRAS domain of RHT-D1a, suggesting a role for the TaPILs in the GA response pathway. The third aim of this project was to investigate the phenotypic effects of reduced and increased *TaPIL* expression on the phenotype of wheat. Overexpression of *OsPIL1* in wheat was found to promote stem and ear elongation, with an indication that it repressed the transition to flowering. While TaPIL1 overexpression did not have the same effect on stem extension, there was an indication that it promoted ear elongation and in one line strongly delayed heading and anthesis. The results from the reduction of *TaPIL1* expression by RNAi provided some evidence of a role for TaPIL1 in the regulation of stem elongation although phenotypes were not consistent. The TaPIL1 RNAi line also displayed decreased ear length and provided further evidence that TaPIL1 regulates heading and flowering. A triple mutant TaPIL1 plant was produced through TILLING. This mutant displayed a reduction in stem elongation in comparison to a single mutant line, indicating that TaPIL1 may be involved in the promotion of stem elongation. A TaPIL3 triple mutant was also produced though TILLING, and this line displayed a reduced stem elongation and reduced tillering phenotype when compared to a wild-type line, indicating that TaPIL3 also promotes stem elongation and tillering. These phenotypes resulting from altered *PIL* expression are consistent with a role for TaPIL1 and TaPIL3 in the regulation of GA responses. A further aim of this project was to identify downstream RHT-1 interactors which could be potential targets for manipulating stem elongation. Screening of a yeast two-hybrid library from internode mRNA using RHT-D1a as the bait identified a number of downstream interactors, including a BOI, ERF, SPL, a bHLH transcription factor and IDD. These results demonstrate that RHT-1 regulates the GA response in wheat stems by interacting with multiple protein partners. This research has therefore been able to identify a novel family of PIF-like proteins in wheat, and has demonstrated an interaction between the wheat DELLA RHT-1 and the TaPIL proteins. The results also suggest that both TaPIL1 and TaPIL3 are involved in the regulation of wheat architecture.

6.1.2 TaPIL1, TaPIL2 and TaPIL3 represent a subgroup of PIF-like proteins in wheat.

Most plant species encode a family of PIF proteins that redundantly regulate light responses. *Arabidopsis* contains a family of 7 PIFs: PIF1, PIF3, PIF4, PIF5, PIF6, PIF7 and PIF8 (Khanna et al., 2004). In *Solanum lycopersicum* (tomato) a family of 8 PIF-like genes have been identified, named *SlPIF1a*, *SlPIF1b, SlPIF3, SlPIF4, SlPIF7a, SlPIF7b, SlPIF8a* and *SlPIF8b*, although only

SlPIF1a has been confirmed to function as a PIF (Llorente et al., 2016, Rosado et al., 2016). *P. patens* also contains a PIF family, with 4 members, PpPIF1-4, which interact with PhyA and PhyB (Possart et al., 2017). Rice has been shown to encode a family of 6 PIL proteins termed OsPIL11-16 (OsPIL13 is also known as OsPIL1) (Nakamura et al., 2007a). Marchantia (liverwort) encodes only one PIF-like protein, MpPIF which appears to regulate multiple light response phenotypes. (Inoue et al., 2016). The identification of the *TaPIL1-3* sequences represents the first description of wheat PIL sequences.

Phenotypic analysis indicated that the clade of TaPILs identified in this project were homologous to the *Arabidopsis* PIF4 and PIF5 proteins. *Arabidopsis* PIF4 has been shown to negatively control the plant response to red light (Huq & Quail, 2002), regulate the stomatal index in response to phytochrome B signalling (Casson et al., 2009), regulate the high temperature response (Hwang et al., 2017), promote flowering in response to high temperature (Kumar et al., 2012) and promote hypocotyl elongation (de Lucas et al., 2008). *Arabidopsis* PIF5 is involved in the repression of anthocyanin accumulation in red light via the repression of anthocyanin biosynthesis genes (Liu et al., 2015) and regulates senescence by promoting the expression of ABA- and ET-induced genes, which positively regulate senescence (Sakuraba et al., 2014). The TaPIL1-3 proteins could therefore be expected to regulate equivalent responses in wheat. Phenotypic analysis also suggested that each TaPIL was homologous to a separate OsPIL1 sequence, with TaPIL1 being most homologous to OsPIL1, TaPIL2 being most homologous to OsPIL11 and OsPIL12 and TaPIL3 being most homologous to OsPIL14. OsPIL1 has been shown to promote stem elongation (Todaka et al., 2012), chlorophyll biosynthesis (Sakuraba et al., 2017a) and negatively regulate senescence in rice (Sakuraba et al., 2017b). The homology in sequence between OsPIL1 and TaPIL1 could therefore indicate that TaPIL1 would regulate these processes in wheat. OsPIL11 has been shown to be involved in red light induced de-etiolation and may be regulated by ABA, JA and SA. However, its phenotypic role has only been investigated by transgenic expression in tobacco, so further analysis is needed to confirm its role in rice (Li et al., 2012c). The similarity between TaPIL2 and OsPIL11 indicates that TaPIL2 may play similar roles in wheat. OsPIL14 has been shown to bind the promoter of stress response genes and promote their expression. TaPIL3 could therefore be expected to play a role in the promotion of stress responses in wheat (Cordeiro et al., 2016).

The findings of Nakamura et al. (2007a) indicated that multiple OsPIL sequences were homologous to each *Arabidopsis* PIF sequence, with OsPIL15 and OsPIL16 being homologous to PIF3, OsPIL13 and OsPIL14 having homology to PIF4 and OsPIL11 and OsPIL12 not grouping with any *Arabidopsis* PIFs. No TaPIL identified in this project had close homology to other

Arabidopsis PIFs such as PIF3 or PIF1, however this project did not aim to identify all PIF-like wheat sequences so it is likely that there are more wheat PIF-like sequences, some of which will have homology to other *Arabidopsis* PIFs. In fact, a wheat PIF3-like sequence has been identified which has homology to OsPIL15, OsPIL16 and *Arabidopsis* PIF3 (Sibbett, Thomas, Hedden, Williams and Terry, unpublished). The results presented here support the findings of Nakamura et al. (2007a) in that groups of TaPILs appear to be homologous to distinct *Arabidopsis* PIFs, and indicate that each TaPIL has one or two orthologous sequences from rice.

The *Arabidopsis* PIF proteins contain two conserved domains, the N-terminal APB domain which facilitates phyB-PIF binding (Khanna et al., 2004), and a C-terminal bHLH DNA binding domain (Huq and Quail, 2002a). Both these domains were identified in all three TaPIL sequences supporting that the TaPILs represent a genuine, novel family of PIL proteins. APB and bHLH domains have also been identified in all rice (Nakamura et al., 2007a), tomato (Rosado et al., 2016), maize (Kumar et al., 2016) and *P. patens* (Possart et al., 2017) PIF protein sequences. The identification of these domains in the wheat TaPILs confirms their roles as PIF-like proteins. However, the identification of an APB domain does not necessarily confirm the ability to bind phyB. Although an APB domain has been identified in OsPIL1, a yeast two hybrid screen was unable to detect an interaction with phyB (Todaka et al., 2012). It would therefore be important to demonstrate the interaction between phytochrome and the TaPILs to confirm their role as PILs in wheat.

6.1.3 ALL three wheat PILs interact with RHT-1.

In *Arabidopsis*, PIF3 and PIF4 have been shown to interact with all five *Arabidopsis* DELLA proteins (Feng et al., 2008, de Lucas et al., 2008). This interaction involved the bHLH DNA binding domain of the PIFs and the leucine heptad repeat (LHR) region of the RGA/GAI GRAS domain. Through this interaction DELLAs sequester PIFs and block their DNA binding ability preventing them from binding promoters of target genes (Feng et al., 2008, de Lucas et al., 2008). This interaction also promotes the degradation of PIFs through the ubiquitin–proteasome system (Li et al., 2016a). This interaction had not previously been demonstrated in any cereal. All three TaPIL proteins were able to interact with the GRAS domain of RHT-D1a in the yeast two-hybrid assays. These findings are the first to extend the demonstration of DELLA-PIF interactions and indicate that DELLA binding may be a general property of at least some PIFs in all species. Based on the *Arabidopsis* model it could be suggested that the interaction between the TaPILs and RHT-D1a is dependent on the bHLH domain of the TaPILs and the LHR domain of RHT-1, and that the interaction causes the repression of TaPIL function through sequestration and also degradation. The interaction between RHT-1 and the wheat PILs also

supports findings that DELLAs are capable of binding bHLH domain-containing proteins, to repress their transcriptional activity as part of the GA response. The bHLH transcription factor ALCATRAZ (ALC) binds to GAI, RGA and RGL2, in an interaction that represses ALC transcriptional activity (Arnaud et al., 2010). This interaction allows DELLAs to repress fruit patterning at low GA levels (Arnaud et al., 2010). The *Arabidopsis* MYC2, MYC3 and MYC4 bHLH transcription factors have been shown to bind all 5 DELLAs using a yeast two-hybrid screen. This interaction allows DELLAs to repress MYC promotion of the JA response in the absence of GA (Hong et al., 2012a).

The interaction between RHT-1 and the TaPILs was demonstrated using only one method. Ideally this interaction should be confirmed using additional methods such as a pull-down assay, and also demonstrated in vivo using BiFC. The interaction between the *Arabidopsis* DELLAs and PIF3/4 was confirmed *in vitro* and *in vivo* using these methods (de Lucas et al., 2008, Feng et al., 2008). The domains required for the interaction between RHT-1 and the TaPILs should also be confirmed using deletion studies, to determine whether the bHLH domain is required.

6.1.4 Altering PIL expression resulted in stem elongation phenotypes.

The overexpression of *OsPIL1* in wheat lead to an increased stem elongation phenotype in two of the three transgenic lines. These results support the findings of Todaka et al. (2012), who found that *OsPIL1*-overexpression lines in rice also had an increased stem elongation phenotype. The rice *OsPIL1*-overexpression lines had increased expression of genes involved in cell wall development, organisation and biogenesis, which promoted cell elongation and hence stem elongation (Todaka et al., 2012). These results suggest that OsPIL1 can also bind the promoters and drive the expression of these cell wall modifying genes in wheat.

The orthologous relationship between TaPIL1 and OsPIL1 gave rise to the hypothesis that TaPIL1 would be involved in the promotion of stem elongation in wheat. However, the *TaPIL1* RNAi and overexpression lines displayed no overall decrease or increase in stem elongation. A comparison between the transgenic and null RNAi lines identified both an increase and decrease in elongation of some internodes, and when the RNAi lines were compared to the wild-type Cadenza control, one RNAi line had a significant reduction in the length of three internodes. These results indicate that TaPIL1 may have some involvement in the regulation of plant height and, if so, that this regulation is positive. However, it is not possible to draw solid conclusions about what role TaPIL1 plays in this regulation due to the inconsistent phenotypes. To further complicate the conclusions, the *TaPIL1* overexpression lines displayed no stem or

internode elongation phenotype. The homozygous triple *tapil1* (aabbdd) mutant which is hypothesised to have a loss of TaPIL1 function, displayed a small reduction in stem elongation compared to a single mutant line, indicating that TaPIL1 does have a role in the promotion of stem elongation. In addition, the triple mutant *tapil3* line also displayed a reduction in stem elongation along with a decrease in tiller number when compared to a wild-type line, indicating that TaPIL3 also regulates stem elongation.

These results suggest that TaPIL1 may not be as central to stem elongation regulation in wheat, as OsPIL1 is in rice. If these proteins are involved in the regulation of different processes in plant growth, it suggests that although the wheat and rice PIL genes are orthologous in sequence, their biological functions may not be conserved. TaPIL1 was also shown to be homologous to *Arabidopsis* PIF4 and PIF5, which have also been indicated in the regulation of stem elongation. de Lucas et al. (2008) demonstrated that PIF4 promotes cell elongation resulting in hypocotyl elongation in seedlings overexpressing PIF4. In contrast, the *pif4* mutant displayed short hypocotyls (de Lucas et al., 2008). Although, put together, the phenotypes from the RNAi and triple mutant TaPIL1 lines suggest that TaPIL1 does play some role in the promotion of stem elongation, the results are not consistent enough to draw a strong conclusion. The unclear role of TaPIL1 in stem elongation could be due to the limitations of the overexpression and RNAi to effectively alter expression levels. For example, the level of expression of *TaPIL1* at 4-fold and 10-fold in the overexpression lines may not be high enough to cause the expected increase in stem elongation. The level of *TaPIL1* expression may also be at a saturating level, although this is unlikely since overexpression of other PIF and PIL proteins has been successful in increasing stem length (de Lucas et al., 2008, Todaka et al., 2012). The RNAi lines may also not show a strong enough phenotype due to residual expression of *TaPIL1*, particularly in lines where expression was only reduced by 20%.Todaka et al. (2012) were unable to reduce OsPIL1 expression through RNAi, instead using a repression domain to repress transcription of its target genes. Therefore, a precedent for difficulties in reducing PIL expression has been previously described. Another possibility is that the TaPILs may redundantly promote stem elongation, meaning knockdown of one PIL is not enough to observe a strong phenotype. The reduced stem elongation of the *TaPIL3* triple mutant line strongly supports this possibility.

6.1.5 Alteration of PIL expression demonstrates a role for PILs in the promotion of ear elongation.

Both the *OsPIL1* and *TaPIL1* overexpression lines displayed a significant increase in ear length while one *TaPIL1* RNAi line displayed a significant reduction in ear length. These results indicate a potential involvement of TaPIL1 in the regulation of ear elongation. This phenotype has not been demonstrated in studies with the OsPILs, so could represent a new set of PIL target genes. It is possible that the altered ear length in the transgenic lines is actually due to changes to the elongation of the rachis internode, which then develops into the ear later in wheat development. The ear elongation phenotype could therefore be a by-product of the expected internode elongation phenotype. The elongation of the Rachis internode has been demonstrated to be promoted by GA in barley (Nicholls, 1978). It would be ideal to establish whether the increased ear length leads to an increase in the number or weight of grain in these lines, as this could provide a new mechanism to increase yields.

6.1.6 Alteration of PIL expression levels indicated a role for PILs in the repression of heading and flowering

The *OsPIL1* and *TaPIL1* transgenic lines demonstrated a negative role for PILs in the regulation of flowering. The *OsPIL1* overexpression line with the highest level of *OsPIL1* expression, and the strongest stem elongation phenotype, displayed an increased number of days to anthesis. This phenotype was also observed in the *TaPIL1* transgenic lines. One overexpression line, with the highest level of *TaPIL1* expression had a significant increase in the number of days to heading and anthesis, while both these parameters were significantly reduced in two RNAi lines. These results suggest that PILs are involved in repressing reproductive development.

Arabidopsis PIF4 has been demonstrated to have a role in the regulation of flowering, although this role was positive rather than negative. Kumar et al. (2012) demonstrated that PIF4 could promote flowering in response to high temperature by binding the transcriptional start site of FT in a temperature-dependent manner to promote expression. OsPIL1 has also been previously shown to regulate flowering through an interaction with other proteins (Zhao et al., 2011). *OsLF* encodes an HLH protein which causes a delay in flowering when overexpressed. OsLF was shown to interact with two OsPIL proteins, OsPIL1 (OsPIL13) and OsPIL15, in yeast two-hybrid assays and colocalization experiments. The interaction between HLH proteins and bHLH transcription factors usually involves the inhibition of bHLH DNA binding ability through the formation of heterodimers. Therefore the model for OsLF-OsPIL interaction is as follows: both OsLF and OsPRR1, a circadian clock regulator involved in the positive regulation of

flowering, compete to bind and regulate the activity of OsPIL13 and OsPIL15, which results in either the repression or promotion of flowering genes (Zhao et al., 2011). This model would also indicate a positive role for OsPIL1 in the regulation of flowering, where binding of OsLF represses its positive activity, and OsPRR1 relieves this repression to allow flowering. This contrasts with the late flowering phenotype of the *OsPIL1* overexpression lines. GA is also involved in the promotion of flowering (Achard et al., 2007), meaning that if PILs are involved in promoting the expression of GA response genes, their role in flowering would be expected to be positive rather than negative.

Previous findings only demonstrate a role for PIFs and GA in the positive regulation of flowering. The findings from the *OsPIL1* and *TaPIL1* transgenic lines could therefore represent a novel role for PILs in the repression of development and timing of flowering. This phenotype could be characterised further by determining if TaPIL1 binds to promoters of any flowering genes, and characterizing the late flowering phenotype in detail.

6.1.7 Model for TaPIL function in wheat.

This work has demonstrated for the first time an interaction between DELLAs and PIFs in wheat, with yeast two-hybrid results demonstrating that TaPIL1, TaPIL2 and TaPIL3 all interact with RHT-1. This research has also shed some light on the previously unknown role of wheat PILs in the regulation of architecture. Results indicate that TaPIL1 is involved in the regulation of heading and flowering time, ear extension, and possibly stem elongation. The stem elongation response is also displayed in TaPIL3 mutants, suggesting that stem elongation is regulated redundantly by TaPIL1, TaPIL3, and possibly TaPIL2. The model proposed by these findings (**Figure 6.1**) is that in the absence of GA and/or a high R:FR ratio, the TaPIL proteins are sequestered and degraded though their interaction with RHT-1 or phytochrome. The interaction between the TaPILs and RHT-1 would involve RHT-1 binding the bHLH domain of the TaPILs and blocking their transcriptional activity, then promoting their degradation. The interaction between the TaPILs and phytochrome would involve phyB binding to the TaPIL APB domain and blocking their transcriptional activity and promoting their degradation. The blocking of TaPIL activity would prevent them from driving the expression of genes involved in stem elongation and ear elongation. In the presence of GA and/or a low R:FR light ratio, the TaPILs are not sequestered or degraded in response to RHT-1 or phytochromes, so are free to regulate transcription of genes involved in the GA response and shade avoidance. The TaPILs would therefore promote the expression of genes involved in ear elongation, and possibly stem elongation. This model indicates that the TaPILs are involved in the regulation of stem

elongation downstream of RHT-1, making them a viable target for the specific manipulation of stem elongation, avoiding the pleiotropic effects of *Rht-1* mutants.

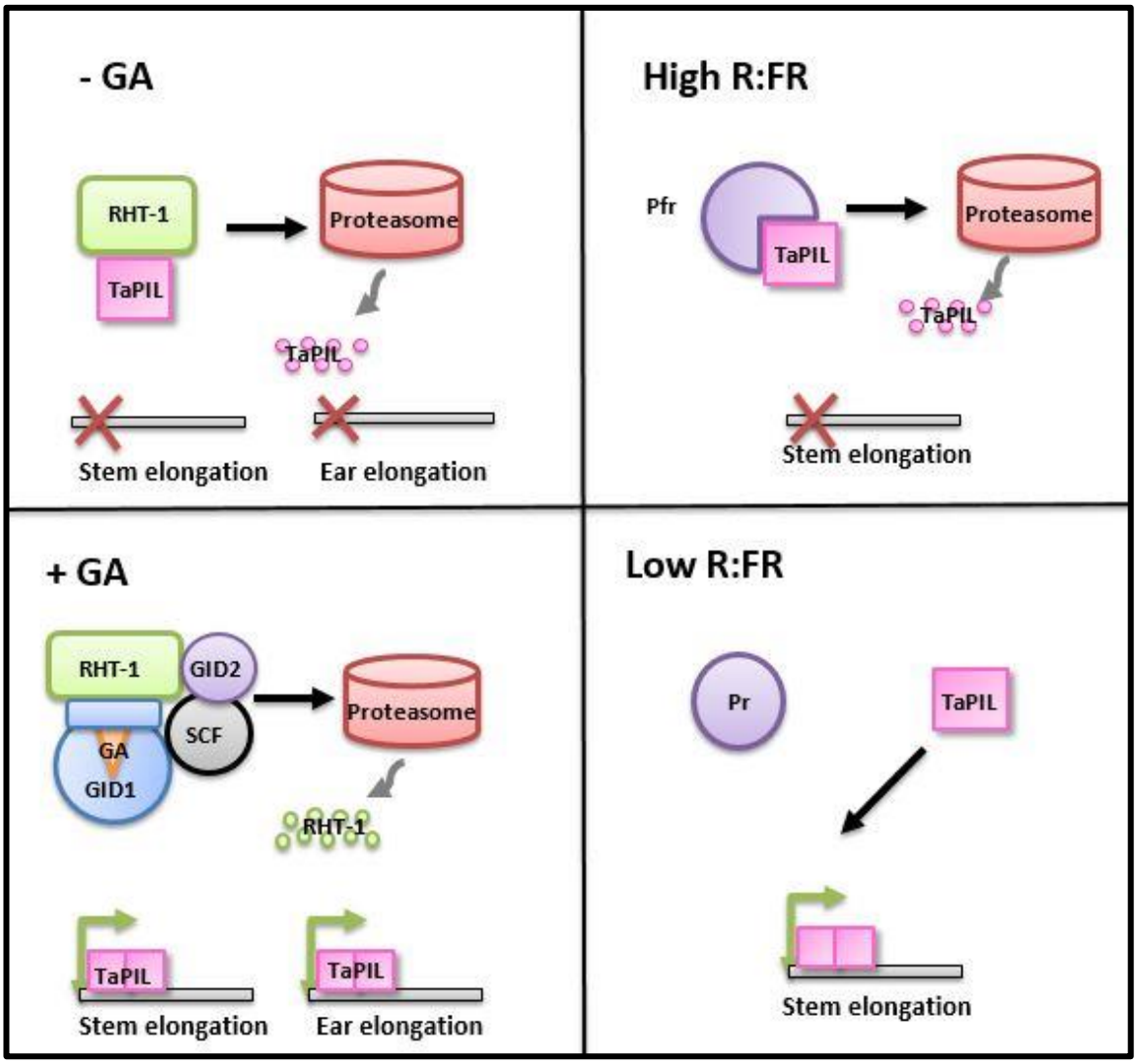

Figure 6.1 A model for RHT-1 regulation of TaPIL activity. In the absence of GA, RHT-1 binds the TaPILs, repressing their activity by sequestration and promoting their degradation by the proteasome. In the absence of TaPILs genes involved in stem elongation and ear elongation are repressed. In the presence of GA, RHT-1 is degraded by the proteasome, leaving the TaPILs free to dimerise and drive the expression of genes involved in the regulation of stem and ear elongation. When the R:FR ratio is high, phytochrome is present in the Pfr form, with can bind to PIFs, repressing their activity and promoting their degradation by the proteasome, leading to the repression of genes involved in stem elongation. When the R:FR ratio is low, phytochrome is present in the Pr form, which cannot bind PIFs. PIFs are therefore able to promote the expression of genes involved in stem elongation.

6.1.8 Identification of multiple RHT-1 interactors in the wheat stem.

One hypothesis of this research was that RHT-1 would regulate stem elongation though an interaction with numerous proteins in various signalling pathways. The yeast two-hybrid

library screen identified multiple new interactors of RHT-1 in the wheat stem. This supports findings from *Arabidopsis* that DELLAs regulate transcription through their interaction with multiple protein partners including transcription factors. A detailed description of the proteins identified can be found in chapter 4 sections 4.4.3-4.4.10.

Several proteins were identified that have also been described as DELLA binding partners in *Arabidopsis,* and this research represents the first time these proteins have been shown to interact with RHT-1 in wheat. A BOI-related protein was identified in the screen. In *Arabidopsis* BOIs interact with DELLAs via their RING domain, which allows the DELLA-BOI complex to target the promoters of a subset of GA responsive genes (Park et al. (2013). An INDETERMINATE DOMAIN (IDD)-like protein was also identified in the screen. In *Arabidopsis*, the interaction between DELLAs and IDDs results in the formation of a complex able to bind to the promoters of *GA* responsive genes and drive their expression. This model provides a mechanism by which RHT-1 could positively regulate the activity of a group of transcription factors in wheat. One protein identified from the screen is an ethylene responsive element binding (ERF)-like protein. DELLAs have been shown to bind ERFs in *Arabidopsis* and repress their transcriptional activation activity (Marin-de la Rosa et al., 2014, Zhou et al., 2016). The identification of an ERF-like protein provides one of the most promising targets for the manipulation of stem elongation. ERF11 has been shown to promote stem elongation redundantly with other closely related ERFs, 4, 8 and 10, by promoting GA biosynthesis at the same time as repressing DELLA activity (Zhou et al., 2016). In addition, rice ERF proteins, OsSUB1A, SNORKEL1 and SNORKEL2, have been linked to the regulation of stem elongation (Hattori et al., 2009, Xu et al., 2006). This indicates that if the expression levels of the wheat ERF protein were manipulated, the stem elongation phenotype could be altered.

Two homoeologues of a SQUAMOSA PROMOTER BINDING-LIKE (SPL) protein were identified. The SPL-DELLA interaction causes repression of SPL transcriptional activity, allowing the repression of the juvenile to adult phase transition (Yu et al., 2012, and the promotion of tillering in the absence of GA (Luo et al., 2012). A bHLH domain containing protein was also identified in the screen. DELLAS have been shown to bind to and repress the DNA binding ability of multiple bHLH transcription factors in *Arabidopsis*, including PIFs (Hong et al., 2012a, Arnaud et al., 2010). The identification of this protein in the screen indicates that RHT-1 also binds bHLH domain-containing proteins in the wheat stem. Identification of these known DELLA interacting proteins supports evidence from *Arabidopsis* that DELLAs are capable of binding to these classes of protein.

The screen also identified several novel RHT-1 interactors that have not previously been shown to interact with DELLAs. A Rho-GTPase-like protein was identified in the screen. Although Rho-GTPases have not been implicated in the GA signalling pathway, or as DELLA interactors, they have been demonstrated to be activated by auxin to promote cell expansion (Xu et al., 2010). The interaction with RHT-1 could indicate that this Rho-GTPase is capable of promoting cell expansion in response to GA, which could indicate a role in regulating stem elongation. This Rho-GTPase (TRIAE_CS42_2BS_TGACv1_146333_AA0462840) was also identified in a yeast two-hybrid library screen of the wheat grain aleurone layer, using RHT-D1a as the bait (personal communication, Patrycja Sokolowska). A FAR1-related protein was also identified in the screen. There has been no role in GA signalling or interaction with DELLAs characterised for FAR1, however, it has been shown be regulated by light signals like the PIF proteins. FAR1 promotes phyA-mediated development in response to R and FR light by dimerizing with FAR-RED ELONGATED HYPOCOTYL 3 (FHY3) to promote the expression of genes involved in the inhibition of hypocotyl elongation, opening of apical hook, expansion of cotyledons and greening (Deng and Quail, 1999, Lin, 2007, Siddiqui et al., 2016). This could provide more evidence of the interaction between light and GA signalling for the regulation of plant development. The role of FAR1 in repressing hypocotyl elongation could indicate a potential role in regulating stem elongation in wheat. Finally, a defensin-like protein was identified in the screen. No interaction between defensins and GA or DELLAs has been previously identified. However, GA has a well characterised role in regulating defence by interacting with components of the JA response pathway (Wild et al., 2012, Fernandez-Calvo et al., 2011). The interaction between RHT-1 and defensin could demonstrate another point of crosstalk between the GA and defence pathways.

6.1.9 Conclusions and future research directions

Overexpression of the rice gene *OsPIL1* increased height in wheat, confirming its function in promoting stem extension. However, overexpression of the closest wheat homologue to *OsPIL1, TaPIL1*, did not promote stem growth significantly, perhaps due to insufficient expression or divergence of function. Results from RNAi of *TaPIL1* were inconsistent, although there was an indication of height reduction in some lines, and a triple mutant knockout line demonstrated a small decrease in stem elongation. A *TaPIL3* triple mutant knockout line also had a reduced stem elongation phenotype. This suggests that both TaPIL1 and TaPIL3 are redundantly regulating stem elongation, which could explain the lack of strong phenotype in the RNAi *TaPIL1* transgenic lines. Future work could therefore include the production of *tapil1tapil3* knockout lines to investigate the effect of knocking out both proteins. It would also

be useful to produce *tapil2*, and *tapil1tapil2tapil3* knockout lines to investigate the effects of TaPIL2 on phenotype, and to see if knocking out all three TaPILs produces a strong stem elongation phenotype. These lines could be produced using the TILLING mutants, or by genome editing. Genome editing using CRISPR/Cas9 (Clustered Regularly Interspaced Short Palindromic Repeats/CRISPR-Associated Protein 9) could provide the most effective method to knockdown all homoeologues. CRISPR/Cas9 uses a guide RNA complementary to the gene of interest and a cas9 endonuclease to introduce double stand breaks in targeted loci. Mutations are then introduced when the stand breaks are repaired by the endogenous DNA repair system, via non-homologous end joining (NHEJ) (Lieberman-Lazarovich and Levy, 2011). CRISPR/Cas9 has been previously used to produce transgenic wheat lines (Liang et al., 2017, Zong et al., 2017), and recently has been used in bread wheat to simultaneously produce frameshift mutations in all three homoeologues of RHT-1 (Martignago, Rafter, Sparks, Edwards, Hanley, Thomas, Huttley, unpublished). For this reason, CRISPR/Cas9 provides a faster and more reliable method of producing knockout mutants in wheat.

In the immediate future, the *TaPIL1* and *TaPIL3* TILLING lines should be backcrossed to remove any background mutations, which could be masking or exaggerating the true phenotypes of *TaPIL1/3* knockdown. The effect of the mutations also needs to be confirmed to ensure the thee homoeologous copies of each gene are non-functional. Once these lines have been produced it is important to investigate the effect of altered expression on yield. In particular, it would be interesting to investigate if the elongated ear phenotype in the overexpression lines leads to an increase in grain number or weight. Other phenotypes associated with altered light or GA response in wheat could also be investigated. For example, light conditions and GA levels have been shown to affect leaf elongation (Xu et al., 2016, Barnes and Bugbee, 1991). A reduction in leaf elongation could therefore indicate a disrupted GA and/or phytochrome response. Chlorophyll accumulation could also be investigated in the transgenic lines. DELLAs have been shown to promote chlorophyll accumulation (Cheminant et al., 2011), while PIFs repress this response in *Arabidopsis* (Leivar et al., 2009). These phenotypes should be characterised in the transgenic PIL lines to characterise any changes in GA or phytochrome response.

TaPIL1 and its close paralogues TaPIL2 and TaPIL3 interacted with RHT-1 in yeast two-hybrid assays consistent with them having a role in GA-regulated development. This hypothesis should be tested by using a ChIP experiment to determine which genes are targeted by the TaPILs to confirm their role in the GA response. The interaction with RHT-1 should also be characterised, by using a ChIP experiment to demonstrate that RHT-1 prevents PIL binding to target promoters.

Several other RHT-1-interacting proteins identified in the wheat stem from a yeast two-hybrid screen may be involved in regulating different aspects of growth and development. The model suggested by these findings would be that in the absence of GA, RHT-1 binds to and either represses the activity of multiple proteins, which promote the GA response, or binds to and promotes the activity of proteins involved in repressing the GA response. All of the proteins identified in this screen must be further characterised to confirm the interaction with RHT-D1a and to characterise the effects of this interaction. For library proteins 51, 143 and 221, where no previous interaction with DELLAs has been established, a role for these proteins in GA responses must be determined. For example, knockout mutants in *Arabidopsis* should be characterised, to identify the phenotypic effects of eliminating this protein. The interaction between RHT-D1a and the library proteins would also need to be confirmed using additional methods. A pull-down assay could be employed to confirm the interaction in vitro, while BiFC would be used to demonstrate the interaction in vivo.

Once the interactions had been confirmed, the expression of the RHT-D1a interacting proteins would need to be altered in wheat to assess the effects of each protein on phenotype. For each protein, the homoeologous sequences would need to be identified, so that all three copies of each protein could be targeted. The expression of all three homoeologues of each gene would then be knocked down either by RNAi, mutagenesis or genome editing. The knockout and overexpression lines for each library protein would then be analysed for phenotypes associated with GA signalling such as germination, stem elongation or flowering time. This would indicate which library proteins have roles in regulating DELLA target genes, and in particular, which library proteins would be potential targets to manipulate stem elongation.

The target genes affected by the RHT-1-library protein interaction could then be investigated using ChIP-seq. This would identify which library proteins were involved in regulating the transcription of GA-regulated genes. Finally, the nature of the interaction with RHT-D1a would have to be investigated, i.e. if the library proteins are positively or negatively regulated by RHT-1. The expression of target genes could be monitored using reporter proteins, in the presence and absence of RHT-1, to determine the effect of the interaction. For non-transcription factor library proteins, the expression of genes downstream of their signalling pathway could be monitored. Any library proteins that regulate genes involved in stem elongation could then be used as new targets for the manipulation of plant height to improve yield.

This project has characterised the interaction between RHT-1 and the wheat PIL1-3 proteins, and demonstrated that both PIL1 and PIL3 play a role in the regulation of stem elongation. In

addition, further RHT-1 binding partners have been identified from the yeast two-hybrid library screen. The results indicate that the TaPILs are viable targets for the manipulation of stem elongation, along with other traits such as ear elongation which could improve yields, avoiding the pleiotropic effects of *Rht-1* mutations.

Chapter 7: Appendix: Supplementary Data

7.1 The coding sequences of TaPIL1, TaPIL2 and TaPIL3

```
TaPIL1 5AL ATGGACGGCAATGGGAGATCGGCGGCGAGTCACAAGAAGCCTCTCGTCGCGGACAACGACCTGGTGGAGCTG 72
TaPIL1 5BL ATGGACGGCAATGGGAGATCGGCGGCGAGACACAAGAAGCCTCTCGTCGCGGACAACGACCTGGTGGAGCTG 72
TaPIL1 5DL ATGGACGGCAATGGGAGATCGGCGGCGAGCCACAAGAAGCCTCTCGTCGCGGACAACGACCTGGTGGAGCTG 72

TaPIL1 5AL CTGTGGCACAACGGGGCGTCGTCGCGCAGCCGCAGACGCACCCGAGGCCGGCGCCCAGCGGCCTCGCCGGC 144
TaPIL1 5BL CTGTGGCACAACGGGGCCGTCGTCGCGCAGCCGCAGACGCACCCGAGGCCGGCGCCCAGCGGCCTCGCCGGC 144
TaPIL1 5DL CTGTGGCACAACGGGGGCGTCGTCGCGCAGCCGCAGACGCACCCGAGGCCGGCGCCCAGCGGCCTCGCCGGC 144

TaPIL1 5AL GGTGGCGGGGAGACGGCCGCGTGGTTCGCGGACGACGTCGACGCGCTGGGGAACGACGTGTACGCGCAGCTC 216
TaPIL1 5BL GGTGGCGGGGAGACGGCCGCGTGGTTCCGGGCGACGTCGACGTGCTGGGAAACGACGTCTACGCGCAGCTC 216
TaPIL1 5DL GGTGGCGGGGAGACGGCCGCGTGGTTCCAGGACGACGTCGACGCGCTGGGGAACGACGTCTACGCACAGCTC 216

TaPIL1 5AL TGGAACAGCATTGCGGTGGGCGCCGCCCCGGACGTCGCGTGCGCGGCGCTCCCGGGGCCCAGCTCCCACCCT 288
TaPIL1 5BL TGGAACAGCATTGCGGTGGGCGCCGCCCCGGACGTCGCGTGCGCGGCGCTCCCGGGGCCCAGCTCCCACCCT 288
TaPIL1 5DL TGGAACAGCATTGCGGTGGGCGCCGCCCCGGAGGTCGCGTGCGCGGCGCTCCCGGGGCCCAGCTCCCACCCT 288

TaPIL1 5AL CCCCCGCCGC---CGCCGCCGCCGCCGATGCCGAGCGGCATCGCCTCCAGCTGGACCGGTGGCGACATCGGC 357
TaPIL1 5BL CCCCCGCCG----------CCGCCGCCGATGCGGAGCCGCATCGCCTCCAGCTGGACCGGCGGCGACATCGGC 351
TaPIL1 5DL CCCCCGCCGCAGCTGCCGCCGCCGCCGATGCGGAGCGGCATCGCCTCCAGCTGGACCGGGGGCGACATCGGC 360

TaPIL1 5AL TCCACCTTCTGCGGCAGCAGCCTGGTCCCGGAGGTGCCGGCGGGGGGCAGGGAGGAAGCCAGCGCCGCACCG 429
TaPIL1 5BL TCCACCTTCTGCGGCAGCAACCTGGTCCCGGAGGTGCCGGCGGGGGGCAGGGAGGAAGCGAGCGCCGCGCCG 423
TaPIL1 5DL TCCACCTTCTGCGGCAGCAACCTGGTCCCGGAGGTGCCGGCGGGGGGACAGAGAGGAGGCGAGCGCCGCGCCG 432

TaPIL1 5AL CCGTCGGAGGGGACGCGCGAGGCCAGCACGCGCGACGGCGGCGCCGGCACCTCGTCGTCCGGCGGGTCCGGG 501
TaPIL1 5BL CCGTCCGAGGGGACGCGCGGGGCGAGCACCGCGCGACGGCGGCGCCGGCACCTCGTCGTCCGGCGGGTCCGGG 495
TaPIL1 5DL CCGTCGGAGGGGACGCGCGGGGCGAGCACGCGCGACGGCGGCGCCGGCACCTCGTCGTCCGGCGGGTCCGGG 504

TaPIL1 5AL AGCAACTTCGGGGGCTCCGGCCTGCCGAGCGAGAGCGGCGGCCATGCCCACAAGAGGAAGGGCAGGGGCAAA 573
TaPIL1 5BL AGCAACTTCGGGGGCTCCGGCCTGCCGAGCGAGAGCGGCGGCCATGCCCACAAGAGGAAGGGGAGGGGCAAA 567
TaPIL1 5DL AGCAACTTCGGGGGCTCCGGCCTGCCGAGCGAGAGCGGCGGCCATGCCCACAAGAGGAAGGGGAGGGGCAAA 576

TaPIL1 5AL GACGACTCTGATAGCCGCAGCGAGGATGTGGAGTGTGAGGCCACTGAAGAGACCAAATCGTCGAGGCGGCAC 645
TaPIL1 5BL GACGACTACGATAGCCGCAGCGAGGATGTGGAGTGTGAGGCGACCGAGGAGACCAAATCGTCGAGGCGACAC 639
TaPIL1 5DL GACGACTCCGATAGCCGCAGCGAGGATGTGGAGTGTGAGGCGACCGAGGAGACCAAATCGTCGAGGCGGCAC 648

TaPIL1 5AL GGGTCGAAGCGGAGGAGCAGGGCAGCTGAAGTTCATAACCAGTCAGAGAGGAGACGAAGGGACCGGATCAAC 717
TaPIL1 5BL GGGTCGAAGCGGAGGAGCAGAGCAGCTGAAGTTCATAACCAGTCAGAGAGGAGACGAAGGGACCGGATAAAC 711
TaPIL1 5DL GGGTCGAAGCGGAGGAGCAGGGCAGCTGAGGTTCATAACCAGTCAGAGAGGAGGCGAAGGGACCGGATCAAC 720

TaPIL1 5AL GAAAAGATGCGGTCACTGCAAGAACTCATACCCCACTGCAACAAGGCTGACAAAGCATCAATATTAGATGAG 789
TaPIL1 5BL GAAAAGATGCGGTCACTTCAAGAACTCATACCCCACTGCAACAAGGCTGACAAAGCATCAATATTAGATGAG 783
TaPIL1 5DL GAAAAGATGCGGTCGTTGCAAGAACTCATACCCCACTGCAACAAGGCTGACAAAGCATCAATATTAGATGAG 792

TaPIL1 5AL GCGATCGAGTACTTAAAGTCCCTCCAAATGCAAGTTCAGATTATGTGGATGACCACCGGGATGGCGCCAATG 861
TaPIL1 5BL GCGATCGAGTACTTAAAGTCCCTCCAAATGCAAGTTCAGATCATGTGGATGACCACCGGGATGGCGCCAATG 855
TaPIL1 5DL GCGATCGAGTACTTAAAGTCCCTCCAAATGCAAGTTCAGATTATGTGGATGACCACCGGGATGGCGCCAATG 864

TaPIL1 5AL ATGTTTCCTGGTTCTCACCAGTTCATGCCGCCGATGGCCGTGGGCATGAATTCGGCATGCATGCCTGCGGCA 933
TaPIL1 5BL ATGTTTCCTGGTGCTCACCAGTTCATGCCGCCGATGGCCGTGGGCATGAATTCGGCATGCATGCCTGCGGCA 927
TaPIL1 5DL ATGTTTCCTGGTTCTCACCAGTTCATGCCGCCGATGGCCGTGGGCATGAACTCGGCATGCATGCCTGCGGCA 936

TaPIL1 5AL CAGGGTCTAAATCAGATGGCAAGAGTGCCATACATGAACCATTCTTTGTCAAATCACATCCCTATGAGCCCA 1005
TaPIL1 5BL CAGGGTCTAAATCAGATGGCAAGAATGCCATACATGAACCATTCCTTGTCAAACCACATCCCTATGAACCCA 999
TaPIL1 5DL CAGGGTCTAAATCAGATGGCAAGAGTGCCATACATGAACCATTCCTTGTCAAATCACATCCCTATGAACCCA 1008
```

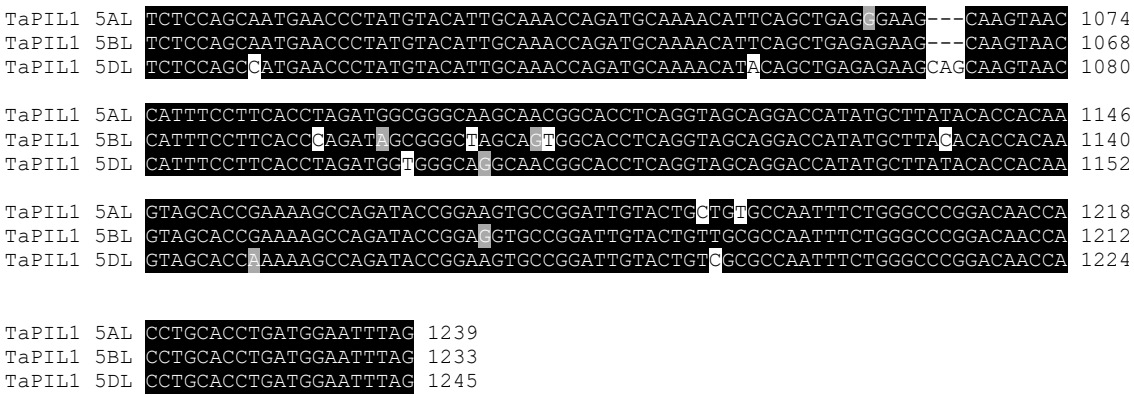

Figure S.1 The cDNA sequence of the A, B and D homoeologues of TaPIL1. The coding sequences of the TaPIL1 homoeologues were aligned in a T-coffee alignment. Highly conserved residues are shown in reverse, similar residues are shown in grey.

```
TaPIL2 5AL ATGAGCCAGTTCGTGCCAGATTGGGGGAACATGGGGGACATCTCCAGGCCACTCGGCGAAGACGATGACCTC 75
TaPIL2 5BL ATGAGCCAATTCGTGCCAGATTGGGGAAACATGGGCGACATCTCCAGGCCACTCGGGGAAGACGATGACCTC 75
TaPIL2 5DL ATGAGCCAATTCGTGCCAGATTGGGGAAACATGGGGGACATCTCCAGGCCACTCGGCGAGGACGATGACCTC 75

TaPIL2 5AL ATGGAGCTGCTGTGGTGCAACGGCAATGTCGTCATGCAGAGCCAGGGTCATCGGAAGCTGCCGCCGAGGCCT 147
TaPIL2 5BL ATGGAGCTGCTGTGGTGCAACGGCAATGTCGTCATGCAGAGCCAGGGTCATCGGAAGCTGCCGCCGAGGCCT 147
TaPIL2 5DL ATGGAGCTGCTGTGGTGCAACGGCAATGTCGTCATGCAGAGCCAGGGTCATCGGAAGCTGCCGCCGAGGCCT 147

TaPIL2 5AL GAGAAGGTCCCGGCGCCGCCGGTGGTGCAAGAAGACGATGCCGGCCTCTGGTTCCCGTTCGCGCTCGCCGAC 219
TaPIL2 5BL GAGAAGGTTCCGGCGCCGCCGGTGGTGCAAGAAGACGAGGCCGGCCTGTGGTTCCCGTTCGCCCTCGCTGAC 219
TaPIL2 5DL GAGAAGGTTCCGGCGCCGCCGGTGGTGCAAGAAGACGAGGCCGGCCTGTGGTTCCCGTTCGCGCTCGCCGAC 219

TaPIL2 5AL TCGCTCGACAAGGACATCTTCCAGGACCTTTTCTGCGAGGAACCACCGGGGGCGGCCGGCGTCGACGGCGCC 291
TaPIL2 5BL TCGCTCGACAAGGACATCTTCCAG GACCTCTTCTGCGAAGAACCACCGGGGGCGGCCGG---------- 278
TaPIL2 5DL TCGCTCGACAAGGACATCTTCACG GACCTCTTCTGCGAGGAACCACCGGGGG---------TCGA---CGC 278

TaPIL2 5AL GGCAAGATCGGCAGGGACGGTGTACCAGTATTAGGGGAT---GACAGGCGCAGCAGCCAGTCGTCCGCGGTG 360
TaPIL2 5BL ----------------------------------------------------------------------C 279
TaPIL2 5DL CGGCAAGGCCGGCAGGGACGGTGCCCCAGTGTTAGGGGACGCCGACAGGCGCAGCAGCCAGTCGTCCGCGGT 350

TaPIL2 5AL TCGGCGGCGAGCGACCTGATGCCCCCTCCCAAGTCCACGCACGTCTCCTGCTCCAGCAGGCAGCAATCGATG 432
TaPIL2 5BL GTCGA----------------------------------C---------GGCTCCAGCAGGCAGCAATCGATG 309
TaPIL2 5DL GTCGGCGGCGAGCGACCTGATGCCCCTCCCAAGTCCACGCACGTGTCCTGCTCCAGCAGGCAGCAATCGATG 423

TaPIL2 5AL AGCCTGGCCGACTGCGGCGACAACGCCGGCGGCGTCCTGTCGGACCTCGTCCAGGCTCGCGCCGGGAAGGCG 504
TaPIL2 5BL AGCCTGGCCGACTGCGGCGACAACGCCGGCGGCTTCCAGTCAGACCTCGTCCAGGCTCGCGCCGGGAAGGCA 381
TaPIL2 5DL AGCCTGGCCGACTGCGGCGACAACGCCGGCGGCGTCCTGTCGGACCTCGTCCAGGCTCGGCCGGGAAGGCG 506

TaPIL2 5AL GCGATGGAGGAGGGCGCGTCGTCGACGCTGAGCGCGATGGGGGCGAGCTTCTGCGGGAGCAACCAGGTGCAG 576
TaPIL2 5BL GCGATGGAGGAGGGCGCGTCGTCGACGCTGAGCGCGATGGGGGCGAGCTTCTGCGGGAGCAACCAGGTGCAG 543
TaPIL2 5DL GCGATGGAGGAGGGCGCGTCGTCGACGCTGAGCGCGATGGGGGCGAGCTTCTGCGGGAGCAACCAGGTGCAG 567

TaPIL2 5AL GTGCAGGGCGCGGTGAGCGAGCAGGGGCGCGCCGGCCACACCACTGCCTATGGCGGCGGCGGAGCGGGCAGC 648
TaPIL2 5BL GTGCAGGGCGCGGTGAGCGACCACGGGCGCGCCGGCCACCCCACTGCCTATGGCGACGGCGGAGCGGGCAGC 523
TaPIL2 5DL GTGCAGGGCGCGGTGAGCGAGCAGGGGCGCGCCGGCCACACCACTGCCTATGGCGGCAGCGGCGCAGGCAGC 627

TaPIL2 5AL GCTCTGCCTTCGGCGGTAGGGAGCGGAAATGCAAACGCCAGAGGCAGGGGCCACGAGGCCACCGTGGCCTCC 720
TaPIL2 5BL GCTCTGCCCTCGGCGGTGGGGAGCGTAAATGCAAACGCCAGAGGCAGGGGCCACGAGGCCACCGTGGCCTCC 597
TaPIL2 5DL GCTCTGCCCTCGGCGGTGGGGAGCGGAAATGCAAACGCCAGAGGCAGGGGCTACGAGGCCACGGTCGCCTCC 711

TaPIL2 5AL TCGTCGGGCCGGTCCAACTACAGCTTCGGCGTGACCA----------CCACCACTGGCACCGAGCCGACG 780
TaPIL2 5BL TCGTCGGGGCGGTCCAACTACAGCTTCGGCGTCACCGCCACTACCACCACCACCGGCACCGAGCCGACG 669
TaPIL2 5DL TCGTCGGGGCGGTCCAACTACAGCTTCGGCGTGACCGCCAC---CACGGCCACCACCGGCACCGAGCCGACG 780

TaPIL2 5AL AGCACGAGCCACCGGAGCAGCAAGCGCAAGCGGGGGCTGGACACGGAGGACTCGGAGAGCCCCAGCGAGGAC 852
TaPIL2 5BL CAACCGGAGCAGCAAGAGCAAGCGGGGGCTCGACACGGAGGACTCGGAGAGCCCCAGCGAGGACGCCGAGTC 741
TaPIL2 5DL CAACCGGAGCAGCAAGCGCAAGCGGGGACTGGACACGGAGGACTCGGAGAGCCCCAGCGAGGACGCCGAGTC 852

TaPIL2 5AL GCCGAGTCGGAGTCGTTGGCGCTTGAGCGCAAGCCGCCGCAGAAGCTCACGACGGCGAGGAGGAGCCGCGCC 924
TaPIL2 5BL AGAGTCCTAGCACGAGTGGTGCTGGAGCGCAAGCCGCCCCAGAAGCTCACGACGGCGCGGAGGAGCCGCGCC 813
TaPIL2 5DL GGATCCTAGCACGAGTGGCGCTTGAGCGCAAGCCGCCGCAGAAGCTCACGACGGCGCGGAGGAGCCGCGCC 924

TaPIL2 5AL GCCGAGGTGCACAACCTCTCCGAGAGGAGGAGACGAGACAGGATCAACGAGAAGATGCGAGCACTGCAAGAG 996
TaPIL2 5BL GCCGAGGTGCACAACCTCTCCGAGAGGAGGAGACGAGACAGGATCAACGAGAAGATGCGAGCCCTGCAAGAG 885
TaPIL2 5DL GCCGAGGTGCACAACCTCTCCGAGAGGAGGAGACGAGACAGGATCAACGAGAAGATGCGAGCGCTGCAAGAG 996

TaPIL2 5AL CTCATACCCCACTGCAACAAGACTGACAAGGCGTCGATGCTGGACGAGGCGATCGAGTACCTGAAGACGCTG 1068
TaPIL2 5BL CTCATACCCCACTGCAACAAGACTGACAAGGCGTCGATGCTGGACGAGGCGATCGAGTACCTGAAGACGCTG 957
TaPIL2 5DL CTCATACCCCACTGCAACAAGACTGACAAGGCGTCGATGCTGGACGAGGCGATCGAGTACCTGAAGACGCTG 1068

TaPIL2 5AL CAGATGCAGGTGCAGATGATGTGGATGGGCGGCGGTATGGCGCCGCCGGCGGTGATGTTCCCGGGCATGCAG 1140
TaPIL2 5BL CAGATGCAGGTGCAGATGATGTGGATGGGCAGCGGCATGGCGCCGCCGGCGGTGATGTTCCCGGGCATGCAG 1029
TaPIL2 5DL CAGATGCAGGTGCAGATGATGTGGATGGGCAGCGGCATGGCGCCGCCGGCGGTGATGTTCCCGGGCATGCAG 1140

TaPIL2 5AL ATGCACCAGTACCTGCCGCAGATGGGGCCGCCGTCCATGGCGCGGATGCCCTTCATGGCGCCGCCGCAGCAG 1212
TaPIL2 5BL ATGCACCAGTACCTGCCGCAGATGGGC---CCGTCCATGGCGCGGATGCCCTTCATGGCGCCGCCGCAGCAG 1098
TaPIL2 5DL ATGCACCAGTACCTGCCGCAGATGGGGCCGCCGTCCATGGCGCGGATGCCCTTCATGGCGCCGCCGCAGCAG 1212

TaPIL2 5AL GGCCACGGCGTGAGCCTGCCGGAGCAGTACGCGCACTTCCTCGGCGTCAACCCCCAC---CACCTGCAGCCG 1281
TaPIL2 5BL GGCCACGGCGTGAGCCTGCCGGAGCAGTACGCGCACTTCCTCGGCGTCAACCCCCACCACCACCTGCAGCCG 1170
TaPIL2 5DL GGCCACGGCGTGAGCCTGCCGGAGCAGTACGCGCACTTCCTCGGCGTCAACCCCCAC---CACCTGCAGCCG 1281

TaPIL2 5AL CCCTCCCACCACCCCACCACCAGCATTTCGCGCAGGGGGTGGGCTACTACCCGCTAGGGGCGAAGGCCCTG 1353
TaPIL2 5BL CCGGCCCACCA-------CCACCAGCATTTCGCGCAGGGGCTGGGCTACTACCCGCTAGGGGCGAAGGCCCTG 1236
TaPIL2 5DL CCGGCCCACCACCATCACCATCAGCATTTCGCGCAGGGGGTGGGCTACTACCCGCTAGGGGCGAAGGCCCTG 1353

TaPIL2 5AL CAGCAGAGTCCGGCGCTCCACCACGTGCCCAATGGCAACACTGGCGCCGGCGCGCCTGCCGCTACCGCCAAC 1425
TaPIL2 5BL CAGCAAAGTCCGGCGCTCCACCACGTGTCCAATGGCAACGCCGGCGGTGGCACGCCTGCCGCTACCGCCAAC 1308
TaPIL2 5DL CAGCAGAGTCCGGCGCTCCACCACGTGTCCAATGGCAACACCGGCGGTGGCACGCCTGCCGCTACCGCCAAC 1425
```

Figure S.2 The cDNA sequences of TaPIL2. The three A, B and D homoeologous sequences of TaPIL2 were aligned using the T-coffee alignment tool. Highly conserved residues are shown in reverse, similar residues are shown in grey.

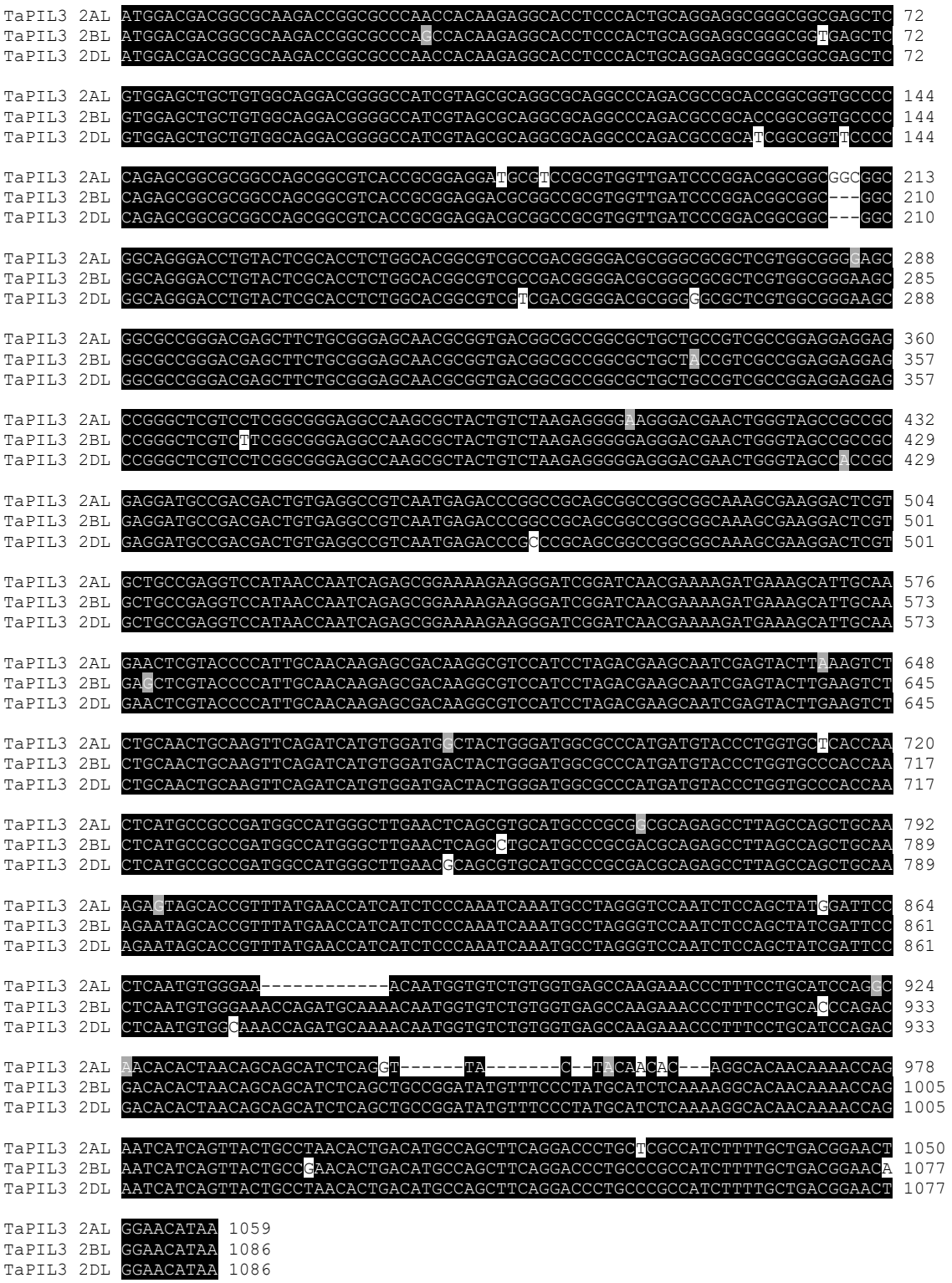

Figure S.3 The cDNA sequences of TaPIL3. The three A, B and D homoeologous sequences of TaPIL2 were aligned using the T-coffee alignment tool. Highly conserved residues are shown in reverse, similar residues are shown in grey.

7.2 The protein sequences of TaPIL1, TaPIL2 and TaPIL3.

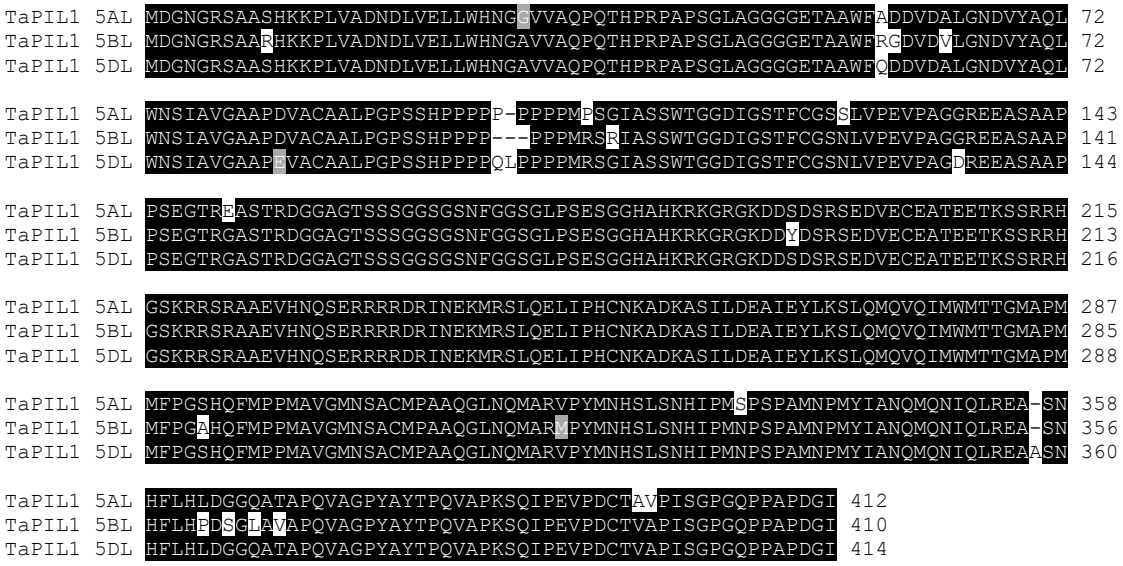

Figure S.4 The Protein Sequence of TaPIL1. The three homoeologous A, B and D protein sequences of TaPIL1 were aligned using a T-coffee alignment. Highly conserved residues are shown in reverse, similar residues are shown in grey.

Figure S.5 The protein sequences of TaPIL2. The three homoeologous A, B and D protein sequences of TaPIL2 were aligned using a T-coffee alignment. Highly conserved residues are shown in reverse, similar residues are shown in grey.

```
TaPIL3 2AL MDDGARPAPNHKRHLPLQEAGGELVELLWQDGAIVAQAQAQTPHRRCPQSGAASGVTAEDASAWLIPDGGGG 72
TaPIL3 2BL MDDGARPAPSHKRHLPLQEAGGELVELLWQDGAIVAQAQAQTPHRRCPQSGAASGVTAEDAAAWLIPDGG-G 71
TaPIL3 2DL MDDGARPAPNHKRHLPLQEAGGELVELLWQDGAIVAQAQAQTPHRRFPQSGAASGVTAEDAAAWLIPDGG-G 71

TaPIL3 2AL GRDLYSHLWHGVADGDAGALVAGSGAGTSFCGSNAVTAPALLPSPEEEPGSSSAGGQALLSKRGRDELGSRR 144
TaPIL3 2BL GRDLYSHLWHGVADGDAGALVAGSGAGTSFCGSNAVTAPALLPSPEEEPGSSSAGGQALLSKRGRDELGSRR 143
TaPIL3 2DL GRDLYSHLWHGVVDGDAGALVAGSGAGTSFCGSNAVTAPALLPSPEEEPGSSSAGGQALLSKRGRDELGSHR 143

TaPIL3 2AL EDADDCEAVNETRPQRPAAKRRTRAAEVHNQSERKRRDRINEKMKALQELVPHCNKSDKASILDEAIEYLKS 216
TaPIL3 2BL EDADDCEAVNETRPQRPAAKRRTRAAEVHNQSERKRRDRINEKMKALQELVPHCNKSDKASILDEAIEYLKS 215
TaPIL3 2DL EDADDCEAVNETRPQRPAAKRRTRAAEVHNQSERKRRDRINEKMKALQELVPHCNKSDKASILDEAIEYLKS 215

TaPIL3 2AL LQLQVQIMWMATGMAPMMYPGAHQLMPPMAMGLNSACMPAAQSLSQLQRVAPFMNHHLPNQMPRVQSPAMDS 288
TaPIL3 2BL LQLQVQIMWMTTGMAPMMYPGAHQLMPPMAMGLNSACMPATQSLSQLQRIAPFMNHHLPNQMPRVQSPAIDS 287
TaPIL3 2DL LQLQVQIMWMTTGMAPMMYPGAHQLMPPMAMGLNAACMPATQSLSQLQRIAPFMNHHLPNQMPRVQSPAIDS 287

TaPIL3 2AL LNVG----NNGVCGEPRNPFLHPGNTLTAASQVT------TTQAQQNQNHQLLPNTDMPASGPCSPSFADGT 350
TaPIL3 2BL LNVGNQMQNNGVCGEPRNPFLHPDDTLTAASQLPDMFPYASQKAQQNQNHQLLPNTDMPASGPCPPSFADGT 359
TaPIL3 2DL LNVANQMQNNGVCGEPRNPFLHPDDTLTAASQLPDMFPYASQKAQQNQNHQLLPNTDMPASGPCPPSFADGT 359

TaPIL3 2AL GT 352
TaPIL3 2BL GT 361
TaPIL3 2DL GT 361
```

Figure S.6 The protein sequence of TaPIL3. The three homoeologous A, B and D protein sequences of TaPIL3 were aligned using a T-coffee alignment. Highly conserved residues are shown in reverse, similar residues are shown in grey.

7.3 Primer Sequences

Table S.1 Primer Sequences. The 5'-3' sequences of all primers used in this project are shown.

Name	*Sequence (5' to 3')*
TaPIL1 F	ATGGACGGCAATGGGAGATC
TaPIL1 R	CTAAATTCCATCAGGTGCAG
TaPIL1 F 2	AATGCAAGTTCAGATCATGT
TaPIL1 F 3	AAGTTCATAACCAGTCAGAG
TaPIL1 F 4	AAAGACGACTCCGATAGCC
TaPIL1 F 5	ACAGCTCTGGAACAGCATT
TaPIL1 UTR F	ATCTTCCTTGCAGTCCCAGC
TaPIL1 UTR R	TCAACGGCATTTGTGATGTCT
TaPIL2 F	ATGAGCCAATTCGTGCCAGAT
TaPIL2 R	TCATCTTTTCTTTCCCTCTATCG
TaPIL2 F 2	ACAAGGCGTCGATGCTGGA
TaPIL2 F 3	CGGAATCATTGGCGCTTGAG
TaPIL2 UTR F	CGGTCGATGCTTGTGATGAT
TaPIL2 UTR R	TCTCTTCCCTTCTCCAGGCA
TaPIL3 F	ATGGACGACGGCGCAAGAC
TaPIL3 R	TCATCTTGCTTGAAACTGCCTGG
TaPIL3 F 2	GATGGCGCCCATGATGTACC
TaPIL3 F 3	CCCATTGCAACAAGAGCGAC
TaPIL3 UTR F	AAGTGGAGAGGCCCGTCA
TaPIL3 UTR R	AGGCAGTTTCAAGCAAGATGA
TaPIL1-A genotyping F	CCTGGAAGGCCTGGATTC
TaPIL1-A genotyping R	ACTGATGCCGTATTTCTCTCTC
TaPIL1-B genotyping F	GATGCTACTTCTGTTGTAGTA
TaPIL1-B genotyping R	ATAATAGATGCCATATTTCTATCG
TaPIL1-D genotyping F	TACATACAGCTGAGAGAAGCAGC
TaPIL1-D genotyping R	CGACAGTACAATCCGGCACT
TaPIL3-A genotyping F	CACTTATTAAGTTTGTGTATAGTCT
TaPIL3-A genotyping R	ACAAATGTAACAATGATTCAAGA
TaPIL3-B genotyping F	ACGGTACTCGACTGACAGC
TaPIL3-B genotyping R	CCTTATGTTCCTGTTCCGTCAG
TaPIL3-D genotyping F	CCACACTCCACACTCCACACC
TaPIL3-D genotyping R	AACCGCCGATGCGGCG
TaPIL1 qPCR F	ACTCATACCCCACTGCAACA
TaPIL1 qPCR R	ACCAGGAAACA CATGGCG
OsPIL1 qPCR F	ACAAGACCGACAAGGCATCT
OsPIL1 qPCR F	GGTGCCATCCCAGTAGTCAT
Ta2526 F	GATCGACCAGAATGGGATGACAAGGAAGATG
Ta2526 F	CCAGTCATCCTC CCATTGCTGGACAG
TaCellDevC F	GAGGAGGATGAGGTGGATGA
TaCellDevC R	CCTGGTACTTGCGGATGTCT
TaActin F	TTGCTGACCGTATGAGCAAG
TaActin R	ACCCTCCAATCCAGACACTG

7.4 Sequencing of clones identified in the yeast two-hybrid library screen

Table S.2 Annotations for the clones identified in the yeast two-hybrid library screen. Clones identified as interactors with RHT-1 were sequenced using one of two methods. Some clones had their cDNA inserts amplified with PCR. Clines with only one cDNA insert had the PCR products purified and sequences. Clones with multiple cDNA inserts were transformed into bacteria for proliferation, and were then extracted as a plasmid prep and sequenced. The table shown the corresponding TGACv1 cDNA sequence for each cDNA and the most closely related rice sequence.

LIBRARY COLONY	WHEAT CDNA	WHEAT ANNOTATION	RICE ORTHOLOGUE	RICE ANNOTATION
287	*TRIAE_CS42_1AL_TGACv1_000318_AA0008620*	Eukaryotic translation initiation factor 3 subunit D	*LOC_Os05g49160.1*	cAMP regulated phosphoprotein
261	*TRIAE_CS42_1AL_TGACv1_002883_AA0045850*	RNA-binding KH domain-containing PEPPER	*LOC_Os10g41440.1*	RNA-binding KH domain-containing protein
101	*TRIAE_CS42_1AL_TGACv1_003073_AA0047440*	NADH dehydrogenase [ubiquinone] 1 beta subcomplex subunit 10-B	*LOC_Os07g34570*	hiazole biosynthetic enzyme, chloroplast
409	*TRIAE_CS42_1BL_TGACv1_032638_AA0132190*	histone -like	*LOC_Os01g05610*	Histone superfamily protein
410	*TRIAE_CS42_1BL_TGACv1_032638_AA0132190*	histone -like	*LOC_Os01g05610*	Histone superfamily protein
73	*TRIAE_CS42_1BS_TGACv1_049491_AA0154730*	Nuclear receptor corepressor 1		
64.3	*TRIAE_CS42_1BS_TGACv1_050766_AA0175240*	Histone H2A	*LOC_Os05g02300*	histone H2A 12
	TRIAE_CS42_1DL_TGACv1_061172_AA0187770	histone H4		
167	*TRIAE_CS42_1DL_TGACv1_062960_AA0222280*	Nucleoside diphosphate kinase 1	*LOC_Os10g41410*	Nucleoside diphosphate kinase
76	*TRIAE_CS42_1DL_TGACv1_064263_AA0233610*	histone H4	*LOC_Os01g61920*	Histone superfamily protein||AT5G59970
234	*TRIAE_CS42_1DS_TGACv1_080285_AA0245220*	predicted protein, partial	*LOC_Os05g01690*	AT2G19390.1
64.1	*TRIAE_CS42_1DS_TGACv1_080822_AA025413*	dnaJ homolog 1	*LOC_Os05g03630*	DNAJ heat shock family protein

	0			
64.2	*TRIAE_CS42_1DS_TGACv1_080822_AA0254130*	dnaJ homolog 1	*LOC_Os05g03630*	DNAJ heat shock family protein
231	*TRIAE_CS42_2AS_TGACv1_113484_AA0356720*	probable small nuclear ribonucleo G	*LOC_Os03g29740*	probable small nuclear ribonucleoprotein G|SNRNP-G|AT2G23930
68	*TRIAE_CS42_2AS_TGACv1_113570_AA0357990*	60S ribosomal L19-1	*LOC_Os02g37440*	
105	*TRIAE_CS42_2AS_TGACv1_113808_AA0360930*	trafficking particle complex subunit 3	*LOC_Os07g44790*	Transport protein particle (TRAPP) component
291	*TRIAE_CS42_2AS_TGACv1_114803_AA0369430*	rho GTPase-activating 7-like	*LOC_Os07g46450.1*	Rho GTPase activation protein with PH domain
95	*TRIAE_CS42_2BL_TGACv1_130221_AA0406630*	peptidyl-tRNA hydrolase PTRHD1	*LOC_Os01g72950*	NAD(P)H:plastoquinone dehydrogenase complex subunit O|NDH-O|AT1G74880
402	*TRIAE_CS42_2BS_TGACv1_145943_AA0450190*	NADH dehydrogenase [ubiquinone] iron-sulfur mitochondrial	*LOC_Os07g39710*	NADH-ubiquinone oxidoreductase-related|FRO1
51	*TRIAE_CS42_2BS_TGACv1_146333_AA0462840*	rho GTPase-activating 7-like	*LOC_Os07g46450*	Rho GTPase activation protein (RhoGAP) with PH domain
178	*TRIAE_CS42_2BS_TGACv1_146333_AA0462840*	rho GTPase-activating 7-like	*LOC_Os07g46450*	Pleckstrin homology domain-containing protein
237	*TRIAE_CS42_2DL_TGACv1_157896_AA0500880*	photosystem II 5 kDa chloroplastic-like	*LOC_Os02g37060*	Photosystem II 5 kD protein||AT1G51400.1
58.1	*TRIAE_CS42_2DL_TGACv1_160015_AA0545600*	hypothetical protein F775_26589		
58.3	*TRIAE_CS42_2DL_TGACv1_160015_AA0545600*	hypothetical protein F775_26589	*LOC_Os04g57690*	Protein of unknown function
67	*TRIAE_CS42_3AL_TGACv1_193736_AA0618750*	1-interacting 1	*LOC_Os01g65560*	cobalt ion binding||AT1G71310.1
202	*TRIAE_CS42_3AS_TGACv1_210742_AA0678170*	transcription factor bHLH35-like	*LOC_Os04g23550*	basic helix-loop-helix (bHLH) DNA-binding superfamily protein||AT5G57150

216	*TRIAE_CS42_3AS_TGACv1_210742_AA0678170*	transcription factor bHLH35-like	*LOC_Os04g23440*	basic helix-loop-helix (bHLH) DNA-binding superfamily protein||AT5G57150
235	*TRIAE_CS42_3AS_TGACv1_213057_AA0705070*	60S ribosomal L9	*LOC_Os09g31180*	Ribosomal protein L6 family
125	*TRIAE_CS42_3B_TGACv1_220646_AA0713530*	Soluble inorganic pyrophosphatase	*LOC_Os01g64670*	pyrophosphorylase 1
116	*TRIAE_CS42_3B_TGACv1_220750_AA0718020*	N/A	*LOC_Os01g05060*	Mitochondrial glycoprotein family protein
134	*TRIAE_CS42_3B_TGACv1_220750_AA0718020*	n/a	*LOC_Os01g05060*	Mitochondrial glycoprotein family protein
57.2	*TRIAE_CS42_3B_TGACv1_220750_AA0718020*	unnamed protein product	*LOC_Os01g05060*	Mitochondrial glycoprotein family protein
163	*TRIAE_CS42_3B_TGACv1_220750_AA0718020*	unnamed protein product	*LOC_Os01g05060*	Mitochondrial glycoprotein
93	*TRIAE_CS42_3B_TGACv1_221518_AA0742720*	1-interacting 1	*LOC_Os01g65560*	cobalt ion binding||AT1G71310
286	*TRIAE_CS42_3DS_TGACv1_272104_AA0914870*	mitochondrial glyco	*LOC_Os01g05010.1*	Mitochondrial glycoprotein family protein
157	*TRIAE_CS42_3DS_TGACv1_272109_AA0915030*	50S ribosomal L3- chloroplastic	*LOC_Os01g14830*	Ribosomal protein
117	*TRIAE_CS42_4AL_TGACv1_288184_AA0940030*	hypothetical protein TRIUR3_13201	*n/a*	
262	*TRIAE_CS42_4AL_TGACv1_288293_AA0943850*	rho GTPase-activating 7-like isoform X2	*LOC_Os03g24180.1*	Rho GTPase activation protein with PH domain
57.3	*TRIAE_CS42_4AL_TGACv1_288766_AA0957540*	nucleotide pyrophosphatase phosphodiesterase-like	*LOC_Os08g41880*	purple acid phosphatase
59.2	*TRIAE_CS42_4AL_TGACv1_288766_AA0957540*	nucleotide pyrophosphatase phosphodiesterase-like	*LOC_Os08g41880*	purple acid phosphatase 27
204	*TRIAE_CS42_4AL_TGACv1_288783_AA0958150*	histone H3-like centromeric CSE4	*LOC_Os06g06460*	Histone superfamily protein||AT1G09200
268	*TRIAE_CS42_4AL_TGACv1_289736_AA0976130*	coiled-coil-helix-coiled-coil-helix domain-containing mitochondrial	*LOC_Os03g48080.1*	Cox 19-like CHCH family protein
63	*TRIAE_CS42_4AS_TGACv1_307286_AA1019140*	probable BOI-related E3 ubiquitin- ligase 3	*LOC_Os01g04650*	Octicosapeptide/Phox/Bem1p family protein||AT2G01190

220	*TRIAE_CS42_4AS_TGACv1_307707_AA1022890*	ETHYLENE INSENSITIVE 3-like 1	*LOC_Os03g20780*	Ethylene insensitive 3 family protein
443	*TRIAE_CS42_4BL_TGACv1_320493_AA1041240*	n/a		
66.1	*TRIAE_CS42_4BL_TGACv1_320880_AA1050780*	40S ribosomal S3a	*LOC_Os03g10340*	Ribosomal protein S3Ae
266	*TRIAE_CS42_4BS_TGACv1_328499_AA1088840*	40S ribosomal S27	*LOC_Os04g27860.1*	Ribosomal protein S27
65.1	*TRIAE_CS42_4BS_TGACv1_328898_AA1095230*	probable xyloglucan endotransglucosylase hydrolase	*LOC_Os11g33270*	xyloglucan endotransglucosylase/hydrolase 5
69.1	*TRIAE_CS42_4BS_TGACv1_329257_AA1099310*	cystathionine gamma-synthase chloroplastic	*LOC_Os03g25940*	Pyridoxal phosphate (PLP)-dependent transferases superfamily protein
69.2	*TRIAE_CS42_4BS_TGACv1_329257_AA1099310*	cystathionine gamma-synthase chloroplastic	*LOC_Os03g25940*	Pyridoxal phosphate (PLP)-dependent transferases superfamily protein
69.3	*TRIAE_CS42_4BS_TGACv1_329257_AA1099310*	cystathionine gamma-synthase chloroplastic	*LOC_Os03g25940*	Pyridoxal phosphate (PLP)-dependent transferases superfamily protein
444	*TRIAE_CS42_4BS_TGACv1_330766_AA1108750*	Zinc finger 593	*LOC_Os08g45040*	zinc finger (C2H2 type) family protein
229	*TRIAE_CS42_4DL_TGACv1_343323_AA1133270*	lipase 1-like	*LOC_Os03g08100*	alpha/beta-Hydrolases superfamily protein||AT5G21950
221	*TRIAE_CS42_4DL_TGACv1_343378_AA1133790*	Defensin 1	*LOC_Os03g03810*	low-molecular-weight cysteine-rich 69
226	*TRIAE_CS42_4DL_TGACv1_343378_AA1133790*	Defensin 1	*LOC_Os03g03810*	low-molecular-weight cysteine-rich 69
59.1	*TRIAE_CS42_4DL_TGACv1_344008_AA1142470*	probable BOI-related E3 ubiquitin- ligase 3	*LOC_Os03g15730*	S-ribonuclease binding protein 1
119	*TRIAE_CS42_4DL_TGACv1_344008_AA1142470*	probable BOI-related E3 ubiquitin- ligase 3	*LOC_Os03g15730*	S-ribonuclease binding protein 1
62	*TRIAE_CS42_5AL_TGACv1_374363_AA1198110*	small heat shock chloroplastic	*LOC_Os06g39390*	HXXXD-type acyl-transferase family protein||AT3G62160
62.2	*TRIAE_CS42_5AL_TGACv1_374363_AA1198110*	small heat shock chloroplastic		
62.3	*TRIAE_CS42_5AL_TGACv1_374363_AA1198110*	small heat shock chloroplastic		

401	*TRIAE_CS42_5AL_TGACv1_374363_AA1198110*	small heat shock chloroplastic		
297	*TRIAE_CS42_5AL_TGACv1_377393_AA1246520*	squamosa promoter-binding 18	*LOC_Os09g32944.1*	Squamasoa promoter-binding protein-like
297	*TRIAE_CS42_5AL_TGACv1_377393_AA1246520*	squamosa promoter-binding 18	*LOC_Os12g40900.1*	AUX/IAA transcriptional regulator family protein
224	*TRIAE_CS42_5AL_TGACv1_377798_AA1249570*	chlorophyll a-b binding chloroplastic	*LOC_Os09g26810*	photosystem I light harvesting complex gene 6
140	*TRIAE_CS42_5AL_TGACv1_378438_AA1253310*	Cytochrome b-c1 complex subunit 7		
292	*TRIAE_CS42_5AS_TGACv1_392869_AA1265640*	auxin-responsive IAA31-like	*LOC_Os03g43410.1*	Indole 3 acetic acid inducible ARX5, IAA1
61.1	*TRIAE_CS42_5AS_TGACv1_394228_AA1279010*	nucleoside diphosphate kinase chloroplastic	*LOC_Os12g36194*	nucleoside diphosphate kinase 2
61.2	*TRIAE_CS42_5AS_TGACv1_394228_AA1279010*	nucleoside diphosphate kinase chloroplastic		
91	*TRIAE_CS42_5BL_TGACv1_404297_AA1294450*	GATA transcription factor 16-like isoform X2	*LOC_Os01g74540*	GATA transcription factor 16|GATA16|AT5G49300
254	*TRIAE_CS42_5BL_TGACv1_404326_AA1295610*	TaPIL2 - stress-responsive bHLH transcription factor	*LOC_Os03g43810.1*	PIF1/PIL5
58.2	*TRIAE_CS42_5BL_TGACv1_404504_AA1302310*	Protein NEDD1	*LOC_Os09g09470*	Transducin/WD40 repeat-like superfamily protein
215	*TRIAE_CS42_5BL_TGACv1_404508_AA1302500*	small heat shock chloroplastic		
205	*TRIAE_CS42_5BL_TGACv1_404876_AA1313820*	30S ribosomal S6 chloroplastic	*LOC_Os03g62630*	Translation elongation factor EF1B/ribosomal protein S6 family protein||AT1G64510
247	*TRIAE_CS42_5BL_TGACv1_405054_AA1318940*	20 kDa chloroplastic	*LOC_Os02g54060*	chaperonin 20
415	*TRIAE_CS42_5BL_TGACv1_405054_AA1318940*	20 kDa chloroplastic	*LOC_Os09g26730*	chaperonin 20
121	*TRIAE_CS42_5BL_TGACv1_405212_AA1322260*	hypothetical protein F775_08920	*n/a*	

137	*TRIAE_CS42_5BL_TGACv1_406028_AA1339440*	squamosa promoter-binding 18 isoform X1	*LOC_Os09g32944*	quamosa promoter-binding protein-like (SBP domain) transcription factor family protein
59.3	*TRIAE_CS42_5DL_TGACv1_433130_AA1403020*	pop3 peptide	*LOC_Os11g05290*	Stress responsive A/B Barrel Domain
438	*TRIAE_CS42_5DL_TGACv1_434074_AA1428410*	nucleolar 58 isoform X1		
77	*TRIAE_CS42_5DL_TGACv1_434302_AA1433530*	CCG-binding partial	*LOC_Os03g55670*	maternal effect embryo arrest 14|MEE14|AT2G15890
70.1	*TRIAE_CS42_5DL_TGACv1_436069_AA1457640*	30S ribosomal S6 chloroplastic	*LOC_Os03g62630*	Translation elongation factor EF1B/ribosomal protein S6 family protein
70.2	*TRIAE_CS42_5DL_TGACv1_436069_AA1457640*	30S ribosomal S6 chloroplastic	*LOC_Os03g62630*	Translation elongation factor EF1B/ribosomal protein S6 family protein
70.3	*TRIAE_CS42_5DL_TGACv1_436069_AA1457640*	30S ribosomal S6 chloroplastic	*LOC_Os03g62630*	Translation elongation factor EF1B/ribosomal protein S6 family protein
71.3	*TRIAE_CS42_5DL_TGACv1_436069_AA1457640*	30S ribosomal S6 chloroplastic	*LOC_Os03g62630*	Translation elongation factor EF1B/ribosomal protein S6 family protein
94	*TRIAE_CS42_5DL_TGACv1_436069_AA1457640*	30S ribosomal S6 chloroplastic	*LOC_Os03g62630*	Translation elongation factor EF1B/ribosomal protein S6 family protein||AT1G64510
428	*TRIAE_CS42_5DL_TGACv1_436069_AA1457640*	30S ribosomal S6 chloroplastic	*LOC_Os03g62630*	Translation elongation factor EF1B/ribosomal protein S6 family protein
447	*TRIAE_CS42_5DL_TGACv1_436069_AA1457640*	30S ribosomal S6 chloroplastic	*LOC_Os03g62630*	ranslation elongation factor EF1B/ribosomal protein S6 family protein
239	*TRIAE_CS42_5DL_TGACv1_436696_AA1462780*	hypothetical protein F775_08920	*LOC_Os08g37920*	methyl-CPG-binding domain 8
168	*TRIAE_CS42_5DS_TGACv1_458113_AA1492120*	SKIP interacting 15	*LOC_Os12g31790*	

98	*TRIAE_CS42_5DS_TGACv1_458160_AA1492440*	nucleoside diphosphate kinase chloroplastic		
408	*TRIAE_CS42_5DS_TGACv1_458160_AA1492440*	nucleoside diphosphate kinase chloroplastic	*LOC_Os12g36194*	nucleoside diphosphate kinase 2
449	*TRIAE_CS42_5DS_TGACv1_458160_AA1492440*	nucleoside diphosphate kinase chloroplastic		
432	*TRIAE_CS42_6AL_TGACv1_471983_AA1516620*	60S ribosomal L37-3	*LOC_Os02g56990*	Zinc-binding ribosomal protein family protein
56.1	*TRIAE_CS42_6AL_TGACv1_472185_AA1518720*	soluble inorganic pyrophosphatase	*LOC_Os02g47600*	pyrophosphorylase 1
56.2	*TRIAE_CS42_6AL_TGACv1_472185_AA1518720*	soluble inorganic pyrophosphatase	*LOC_Os02g47600*	pyrophosphorylase 1
56.3	*TRIAE_CS42_6AL_TGACv1_472185_AA1518720*	soluble inorganic pyrophosphatase	*LOC_Os02g47600*	pyrophosphorylase 1
279	*TRIAE_CS42_6AL_TGACv1_472185_AA1518720*	soluble inorganic pyrophosphatase	*LOC_Os02g47600.1*	Pyrophosphorylase 1
66.3	*TRIAE_CS42_6AL_TGACv1_473088_AA1528560*	glyceraldehyde-3-phosphate dehydrogenase	*LOC_Os02g38920*	glyceraldehyde-3-phosphate dehydrogenase C subunit 1
257	*TRIAE_CS42_6AS_TGACv1_487662_AA1572230*	acylamino-acid-releasing enzyme-like	*LOC_Os10g28030.1*	Acylaminoacyl peptidase related.
72	*TRIAE_CS42_6BS_TGACv1_513480_AA1642900*	hypothetical protein F775_11456		
442	*TRIAE_CS42_6BS_TGACv1_513480_AA1642900*	hypothetical protein F775_11456		
277	*TRIAE_CS42_6DL_TGACv1_527484_AA1704710*	predicted protein	*LOC_Os08g19370.1*	AT4G39630.1
417	*TRIAE_CS42_6DL_TGACv1_527727_AA1708000*	acetohydroxyacid partial	*LOC_Os02g30630*	chlorsulfuron/imidazolinone resistant
61.3	*TRIAE_CS42_6DS_TGACv1_543026_AA1734280*	U5 small nuclear ribonucleo 200 kDa helicase	*0*	
54	*TRIAE_CS42_6DS_TGACv1_543132_AA1735890*	hypothetical protein TRIUR3_22378		
53	*TRIAE_CS42_7AL_TGACv1_557230_AA1778570*	#N/A	*LOC_Os07g34570*	thiazole biosynthetic enzyme, chloroplast (ARA6) (THI1) (THI4)

80	*TRIAE_CS42_7AL_TGACv1_557230_AA1778570*	#N/A	*LOC_Os02g16680*	basic leucine zipper 9|ATBZIP9
153	*TRIAE_CS42_7AL_TGACv1_557230_AA1778570*	#N/A	*LOC_Os07g34570*	thiazole biosynthetic enzyme, chloroplast
206	*TRIAE_CS42_7AL_TGACv1_557230_AA1778570*	#N/A	*LOC_Os07g34570*	thiazole biosynthetic enzyme, chloroplast
214	*TRIAE_CS42_7AL_TGACv1_557230_AA1778570*	#N/A	*LOC_Os02g16680*	basic leucine zipper 9
299	*TRIAE_CS42_7AL_TGACv1_557230_AA1778570*	#N/A	*LOC_Os07g34570.1*	Thiazole biosynthetic enzyme, chloroplast (ARA6)
446	*TRIAE_CS42_7AL_TGACv1_557819_AA1786560*	14 kDa zinc-binding	*LOC_Os06g45660*	HISTIDINE TRIAD NUCLEOTIDE-BINDING 2
212	*TRIAE_CS42_7AS_TGACv1_569962_AA1827770*	RNA-binding 1-like	*LOC_Os08g43360*	nucleotide binding;nucleic acid binding||AT1G21320
421	*TRIAE_CS42_7AS_TGACv1_570151_AA1831280*	predicted protein		
65.3	*TRIAE_CS42_7AS_TGACv1_570423_AA1835500*	ethylene-responsive element binding	*LOC_Os02g54160.*	related to AP2 12
65.2	*TRIAE_CS42_7AS_TGACv1_570423_AA1835500*	ethylene-responsive element binding	*LOC_Os02g54160*	related to AP2 12
74	*TRIAE_CS42_7AS_TGACv1_570423_AA1835500*	ethylene-responsive element binding	*LOC_Os01g68390*	Protein of unknown function (DUF185)||AT1G04900
273	*TRIAE_CS42_7AS_TGACv1_570423_AA1835500*	ethylene-responsive element binding	*LOC_Os06g09390.1*	Related to AP2 12
292	*TRIAE_CS42_7AS_TGACv1_570936_AA1842670*	nucleotide pyrophosphatase phosphodiesterase-like	*LOC_Os08g41880.1*	Purple acid phosphatase 2
104	*TRIAE_CS42_7BS_TGACv1_592265_AA1934530*	60S ribosomal L35a-1	*n/a*	
55.1	*TRIAE_CS42_7BS_TGACv1_592615_AA1941460*	E3 ubiquitin- ligase HERC1		
55.2	*TRIAE_CS42_7BS_TGACv1_592615_AA1941460*	E3 ubiquitin- ligase HERC1		
55.3	*TRIAE_CS42_7BS_TGACv1_592615_AA194146*	E3 ubiquitin- ligase HERC1		

	0			
	TRIAE_CS42_7BS_TGACv1_594836_AA1958510	ethylene-responsive element binding		
60.1	*TRIAE_CS42_7DL_TGACv1_602628_AA1963110*	60S ribosomal L34	*LOC_Os08g06040*	Ribosomal protein L34e superfamily protein
60.2	*TRIAE_CS42_7DL_TGACv1_602628_AA1963110*	60S ribosomal L34	*LOC_Os08g06040*	Ribosomal protein L34e superfamily protein
60.3	*TRIAE_CS42_7DL_TGACv1_602628_AA1963110*	60S ribosomal L34	*LOC_Os08g06040*	Ribosomal protein L34e superfamily protein
71.1	*TRIAE_CS42_7DL_TGACv1_602822_AA1969410*	AF464738_3 transposase		
71.2	*TRIAE_CS42_7DL_TGACv1_602822_AA1969410*	AF464738_3 transposase		
274	*TRIAE_CS42_7DL_TGACv1_602857_AA1970150*	thiamine thiazole synthase chloroplastic	*LOC_Os07g34570.1* *|*	Thiazole biosynthetic enzyme, chloroplast (ARA6)
	TRIAE_CS42_7DL_TGACv1_602857_AA1970150	thiamine thiazole synthase chloroplastic		
159	*TRIAE_CS42_7DL_TGACv1_602857_AA1970160*	hypothetical protein G7K_0011-t1	*LOC_Os07g34570*	Thiazole biosynthetic enzyme, chloroplast (ARA6)
256	*TRIAE_CS42_7DL_TGACv1_602857_AA1970160*	hypothetical protein G7K_0011-t1	*LOC_Os07g34570.1*	Thiazole biosynthetic enzyme, chloroplast (ARA6)
236	*TRIAE_CS42_7DL_TGACv1_603063_AA1974950*	bHLH DNA-binding domain superfamily	*LOC_Os01g70310*	basic helix-loop-helix (bHLH) DNA-binding superfamily protein
130	*TRIAE_CS42_7DS_TGACv1_622192_AA2034890*	kDa heat-shock	*LOC_Os06g11610*	HSP20-like chaperones superfamily protein
416	*TRIAE_CS42_7DS_TGACv1_623153_AA2050180*	hypothetical protein F775_29406	*LOC_Os08g27070*	HSP20-like chaperones superfamily protein
422	*TRIAE_CS42_U_TGACv1_641036_AA2082900*	kDa heat-shock	*LOC_Os06g11610*	HSP20-like chaperones superfamily protein
139	*TRIAE_CS42_U_TGACv1_641253_AA2089820*	CURVATURE THYLAKOID chloroplastic		
87	*TRIAE_CS42_U_TGACv1_641729_AA2102670*	Thiol protease	*LOC_Os03g56690*	Cysteine proteinases superfamily protein||AT5G50260
259	*TRIAE_CS42_U_TGACv1_641729_AA2102670*	Thiol protease	*LOC_Os03g56690.1*	Cysteine proteinases superfamily

276	*TRIAE_CS42_U_TGACv1_642001_AA2109140*	tricin synthase 2-like	*LOC_Os08g38920.1*	S-adenosyl-L-methionone-dependent methyltransferases superfamily
165	*TRIAE_CS42_U_TGACv1_642183_AA2112810*	polyamine transporter PUT1 isoform X1	*LOC_Os02g47210*	Amino acid permease family protein
52	*TRIAE_CS42_U_TGACv1_642369_AA2116430*	hypothetical protein TRIUR3_22378	*LOC_Os05g06480*	Inorganic H pyrophosphatase family protein
52	*TRIAE_CS42_U_TGACv1_642369_AA2116430*	hypothetical protein TRIUR3_22378		
143	*TRIAE_CS42_U_TGACv1_642981_AA2125590*	FAR1-RELATED SEQUENCE 5-like		
89	*TRIAE_CS42_U_TGACv1_643998_AA2136370*	histone H3	*LOC_Os01g64640*	Histone superfamily protein||AT1G09200.1
66.2			*LOC_Os10g38216*	Tetratricopeptide repeat (TPR)-like superfamily protein

Chapter 8: Reference List

AACH, H., BODE, H., ROBINSON, D. G. & GRAEBE, J. E. 1997. ent-kaurene synthase is located in proplastids of meristematic shoot tissues. *Planta,* 202**,** 211-219.

ACHARD, P., BAGHOUR, M., CHAPPLE, A., HEDDEN, P., VAN DER STRAETEN, D., GENSCHIK, P., MORITZ, T. & HARBERD, N. P. 2007. The plant stress hormone ethylene controls floral transition via DELLA-dependent regulation ot floral meristem-identity genes. *Proceedings of the National Academy of Sciences of the United States of America,* 104**,** 6484-6489.

ACHARD, P., VRIEZEN, W. H., VAN DER STRAETEN, D. & HARBERD, N. P. 2003. Ethylene regulates Arabidopsis development via the modulation of DELLA protein growth repressor function. *Plant Cell,* 15**,** 2816-2825.

AL-SADY, B., NI, W. M., KIRCHER, S., SCHAFER, E. & QUAIL, P. H. 2006. Photoactivated phytochrome induces rapid PIF3 phosphorylation prior to proteasorne-mediated degradation. *Molecular Cell,* 23**,** 439-446.

ALABADI, D., BLAZQUEZ, M. A., CARBONELL, J., FERRANDIZ, C. & PEREZ-AMADOR, M. A. 2009. Instructive roles for hormones in plant development. *International Journal of Developmental Biology,* 53**,** 1597-1608.

ALGHABARI, F., LUKAC, M., JONES, H. E. & GOODING, M. J. 2014. Effect of Rht alleles on the tolerance of wheat grain set to high temperature and drought stress during booting and anthesis. *Journal of Agronomy and Crop Science,* 200**,** 36-45.

ARNAUD, N., GIRIN, T., SOREFAN, K., FUENTES, S., WOOD, T. A., LAWRENSON, T., SABLOWSKI, R. & OSTERGAARD, L. 2010. Gibberellins control fruit patterning in Arabidopsis thaliana. *Genes & Development,* 24**,** 2127-2132.

AYANO, M., KANI, T., KOJIMA, M., SAKAKIBARA, H., KITAOKA, T., KUROHA, T., ANGELES-SHIM, R. B., KITANO, H., NAGAI, K. & ASHIKARI, M. 2014. Gibberellin biosynthesis and signal transduction is essential for internode elongation in deepwater rice. *Plant Cell and Environment,* 37**,** 2313-2324.

BAE, G. & CHOI, G. 2008. Decoding of light signals by plant phytochromes and their interacting proteins. *Annual Review of Plant Biology,* 59**,** 281-311.

BAILEY, P. C., MARTIN, C., TOLEDO-ORTIZ, G., QUAIL, P. H., HUQ, E., HEIM, M. A., JAKOBY, M., WERBER, M. & WEISSHAAR, B. 2003. Update on the basic helix-loop-helix transcription factor gene family in Arabidopsis thaliana. *Plant Cell,* 15**,** 2497-2501.

BAIMA, S., POSSENTI, M., MATTEUCCI, A., WISMAN, E., ALTAMURA, M. M., RUBERTI, I. & MORELLI, G. 2001. The Arabidopsis ATHB-8 HD-zip protein acts as a differentiation-promoting transcription factor of the vascular meristems. *Plant Physiology,* 126**,** 643-655.

BALLARE, C. L., SCOPEL, A. L. & SANCHEZ, R. A. 1989. Photomodulation of axis extension in sparse canopies - role of the stem in the perception of light-quality signals of stand density. *Plant Physiology,* 89**,** 1324-1330.

BARNES, C. & BUGBEE, B. 1991. Morphological responses of wheat to changes in phytochrome photoequilibrium. *Plant Physiology,* 97**,** 359-365.

BASU, D., DEHESH, K., SCHNEIDER-POETSCH, H. J., HARRINGTON, S. E., MCCOUCH, S. R. & QUAIL, P. H. 2000. Rice PHYC gene: structure, expression, map position and evolution. *Plant Molecular Biology,* 44**,** 27-42.

BAUER, D., VICZIAN, A., KIRCHER, S., NOBIS, T., NITSCHKE, R., KUNKEL, T., PANIGRAHI, K. C. S., ADAM, E., FEJES, E., SCHAFER, E. & NAGY, F. 2004. Constitutive photomorphogenesis 1 and multiple photoreceptors control degradation of phytochrome interacting factor 3, a transcription factor required for light signaling in Arabidopsis. *Plant Cell,* 16**,** 1433-1445.

BEDDINGTON, J. 2010. Food security: contributions from science to a new and greener revolution. *Philosophical Transactions of the Royal Society B: Biological Sciences,* 365**,** 61-71.

BEEVERS, L., LOVEYS, B., PEARSON, J. A. & WAREING, P. F. 1970. Phytochrome and hormonal control of expansion and greening of etiolated wheat leaves. *Planta,* 90**,** 286-&.

BETHKE, P. C., SCHUURINK, R. & JONES, R. L. 1997. Hormonal signalling in cereal aleurone. *Journal of Experimental Botany,* 48**,** 1337-1356.

BIRMINGHAM, A., ANDERSON, E. M., REYNOLDS, A., ILSLEY-TYREE, D., LEAKE, D., FEDOROV, Y., BASKERVILLE, S., MAKSIMOVA, E., ROBINSON, K., KARPILOW, J., MARSHALL, W. S. & KHVOROVA, A. 2006. 3'UTR seed matches, but not overall identity, are associated with RNAi off-targets. *Nature Methods,* 3**,** 199-204.

BLAKELEY, S. D., THOMAS, B., HALL, J. L. & VINCEPRUE, D. 1983. Regulation of swelling of etiolated-wheat-leaf protoplasts by phytochrome and gibberellic-acid. *Planta,* 158**,** 416-421.

BLAZQUEZ, M. A., GREEN, R., NILSSON, O., SUSSMAN, M. R. & WEIGEL, D. 1998. Gibberellins promote flowering of Arabidopsis by activating the LEAFY promoter. *Plant Cell,* 10**,** 791-800.

BORNER, A., PLASCHKE, J., KORZUN, V. & WORLAND, A. J. 1996. The relationships between the dwarfing genes of wheat and rye. *Euphytica,* 89**,** 69-75.

BOULY, J. P., SCHLEICHER, E., DIONISIO-SESE, M., VANDENBUSSCHE, F., VAN DER STRAETEN, D., BAKRIM, N., MEIER, S., BATSCHAUER, A., GALLAND, P., BITTL, R. & AHMAD, M. 2007. Cryptochrome blue light photoreceptors are activated through interconversion of flavin redox states. *Journal of Biological Chemistry,* 282**,** 9383-9391.

BOYLAN, M. T. & QUAIL, P. H. 1991. Phytochrome-A overexpression inhibits hypocotyl elongation in transgenic Arabidopsis. *Proceedings of the National Academy of Sciences of the United States of America,* 88**,** 10806-10810.

BRENCHLEY, R., SPANNAGL, M., PFEIFER, M., BARKER, G. L., D'AMORE, R., ALLEN, A. M., MCKENZIE, N., KRAMER, M., KERHORNOU, A., BOLSER, D., KAY, S., WAITE, D., TRICK, M., BANCROFT, I., GU, Y., HUO, N., LUO, M. C., SEHGAL, S., GILL, B., KIANIAN, S., ANDERSON, O., KERSEY, P., DVORAK, J., MCCOMBIE, W. R., HALL, A., MAYER, K. F., EDWARDS, K. J., BEVAN, M. W. & HALL, N. 2012. Analysis of the bread wheat genome using whole-genome shotgun sequencing. *Nature,* 491**,** 705-10.

BREWER, P. B., KOLTAI, H. & BEVERIDGE, C. A. 2013. Diverse roles of strigolactones in plant development. *Molecular Plant,* 6**,** 18-28.

BRIGGS, W. R. 2014. Phototropism: some history, some puzzles, and a look ahead. *Plant Physiology,* 164**,** 13-23.

BRIGGS, W. R. & CHRISTIE, J. M. 2002. Phototropins 1 and 2: versatile plant blue-light receptors. *Trends in Plant Science,* 7**,** 204-210.

BRIGGS, W. R. & OLNEY, M. A. 2001. Photoreceptors in plant photomorphogenesis to date. Five phytochromes, two cryptochromes, one phototropin, and one superchrome. *Plant Physiology,* 125**,** 85-88.

BROCK, M. T., MALOOF, J. N. & WEINIG, C. 2010. Genes underlying quantitative variation in ecologically important traits: PIF4 (phytochrome interacting factor 4) is associated with variation in internode length, flowering time, and fruit set in Arabidopsis thaliana. *Molecular Ecology,* 19**,** 1187-99.

BUCHANAN WOLLASTON, V. 1997. The molecular biology of leaf senescence. *Journal of Experimental Botany,* 48**,** 181-199.

CASAL, J. J., DEREGIBUS, V. A. & SANCHEZ, R. A. 1985. Variations in tiller dynamics and morphology in lolium multiflorum Lam. vegetative and reproductive plants as affected by differences in red/far-red Irradiation. *Annals of Botany***,** 553-559.

CASSON, S. A., FRANKLIN, K. A., GRAY, J. E., GRIERSON, C. S., WHITELAM, G. C. & HETHERINGTON, A. M. 2009. Phytochrome B and PIF4 regulate stomatal development in response to light quantity. *Comparative Biochemistry and Physiology - Part A: Molecular & Integrative Physiology,* 153A**,** S209-S209.

CHAKRABORTY, S. & NEWTON, A. C. 2011. Climate change, plant diseases and food security: an overview. *Plant Pathology,* 60**,** 2-14.

CHANDLER, P. M., MARION-POLL, A., ELLIS, M. & GUBLER, F. 2002. Mutants at the Slender1 locus of barley cv Himalaya. molecular and physiological characterization. *Plant Physiology,* 129**,** 181-190.

CHAO, L. M., LIU, Y. Q., CHEN, D. Y., XUE, X. Y., MAO, Y. B. & CHEN, X. Y. 2017. Arabidopsis transcription factors SPL1 and SPL12 confer plant thermotolerance at reproductive stage. *Molecular Plant,* 10**,** 735-748.

CHAPMAN, J. A., MASCHER, M., BULUC, A., BARRY, K., GEORGANAS, E., SESSION, A., STRNADOVA, V., JENKINS, J., SEHGAL, S., OLIKER, L., SCHMUTZ, J., YELICK, K. A., SCHOLZ, U., WAUGH, R., POLAND, J. A., MUEHLBAUER, G. J., STEIN, N. & ROKHSAR, D. S. 2015. A whole-genome shotgun approach for assembling and anchoring the hexaploid bread wheat genome. *Genome Biology,* 16.

CHAUDHURY, A. M., LETHAM, S., CRAIG, S. & DENNIS, E. S. 1993. Amp1 - a mutant with high cytokinin levels and altered embryonic pattern, faster vegetative growth, constitutive photomorphogenesis and precocious flowering. *Plant Journal,* 4**,** 907-916.

CHEMINANT, S., WILD, M., BOUVIER, F., PELLETIER, S., RENOU, J. P., ERHARDT, M., HAYES, S., TERRY, M. J., GENSCHIK, P. & ACHARD, P. 2011. DELLAs regulate chlorophyll and carotenoid biosynthesis to prevent photooxidative damage during seedling deetiolation in Arabidopsis. *Plant Cell,* 23**,** 1849-1860.

CHEN, A. & DUBCOVSKY, J. 2012. Wheat TILLING mutants show that the vernalization gene VRN1 down-regulates the flowering repressor VRN2 in leaves but is not essential for flowering. *Plos Genetics,* 8.

CHEN, M. & CHORY, J. 2011. Phytochrome signaling mechanisms and the control of plant development. *Trends in Cell Biology,* 21**,** 664-671.

CHIBA, Y., SHIMIZU, T., MIYAKAWA, S., KANNO, Y., KOSHIBA, T., KAMIYA, Y. & SEO, M. 2015. Identification of Arabidopsis thaliana NRT1/PTR FAMILY (NPF) proteins capable of transporting plant hormones. *Journal of Plant Research,* 128**,** 679-686.

CHIEN, C. T., BARTEL, P. L., STERNGLANZ, R. & FIELDS, S. 1991. The 2-hybrid system - a method to identify and clone genes for proteins that interact with a protein of interest. *Proceedings of the National Academy of Sciences of the United States of America,* 88**,** 9578-9582.

CHIN ATKINS, A. N., CRAIG, S., HOCART, C. H., DENNIS, E. S. & CHAUDHURY, A. M. 1996. Increased endogenous cytokinin in the Arabidopsis amp1 mutant corresponds with de-etiolation responses. *Planta,* 198**,** 549-556.

CHRISTENSEN, A. H. & QUAIL, P. H. 1989. Structure and expression of a maize phytochrome-encoding gene. *Gene,* 85**,** 381-390.

CHRISTIE, J. M., ARVAI, A. S., BAXTER, K. J., HEILMANN, M., PRATT, A. J., O'HARA, A., KELLY, S. M., HOTHORN, M., SMITH, B. O., HITOMI, K., JENKINS, G. I. & GETZOFF, E. D. 2012. Plant UVR8 photoreceptor senses UV-B by tryptophan-mediated disruption of cross-dimer salt bridges. *Science,* 335**,** 1492-1496.

CHRISTIE, J. M., SALOMON, M., NOZUE, K., WADA, M. & BRIGGS, W. R. 1999. LOV (light, oxygen, or voltage) domains of the blue-light photoreceptor phototropin (nph1): Binding sites for the chromophore flavin mononucleotide. *Proceedings of the National Academy of Sciences of the United States of America,* 96**,** 8779-8783.

CIMMYT, B., ICRISAT, IFPRI, ILRI, IRRI AND IWMI 2011. Wheat - global alliance for improving food security and the livelihoods of the resource poor in the developing world. *In:* CIMMYT (ed.). Mexico.

CLACK, T., MATHEWS, S. & SHARROCK, R. A. 1994. The phytochrome apoprotein family in Arabidopsis is encoded by 5 genes - the sequences and expression of PHYD and PYHE. *Plant Molecular Biology,* 25**,** 413-427.

CLAEYS, H., DE BODT, S. & INZE, D. 2014. Gibberellins and DELLAs: central nodes in growth regulatory networks. *Trends in Plant Science,* 19**,** 231-239.

CLAVIJO, B. J., VENTURINI, L., SCHUDOMA, C., ACCINELLI, G. G., KAITHAKOTTIL, G., WRIGHT, J., BORRILL, P., KETTLEBOROUGH, G., HEAVENS, D., CHAPMAN, H., LIPSCOMBE, J., BARKER, T., LU, F. H., MCKENZIE, N., RAATS, D., RAMIREZ-GONZALEZ, R. H., COINCE, A., PEEL, N., PERCIVAL-ALWYN, L., DUNCAN, O., TROSCH, J., YU, G. T., BOLSER, D. M., NAMAATI, G., KERHORNOU, A., SPANNAGL, M., GUNDLACH, H., HABERER, G., DAVEY, R. P., FOSKER, C., DI PALMA, F., PHILLIPS, A. L., MILLAR, A. H., KERSEY, P. J., UAUY, C., KRASILEVA, K. V., SWARBRECK, D., BEVAN, M. W. & CLARK, M. D. 2017. An improved assembly and annotation of the allohexaploid wheat genome identifies complete families of agronomic genes and provides genomic evidence for chromosomal translocations. *Genome Research,* 27**,** 885-896.

CLOUSE, S. D. & SASSE, J. M. 1998. Brassinosteroids: Essential regulators of plant growth and development. *Annual Review of Plant Physiology and Plant Molecular Biology,* 49**,** 427-451.

COELHO, M., COLEBROOK, E. H., LLOYD, D. P. A., WEBSTER, C. P., MOONEY, S. J., PHILLIPS, A. L., HEDDEN, P. & WHALLEY, W. R. 2013. The involvement of gibberellin signalling in the effect of soil resistance to root penetration on leaf elongation and tiller number in wheat. *Plant and Soil,* 371**,** 81-94.

COLASANTI, J., TREMBLAY, R., WONG, A. Y., CONEVA, V., KOZAKI, A. & MABLE, B. K. 2006. The maize INDETERMINATE1 flowering time regulator defines a highly conserved zinc finger protein family in higher plants. *BMC Genomics,* 7**,** 158.

CORDEIRO, A. M., FIGUEIREDO, D. D., TEPPERMAN, J., BORBA, A. R., LOURENCO, T., ABREU, I. A., OUWERKERK, P. B. F., QUAIL, P. H., OLIVEIRA, M. M. & SAIBO, N. J. M. 2016. Rice phytochrome-interacting factor protein OsPIF14 represses OsDREB1B gene expression through an extended N-box and interacts preferentially with the active form of phytochrome B. *Biochimica Et Biophysica Acta-Gene Regulatory Mechanisms,* 1859**,** 393-404.

CORDELL, D., DRANGERT, J.-O. & WHITE, S. 2009. The story of phosphorus: Global food security and food for thought. *Global Environmental Change,* 19**,** 292-305.

CORNEJO, M. J., LUTH, D., BLANKENSHIP, K. M., ANDERSON, O. D. & BLECHL, A. E. 1993. Activity of a maize ubiquitin promoter in transgenic rice. *Plant Molecular Biology,* 23**,** 567-581.

DAI, M. Q., HU, Y. F., ZHAO, Y., LIU, H. F. & ZHOU, D. X. 2007. A WUSCHEL-LIKE HOMEOBOX gene represses a YABBY gene expression required for rice leaf development. *Plant Physiology,* 144**,** 380-390.

DAVIERE, J. M. & ACHARD, P. 2013. Gibberellin signaling in plants. *Development,* 140**,** 1147-1151.

DE BEER, A. & VIVIER, M. A. 2011. Four plant defensins from an indigenous South African Brassicaceae species display divergent activities against two test pathogens despite high sequence similarity in the encoding genes. *BMC Research Notes,* 4**,** 459.

DE CONINCK, B., CAMMUE, B. P. A. & THEVISSEN, K. 2013. Modes of antifungal action and in planta functions of plant defensins and defensin-like peptides. *Fungal Biology Reviews,* 26**,** 109-120.

DE GRAUWE, L., VRIEZEN, W. H., BERTRAND, S., PHILLIPS, A., VIDAL, A. M., HEDDEN, P. & VAN DER STRAETEN, D. 2007. Reciprocal influence of ethylene and gibberellins on response-gene expression in Arabidopsis thaliana. *Planta,* 226**,** 485-498.

DE LUCAS, M., DAVIERE, J. M., RODRIGUEZ-FALCON, M., PONTIN, M., IGLESIAS-PEDRAZ, J. M., LORRAIN, S., FANKHAUSER, C., BLAZQUEZ, M. A., TITARENKO, E. & PRAT, S. 2008. A molecular framework for light and gibberellin control of cell elongation. *Nature,* 451**,** 480-U11.

DE LUCAS, M. & PRAT, S. 2014. PIFs get BRright: PHYTOCHROME INTERACTING FACTORs as integrators of light and hormonal signals. *New Phytologist,* 202**,** 1126-41.

DE WIT, M., GALVAO, V. C. & FANKHAUSER, C. 2016. Light-mediated hormonal regulation of plant growth and development. *Annual Review of Plant Biology,* 67**,** 513-537.

DEHESH, K., TEPPERMAN, J., CHRISTENSEN, A. H. & QUAIL, P. H. 1991. Phyb is evolutionarily conserved and constitutively expressed in rice seedling shoots. *Molecular & General Genetics,* 225**,** 305-313.

DENG, X. W., MATSUI, M., WEI, N., WAGNER, D., CHU, A. M., FELDMANN, K. A. & QUAIL, P. H. 1992. Cop1, an Arabidopsis regulatory gene, encodes a protein with both a zinc-binding motif and a G-beta homologous domain. *Cell,* 71**,** 791-801.

DENG, X. W. & QUAIL, P. H. 1999. Signalling in light-controlled development. *Seminars in Cell & Developmental Biology,* 10**,** 121-129.

DEREGIBUS, V. A., SANCHEZ, R. A. & CASAL, J. J. 1983. Effects of light quality on tiller production in Lolium spp. *Plant Physiology***,** 900-902.

DILL, A., JUNG, H. S. & SUN, T. P. 2001. The DELLA motif is essential for gibberellin-induced degradation of RGA. *Proceedings of the National Academy of Sciences of the United States of America,* 98**,** 14162-14167.

DIXON, J., H.-J. BRAUN, P. KOSINA, AND J. CROUCH (EDS.) 2009. Wheat facts and futures. *In:* CIMMYT (ed.) *D.F.* Mexico.

DJAKOVIC-PETROVIC, T., DE WIT, M., VOESENEK, L. A. C. J. & PIERIK, R. 2007. DELLA protein function in growth responses to canopy signals. *Plant Journal,* 51**,** 117-126.

DO, P. T., DE TAR, J. R., LEE, H., FOLTA, M. K. & ZHANG, Z. Y. J. 2016. Expression of ZmGA20ox cDNA alters plant morphology and increases biomass production of switchgrass (Panicum virgatum L.). *Plant Biotechnology Journal,* 14**,** 1532-1540.

DOMAGALSKA, M. A., SCHOMBURG, F. M., AMASINO, R. M., VIERSTRA, R. D., NAGY, F. & DAVIS, S. J. 2007. Attenuation of brassinosteroid signaling enhances FLC expression and delays flowering. *Development,* 134**,** 2841-2850.

DOMINGUEZ, F. & CEJUDO, F. J. 1999. Patterns of starchy endosperm acidification and protease gene expression in wheat grains following germination. *Plant Physiology,* 119**,** 81-87.

DOU, M., CHENG, S., ZHAO, B., XUAN, Y. & SHAO, M. 2016. The indeterminate domain protein ROC1 regulates chilling tolerance via activation of DREB1B/CBF1 in rice. *International Journal of Molecular Sciences,* 17**,** 233.

DUEK, P. D., ELMER, M. V., VAN OOSTEN, V. R. & FANKHAUSER, C. 2004. The degradation of HFR1, a putative bHLH class transcription factor involved in light signaling, is regulated by phosphorylation and requires COP1. *Current Biology,* 14**,** 2296-2301.

DUEK, P. D. & FANKHAUSER, C. 2005. bHLH class transcription factors take centre stage in phytochrome signalling. *Trends in Plant Science,* 10**,** 51-54.

EDWARDS, D., BATLEY, J. & SNOWDON, R. J. 2013a. Accessing complex crop genomes with next-generation sequencing. *Theoretical and Applied Genetics,* 126**,** 1-11.

EDWARDS, D., BATLEY, J. & SNOWDON, R. J. 2013b. Accessing complex crop genomes with next-generation sequencing. *Theoretical and Applied Genetic,* 126**,** 1-11.

ELLIS, M. H., REBETZKE, G. J., CHANDLER, P., BONNETT, D., SPIELMEYER, W. & RICHARDS, R. A. 2004. The effect of different height reducing genes on the early growth of wheat. *Functional Plant Biology,* 31**,** 583-589.

ERIKSSON, S., BOHLENIUS, H., MORITZ, T. & NILSSON, O. 2006. GA(4) is the active gibberellin in the regulation of LEAFY transcription and Arabidopsis floral initiation. *Plant Cell,* 18**,** 2172-2181.

EVENSON, R. E. & GOLLIN, D. 2003. Assessing the impact of the Green Revolution, 1960 to 2000. *Science,* 300**,** 758-762.

FAN, W. H. & DONG, X. N. 2002. In vivo interaction between NPR1 and transcription factor TGA2 leads to salicylic acid-mediated gene activation in Arabidopsis. *The Plant Cell,* 14**,** 1377-1389.

FAO 2016. The state of food and agriculture 2016. *State of Food and Agriculture.*

FAO, I. A. W. 2013. The state of food insecurity in the world: The multiple dimensions of food security. *In:* NATIONS, F. A. A. O. O. T. U. (ed.). Rome: FAO.

FELLER, A., MACHEMER, K., BRAUN, E. L. & GROTEWOLD, E. 2011. Evolutionary and comparative analysis of MYB and bHLH plant transcription factors. *Plant Journal,* 66**,** 94-116.

FENG, S. H., MARTINEZ, C., GUSMAROLI, G., WANG, Y., ZHOU, J. L., WANG, F., CHEN, L. Y., YU, L., IGLESIAS-PEDRAZ, J. M., KIRCHER, S., SCHAFER, E., FU, X. D., FAN, L. M. & DENG, X. W. 2008. Coordinated regulation of Arabidopsis thaliana development by light and gibberellins. *Nature,* 451**,** 475-U9.

FERNANDEZ-CALVO, P., CHINI, A., FERNANDEZ-BARBERO, G., CHICO, J. M., GIMENEZ-IBANEZ, S., GEERINCK, J., EECKHOUT, D., SCHWEIZER, F., GODOY, M., FRANCO-ZORRILLA, J. M., PAUWELS, L., WITTERS, E., PUGA, M. I., PAZ-ARES, J., GOOSSENS, A., REYMOND, P., DE JAEGER, G. & SOLANO, R. 2011. The Arabidopsis bHLH transcription factors MYC3 and MYC4 are targets of JAZ repressors and act additively with MYC2 in the activation of jasmonate responses. *Plant Cell,* 23**,** 701-715.

FEURTADO, J. A., HUANG, D. Q., WICKI-STORDEUR, L., HEMSTOCK, L. E., POTENTIER, M. S., TSANG, E. W. T. & CUTLER, A. J. 2011. The Arabidopsis C2H2 zinc finger INDETERMINATE DOMAIN1/ENHYDROUS promotes the transition to germination by regulating light and hormonal signaling during seed maturation. *Plant Cell,* 23**,** 1772-1794.

FIELDS, S. & SONG, O. K. 1989. A novel genetic system to detect protein-protein interactions. *Nature,* 340**,** 245-246.

FINLAYSON, S. A., KRISHNAREDDY, S. R., KEBROM, T. H. & CASAL, J. J. 2010. Phytochrome regulation of branching in Arabidopsis. *Plant Physiology,* 152**,** 1914-1927.

FIRE, A., XU, S. Q., MONTGOMERY, M. K., KOSTAS, S. A., DRIVER, S. E. & MELLO, C. C. 1998. Potent and specific genetic interference by double-stranded RNA in Caenorhabditis elegans. *Nature,* 391**,** 806-811.

FLINTHAM, J. E., ANGUS, W. J. & GALE, M. D. 1997a. Heterosis, overdominance for grain yield, and alpha-amylase activity in F-1 hybrids between near-isogenic Rht dwarf and tall wheats. *Journal of Agricultural Science,* 129**,** 371-378.

FLINTHAM, J. E., BORNER, A., WORLAND, A. J. & GALE, M. D. 1997b. Optimizing wheat grain yield: Effects of Rht (gibberellin-insensitive) dwarfing genes. *Journal of Agricultural Science,* 128**,** 11-25.

FOLEY, J. A., RAMANKUTTY, N., BRAUMAN, K. A., CASSIDY, E. S., GERBER, J. S., JOHNSTON, M., MUELLER, N. D., O'CONNELL, C., RAY, D. K., WEST, P. C., BALZER, C., BENNETT, E. M., CARPENTER, S. R., HILL, J., MONFREDA, C., POLASKY, S., ROCKSTROM, J., SHEEHAN, J., SIEBERT, S., TILMAN, D. & ZAKS, D. P. 2011. Solutions for a cultivated planet. *Nature,* 478**,** 337-42.

FOO, E., PLATTEN, J. D., WELLER, J. L. & REID, J. B. 2006. PhyA and cry1 act redundantly to regulate gibberellin levels during de-etiolation in blue light. *Physiologia Plantarum,* 127**,** 149-156.

FRANKLIN, K. A. 2008. Shade avoidance. *New Phytologist,* 179**,** 930-944.

FRIGERIO, M., ALABADI, D., PEREZ-GOMEZ, J., GARCIA-CARCEL, L., PHILLIPS, A. L., HEDDEN, P. & BLAZQUEZ, M. A. 2006. Transcriptional regulation of gibberellin metabolism genes by auxin signaling in arabidopsis. *Plant Physiology,* 142**,** 553-563.

FRIML, J., WISNIEWSKA, J., BENKOVA, E., MENDGEN, K. & PALME, K. 2002. Lateral relocation of auxin efflux regulator PIN3 mediates tropism in Arabidopsis. *Nature,* 415**,** 806-809.

FU, X. D. & HARBERD, N. P. 2003. Auxin promotes Arabidopsis root growth by modulating gibberellin response. *Nature,* 421**,** 740-743.

FU, X. D., RICHARDS, D. E., AIT-ALI, T., HYNES, L. W., OUGHAM, H., PENG, J. R. & HARBERD, N. P. 2002. Gibberellin-mediated proteasome-dependent degradation of the barley DELLA protein SLN1 repressor. *Plant Cell,* 14**,** 3191-3200.

FU, X. D., SUDHAKAR, D., PENG, J. R., RICHARDS, D. E., CHRISTOU, P. & HARBERD, N. P. 2001. Expression of arabidopsis GAI in transgenic rice represses multiple gibberellin responses. *Plant Cell,* 13**,** 1791-1802.

FUKAZAWA, J., NAKATA, M., ITO, T., MATSUSHITA, A., YAMAGUCHI, S. & TAKAHASHI, Y. 2011. bZIP transcription factor RSG controls the feedback regulation of NtGA20ox1 via intracellular localization and epigenetic mechanism. *Plant Signaling & Behavior,* 6**,** 26-8.

FUKAZAWA, J., NAKATA, M., ITO, T., YAMAGUCHI, S. & TAKAHASHI, Y. 2010. The transcription factor RSG regulates negative feedback of NtGA20ox1 encoding GA 20-oxidase. *Plant Journal,* 62**,** 1035-1045.

FUKAZAWA, J., TERAMURA, H., MURAKOSHI, S., NASUNO, K., NISHIDA, N., ITO, T., YOSHIDA, M., KAMIYA, Y., YAMAGUCHI, S. & TAKAHASHI, Y. 2014. DELLAs function as coactivators of GAI-ASSOCIATED FACTOR1 in regulation of gibberellin homeostasis and signaling in Arabidopsis. *Plant Cell,* 26**,** 2920-2938.

GALLAGHER, S., SHORT, T. W., RAY, P. M., PRATT, L. H. & BRIGGS, W. R. 1988. Light-mediated changes in 2 proteins found associated with plasma-membrane fractions from pea stem sections. *Proceedings of the National Academy of Sciences of the United States of America,* 85**,** 8003-8007.

GAN, S. S. & AMASINO, R. M. 1995. Inhibition of leaf senescence by autoregulated production of cytokinin. *Science,* 270**,** 1986-1988.

GAO, Y., JIANG, W., DAI, Y., XIAO, N., ZHANG, C. Q., LI, H., LU, Y., WU, M. Q., TAO, X. Y., DENG, D. X. & CHEN, J. M. 2015. A maize phytochrome-interacting factor 3 improves drought and salt stress tolerance in rice. *Plant Molecular Biology,* 87**,** 413-428.

GODFRAY, H. C. J., BEDDINGTON, J. R., CRUTE, I. R., HADDAD, L., LAWRENCE, D., MUIR, J. F., PRETTY, J., ROBINSON, S., THOMAS, S. M. & TOULMIN, C. 2010. Food security: The challenge of feeding 9 billion people. *Science,* 327**,** 812-818.

GOESCHL, J. D., RAPPAPORT, L. & PRATT, H. K. 1966. Ethylene as a factor regulating growth of pea epicotyls subjected to physical stress. *Plant Physiology,* 41**,** 877-+.

GOINS, G. D., YORIO, N. C., SANWO, M. M. & BROWN, C. S. 1997. Photomorphogenesis, photosynthesis, and seed yield of wheat plants grown under red light-emitting diodes (LEDs) with and without supplemental blue lighting. *Journal of Experimental Botany,* 48**,** 1407-1413.

GOMEZ-CADENAS, A., ZENTELLA, R., WALKER-SIMMONS, M. K. & HO, T. H. D. 2001. Gibberellin/abscisic acid antagonism in barley aleurone cells: Site of action of the protein kinase PKABA1 in relation to gibberellin signaling molecules. *Plant Cell,* 13**,** 667-679.

GOMI, K., SASAKI, A., ITOH, H., UEGUCHI-TANAKA, M., ASHIKARI, M., KITANO, H. & MATSUOKA, M. 2004. GID2, an F-box subunit of the SCF E3 complex, specifically interacts with phosphorylated SLR1 protein and regulates the gibberellin-dependent degradation of SLR1 in rice. *Plant Journal,* 37**,** 626-634.

GRIFFITHS, J., MURASE, K., RIEU, I., ZENTELLA, R., ZHANG, Z. L., POWERS, S. J., GONG, F., PHILLIPS, A. L., HEDDEN, P., SUN, T. P. & THOMAS, S. G. 2006. Genetic characterization and functional analysis of the GID1 gibberellin receptors in Arabidopsis. *Plant Cell,* 18**,** 3399-3414.

HAMMOND, S. M., CAUDY, A. A. & HANNON, G. J. 2001. Post-transcriptional gene silencing by double-stranded RNA. *Nature Reviews Genetics,* 2**,** 110-119.

HAN, F. M. & ZHU, B. G. 2011. Evolutionary analysis of three gibberellin oxidase genesin rice, Arabidopsis, and soybean. *Gene,* 473**,** 23-35.

HARPHAM, N. V. J., BERRY, A. W., KNEE, E. M., ROVEDAHOYOS, G., RASKIN, I., SANDERS, I. O., SMITH, A. R., WOOD, C. K. & HALL, M. A. 1991. The effect of ethylene on the growth and development of wild-type and mutant Arabidopsis-thaliana (L) heynh. *Annals of Botany,* 68**,** 55-61.

HATTORI, Y., NAGAI, K., FURUKAWA, S., SONG, X. J., KAWANO, R., SAKAKIBARA, H., WU, J. Z., MATSUMOTO, T., YOSHIMURA, A., KITANO, H., MATSUOKA, M., MORI, H. & ASHIKARI, M. 2009. The ethylene response factors SNORKEL1 and SNORKEL2 allow rice to adapt to deep water. *Nature,* 460**,** 1026-U116.

HAY, A., CRAFT, J. & TSIANTIS, M. 2004. Plant hormones and homeoboxes: Bridging the gap? *Bioessays,* 26**,** 395-404.

HE, C., HOLME, J. & ANTHONY, J. 2014. SNP genotyping: the KASP assay. *Methods Mol Biol,* 1145**,** 75-86.

HEDDEN, P. 1997. The oxidases of gibberellin biosynthesis: Their function and mechanism. *Physiologia Plantarum,* 101**,** 709-719.

HEDDEN, P. 2003. The genes of the Green Revolution. *Trends in Genetics,* 19**,** 5-9.

HEDDEN, P. & PHILLIPS, A. L. 2000. Gibberellin metabolism: new insights revealed by the genes. *Trends in Plant Science,* 5**,** 523-530.

HEDDEN, P. & THOMAS, S. G. 2012. Gibberellin biosynthesis and its regulation. *Biochemical Journal,* 444**,** 11-25.

HEGEDUS, N. & MARX, F. 2013. Antifungal proteins: More than antimicrobials? *Fungal Biology Reviews,* 26**,** 132-145.

HEIJDE, M. & ULM, R. 2012. UV-B photoreceptor-mediated signalling in plants. *Trends in Plant Science,* 17**,** 230-237.

HEIM, M. A., JAKOBY, M., WERBER, M., MARTIN, C., WEISSHAAR, B. & BAILEY, P. C. 2003. The basic helix-loop-helix transcription factor family in plants: A genome-wide study of protein structure and functional diversity. *Molecular Biology and Evolution,* 20**,** 735-747.

HELLIWELL, C. A., CHANDLER, P. M., POOLE, A., DENNIS, E. S. & PEACOCK, W. J. 2001. The CYP88A cytochrome P450, ent-kaurenoic acid oxidase, catalyzes three steps of the gibberellin biosynthesis pathway. *Proceedings of the National Academy of Sciences of the United States of America,* 98**,** 2065-2070.

HELLIWELL, C. A., POOLE, A., PEACOCK, W. J. & DENNIS, E. S. 1999. Arabidopsis ent-kaurene oxidase catalyzes three steps of gibberellin biosynthesis. *Plant Physiology,* 119**,** 507-510.

HELLIWELL, C. A. & WATERHOUSE, P. M. 2005. Constructs and methods for hairpin RNA-mediated gene silencing in plants. *Methods in Enzymology,* 392**,** 24-35.

HIRANO, K., KOUKETU, E., KATOH, H., AYA, K., UEGUCHI-TANAKA, M. & MATSUOKA, M. 2012. The suppressive function of the rice DELLA protein SLR1 is dependent on its transcriptional activation activity. *Plant Journal,* 71**,** 443-453.

HIROSE, F., SHINOMURA, T., TANABATA, T., SHIMADA, H. & TAKANO, M. 2006. Involvement of rice cryptochromes in de-etiolation responses and flowering. *Plant and Cell Physiology,* 47**,** 915-925.

HIRSCH, S., KIM, J., MUNOZ, A., HECKMANN, A. B., DOWNIE, J. A. & OLDROYD, G. E. 2009. GRAS proteins form a DNA binding complex to induce gene expression during nodulation signaling in Medicago truncatula. *Plant Cell,* 21**,** 545-57.

HONG, G. J., XUE, X. Y., MAO, Y. B., WANG, L. J. & CHEN, X. Y. 2012a. Arabidopsis MYC2 interacts with DELLA proteins in regulating sesquiterpene synthase gene expression. *Plant Cell,* 24**,** 2635-2648.

HONG, M. J., KIM, D. Y., KANG, S. Y., KIM, D. S., KIM, J. B. & SEO, Y. W. 2012b. Wheat F-box protein recruits proteins and regulates their abundance during wheat spike development. *Molecular Biology Reports,* 39**,** 9681-9696.

HONG, M. J., KIM, D. Y. & SEO, Y. W. 2013. SKP1-like-related genes interact with various F-box proteins and may form SCF complexes with Cullin-F-box proteins in wheat. *Molecular Biology Reports,* 40**,** 969-981.

HONG, M. J., KIM, D. Y. & SEO, Y. W. 2014. Cullin, a component of the SCF complex, interacts with TaRMD5 during wheat spike development. *Biologia Plantarum,* 58**,** 218-230.

HOU, X. L., HU, W. W., SHEN, L. S., LEE, L. Y. C., TAO, Z., HAN, J. H. & YU, H. 2008. Global identification of DELLA target genes during Arabidopsis flower development. *Plant Physiology,* 147**,** 1126-1142.

HU, J. H., MITCHUM, M. G., BARNABY, N., AYELE, B. T., OGAWA, M., NAM, E., LAI, W. C., HANADA, A., ALONSO, J. M., ECKER, J. R., SWAIN, S. M., YAMAGUCHI, S., KAMIYA, Y. & SUN, T. P. 2008. Potential sites of bioactive gibberellin production during reproductive growth in Arabidopsis. *Plant Cell,* 20**,** 320-336.

HUQ, E., AL-SADY, B., HUDSON, M., KIM, C., APEL, K. & QUAIL, P. H. 2004a. PHYTOCHROME-INTERACTING FACTOR 1 Is a Critical bHLH Regulator of Chlorophyll Biosynthesis. *Science,* 305**,** 1937-1941.

HUQ, E., AL-SADY, B., HUDSON, M., KIM, C. H., APEL, M. & QUAIL, P. H. 2004b. PHYTOCHROME-INTERACTING FACTOR 1 is a critical bHLH regulator of chlorophyll biosynthesis. *Science,* 305**,** 1937-1941.

HUQ, E. & QUAIL, P. H. 2002a. PIF4, a phytochrome-interacting bHLH factor, functions as a negative regulator of phytochrome B signaling in *Arabidopsis*. *The Embo Journal,* 21**,** 2441-2450.

HUQ, E. & QUAIL, P. H. 2002b. PIF4, a phytochrome-interacting bHLH factor, functions as a negative regulator of phytochrome B signaling in Arabidopsis. *Embo Journal,* 21**,** 2441-2450.

HUSSAIN, A., CAO, D. N., CHENG, H., WEN, Z. L. & PENG, J. R. 2005. Identification of the conserved serine/threonine residues important for gibberellin-sensitivity of *Arabidopsis* RGL2 protein. *Plant Journal,* 44**,** 88-99.

HUSSAIN, A., CAO, D. N. & PENG, J. R. 2007. Identification of conserved tyrosine residues important for gibberellin sensitivity of Arabidopsis RGL2 protein. *Planta,* 226**,** 475-483.

HWANG, G., ZHU, J. Y., LEE, Y. K., KIM, S., NGUYEN, T. T., KIM, J. & OH, E. 2017. PIF4 Promotes Expression of LNG1 and LNG2 to Induce Thermomorphogenic Growth in Arabidopsis. *Frontiers in Plant Science,* 8.

IKEDA, A., UEGUCHI-TANAKA, M., SONODA, Y., KITANO, H., KOSHIOKA, M., FUTSUHARA, Y., MATSUOKA, M. & YAMAGUCHI, J. 2001. slender rice, a constitutive gibberellin response mutant, is caused by a null mutation of the SLR1 gene, an ortholog of the height-regulating gene GAI/RGA/RHT/D8. *Plant Cell,* 13**,** 999-1010.

INOUE, K., NISHIHAMA, R., KATAOKA, H., HOSAKA, M., MANABE, R., NOMOTO, M., TADA, Y., ISHIZAKI, K. & KOHCHI, T. 2016. Phytochrome Signaling Is Mediated by PHYTOCHROME INTERACTING FACTOR in the Liverwort Marchantia polymorpha. *Plant Cell,* 28**,** 1406-1421.

INTERNATIONAL WHEAT GENOME SEQUENCING, C. 2014. A chromosome-based draft sequence of the hexaploid bread wheat (Triticum aestivum) genome. *Science,* 345**,** 1251788.

ITOH, H., UEGUCHI-TANAKA, M., SATO, Y., ASHIKARI, M. & MATSUOKA, M. 2002. The gibberellin signaling pathway is regulated by the appearance and disappearance of SLENDER RICE1 in nuclei. *Plant Cell,* 14**,** 57-70.

JANG, I. C., HENRIQUES, R., SEO, H. S., NAGATANI, A. & CHUA, N. H. 2010. Arabidopsis PHYTOCHROME INTERACTING FACTOR proteins promote phytochrome B polyubiquitination by COP1 E3 ligase in the nucleus. *Plant Cell,* 22**,** 2370-83.

JASINSKI, S., PIAZZA, P., CRAFT, J., HAY, A., WOOLLEY, L., RIEU, I., PHILLIPS, A., HEDDEN, P. & TSIANTIS, M. 2005. KNOX action in Arabidopsis is mediated by coordinate regulation of cytokinin and gibberellin activities. *Current Biology,* 15**,** 1560-1565.

JEONG, J. & CHOI, G. 2013. Phytochrome-interacting factors have both shared and distinct biological roles. *Molecules and Cells,* 35**,** 371-80.

JIANG, X. S., LI, H. Y., WANG, T., PENG, C. L., WANG, H. Y., WU, H. & WANG, X. J. 2012. Gibberellin indirectly promotes chloroplast biogenesis as a means to maintain the chloroplast population of expanded cells. *Plant Journal,* 72**,** 768-780.

JOSSE, E. M., GAN, Y. B., BOU-TORRENT, J., STEWART, K. L., GILDAY, A. D., JEFFREE, C. E., VAISTIJ, F. E., MARTINEZ-GARCIA, J. F., NAGY, F., GRAHAM, I. A. & HALLIDAY, K. J. 2011. A DELLA in disguise: SPATULA restrains the growth of the developing Arabidopsis seedling. *Plant Cell,* 23**,** 1337-1351.

KAISERLI, E. & JENKINS, G. I. 2007. UV-B promotes rapid nuclear translocation of the Arabidopsis UV-B-specific signaling component UVR8 and activates its function in the nucleus. *Plant Cell,* 19**,** 2662-2673.

KAMATH, R. S., FRASER, A. G., DONG, Y., POULIN, G., DURBIN, R., GOTTA, M., KANAPIN, A., LE BOT, N., MORENO, S., SOHRMANN, M., WELCHMAN, D. P., ZIPPERLEN, P. & AHRINGER, J. 2003. Systematic functional analysis of the Caenorhabditis elegans genome using RNAi. *Nature,* 421**,** 231-237.

KANAOKA, M. M., PILLITTERI, L. J., FUJII, H., YOSHIDA, Y., BOGENSCHUTZ, N. L., TAKABAYASHI, J., ZHU, J. K. & TORII, K. U. 2008. SCREAM/ICE1 and SCREAM2 specify three cell-state transitional steps leading to Arabidopsis stomatal differentiation. *Plant Cell,* 20**,** 1775-85.

KANEKO, M., ITOH, H., INUKAI, Y., SAKAMOTO, T., UEGUCHI-TANAKA, M., ASHIKARI, M. & MATSUOKA, M. 2003. Where do gibberellin biosynthesis and gibberellin signaling occur in rice plants? *Plant Journal,* 35**,** 104-115.

KASAHARA, H., HANADA, A., KUZUYAMA, T., TAKAGI, M., KAMIYA, Y. & YAMAGUCHI, S. 2002. Contribution of the mevalonate and methylerythritol phosphate pathways to the biosynthesis of gibberellins in Arabidopsis. *Journal of Biological Chemistry,* 277**,** 45188-45194.

KAY, S. A., KEITH, B., SHINOZAKI, K. & CHUA, N. H. 1989. The sequence of the rice phytochrome gene. *Nucleic Acids Research,* 17**,** 2865-2866.

KHANNA, R., HUQ, E., KIKIS, E. A., AL-SADY, B., LANZATELLA, C. & QUAIL, P. H. 2004. A novel molecular recognition motif necessary for targeting photoactivated phytochrome signaling to specific basic helix-loop-helix transcription factors. *Plant Cell,* 16**,** 3033-3044.

KIDOKORO, S., MARUYAMA, K., NAKASHIMA, K., IMURA, Y., NARUSAKA, Y., SHINWARI, Z. K., OSAKABE, Y., FUJITA, Y., MIZOI, J., SHINOZAKI, K. & YAMAGUCHI-SHINOZAKI, K. 2009. The phytochrome-interacting factor PIF7 negatively regulates DREB1 expression under circadian control in Arabidopsis. *Plant Physiology,* 151**,** 2046-2057.

KIM, J., HARTER, K. & THEOLOGIS, A. 1997. Protein-protein interactions among the Aux/IAA proteins. *Proceedings of the National Academy of Sciences of the United States of America,* 94**,** 11786-11791.

KIM, J., SONG, K., PARK, E., KIM, K., BAE, G. & CHOI, G. 2016. Epidermal phytochrome B inhibits hypocotyl negative gravitropism non-cell-autonomously. *Plant Cell,* 28**,** 2770-2785.

KING, R. W., MORITZ, T., EVANS, L. T., JUNTTILA, O. & HERLT, A. J. 2001. Long-day induction of flowering in Lolium temulentum involves sequential increases in specific gibberellins at the shoot apex. *Plant Physiology,* 127**,** 624-632.

KLIEBENSTEIN, D. J., LIM, J. E., LANDRY, L. G. & LAST, R. L. 2002. Arabidopsis UVR8 regulates ultraviolet-B signal transduction and tolerance and contains sequence similarity to human Regulator of Chromatin Condensation 1. *Plant Physiology,* 130**,** 234-243.

KOINI, M. A., ALVEY, L., ALLEN, T., TILLEY, C. A., HARBERD, N. P., WHITELAM, G. C. & FRANKLIN, K. A. 2009. High temperature-medated adaptations in plant architecture require the bHLH transcription factor PIF4. *Current Biology,* 19**,** 408-413.

KOORNNEEF, M., ELGERSMA, A., HANHART, C. J., VANLOENENMARTINET, E. P., VANRIJN, L. & ZEEVAART, J. A. D. 1985. A gibberellin insensitive mutant of Arabidopsis thaliana. *Physiologia Plantarum,* 65**,** 33-39.

KOORNNEEF, M. & VANDERVEEN, J. H. 1980. Induction and Analysis of Gibberellin Sensitive Mutants in Arabidopsis-Thaliana (L) Heynh. *Theoretical and Applied Genetics,* 58**,** 257-263.

KRASILEVA, K. V., VASQUEZ-GROSS, H. A., HOWELL, T., BAILEY, P., PARAISO, F., CLISSOLD, L., SIMMONDS, J., RAMIREZ-GONZALEZ, R. H., WANG, X. D., BORRILL, P., FOSKER, C., AYLING, S., PHILLIPS, A. L., UAUY, C. & DUBCOVSKY, J. 2017. Uncovering hidden variation in polyploid wheat. *Proceedings of the National Academy of Sciences of the United States of America,* 114**,** E913-E921.

KRZANOWSKI, W. J. 2000. *Principles of multivariate analysis: a user's perspective. Revised edition*, Clarendon Press, Oxford, UK.

KUCERA, B., COHN, M. A. & LEUBNER-METZGER, G. 2005. Plant hormone interactions during seed dormancy release and germination. *Seed Science Research,* 15**,** 281-307.

KUMAR, I., SWAMINATHAN, K., HUDSON, K. & HUDSON, M. E. 2016. Evolutionary divergence of phytochrome protein function in Zea mays PIF3 signaling. *Journal of Experimental Botany,* 67**,** 4231-4240.

KUMAR, S. V., LUCYSHYN, D., JAEGER, K. E., ALOS, E., ALVEY, E., HARBERD, N. P. & WIGGE, P. A. 2012. Transcription factor PIF4 controls the thermosensory activation of flowering. *Nature,* 484**,** 242-5.

KUMARAN, M. K., BOWMAN, J. L. & SUNDARESAN, V. 2002. YABBY polarity genes mediate the repression of KNOX homeobox genes in Arabidopsis. *The Plant Cell,* 14**,** 2761-2770.

KUNIHIRO, A., YAMASHINO, T. & MIZUNO, T. 2010. PHYTOCHROME-INTERACTING FACTORS PIF4 and PIF5 are implicated in the regulation of hypocotyl elongation in response to blue light in Arabidopsis thaliana. *Bioscience Biotechnology and Biochemistry,* 74**,** 2538-2541.

KUNIHIRO, A., YAMASHINO, T., NAKAMICHI, N., NIWA, Y., NAKANISHI, H. & MIZUNO, T. 2011. Phytochrome-interacting factor 4 and 5 (PIF4 and PIF5) activate the homeobox ATHB2 and auxin-inducible IAA29 genes in the coincidence mechanism underlying photoperiodic control of plant growth of Arabidopsis thaliana. *Plant Cell Physiol,* 52**,** 1315-29.

LAGARIAS, J. C. & MERCURIO, F. M. 1985. Structure-function studies on phytochrome - identification of light-induced conformational-changes in 124-Kda avena phytochrome invitro. *Journal of Biological Chemistry,* 260**,** 2415-2423.

LANCET, T. 2013. Maternal and Child Nutrition. *In:* LANCET, T. (ed.).

LANGRIDGE, J. 1957. Effect of Day-Length and Gibberellic Acid on the Flowering of Arabidopsis. *Nature,* 180**,** 36-37.

LAWIT, S. J., WYCH, H. M., XU, D. P., KUNDU, S. & TOMES, D. T. 2010. Maize DELLA proteins dwarf plant8 and dwarf plant9 as modulators of plant development. *Plant and Cell Physiology,* 51**,** 1854-1868.

LEE, J., HE, K., STOLC, V., LEE, H., FIGUEROA, P., GAO, Y., TONGPRASIT, W., ZHAO, H. Y., LEE, I. & DENG, X. 2007. Analysis of transcription factor HY5 genomic binding sites revealed its hierarchical role in light regulation of development. *Plant Cell,* 19**,** 731-749.

LEE, K. P., PISKUREWICZ, U., TURECKOVA, V., CARAT, S., CHAPPUIS, R., STRNAD, M., FANKHAUSER, C. & LOPEZ-MOLINA, L. 2012. Spatially and genetically distinct control of seed germination by phytochromes A and B. *Genes & Development,* 26**,** 1984-1996.

LEE, S. C., CHENG, H., KING, K. E., WANG, W. F., HE, Y. W., HUSSAIN, A., LO, J., HARBERD, N. P. & PENG, J. R. 2002. Gibberellin regulates Arabidopsis seed germination via RGL2, a GAI/RGA-like gene whose expression is up-regulated following imbibition. *Genes & Development,* 16**,** 646-658.

LEIVAR, P., MONTE, E., AL-SADY, B., CARLE, C., STORER, A., ALONSO, J. M., ECKER, J. R. & QUAIL, P. H. 2008a. The Arabidopsis phytochrome-interacting factor PIF7, together with PIF3 and PIF4, regulates responses to prolonged red light by modulating phyB levels. *Plant Cell,* 20**,** 337-52.

LEIVAR, P., MONTE, E., OKA, Y., LIU, T., CARLE, C., CASTILLON, A., HUQ, E. & QUAIL, P. H. 2008b. Multiple phytochrome-interacting bHLH transcription factors repress premature seedling photomorphogenesis in darkness. *Current Biology,* 18**,** 1815-1823.

LEIVAR, P., TEPPERMAN, J. M., MONTE, E., CALDERON, R. H., LIU, T. L. & QUAIL, P. H. 2009. Definition of early transcriptional circuitry involved in light-induced reversal of PIF-imposed repression of photomorphogenesis in young Arabidopsis seedlings. *Plant Cell,* 21**,** 3535-53.

LELE, U. 2010. Food security for a billion poor. *Science,* 327**,** 1554-1554.

LEWANDOWSKA, M. A. 2013. The missing puzzle piece: splicing mutations. *International Journal of Clinical and Experimental Pathology,* 6**,** 2675-2682.

LI, K. L., YU, R. B., FAN, L. M., WEI, N., CHEN, H. D. & DENG, X. W. 2016a. DELLA-mediated PIF degradation contributes to coordination of light and gibberellin signalling in Arabidopsis. *Nature Communications,* 7.

LI, L., LJUNG, K., BRETON, G., SCHMITZ, R. J., PRUNEDA-PAZ, J., COWING-ZITRON, C., COLE, B. J., IVANS, L. J., PEDMALE, U. V., JUNG, H. S., ECKER, J. R., KAY, S. A. & CHORY, J. 2012a. Linking photoreceptor excitation to changes in plant architecture. *Genes & Development,* 26**,** 785-90.

LI, L., PENG, W.-F., LIU, Q.-Q., ZHOU, J.-J., LIANG, W.-H. & XIE, X.-Z. 2012b. Expression patterns of OsPIL11, a phytochrome-interacting factor in rice, and preliminary analysis of its roles in light signal transduction. *Rice Science,* 19**,** 263-268.

LI, L., PENG, W. F., LIU, Q., ZHOU, J. J., LIANG, W. H. & XIE, X. Z. 2012c. Expression patterns of OsPIL11, a phytochrome-interacting factor in rice, and preliminary analysis of its roles in light signal transduction. *Rice Science,* 19**,** 263-268.

LI, M. Z., AN, F. Y., LI, W. Y., MA, M. D., FENG, Y., ZHANG, X. & GUO, H. W. 2016b. DELLA proteins interact with FLC to repress flowering transition. *Journal of Integrative Plant Biology,* 58**,** 642-655.

LI, Q. F., WANG, C. M., JIANG, L., LI, S., SUN, S. S. M. & HE, J. X. 2012d. An interaction between BZR1 and DELLAs mediates direct signaling crosstalk between brassinosteroids and gibberellins in *Arabidopsis*. *Science Signaling,* 5.

LI, S. X., CONG, Y. H., LIU, Y. P., WANG, T. T., SHUAI, Q., CHEN, N. N., GAI, J. Y. & LI, Y. 2017. Optimization of agrobacterium-mediated transformation in soybean. *Frontiers in Plant Science,* 8.

LI, W., WANG, H. P. & YU, D. Q. 2016c. Arabidopsis WRKY transcription factors WRKY12 and WRKY13 oppositely regulate flowering under short-day conditions. *Molecular Plant,* 9**,** 1492-1503.

LIANG, Z., CHEN, K. L., LI, T. D., ZHANG, Y., WANG, Y. P., ZHAO, Q., LIU, J. X., ZHANG, H. W., LIU, C. M., RAN, Y. D. & GAO, C. X. 2017. Efficient DNA-free genome editing of bread wheat using CRISPR/Cas9 ribonucleoprotein complexes. *Nature Communications,* 8.

LIEBERMAN-LAZAROVICH, M. & LEVY, A. A. 2011. Homologous recombination in plants: an antireview. *Methods in Molecular Biology,* 701**,** 51-65.

LIEBSCH, D. & KEECH, O. 2016. Dark-induced leaf senescence: new insights into a complex light-dependent regulatory pathway. *New Phytologist,* 212**,** 563-570.

LILJEGREN, S. J., DITTA, G. S., ESHED, H. Y., SAVIDGE, B., BOWMAN, J. L. & YANOFSKY, M. F. 2000. SHATTERPROOF MADS-box genes control seed dispersal in Arabidopsis. *Nature,* 404**,** 766-770.

LIN, C. T., ROBERTSON, D. E., AHMAD, M., RAIBEKAS, A. A., JORNS, M. S., DUTTON, P. L. & CASHMORE, A. R. 1995. Association of flavin adenine-dinucleotide with the *Arabidopsis* blue-light receptor Cry1. *Science,* 269**,** 968-970.

LIN, R. 2007. Transposase-derived transcription factors regulate light signaling in Arabidopsis. *Science,* 318**,** 1866-1866.

LIN, R. C., DING, L., CASOLA, C., RIPOLL, D. R., FESCHOTTE, C. & WANG, H. Y. 2007. Transposase-derived transcription factors regulate light signaling in Arabidopsis. *Science,* 318**,** 1302-1305.

LIN, R. C. & WANG, H. Y. 2004. *Arabidopsis* FHY3/FAR1 gene family and distinct roles of its members in light control of *Arabidopsis* development. *Plant Physiology,* 136**,** 4010-4022.

LISCUM, E. & BRIGGS, W. R. 1995. Mutations in the Nph1 locus of *Arabidopsis* disrupt the perception of phototropic stimuli. *Plant Cell,* 7**,** 473-485.

LIU, H. T., LIU, B., ZHAO, C. X., PEPPER, M. & LIN, C. T. 2011. The action mechanisms of plant cryptochromes. *Trends in Plant Science,* 16**,** 684-691.

LIU, H. T., YU, X. H., LI, K. W., KLEJNOT, J., YANG, H. Y., LISIERO, D. & LIN, C. T. 2008. Photoexcited CRY2 interacts with CIB1 to regulate transcription and floral initiation in *Arabidopsis*. *Science,* 322**,** 1535-1539.

LIU, J., ZHANG, F., ZHOU, J. J., CHEN, F., WANG, B. S. & XIE, X. Z. 2012. Phytochrome B control of total leaf area and stomatal density affects drought tolerance in rice. *Plant Molecular Biology,* 78**,** 289-300.

LIU, Q. H. & PAROO, Z. 2010. Biochemical principles of small RNA pathways. *Annual Review of Biochemistry,* 79**,** 295-319.

LIU, Z. J., ZHANG, Y. Q., WANG, J. F., LI, P., ZHAO, C. Z., CHEN, Y. D. & BI, Y. R. 2015. Phytochrome-interacting factors PIF4 and PIF5 negatively regulate anthocyanin biosynthesis under red light in Arabidopsis seedlings. *Plant Science,* 238**,** 64-72.

LLORENTE, B., D'ANDREA, L., RUIZ-SOLA, M. A., BOTTERWEG, E., PULIDO, P., ANDILLA, J., LOZA-ALVAREZ, P. & RODRIGUEZ-CONCEPCION, M. 2016. Tomato fruit carotenoid biosynthesis is adjusted to actual ripening progression by a light-dependent mechanism. *Plant Journal,* 85**,** 107-119.

LOUKOIANOV, A., YAN, L. L., BLECHL, A., SANCHEZ, A. & DUBCOVSKY, J. 2005. Regulation of VRN-1 vernalization genes in normal and transgenic polyploid wheat. *Plant Physiology,* 138**,** 2364-2373.

LUCCIONI, L. G., OLIVERIO, K. A., YANOVSKY, M. J., BOCCALANDRO, H. E. & CASAL, J. J. 2002. Brassinosteroid mutants uncover fine tuning of phytochrome signaling. *Plant Physiology,* 128**,** 173-181.

LUO, H. L., LALUK, K., LAI, Z. B., VERONESE, P., SONG, F. M. & MENGISTE, T. 2010. The *Arabidopsis* botrytis susceptible1 interactor defines a subclass of RING E3 Ligases that regulate pathogen and stress responses. *Plant Physiology,* 154**,** 1766-1782.

LUO, L., LI, W. Q., MIURA, K., ASHIKARI, M. & KYOZUKA, J. 2012. Control of tiller growth of rice by OsSPL14 and strigolactones, which work in two independent pathways. *Plant and Cell Physiology,* 53**,** 1793-1801.

MARCUSSEN, T., SANDVE, S. R., HEIER, L., SPANNAGL, M., PFEIFER, M., JAKOBSEN, K. S., WULFF, B. B. H., STEUERNAGEL, B., MAYER, K. F. X., OLSEN, O. A. & SEQUENCING, I. W. G. 2014. Ancient hybridizations among the ancestral genomes of bread wheat. *Science,* 345.

MARIN-DE LA ROSA, N., SOTILLO, B., MISKOLCZI, P., GIBBS, D. J., VICENTE, J., CARBONERO, P., ONATE-SANCHEZ, L., HOLDSWORTH, M. J., BHALERAO, R., ALABADI, D. & BLAZQUEZ, M. A. 2014. Large-scale identification of gibberellin-related transcription factors defines group VII ETHYLENE RESPONSE FACTORS as functional DELLA partners. *Plant Physiology,* 166**,** 1022-1032.

MARTINEZ-GARCIA, J. F., HUQ, E. & QUAIL, P. H. 2000. Direct targeting of light signals to a promoter element-bound transcription factor. *Science,* 288**,** 859-863.

MATHEWS, S. & SHARROCK, R. A. 1996. The phytochrome gene family in grasses (*Poaceae*): A phylogeny and evidence that grasses have a subset of the loci found in dicot angiosperms. *Molecular Biology and Evolution,* 13**,** 1141-1150.

MATSUBARA, K., YAMANOUCHI, U., WANG, Z. X., MINOBE, Y., IZAWA, T. & YANO, M. 2008. Ehd2, a rice ortholog of the maize *INDETERMINATE*1 gene, promotes flowering by up-regulating Ehd1. *Plant Physiology,* 148**,** 1425-1435.

MATSUMOTO, N., HIRANO, T., IWASAKI, T. & YAMAMOTO, N. 2003. Functional analysis and intracellular localization of rice cryptochromes. *Plant Physiology,* 133**,** 1494-1503.

MATSUSHITA, A., FURUMOTO, T., ISHIDA, S. & TAKAHASHI, Y. 2007. AGF1, an AT-hook protein, is necessary for the negative feedback of AtGA3ox1 encoding GA 3-oxidase. *Plant Physiology,* 143**,** 1152-1162.

MCCALLUM, C. M., COMAI, L., GREENE, E. A. & HENIKOFF, S. 2000a. Targeted screening for induced mutations. *Nature Biotechnology,* 18**,** 455-457.

MCCALLUM, C. M., COMAI, L., GREENE, E. A. & HENIKOFF, S. 2000b. Targeting induced local lesions in genomes (TILLING) for plant functional genomics. *Plant Physiology,* 123**,** 439-442.

MCELROY, D., BLOWERS, A. D., JENES, B. & WU, R. 1991. Construction of expression vectors based on the rice actin-1 (Act1) 5' region for use in monocot transformation. *Molecular & General Genetics,* 231**,** 150-160.

MCGINNIS, K. M., THOMAS, S. G., SOULE, J. D., STRADER, L. C., ZALE, J. M., SUN, T. P. & STEBER, C. M. 2003. The *Arabidopsis SLEEPY1* gene encodes a putative F-box subunit of an SCF E3 ubiquitin ligase. *Plant Cell,* 15**,** 1120-1130.

MITCHUM, M. G., YAMAGUCHI, S., HANADA, A., KUWAHARA, A., YOSHIOKA, Y., KATO, T., TABATA, S., KAMIYA, Y. & SUN, T. P. 2006. Distinct and overlapping roles of two gibberellin 3-oxidases in Arabidopsis development. *Plant Journal,* 45**,** 804-18.

MIURA, K., IKEDA, M., MATSUBARA, A., SONG, X. J., ITO, M., ASANO, K., MATSUOKA, M., KITANO, H. & ASHIKARI, M. 2010. OsSPL14 promotes panicle branching and higher grain productivity in rice. *Nature Genetics,* 42**,** 545-U102.

MIZUTANI, M. & OHTA, D. 2010. Diversification of P450 genes during land plant evolution. *Annual Review of Plant Biology,* 61**,** 291-315.

MOCHIDA, K., YOSHIDA, T., SAKURAI, T., OGIHARA, Y. & SHINOZAKI, K. 2009. TriFLDB: A Database of Clustered Full-Length Coding Sequences from Triticeae with Applications to Comparative Grass Genomics. *Plant Physiology,* 150**,** 1135-1146.

MOOLHUIJZEN, P., DUNN, D. S., BELLGARD, M., CARTER, M., JIA, J., KONG, X., GILL, B. S., FEUILLET, C., BREEN, J. & APPELS, R. 2007. Wheat genome structure and function: genome sequence data and the International Wheat Genome Sequencing Consortium. *Australian Journal of Agricultural Research,* 58**,** 470.

MORISON, J. I., BAKER, N. R., MULLINEAUX, P. M. & DAVIES, W. J. 2008. Improving water use in crop production. *Philosophical transactions of the Royal Society of London. Series B, Biological sciences,* 363**,** 639-58.

MORITA, M. T., SAKAGUCHI, K., KIYOSE, S. I., TAIRA, K., KATO, T., NAKAMURA, M. & TASAKA, M. 2006. A C2H2-type zinc finger protein, SGR5, is involved in early events of gravitropism in Arabidopsis inflorescence stems. *Plant Journal,* 47**,** 619-628.

MURASE, K., HIRANO, Y., SUN, T. P. & HAKOSHIMA, T. 2008. Gibberellin-induced DELLA recognition by the gibberellin receptor GID1. *Nature,* 456**,** 459-U15.

NAGATANI, A. 2004. Light-regulated nuclear localization of phytochromes. *Current Opinion in Plant Biology,* 7**,** 708-711.

NAKAJIMA, M., SHIMADA, A., TAKASHI, Y., KIM, Y. C., PARK, S. H., UEGUCHI-TANAKA, M., SUZUKI, H., KATOH, E., IUCHI, S., KOBAYASHI, M., MAEDA, T., MATSUOKA, M. & YAMAGUCHI, I. 2006. Identification and characterization of Arabidopsis gibberellin receptors. *Plant Journal,* 46**,** 880-889.

NAKAMURA, Y., KATO, T., YAMASHINO, T., MURAKAMI, M. & MIZUNO, T. 2007a. Characterization of a set of phytochrome-interacting factor-like bHLH proteins in Oryza sativa. *Bioscience Biotechnology and Biochemistry,* 71**,** 1183-1191.

NAKAMURA, Y., KATO, T., YAMASHINO, T., MURAKAMI, M. & MIZUNO, T. 2007b. Characterization of a set of phytochrome-interacting factor-like bHLH proteins in Oryza sativa. *Biosci Biotechnol Biochem,* 71**,** 1183-91.

NEHRA, N. S., CHIBBAR, R. N., LEUNG, N., CASWELL, K., MALLARD, C., STEINHAUER, L., BAGA, M. & KARTHA, K. K. 1994. Self-fertile transgenic wheat plants regenerated from isolated scutellar tissues following microprojectile bombardment with 2 distinct gene constructs. *The Plant Journal,* 5**,** 285-297.

NGUYEN, K. T., PARK, J., PARK, E., LEE, I. & CHOI, G. 2015. The Arabidopsis RING domain protein BOI inhibits flowering via CO-dependent and CO-independent mechanisms. *Molecular Plant,* 8**,** 1725-1736.

NI, M., TEPPERMAN, J. M. & QUAIL, P. H. 1998. PIF3, a phytochrome-interacting factor necessary for normal photoinduced signal transduction, is a novel basic helix-loop-helix protein. *Cell,* 95**,** 657-667.

NI, W., XU, S. L., CHALKLEY, R. J., PHAM, T. N., GUAN, S., MALTBY, D. A., BURLINGAME, A. L., WANG, Z. Y. & QUAIL, P. H. 2013. Multisite light-induced phosphorylation of the transcription factor PIF3 is necessary for both its rapid degradation and concomitant negative feedback modulation of photoreceptor phyB levels in Arabidopsis. *Plant Cell,* 25**,** 2679-98.

NI, W. M., XU, S. L., GONZALEZ-GRANDIO, E., CHALKLEY, R. J., HUHMER, A. F. R., BURLINGAME, A. L., WANG, Z. Y. & QUAIL, P. H. 2017. PPKs mediate direct signal transfer from phytochrome photoreceptors to transcription factor PIF3. *Molecular & Cellular Proteomics,* 16**,** S21-S21.

NI, W. M., XU, S. L., TEPPERMAN, J. M., STANLEY, D. J., MALTBY, D. A., GROSS, J. D., BURLINGAME, A. L., WANG, Z. Y. & QUAIL, P. H. 2014. A mutually assured destruction mechanism attenuates light signaling in Arabidopsis. *Science,* 344**,** 1160-1164.

NIBAU, C., TAO, L. Z., LEVASSEUR, K., WU, H. M. & CHEUNG, A. Y. 2013. The *Arabidopsis* small GTPase AtRAC7/ROP9 is a modulator of auxin and abscisic acid signalling. *Journal of Experimental Botany,* 64**,** 3425-3437.

NICHOLLS, P. B. 1978. Response of barley shoot apices to application of gibberellic-acid and abscisic-acid - dependence on tissue sensitivity. *Australian Journal of Plant Physiology,* 5**,** 581-588.

NIU, Y. J., FIGUEROA, P. & BROWSE, J. 2011. Characterization of JAZ-interacting bHLH transcription factors that regulate jasmonate responses in *Arabidopsis*. *Journal of Experimental Botany,* 62**,** 2143-2154.

O'NEILL, D. P. & ROSS, J. J. 2002. Auxin regulation of the gibberellin pathway in pea. *Plant Physiology,* 130**,** 1974-1982.

OH, E., YAMAGUCHI, S., HU, J., YUSUKE, J., JUNG, B., PAIK, I., LEE, H. S., SUN, T. P., KAMIYA, Y. & CHOI, G. 2007. PIL5, a phytochrome-interacting bHLH protein, regulates gibberellin responsiveness by binding directly to the GAI and RGA promoters in Arabidopsis seeds. *Plant Cell,* 19**,** 1192-208.

OH, E., YAMAGUCHI, S., KAMIYA, Y., BAE, G., CHUNG, W. I. & CHOI, G. 2006. Light activates the degradation of PIL5 protein to promote seed germination through gibberellin in Arabidopsis. *Plant Journal,* 47**,** 124-39.

OH, E., ZHU, J. Y., BAI, M. Y., ARENHART, R. A., SUN, Y. & WANG, Z. Y. 2014. Cell elongation is regulated through a central circuit of interacting transcription factors in the Arabidopsis hypocotyl. *eLife,* 3.

OH, E., ZHU, J. Y. & WANG, Z. Y. 2012. Interaction between BZR1 and PIF4 integrates brassinosteroid and environmental responses. *Nature Cell Biology,* 14**,** 802-9.

OONO, Y., KOBAYASHI, F., KAWAHARA, Y., YAZAWA, T., HANDA, H., ITOH, T. & MATSUMOTO, T. 2013. Characterisation of the wheat (triticum aestivum L.) transcriptome by de novo assembly for the discovery of phosphate starvation-responsive genes: gene expression in Pi-stressed wheat. *Bmc Genomics,* 14.

ORAVECZ, A., BAUMANN, A., MATE, Z., BRZEZINSKA, A., MOLINIER, J., OAKELEY, E. J., ADAM, E., SCHAFER, E., NAGY, F. & ULM, R. 2006. CONSTITUTIVELY PHOTOMORPHOGENIC1 is required for the UV-B response in Arabidopsis. *Plant Cell,* 18**,** 1975-1990.

OSTERLUND, M. T., HARDTKE, C. S., WEI, N. & DENG, X. W. 2000. Targeted destabilization of HY5 during light-regulated development of Arabidopsis. *Nature,* 405**,** 462-466.

OUYANG, X. H., LI, J. G., LI, G., LI, B. S., CHEN, B. B., SHEN, H. S., HUANG, X., MO, X. R., WAN, X. Y., LIN, R. C., LI, S. G., WANG, H. Y. & DENG, X. W. 2011. Genome-wide binding site analysis of FAR-RED ELONGATED HYPOCOTYL3 reveals its novel function in Arabidopsis development. *Plant Cell,* 23**,** 2514-2535.

PADMANABHAN, M. S., MA, S. S., BURCH-SMITH, T. M., CZYMMEK, K., HUIJSER, P. & DINESH-KUMAR, S. P. 2013. Novel positive regulatory role for the SPL6 transcription factor in the N TIR-NB-LRR receptor-mediated plant innate immunity. *Plos Pathogens,* 9.

PAPDI, C., PEREZ-SALAMO, I., JOSEPH, M. P., GIUNTOLI, B., BOGRE, L., KONCZ, C. & SZABADOS, L. 2015. The low oxygen, oxidative and osmotic stress responses synergistically act through the ethylene response factor VII genes RAP2.12, RAP2.2 and RAP2.3. *Plant Journal,* 82**,** 772-784.

PARK, E., KIM, J., LEE, Y., SHIN, J., OH, E., CHUNG, W. I., LIU, J. R. & CHOI, G. 2004. Degradation of phytochrome interacting factor 3 in phytochrome-mediated light signaling. *Plant and Cell Physiology,* 45**,** 968-975.

PARK, E., PARK, J., KIM, J., NAGATANI, A., LAGARIAS, J. C. & CHOI, G. 2012. Phytochrome B inhibits binding of phytochrome-interacting factors to their target promoters. *Plant Journal,* 72**,** 537-46.

PARK, J., NGUYEN, K. T., PARK, E., JEON, J. S. & CHOI, G. 2013. DELLA proteins and their interacting RING finger proteins repress gibberellin responses by binding to the promoters of a subset of gibberellin-responsive genes in Arabidopsis. *Plant Cell,* 25**,** 927-943.

PARRY, M. A. J. & HAWKESFORD, M. J. 2010. Food security: increasing yield and improving resource use efficiency. *Proceedings of the Nutrition Society,* 69**,** 592-600.

PEARCE, S., SAVILLE, R., VAUGHAN, S. P., CHANDLER, P. M., WILHELM, E. P., SPARKS, C. A., AL-KAFF, N., KOROLEV, A., BOULTON, M. I., PHILLIPS, A. L., HEDDEN, P., NICHOLSON, P. & THOMAS, S. G. 2011. Molecular characterization of Rht-1 dwarfing genes in hexaploid wheat. *Plant Physiology,* 157**,** 1820-1831.

PENFIELD, S., JOSSE, E. M., KANNANGARA, R., GILDAY, A. D., HALLIDAY, K. J. & GRAHAM, I. A. 2005. Cold and light control seed germination through the bHLH transcription factor SPATULA. *Current Biology,* 15**,** 1998-2006.

PENG, J. R., CAROL, P., RICHARDS, D. E., KING, K. E., COWLING, R. J., MURPHY, G. P. & HARBERD, N. P. 1997. The Arabidopsis *GAI* gene defines a signaling pathway that negatively regulates gibberellin responses. *Genes & Development,* 11**,** 3194-3205.

PENG, J. R. & HARBERD, N. P. 1993. Derivative alleles of the Arabidopsis gibberellin-insensitive (Gai) mutation confer a wild-type phenotype. *Plant Cell,* 5**,** 351-360.

PENG, J. R., RICHARDS, D. E., HARTLEY, N. M., MURPHY, G. P., DEVOS, K. M., FLINTHAM, J. E., BEALES, J., FISH, L. J., WORLAND, A. J., PELICA, F., SUDHAKAR, D., CHRISTOU, P., SNAPE, J. W., GALE, M. D. & HARBERD, N. P. 1999. 'Green revolution' genes encode mutant gibberellin response modulators. *Nature,* 400**,** 256-261.

PENG, L. L., LIU, WEI-FENG, ZHOU, QIAN-QIAN, LIANG, JIN-JUN, WEI-HONG, XIE XIAN-ZHI 2012. Expression patterns of OsPIL11, a phytochrome-interacting factor in rice, and preliminary analysis of its roles in light signal transduction. *Rice Science,* 19**,** 263-268.

PENNINCKX, I. A. M. A., THOMMA, B. P. H. J., BUCHALA, A., METRAUX, J. P. & BROEKAERT, W. F. 1998. Concomitant activation of jasmonate and ethylene response pathways is required for induction of a plant defensin gene in Arabidopsis. *Plant Cell,* 10**,** 2103-2113.

PEROCHON, A., JIANGUANG, J., KAHLA, A., ARUNACHALAM, C., R., S. S., BOWDEN, S., WALLINGTON, E. & DOOHAN, F. M. 2015a. TaFROG encodes a pooideae orphan protein that interacts with SnRK1 and enhances resistance to the mycotoxigenic fungus Fusarium graminearum. *Plant Physiology,* 169**,** 2895-2906.

PEROCHON, A., JIANGUANG, J., KAHLA, A., ARUNACHALAM, C., R., S. S., BOWDEN, S., WALLINGTON, E. & DOOHAN, F. M. 2015b. TaFROG encodes a pooideae orphan protein that interacts with SnRK1 and enhances resistance to the mycotoxigenic fungus fusarium graminearum. *Plant Physiology,* 169**,** 2895-2906.

PETERSEN, G., SEBERG, O., YDE, M. & BERTHELSEN, K. 2006. Phylogenetic relationships of *Triticum* and *Aegilops* and evidence for the origin of the A, B, and D genomes of common wheat (*Triticum aestivum*). *Molecular Phylogenetics and Evolution,* 39**,** 70-82.

PHILLIPS, A. L., WARD, D. A., UKNES, S., APPLEFORD, N. E., LANGE, T., HUTTLY, A. K., GASKIN, P., GRAEBE, J. E. & HEDDEN, P. 1995. Isolation and expression of three gibberellin 20-oxidase cDNA clones from Arabidopsis. *Plant Physiology,* 108**,** 1049-57.

PONTIER, D., MIAO, Z. H. & LAM, E. 2001. Trans-dominant suppression of plant TGA factors reveals their negative and positive roles in plant defense responses. *The Plant Journal,* 27**,** 529-538.

POSSART, A., XU, T. F., PAIK, I., HANKE, S., KEIM, S., HERMANN, H. M., WOLF, L., HISS, M., BECKER, C., HUQ, E., RENSING, S. A. & HILTBRUNNER, A. 2017. Characterization of phytochrome interacting factors from the moss Physcomitrella patens illustrates conservation of phytochrome signaling modules in land plants. *Plant Cell,* 29**,** 310-330.

PYSH, L. D., WYSOCKA-DILLER, J. W., CAMILLERI, C., BOUCHEZ, D. & BENFEY, P. N. 1999. The GRAS gene family in Arabidopsis: sequence characterization and basic expression analysis of the SCARECROW-LIKE genes. *Plant Journal,* 18**,** 111-119.

QI, L. L., ECHALIER, B., CHAO, S., LAZO, G. R., BUTLER, G. E., ANDERSON, O. D., AKHUNOV, E. D., DVORAK, J., LINKIEWICZ, A. M., RATNASIRI, A., DUBCOVSKY, J., BERMUDEZ-KANDIANIS, C. E., GREENE, R. A., KANTETY, R., LA ROTA, C. M., MUNKVOLD, J. D., SORRELLS, S. F., SORRELLS, M. E., DILBIRLIGI, M., SIDHU, D., ERAYMAN, M., RANDHAWA, H. S., SANDHU, D., BONDAREVA, S. N., GILL, K. S., MAHMOUD, A. A., MA, X. F., MIFTAHUDIN, GUSTAFSON, J. P., CONLEY, E. J., NDUATI, V., GONZALEZ-HERNANDEZ, J. L., ANDERSON, J. A., PENG, J. H., LAPITAN, N. L. V., HOSSAIN, K. G., KALAVACHARLA, V., KIANIAN, S. F., PATHAN, M. S., ZHANG, D. S., NGUYEN, H. T., CHOI, D. W., FENTON, R. D., CLOSE, T. J., MCGUIRE, P. E., QUALSET, C. O. & GILL, B. S. 2004. A chromosome bin map of 16,000 expressed sequence tag loci and distribution of genes among the three genomes of polyploid wheat. *Genetics,* 168**,** 701-712.

RAJANI, S. & SUNDARESAN, V. 2001. The Arabidopsis myc/bHLH gene ALCATRAZ enables cell separation in fruit dehiscence. *Current Biology,* 11**,** 1914-1922.

REED, J. W., NAGATANI, A., ELICH, T. D., FAGAN, M. & CHORY, J. 1994. Phytochrome-A and phytochrome-B have overlapping but distinct functions in Arabidopsis development. *Plant Physiology,* 104**,** 1139-1149.

REGNAULT, T., DAVIERE, J. M. & ACHARD, P. 2016. Long-distance transport of endogenous gibberellins in Arabidopsis. *Plant Signaling & Behavior,* 11.

REYNOLDS, M. P., RAJARAM, S. & SAYRE, K. D. 1999. Physiological and genetic changes of irrigated wheat in the post-green revolution period and approaches for meeting projected global demand. *Crop Science,* 39**,** 1611-1621.

RICHARDS, D. E., KING, K. E., AIT-ALI, T. & HARBERD, N. P. 2001. How gibberellin regulates plant growth and development: A molecular genetic analysis of gibberellin signaling. *Annual Review of Plant Physiology and Plant Molecular Biology,* 52**,** 67-88.

RIEU, I., ERIKSSON, S., POWERS, S. J., GONG, F., GRIFFITHS, J., WOOLLEY, L., BENLLOCH, R., NILSSON, O., THOMAS, S. G., HEDDEN, P. & PHILLIPS, A. L. 2008. Genetic analysis reveals that C-19-GA 2-oxidation is a major gibberellin inactivation pathway in Arabidopsis. *Plant Cell,* 20**,** 2420-2436.

ROBERTSON, M. 2004. Two transcription factors are negative regulators of gibberellin response in the HvSPY-signaling pathway in barley aleurone. *Plant Physiology,* 136**,** 2747-2761.

ROCHELEAU, C. E., DOWNS, W. D., LIN, R. L., WITTMANN, C., BEI, Y. X., CHA, Y. H., ALI, M., PRIESS, J. R. & MELLO, C. C. 1997. Wnt signaling and an APC-related gene specify endoderm in early C. elegans embryos. *Cell,* 90**,** 707-716.

ROCKWELL, N. C., SU, Y. S. & LAGARIAS, J. C. 2006. Phytochrome structure and signaling mechanisms. *Annual Review of Plant Biology,* 57**,** 837-858.

ROOKE, L., BYRNE, D. & SALGUEIRO, S. 2000. Marker gene expression driven by the maize ubiquitin promoter in transgenic wheat. *Annals of Applied Biology,* 136**,** 167-172.

ROSADO, D., GRAMEGNA, G., CRUZ, A., LIRA, B. S., FRESCHI, L., DE SETTA, N. & ROSSI, M. 2016. Phytochrome interacting factors (PIFs) in Solanum lycopersicum: diversity, evolutionary history and expression profiling during different developmental processes. *Plos One,* 11.

ROSS, J. J., O'NEILL, D. P., SMITH, J. J., KERCKHOFFS, L. H. J. & ELLIOTT, R. C. 2000. Evidence that auxin promotes gibberellin A(1) biosynthesis in pea. *Plant Journal,* 21**,** 547-552.

SAIJO, Y., SULLIVAN, J. A., WANG, H. Y., YANG, J. P., SHEN, Y. P., RUBIO, V., MA, L. G., HOECKER, U. & DENG, X. W. 2003. The COP1-SPA1 interaction defines a critical step in phytochrome A-mediated regulation of HY5 activity. *Genes & Development,* 17**,** 2642-2647.

SAITO, H., OIKAWA, T., HAMAMOTO, S., ISHIMARU, Y., KANAMORI-SATO, M., SASAKI-SEKIMOTO, Y., UTSUMI, T., CHEN, J., KANNO, Y., MASUDA, S., KAMIYA, Y., SEO, M., UOZUMI, N., UEDA, M. & OHTA, H. 2015. The jasmonate-responsive GTR1 transporter is required for gibberellin-mediated stamen development in Arabidopsis. *Nature Communications,* 6.

SAKAI, T., KAGAWA, T., KASAHARA, M., SWARTZ, T. E., CHRISTIE, J. M., BRIGGS, W. R., WADA, M. & OKADA, K. 2001. Arabidopsis nph1 and npl1: Blue light receptors that mediate both phototropism and chloroplast relocation. *Proceedings of the National Academy of Sciences of the United States of America,* 98**,** 6969-6974.

SAKAMOTO, T., KAMIYA, N., UEGUCHI-TANAKA, M., IWAHORI, S. & MATSUOKA, M. 2001. KNOX homeodomain protein directly suppresses the expression of a gibberellin biosynthetic gene in the tobacco shoot apical meristem. *Genes & Development,* 15**,** 581-590.

SAKURABA, Y., JEONG, J., KANG, M. Y., KIM, J., PAEK, N. C. & CHOI, G. 2014. Phytochrome-interacting transcription factors PIF4 and PIF5 induce leaf senescence in Arabidopsis. *Nature Communications,* 5**,** 4636.

SAKURABA, Y., KIM, E. Y., HAN, S. H., PIAO, W., AN, G., TODAKA, D., YAMAGUCHI-SHINOZAKI, K. & PAEK, N. C. 2017a. Rice Phytochrome-Interacting Factor-Like1 (OsPIL1) is involved in the promotion of chlorophyll biosynthesis through feed-forward regulatory loops. *Journal of Experimental Botany,* 68**,** 4103–4114.

SAKURABA, Y., KIM, E. Y. & PAEK, N. C. 2017b. Roles of rice PHYTOCHROME-INTERACTING FACTOR-LIKE1 (OsPIL1) in leaf senescence. *Plant Signaling & Behavior***,** 0.

SALTER, M. G., FRANKLIN, K. A. & WHITELAM, G. C. 2003. Gating of the rapid shade-avoidance response by the circadian clock in plants. *Nature,* 426**,** 680-683.

SANG, Y., LI, Q. H., RUBIO, V., ZHANG, Y. C., MAO, J., DENG, X. W. & YANG, H. Q. 2005. N-terminal domain-mediated homodimerization is required for photoreceptor activity of Arabidopsis CRYPTOCHROME 1. *Plant Cell,* 17**,** 1569-1584.

SASAKI, A., ITOH, H., GOMI, K., UEGUCHI-TANAKA, M., ISHIYAMA, K., KOBAYASHI, M., JEONG, D. H., AN, G., KITANO, H., ASHIKARI, M. & MATSUOKA, M. 2003. Accumulation of phosphorylated repressor for gibberellin signaling in an F-box mutant. *Science,* 299**,** 1896-1898.

SCHOMBURG, F. M., BIZZELL, C. M., LEE, D. J., ZEEVAART, J. A. D. & AMASINO, R. M. 2003. Overexpression of a novel class of gibberellin 2-oxidases decreases gibberellin levels and creates dwarf plants. *Plant Cell,* 15**,** 151-163.

SCHWARZ, S., GRANDE, A. V., BUJDOSO, N., SAEDLER, H. & HUIJSER, P. 2008. The microRNA regulated SBP-box genes SPL9 and SPL15 control shoot maturation in Arabidopsis. *Plant Molecular Biology,* 67**,** 183-195.

SEO, P. J., RYU, J., KANG, S. K. & PARK, C. M. 2011. Modulation of sugar metabolism by an INDETERMINATE DOMAIN transcription factor contributes to photoperiodic flowering in Arabidopsis. *Plant Journal,* 65**,** 418-429.

SHALITIN, D., YANG, H. Y., MOCKLER, T. C., MAYMON, M., GUO, H. W., WHITELAM, G. C. & LIN, C. T. 2002. Regulation of Arabidopsis cryptochrome 2 by blue-light-dependent phosphorylation. *Nature,* 417**,** 763-767.

SHEEHAN, M. J., FARMER, P. R. & BRUTNELL, T. P. 2004. Structure and expression of maize phytochrome family homeologs. *Genetics,* 167**,** 1395-1405.

SHEN, Y., KHANNA, R., CARLE, C. M. & QUAIL, P. H. 2007. Phytochrome induces rapid PIF5 phosphorylation and degradation in response to red-light activation. *Plant Physiology,* 145**,** 1043-1051.

SHIFERAW, B., SMALE, M., BRAUN, H. J., DUVEILLER, E., REYNOLDS, M. & MURICHO, G. 2013. Crops that feed the world 10. Past successes and future challenges to the role played by wheat in global food security. *Food Security,* 5**,** 291-317.

SHIKATA, M., KOYAMA, T., MITSUDA, N. & OHME-TAKAGI, M. 2009. Arabidopsis SBP-box genes SPL10, SPL11 and SPL2 control morphological change in association with shoot maturation in the reproductive phase. *Plant and Cell Physiology,* 50**,** 2133-2145.

SHIMADA, A., UEGUCHI-TANAKA, M., NAKATSU, T., NAKAJIMA, M., NAOE, Y., OHMIYA, H., KATO, H. & MATSUOKA, M. 2008. Structural basis for gibberellin recognition by its receptor GID1. *Nature,* 456**,** 520-U44.

SHIN, A. Y., HAN, Y. J., BAEK, A., AHN, T., KIM, S. Y., NGUYEN, T. S., SON, M., LEE, K. W., SHEN, Y., SONG, P. S. & KIM, J. I. 2016. Evidence that phytochrome functions as a protein kinase in plant light signalling. *Nature Communications,* 7.

SHIN, J., KIM, K., KANG, H., ZULFUGAROV, I. S., BAE, G., LEE, C. H., LEE, D. & CHOI, G. 2009. Phytochromes promote seedling light responses by inhibiting four negatively-acting phytochrome-interacting factors. *Proceedings of the National Academy of Sciences of the United States of America,* 106**,** 7660-5.

SI, L. Z., CHEN, J. Y., HUANG, X. H., GONG, H., LUO, J. H., HOU, Q. Q., ZHOU, T. Y., LU, T. T., ZHU, J. J., SHANGGUAN, Y. Y., CHEN, E. W., GONG, C. X., ZHAO, Q., JING, Y. F., ZHAO, Y., LI, Y., CUI, L. L., FAN, D. L., LU, Y. Q., WENG, Q. J., WANG, Y. C., ZHAN, Q. L., LIU, K. Y., WEI, X. H., AN, K., AN, G. & HAN, B. 2016. OsSPL13 controls grain size in cultivated rice. *Nature Genetics,* 48**,** 447-+.

SIDDIQUI, H., KHAN, S., RHODES, B. M. & DEVLIN, P. F. 2016. FHY3 and FAR1 act downstream of light stable phytochromes. *Frontiers in Plant Science,* 7.

SILVERSTONE, A. L., CHANG, C. W., KROL, E. & SUN, T. P. 1997. Developmental regulation of the gibberellin biosynthetic gene GA1 in Arabidopsis thaliana. *Plant Journal,* 12**,** 9-19.

SILVERSTONE, A. L., CIAMPAGLIO, C. N. & SUN, T. P. 1998. The Arabidopsis RGA gene encodes a transcriptional regulator repressing the gibberellin signal transduction pathway. *Plant Cell,* 10**,** 155-169.

SLADE, A. J., FUERSTENBERG, S. I., LOEFFLER, D., STEINE, M. N. & FACCIOTTI, D. 2005. A reverse genetic, nontransgenic approach to wheat crop improvement by TILLING. *Nature Biotechnology,* 23**,** 75-81.

SMALL, I. 2007. RNAi for revealing and engineering plant gene functions. *Current Opinion in Biotechnology,* 18**,** 148-153.

SMITH, H. & JACKSON, G. M. 1987. Rapid phytochrome regulation of wheat seedling extension - light pretreatment extends coupling time, increases response lag, and decreases light sensitivity. *Plant Physiology,* 84**,** 1059-1062.

SMITH, N. A., SINGH, S. P., WANG, M. B., STOUTJESDIJK, P. A., GREEN, A. G. & WATERHOUSE, P. M. 2000. Gene expression - total silencing by intron-spliced hairpin RNAs. *Nature,* 407**,** 319-320.

SMITH, V. A., KNATT, C. J., GASKIN, P. & REID, J. B. 1992. The distribution of gibberellins in vegetative tissues of Pisum. Sativum L .1. biological and biochemical consequences of the le mutation. *Plant Physiology,* 99**,** 368-371.

SOOD, S., GUPTA, V. & TRIPATHY, B. C. 2005. Photoregulation of the greening process of wheat seedlings grown in red light. *Plant Molecular Biology,* 59**,** 269-287.

SOY, J., LEIVAR, P., GONZALEZ-SCHAIN, N., SENTANDREU, M., PRAT, S., QUAIL, P. H. & MONTE, E. 2012. Phytochrome-imposed oscillations in PIF3 protein abundance regulate hypocotyl growth under diurnal light/dark conditions in Arabidopsis. *Plant Journal,* 71**,** 390-401.

SPARKS, C. A. & JONES, H. D. 2014. Genetic transformation of wheat via particle bombardment. *Methods in Molecular Biology,* 1099**,** 201-18.

STEPHENSON, P. G., FANKHAUSER, C. & TERRY, M. J. 2009. PIF3 is a repressor of chloroplast development. *Proceedings of the National Academy of Sciences of the United States of America,* 106**,** 7654-9.

SUN, J. Q., QI, L. L., LI, Y. A., ZHAI, Q. Z. & LI, C. Y. 2013. PIF4 and PIF5 transcription factors link blue light and auxin to regulate the phototropic response in Arabidopsis. *Plant Cell,* 25**,** 2102-2114.

SUN, Y., FAN, X. Y., CAO, D. M., TANG, W. Q., HE, K., ZHU, J. Y., HE, J. X., BAI, M. Y., ZHU, S. W., OH, E., PATIL, S., KIM, T. W., JI, H. K., WONG, W. H., RHEE, S. Y. & WANG, Z. Y. 2010. Integration of brassinosteroid signal transduction with the transcription network for plant growth regulation in Arabidopsis. *Developmental Cell,* 19**,** 765-777.

SWAIN, S. M., ROSS, J. J., REID, J. B. & KAMIYA, Y. 1995. Gibberellins and pea seed development - expression of the Lh(I) Ls and Le(5839) mutations. *Planta,* 195**,** 426-433.

SWAIN, S. M. & SINGH, D. P. 2005. Tall tales from sly dwarves: novel functions of gibberellins in plant development. *Trends in Plant Science,* 10**,** 123-129.

TAKANO, M., KANEGAE, H., SHINOMURA, T., MIYAO, A., HIROCHIKA, H. & FURUYA, W. 2001. Isolation and characterization of rice phytochrome A mutants. *Plant Cell,* 13**,** 521-534.

TAKUMI, S., MOTOYASU, O. & TAKIKO, S. 1994. Effect of six promoter-intron combinations on transient reporter gene expression in einkorn, emmer and common wheat cells by particle bombardment. *Plant Science* 103**,** 161-166.

TALON, M., KOORNNEEF, M. & ZEEVAART, J. A. D. 1990. Accumulation of C19-gibberellins in the gibberellin-insensitive dwarf mutant Gai of Arabidopsis. thaliana (L) heynh. *Planta,* 182**,** 501-505.

TANAKA, H., DHONUKSHE, P., BREWER, P. B. & FRIML, J. 2006. Spatiotemporal asymmetric auxin distribution: a means to coordinate plant development. *Cellular and Molecular Life Sciences,* 63**,** 2738-2754.

TAO, Y., FERRER, J. L., LJUNG, K., POJER, F., HONG, F. X., LONG, J. A., LI, L., MORENO, J. E., BOWMAN, M. E., IVANS, L. J., CHENG, Y. F., LIM, J., ZHAO, Y. D., BALLARE, C. L., SANDBERG, G., NOEL, J. P. & CHORY, J. 2008. Rapid synthesis of auxin via a new tryptophan-dependent pathway is required for shade avoidance in plants. *Cell,* 133**,** 164-176.

TERPE, K. 2003. Overview of tag protein fusions: from molecular and biochemical fundamentals to commercial systems. *Applied Microbiology and Biotechnology,* 60**,** 523-533.

THINES, B. C., YOUN, Y. W., DUARTE, M. I. & HARMON, F. G. 2014. The time of day effects of warm temperature on flowering time involve PIF4 and PIF5. *Journal of Experimental Botany,* 65**,** 1141-1151.

THOMAS, S. G., PHILLIPS, A. L. & HEDDEN, P. 1999. Molecular cloning and functional expression of gibberellin 2-oxidases, multifunctional enzymes involved in gibberellin deactivation. *Proceedings of the National Academy of Sciences of the United States of America,* 96**,** 4698-4703.

TODAKA, D., NAKASHIMA, K., MARUYAMA, K., KIDOKORO, S., OSAKABE, Y., ITO, Y., MATSUKURA, S., FUJITA, Y., YOSHIWARA, K., OHME-TAKAGI, M., KOJIMA, M., SAKAKIBARA, H., SHINOZAKI, K. & YAMAGUCHI-SHINOZAKI, K. 2012. Rice phytochrome-interacting factor-like protein OsPIL1 functions as a key regulator of internode elongation and induces a morphological response to drought stress. *Proceedings of the National Academy of Sciences of the United States of America,* 109**,** 15947-15952.

TOLEDO-ORTIZ, G., HUQ, E. & QUAIL, P. H. 2003. The Arabidopsis basic/helix-loop-helix transcription factor family. *Plant Cell,* 15**,** 1749-1770.

TOYOMASU, T., KAGAHARA, T., HIROSE, Y., USUI, M., ABE, S., OKADA, K., KOGA, J., MITSUHASHI, W. & YAMANE, H. 2009. Cloning and characterization of cDNAs encoding ent-copalyl diphosphate synthases in wheat: insight into the evolution of rice phytoalexin biosynthetic genes. *Bioscience Biotechnology and Biochemistry,* 73**,** 772-775.

TRAVELLA, S., KLIMM, T. E. & KELLER, B. 2006. RNA interference-based gene silencing as an efficient tool for functional genomics in hexaploid bread wheat. *Plant Physiology,* 142**,** 6-20.

UEGUCHI-TANAKA, M., NAKAJIMA, M., KATOH, E., OHMIYA, H., ASANO, K., SAJI, S., XIANG, H. Y., ASHIKARI, M., KITANO, H., YAMAGUCHI, I. & MATSUOKAA, M. 2007. Molecular interactions of a soluble gibberellin receptor, GID1, with a rice DELLA protein, SLR1, and gibberellin. *Plant Cell,* 19**,** 2140-2155.

VAN DEN HEUVEL, K. J. P. T., HULZINK, J. M. R., BARENDSE, G. W. M. & WULLEMS, G. J. 2001. The expression of tgas118, encoding a defensin in Lycopersicon esculentum, is regulated by gibberellin. *Journal of Experimental Botany,* 52**,** 1427-1436.

VANNESTE, S. & FRIML, J. 2009. Auxin: A trigger for change in plant development. *Cell,* 136**,** 1005-1016.

VARBANOVA, M., YAMAGUCHI, S., YANG, Y., MCKELVEY, K., HANADA, A., BOROCHOV, R., YU, F., JIKUMARU, Y., ROSS, J., CORTES, D., MA, C. J., NOEL, J. P., MANDER, L., SHULAEV, V., KAMIYA, Y., RODERMEL, S., WEISS, D. & PICHERSKY, E. 2007. Methylation of gibberellins by Arabidopsis GAMT1 and GAMT2. *Plant Cell,* 19**,** 32-45.

VAUCHERET, H., BECLIN, C. & FAGARD, M. 2001. Post-transcriptional gene silencing in plants. *Journal of Cell Science,* 114**,** 3083-3091.

VON ARNIM, A. & DENG, X. W. 1996. Light control of seedling development. *Annual Review of Plant Physiology and Plant Molecular Biology,* 47**,** 215-243.

VRIEZEN, W. H., ACHARD, P., HARBERD, N. P. & VAN DER STRAETEN, D. 2004. Ethylene-mediated enhancement of apical hook formation in etiolated Arabidopsis thaliana seedlings is gibberellin dependent. *Plant Journal,* 37**,** 505-516.

WANG, H., NUSSBAUM-WAGLER, T., LI, B. L., ZHAO, Q., VIGOUROUX, Y., FALLER, M., BOMBLIES, K., LUKENS, L. & DOEBLEY, J. F. 2005a. The origin of the naked grains of maize. *Nature,* 436**,** 714-719.

WANG, J. W., CZECH, B. & WEIGEL, D. 2009. miR156-regulated SPL transcription factors define an endogenous flowering pathway in Arabidopsis thaliana. *Cell,* 138**,** 738-749.

WANG, L., SUN, S. Y., JIN, J. Y., FU, D. B., YANG, X. F., WENG, X. Y., XU, C. G., LI, X. H., XIAO, J. H. & ZHANG, Q. F. 2015a. Coordinated regulation of vegetative and reproductive branching in rice. *Proceedings of the National Academy of Sciences of the United States of America,* 112**,** 15504-15509.

WANG, S. K., LI, S., LIU, Q., WU, K., ZHANG, J. Q., WANG, S. S., WANG, Y., CHEN, X. B., ZHANG, Y., GAO, C. X., WANG, F., HUANG, H. X. & FU, X. D. 2015b. The OsSPL16-GW7 regulatory module determines grain shape and simultaneously improves rice yield and grain quality. *Nature Genetics,* 47**,** 949-+.

WANG, S. K., WU, K., YUAN, Q. B., LIU, X. Y., LIU, Z. B., LIN, X. Y., ZENG, R. Z., ZHU, H. T., DONG, G. J., QIAN, Q., ZHANG, G. Q. & FU, X. D. 2012. Control of grain size, shape and quality by OsSPL16 in rice. *Nature Genetics,* 44**,** 950-+.

WANG, T., IYER, L. M., PANCHOLY, R., SHI, X. Y. & HALL, T. C. 2005b. Assessment of penetrance and expressivity of RNAi-mediated silencing of the Arabidopsis phytoene desaturase gene. *New Phytologist,* 167**,** 751-760.

WARPEHA, K. M. & MONTGOMERY, B. L. 2016. Light and hormone interactions in the seed-to-seedling transition. *Environmental and Experimental Botany,* 121**,** 56-65.

WEEKS, J. T., ANDERSON, O. D. & BLECHL, A. E. 1993. Rapid production of multiple independent lines of fertile transgenic wheat (Triticum-aestivum). *Plant Physiology,* 102**,** 1077-1084.

WELCH, D., HASSAN, H., BLILOU, I., IMMINK, R., HEIDSTRA, R. & SCHERES, B. 2007. Arabidopsis JACKDAW and MAGPIE zinc finger proteins delimit asymmetric cell division and stabilize tissue boundaries by restricting SHORT-ROOT action. *Genes & Development,* 21**,** 2196-204.

WESLEY, S. V., HELLIWELL, C. A., SMITH, N. A., WANG, M. B., ROUSE, D. T., LIU, Q., GOODING, P. S., SINGH, S. P., ABBOTT, D., STOUTJESDIJK, P. A., ROBINSON, S. P., GLEAVE, A. P., GREEN, A. G. & WATERHOUSE, P. M. 2001. Construct design for efficient, effective and high-throughput gene silencing in plants. *The Plant Journal,* 27**,** 581-590.

WESTON, D. E., ELLIOTT, R. C., LESTER, D. R., RAMEAU, C., REID, J. B., MURFET, I. C. & ROSS, J. J. 2008. The pea DELLA proteins LA and CRY are important regulators of gibberellin synthesis and root growth. *Plant Physiology,* 147**,** 199-205.

WICKER, T., MAYER, K. F., GUNDLACH, H., MARTIS, M., STEUERNAGEL, B., SCHOLZ, U., SIMKOVA, H., KUBALAKOVA, M., CHOULET, F., TAUDIEN, S., PLATZER, M., FEUILLET, C., FAHIMA, T., BUDAK, H., DOLEZEL, J., KELLER, B. & STEIN, N. 2011. Frequent gene movement and pseudogene evolution is common to the large and complex genomes of wheat, barley, and their relatives. *Plant Cell,* 23**,** 1706-18.

WILD, M., DAVIERE, J. M., CHEMINANT, S., REGNAULT, T., BAUMBERGER, N., HEINTZ, D., BALTZ, R., GENSCHIK, P. & ACHARD, P. 2012. The Arabidopsis DELLA RGA-LIKE3 is a direct target of MYC2 and modulates jasmonate signaling responses. *Plant Cell,* 24**,** 3307-3319.

WILLEMS, A. R., SCHWAB, M. & TYERS, M. 2004. A hitchhiker's guide to the cullin ubiquitin ligases: SCF and its kin. *Biochimica Et Biophysica Acta-Molecular Cell Research,* 1695**,** 133-170.

WILSON, R. N., HECKMAN, J. W. & SOMERVILLE, C. R. 1992. Gibberellin is required for flowering in Arabidopsis. thaliana under short days. *Plant Physiology,* 100**,** 403-408.

WINKLER, R. G. & FREELING, M. 1994. Physiological genetics of the dominant gibberellin-nonresponsive maize dwarfs, Dwarf-8 and Dwarf-9. *Planta,* 193**,** 341-348.

WU, G., PARK, M. Y., CONWAY, S. R., WANG, J. W., WEIGEL, D. & POETHIG, R. S. 2009. The sequential action of miR156 and miR172 regulates developmental timing in Arabidopsis. *Cell,* 138**,** 750-759.

WU, G. & POETHIG, R. S. 2006. Temporal regulation of shoot development in Arabidopsis thaliana by miR156 and its target SPL3. *Development,* 133**,** 3539-3547.

WU, G. & SPALDING, E. P. 2007. Separate functions for nuclear and cytoplasmic cryptochrome 1 during photomorphogenesis of Arabidopsis seedlings. *Proceedings of the National Academy of Sciences of the United States of America,* 104**,** 18813-18818.

WU, J., KONG, X. Y., WAN, J. M., LIU, X. Y., ZHANG, X., GUO, X. P., ZHOU, R. H., ZHAO, G. Y., JING, R. L., FU, X. D. & JIA, J. Z. 2011. Dominant and pleiotropic effects of a GAI gene in wheat results from a lack of interaction between DELLA and GID1. *Plant Physiology,* 157**,** 2120-2130.

WU, X., TANG, D., LI, M., WANG, K. & CHENG, Z. 2013. Loose plant architecture 1, an INDETERMINATE DOMAIN protein involved in shoot gravitropism, regulates plant architecture in rice. *Plant Physiology,* 161**,** 317-29.

XIE, X. Z., KAGAWA, T. & TAKANO, M. 2014. The phytochrome B/phytochrome C heterodimer is necessary for phytochrome C-mediated responses in rice seedlings. *Plos One,* 9.

XIE, Y., TAN, H. J., MA, Z. X. & HUANG, J. R. 2016. DELLA proteins promote anthocyanin biosynthesis via sequestering MYBL2 and JAZ suppressors of the MYB/bHLH/WD40 complex in Arabidopsis thaliana. *Molecular Plant,* 9**,** 711-721.

XIE, Z., ZHANG, Z. L., ZOU, X. L., YANG, G. X., KOMATSU, S. & SHEN, Q. X. J. 2006. Interactions of two abscisic-acid induced WRKY genes in repressing gibberellin signaling in aleurone cells. *Plant Journal,* 46**,** 231-242.

XU, K., XU, X., FUKAO, T., CANLAS, P., MAGHIRANG-RODRIGUEZ, R., HEUER, S., ISMAIL, A. M., BAILEY-SERRES, J., RONALD, P. C. & MACKILL, D. J. 2006. Sub1A is an ethylene-response-factor-like gene that confers submergence tolerance to rice. *Nature,* 442**,** 705-708.

XU, M. M., WILDERMAN, P. R., MORRONE, D., XU, J. J., ROY, A., MARGIS-PINHEIRO, M., UPADHYAYA, N. M., COATES, R. M. & PETERS, R. J. 2007. Functional characterization of the rice kaurene synthase-like gene family. *Phytochemistry,* 68**,** 312-326.

XU, P., XIANG, Y., ZHU, H. L., XU, H. B., ZHANG, Z. Z., ZHANG, C. Q., ZHANG, L. X. & MA, Z. Q. 2009. Wheat cryptochromes: subcellular localization and involvement in photomorphogenesis and osmotic stress responses. *Plant Physiology,* 149**,** 760-774.

XU, Q., KRISHNAN, S., MEREWITZ, E., XU, J. C. & HUANG, B. R. 2016. Gibberellin-regulation and genetic variations in leaf elongation for tall fescue in association with differential gene expression controlling cell expansion. *Scientific Reports,* 6.

XU, T. D., WEN, M. Z., NAGAWA, S., FU, Y., CHEN, J. G., WU, M. J., PERROT-RECHENMANN, C., FRIML, J., JONES, A. M. & YANG, Z. B. 2010. Cell surface and Rho GTPase-based auxin signaling controls cellular interdigitation in Arabidopsis. *Cell,* 143**,** 99-110.

YAMAGUCHI, A., WU, M. F., YANG, L., WU, G., POETHIG, R. S. & WAGNER, D. 2009. The microRNA-regulated SBP-box transcription factor SPL3 is a direct upstream activator of LEAFY, FRUITFULL, and APETALA1. *Developmental Cell,* 17**,** 268-278.

YAMAGUCHI, S. 2008. Gibberellin metabolism and its regulation. *Annual Review of Plant Biology,* 59**,** 225-251.

YAMAGUCHI, S. & KAMIYA, Y. 2001. Gibberellins and light-stimulated seed germination. *Journal of Plant Growth Regulation,* 20**,** 369-376.

YAMAGUCHI, S., KAMIYA, Y. & SUN, T. P. 2001. Distinct cell-specific expression patterns of early and late gibberellin biosynthetic genes during Arabidopsis seed germination. *Plant Journal,* 28**,** 443-453.

YAMASAKI, H., HAYASHI, M., FUKAZAWA, M., KOBAYASHI, Y. & SHIKANAI, T. 2009. SQUAMOSA Promoter Binding Protein-Like7 Is a Central Regulator for Copper Homeostasis in Arabidopsis. *Plant Cell,* 21**,** 347-61.

YAMASAKI, T., MIYASAKA, H. & OHAMA, T. 2008. Unstable RNAi effects through epigenetic silencing of an inverted repeat transgene in Chlamydomonas reinhardtii. *Genetics,* 180**,** 1927-1944.

YAN, L. L., LOUKOIANOV, A., BLECHL, A., TRANQUILLI, G., RAMAKRISHNA, W., SANMIGUEL, P., BENNETZEN, J. L., ECHENIQUE, V. & DUBCOVSKY, J. 2004. The wheat VRN2 gene is a flowering repressor down-regulated by vernalization. *Science,* 303**,** 1640-1644.

YANAI, O., SHANI, E., DOLEZAL, K., TARKOWSKI, P., SABLOWSKI, R., SANDBERG, G., SAMACH, A. & ORI, N. 2005. Arabidopsis KNOXI proteins activate cytokinin biosynthesis. *Current Biology,* 15**,** 1566-1571.

YANO, R., KANNO, Y., JIKUMARU, Y., NAKABAYASHI, K., KAMIYA, Y. & NAMBARA, E. 2009. CHOTTO1, a putative double APETALA2 repeat transcription factor, is involved in abscisic acid-mediated repression of gibberellin biosynthesis during seed germination in Arabidopsis. *Plant Physiology,* 151**,** 641-654.

YI, C. L. & DENG, X. W. 2005. COP1 - from plant photomorphogenesis to mammalian tumorigenesis. *Trends in Cell Biology,* 15**,** 618-625.

YOSHIDA, H., HIRANO, K., SATO, T., MITSUDA, N., NOMOTO, M., MAEO, K., KOKETSU, E., MITANI, R., KAWAMURA, M., ISHIGURO, S., TADA, Y., OHME-TAKAGI, M., MATSUOKA, M. & UEGUCHI-TANAKA, M. 2014. DELLA protein functions as a transcriptional

activator through the DNA binding of the INDETERMINATE DOMAIN family proteins. *Proceedings of the National Academy of Sciences of the United States of America,* 111**,** 7861-7866.

YU, L. X., SHEN, X. & SETTER, T. L. 2015. Molecular and functional characterization of two drought-induced zinc finger proteins, ZmZnF1 and ZmZnF2 from maize kernels. *Environmental and Experimental Botany,* 111**,** 13-20.

YU, S., GALVAO, V. C., ZHANG, Y. C., HORRER, D., ZHANG, T. Q., HAO, Y. H., FENG, Y. Q., WANG, S., SCHMID, M. & WANG, J. W. 2012. Gibberellin regulates the Arabidopsis floral transition through miR156-targeted SQUAMOSA PROMOTER BINDING-LIKE transcription factors. *Plant Cell,* 24**,** 3320-3332.

YU, X., KLEJNOT, J., ZHAO, X., SHALITIN, D., MAYMON, M., YANG, H., LEE, J., LIU, X., LOPEZ, J. & LIN, C. 2007. Arabidopsis cryptochrome 2 completes its posttranslational life cycle in the nucleus. *Plant Cell,* 19**,** 3146-3156.

ZENTELLA, R., SUI, N., BARNHILL, B., HSIEH, W. P., HU, J. H., SHABANOWITZ, J., BOYCE, M., OLSZEWSKI, N. E., ZHOU, P., HUNT, D. F. & SUN, T. P. 2017. The Arabidopsis O-fucosyltransferase SPINDLY activates nuclear growth repressor DELLA. *Nature Chemical Biology,* 13**,** 479-+.

ZHANG, W. G., MCELROY, D. & WU, R. 1991. Analysis of rice Act1 5' region activity in transgenic rice plants. *The Plant Cell,* 3**,** 1155-1165.

ZHANG, Y., SCHWARZ, S., SAEDLER, H. & HUIJSER, P. 2007. SPL8, a local regulator in a subset of gibberellin-mediated developmental processes in Arabidopsis. *Plant Molecular Biology,* 63**,** 429-439.

ZHAO, X. L., SHI, Z. Y., PENG, L. T., SHEN, G. Z. & ZHANG, J. L. 2011. An atypical HLH protein OsLF in rice regulates flowering time and interacts with OsPIL13 and OsPIL15. *New Biotechnology,* 28**,** 788-797.

ZHOU, J., LIU, Q., ZHANG, F., WANG, Y., ZHANG, S., CHENG, H., YAN, L., LI, L., CHEN, F. & XIE, X. 2014a. Overexpression of OsPIL15, a phytochrome-interacting factor-like protein gene, represses etiolated seedling growth in rice. *Journal of integrative plant biology,* 56**,** 373-87.

ZHOU, J. J., LIU, Q. Q., ZHANG, F., WANG, Y. Y., ZHANG, S. Y., CHENG, H. M., YAN, L. H., LI, L., CHEN, F. & XIE, X. Z. 2014b. Overexpression of OsPIL15, a phytochromeinteracting factor- like protein gene, represses etiolated seedling growth in rice. *Journal of Integrative Plant Biology,* 56**,** 373-387.

ZHOU, Q. Q., HARE, P. D., YANG, S. W., ZEIDLER, M., HUANG, L. F. & CHUA, N. H. 2005. FHL is required for full phytochrome A signaling and shares overlapping functions with FHY1. *Plant Journal,* 43**,** 356-370.

ZHOU, X., ZHANG, Z. L., PARK, J., TYLER, L., YUSUKE, J., QIU, K., NAM, E. A., LUMBA, S., DESVEAUX, D., MCCOURT, P., KAMIYA, Y. & SUN, T. P. 2016. The ERF11 transcription factor promotes internode elongation by activating gibberellin biosynthesis and signaling. *Plant Physiology,* 171**,** 2760-2770.

ZHU, Y. X., TEPPERMAN, J. M., FAIRCHILD, C. D. & QUAIL, P. H. 2000. Phytochrome B binds with greater apparent affinity than phytochrome A to the basic helix-loop-helix factor PIF3 in a reaction requiring the PAS domain of PIF3. *Proceedings of the National Academy of Sciences of the United States of America,* 97**,** 13419-13424.

ZHU, Y. Y., NOMURA, T., XU, Y. H., ZHANG, Y. Y., PENG, Y., MAO, B. Z., HANADA, A., ZHOU, H. C., WANG, R. X., LI, P. J., ZHU, X. D., MANDER, L. N., KAMIYA, Y., YAMAGUCHI, S. & HE, Z. H. 2006. ELONGATED UPPERMOST INTERNODE encodes a cytochrome P450 monooxygenase that epoxidizes gibberellins in a novel deactivation reaction in rice. *Plant Cell,* 18**,** 442-456.

ZONG, Y., WANG, Y., LI, C., ZHANG, R., CHEN, K., RAN, Y., QIU, J. L., WANG, D. & GAO, C. 2017. Precise base editing in rice, wheat and maize with a Cas9-cytidine deaminase fusion. *Nature Biotechnology,* 35**,** 438-440.